frontiers | Research Topics

Bacteria-host interactions: from infection to carcinogenesis

Edited by
Marco Antonio Hernández-Luna and Maurizio Sanguinetti

Published in
Frontiers in Cellular and Infection Microbiology

ISSN 1664-8714
ISBN 978-2-8325-6498-1
DOI 10.3389/978-2-8325-6498-1

Generative AI statement
Any alternative text (Alt text) provided alongside figures in the articles in this ebook has been generated by Frontiers with the support of artificial intelligence and reasonable efforts have been made to ensure accuracy, including review by the authors wherever possible. If you identify any issues, please contact us.

About Frontiers

Frontiers is more than just an open access publisher of scholarly articles: it is a pioneering approach to the world of academia, radically improving the way scholarly research is managed. The grand vision of Frontiers is a world where all people have an equal opportunity to seek, share and generate knowledge. Frontiers provides immediate and permanent online open access to all its publications, but this alone is not enough to realize our grand goals.

Frontiers journal series

The Frontiers journal series is a multi-tier and interdisciplinary set of open-access, online journals, promising a paradigm shift from the current review, selection and dissemination processes in academic publishing. All Frontiers journals are driven by researchers for researchers; therefore, they constitute a service to the scholarly community. At the same time, the *Frontiers journal series* operates on a revolutionary invention, the tiered publishing system, initially addressing specific communities of scholars, and gradually climbing up to broader public understanding, thus serving the interests of the lay society, too.

Dedication to quality

Each Frontiers article is a landmark of the highest quality, thanks to genuinely collaborative interactions between authors and review editors, who include some of the world's best academicians. Research must be certified by peers before entering a stream of knowledge that may eventually reach the public - and shape society; therefore, Frontiers only applies the most rigorous and unbiased reviews. Frontiers revolutionizes research publishing by freely delivering the most outstanding research, evaluated with no bias from both the academic and social point of view. By applying the most advanced information technologies, Frontiers is catapulting scholarly publishing into a new generation.

What are Frontiers Research Topics?

Frontiers Research Topics are very popular trademarks of the *Frontiers journals series*: they are collections of at least ten articles, all centered on a particular subject. With their unique mix of varied contributions from Original Research to Review Articles, Frontiers Research Topics unify the most influential researchers, the latest key findings and historical advances in a hot research area.

Find out more on how to host your own Frontiers Research Topic or contribute to one as an author by contacting the Frontiers editorial office: frontiersin.org/about/contact

Bacteria-host interactions: from infection to carcinogenesis

Topic editors
Marco Antonio Hernández-Luna — University of Guanajuato, Mexico
Maurizio Sanguinetti — Catholic University of the Sacred Heart, Italy

Citation
Hernández-Luna, M. A., Sanguinetti, M., eds. (2025). *Bacteria-host interactions: from infection to carcinogenesis*. Lausanne: Frontiers Media SA.
doi: 10.3389/978-2-8325-6498-1

Table of contents

frontiers | Frontiers in Cellular and Infection Microbiology

TYPE Editorial
PUBLISHED 11 June 2025
DOI 10.3389/fcimb.2025.1634299

OPEN ACCESS

EDITED AND REVIEWED BY
Mariola J. Ferraro,
University of Florida, United States

*CORRESPONDENCE
Marco A. Hernández-Luna
marco.hernandez@ugto.mx

RECEIVED 24 May 2025
ACCEPTED 29 May 2025
PUBLISHED 11 June 2025

CITATION
Hernández-Luna MA (2025) Editorial: Bacteria-host interactions: from infection to carcinogenesis.
Front. Cell. Infect. Microbiol. 15:1634299.
doi: 10.3389/fcimb.2025.1634299

Editorial: Bacteria-host interactions: from infection to carcinogenesis

Marco A. Hernández-Luna*

Department of Medicine and Nutrition, Division of Health Science, University of Guanajuato, León, Mexico

KEYWORDS

bacteria-host interaction, carcinogenesis, tumoral microbiome, bacterial infection, viral infection

Editorial on the Research Topic
Bacteria-host interactions: from infection to carcinogenesis

An increasing number of microorganisms are being associated with the development and progression of cancer. The advent of techniques such as Next Generation Sequencing (NGS) has enabled the study of the tumor microbiome, opening a new field of research aimed at understanding the role of microorganisms—such as viruses and bacteria—in carcinogenesis.

This Research Topic, titled "*Bacteria–Host Interactions: From Infection to Carcinogenesis*," includes twelve publications: eight original research articles and four review articles, all of which describe the mechanisms through which microorganisms contribute to carcinogenesis.

Human papillomavirus (HPV) is a well-known infectious agent closely associated with various types of cancer. Persistent infection with HPV types 16 and 18 leads to the production of E6 and E7 viral proteins, which inactivate tumor suppressor genes such as p53 and pRb. This alters the cell cycle and promotes uncontrolled cell proliferation. While the mechanisms by which HPV induces carcinogenesis have been extensively studied, its impact on the vaginal microbiome remains less understood. In this regard, Li and Wu explored the association between HPV infection, cervical lesion severity, and the composition of the vaginal microbiome, proposing that microbial changes may influence cervical cancer progression.

Helicobacter pylori (*H. pylori*) has been identified as a major risk factor for gastric cancer (GC). Chronic infection results in persistent gastric mucosal inflammation, which can evolve into gastric atrophy, intestinal metaplasia, dysplasia, and, eventually, cancer. However, the mechanisms enabling this bacterium to colonize tumor tissue are not yet fully understood. Liu et al. investigated the relationship between progranulin (PGRN), a multifunctional protein dysregulated in various cancers, and *H. pylori* colonization. Their study describes how increased PGRN expression—induced by *H. pylori*—inhibits autophagy via the mTOR pathway, thereby facilitating bacterial internalization. These findings may contribute to the development of new therapeutic targets for reducing the risk of *H. pylori*–associated gastric cancer.

Moreover, *H. pylori* has been shown to promote carcinogenesis through other mechanisms, including mitochondrial DNA (mtDNA) damage. Shahi et al. published a review examining how *H. pylori* compromises mitochondrial genomic integrity by affecting the base excision repair mechanisms involving proteins such as POLG, TFAM, and MGME1. These alterations may lead to mtDNA deletions, increasing susceptibility to chronic inflammatory diseases linked to bacterial infections. The review also discusses how mtDNA damage and repair influence immune responses during *H. pylori* infection.

H. pylori has likewise been associated with programmed cell death (PCD) mechanisms, including apoptosis, autophagy, and necroptosis. Lin et al. reviewed how *H. pylori* activates PCD pathways. The bacterium interferes with apoptosis, leading to gastric tissue damage, and can also promote pyroptosis via the NLRP3 inflammasome pathway, which contributes to gastric tumor growth. The review further addresses how *H. pylori*–induced inhibition of autophagy could support carcinogenesis. Additional forms of cell death, such as necroptosis and ferroptosis, are also discussed in the context of bacterial involvement.

The available experimental models present significant challenges for understanding bacterial infections like that caused by *H. pylori*. Both *in vitro* and *in vivo* models are essential tools in this field. *In vitro* models provide a controlled environment to study bacteria–host interactions, while *in vivo* models offer insights into the progression of infection in a whole organism. However, the degree to which these models accurately replicate human infection remains a topic of debate. Patil et al. reviewed various infection models for *H. pylori* and discussed their applications in vaccine and drug development.

NGS technologies have allowed researchers to analyze changes in the tumor microbiome, revealing potential links between microbiota composition and cancer progression. Liu et al. investigated correlations between body mass index in GC patients, tumor-associated microbiota, and prognosis. Their findings suggest that the presence of bacteria from the genus *Abiotrophia*, which are associated with immune evasion, may promote tumor progression. This opens the possibility of antibiotic-based cancer therapies that target specific bacteria within the tumor microenvironment.

Oral cancer is a malignancy affecting tissues in the oral cavity, including the lips, tongue, gums, palate, and buccal mucosa. It has been strongly linked to tobacco and alcohol use, as well as infections such as HPV. In recent years, bacteria like *Fusobacterium nucleatum* (*F. nucleatum*) have also been associated with various gastrointestinal cancers, including those of the oral cavity. Although the precise mechanisms remain unclear, Selvaraj et al. reported that *F. nucleatum*'s adhesion to and invasion of oral epithelial cells enhances cell migration and invasion, potentially favoring metastasis in gastrointestinal tumors.

The oral microbiota comprises over 700 species of commensal bacteria, with the genus Streptococcus being among the most abundant. Its role in carcinogenesis is not fully understood. Inui et al. used an *in vitro* model found that *Streptococcus mitis* have a protective effect. The bacterium inhibited cell proliferation in oral squamous cell carcinoma (OSCC) by regulating the cell cycle, suggesting that certain commensal bacteria may play a role in controlling carcinogenesis and could be explored as therapeutic agents for oral cancers.

Global Transcriptomic Network Analysis allows large-scale exploration of gene interactions by integrating gene expression profiles. This approach enables the identification of patterns and contributes to the discovery of novel therapeutic targets. Using this method, Otálora-Otálora et al. found that neoplasms such as stomach and lung cancers share similarities in the expression of transcription factors regulating genes for receptors that interact with viruses such as HTLV-1, HPV, EBV, and SARS-CoV-2. Their research furthers our understanding of how microorganisms may influence cancer development and provides foundational data for improving diagnosis and treatment strategies for gastrointestinal and lung cancers.

Vimentin plays a pivotal role in cancer progression, being associated with epithelial–mesenchymal transition (EMT) and metastasis. Overexpression of vimentin in tumor cells enhances cell motility, invasiveness, and resistance to apoptosis. The factors driving vimentin upregulation remain unclear. In this context, Jang et al. reported that *Staphylococcus aureus* (*S. aureus*) induces vimentin expression via the TLR2 signaling pathway, facilitating its internalization into keratinocytes. Their study not only highlights vimentin as a potential therapeutic target for managing *S. aureus* infections, but also suggests that pathogenic microorganisms may promote tumor progression by enhancing vimentin expression.

Finally, an increasing number of bacterial species are being implicated in the carcinogenic process. Solomon et al. reviewed the role of *Ehrlichia chaffeensis* (*E. chaffeensis*), an intracellular bacterium that evades the host immune system and activates carcinogenic signaling pathways such as Wnt, Notch, and Hedgehog via Short Linear Motifs (SLiMs). Activation of these pathways by *E. chaffeensis* results in apoptosis inhibition, enhanced cell survival, and increased proliferation. Understanding the mechanisms by which *E. chaffeensis* modulates these cellular pathways could facilitate the development of new anticancer therapies and the identification of novel therapeutic targets.

Author contributions

MH-L: Writing – original draft, Writing – review & editing.

Acknowledgments

I thank Dr. Maurizio Sanguinetti, from the Department of Basic Biotechnological Sciences, Intensive and Perioperative Clinics, Catholic University of the Sacred Heart, Rome, Italy., for his invaluable work as part of the team of guest editors for this Research Topic.

Conflict of interest

The author declares that this research was conducted without any commercial or financial relationships that could be construed as potential conflicts of interest.

Generative AI statement

The author(s) declare that no Generative AI was used in the creation of this manuscript.

Publisher's note

frontiers | Frontiers in Cellular and Infection Microbiology

TYPE Original Research
PUBLISHED 31 July 2024
DOI 10.3389/fcimb.2024.1425367

OPEN ACCESS

EDITED BY
Maurizio Sanguinetti,
Catholic University of the Sacred Heart, Italy

REVIEWED BY
Shintaro Nakajima,
California Institute of Technology,
United States
Jie Chen,
Shanghai Jiao Tong University, China

*CORRESPONDENCE
Panpan Li
lipanpan@sdsmu.edu.cn
Hongyan Wang
wanghy@sdsmu.edu.cn

†These authors have contributed equally to this work and share first authorship

RECEIVED 29 April 2024
ACCEPTED 11 July 2024
PUBLISHED 31 July 2024

CITATION
Liu L, Xiang M, Zhou J, Ren Z, Shi W, Du X, Fu X, Li P and Wang H (2024) Progranulin inhibits autophagy to facilitate intracellular colonization of *Helicobacter pylori* through the PGRN/mTOR/DCN axis in gastric epithelial cells.
Front. Cell. Infect. Microbiol. 14:1425367.
doi: 10.3389/fcimb.2024.1425367

Progranulin inhibits autophagy to facilitate intracellular colonization of *Helicobacter pylori* through the PGRN/mTOR/DCN axis in gastric epithelial cells

Linlin Liu[1,2†], Miao Xiang[1,2†], Jiaqi Zhou[1,3†], Zongjiao Ren[1,2†], Wenjing Shi[4], Xianhong Du[1], Xiaoyan Fu[1], Panpan Li[1,2*] and Hongyan Wang[1,2*]

[1]Key Laboratory of Immune Microenvironment and Inflammatory Disease Research in Universities of Shandong Province, School of Basic Medical Sciences, Shandong Second Medical University, Weifang, China, [2]Department of Pathogenic Biology, School of Basic Medical Sciences, Shandong Second Medical University, Weifang, China, [3]Health Toxicology Laboratory, School of Public Health, Shandong Second Medical University, Weifang, China, [4]School Hospital, Shandong Second Medical University, Weifang, China

Helicobacter pylori (*H. pylori*) infection is the primary risk factor for the progress of gastric diseases. The persistent stomach colonization of *H. pylori* is closely associated with the development of gastritis and malignancies. Although the involvement of progranulin (PGRN) in various cancer types has been well-documented, its functional role and underlying mechanisms in gastric cancer (GC) associated with *H. pylori* infection remain largely unknown. This report demonstrated that PGRN was up-regulated in GC and associated with poor prognosis, as determined through local and public database analysis. Additionally, *H. pylori* induced the up-regulation of PGRN in gastric epithelial cells both *in vitro* and *in vivo*. Functional studies have shown that PGRN promoted the intracellular colonization of *H. pylori*. Mechanistically, *H. pylori* infection induced autophagy, while PGRN inhibited autophagy to promote the intracellular colonization of *H. pylori*. Furthermore, PGRN suppressed *H. pylori*-induced autophagy by down-regulating decorin (DCN) through the mTOR pathway. In general, PGRN inhibited autophagy to facilitate intracellular colonization of *H. pylori* via the PGRN/mTOR/DCN axis. This study provides new insights into the molecular mechanisms underlying the progression of gastric diseases, suggesting PGRN as a potential therapeutic target and prognostic predictor for these disorders.

KEYWORDS

Helicobacter pylori, autophagy, PGRN, intracellular colonization, DCN

1 Introduction

Helicobacter pylori (*H. pylori*) is a Gram-negative microaerobic bacterium that colonizes the gastric mucosa. It initiates a chronic inflammatory response, which progresses through a multi-step gastric tumorigenesis cascade known as Correa's cascade (Thrift et al., 2023). Upon infection, *H. pylori* establishes long-term colonization on the gastric mucosal surface and subsequently invades large cytoplasmic vacuoles, where it continues to survive and alter the molecular composition of the vacuole (Amieva et al., 2002). *H. pylori* internalization in gastric epithelial cells exhibit greater resistance to immune response and antibiotic treatment and played a major role in tumor progression (Sit et al., 2020). Therefore, despite acting as an extracellular pathogen, a comprehensive understanding of the intracellular colonization mechanisms of *H. pylori* is crucial for preventing and treating persistent infections.

Autophagy is an intracellular degradation process that cells use to degrade and recycle cellular components. The process involves the formation of special structures called autophagosomes, which engulf damaged organelles, proteins, other cellular components and invading pathogens. These autophagosomes then fuse with lysosomes, which contain enzymes that break down the contents of the autophagosome for recycling. Autophagy plays a crucial role in maintaining cellular homeostasis, eliminating damaged components (Miller and Thorburn, 2021; Debnath et al., 2023). Pathogenic microorganisms have evolved multiple strategies to regulate or impede autophagy, leading to sustained intracellular survival (Kim et al., 2019; Chidambaram et al., 2022; Zhou et al., 2023). Autophagy has been found to have a complex role in regulating the survival of *H. pylori*, although the specific mechanisms involved are not yet well understood.

Progranulin (PGRN), known as GEP, GP88, or PC cell-derived multifunctional growth factor, consists of 593 amino acid residues (Anakwe and Gerton, 1990). It is involved in various physiological processes, including cell development, cell cycle progression, vascular and tissue repair, as well as the growth of bone and cartilage (Chen Q. et al., 2022). Numerous studies have shown the abnormal expression of PGRN in various cancers, including gastric cancer (GC), where its overexpression is closely associated with tumor proliferation, aggressiveness and adverse prognostic outcomes (Chen S. et al., 2022; Zhao et al., 2020; Do et al., 2021; Purrahman et al., 2022). Our preceding investigation revealed that *H. pylori* infection upregulated PGRN expressions in gastric epithelial cells and activated related signaling pathways, thereby enhancing the proliferation and migration of gastric cancer cells (Wang et al., 2011). Therefore, we aim to further investigate the mechanism through which PGRN exerts its oncogenic role. It has been documented that PGRN inhibits autophagy, thereby reducing MHC class I (MHC I) expression, limiting $CD8^+$ T cell infiltration, and promoting immune evasion in pancreatic ductal adenocarcinoma (Cheung et al., 2022). However, the interplay between PGRN and autophagy within gastric mucosal epithelial cells has not been investigated, and it remains unclear whether the upregulation of PGRN triggered by *H. pylori* infection influences autophagy, potentially facilitating the colonization of *H. pylori* in these cells.

To further elucidate the mechanism by which PGRN modulates autophagy and contributes to *H. pylori* colonization, we employed gene chip analysis and identified that decorin (DCN), as the primary target protein of PGRN, indicating its role in regulating *H. pylori* intracellular colonization. DCN, a small leucine-rich proteoglycan, is crucial in mediating a variety of cellular functions, including proliferation, differentiation, and inflammatory responses, by interacting with multiple growth factors and receptors (Schneider et al., 2021). Moreover, DCN functions as a tumor suppressor in GC, with its expression levels significantly associated with angiogenesis and patient prognosis, suggesting its potential as a therapeutic target for GC (Basak et al., 2021). Recent research has demonstrated that DCN can modulate the tumor microenvironment, thus inhibiting tumor progression by inducing autophagy and apoptosis (Wang et al., 2020; Liu et al., 2022). However, the precise role of DCN in PGRN-mediated autophagy warrants further investigation.

In this study, we elucidated the association between *H. pylori* intracellular colonization and autophagy, analyzing the impact of PGRN on the internalization of *H. pylori* and its mechanistic role in inhibiting autophagy via the PGRN/mTOR/DCN pathway.

2 Materials and methods

2.1 Cell culture and reagents

Human immortalized gastric epithelial cell line GES−1 and human GC cell lines BGC-823 were cultured in RPMI−1640 medium (Gibco, USA), supplemented with 10% newborn bovine serum (Gibco, USA) and maintained in a humidified atmosphere containing 5% CO_2 at 37°C. The autophagy inhibitor 3-MA (Selleck, USA) and mTOR inhibitor Everolimus (Selleck, USA) were dissolved in dimethyl sulfoxide (DMSO, China) for use in experiments.

2.2 Bacterial culture

As previously described, the wild-type *H. pylori* strain 26695 and SS1 were maintained in our laboratory. Briefly, the *H. pylori* strains were cultured in Brucella broth containing 5% FBS at 37°C under microaerobic conditions. Gastric cells were cocultured with *H. pylori* 26695 as a concentration of different multiplicity of infection (MOI) for designated durations.

2.3 Clinical samples

Atrophic gastric specimens were collected from 43 patients undergoing gastroscopic examination at the Affiliated Hospital of Shandong Second Medical University. These samples included *H. pylori*-positive chronic gastritis (n=24) and *H. pylori*-negative controls (n=19). 16S rRNA test and ^{13}C-urea breath test were used to demonstrate *H. pylori* infection status. Patients were regarded as being *H. pylori*-positive if two tests yielded positive results. None of

the patients had taken nonsteroidal anti-inflammatory drugs, antibiotics or proton pump inhibitors in the four weeks prior to the study. Additionally, 35 samples of paraneoplastic tissues and 50 GC tissue specimens were collected. The GC tissue specimens included *H. pylori*-negative samples (n=11), *H. pylori*-positive samples (n=32), and 7 samples that were not tested with ^{13}C-urea breath test. Informed consent was obtained from each patient before participation. Data on age, gender, and pertinent clinical history were collected for all subjects in accordance with the approval from the Ethics Committee at Shandong Second Medical University (2022YX045).

2.4 Animal models

Specific pathogen-free (SPF) C56BL/6 mice (female, four weeks old) were used for *H. pylori* SS1 infection *in vivo* and purchased from Beijing Huafukang Bio-technology Co (SCXK(Beijing)2019–0008). All mice were randomly divided into two groups: uninfected (n=6) and *H. pylori*-infected (n=6) based on "complete randomization" rules. Mice were inoculated via oral gavage with 2.2×10^8 colony forming units of *H. pylori* strain SS1 every other day for one month. Gastric tissues were collected 24 weeks later for rapid urease testing to confirm successful colonization of *H. pylori*, followed by additional analyses. All procedures and animal experiments were approved by the Animal Care and Use Committee of Shandong Second Medical University (2021SDL555).

2.5 Database and gene enrichment analysis

The gene expression levels of PGRN in GC and the clinical information of GC patients were derived from the Gene Expression Profiling Interactive Analysis (GEPIA, http://gepia.cancer-pku.cn/) and The Cancer Genome Atlas Program (TCGA, https://www.cancer.gov/ccg/research/genome-sequencing/tcga) database. Analysis of PGRN malignant expression in GC microenvironment by CTD database (https://www.ctdbase.org/) and TISCH database (http://tisch.comp-genomics.org/home/). Based on the expression of PGRN in patients, the expression levels were classified as high or low using the median expression level as the standard, survival analysis for GC patients was performed using the Kaplan–Meier Plotter (https://kmplot.com/analysis/). Gene set enrichment analysis (GSEA, https://www.gsea-msigdb.org/gsea/index.jsp) algorithm was employed to identify pathways significantly enriched between PGRN low and high tumor cells.

2.6 Immunohistochemical staining

Gastric tissues were fixed in 4% paraformaldehyde, paraffin-embedded, sectioned, deparaffinized with xylene, and rehydrated in ethanol. Following standard protocols, immunohistochemistry was conducted. Color development was achieved using DAB chromogenic solution (ZSGB Biotech), with subsequent hematoxylin staining of nuclei. Observations were made with an orthogonal fluorescence microscope (Olympus, Japan). The AOD is displayed in the bar chart as the measurement metric, which were assessed by ImageJ and checked by the individual pathologist.

2.7 Plasmids and siRNAs

The plasmid overexpressing PGRN and its corresponding negative control vector (pcDNA3.1) were successfully constructed and preserved in the laboratory. The PGRN and DCN siRNAs were purchased from Genepharma along with control siRNA (siNC). The lipofectamine 2000 (Invitrogen, USA) facilitated the transfection of plasmids and siRNA into GC cells. All experimental procedures are performed according to the manufacturer's instructions.

2.8 RNA extraction and quantitative real-time PCR

Trizol reagent (Invitrogen) was used to extract the total RNA from the GC cells or gastric tissues according to the manufacturer's protocol. RNA was reverse-transcribed into cDNA with a ReverTra Ace qPCR RT Kit (Toyobo, Japan). The mRNA expression levels of PGRN, DCN and *H. pylori* 16S rRNA were determined by using SYBR Green kit (AG, China) and the QuantStudio™ 1 Plus System (Applied Biosystems, USA) according to the protocol of manufacturer. Calculation of target mRNA levels was based on the CT method and normalization to human β-actin expression. The primer sequences are as follows:

PGRN, forward-5'-GGACAGTACTGAAGACTCTG-3', reverse-5'-GGATGGCAGCTTGTAATGTG-3';

DCN, forward-5'-GACAACAACAAGCTTACCAGAG-3', reverse-5'-TGAAAAGACTCACACCCGAATA-3';

β-actin, forward-5'-AGTTGCGTTACACCCTTTCTTG-3', reverse-5'-CACCTTCACCGTTCCAGTTTT-3';

16S rRNA, forward-5'-TGAGTACAAGACCCGGGAAC, reverse-5'-CAGTTCGGATTGTAGGCTGC-3'.

2.9 Western blot

Cell and tissue proteins were lysed using RIPA buffer containing PMSF protease inhibitor (Solarbio, China). The total protein concentration was quantified using a NanoDrop Lite Spectrophotometer (Thermo Scientific, USA). Proteins were then resolved by SDS-PAGE using either 10% or 12% gels and subsequently transferred onto PVDF membranes. The membranes were blocked with 5% nonfat milk at room temperature for one hour before overnight incubation with specific primary antibodies at 4°C. Following primary antibody binding, the membranes were washed and incubated with HRP-conjugated secondary antibodies. HRP-linked anti-mouse IgG

(7076) and anti-rabbit IgG (7074) antibodies were from Cell Signal Technology. The protein bands were visualized using an enhanced chemiluminescence (ECL) detection system (EMD Millipore, USA). The bar graph was the intensities of the corresponding bands, which were measured using ImageJ software and normalized to β-actin, dividing the target protein band intensity by the internal control protein band intensity. PGRN (sc-377036), β-actin (sc-47778) antibodies were from Santa Cruz Biotechnology. LC3B (ab192890), DCN (ab277636) antibodies were from Abcam, mTOR (A2445) and phospho-mTOR (AP0115) antibodies were from Abconal Biotechnology.

2.10 Transmission electron microscopy

Cells were collected, fixed in 2% paraformaldehyde, 0.1% glutaraldehyde and in 0.1 mol/L sodium cacodylate for 2 h, subsequently post-fixed in 1% osmium tetroxide (OsO_4) for 1.5 h, and then stained with 3% aqueous uranyl acetate for 1 h. Following an additional wash, cells were dehydrated through a graded series of and embedded in Epon-Araldite resin (Canemco, Canada). Ultrathin sections (0.05 μm) were prepared using an ultramicrotome, counterstained with 0.3% lead citrate, and examined on HT7700 (Hitachi, Japan) electron microscopy.

2.11 Confocal laser scanning microscope

Cells were infected with RFP-LC3B-expressing lentivirus and selected using 2 μg/ml puromycin. Subsequently, they were co-transfected with either PGRN plasmids or siRNAs, followed by infection with *H. pylori* at MOI 100:1 for 12 h. The formation of LC3B autophagic puncta was then monitored through sequential scanning with confocal laser scanning microscopy (CLSM) (Leica, Germany).

2.12 Gentamicin protection assay

The GPA was performed as previous studies to assess the invasion of gastric cells by *H. pylori*. *H. pylori* was introduced to gastric cells seeded in 24-well plates with antibiotic-free RPMI 1640 medium at an MOI of 100:1 for various durations. Unattached bacteria were removed by washing with 1 mL of warm PBS per well, followed by gentamicin (100 μg/ml, G1272, Sigma) treatment for 1 h to eliminate extracellular bacteria. After incubation, cells were washed and lysed with 0.5% saponin (47036, Sigma) in PBS at 37°C for 15 min. The lysates were then serially diluted from 10^1 to 10^3 into Brucella broth solid medium to culture viable intracellular *H. pylori* and the colonies were counted after an incubation period of 3–5 days.

2.13 Statistical analysis

The experimental data were statistically processed using SPSS 24.0 statistical software. Experimental data of three independent repeats were shown as mean ± standard deviation (SD). Paired t-test was used to compare the means between two groups; one-way ANOVA and multi way ANOVA was used for multiple groups. Survival analysis was performed using Kaplan-Meier. Figures were created in GraphPad Prism 8.0. $P<0.01$ and $P<0.05$ were considered statistically significant.

3 Results

3.1 PGRN is up-regulated in GC and associated with poor prognosis

PGRN plays a significant and pivotal role in the modulation and progression of tumorous growths (Dong et al., 2023). We firstly elucidated the relationship between PGRN and GC. Our findings revealed a marked upregulation of PGRN in GC specimens compared with normal gastric tissues based on TCGA database (Figures 1A, B). Furthermore, PGRN levels were significantly higher in malignant cells than in other cellular constituents of the GC microenvironment (Figure 1C). Notably, PGRN was highest in inflammation phenotype among the various malignant phenotypes studied (Figure 1D). Building on previous studies that linked increased PGRN with poor prognosis in certain cancers, Kaplan-Meier Plotter survival analysis also showed that higher PGRN expression is associated with poorer overall survival in GC patients (Figure 1E). To evaluate the association between PGRN expression and clinicopathological parameters, we analysed PGRN mRNA expression in TCGA database. The results showed that up-regulation of PGRN corresponded with advanced tumor/node/metastasis (TNM) stage and correlated with the increased tumor size and/or the extent of invasion into adjacent tissues (Supplementary Table 1). We further used clinical gastric tissues to prove the correlation between PGRN and GC, demonstrating higher expression of PGRN in GC compared to normal gastric tissues (Figure 1F). Collectively, these findings indicate that PGRN is up-regulated in GC and is indicative of poor prognosis.

3.2 *H. pylori* induces the up-regulation of PGRN in gastric epithelial cells

H. pylori infection is one of the major causes of chronic gastritis and GC. We further explore the association between *H. pylori* infection and PGRN. GSEA confirmed a significant association between PGRN mRNA expression and *H. pylori* infection (Figure 2A). To elucidate the clinical significance of PGRN in gastritis, we analyzed gastric tissues from patients at varying stages of gastritis and found a progressive increase in PGRN expression, ranging from normal gastric mucosa through superficial gastritis to atrophic gastritis (Figure 2B). Furthermore, comparative analysis revealed that PGRN mRNA expression in *H. pylori*-positive chronic gastritis tissues was higher than that in *H. pylori*-negative counterparts (Figure 2C). *In vitro* experiments demonstrated that *H. pylori* infection promoted PGRN expression

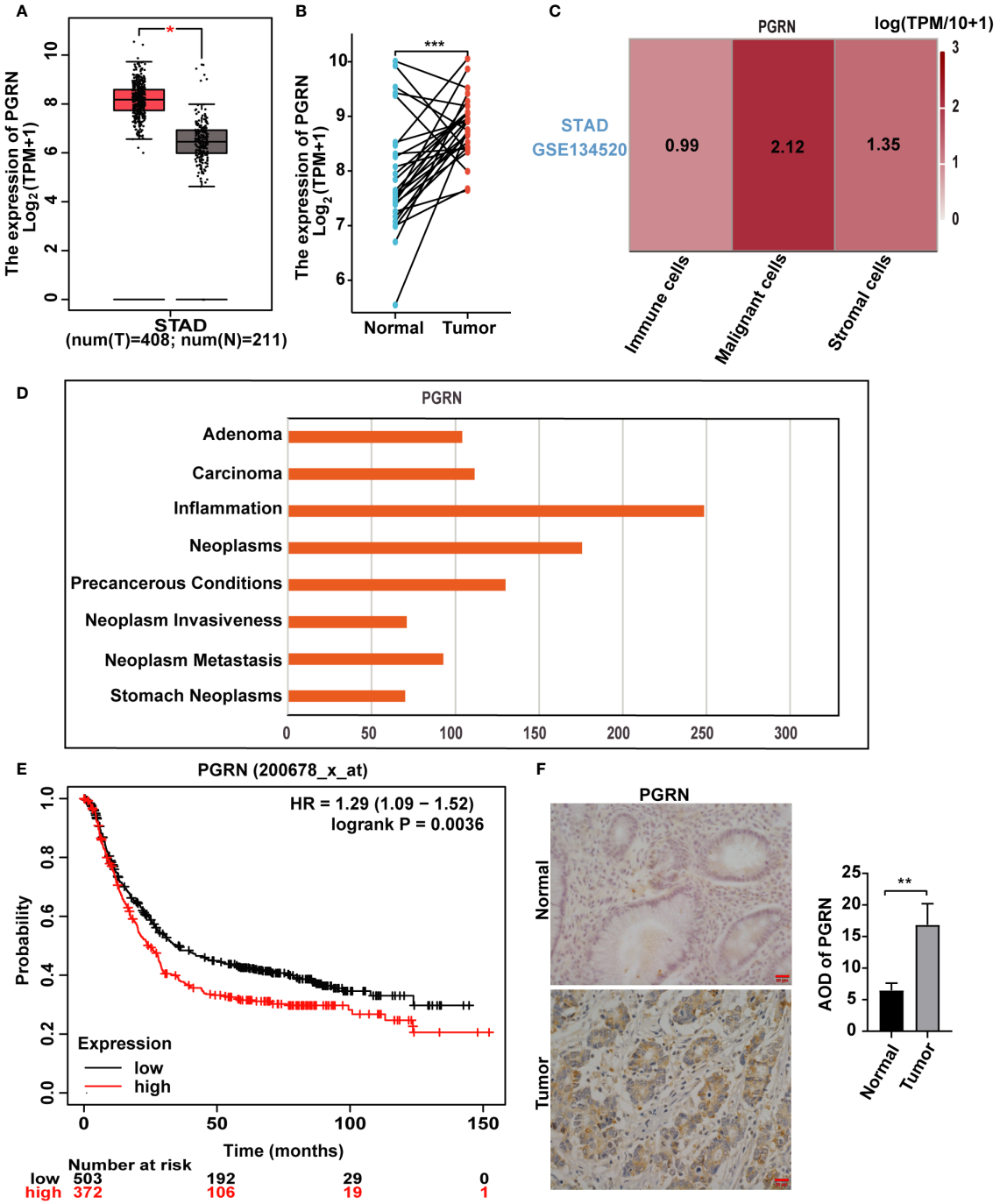

FIGURE 1
PGRN is up-regulated in GC and associated with poor prognosis. **(A)** Analysis of mRNA expression level of PGRN in GC tissues and non-tumor tissues according to TCGA database, with T representing GC tissue and N representing normal gastric mucosal epithelial tissue. **(B)** PGRN expression levels in GC and adjacent normal tissues across TCGA. The lines between the samples are one-to-one paired GC and para-cancerous tissue. **(C)** TISCH database analysis of PGRN expression in the microenvironment of GC (STAD-GSE134520). The number means the expression levels of PGRN in different cell types. **(D)** CTD database analysis of PGRN expression in malignant phenotype. **(E)** Kaplan-Meier analysis of overall survival (OS) in GC patients based on PGRN expression level. **(F)** Immunohistochemistry staining of PGRN in human adjacent normal and GC tissues. Scale bars, 20 μm. (*P<0.05, **P<0.01, ***P<0.001).

in gastric epithelial cells (Figure 2D). This up-regulation was corroborated *in vivo* both in *H. pylori*-negative, *H. pylori*-positive GC tissues and a mouse model infected with *H. pylori* (Figures 2E–G). Therefore, it is evident that *H. pylori* triggers the up-regulation of PGRN in gastric epithelial cells.

3.3 PGRN promotes the intracellular colonization of *H. pylori*

Although *H. pylori* was previously considered an extracellular bacterium, increasing evidence has shown that it can survive and even

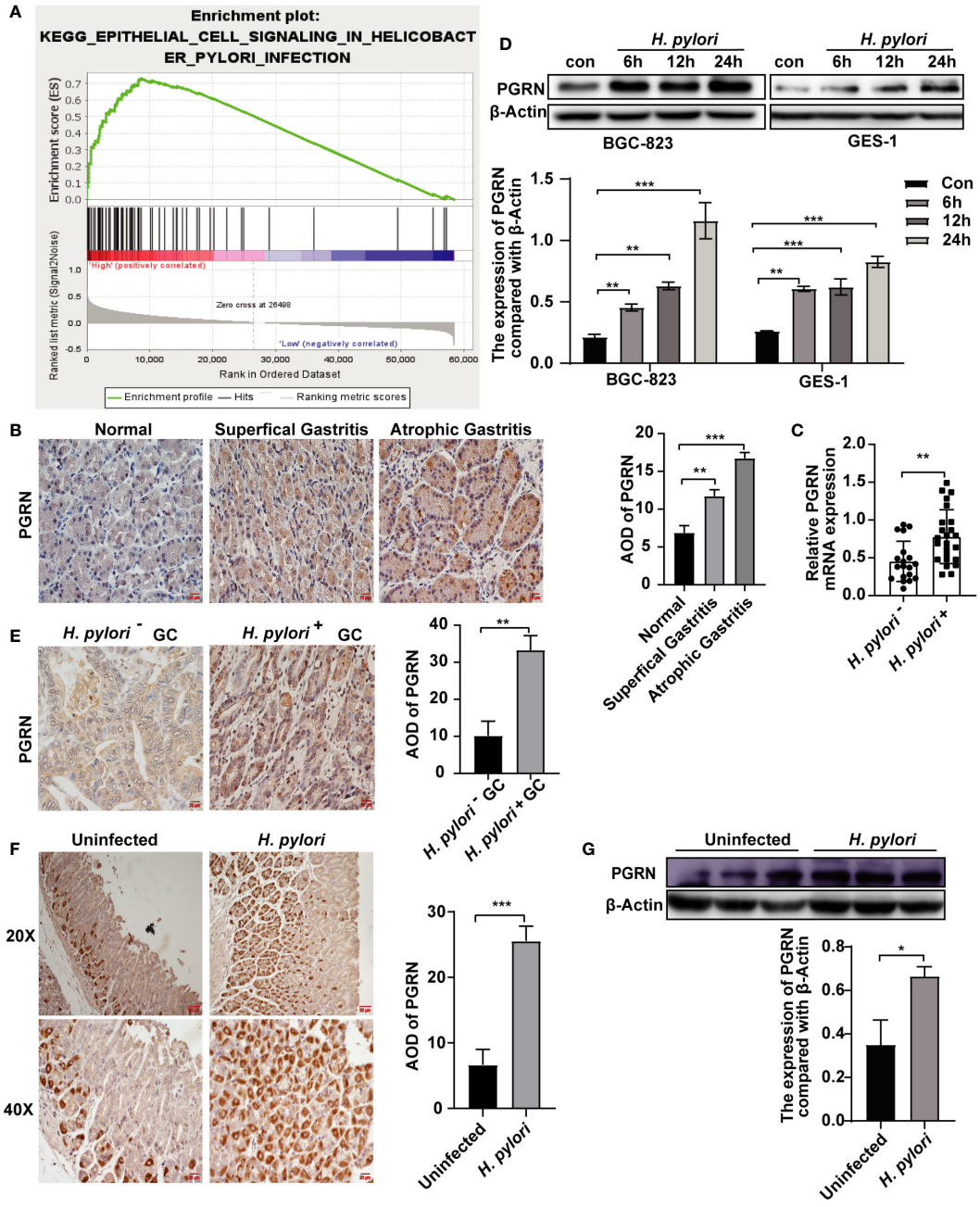

FIGURE 2
H. pylori induces the up-regulation of PGRN in gastric epithelial cells. **(A)** Enrichment plots of gene expression signatures for *H. pylori* infection according to PGRN mRNA expression in a GSEA analysis of TCGA. **(B)** Immunohistochemistry staining of PGRN in human normal, superficial gastritis and atrophic gastritis tissues. Scale bars, 20 μm. **(C)** qRT-PCR analysis of PGRN mRNA expression level in *H. pylori*-negative (n=19) and *H. pylori*-positive (n=24) chronic gastritis tissue samples. **(D)** Western blot of PGRN in in BGC-823 and GES-1 cells infected with *H. pylori* (MOI = 100) for 0, 6, 12 and 24 h. **(E)** Immunohistochemistry staining of PGRN in *H. pylori*-negative (n=11) and *H. pylori*-positive (n=32) GC tissues. Scale bars, 20 μm. **(F)** Immunohistochemistry staining of PGRN in containing *H. pylori*-negative and *H. pylori*- positive gastric tissues of mice. Scale bars, 50 μm (20X), 20 μm (40X). **(G)** Western blot of PGRN in *H. pylori*-negative and *H. pylori*-positive gastric tissues of mice. (**P*<0.05, ***P*<0.01, ****P*<0.001).

multiply inside gastric epithelial cells (Dubois and Borén, 2007). Therefore, our study aimed to investigate the impact of PGRN on the intracellular colonization of *H. pylori*. Utilizing *H. pylori* 16S rRNA and colony forming units assay followed by gentamicin treatment, we demonstrated the colonization of *H. pylori* within gastric epithelial cells (Figures 3A, B). Furthermore, overexpression of PGRN promoted the intracellular colonization of *H. pylori* into gastric epithelial cells, whereas knockdown of PGRN got the opposite effect (Figures 3C–E). These results indicate that PGRN promotes the intracellular colonization of *H. pylori*.

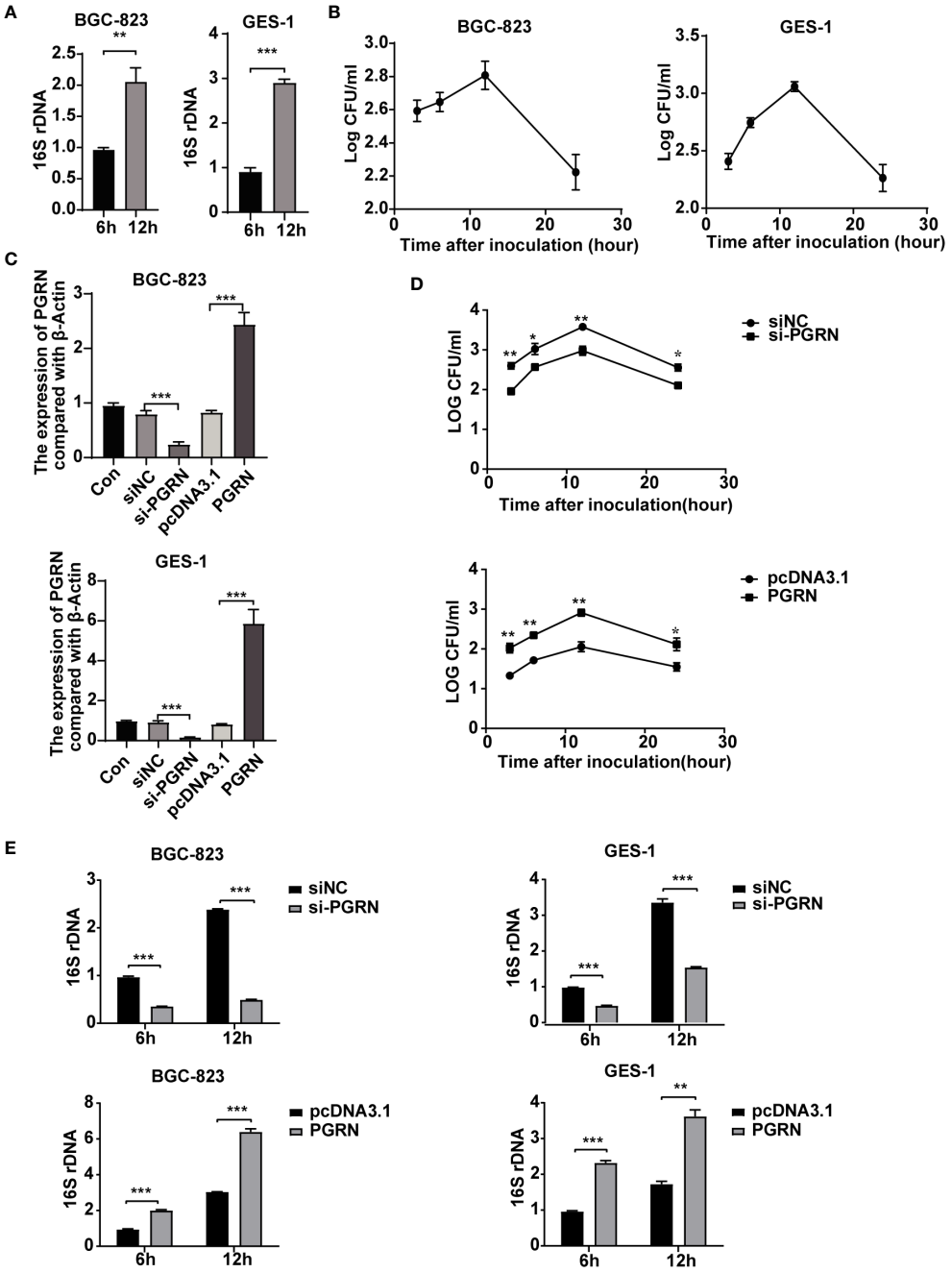

FIGURE 3
PGRN promotes the intracellular colonization of *H. pylori*. **(A)** qRT-PCR analysis of 16S rRNA in BGC-823 and GES-1 cells infected with *H. pylori* for 6 h, 12 h (n=3). **(B)** CFU analysis in BGC-823 and GES-1 cells infected with *H. pylori* (MOI = 100) for 3, 6, 12 and 24 h, then followed with gentamicin protection assay. **(C)** qRT-PCR analysis of PGRN mRNA expression level in BGC-823 and GES-1 cells transfected with PGRN siRNA or WT PGRN (n=3). **(D)** CFU analysis in BGC-823 cells transfected with PGRN siRNA or WT PGRN following *H. pylori* infection for indicated times, then followed with gentamicin protection assay (n=3). **(E)** qRT-PCR analysis of 16S rRNA levels in BGC-823 and GES-1 cells transfected with PGRN siRNA or WT PGRN following *H. pylori* infection for 6 h, 12 h (n=3). (**P*<0.05, ***P*<0.01, ****P*<0.001).

3.4 PGRN inhibits autophagy to promote intracellular colonization of *H. pylori*

Autophagy is involved in multiple biological processes regulated by *H. pylori* infection (Yang et al., 2022). To ascertain the effect of *H. pylori* on autophagy within gastric epithelial cells, we investigated the expression of LC3BI/II and the formation of RFP-LC3B puncta, a reliable autophagy marker, following *H. pylori* infection. Our findings showed that *H. pylori* infection promoted LC3B expression and RFP-LC3B puncta formation (Supplementary Figures 1A, B). These results indicate that *H. pylori* infection induces autophagy in gastric epithelial cells.

In order to investigate the underlying mechanism of PGRN in facilitating intracellular colonization of *H. pylori*, we employed gene

10.3389/fcimb.2024.1425367

microarray high pathway screening to examine the functions of PGRN involved in the regulation, revealing a close association between PGRN and the autophagic process in gastric epithelial cells (Supplementary Figure 1C). Meanwhile, GSEA highlighted the involvement of PGRN in regulating lysosome-associated pathways and cellular endocytosis (Supplementary Figures 1D, E), indicating a potential mechanism through which PGRN may influence *H. pylori*-induced autophagy. Furthermore, we found that down-regulation of PGRN significantly increased the expression of LC3B, while overexpression of PGRN had the opposite effects (Figure 4A).

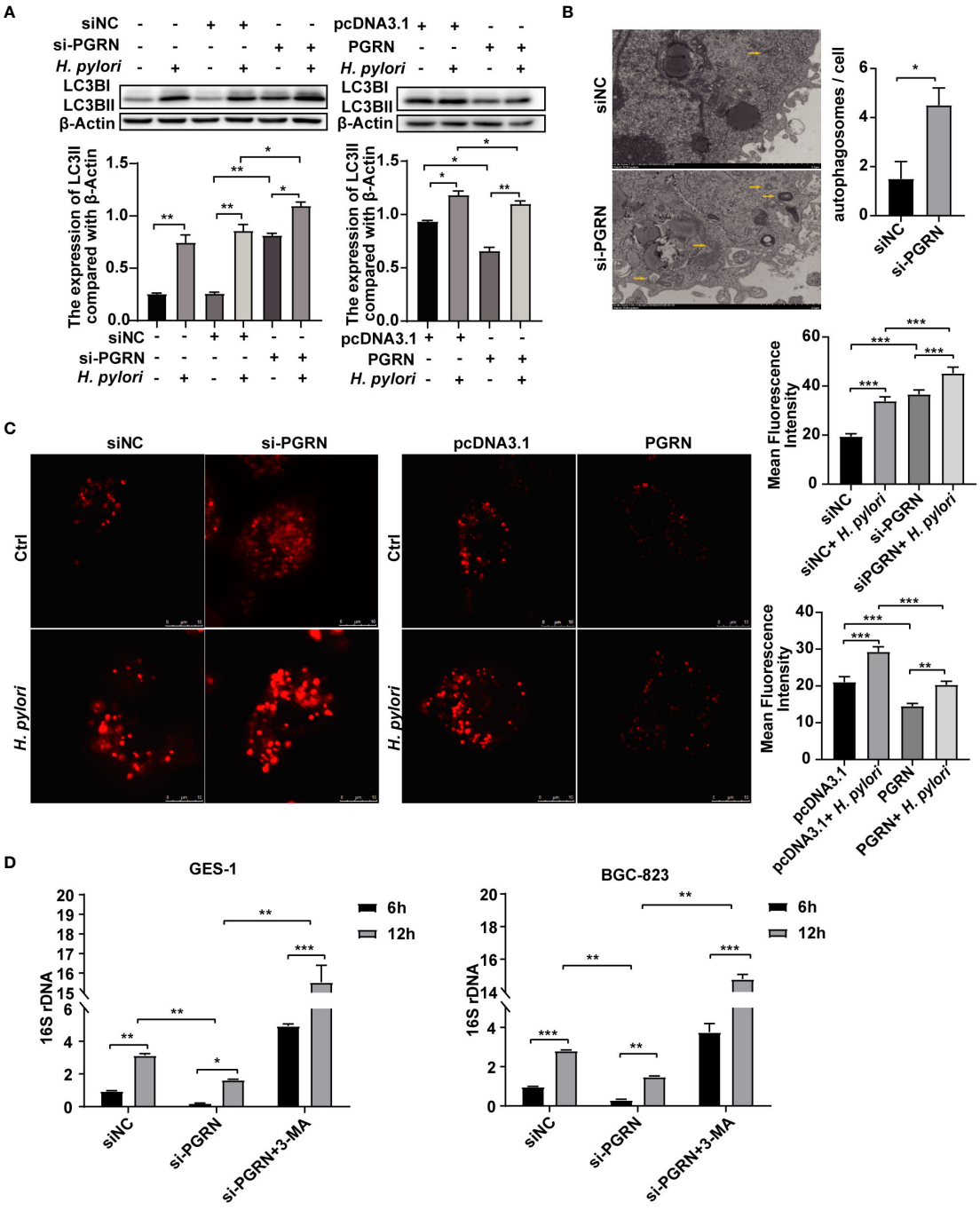

FIGURE 4
PGRN inhibits autophagy to promote intracellular colonization of *H. pylori*. **(A)** Western blot of LC3B in BGC-823 cells transfected with PGRN siRNA or WT PGRN following *H. pylori* infection for 12 h. **(B)** TEM images of autophagosomes in BGC-823 cells transfected with PGRN siRNA. Scale bars, 2 μm. **(C)** CLSM images of LC3B autophagy puncta in BGC-823 cells with stably expressing RFP-LC3B transfected with PGRN siRNA or WT PGRN following *H. pylori* infection. Scale bars, 10 μm. **(D)** qRT-PCR analysis of 16S rRNA levels in BGC-823 and GES-1 cells transfected with PGRN siRNA or WT PGRN following *H. pylori* infection for 12 h (MOI=100:1), with or without a pretreatment of the autophagy inhibitor 3-MA (10 nM, 2 h) (n=3). (**P*<0.05, ***P*<0.01, ****P*<0.001).

10.3389/fcimb.2024.1425367

Using TEM, we also observed a significant increase in autophagosome formation in gastric epithelial cells following PGRN interference (Figure 4B). CLSM analysis further confirmed the difference in LC3B autophagy puncta formation corresponding with PGRN expression (Figure 4C). More importantly, the inhibition of 16S rRNA of *H. pylori* due to PGRN knockdown could be rescued in the cells pretreated with 3-MA (Figure 4D). Taken together, we confirm that PGRN promotes *H. pylori* colonization in gastric epithelial cells by inhibiting cellular autophagy.

3.5 PGRN suppresses *H. pylori*-induced autophagy via down-regulation of DCN

To investigate the role of PGRN in regulating autophagy, a gene microarray was conducted to predict the interaction proteins of PGRN, and several genes were identified as a potential PGRN-associated protein (Figure 5A; Supplementary Table 2). Subsequent validation experiments confirmed that PGRN could negatively regulate DCN expression (Figure 5B). To confirm the effects of

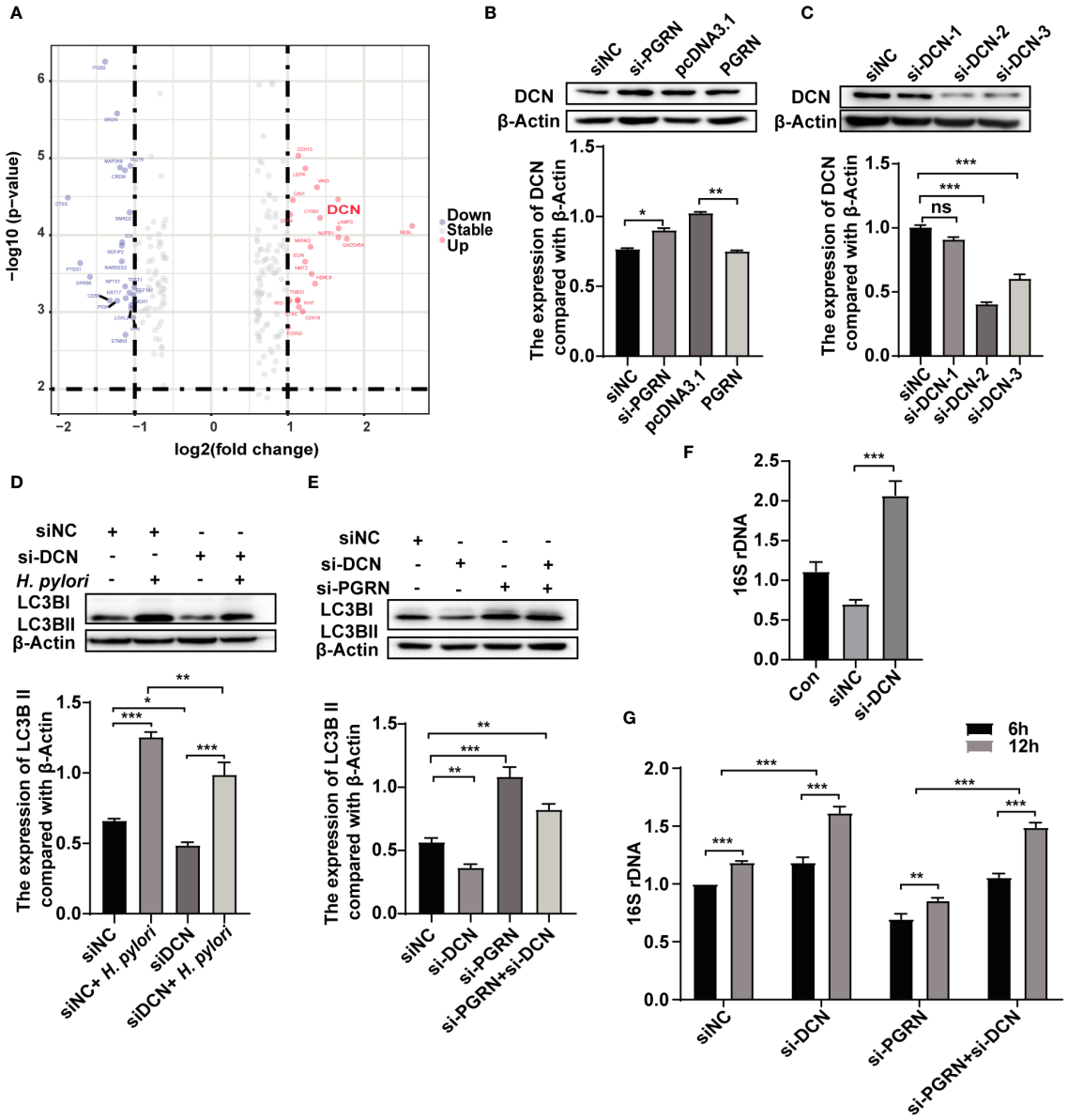

FIGURE 5
PGRN suppresses *H. pylori*-induced autophagy via down-regulation of DCN. **(A)** Gene microarray analysis of PGRN downstream target genes shown as volcano plots. **(B)** Western blot of DCN in BGC-823 cells transfected with WT PGRN and PGRN siRNA. **(C)** Western blot of DCN in BGC-823 cells transfected with DCN siRNA. **(D)** Western blot of LC3B in BGC-823 cells transfected with DCN siRNA following *H. pylori* infection for 12 h. **(E)** Western blot of LC3B in BGC-823 cells transfected with PGRN or/and DCN siRNA. **(F)** qRT-PCR analysis of 16S rRNA levels in BGC-823 cells transfected with DCN siRNA following *H. pylori* infection for 12 h (n=3). **(G)** qRT-PCR analysis of 16S rRNA levels in BGC-823 cells transfected with DCN siRNA, PGRN siRNA following *H. pylori* infection for 6, 12 h (n=3). (**P*<0.05, ***P*<0.01, ****P*<0.001, ns, not significant).

DCN on autophagy in gastric epithelial cells, we detected LC3B expression after down-regulation of DCN. Results showed that DCN knockdown inhibited autophagy induced by *H. pylori* infection (Figures 5C, D). Additionally, down-regulation of DCN rescued the level of LC3B, which was increased by PGRN knockdown (Figure 5E). Subsequently, the effect of DCN on intracellular bacterial colonization was investigated, showing that down-regulation of DCN enhanced the intracellular colonization of *H. pylori* (Figure 5F). Furthermore, co-transfection with si-PGRN and si-DCN attenuated the reduction of intracellular *H. pylori* colonization initially induced by PGRN knockdown (Figure 5G). These findings indicate that PGRN inhibits *H. pylori*-induced autophagy via down-regulation of DCN.

3.6 PGRN down-regulates DCN by inhibiting the mTOR pathway

The biogenesis of autophagic vesicles is intricately linked to the regulation by upstream pathways, including the mechanistic target of the rapamycin (mTOR) pathway (Pei et al., 2023). GSEA analysis revealed the involvement of PGRN in modulating the mTOR pathway (Figure 6A), suggesting that PGRN may regulate autophagy by influencing DCN expression through the mTOR signaling pathway. Upon the siRNA-mediated down-regulation of PGRN, an increase in phosphorylated mTOR (p-mTOR) levels was observed, with a corresponding alteration following PGRN overexpression (Figure 6B). Furthermore, up-regulation of DCN by si-PGRN was rescued via inhibiting mTOR (Figure 6C). Taken together, we confirmed that PGRN down-regulated DCN by inhibiting the mTOR pathway. And these findings highlight the crucial role of the mTOR pathway in mediating the effects of PGRN on DCN expression, autophagy and intracellular colonization.

4 Discussion

H. pylori, a significant risk factor closely associated with gastric carcinogenesis, has become a focal point of current research due to the urgent need to improve diagnostic and therapeutic strategies (Malfertheiner et al., 2023). Once individuals acquire *H. pylori* infection, the pathogen can persists in the gastric mucosa for a

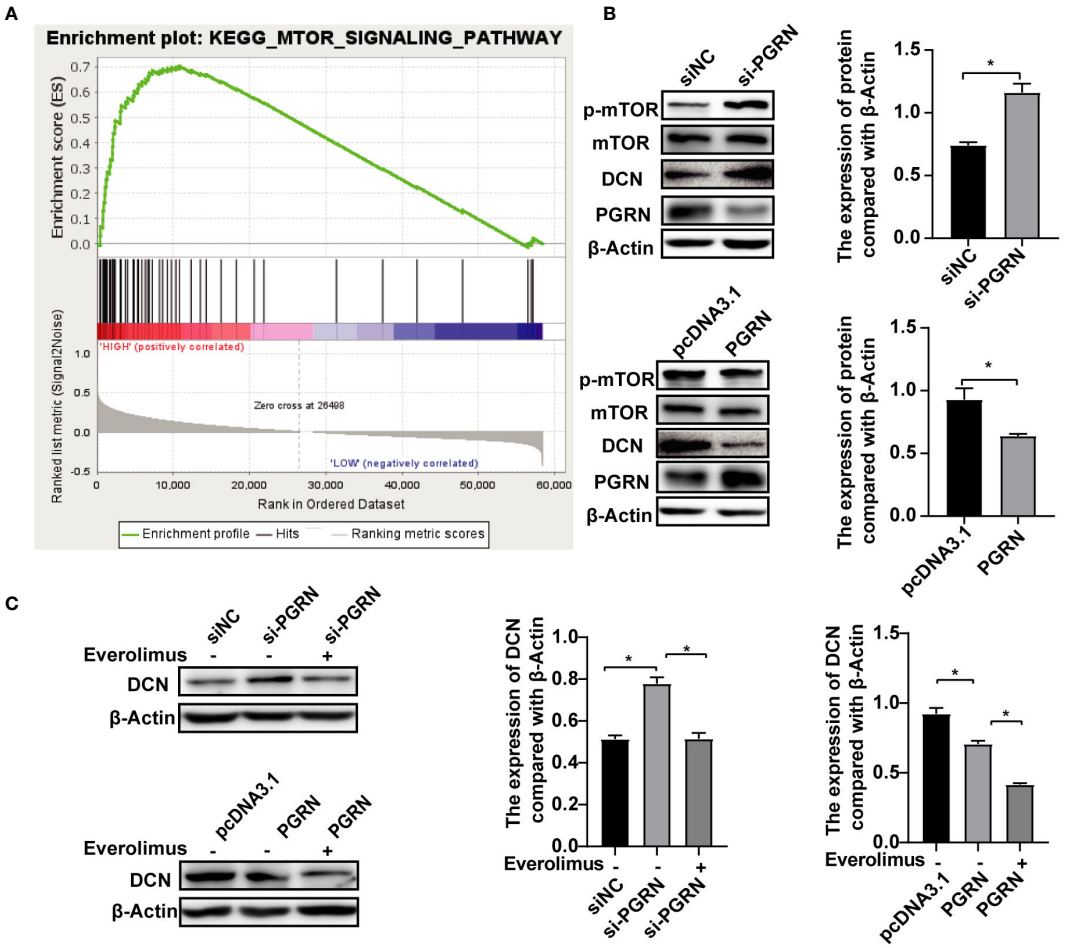

FIGURE 6
PGRN down-regulates DCN by inhibiting the mTOR pathway. **(A)** GSEA analyzed the involvement of PGRN in the mTOR pathway. **(B)** Western blot of mTOR signaling in BGC-823 cells transfected with PGRN siRNA or WT PGRN. **(C)** Western blot of DCN in BGC-823 cells transfected with PGRN siRNA or WT PGRN, then treated with Everolious (10 nM) for 2 h. (*P<0.05).

lifetime if left untreated. Although *H. pylori* is considered an extracellular pathogen, it also has the ability to invade and colonize host cells, thereby evading clearance by the immune system and causing long-term infection. Zhang discovered that *H. pylori* infection can reduce the sensitivity of Toll-like receptors 6 (TLR6) and down-regulate the expression of inflammatory factors, leading to persistent infection (Zhang et al., 2024). Our study also found that *H. pylori* is capable of intracellular invasion, colonization, and survival, with this ability increasing over time, as shown by intracellular 16S rRNA detection and colony formation after gentamicin treatment. However, the mechanisms underlying *H. pylori*-induced intracellular colonization remain unclear.

Autophagy is a cellular "cleanup" process that cells use to degrade and recycle unnecessary or dysfunctional cellular components. It plays a crucial role in maintaining cellular homeostasis, removing damaged organelles, clearing protein aggregates, and combating invading pathogens like bacteria, parasites, and viruses. However, pathogens can evade host cell elimination through various mechanisms, resulting in persistent bacterial infections. Studies has shown that the heparin-binding hemagglutinin (HBHA) of *Mycobacterium tuberculosis* inhibited autophagy in macrophages via Toll-like receptor 4, thereby promoting intracellular survival (Zheng et al., 2024). Similarly, Uropathogenic *Escherichia coli* PldA suppressed pre-autophagosomal structures, decreasing lysosomal cytotoxicity and escaping host immunity (Li et al., 2024). Furthermore, *H. pylori* also developed highly evolved mechanisms to escape autophagic degradation, manipulate autophagic pathways, and reconstruct autophagosomal compartments for survival in gastric cells (Capurro et al., 2020). Therefore, a key mechanism for *H. pylori* to evade host immune responses and maintain infection involves inhibiting autophagy and facilitating intracellular colonization in gastric epithelial cells. In our study, we discovered that *H. pylori* infection promoted the formation of LC3B autophagy puncta and up-regulated the expression of the autophagy-associated protein LC3B, while inhibiting autophagy using 3-MA resulted in increased intracellular bacterial loading and survival. However, the mechanism by which *H. pylori* regulates autophagy are complex and requires further study.

PGRN is a growth factor that plays a crucial role in various biological processes, including inflammation, wound healing, neurodegeneration and cancer development and progression. It has been reported that PGRN modulates PD-1 expression in tumor-associated macrophages (TAMs), promotes $CD8^+$ T cell rejection, and induces immune escape from breast cancer (Fang et al., 2021). Our previous research indicated that *H. pylori* can upregulate the expression of PGRN in gastric mucosal epithelial cells through the p38 MAPK and MEK1/2 signaling pathways. The elevated expression of PGRN can subsequently modulate G2/M stage and CDK4 to promote cell cycle progression, leading to the proliferation and migration of gastric cancer cells (Wang et al., 2011; Yang et al., 2017; Ren et al., 2022). While the intricate mechanisms by which PGRN regulate cell cycle and promote proliferation requires further study. Additionally, several studies have demonstrated that PGRN possesses pro-lysosomal functions, such as regulating protease activity, promoting lysosomal acidification, and facilitating protein trafficking (Tanaka et al., 2017; Zhou et al., 2017a, Zhou et al., 2017b). Therefore, it is worth investigating how *H. pylori*-induced upregulation of PGRN expression promotes lysosomal function in gastric mucosal epithelial cells. In this study, we present evidence that *H. pylori*-mediated PGRN induction, both *in vitro* and *in vivo*, suppresses autophagy, thus promoting the intracellular colonization and survival of *H. pylori* in gastric epithelial cells. Therefore, our findings may provide a novel mechanism that high expression of PGRN can inhibit autophagy in gastric mucosal cells, suppress pro-lysosomal functions, leading to the failure in eliminating

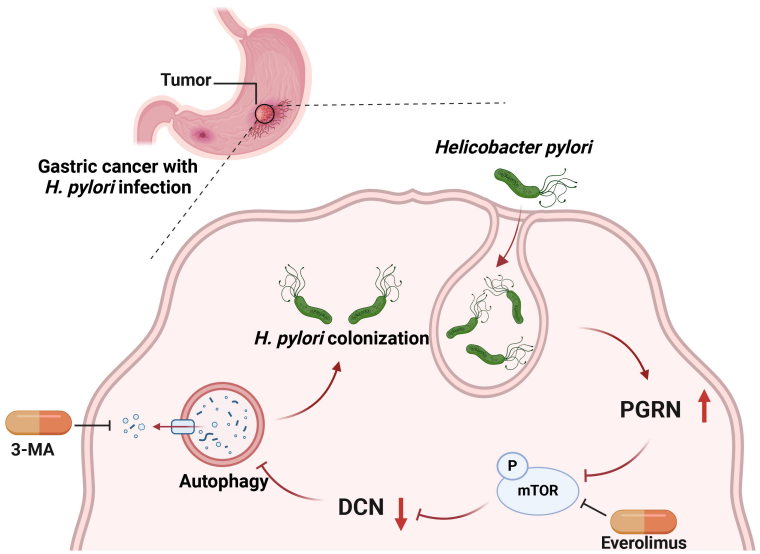

FIGURE 7
Working model for PGRN regulate autophagy and intracellular colonization in GC.

intracellular *H. pylori*, resulting in persistent infection and proliferation of *H. pylori* in the host cells.

To elucidate the molecular mechanisms underlying PGRN function, we employed high-throughput gene chip screening and bioinformatic analyses, which identified DCN as a probable functional target. Our findings demonstrated that DCN expression is up-regulated in PGRN-knockdown gastric epithelial cells. As a matrix-derived proteoglycan, DCN functions as a partial agonist for a variety of biological activities, directly interacting with a wide range of receptor tyrosine kinases (RTKs) and activating autophagy (Neill et al., 2017). Our data indicated that *H. pylori* infection triggered autophagy in gastric epithelial cells, while downregulation of DCN expression curtailed autophagy thus facilitating intracellular *H. pylori* colonization. Meanwhile, PGRN-mediated cellular autophagy and intracellular colonization were rescued by DCN. The autophagy inhibited by DCN downregulation may result from reduced interactions with PTKs, which will be further investigated in subsequent studies. Additionally, PGRN is significantly enriched in the mTOR pathway. The mTOR complex plays a critical role not only in gene transcription regulation and tumor metabolism but also in the regulation of autophagy and apoptosis. Our study shows that PGRN can inhibit mTOR phosphorylation to down-regulate DCN expression. Chen et al. indicated that Nobiletin can inhibit the protective effect of autophagy in GC cells through the PI3K/Akt/mTOR pathway (Chen et al., 2024). Additionally, Wang et al. proposed that Vitamin D3 promotes autophagy in GC cells by mediating AMPK/mTOR pathway (Wang et al., 2024). Therefore, the upregulated PGRN by *H. pylori* may inhibit mTOR phosphorylation through the regulation of PI3K/AKT and AMPK. Additional experiments using the mTOR inhibitor Everolimus confirmed that PGRN impeded *H. pylori*-induced autophagy in gastric epithelial cells by modulating DCN expression through the mTOR pathway.

In conclusion, *H. pylori*, previously regarded as an extracellular bacterium, can colonize and even multiply inside gastric epithelial cells. Our study revealed that *H. pylori* infection induces upregulation of PGRN, which in turn facilitates the intracellular colonization of *H. pylori* by attenuating cellular autophagy. This suppression occurs via the downregulation of DCN, mediated by the inhibition of the mTOR pathway (Figure 7). Our findings provide a novel mechanism by which PGRN enhances *H. pylori* colonization and promotes proliferation of gastric epithelial cells. Targeting PGRN in *H. pylori* infection and GC may offer new opportunities for treatment strategies in the future.

Data availability statement

The datasets presented in this study can be found in online repositories. The name of the repository and accession number can be found below: https://www.ncbi.nlm.nih.gov/geo/, GSE266076.

Ethics statement

The studies involving humans were approved by the Ethics Committee at Shandong Second Medical University (2022YX045). The studies were conducted in accordance with the local legislation and institutional requirements. The participants provided their written informed consent to participate in this study. The animal study was approved by the Animal Care and Use Committee of Shandong Second Medical University (2021SDL555). The study was conducted in accordance with the local legislation and institutional requirements. Written informed consent was obtained from the individual(s) for the publication of any potentially identifiable images or data included in this article.

Author contributions

LL: Writing – original draft, Project administration, Methodology, Investigation, Software. MX: Writing – original draft, Methodology, Investigation, Software, Project administration. JZ: Writing – original draft, Investigation, Project administration, Software, Methodology. ZR: Writing – original draft, Investigation, Methodology, Project administration, Software. WS: Writing – original draft, Funding acquisition, Methodology. XD: Writing – original draft, Methodology. XF: Writing – original draft, Methodology. PL: Writing – original draft, Writing – review & editing, Funding acquisition, Project administration, Validation, Formal analysis, Supervision, Software, Investigation, Methodology, Visualization, Resources. HW: Writing – original draft, Writing – review & editing, Supervision, Project administration, Validation, Methodology, Investigation, Formal analysis, Funding acquisition, Visualization, Resources, Software.

Funding

The author(s) declare financial support was received for the research, authorship, and/or publication of this article. This work was supported by grants from the Natural Science Foundation of Shandong Province (ZR2022MH172, ZR2022QH165), Development Programme for Young Innovation Teams in Shandong Higher Education Institutions (2023KJ254) and Weifang Science and Technology Development Programme (2023YX042).

Acknowledgments

We would like to give our sincere gratitude to the reviewers for their constructive comments, and members of our research laboratories for reading and guidance.

Conflict of interest

The authors declare that the research was conducted in the absence of any commercial or financial relationships that could be construed as a potential conflict of interest.

Publisher's note

All claims expressed in this article are solely those of the authors and do not necessarily represent those of their affiliated organizations, or those of the publisher, the editors and the reviewers. Any product that may be evaluated in this article, or claim that may be made by its manufacturer, is not guaranteed or endorsed by the publisher.

Supplementary material

The Supplementary Material for this article can be found online at: https://www.frontiersin.org/articles/10.3389/fcimb.2024.1425367/full#supplementary-material

References

Amieva, M. R., Salama, N. R., Tompkins, L. S., and Falkow, S. (2002). *Helicobacter pylori* enter and survive within multivesicular vacuoles of epithelial cells. *Cell Microbiol.* 4, 677–690. doi: 10.1046/j.1462-5822.2002.00222.x

Anakwe, O. O., and Gerton, G. L. (1990). Acrosome biogenesis begins during meiosis: evidence from the synthesis and distribution of an acrosomal glycoprotein, acrogranin, during Guinea pig spermatogenesis. *Biol. Reprod.* 42, 317–328. doi: 10.1095/biolreprod42.2.317

Basak, D., Jamal, Z., Ghosh, A., Mondal, P. K., Dey Talukdar, P., Ghosh, S., et al. (2021). Reciprocal interplay between asporin and decorin: Implications in gastric cancer prognosis. *PloS One* 16, e0255915. doi: 10.1371/journal.pone.0255915

Capurro, M. I., Prashar, A., and Jones, N. L. (2020). MCOLN1/TRPML1 inhibition - a novel strategy used by *Helicobacter pylori* to escape autophagic killing and antibiotic eradication therapy in *vivo*. *Autophagy* 16, 169–170. doi: 10.1080/15548627.2019.1677322

Chen, S., Bie, M., Wang, X., Fan, M., Chen, B., Shi, Q., et al. (2022). PGRN exacerbates the progression of non-small cell lung cancer via PI3K/AKT/Bcl-2 antiapoptotic signaling. *Genes Dis.* 9, 1650–1661. doi: 10.1016/j.gendis.2021.05.005

Chen, M., Li, H., Zheng, S., Shen, J., Chen, Y., Li, Y., et al. (2024). Nobiletin targets SREBP1/ACLY to induce autophagy-dependent cell death of gastric cancer cells through PI3K/Akt/mTOR signaling pathway. *Phytomedicine* 128, 155360. doi: 10.1016/j.phymed.2024.155360

Chen, Q., Wu, Z., and Xie, L. (2022). Progranulin is essential for bone homeostasis and immunology. *Ann. N Y Acad. Sci.* 1518, 58–68. doi: 10.1111/nyas.14905

Cheung, P. F., Yang, J., Fang, R., Borgers, A., Krengel, K., Stoffel, A., et al. (2022). Progranulin mediates immune evasion of pancreatic ductal adenocarcinoma through regulation of MHCI expression. *Nat. Commun.* 13, 156. doi: 10.1038/s41467-021-27088-9

Chidambaram, S. B., Essa, M. M., Rathipriya, A. G., Bishir, M., Ray, B., Mahalakshmi, A. M., et al. (2022). Gut dysbiosis, defective autophagy and altered immune responses in neurodegenerative diseases: Tales of a vicious cycle. *Pharmacol. Ther.* 231, 107988. doi: 10.1016/j.pharmthera.2021.107988

Debnath, J., Gammoh, N., and Ryan, K. M. (2023). Autophagy and autophagy-related pathways in cancer. *Nat. Rev. Mol. Cell Biol.* 24, 560–575. doi: 10.1038/s41580-023-00585-z

Do, I. G., Jung, K. U., Koo, D. H., Lee, Y. G., Oh, S., Kim, K., et al. (2021). Clinicopathological characteristics and outcomes of gastrointestinal stromal tumors with high progranulin expression. *PloS On.* 16, e0245153. doi: 10.1371/journal.pone.0245153

Dong, Y., Tan, H., Wang, L., and Liu, Z. (2023). Progranulin promoted the proliferation, metastasis, and suppressed apoptosis *via* JAK2-STAT3/4 signaling pathway in papillary thyroid carcinoma. *Cancer Cell In.* 23, 191. doi: 10.1186/s12935-023-03033-2

Dubois, A., and Borén, T. (2007). *Helicobacter pylori* is invasive and it may be a facultative intracellular organism. *Cell Microbiol.* 9, 1108–1116. doi: 10.1111/j.1462-5822.2007.00921.x

Fang, W., Zhou, T., Shi, H., Yao, M., Zhang, D., Qian, H., et al. (2021). Progranulin induces immune escape in breast cancer *via* up-regulating PD-L1 expression on tumor-associated macrophages (TAMs) and promoting CD8(+) T cell exclusion. *J. Exp. Clin. Cancer Res.* 40, 4. doi: 10.1186/s13046-020-01786-6

Kim, T. S., Jin, Y. B., Kim, Y. S., Kim, S., Kim, J. K., Lee, H. M., et al. (2019). SIRT3 promotes antimycobacterial defenses by coordinating mitochondrial and autophagic functions. *Autophagy* 15, 1356–1375. doi: 10.1080/15548627.2019.1582743

Li, X., Jiang, L., Zhang, S., Zhou, J., Liu, L., Jin, C., et al. (2024). Uropathogenic Escherichia coli subverts host autophagic defenses by stalling pre-autophagosomal structures to escape lysosome exocytosis. *J. Infect. Dis.* 8, jiae063. doi: 10.1093/infdis/jiae063

Liu, J., Zhu, S., Zeng, L., Li, J., Klionsky, D. J., Kroemer, G., et al. (2022). DCN released from ferroptotic cells ignites AGER-dependent immune responses. *Autophagy* 18, 2036–2049. doi: 10.1080/15548627.2021.2008692

Malfertheiner, P., Camargo, M. C., El-Omar, E., Liou, J. M., Peek, R., Schulz, C., et al. (2023). *Helicobacter pylori* infection. *Nat. Rev. Dis. Primers.* 9, 19. doi: 10.1038/s41572-023-00431-8

Miller, D. R., and Thorburn, A. (2021). Autophagy and organelle homeostasis in cancer. *Dev. Cell.* 56, 906–918. doi: 10.1016/j.devcel.2021.02.010

Neill, T., Sharpe, C., Owens, R. T., and Iozzo, R. V. (2017). Decorin-evoked paternally expressed gene 3 (PEG3) is an upstream regulator of the transcription factor EB (TFEB) in endothelial cell autophagy. *J. Biol. Chem.* 292, 16211–16220. doi: 10.1074/jbc.M116.769950

Pei, F., Ma, L., Jing, J., Feng, J., Yuan, Y., Guo, T., et al. (2023). Sensory nerve niche regulates mesenchymal stem cell homeostasis *via* FGF/mTOR/autophagy axis. *Nat. Commun.* 14, 344. doi: 10.1038/s41467-023-35977-4

Purrahman, D., Mahmoudian-Sani, M. R., Saki, N., Wojdasiewicz, P., Kurkowska-Jastrzębska, I., and Poniatowski Ł, A. (2022). Involvement of progranulin (PGRN) in the pathogenesis and prognosis of breast cancer. *Cytokine* 151, 155803. doi: 10.1016/j.cyto.2022.155803

Ren, Z., Li, J., Du, X., Shi, W., Guan, F., Wang, X., et al. (2022). *Helicobacter pylori*-induced progranulin promotes the progression of the gastric epithelial cell cycle by regulating CDK4. *J. Microbiol. Biotechnol.* 28, 844–854. doi: 10.4014/jmb.2203.03053

Schneider, M., Dillinger, A. E., Ohlmann, A., Iozzo, R. V., and Fuchshofer, R. (2021). Decorin-an antagonist of TGF-β in astrocytes of the optic nerve. *Int. J. Mol. Sci.* 22, 7660. doi: 10.3390/ijms22147660

Sit, W. Y., Chen, Y. A., Chen, Y. L., Lai, C. H., and Wang, W. C. (2020). Cellular evasion strategies of *Helicobacter pylori* in regulating its intracellular fate. *Semin. Cell Dev. Biol.* 101, 59–67. doi: 10.1016/j.semcdb.2020.01.007

Tanaka, Y., Suzuki, G., Matsuwaki, T., Hosokawa, M., Serrano, G., Beach, T. G., et al. (2017). Progranulin regulates lysosomal function and biogenesis through acidification of lysosomes. *Hum. Mol. Genet.* 1, 969–988. doi: 10.1093/hmg/ddx011

Thrift, A. P., Wenker, T. N., and El-Serag, H. B. (2023). Global burden of gastric cancer: epidemiological trends, risk factors, screening and prevention. *Nat. Rev. Clin. Oncol.* 20, 338–349. doi: 10.1038/s41571-023-00747-0

Wang, Y., He, Q., Rong, K., Zhu, M., Zhao, X., Zheng, P., et al. (2024). Vitamin D3 promotes gastric cancer cell autophagy by mediating p53/AMPK/mTOR signaling. *Front. Pharmacol.* 14. doi: 10.3389/fphar.2023.1338260

Wang, H., Sun, Y., Liu, S., Yu, H., Li, W., Zeng, J., et al. (2011). Upregulation of progranulin by *Helicobacter pylori* in human gastric epithelial cells *via* p38MAPK and MEK1/2 signaling pathway: role in epithelial cell proliferation and migration. *FEMS Immunol. Med. Microbiol.* 63, 82–92. doi: 10.1111/j.1574-695X.2011.00833.x

Wang, Y., Zhang, H., Zhang, Y., Li, X., Hu, X., and Wang, X. (2020). Decorin promotes apoptosis and autophagy *via* suppressing c-Met in HTR-8 trophoblasts. *Reproduction* 159, 669–677. doi: 10.1530/REP-19-0458

Yang, D., Li, R., Wang, H., Wang, J., Han, L., Pan, L., et al. (2017). Clinical implications of progranulin in gastric cancer and its regulation *via* a positive feedback loop involving AKT and ERK signaling pathways. *Mol. Med. Rep.* 16, 9685–9691. doi: 10.3892/mmr.2017.7796

Yang, Y., Shu, X., and Xie, C. (2022). An overview of autophagy in *Helicobacter pylori* infection and related gastric cancer. *Front. Cell Infect. Microbiol.* 12. doi: 10.3389/fcimb.2022.847716

Zhang, X., He, Y., Zhang, X., Fu, B., Song, Z., Wang, L., et al. (2024). Sustained exposure to *Helicobacter pylori* induces immune tolerance by desensitizing TLR6. *Gastric Cancer*. 27, 324–342. doi: 10.1007/s10120-023-01461-7

Zhao, Z., Li, E., Luo, L., Zhao, S., Liu, L., Wang, J., et al. (2020). A PSCA/PGRN-NF-κB-integrin-α4 axis promotes prostate cancer cell adhesion to bone marrow endothelium and enhances metastatic potential. *Mol. Cancer Res.* 18, 501–513. doi: 10.1158/1541-7786.MCR-19-0278

Zheng, Q., Li, Z., Zhou, Y., Li, Y., Gong, M., Sun, H., et al. (2024). Heparin-binding hemagglutinin of *Mycobacterium tuberculosis* inhibits autophagy *via* TLR4 and drives M2 polarization in macrophages. *J. Infect. Dis.* 24, jiae030. doi: 10.1093/infdis/jiae030

Zhou, X., Paushter, D. H., Feng, T., Pardon, C. M., Mendoza, C. S., and Hu, F. (2017a). Regulation of cathepsin D activity by the FTLD protein progranulin. *Acta Neuropathol.* 134, 151–153. doi: 10.1007/s00401-017-1719-5

Zhou, X., Sun, L., Bracko, O., Choi, J. W., Jia, Y., Nana, A. L., et al. (2017b). Impaired prosaposin lysosomal trafficking in frontotemporal lobar degeneration due to progranulin mutations. *Nat. Commun.* 25, 15277. doi: 10.1038/ncomms15277

Zhou, Y., Xiong, D., Guo, Y., Liu, Y., Kang, X., Song, H., et al. (2023). Salmonella Enteritidis RfbD enhances bacterial colonization and virulence through inhibiting autophagy. *Microbiol. Res.* 270, 127338. doi: 10.1016/j.micres.2023.127338

frontiers | Frontiers in Cellular and Infection Microbiology

TYPE Review
PUBLISHED 31 July 2024
DOI 10.3389/fcimb.2024.1416819

OPEN ACCESS

EDITED BY
Maurizio Sanguinetti,
Catholic University of the Sacred Heart, Italy

REVIEWED BY
Diane Bimczok,
Montana State University, United States
Giuseppe Losurdo,
University of Bari Medical School, Italy

*CORRESPONDENCE
Fafeng Cheng
700477@bucm.edu.cn
Changming Zhai
drzcm@bucm.edu.cn

†These authors have contributed equally to this work

RECEIVED 13 April 2024
ACCEPTED 08 July 2024
PUBLISHED 31 July 2024

CITATION
Lin Y, Liu K, Lu F, Zhai C and Cheng F (2024) Programmed cell death in *Helicobacter pylori* infection and related gastric cancer. *Front. Cell. Infect. Microbiol.* 14:1416819. doi: 10.3389/fcimb.2024.1416819

Programmed cell death in *Helicobacter pylori* infection and related gastric cancer

Yukun Lin[1†], Kunjing Liu[1†], Fang Lu[2], Changming Zhai[3*] and Fafeng Cheng[1*]

[1]School of Traditional Chinese Medicine, Beijing University of Chinese Medicine, Beijing, China, [2]School of Life Sciences, Beijing University of Chinese Medicine, Beijing, China, [3]Department of Rheumatism, Beijing University of Chinese Medicine Third Affiliated Hospital, Beijing, China

Programmed cell death (PCD) plays a crucial role in maintaining the normal structure and function of the digestive tract in the body. Infection with *Helicobacter pylori* (*H. pylori*) is an important factor leading to gastric damage, promoting the Correa cascade and accelerating the transition from gastritis to gastric cancer. Recent research has shown that several PCD signaling pathways are abnormally activated during *H. pylori* infection, and the dysfunction of PCD is thought to contribute to the development of gastric cancer and interfere with treatment. With the deepening of studies on *H. pylori* infection in terms of PCD, exploring the interaction mechanisms between *H. pylori* and the body in different PCD pathways may become an important research direction for the future treatment of *H. pylori* infection and *H. pylori*-related gastric cancer. In addition, biologically active compounds that can inhibit or induce PCD may serve as key elements for the treatment of this disease. In this review, we briefly describe the process of PCD, discuss the interaction between different PCD signaling pathways and the mechanisms of *H. pylori* infection or *H. pylori*-related gastric cancer, and summarize the active molecules that may play a therapeutic role in each PCD pathway during this process, with the expectation of providing a more comprehensive understanding of the role of PCD in *H. pylori* infection.

KEYWORDS

***Helicobacter pylori*, programmed cell death, gastric cancer, infection, therapy**

Introduction

Programmed cell death is an active, inherent phenomenon. It supports normal physiological activities during development and homeostasis after birth by eliminating damaged, infected or superannuated cells. In 1972, Kerr et al. made a groundbreaking discovery by describing a phenomenon known as apoptosis (Kerr et al., 1972). This phenomenon involves a programmed condensation of the nucleus and cytoplasm, leading to fragmentation of the cell into a series of membrane-bound, structurally well-preserved

fragments. Subsequently, these fragments are either shed from the epithelial-lined surfaces or taken up by other cells and rapidly degraded by lysosomal enzymes from macrophages. Subsequently, different forms of PCD were gradually discovered (Table 1). Today, programmed cell death includes genetically programmed suicide mechanisms, such as apoptosis, necroptosis and pyroptosis (Newton et al., 2024). It can also result from highly conserved processes to degrade macromolecular structures and even entire organelles, as in autophagy (Cadwell, 2016), or from dysregulated metabolism, as observed in ferroptosis (Tang et al., 2021).

Although the PCD plays a crucial role in maintaining homeostasis in our body and keeping it in a stable state, its normal processes can be disrupted by the invasion of pathogens, especially *H. pylori* infection. This disruption can unbalance our internal environment and possibly even trigger gastric cancer (Meng et al., 2015). In the early stage of infection, *H. pylori* can induce the expression of programmed death ligand 1 (PD-L1) on the epithelial cells of the stomach, for example via the Shh signaling pathway (Holokai et al., 2019). PD-L1, which interacts with programmed death 1 (PD1) on the surface of cytotoxic T lymphocytes (CTLs), can inhibit CTLs to induce PCD (Sun et al., 2007). In this way, cells infected with *H. pylori* can be protected from the immune response. In addition, *H. pylori* infection causes visible damage to both the superficial epithelial cells and the cells that form pits and glands in the stomach, caused directly by the bacteria or by PCD-mediated mechanisms (Genta, 1997). Once the destroyed glands can no longer regenerate, fibroblasts and extracellular matrix fill the space they previously occupied in the lamina propria. This leads to an irreversible loss of functional structure known as atrophy, a condition thought to be a precursor to gastric cancer (Correa, 1995). In addition, *H. pylori* infection triggers several intracellular signaling pathways, such as mitogen-activated protein kinase (MAPK), nuclear factor kappa B (NF-κB) and phosphatidylinositol 3-kinase (PI3K). These signaling pathways in turn have a direct and indirect effect on the proliferation, differentiation and programmed cell death of the gastric epithelium and ultimately lead to the conversion of epithelial cells into oncogenic units (Kato et al., 2008; Yousefi et al., 2019).

Overall, it is clear that PCD plays an important role in *H. pylori* infection. However, the relationship between PCD and *H. pylori* infection is complicated and not simply linear. During the infection process, *H. pylori* can both promote and inhibit PCD. For example, *H. pylori* infection can trigger both ROS formation and DNA fragmentation, leading to the activation of caspase-3 and caspase-8. This suggests that oxidative stress can be exerted on gastric epithelial cells during *H. pylori* infection, leading to apoptosis (Ding et al., 2007). However, other studies have shown that the gamma-glutamyl transpeptidase (GGT) of *H. pylori* can inhibit apoptosis and induce proliferation of gastric epithelial cells through the induction of cyclooxygenase-2, epidermal growth factor-related peptides and interleukin-8 (Ricci et al., 2014).

In this review, we provide a brief overview of the different pathways of PCD, including apoptosis, necroptosis, pyroptosis, autophagy and ferroptosis. We discuss their known and proposed roles in *H. pylori* infection to elucidate the intricate relationships. In addition, we describe proposed therapeutic strategies for the treatment of *H. pylori* infection that target key regulators of various PCD signaling pathways.

TABLE 1 Programmed cell death pathways with their morphological and biochemical features.

Programmed cell death	Morphological features and key pathway components	References
Apoptosis	Nuclear and cytoplasmic condensation (pyknosis), formation of extracellular vesicles (apoptotic bodies) and phagocytosis by surrounding cells.	(Kerr et al., 1972)
	Pro-apoptotic proteins of the BCL-2 family, MOMP, caspase activation (e.g. Apaf-1 in intrinsic apoptosis or FADD in extrinsic apoptosis), cleavage of caspase substrates and ROS production.	(Li et al., 1997) (Stennicke et al., 1998)
Necroptosis	Cell swelling, rupture of the plasma membrane, swelling of the cytoplasmic organelles and release of intracellular contents.	(Degterev et al., 2005)
	Inhibition of caspase-8, activation of RIPK1 and RIPK3, formation of the necrosome complex, phosphorylation of MLKL, inflammatory response and release of DAMPs (also called PAMPs in pathogenically infected cells).	(Li and Beg, 2000) (Holler et al., 2000)
Pyroptosis	Cell swelling or lack of cell swelling, rupture of the plasma membrane and release of intracellular contents (inflammation-related).	(Cookson and Brennan, 2001) (Moujalled et al., 2021)
	Activation of the inflammasome, cleavage of the GSDMD protein, release of pro-inflammatory cytokines (e.g. IL-18).	(Galluzzi et al., 2018)
Autophagy	Vacuolization of the cytoplasm, formation of autophagosomes, without chromatin condensation.	(Mizushima and Komatsu, 2011)
	ATG family proteins and the conversion of LC3-I to LC3-II (e.g. ATG7 and ATG3 are involved in the phosphorylation and lipidation of LC3 and promote the conversion).	(Bergmann, 2007)
Ferroptosis	Mitochondria that appear smaller than normal, with increased membrane density.	(Dixon et al., 2012)
	Excessive accumulation of iron, peroxidation of membrane lipids and glutathione depletion.	(Stockwell, 2022)

B-cell lymphoma gene 2 (BCL-2), Mitochondrial outer membrane permeabilization (MOMP), Apoptotic peptidase activating factor 1 (Apaf-1), FAS-associated death domain (FADD), Reactive oxygen species (ROS), Receptor-interacting serine/threonine-protein kinase 1 (RIPK1) activation, Mixed lineage kinase domain-like protein (MLKL), Damage-associated molecular patterns (DAMPs), Gasdermin D (GSDMD), Interleukin-18 (IL-18), Autophagy-related protein (ATG), Microtubule-associated protein 1A/1B-light chain 3 (LC3).

Programmed cell death in *H. pylori* infection and related gastric cancer

Apoptosis, common in *H. pylori* infection

The term "apoptosis" comes from the Greek and means "falling away", which reflects the characteristic property of apoptotic cells to disintegrate and fragment in a controlled manner. At the molecular level, apoptosis is triggered by either intrinsic or extrinsic signaling pathways, both of which converge in a common execution phase (Green, 2000). Intrinsic apoptosis is triggered by intracellular signals such as DNA damage, oxidative stress or growth factor deficiency and leads to the activation of pro-apoptotic proteins of the BCL-2 family, including BAX and BAK (Puthalakath and Strasser, 2002). These proteins promote permeabilization of the outer mitochondrial membrane, leading to the release of cytochrome c into the cytoplasm (Jost and Vucic, 2020). Cytochrome c then activates the caspase cascades, which ultimately leads to cell death. Extrinsic apoptosis, on the other hand, is triggered by extracellular signals, e.g. by the binding of death ligands to death receptors on the cell surface, such as tumor necrosis factor receptor 1 (TNFR1) or FAS. This interaction recruits and activates caspase-8, which can directly cleave and activate downstream effector caspases or trigger the mitochondrial signaling pathway through BID cleavage (Czabotar et al., 2014).

With the exponential increase in the number of publications on *H. pylori* as well as those written on apoptosis, it is clear that apoptosis is closely intertwined with *H. pylori* infection (Shirin and Moss, 1998). In the context of infection, there are changes in the extent of cell apoptosis, accompanied by changes in cell proliferation, migration and cytokine production (Alzahrani et al., 2014). In addition to directly triggering apoptosis, *H. pylori* induces sensitivity to various epithelial signaling pathways and events in the host. Certain mechanisms are triggered by *H. pylori* binding to cell surface receptors or by soluble virulence factors entering the epithelium, leading to the initiation of gastric pathologies, including inflammation, mucosal damage, and even the development of gastric cancer (Figure 1) (Tsai and Hsu, 2017).

Different apoptotic effects in *H. pylori* infection

Infection with *H. pylori* has different apoptotic effects on different types of host cells. In most cells, *H. pylori* infection increases apoptosis. In gastric epithelial cells, acute *H. pylori* infection significantly accelerated GES-1 apoptosis by increasing the expression of BAX and cleaved caspase-3, while decreasing the expression of BCL-2 (Liu et al., 2021). In lymphocytes, the researchers observed the transfer of apoptosis-inducing factor (AIF) from the mitochondria to the nucleus.

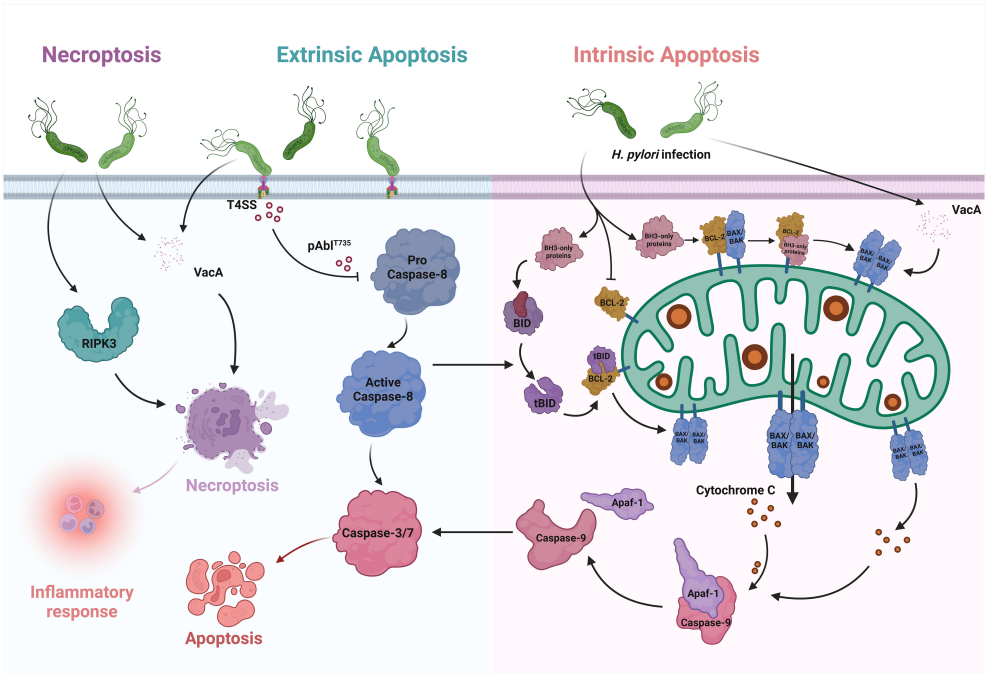

FIGURE 1
Apoptosis and Necroptosis in *H. pylori* infection. In the intrinsic pathway of apoptosis, only BH3 proteins are upregulated after *H. pylori* infection. They interact with the BCL-2 proteins, which are essential for survival, and thus override the inhibition of BAX and BAK. As a result, BAX and BAK oligomerize, leading to MOMP. After its release into the cytoplasm, cytochrome c binds to Apaf-1, which activates the initiator caspases and induces apoptosis. VacA, which causes the translocation of BAX and increases cytochrome c, can also enhance apoptosis. BID is one of the pure BH3 proteins. It can be cleaved by activated caspase-8 and releases BAX and BAK to activate intrinsic apoptosis via the MOMP pathway. In the extrinsic pathway, *H. pylori* promotes the formation of pAblT735 via the type IV secretion system (T4SS), thereby attenuating caspase-8-dependent cell apoptosis. In necroptosis, infection with *H. pylori* leads to an increase in the key factor RIPK3, which promotes the occurrence of inflammatory reactions. VacA also triggers necroptosis and releases considerable amounts of inflammatory mediators.

In addition, apoptosis of both T and B cells was significantly increased in *H. pylori* infected cells compared to uninfected controls (Singh et al., 2006). *H. pylori* induces apoptosis in T and B cell lines and translocates AIF. The destruction of T and B cells by apoptosis could explain the persistence of *H. pylori* infection. In the mononuclear phagocyte system, macrophages under infection have also shown the ability to induce apoptosis by the protein HP1286 secreted by *H. pylori* (Tavares and Pathak, 2017). Co-culturing *H. pylori* with peripheral blood monocytes, THP-1 or U937 cells leads to increased apoptosis (Zhang et al., 2017a). However, the researchers found that suppressing the expression of leukocyte-associated immunoglobulin-like receptor-1 (LAIR-1) on THP-1 cells can reduce this process (Zhang et al., 2017b). The results suggest that LAIR-1 modulates cell apoptosis and secretion of inflammatory cytokines in THP-1 cells, which may help to maintain inflammation and prevent the clearance of bacteria by the immune response. In gastric cancer cells, infection with *H. pylori* resulted in cell cycle arrest, decreased proliferation and increased apoptosis (Ding et al., 2008). *H. pylori* increased apoptosis in AGS cells with chromatin condensation and decreased BCL-2 levels, which was associated with NF-κB activation (Chu et al., 2003). In addition, *H. pylori* induced cullin 1-RING ubiquitin ligase (CRL1) and 26S proteasome-dependent degradation of STAMBPL1 in AGS (Chaithongyot and Naumann, 2022). STAMBPL1, which functions as a deubiquitinase of the anti-apoptotic protein survivin, balances the extent of survivin degradation with the E3 ligase CRL1 and thus regulates apoptotic cell death. Thus, the degradation of STAMBPL1 promotes apoptotic cell death.

However, there are always exceptions. Yang et al. found that *H. pylori* infection promotes apoptosis of MGC-803 cells, but high expression of FRA-1 induced by *H. pylori* suppresses this cell death (Yang et al., 2021). Liu et al. showed that acute infection with *H. pylori* significantly accelerated the apoptosis of GES-1, but the apoptosis rate of GES-1 cells with chronic *H. pylori* infection decreased significantly (Liu et al., 2021). Zhang et al. also demonstrated a novel mechanism by which *H. pylori* escapes from monocytes by upregulating early apoptosis and inhibiting late apoptosis (Zhang et al., 2017a). These studies have shown that inhibition of apoptosis of gastric epithelial cells due to chronic *H. pylori* infection is a contributing factor to severe gastric diseases, leading us to realize that the influence of *H. pylori* on cell apoptosis may not be unidirectional. An imbalance between apoptosis and proliferation may contribute to *H. pylori*-associated gastric carcinogenesis. Clinical research has also confirmed that dysregulation of apoptosis control in gastric intestinal metaplasia could further exacerbate gastric carcinogenesis, while elimination of *H. pylori* could potentially delay this process (Leung et al., 2001). It is worth noting that cell escape from apoptosis is an important link in the process of carcinogenesis.

Key virulence factors in apoptosis

H. pylori affects apoptosis through several virulence factors (Gonciarz et al., 2019). Among the numerous factors, the importance of Vacuolating cytotoxin A (VacA) and Cytotoxin-associated gene A (CagA) is obvious. Clinical studies have shown that gastric mucosal proliferation significantly correlates with the severity of acute gastritis in individuals infected with CagA+ VacA s1a strains of *H. pylori*. However, this increased proliferation was not accompanied by a parallel increase in apoptosis (Peek et al., 1997). The increased cell proliferation in the absence of a corresponding increase in apoptosis may explain the increased risk of gastric carcinoma associated with infection by CagA+ VacA s1a strains of *H. pylori*. VacA is observed in almost all clinical strains of *H. pylori*. While only certain strains produce the toxic and pathogenic VacA, this variant can induce vacuolization and apoptosis of cells (Ansari and Yamaoka, 2020). VacA can affect immune cells such as T cells and dendritic cells, leading to increased cell apoptosis (Winter et al., 2014; Kim et al., 2015). In addition, VacA can induce apoptosis in gastric cancer cells such as AGS and AZ-521 via low-density lipoprotein receptor-related protein-1 (LRP1) (Yahiro et al., 2012). But in some situations, the effect of VacA on cell apoptosis is also dual. In the response to *H. pylori* infection, infiltration of numerous inflammatory cells such as eosinophils occurs. VacA caused the translocation of cytoplasmic BAX to mitochondria and increased cytochrome c to facilitate apoptosis, while the expression of cellular apoptosis inhibitory protein (c-IAP)-2 was upregulated in the early phase of VacA stimulation (Kim et al., 2010). Another important virulence factor of *H. pylori* is the Cag secretion system. This system translocates CagA and peptidoglycan into the host cells, leading to the activation of PI3K signaling pathways. Activation of PI3K attenuated apoptosis in response to infection and was required for cell migration induced by *H. pylori* (Nagy et al., 2009). CagA can also inhibit cell apoptosis by reducing the expression of the tumor-suppressive E3 ubiquitin ligase proteins SIVA1 and ULF in SNU1 cells, possibly promoting the development of gastric cancer (Palrasu et al., 2022).

Having discussed the main virulence factors in *H. pylori* infection, we must not overlook other factors. *H. pylori* outer inflammatory protein A (OipA) is an outer membrane protein that contributes to gastric inflammation. It can trigger toxic events and initiate the apoptotic cascade in AGS through the intrinsic pathway (Teymournejad et al., 2017). In addition, Zhao et al. have shown that OipA affects apoptosis and cell cycle of AGS cells independent of its gene copy number (Zhao et al., 2020). However, Al-Maleki et al. reported that OipA "off" and ΔOipA cause a higher level of apoptosis in AGS cells than OipA "on" strains, and deletion of OipA increased bacterial VacA production (Al-Maleki et al., 2017). Virulence factors secreted by *H. pylori*, such as lipopolysaccharide (LPS) and the antigen complex glycic acid extract (GE), are also responsible for triggering apoptosis in gastric epithelial cells (Piotrowski et al., 1997; Gonciarz et al., 2020). In addition, the *H. pylori* T4SS effector D-glycero-β-D-manno-heptose-1,7-bisphosphate (βHBP) can trigger strong c-Abl threonine 735 phosphorylation and the process attenuates extrinsic apoptosis (Posselt et al., 2019). All these reports suggest that various virulence factors produced by *H. pylori* can regulate apoptosis through multiple signaling pathways. In addition to the bacterial virulence factors, the outer membrane vesicles (OMVs) secreted by *H. pylori*, which are involved in the transport of these factors, can also influence apoptosis through their various biologically active compounds (Chmiela et al., 2018). These metabolic by-products of *H. pylori* affect the migration,

proliferation and apoptosis of normal gastric cells, while they do not affect the proliferation and migration of gastric cancer cells (He et al., 2020). This creates the conditions for the transition from gastritis to gastric cancer under *H. pylori* infection.

Dysregulation of apoptosis, from infection to gastric cancer

Apoptosis triggered by *H. pylori* may play a key role in the development of gastric cancer (Xia and Talley, 2001). Dysregulation of apoptosis within the gastric epithelium and the surrounding microenvironment is a characteristic feature of *H. pylori* infection and contributes to the development of gastric cancer (Lim et al., 2023). *H. pylori* leads to chronic inflammation because the host is unable to eradicate the infection. The chronic inflammation leads to oxidative stress originating from immune cells and within the epithelial cells of the stomach (Hardbower et al., 2013). *H. pylori* infection can synergistically interact with the tumor microenvironment (TME) and lead to DNA damage, abnormal gene expression and activation of signaling pathways. In addition, it affects the host immune system to promote tumor cell proliferation and metastasis, facilitate epithelial-mesenchymal transition (EMT), suppress apoptosis, and provide energy for tumor growth (Zhu et al., 2022). EMT is the most important biological event in epithelial cell invasion or metastasis. Yu et al. investigated that *H. pylori* CagA also triggers EMT in gastric cancer cells and promotes the mobility of gastric cancer cells by regulating PDCD4 (Yu et al., 2014).

The pathways by which *H. pylori* triggers carcinogenesis and progression of gastric cancer are complex and include nitration and oxidation of DNA by mutagenic factors, epigenetic alterations by *H. pylori*, disruption of the balance between cell proliferation and apoptosis, and promotion of cancer cell invasion and metastasis by *H. pylori* (Meng et al., 2015). A clinical report showed that dysregulation of the BAX/BCL-2 system was observed in gastric cancer with a significant down-regulation of the pro-apoptotic effect. This uncontrolled cell proliferation is coupled with various proto-oncogenes that contribute to this process, resulting in inhibition of apoptosis and increased cell survival, ultimately promoting tumor growth (Figure 2) (Konturek et al., 2001). Rosania et al. also reported that BCL-2 gene expression decreased in preneoplastic gastric lesions such as atrophic gastritis and intestinal metaplasia. However, they found that proliferation and apoptosis did not correlate with the status of *H. pylori* infection (Rosania et al., 2017).

Necroptosis in *H. pylori* infection

Necroptosis is a form of PCD that differs from apoptosis in both its morphological and biochemical characteristics. While apoptosis is generally considered to be a process involving controlled shrinkage and fragmentation of the cell, necroptosis is a programmed form of

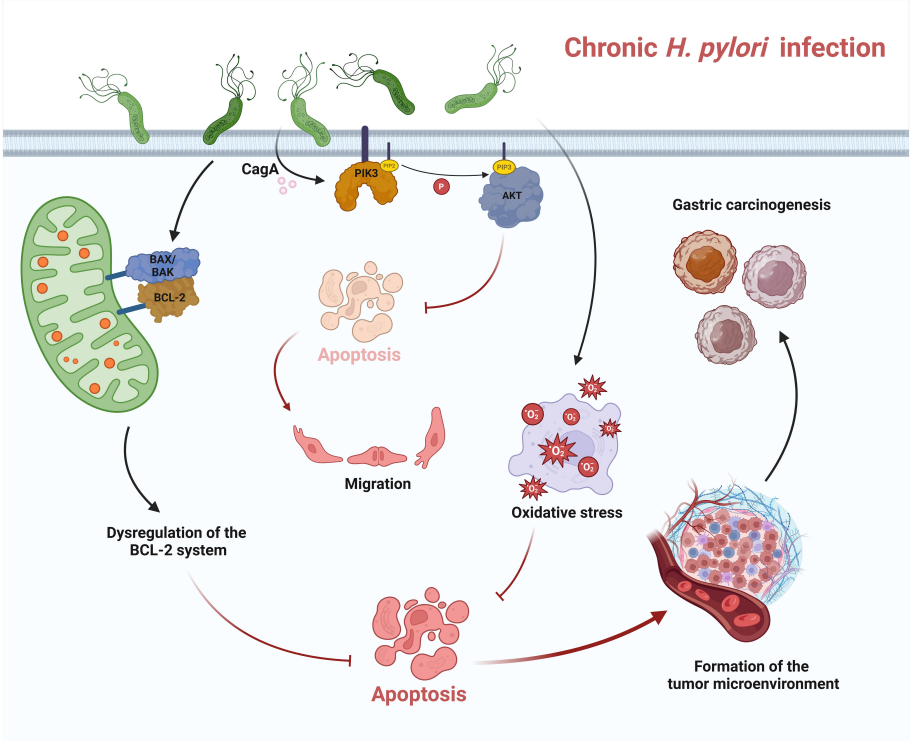

FIGURE 2
Apoptosis in chronic *H. pylori* infection. In chronic infection, *H. pylori* can trigger dysregulation of the BCL-2 system and downregulate apoptosis. *H. pylori* also leads to chronic inflammation, triggers oxidative stress and inhibits apoptosis. CagA, the virulence factor released by *H. pylori*, can regulate the activation of PI3K and AKT. AKT-dependent phosphorylation of caspase-9 attenuates apoptosis. All these dysregulations of apoptosis in chronic infection lead to the formation of a tumor microenvironment and ultimately contribute to the development of gastric cancer.

necrosis leading to cell swelling, rupture of the plasma membrane and release of cell contents, which in turn results in inflammation and immune activation (Degterev et al., 2005). At the molecular level, necroptosis is initiated by the activation of RIPKs, in particular RIPK1 and RIPK3 (Sun et al., 2012). During necroptosis, these kinases form a complex known as the necrosome, which phosphorylates and activates the pseudokinase MLKL. The activated MLKL oligomerizes and translocates to the plasma membrane, where it disrupts membrane integrity and leads to cell lysis (Murphy et al., 2013). Necroptosis can be triggered in response to various stimuli, including death receptor activation, toll-like receptor signaling, or cellular stress such as DNA damage or viral infection (Mocarski et al., 2011). In contrast to apoptosis, which is often inhibited by the activation of caspases, necroptosis can occur when caspase-8 is blocked, making it a potential surrogate mechanism for cell death in conditions where apoptosis is impaired (Tummers and Green, 2017).

Signs of necroptosis were found in *H. pylori* infection. Virulence factors, such as VacA, induce necroptosis in immune cells and release high levels of inflammatory mediators. In the tissues of patients with clinical *H. pylori* infection, increased expression of the necroptosis key factor RIPK3-positive cells was found in both gastritis and atrophic lesions (Figure 1) (Cui et al., 2022). Phenotypic analysis showed that numerous RIPK3-positive cells in the gastric glands were identified as H + K+ ATPase-positive parietal cells, while in the lamina propria they were mainly CD3-positive T lymphocytes and CD68-positive macrophages.

Pyroptosis dysregulation in *H. pylori* infection

Pyroptosis is a form of PCD characterized by inflammatory reactions and cell lysis. It is distinct from apoptosis and necroptosis and plays a crucial role in the defense against microbial infections as well as in various inflammatory diseases (Pachathundikandi et al., 2016). Pyroptosis is triggered by the activation of specific intracellular signaling pathways that lead to the formation of large pores in the plasma membrane and subsequent cell swelling and lysis (Cookson and Brennan, 2001). At the molecular level, pyroptosis is mainly mediated by a group of proteins known as inflammasomes. These are intracellular multiprotein complexes that recognize microbial infections or cell damage (Martinon et al., 2002). In response to these stimuli, the inflammasomes assemble and activate caspase-1, also known as interleukin-1β (IL-1β)-converting enzyme, which cleaves GSDMD, a key executioner protein of pyroptosis (Shi et al., 2015). Cleaved GSDMD forms pores in the plasma membrane, leading to osmotic swelling and eventual cell lysis. The activation of inflammasomes can be triggered by various DAMPs (also called PAMPs in pathogen-infected cells) that originate from microbial infections or host cells (Rathinam et al., 2010). These include bacterial LPS, bacterial DNA and host-derived molecules such as ATP and uric acid crystals (Kayagaki et al., 2013). When these signals are sensed, oligomerization of inflammasomes occurs, particularly the NLRP3 inflammasome (Nucleotide-Binding Oligomerization Domain-like Receptor Family, Pyrin Domain-Containing 3), which recruits the adaptor protein ASC and leads to activation of caspase-1 and subsequent pyroptosis (Pachathundikandi et al., 2020). Pyroptosis is associated with the release of pro-inflammatory cytokines, including IL-1β and IL-18, which are synthesized as inactive precursors and require cleavage by activated caspase-1 for activation and secretion. The release of these cytokines amplifies the inflammatory response, recruits immune cells to the site of infection and helps eliminate pathogens (Galluzzi et al., 2018).

Pyroptosis dysregulation is associated with *H. pylori* infection. *H. pylori* can regulate the key steps of pyroptosis through various virulence factors such as UreB, CagA and VacA, thereby initiating the inflammatory cascade (Figure 3) (Kumar and Dhiman, 2018). Although various virulence factors can trigger pyroptosis, the flagellin protein of *H. pylori*, which can trigger NLRC4 phosphorylation, does not activate the inflammasome, suggesting that NLRC4 phosphorylation is not sufficient for inflammasome activation (Matusiak et al., 2015). These results were supported by the observation that S533 is phosphorylated in the inactive NLRC4 monomer (Hu et al., 2013).

The NLRP3 inflammasome

In *H. pylori* infection, IL-1β is highly expressed, leading to gastric acid inhibition, gastric cancer-associated gene methylation and angiogenesis. The NLRP3 inflammasome facilitates the maturation of IL-1β in various cell types such as macrophages, neutrophils and dendritic cells (Yuan et al., 2023). Another study showed that *H. pylori* infection indeed upregulates the expression of pro-IL-1β in human immune cells, but secretes only very low levels of mature IL-1β. However, administration of exogenous control activators such as nigericin or ATP to infected cells immediately triggered the formation of the NLRP3 inflammasome and the subsequent release of substantial amounts of mature IL-1β (Pachathundikandi et al., 2020). This suggests that chronic *H. pylori* infection manipulates inflammasome activation and pyroptosis to promote bacterial persistence.

Nevertheless, this deregulation of the inflammasome during *H. pylori* infection is susceptible to external stimulation by microbial, environmental, or host molecules that act as inflammasome activators, leading to the production of large amounts of mature IL-1β and signal-mediated gastric tumorigenesis in humans. Zhang et al. found that *H. pylori* infection leads to NLRP3 inflammasome activation, generation of intracellular ROS, and increased gastric cancer cell invasion and migration. In addition, ROS inhibition by N-acetyl-L-cysteine (NAC) effectively blocks NLRP3 activation and pyroptosis. Silencing of NLRP3 reduces the effects of *H. pylori* infection on gastric cancer cell migration and invasion (Zhang et al., 2022a). Taken together, this suggests that the role of the NLRP3 inflammasome in *H. pylori* infection deserves attention.

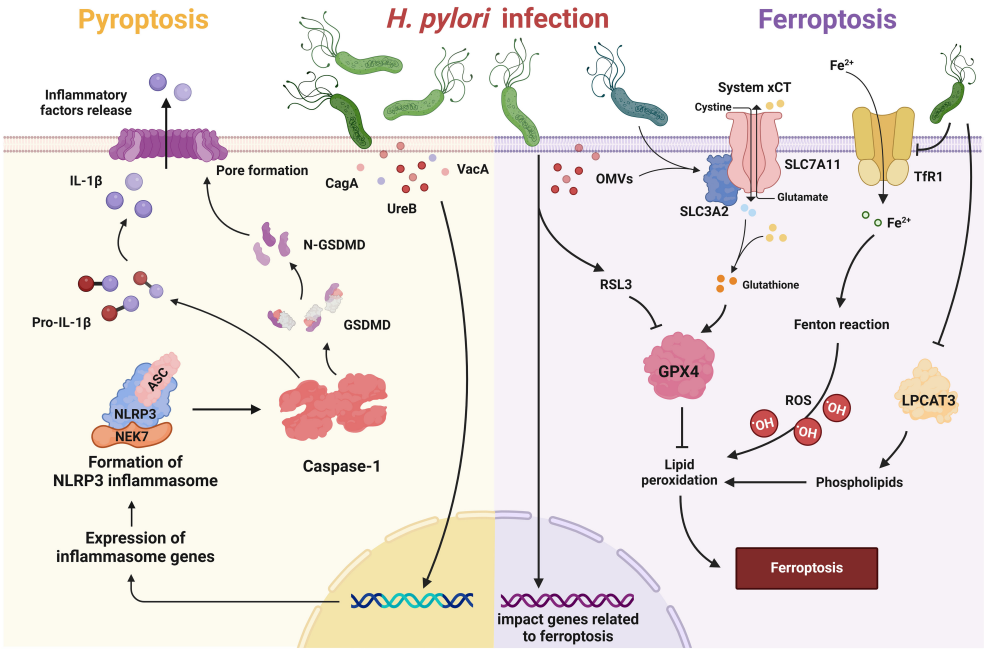

FIGURE 3
Pyroptosis and ferroptosis in *H. pylori* infection. In pyroptosis, *H. pylori* and its virulence factors (e.g. CagA, VacA, UreB) trigger the inflammatory cascade of NLRP3, which leads to the activation of caspase-1. Caspase-1 cleaves pro-IL-1β to generate its active form and also targets GSDMD, leading to recruitment of the N-terminal fragment of GSDMD to the plasma membrane. This leads to pore formation and the subsequent release of inflammatory factors. Upon ferroptosis, *H. pylori* and its OMVs upregulate Solute Carrier Family 3 Member 2 (SLC3A2) to attenuate ferroptosis, while repressing lysophosphatidylcholine acyltransferase 3 (LPCAT3) and downregulating transferrin receptor 1 (TfR1) to attenuate lipid peroxidation. *H. pylori* may also increase susceptibility to RAS-selective lethality 3 (RSL3)-induced ferroptosis by influencing associated genes.

Programmed cell death associated with autophagy

Autophagy, derived from the Greek words "auto" meaning self and "phagy" meaning to eat, is a highly conserved cellular process that is essential for maintaining cellular health and homeostasis (Ohsumi, 2014). It plays a crucial role in various physiological processes such as development, immunity and energy metabolism, and its dysregulation has been found in numerous diseases such as cancer, neurodegenerative disorders and metabolic syndromes. The process of autophagy begins with the formation of a double-membrane structure, the autophagosome. This structure engulfs cellular components to be degraded, such as damaged organelles or protein aggregates. The autophagosome then fuses with lysosomes, organelles filled with digestive enzymes, to form an autolysosome. In the autolysosome, the engulfed cargo is broken down into its individual molecules such as amino acids, fatty acids and sugars, which can then be recycled by the cell to generate energy or build new cell components (Zhang et al., 2014). There are three different types of autophagy, each of which fulfills different functions within the cell. Macroautophagy is the best-studied form of autophagy and involves the massive degradation of cytoplasmic contents. In microautophagy, cytoplasmic components are taken up directly by the lysosomes by invagination of the lysosomal membrane. Chaperone-mediated autophagy (CMA) selectively targets specific proteins for degradation by directing them to the lysosomes with the help of chaperone proteins (Yang and Klionsky, 2020). Under normal circumstances, autophagy can be regarded as a PCD process in cells or organelles (Chesnokov et al., 2024). It is a renewal process in which cellular components are recycled and redistributed to enable a dynamic balance within the cell. It is like tearing down an old wall and using the bricks to build a new house. When autophagy is disrupted, impaired cellular components can aggregate, leading to cellular senescence or autophagic cell death (Nabavi-Rad et al., 2023). Normally, autophagy turns off apoptosis, while activation of pro-apoptotic caspases can interrupt the autophagy process. However, under certain circumstances, autophagy can consume too much cytoplasmic material and promote apoptosis or necrosis, ultimately leading to autophagic cell death (Mariño et al., 2014). Unfortunately, *H. pylori* infection can promote autophagic dysregulation.

Autophagy and *H. pylori* infection

Infection with *H. pylori* has different autophagic effects on various types of host cells. In macrophages, *H. pylori* can secrete cholesterol-α-glucosyltransferase (CGT), which inhibits the fusion of autophagosomes with lysosomes, leading to a significant increase in bacterial load within macrophages, thereby impairing the autophagic process of macrophage clearance (Lai et al., 2018). In gastric epithelial cells, *H. pylori* manipulates the NOX-ROS-Nrf2/HO-1-ROS loop to control intracellular oxidative stress and also

affects ROS-mediated autophagy (Li et al., 2023a). In gastric cancer cells, autophagy is significantly altered after *H. pylori* infection and dysregulation of autophagy may be a causative factor for promoting the production of pro-inflammatory mediators in the human body (Halder et al., 2015; Sakatani et al., 2023). Initially, autophagy is a crucial pathway for controlling infection. However, prolonged exposure of the cells to the toxin VacA disrupts the induction of autophagy. This loss of autophagy leads to an accumulation of ROS, which can exacerbate inflammation and eventually lead to carcinogenesis (Raju et al., 2012). In *H. pylori* infection, the regulation of cellular autophagy can be mediated by microRNAs. Tang et al. showed that MIR30B was upregulated during *H. pylori* infection and favored bacterial replication by directly targeting ATG12 and Beclin1, important proteins involved in autophagy (Tang et al., 2012). Impairment of autophagy by MIR30B allows intracellular *H. pylori* to evade autophagic clearance and thus promotes the persistence of *H. pylori* infection. In another study, a significant correlation was found between MIR155 and immunohistochemical grade in *H. pylori*-positive patients. High expression of MIR155 could significantly reduce *H. pylori* survival by inducing autophagy (Wu et al., 2016). However, too much of a good thing is not always good. The increase of autophagy mediated by the Nrf2-HO-1 axis plays an important role in promoting *H. pylori* induced gastric carcinogenesis (Paik et al., 2019). VacA in *H. pylori* can also induce autophagy by promoting the formation of autophagosomes (Terebiznik et al., 2009). It can impair the activity of the lysosomal calcium channel MCOLN1/TRPML1, leading to the formation of enlarged, dysfunctional lysosomes and autophagosomes (Capurro et al., 2020). These autophagosomes are distinct from the induced large vacuoles and serve as an intracellular niche that allows the bacteria to evade eradication therapy. At this point, inhibition of autophagy stabilizes VacA and reduces vacuolization in the cells, limiting the damage caused by the toxin to the host cells (Raju and Jones, 2010). Thus, when autophagy is weakened, *H. pylori* can proliferate in the human body and its toxins cannot be effectively eliminated. Conversely, when autophagy is strengthened, *H. pylori* can also hide in abnormally increased autophagosomes and thus escape elimination by the host organism. It appears that *H. pylori* interferes with the normal autophagy process independently of the changes in autophagy and thus triggers negative reactions in the body. Furthermore, since there is evidence that autophagy associated with *H. pylori* depends on host cell types and bacterial strains, the ability of *H. pylori* to trigger autophagic responses should not be generalized (Deen et al., 2013).

Key virulence factors in autophagy

While the pathogenic mechanisms of *H. pylori* and its virulence factors are diverse, VacA and CagA play a crucial role in the interaction between *H. pylori* and the host autophagic machinery (Figure 4). VacA plays a key role in the pathogenesis of the disease by exerting pleiotropic effects on the host (Greenfield and Jones, 2013). One effect of acute VacA exposure is the induction of autophagy. However, prolonged exposure to the toxin impedes autophagy by inhibiting the maturation of autolysosomes. Kim et al. reported that the mitochondria-targeting bacterial toxin VacA inhibits a key sensor of host nutritional status, the mammalian target of rapamycin complex 1 (mTORC1), leading to a general cellular shift from biosynthetic to catabolic metabolism and further triggering the autophagic response (Kim et al., 2018). CagA can evade autophagic degradation in the host cells and thus exert its toxic effect (Tsugawa et al., 2019). Xie et al. found that autophagy initially increased and then gradually decreased during the duration of *H. pylori* infection *in vitro*, in a CagA-dependent manner. Moreover, dysregulation of autophagy promoted DNA damage in *H. pylori*-infected cells (Xie et al., 2020).

Dysregulation of autophagy leading to gastric cancer

Dysregulation of autophagy during *H. pylori* infection undoubtedly exacerbates the progression from gastritis to gastric cancer. For example, cagA and vacA can inhibit the activation of upstream signaling pathways of autophagy and thus inhibit autophagy of gastric mucosal cells in precancerous lesions of gastric cancer (Zhang et al., 2022b). The signaling pathways that link gastric cancer to *H. pylori* infection and are mediated by autophagy form a multi-layered protein network for regulation. Different signaling pathways have different functions and can interact with each other. Activation or abnormal induction of one of these pathways can lead to a cascade of cellular immune damage, ultimately culminating in the development of gastric cancer (Yang et al., 2022). For example, *H. pylori* can activate NF-κB and autophagy through nucleotide-binding oligomerization domain 1 (NOD1), allowing the bacterium to persist in the gastric niche and cause carcinogenic consequences (Suarez et al., 2015). In particular, *H. pylori* and its virulence factors can disrupt autophagy, leading to increased EMT (Shi et al., 2019). The occurrence of EMT and chronic inflammation leads to the emergence of cells with tumor stem cell (CSC) characteristics, such as the ability to migrate, invade and form tumor spheres (Courtois et al., 2021). In addition, the complex process of carcinogenesis triggered by *H. pylori* is closely linked to the genetic background of the host. Many of these genes influence cellular signaling pathways that contribute to inflammatory signals, inflammasome formation and autophagy (Mommersteeg et al., 2018). For example, clinical studies have shown that the autophagy gene ATG16L1 (rs2241880, G allele) was genotyped in subjects from different ethnic cohorts (Dutch and Australian) with premalignant gastric lesions of varying severity. The mechanism of the increased risk associated with ATG16L1 rs2441880 could be attributed to its modulation of *H. pylori*-induced ER stress signaling pathways and pro-inflammatory mediators (Mommersteeg et al., 2022).

Ferroptosis and *H. pylori* infection

Ferroptosis is a form of regulated cell death that is characterized by iron-dependent lipid peroxidation and differs from other forms

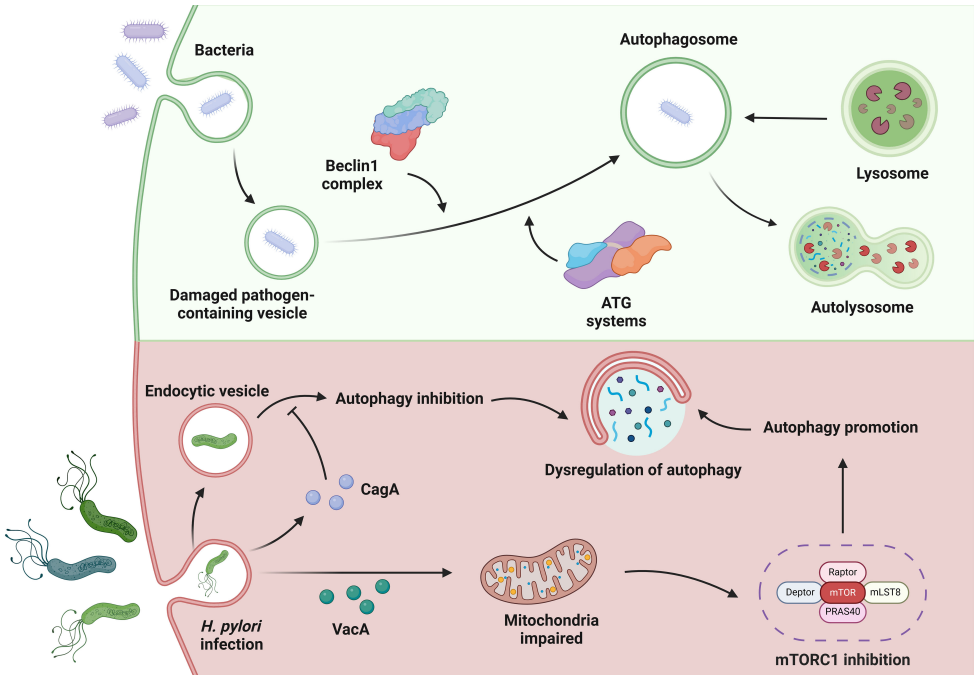

FIGURE 4
Autophagy in *H. pylori* infection. In autophagy, bacteria can be used to form damaged pathogen-containing vesicles. Under the action of the Beclin1 complex and the ATG systems, autophagosomes are formed that cooperate with the lysosomes in the cell to complete autophagy. When infected with *H. pylori*, the bacterial toxin VacA can target mitochondria to inhibit mTORC1 to promote cell autophagy. CagA, another toxin factor secreted by *H. pylori*, can evade autophagic degradation and gradually reduce cell autophagy. These complex circumstances during *H. pylori* infection lead to dysregulation of autophagy.

of programmed cell death such as apoptosis and pyroptosis. This process was first described in 2012 and has since attracted considerable attention due to its role in various physiological and pathological conditions (Dixon et al., 2012). At the molecular level, ferroptosis involves the accumulation of lipid hydroperoxides, particularly phospholipids containing polyunsaturated fatty acids (PUFAs), resulting from the dysregulation of cellular antioxidant systems, including glutathione peroxidase 4 (GPX4) and the cystine/glutamate antiporter system xCT (Stockwell, 2022). GPX4 is a key enzyme responsible for the reduction of lipid hydroperoxides to non-toxic lipid alcohols, thus protecting cells from oxidative damage. Inhibition or depletion of GPX4 leads to an accumulation of lipid peroxides and ultimately triggers ferroptotic cell death (Yang et al., 2014). Several signaling pathways and molecules are involved in the regulation of ferroptosis. For example, the tumor suppressor p53 and the nuclear factor erythroid 2-related factor 2 (Nrf2) have been shown to modulate ferroptotic cell death through their effects on lipid peroxidation and antioxidant defense. In addition, proteins related to iron metabolism, such as ferritin, transferrin and TfR1, play a crucial role in regulating intracellular iron levels and thus influence susceptibility to ferroptosis (Stockwell, 2022).

Infection with *H. pylori* has a considerable influence on the process of ferroptosis (Figure 3). *H. pylori* and its components reduced the expression of LPCAT3, which plays a role in the generation of the lipid peroxide substrate. They also downregulated genes involved in iron uptake, such as TfR1. In addition, they upregulated the cystine/glutamate antiporter subunit SLC3A2 to counteract glutathione depletion, which attenuates ferroptosis (Melo et al., 2024). *H. pylori* infection can also influence the development of gastric cancer by affecting ferroptosis-related genes. Suppressor of cytokine signaling 1 (SOCS1), which is known to be a driver of ferroptosis, showed significant upregulation in both *H. pylori*-infected individuals and patients with gastric adenocarcinoma (STAD). Furthermore, increased SOCS1 expression correlated with an unfavorable prognosis in STAD patients. The increase in SOCS1 was associated with increased infiltration of immune cells and upregulation of immune checkpoints in STAD patients (Yan et al., 2023). Liu et al. demonstrated that the ferroptosis-related gene YWHAE is highly expressed in both *H. pylori*-associated gastritis and gastric cancer. The expression of YWHAE positively correlates with ferroptosis in gastric cancer and is associated with several cancer-related signaling pathways, including MAPK, NF-κB and PI3K (Liu et al., 2023). Zhu et al. also demonstrated that the molecular subtypes regulated by ferroptosis-associated genes correlate with TME cell infiltration and *H. pylori* infection increases the susceptibility of gastric cancer cells to RSL3-triggered ferroptosis (Zhu et al., 2023). To sum up, *H. pylori* appears to trigger pathways that can either enhance or block ferroptosis.

Therapy associated with PCD

Triple or quadruple therapies are the first choice in the treatment of *H. pylori* infections. Although conventional clinical therapies can effectively kill *H. pylori*, the continuous increase in antibiotic resistance has led to a decrease in the efficacy of standard triple and quadruple therapies. In addition, side effects related to *H. pylori* eradication, such as diarrhea, taste disturbance and nausea, have a certain incidence rate among patients (Liang et al., 2022). However, PCD such as autophagy, can play a role in eliminating intracellular *H. pylori* (Huang et al., 2018). With the increasing research on *H. pylori* infection related to PCD dysregulation, exploring the mechanisms of action of *H. pylori* virulence factors and their major targets in the different pathways of PCD may become an important research direction for future treatments of *H. pylori* infection and *H. pylori*-related gastric cancer. Establishing animal and cell models of *H. pylori* infection, exploring different cell death signaling pathways and gaining deeper insights into their importance in the pathogenesis of the disease, and searching for biologically active substances that can inhibit or induce PCD may be crucial for future treatments of *H. pylori* infection and associated gastric cancer (Table 2).

During apoptosis, several biologically active substances act in different phases, mainly influence intrinsic apoptosis. During the initiation phase of intrinsic apoptosis, upregulated BCL-2 homology region 3 proteins bind to survival-associated BCL-2 proteins and release BAX and BAK from their inhibition by survival-associated BCL-2 proteins. Quercetin modulates the balance between proliferation and apoptosis of gastric cells by affecting the levels of BCL-2 and BAX, thereby downregulating apoptosis induced by *H. pylori* infection and exerting a protective effect against gastritis-associated inflammation (Zhang et al., 2017c). In the subsequent steps of intrinsic apoptosis, BAX and BAK form oligomers that trigger mitochondrial events. L-ascorbic acid-2-glucoside (AA2G) reduces *H. pylori*-induced cell apoptosis by modulating the mitochondria-dependent apoptotic signaling pathway. The mechanism may be related to the restoration of mitochondrial ATP level and membrane potential, thereby improving mitochondrial function to protect gastric epithelial cells from *H. pylori* infection (Chen et al., 2018). After the mitochondrial phase, the assembly of the apoptosome scaffold is triggered and the caspase process is activated. Eudesmin inhibits the growth of *H. pylori* and suppresses the activation of caspase-associated proteins (caspase-3, -8, -9) induced by *H. pylori* (Yang et al., 2018). There are also preparations that can regulate intrinsic apoptosis in multiple steps, such as Lactobacillus rhamnosus JB3, which can dose-dependently inhibit proteins involved in the intrinsic apoptotic pathway, including BAX, cytochrome c and caspase-3, thus suppressing cell apoptosis induced by *H. pylori* (Do et al., 2021). The above preparations can all reduce the abnormal increase in apoptosis caused by *H. pylori* infection. However, in the chronic stage of *H. pylori* infection, apoptosis often decreases (Nagy et al., 2009). In chronic infection, treatment with tanshinone IIA significantly increases the expression of apoptosis-related proteins BAX and caspase-9, disrupts mitochondrial transmembrane potential, triggers the release of cytochrome c and activates caspase cascades. It markedly promotes intrinsic cellular apoptosis via the NF-κB and MAPK pathways and exerts a protective effect on host cells in severe inflammation and *H. pylori*-induced gastric cancer (Chen et al., 2016).

In autophagy, *H. pylori* infection can disrupt lysosomal function, leading to the development of enlarged and dysfunctional lysosomes and autophagosomes (Capurro et al., 2020). At the same time, infection leads to upregulation of autophagy-related proteins Beclin1 and LC3B-II, while chloroquine can inhibit this abnormal autophagic expression (Li et al., 2023b). In addition to suppressing abnormal autophagy during *H. pylori* infection, bioactive compounds can also promote the development of beneficial autophagy. The lysosomal autophagy pathway was impaired by an increase in lysosomal membrane permeabilization during *H. pylori* infection. However, glycyrrhizin

TABLE 2 Biologically active compounds targeting cell death pathways in *H. pylori* infection.

Programmed cell death	Compound	Mechanism of action	References
Apoptosis	Tanshinone IIA	Increases apoptotic relevant protein BAX and caspase-9 expressions in *H. pylori* infection.	(Chen et al., 2016)
	Quercetin	Affects the levels of BCL-2 and BAX to protect against apoptosis associated with *H. pylori* infection.	(Zhang et al., 2017c)
	L-ascorbic Acid-2-Glucoside	Improves mitochondrial function by restoring the level of ATP and MMP, inhibits *H. pylori* induced apoptosis.	(Chen et al., 2018)
	Eudesmin	Suppresses the activation of apoptosis associated proteins induced by *H. pylori*.	(Yang et al., 2018)
	Lactobacillus rhamnosus JB3	Inhibits intrinsic apoptosis proteins including BAX, cytochrome c, and caspase-3 mediated by infection.	(Do et al., 2021)
Autophagy	Chloroquine	Inhibits the increased expression of Beclin1 and LC3B-II, thereby reducing autophagy in *H. pylori* infection.	(Li et al., 2023)
	Glycyrrhizin	Restores autolysosomal function by inhibiting HMGB1 to ameliorate *H. pylori* infection.	(Khan et al., 2023)
	Simvastatin	Enhances early endosome maturation and subsequently activates the autophagy pathway.	(Liao et al., 2016)
	Astaxanthin	Induces autophagy through the activation of AMPK and the downregulation of its downstream target, mTOR.	(Lee et al., 2020)
Pyroptosis	Rabeprazole	Inhibits pyroptosis by alleviating GSDMD-executed pyroptosis, leading to decrease IL-1β and IL-18 mature and secretion.	(Xie et al., 2021)

ATP, Adenosine triphosphate; MMP, Mitochondrial membrane potential; HMGB1, High mobility group box 1; AMPK, Adenosine monophosphate-activated protein kinase; mTOR, Mammalian target of rapamycin.

preserves the integrity of the lysosomal membrane, which in turn facilitates the formation of autolysosomes. This restoration of lysosomal function leads to a reduction in intracellular *H. pylori* growth by eliminating the pathogenic niche (Khan et al., 2023). In addition, simvastatin can promote early endosome maturation and subsequently activate the autophagy pathway, which promotes lysosomal fusion and leads to the degradation of sequestered bacteria, thereby alleviating *H. pylori*-triggered inflammation (Liao et al., 2016).

Biologically active compounds can also comprehensively regulate several PCD processes to reduce the damage to normal PCD in the body caused by *H. pylori* infection. For example, astaxanthin induces autophagy by activating AMPK and downregulating its downstream target mTOR. When astaxanthin levels increase, it can also inhibit cell apoptosis induced by *H. pylori* (Lee et al., 2020). In addition, we should emphasize the use of the proton pump inhibitor rabeprazole in triple or quadruple drug regimens. In contrast to conventional acid-suppressive and antimicrobial drugs, rabeprazole acts by modulating PCD (Xie et al., 2021). NLRP3 and GSDMD are significantly increased in the gastric tissue of patients with *H. pylori* infection. Lansoprazole can attenuate GSDMD-induced cell pyroptosis, significantly inhibit the expression of ASC, NLRP3 and caspase-1, and thus lead to a reduction in the maturation and secretion of IL-1β.

Therapeutic interventions targeting regulators and effectors of various cell death pathways hold promise for improving treatment outcomes in patients with *H. pylori* infection. Given the complex nature of *H. pylori* infection, in which multiple cell death mechanisms interact with other cellular processes, effective therapies will likely include combinations of agents targeting different cell death programs, as well as molecules that affect additional cellular pathways. Therefore, the efficacy of the above agents at the animal and cellular level is promising, but their clinical utility needs to be further explored.

Discussion

A comprehensive understanding of programmed cell death has revealed ways to address aberrant situations in *H. pylori* infection. In apoptosis, *H. pylori* infection can cause dynamic changes in apoptosis levels in different cells. The increase in apoptosis in the acute phase may be an important mechanism by which the bacteria damage the stomach, while the decrease in apoptosis in the chronic phase leads to the formation of a tumor microenvironment that promotes the development of gastric cancer. In pyroptosis, the signaling pathway most closely associated with *H. pylori* infection is NLRP3. During infection, the pyroptotic inflammasome is susceptible to external stimuli such as microbes, environmental factors or inflammasome activators, leading to abundant production of inflammatory factors and promoting the occurrence of human gastric tumors. In autophagy, *H. pylori* and its virulence factors disrupt the normal level of autophagy, leading to an accumulation of damaged cellular components in the early stages and triggering autophagic cell death. In the later stages of infection, however, autophagic function is impaired, eventually leading to the development of gastric cancer. As for necroptosis and ferroptosis, there is relatively little research on their processes in *H. pylori* infection. However, animal studies, cell experiments and clinical observations have confirmed the importance of these two forms of cell death in *H. pylori* infection, and further investigation of their interaction is warranted.

The key question is whether blocking or promoting a specific PCD signaling pathway would be beneficial for the clinical treatment of *H. pylori* infection and associated gastric cancer. The prospects of such a therapy should be further investigated. We hope that research on PCD in the context of *H. pylori* infection will continue to progress and eventually lead to valuable life-saving treatments.

Author contributions

YL: Writing – original draft, Writing – review & editing. KL: Writing – original draft, Writing – review & editing. FL: Data curation, Visualization, Writing – review & editing. CZ: Conceptualization, Funding acquisition, Writing – review & editing. FC: Conceptualization, Writing – review & editing.

Funding

The author(s) declare financial support was received for the research, authorship, and/or publication of this article. Our work is supported by National Natural Science Foundation of China (NSFC) #82205069 awarded to CZ.

Acknowledgments

Thanks to BioRender. All these figures are created with BioRender.com.

Conflict of interest

The authors declare that the research was conducted in the absence of any commercial or financial relationships that could be construed as a potential conflict of interest.

Publisher's note

References

Al-Maleki, A. R., Loke, M. F., Lui, S. Y., Ramli, N. S. K., Khosravi, Y., Ng, C. G., et al. (2017). Helicobacter pylori outer inflammatory protein A (OipA) suppresses apoptosis of AGS gastric cells *in vitro*. *Cell. Microbiol.* 19. doi: 10.1111/cmi.v19.12

Alzahrani, S., Lina, T. T., Gonzalez, J., Pinchuk, I. V., Beswick, E. J., and Reyes, V. E. (2014). Effect of Helicobacter pylori on gastric epithelial cells. *World J. Gastroenterol.* 20, 12767–12780. doi: 10.3748/wjg.v20.i36.12767

Ansari, S., and Yamaoka, Y. (2020). Role of vacuolating cytotoxin A in Helicobacter pylori infection and its impact on gastric pathogenesis. *Expert Rev. Anti-Infective Ther.* 18, 987–996. doi: 10.1080/14787210.2020.1782739

Bergmann, A. (2007). Autophagy and cell death: no longer at odds. *Cell* 131, 1032–1034. doi: 10.1016/j.cell.2007.11.027

Cadwell, K. (2016). Crosstalk between autophagy and inflammatory signalling pathways: balancing defence and homeostasis. *Nat. Rev. Immunol.* 16, 661–675. doi: 10.1038/nri.2016.100

Capurro, M. I., Prashar, A., and Jones, N. L. (2020). MCOLN1/TRPML1 inhibition - a novel strategy used by Helicobacter pylori to escape autophagic killing and antibiotic eradication therapy *in vivo*. *Autophagy* 16, 169–170. doi: 10.1080/15548627.2019.1677322

Chaithongyot, S., and Naumann, M. (2022). Helicobacter pylori-induced reactive oxygen species direct turnover of CSN-associated STAMBPL1 and augment apoptotic cell death. *Cell. Mol. Life sciences: CMLS* 79, 86. doi: 10.1007/s00018-022-04135-2

Chen, G.-Y., Shu, Y.-C., Chuang, D.-Y., and Wang, Y.-C. (2016). Inflammatory and apoptotic regulatory activity of tanshinone IIA in *helicobacter pylori* -infected cells. *Am. J. Chin. Med.* 44, 1187–1206. doi: 10.1142/S0192415X1650066X

Chen, X., Liu, R., Liu, X., Xu, C., and Wang, X. (2018). L-ascorbic Acid-2-Glucoside inhibits Helicobacter pylori-induced apoptosis through mitochondrial pathway in Gastric Epithelial cells. *Biomedicine Pharmacotherapy = Biomedecine Pharmacotherapie* 97, 75–81. doi: 10.1016/j.biopha.2017.10.030

Chesnokov, M. S., Mamedova, A. R., Zhivotovsky, B., and Kopeina, G. S. (2024). A matter of new life and cell death: programmed cell death in the mammalian ovary. *J. Biomed. Sci.* 31, 31. doi: 10.1186/s12929-024-01017-6

Chmiela, M., Walczak, N., and Rudnicka, K. (2018). Helicobacter pylori outer membrane vesicles involvement in the infection development and Helicobacter pylori-related diseases. *J. Biomed. Sci.* 25, 78. doi: 10.1186/s12929-018-0480-y

Chu, S. H., Lim, J. W., Kim, K. H., and Kim, H. (2003). NF-kappaB and Bcl-2 in Helicobacter pylori-induced apoptosis in gastric epithelial cells. *Ann. New York Acad. Sci.* 1010, 568–572. doi: 10.1196/annals.1299.106

Cookson, B. T., and Brennan, M. A. (2001). Pro-inflammatory programmed cell death. *Trends Microbiol.* 9, 113–114. doi: 10.1016/S0966-842X(00)01936-3

Correa, P. (1995). Helicobacter pylori and gastric carcinogenesis. *Am. J. Surg. Pathol.* 19, S37–S43.

Courtois, S., Haykal, M., Bodineau, C., Sifré, E., Azzi-Martin, L., Ménard, A., et al. (2021). Autophagy induced by Helicobacter pylori infection is necessary for gastric cancer stem cell emergence. *Gastric Cancer* 24, 133–144. doi: 10.1007/s10120-020-01118-9

Cui, G., Yuan, A., and Li, Z. (2022). Occurrences and phenotypes of RIPK3-positive gastric cells in Helicobacter pylori infected gastritis and atrophic lesions. *Digestive Liver Dis.* 54, 1342–1349. doi: 10.1016/j.dld.2022.04.013

Czabotar, P. E., Lessene, G., Strasser, A., and Adams, J. M. (2014). Control of apoptosis by the BCL-2 protein family: implications for physiology and therapy. Nature Reviews. *Mol. Cell Biol.* 15, 49–63. doi: 10.1038/nrm3722

Deen, N. S., Huang, S. J., Gong, L., Kwok, T., and Devenish, R. J. (2013). The impact of autophagic processes on the intracellular fate of Helicobacter pylori: more tricks from an enigmatic pathogen? *Autophagy* 9, 639–652. doi: 10.4161/auto.23782

Degterev, A., Huang, Z., Boyce, M., Li, Y., Jagtap, P., Mizushima, N., et al. (2005). Chemical inhibitor of nonapoptotic cell death with therapeutic potential for ischemic brain injury. *Nat. Chem. Biol.* 1, 112–119. doi: 10.1038/nchembio711

Ding, S.-Z., Minohara, Y., Fan, X. J., Wang, J., Reyes, V. E., Patel, J., et al. (2007). Helicobacter pylori infection induces oxidative stress and programmed cell death in human gastric epithelial cells. *Infection Immun.* 75, 4030–4039. doi: 10.1128/IAI.00172-07

Ding, S.-Z., Smith, M. F., and Goldberg, J. B. (2008). Helicobacter pylori and mitogen-activated protein kinases regulate the cell cycle, proliferation and apoptosis in gastric epithelial cells. *J. Gastroenterol. Hepatol.* 23, e67–e78. doi: 10.1111/j.1440-1746.2007.04912.x

Dixon, S. J., Lemberg, K. M., Lamprecht, M. R., Skouta, R., Zaitsev, E. M., Gleason, C. E., et al. (2012). Ferroptosis: an iron-dependent form of nonapoptotic cell death. *Cell* 149, 1060–1072. doi: 10.1016/j.cell.2012.03.042

Do, A. D., Chang, C.-C., Su, C.-H., and Hsu, Y.-M. (2021). Lactobacillus rhamnosus JB3 inhibits Helicobacter pylori infection through multiple molecular actions. *Helicobacter* 26, e12806. doi: 10.1111/hel.12806

Galluzzi, L., Vitale, I., Aaronson, S. A., Abrams, J. M., Adam, D., Agostinis, P., et al. (2018). Molecular mechanisms of cell death: recommendations of the Nomenclature Committee on Cell Death 2018. *Cell Death Differentiation* 25, 486–541. doi: 10.1038/s41418-017-0012-4

Genta, R. M. (1997). Helicobacter pylori, inflammation, mucosal damage, and apoptosis: pathogenesis and definition of gastric atrophy. *Gastroenterology* 113, S51–S55. doi: 10.1016/S0016-5085(97)80012-1

Gonciarz, W., Krupa, A., and Chmiela, M. (2020). Proregenerative activity of IL-33 in gastric tissue cells undergoing helicobacter pylori-induced apoptosis. *Int. J. Mol. Sci.* 21, 1801. doi: 10.3390/ijms21051801

Gonciarz, W., Krupa, A., Hinc, K., Obuchowski, M., Moran, A. P., Gajewski, A., et al. (2019). The effect of Helicobacter pylori infection and different H. pylori components on the proliferation and apoptosis of gastric epithelial cells and fibroblasts. *PloS One* 14, e0220636. doi: 10.1371/journal.pone.0220636

Green, D. R. (2000). Apoptotic pathways: paper wraps stone blunts scissors. *Cell* 102, 1–4. doi: 10.1016/S0092-8674(00)00003-9

Greenfield, L. K., and Jones, N. L. (2013). Modulation of autophagy by Helicobacter pylori and its role in gastric carcinogenesis. *Trends Microbiol.* 21, 602–612. doi: 10.1016/j.tim.2013.09.004

Halder, P., Datta, C., Kumar, R., Sharma, A. K., Basu, J., and Kundu, M. (2015). The secreted antigen, HP0175, of Helicobacter pylori links the unfolded protein response (UPR) to autophagy in gastric epithelial cells. *Cell. Microbiol.* 17, 714–729. doi: 10.1111/cmi.12396

Hardbower, D. M., De Sablet, T., Chaturvedi, R., and Wilson, K. T. (2013). Chronic inflammation and oxidative stress: the smoking gun for Helicobacter pylori-induced gastric cancer? *Gut Microbes* 4, 475–481. doi: 10.4161/gmic.25583

He, Y., Wang, C., Zhang, X., Lu, X., Xing, J., Lv, J., et al. (2020). Sustained exposure to helicobacter pylori lysate inhibits apoptosis and autophagy of gastric epithelial cells. *Front. Oncol.* 10. doi: 10.3389/fonc.2020.581364

Holler, N., Zaru, R., Micheau, O., Thome, M., Attinger, A., Valitutti, S., et al. (2000). Fas triggers an alternative, caspase-8-independent cell death pathway using the kinase RIP as effector molecule. *Nat. Immunol.* 1, 489–495. doi: 10.1038/82732

Holokai, L., Chakrabarti, J., Broda, T., Chang, J., Hawkins, J. A., Sundaram, N., et al. (2019). Increased programmed death-ligand 1 is an early epithelial cell response to helicobacter pylori infection. *PloS Pathog.* 15, e1007468. doi: 10.1371/journal.ppat.1007468

Hu, Z., Yan, C., Liu, P., Huang, Z., Ma, R., Zhang, C., et al. (2013). Crystal structure of NLRC4 reveals its autoinhibition mechanism. *Science* 341, 172–175. doi: 10.1126/science.1236381

Huang, Y., Deng, X., Lang, J., and Liang, X. (2018). Modulation of quantum dots and clearance of Helicobacter pylori with synergy of cell autophagy. *Nanomedicine: Nanotechnology Biology Med.* 14, 849–861. doi: 10.1016/j.nano.2017.12.016

Jost, P. J., and Vucic, D. (2020). Regulation of cell death and immunity by XIAP. *Cold Spring Harbor Perspect. Biol.* 12, a036426. doi: 10.1101/cshperspect.a036426

Kato, K., Hasui, K., Wang, J., Kawano, Y., Aikou, T., and Murata, F. (2008). Homeostatic mass control in gastric non-neoplastic epithelia under infection of Helicobacter pylori: an immunohistochemical analysis of cell growth, stem cells and programmed cell death. *Acta Histochemica Et Cytochemica.* 41, 23–38. doi: 10.1267/ahc.07021

Kayagaki, N., Wong, M. T., Stowe, I. B., Ramani, S. R., Gonzalez, L. C., Akashi-Takamura, S., et al. (2013). Noncanonical inflammasome activation by intracellular LPS independent of TLR4. *Science* 341, 1246–1249. doi: 10.1126/science.1240248

Kerr, J. F., Wyllie, A. H., and Currie, A. R. (1972). Apoptosis: a basic biological phenomenon with wide-ranging implications in tissue kinetics. *Br. J. Cancer* 26, 239–257. doi: 10.1038/bjc.1972.33

Khan, U., Karmakar, B. C., Basak, P., Paul, S., Gope, A., Sarkar, D., et al. (2023). Glycyrrhizin, an inhibitor of HMGB1 induces autolysosomal degradation function and inhibits Helicobacter pylori infection. *Mol. Med.* 29, 51. doi: 10.1186/s10020-023-00641-6

Kim, J. M., Kim, J. S., Kim, N., Ko, S. H., Jeon, J. I., and Kim, Y.-J. (2015). Helicobacter pylori vacuolating cytotoxin induces apoptosis via activation of endoplasmic reticulum stress in dendritic cells. *J. Gastroenterol. Hepatol.* 30, 99–108. doi: 10.1111/jgh.12663

Kim, J. M., Kim, J. S., Lee, J. Y., Sim, Y.-S., Kim, Y.-J., Oh, Y.-K., et al. (2010). Dual effects of Helicobacter pylori vacuolating cytotoxin on human eosinophil apoptosis in early and late periods of stimulation. *Eur. J. Immunol.* 40, 1651–1662. doi: 10.1002/eji.200939882

Kim, I.-J., Lee, J., Oh, S. J., Yoon, M.-S., Jang, S.-S., Holland, R. L., et al. (2018). Helicobacter pylori Infection Modulates Host Cell Metabolism through VacA-Dependent Inhibition of mTORC1. *Cell Host Microbe* 23, 583–593.e588. doi: 10.1016/j.chom.2018.04.006

Konturek, P. C., Konturek, S. J., Pierzchalski, P., Bielański, W., Duda, A., Marlicz, K., et al. (2001). Cancerogenesis in Helicobacter pylori infected stomach–role of growth factors, apoptosis and cyclooxygenases. *Med. Sci. Monitor: Int. Med. J. Exp. Clin. Res.* 7, 1092–1107.

Kumar, S., and Dhiman, M. (2018). Inflammasome activation and regulation during Helicobacter pylori pathogenesis. *Microbial Pathogenesis* 125, 468–474. doi: 10.1016/j.micpath.2018.10.012

Lai, C.-H., Huang, J.-C., Cheng, H.-H., Wu, M.-C., Huang, M.-Z., Hsu, H.-Y., et al. (2018). Helicobacter pylori cholesterol glucosylation modulates autophagy for increasing intracellular survival in macrophages. *Cell. Microbiol.* 20, e12947. doi: 10.1111/cmi.v20.12

Lee, H., Lim, J. W., and Kim, H. (2020). Effect of astaxanthin on activation of autophagy and inhibition of apoptosis in helicobacter pylori-infected gastric epithelial cell line AGS. *Nutrients* 12, 1750. doi: 10.3390/nu12061750

Leung, W. K., Yu, J., To, K. F., Go, M. Y., Ma, P. K., Chan, F. K., et al. (2001). Apoptosis and proliferation in Helicobacter pylori-associated gastric intestinal metaplasia. *Alimentary Pharmacol. Ther.* 15, 1467–1472. doi: 10.1046/j.1365-2036.2001.01057.x

Li, M., and Beg, A. A. (2000). Induction of necrotic-like cell death by tumor necrosis factor alpha and caspase inhibitors: novel mechanism for killing virus-infected cells. *J. Virol.* 74, 7470–7477. doi: 10.1128/JVI.74.16.7470-7477.2000

Li, B., Du, Y., He, J., Lv, X., Liu, S., Zhang, X., et al. (2023a). Chloroquine inhibited Helicobacter pylori-related gastric carcinogenesis by YAP-β-catenin-autophagy axis. *Microbial Pathogenesis* 184, 106388. doi: 10.1016/j.micpath.2023.106388

Li, B., Lv, X., Xu, Z., He, J., Liu, S., Zhang, X., et al. (2023b). Helicobacter pylori infection induces autophagy via ILK regulation of NOXs-ROS-Nrf2/HO-1-ROS loop. *World J. Microbiol. Biotechnol.* 39, 284. doi: 10.1007/s11274-023-03710-4

Li, P., Nijhawan, D., Budihardjo, I., Srinivasula, S. M., Ahmad, M., Alnemri, E. S., et al. (1997). Cytochrome c and dATP-dependent formation of Apaf-1/caspase-9 complex initiates an apoptotic protease cascade. *Cell* 91, 479–489. doi: 10.1016/S0092-8674(00)80434-1

Liang, B., Yuan, Y., Peng, X.-J., Liu, X.-L., Hu, X.-K., and Xing, D.-M. (2022). Current and future perspectives for Helicobacter pylori treatment and management: From antibiotics to probiotics. *Front. Cell. Infection Microbiol.* 12. doi: 10.3389/fcimb.2022.1042070

Liao, W.-C., Huang, M.-Z., Wang, M. L., Lin, C.-J., Lu, T.-L., Lo, H.-R., et al. (2016). Statin decreases helicobacter pylori burden in macrophages by promoting autophagy. *Front. Cell. Infection Microbiol.* 6. doi: 10.3389/fcimb.2016.00203

Lim, M. C. C., Jantaree, P., and Naumann, M. (2023). The conundrum of Helicobacter pylori-associated apoptosis in gastric cancer. *Trends Cancer* 9, 679–690. doi: 10.1016/j.trecan.2023.04.012

Liu, J.-F., Guo, D., Kang, E.-M., Wang, Y.-S., Gao, X.-Z., Cong, H.-Y., et al. (2021). Acute and chronic infection of H. pylori caused the difference in apoptosis of gastric epithelial cells. *Microb. Pathogen.* 150, 104717. doi: 10.1016/j.micpath.2020.104717

Liu, D., Peng, J., Xie, J., and Xie, Y. (2024). Comprehensive analysis of the function of helicobacter-associated ferroptosis gene YWHAE in gastric cancer through multi-omics integration, molecular docking, and machine learning. *Apoptosis: Int. J. Programmed Cell Death.* 29 (3-4), 439–456. doi: 10.1007/s10495-023-01916-3

Mariño, G., Niso-Santano, M., Baehrecke, E. H., and Kroemer, G. (2014). Self-consumption: the interplay of autophagy and apoptosis. *Nat. Rev. Mol. Cell Biol.* 15, 81–94. doi: 10.1038/nrm3735

Martinon, F., Burns, K., and Tschopp, J. (2002). The inflammasome: a molecular platform triggering activation of inflammatory caspases and processing of proIL-beta. *Mol. Cell* 10, 417–426. doi: 10.1016/S1097-2765(02)00599-3

Matusiak, M., Van Opdenbosch, N., Vande Walle, L., Sirard, J.-C., Kanneganti, T.-D., and Lamkanfi, M. (2015). Flagellin-induced NLRC4 phosphorylation primes the inflammasome for activation by NAIP5. *Proc. Natl. Acad. Sci. United States America* 112, 1541–1546. doi: 10.1073/pnas.1417945112

Melo, J., Cavadas, B., Pereira, L., Figueiredo, C., and Leite, M. (2024). Transcriptomic remodeling of gastric cells by Helicobacter pylori outer membrane vesicles. *Helicobacter* 29, e13031. doi: 10.1111/hel.13031

Meng, W., Bai, B., Sheng, L., Li, Y., Yue, P., Li, X., et al. (2015). Role of Helicobacter pylori in gastric cancer: advances and controversies. *Discovery Med.* 20, 285–293.

Mizushima, N., and Komatsu, M. (2011). Autophagy: renovation of cells and tissues. *Cell* 147, 728–741. doi: 10.1016/j.cell.2011.10.026

Mocarski, E. S., Upton, J. W., and Kaiser, W. J. (2011). Viral infection and the evolution of caspase 8-regulated apoptotic and necrotic death pathways. *Nat. Rev. Immunol.* 12, 79–88. doi: 10.1038/nri3131

Mommersteeg, M. C., Simovic, I., Yu, B., Van Nieuwenburg, S., Bruno, I. M. J., Doukas, M., et al. (2022). Autophagy mediates ER stress and inflammation in Helicobacter pylori-related gastric cancer. *Gut Microbes* 14, 2015238. doi: 10.1080/19490976.2021.2015238

Mommersteeg, M. C., Yu, J., Peppelenbosch, M. P., and Fuhler, G. M. (2018). Genetic host factors in Helicobacter pylori-induced carcinogenesis: Emerging new paradigms. *Biochim. Et Biophys. Acta Rev. Cancer* 1869, 42–52. doi: 10.1016/j.bbcan.2017.11.003

Moujalled, D., Strasser, A., and Liddell, J. R. (2021). Molecular mechanisms of cell death in neurological diseases. *Cell Death Differentiation* 28, 2029–2044. doi: 10.1038/s41418-021-00814-y

Murphy, J. M., Czabotar, P. E., Hildebrand, J. M., Lucet, I. S., Zhang, J.-G., Alvarez-Diaz, S., et al. (2013). The pseudokinase MLKL mediates necroptosis via a molecular switch mechanism. *Immunity* 39, 443–453. doi: 10.1016/j.immuni.2013.06.018

Nabavi-Rad, A., Yadegar, A., Sadeghi, A., Aghdaei, H. A., Zali, M. R., Klionsky, D. J., et al. (2023). The interaction between autophagy, Helicobacter pylori, and gut microbiota in gastric carcinogenesis. *Trends Microbiol.* 31, 1024–1043. doi: 10.1016/j.tim.2023.04.001

Nagy, T. A., Frey, M. R., Yan, F., Israel, D. A., Polk, D. B., and Peek, R. M. (2009). Helicobacter pylori regulates cellular migration and apoptosis by activation of phosphatidylinositol 3-kinase signaling. *J. Infect. Dis.* 199, 641–651. doi: 10.1086/596660

Newton, K., Strasser, A., Kayagaki, N., and Dixit, V. M. (2024). Cell death. *Cell* 187, 235–256. doi: 10.1016/j.cell.2023.11.044

Ohsumi, Y. (2014). Historical landmarks of autophagy research. *Cell Res.* 24, 9–23. doi: 10.1038/cr.2013.169

Pachathundikandi, S. K., Blaser, N., Bruns, H., and Backert, S. (2020). Helicobacter pylori avoids the critical activation of NLRP3 inflammasome-mediated production of oncogenic mature IL-1β in human immune cells. *Cancers* 12, 803. doi: 10.3390/cancers12040803

Pachathundikandi, S. K., Müller, A., and Backert, S. (2016). Inflammasome activation by helicobacter pylori and its implications for persistence and immunity. *Curr. Topics Microbiol. Immunol.* 397, 117–131. doi: 10.1007/978-3-319-41171-2_6

Paik, J. Y., Lee, H. G., Piao, J.-Y., Kim, S.-J., Kim, D.-H., Na, H.-K., et al. (2019). Helicobacter pylori infection promotes autophagy through Nrf2-mediated heme oxygenase upregulation in human gastric cancer cells. *Biochem. Pharmacol.* 162, 89–97. doi: 10.1016/j.bcp.2019.02.003

Palrasu, M., Zaika, E., Paulrasu, K., Caspa Gokulan, R., Suarez, G., Que, J., et al. (2022). Helicobacter pylori pathogen inhibits cellular responses to oncogenic stress and apoptosis. *PloS Pathog.* 18, e1010628. doi: 10.1371/journal.ppat.1010628

Peek, R. M., Moss, S. F., Tham, K. T., Pérez-Pérez, G. I., Wang, S., Miller, G. G., et al. (1997). Helicobacter pylori cagA+ strains and dissociation of gastric epithelial cell proliferation from apoptosis. *J. Natl. Cancer Institute* 89, 863–868. doi: 10.1093/jnci/89.12.863

Piotrowski, J., Piotrowski, E., Skrodzka, D., Slomiany, A., and Slomiany, B. L. (1997). Induction of acute gastritis and epithelial apoptosis by Helicobacter pylori lipopolysaccharide. *Scandinavian J. Gastroenterol.* 32, 203–211. doi: 10.3109/00365529709000195

Posselt, G., Wiesauer, M., Chichirau, B. E., Engler, D., Krisch, L. M., Gadermaier, G., et al. (2019). Helicobacter pylori-controlled c-Abl localization promotes cell migration and limits apoptosis. *Cell communication signaling: CCS* 17, 10. doi: 10.1186/s12964-019-0323-9

Puthalakath, H., and Strasser, A. (2002). Keeping killers on a tight leash: transcriptional and post-translational control of the pro-apoptotic activity of BH3-only proteins. *Cell Death Differentiation* 9, 505–512. doi: 10.1038/sj.cdd.4400998

Raju, D., Hussey, S., Ang, M., Terebiznik, M. R., Sibony, M., Galindo-Mata, E., et al. (2012). Vacuolating cytotoxin and variants in Atg16L1 that disrupt autophagy promote Helicobacter pylori infection in humans. *Gastroenterology* 142, 1160–1171. doi: 10.1053/j.gastro.2012.01.043

Raju, D., and Jones, N. L. (2010). Methods to monitor autophagy in H. pylori vacuolating cytotoxin A (VacA)-treated cells. *Autophagy* 6, 138–143. doi: 10.4161/auto.6.1.10222

Rathinam, V., Jiang, Z., Waggoner, S. N., Sharma, S., Cole, L. E., Waggoner, L., et al. (2010). The AIM2 inflammasome is essential for host defense against cytosolic bacteria and DNA viruses. *Nat. Immunol.* 11, 395–402. doi: 10.1038/ni.1864

Ricci, V., Giannouli, M., Romano, M., and Zarrilli, R. (2014). Helicobacter pylori gamma-glutamyl transpeptidase and its pathogenic role. *World J. Gastroenterol.* 20, 630–638. doi: 10.3748/wjg.v20.i3.630

Rosania, R., Varbanova, M., Wex, T., Langner, C., Bornschein, J., Giorgio, F., et al. (2017). Regulation of apoptosis is impaired in atrophic gastritis associated with gastric cancer. *BMC Gastroenterol.* 17, 84. doi: 10.1186/s12876-017-0640-7

Sakatani, A., Hayashi, Y., Saiki, H., Kato, M., Uema, R., Inoue, T., et al. (2023). A novel role for Helicobacter pylori cytotoxin-associated gene A in negative regulation of autophagy in human gastric cells. *BMC Gastroenterol.* 23, 326. doi: 10.1186/s12876-023-02944-8

Shi, Y., Yang, Z., Zhang, T., Shen, L., Li, Y., and Ding, S. (2019). SIRT1-targeted miR-543 autophagy inhibition and epithelial-mesenchymal transition promotion in Helicobacter pylori CagA-associated gastric cancer. *Cell Death Dis.* 10, 625. doi: 10.1038/s41419-019-1859-8

Shi, J., Zhao, Y., Wang, K., Shi, X., Wang, Y., Huang, H., et al. (2015). Cleavage of GSDMD by inflammatory caspases determines pyroptotic cell death. *Nature* 526, 660–665. doi: 10.1038/nature15514

Shirin, H., and Moss, S. F. (1998). Helicobacter pylori induced apoptosis. *Gut* 43, 592–594. doi: 10.1136/gut.43.5.592

Singh, M., Prasad, K. N., Saxena, A., and Yachha, S. K. (2006). Helicobacter pylori induces apoptosis of T- and B-cell lines and translocates mitochondrial apoptosis-inducing factor to nucleus. *Curr. Microbiol.* 52, 254–260. doi: 10.1007/s00284-005-0103-1

Stennicke, H. R., Jürgensmeier, J. M., Shin, H., Deveraux, Q., Wolf, B. B., Yang, X., et al. (1998). Pro-caspase-3 is a major physiologic target of caspase-8. *J. Biol. Chem.* 273, 27084–27090. doi: 10.1074/jbc.273.42.27084

Stockwell, B. R. (2022). Ferroptosis turns 10: Emerging mechanisms, physiological functions, and therapeutic applications. *Cell* 185, 2401–2421. doi: 10.1016/j.cell.2022.06.003

Suarez, G., Romero-Gallo, J., Piazuelo, M. B., Wang, G., Maier, R. J., Forsberg, L. S., et al. (2015). Modification of helicobacter pylori peptidoglycan enhances NOD1 activation and promotes cancer of the stomach. *Cancer Res.* 75, 1749–1759. doi: 10.1158/0008-5472.CAN-14-2291

Sun, L., Wang, H., Wang, Z., He, S., Chen, S., Liao, D., et al. (2012). Mixed lineage kinase domain-like protein mediates necrosis signaling downstream of RIP3 kinase. *Cell* 148, 213–227. doi: 10.1016/j.cell.2011.11.031

Sun, J., Xu, K., Wu, C., Wang, Y., Hu, Y., Zhu, Y., et al. (2007). PD-L1 expression analysis in gastric carcinoma tissue and blocking of tumor-associated PD-L1 signaling by two functional monoclonal antibodies. *Tissue Antigens* 69, 19–27. doi: 10.1111/j.1399-0039.2006.00701.x

Tang, D., Chen, X., Kang, R., and Kroemer, G. (2021). Ferroptosis: molecular mechanisms and health implications. *Cell Res.* 31, 107–125. doi: 10.1038/s41422-020-00441-1

Tang, B., Li, N., Gu, J., Zhuang, Y., Li, Q., Wang, H.-G., et al. (2012). Compromised autophagy by MIR30B benefits the intracellular survival of Helicobacter pylori. *Autophagy* 8, 1045–1057. doi: 10.4161/auto.20159

Tavares, R., and Pathak, S. K. (2017). Helicobacter pylori Secreted Protein HP1286 Triggers Apoptosis in Macrophages via TNF-Independent and ERK MAPK-Dependent Pathways. *Front. Cell. Infection Microbiol.* 7. doi: 10.3389/fcimb.2017.00058

Terebiznik, M. R., Raju, D., Vázquez, C. L., Torbricki, K., Kulkarni, R., Blanke, S. R., et al. (2009). Effect of Helicobacter pylori's vacuolating cytotoxin on the autophagy pathway in gastric epithelial cells. *Autophagy* 5, 370–379. doi: 10.4161/auto.5.3.7663

Teymournejad, O., Mobarez, A. M., Hassan, Z. M., and Talebi Bezmin Abadi, A. (2017). Binding of the Helicobacter pylori OipA causes apoptosis of host cells via modulation of Bax/Bcl-2 levels. *Sci. Rep.* 7, 8036. doi: 10.1038/s41598-017-08176-7

Tsai, H.-F., and Hsu, P.-N. (2017). Modulation of tumor necrosis factor-related apoptosis-inducing ligand (TRAIL)-mediated apoptosis by Helicobacter pylori in immune pathogenesis of gastric mucosal damage. *J. Microbiology Immunology Infection = Wei Mian Yu Gan Ran Za Zhi* 50, 4–9. doi: 10.1016/j.jmii.2016.01.002

Tsugawa, H., Mori, H., Matsuzaki, J., Sato, A., Saito, Y., Imoto, M., et al. (2019). CAPZA1 determines the risk of gastric carcinogenesis by inhibiting Helicobacter pylori CagA-degraded autophagy. *Autophagy* 15, 242–258. doi: 10.1080/15548627.2018.1515530

Tummers, B., and Green, D. R. (2017). Caspase-8: regulating life and death. *Immunol. Rev.* 277, 76–89. doi: 10.1111/imr.12541

Winter, J., Letley, D., Rhead, J., Atherton, J., and Robinson, K. (2014). Helicobacter pylori membrane vesicles stimulate innate pro- and anti-inflammatory responses and induce apoptosis in Jurkat T cells. *Infection Immun.* 82, 1372–1381. doi: 10.1128/IAI.01443-13

Wu, K., Zhu, C., Yao, Y., Wang, X., Song, J., and Zhai, J. (2016). MicroRNA-155-enhanced autophagy in human gastric epithelial cell in response to Helicobacter pylori. *Saudi J. Gastroenterol.* 22, 30–36. doi: 10.4103/1319-3767.173756

Xia, H. H., and Talley, N. J. (2001). Apoptosis in gastric epithelium induced by Helicobacter pylori infection: implications in gastric carcinogenesis. *Am. J. Gastroenterol.* 96, 16–26. doi: 10.1111/j.1572-0241.2001.03447.x

Xie, J., Fan, L., Xiong, L., Chen, P., Wang, H., Chen, H., et al. (2021). Rabeprazole inhibits inflammatory reaction by inhibition of cell pyroptosis in gastric epithelial cells. *BMC Pharmacol. Toxicol.* 22, 44. doi: 10.1186/s40360-021-00509-7

Xie, C., Li, N., Wang, H., He, C., Hu, Y., Peng, C., et al. (2020). Inhibition of autophagy aggravates DNA damage response and gastric tumorigenesis via Rad51 ubiquitination in response to H. pylori infection. *Gut Microbes* 11, 1567–1589. doi: 10.1080/19490976.2020.1774311

Yahiro, K., Satoh, M., Nakano, M., Hisatsune, J., Isomoto, H., Sap, J., et al. (2012). Low-density lipoprotein receptor-related protein-1 (LRP1) mediates autophagy and apoptosis caused by Helicobacter pylori VacA. *J. Biol. Chem.* 287, 31104–31115. doi: 10.1074/jbc.M112.387498

Yan, P., Cheng, M., Wang, L., and Zhao, W. (2023). A ferroptosis-related gene in Helicobacter pylori infection, SOCS1, serves as a potential prognostic biomarker and corresponds with tumor immune infiltration in stomach adenocarcinoma: In silico approach. *Int. Immunopharmacol.* 119, 110263. doi: 10.1016/j.intimp.2023.110263

Yang, Y., and Klionsky, D. J. (2020). Autophagy and disease: unanswered questions. *Cell Death Differentiation* 27, 858–871. doi: 10.1038/s41418-019-0480-9

Yang, Y., Shu, X., and Xie, C. (2022). An overview of autophagy in helicobacter pylori infection and related gastric cancer. *Front. Cell. Infection Microbiol.* 12. doi: 10.3389/fcimb.2022.847716

Yang, W. S., Sriramaratnam, R., Welsch, M. E., Shimada, K., Skouta, R., Viswanathan, V. S., et al. (2014). Regulation of ferroptotic cancer cell death by GPX4. *Cell* 156, 317–331. doi: 10.1016/j.cell.2013.12.010

Yang, J.-S., Wang, C.-M., Su, C.-H., Ho, H.-C., Chang, C.-H., Chou, C.-H., et al. (2018). Eudesmin attenuates Helicobacter pylori-induced epithelial autophagy and apoptosis and leads to eradication of H. pylori infection. *Exp. Ther. Med.* 15, 2388–2396. doi: 10.3892/etm.2018.5701

Yang, Y., You, B., Dong, S., and Zhou, C. (2021). FRA-1 suppresses apoptosis of Helicobacter pylori infected MGC-803 cells. *Mol. Biol. Rep.* 48, 611–621. doi: 10.1007/s11033-020-06105-y

Yousefi, B., Mohammadlou, M., Abdollahi, M., Salek Farrokhi, A., Karbalaei, M., Keikha, M., et al. (2019). Epigenetic changes in gastric cancer induction by Helicobacter pylori. *J. Cell. Physiol.* 234, 21770–21784. doi: 10.1002/jcp.28925

Yu, H., Zeng, J., Liang, X., Wang, W., Zhou, Y., Sun, Y., et al. (2014). Helicobacter pylori promotes epithelial-mesenchymal transition in gastric cancer by downregulating programmed cell death protein 4 (PDCD4). *PloS One* 9, e105306. doi: 10.1371/journal.pone.0105306

Yuan, X.-Y., Zhang, Y., Zhao, X., Chen, A., and Liu, P. (2023). IL-1β, an important cytokine affecting Helicobacter pylori-mediated gastric carcinogenesis. *Microbial Pathogenesis.* 174, 105933. doi: 10.1016/j.micpath.2022.105933

Zhang, S., Huang, J., Xie, X., He, Y., Mo, F., and Luo, Z. (2017a). Quercetin from Polygonum capitatum Protects against Gastric Inflammation and Apoptosis Associated with Helicobacter pylori Infection by Affecting the Levels of p38MAPK, BCL-2 and BAX. *Molecules* 22, 744. doi: 10.3390/molecules22050744

Zhang, X., Li, C., Chen, D., He, X., Zhao, Y., Bao, L., et al. (2022b). H. pylori CagA activates the NLRP3 inflammasome to promote gastric cancer cell migration and invasion. *Inflammation Res.* 71, 141–155. doi: 10.1007/s00011-021-01522-6

Zhang, Y., Sun, H., Li, J., Rong, Q., Ji, X., and Li, B. (2017b). The leukocyte-associated immunoglobulin (Ig)-like receptor-1 modulating cell apoptosis and inflammatory cytokines secretion in THP-1 cells after Helicobacter pylori infection. *Microbial Pathogenesis* 109, 292–299. doi: 10.1016/j.micpath.2017.06.012

Zhang, Y., Sun, H., Zhao, H., Chen, X., Li, J., and Li, B. (2017c). Early apoptosis of monocytes induced by Helicobacter pylori infection through multiple pathways. *Dev. Comp. Immunol.* 73, 46–51. doi: 10.1016/j.dci.2017.03.010

Zhang, L., Sung, J. J. Y., Yu, J., Ng, S. C., Wong, S. H., Cho, C. H., et al. (2014). Xenophagy in Helicobacter pylori- and Epstein-Barr virus-induced gastric cancer. *J. Pathol.* 233, 103–112. doi: 10.1002/path.4351

Zhang, J., Wang, W., Yan, S., Li, J., Wei, H., and Zhao, W. (2022a). CagA and VacA inhibit gastric mucosal epithelial cell autophagy and promote the progression of gastric precancerous lesions. *Zhong Nan Da Xue Xue Bao. Yi Xue Ban* 47, 942–951. doi: 10.11817/j.issn.1672-7347.2022.210779

Zhao, Q., Yin, W., Zhao, R., Wang, Y., Song, C., Wang, H., et al. (2020). Outer inflammatory protein of Helicobacter pylori impacts IL-8 expression, adherence, cell apoptosis and cell cycle of gastric cells independent of its copy number. *Med. Microbiol. Immunol.* 209, 621–630. doi: 10.1007/s00430-020-00688-w

Zhu, L., Huang, Y., Li, H., and Shao, S. (2022). Helicobacter pylori promotes gastric cancer progression through the tumor microenvironment. *Appl. Microbiol. Biotechnol.* 106, 4375–4385. doi: 10.1007/s00253-022-12011-z

Zhu, W., Liu, D., Lu, Y., Sun, J., Zhu, J., Xing, Y., et al. (2023). PHKG2 regulates RSL3-induced ferroptosis in Helicobacter pylori related gastric cancer. *Arch. Biochem. Biophysics* 740, 109560. doi: 10.1016/j.abb.2023.109560

frontiers | Frontiers in Cellular and Infection Microbiology

TYPE Original Research
PUBLISHED 20 August 2024
DOI 10.3389/fcimb.2024.1425388

OPEN ACCESS

EDITED BY
Maurizio Sanguinetti,
Catholic University of the Sacred Heart, Italy

REVIEWED BY
Neha Nanda,
Harvard Medical School, United States
Lauren Ford,
Imperial College London, United Kingdom

*CORRESPONDENCE
Beatriz Andrea Otálora-Otálora
baotaloraot@unisanitas.edu.co

RECEIVED 29 April 2024
ACCEPTED 15 July 2024
PUBLISHED 20 August 2024

CITATION
Otálora-Otálora BA, Payán-Gómez C, López-Rivera JJ, Pedroza-Aconcha NB, Aristizábal-Guzmán C, Isaza-Ruget MA and Álvarez-Moreno CA (2024) Global transcriptomic network analysis of the crosstalk between microbiota and cancer-related cells in the oral-gut-lung axis. *Front. Cell. Infect. Microbiol.* 14:1425388. doi: 10.3389/fcimb.2024.1425388

Global transcriptomic network analysis of the crosstalk between microbiota and cancer-related cells in the oral-gut-lung axis

Beatriz Andrea Otálora-Otálora[1*], César Payán-Gómez[2], Juan Javier López-Rivera[3], Natalia Belén Pedroza-Aconcha[2], Claudia Aristizábal-Guzmán[1], Mario Arturo Isaza-Ruget[4] and Carlos Arturo Álvarez-Moreno[5]

[1]Grupo de Investigación INPAC, Unidad de Investigación, Fundación Universitaria Sanitas, Bogotá, Colombia, [2]Dirección Académica, Universidad Nacional de Colombia, Sede de La Paz, La Paz, Colombia, [3]Grupo de Investigación INPAC, Specialized Laboratory, Clinica Universitaria Colombia, Clínica Colsanitas S.A., Bogotá, Colombia, [4]Keralty, Sanitas International Organization, Grupo de Investigación INPAC, Fundación Universitaria Sanitas, Bogotá, Colombia, [5]Infectious Diseases Department, Clinica Universitaria Colombia, Clínica Colsanitas S.A., Bogotá, Colombia

Background: The diagnosis and treatment of lung, colon, and gastric cancer through the histologic characteristics and genomic biomarkers have not had a strong impact on the mortality rates of the top three global causes of death by cancer.

Methods: Twenty-five transcriptomic analyses (10 lung cancer, 10 gastric cancer, and 5 colon cancer datasets) followed our own bioinformatic pipeline based on the utilization of specialized libraries from the R language and DAVID´s gene enrichment analyses to identify a regulatory metafirm network of transcription factors and target genes common in every type of cancer, with experimental evidence that supports its relationship with the unlocking of cell phenotypic plasticity for the acquisition of the hallmarks of cancer during the tumoral process. The network's regulatory functional and signaling pathways might depend on the constant crosstalk with the microbiome network established in the oral-gut-lung axis.

Results: The global transcriptomic network analysis highlighted the impact of transcription factors (SOX4, TCF3, TEAD4, ETV4, and FOXM1) that might be related to stem cell programming and cancer progression through the regulation of the expression of genes, such as cancer-cell membrane receptors, that interact with several microorganisms, including human T-cell leukemia virus 1 (HTLV-1), the human papilloma virus (HPV), the Epstein–Barr virus (EBV), and SARS–CoV–2. These interactions can trigger the MAPK, non-canonical WNT, and IFN signaling pathways, which regulate key transcription factor overexpression during the establishment and progression of lung, colon, and gastric cancer, respectively, along with the formation of the microbiome network.

Conclusion: The global transcriptomic network analysis highlights the important interaction between key transcription factors in lung, colon, and gastric cancer, which regulates the expression of cancer-cell membrane receptors for the interaction with the microbiome network during the tumorigenic process.

KEYWORDS

transcription factors, transcriptional regulatory network, cancer-related cells membrane receptors, microbiota, hallmarks of cancer, oral-gut-lung axis, gut-lung cancer

1 Introduction

Cancers are a leading cause of mortality, accounting for 10 million deaths worldwide every year. Most cancer deaths (75.1%) occur in low- and middle-income countries, where capital spending is lower at 49.5%. In high income countries like the US, where the cancer mortality rate is lower than the median, twice the amount of capital is spent on cancer care than in low-income countries, in an attempt to improve cancer outcomes (Chow et al., 2022). The estimated global economic cost of cancers between 2020 and 2050 is $25.2 trillion international dollars. The three cancers with the highest economic investment are tracheal, bronchus, and lung cancer (15.4%); colon and rectum cancer (10.9%); and breast cancer (7.7%) (Chen et al., 2023). Lung cancer has the second highest incidence (11.4% new cases) after breast cancer (11.7%) and is the leading cause of cancer-associated deaths worldwide (18%) (Siegel et al., 2023). Colon cancer has the third highest incidence (10%) and is the second leading cause of cancer-associated deaths worldwide (9.4%) (Siegel et al., 2023). Gastric cancer has the fifth highest incidence (5.6%), after breast, lung, colorectum and prostate cancer, and is the third leading cause of cancer-associated deaths worldwide (7.7%) (Siegel et al., 2023).

Approximately 80–85% of lung cancers are non-small cell lung cancer (NSCLC), which has three main subtypes: adenocarcinoma, squamous cell carcinoma, and large cell carcinoma. Approximately 10–15% of all lung cancers are small cell lung cancer (SCLC), and its main subtypes are small cell carcinoma and mixed small cell/large cell cancer or combined small cell lung cancer (Zhang et al., 2023). The regions with the highest risk of lung cancer are Polynesia, Micronesia, Eastern Asia, Europe, and Northern America (Siegel et al., 2023). The distinction between SCLC and NSCLC is a key parameter in the therapeutic management of lung cancer, selecting chemotherapy regimens in NSCLC patients lacking targetable EGFR and BRAF mutations, ALK and ROS1 rearrangements, and PD-L1 overexpression (Galli and Rossi, 2021). Targeted therapies based on druggable oncogenic molecular alterations and immunotherapy interfering with the PD1/PD-L1 checkpoint are used in lung cancer treatment (Salmani-Javan et al., 2024).

Colon cancer has three major histological types: adenocarcinoma, mucinous adenocarcinoma, and signet ring cell carcinoma (Wu et al., 2019). Adenocarcinoma originating from epithelial cells of the colorectal mucosa is the most frequent (>90%) type, and well differentiated tumors (>95%) are characterized by glandular formation (Rawla et al., 2019). Rare types include neuroendocrine, squamous cell, adenosquamous, spindle cell, and undifferentiated carcinomas (Fleming et al., 2012). The regions with the highest risk of colon cancer are Europe, Eastern Asia, and North and South America (Siegel et al., 2023). Adenocarcinoma patients have the best prognoses, whereas signet ring cell carcinoma patients have the poorest prognoses, and some patients with these different pathological types have no statistical difference at the early stages of the disease, suggesting that, right now, different treatment strategies specific for a particular histological subset should be applied only in the advanced stages of colon cancer (Ackermann et al., 2018). Currently, there are no established clinical guidelines for the treatment of the different pathological types, as previous studies on the prognostic effects have yielded conflicting results (Ackermann et al., 2018).

Gastric cancer classifications [intestinal type, diffuse type, and mixed type (Lauren, 1965) and the World Health Organization (mixed gastric mucinous adenocarcinoma) (Kushima, 2022)] have been used in clinicopathological diagnoses (Meng et al., 2022a). The well differentiated intestinal type is sporadic and highly associated with environmental factors, especially *Helicobacter pylori* infection (Takenaka et al., 2007). The diffuse type is undifferentiated and characterized by the loss of expression of the adhesion protein E-cadherin, which is related to tumor metastasis (Guilford et al., 1998). Gastric adenocarcinomas are the most frequent (>90%) and are classified as cardia and non-cardia based on their anatomic site, and the main subtypes are intestinal and diffuse (Yang et al., 2011). The regions with the highest risk of gastric cancer risk are East Asia, Eastern Europe, and Central and South America (Siegel et al., 2023). The incidence varies between regions, showing a high heterogeneity attributed to the commensal and infectious microbiota community, environmental factors, epigenetic programming, and genetic traits such as immune response receptors characteristic of every population ancestry (Otálora-Otálora et al., 2023b). Gastric cancer treatment includes chemotherapy, molecularly targeted therapies, and therapeutic agents such as immune checkpoint inhibitors (ICIs) selected for every patient as humanized monoclonal antibodies that target inhibitory receptors (CTLA-4, PD-1, LAG-3, TIM-3, and PD-L1) expressed on T lymphocytes,

antigen presenting cells, and tumor cells, where they elicit an anti-tumor response by stimulating the immune system (Franzin et al., 2020); they are effective in the microsatellite instability and ICI subtypes but quite ineffective in the GS subtype (Kim et al., 2018).

The treatment of gut and lung cancer through histologic characteristics is limited by the high tumor morphological heterogeneity making every case extremely unique, and the identification of genomic biomarkers (Otálora-Otálora et al., 2023b) is still limited by the small number of patients with a specific variation, thus this therapeutic approach has not significantly impacted the mortality rates of the top three global causes of cancer deaths (Siegel et al., 2023). The identification of targetable oncogenic drivers in solid tumor and liquid biopsy using high-throughput deep sequencing methods can change significantly the paradigm of histology determination as one of the mandatory steps in future therapeutic strategies, and genomics as the only sequencing technology involved in the development of treatments against cancer (Galli and Rossi, 2021). We have developed a bioinformatics pipeline that is capable of identifying the most frequently differentially expressed genes (DEGs) and transcription factors (TFs) during the establishment and progression of every type of tumor pathology as key biomarkers due to their association with the regulation of biological processes and signaling pathways related to the acquisition of the hallmarks of cancer (Otálora-Otálora et al., 2023a). We address the great complexity of cancer in a holistic way from the transcriptome. The transcriptome reflects the genetics, epigenetics, and microenvironment of tumor cells that largely determine their phenotype. The identification of co-expressed common and unique DEGs between cancer types and related inflammatory diseases (Otálora-Otálora et al., 2019, Otálora-Otálora et al., 2022a, Otálora-Otálora et al., 2022b, Otálora-Otálora et al., 2023a) helps to identify the following: gene regulatory networks (GRNs), which contain promising targets for the pharmaceutical treatment of cancer (Zhou et al., 2019); co-regulatory networks (CRNs), which contain protein-protein interaction complexes of TFs regulating transcription at every stage of the tumorigenic process (Otálora-Otálora et al., 2023a); and transcriptional regulatory networks (TRNs), which represent the group of TFs that can regulate the all-important DEGs for the acquisition of the hallmarks of cancer (Otálora-Otálora et al., 2023b).

The polymorphic microbiome is a new dimension included in the hallmarks of cancer, along with epigenetic reprogramming, and both are considered constitute distinctive enabling characteristics that facilitate the acquisition of the hallmarks of cancer (Figure 1) (Hanahan, 2022). Our bioinformatic pipeline has evolved to identify a transcriptional regulatory metafirm of gut and lung

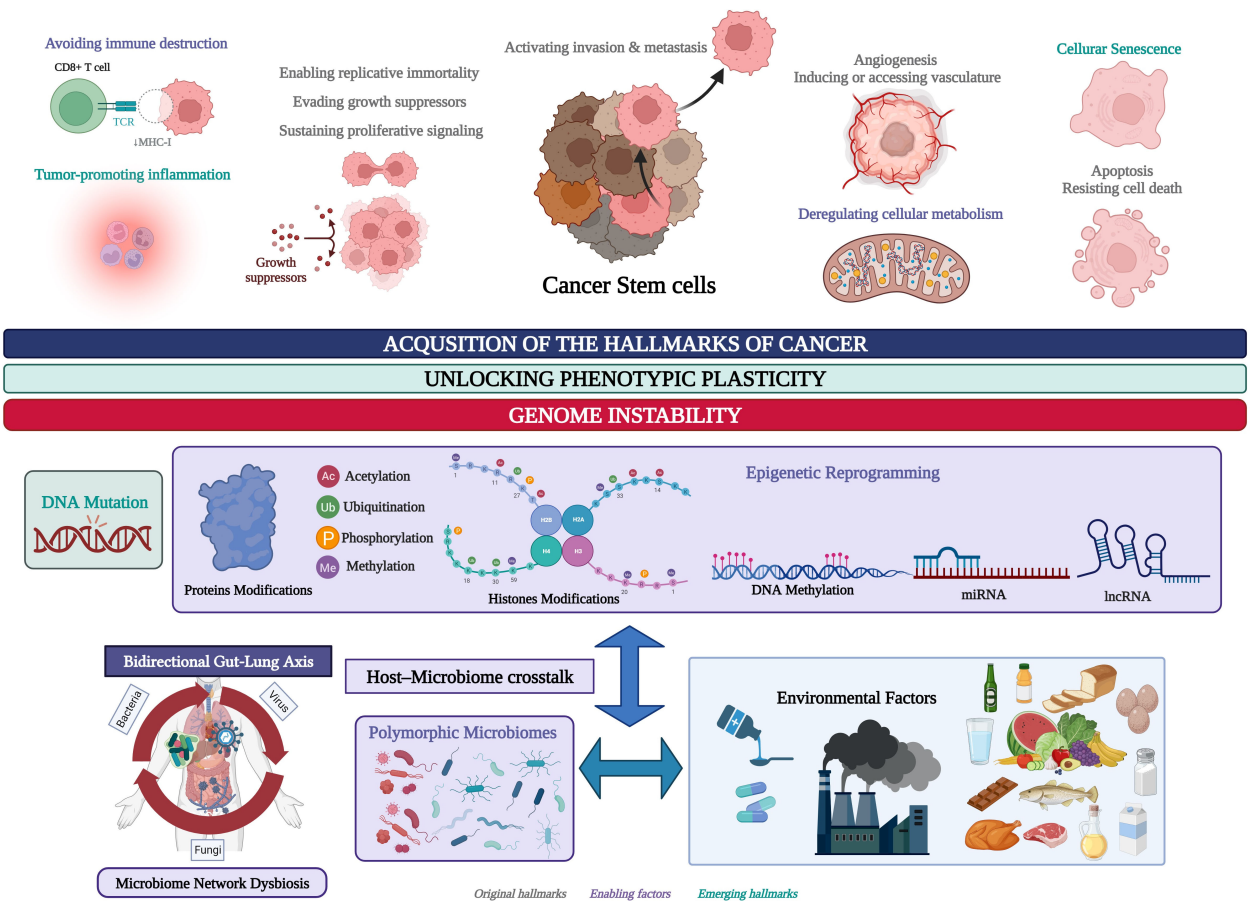

FIGURE 1
Environmental factors and the genomic and epigenomic regulatory processes involved in the unlocking of the phenotypic plasticity in cancer stem cells (CSC) and the acquisition of the hallmarks of cancer. Created with BioRender.com.

cancer, the regulatory function of which might depend on the constant crosstalk with the microbiome network established in the gut-lung axis (Otálora-Otálora et al., 2023b). In this study, we aim to achieve the following: 1) identify the common DEGs in gut and lung cancers, highlighting the *membrane receptors* that are key for the communication between the host cells and the microbiota, and the downstream activation of signaling pathways involved in the regulation of gene expression, particularly the expression of key TFs that control the expression of the other DEGs in every type of cancer; 2) identify the regulatory interactions between the key TFs in a TRN as functional blocks of genes co-expressed for the control of gene expression and the acquisition of the hallmarks of cancer, and analyze its regulatory function over the other DEGs; and 3) perform a *global transcriptomic network analysis* combining the results of gene ontology and network bioinformatic analysis, along with a deep review of the scientific data, which ultimately might highlight the importance of the microbiota in the regulation of genomic (DNA mutations), transcriptomic (RNA expression), epigenomic, (DNA methylation, non-coding RNAs, histone, and protein modifications), proteomic, and metabolomic process stability through the establishment of a specific TRN in cancer-related cells, which in turn may control the interaction with the microbiome network to unlock phenotypic plasticity and acquire the hallmarks of cancer (Figure 1). Therefore, the highlighted TFs in a cancer TRN that could communicate with the microbiome network through specific membrane receptors may become interesting candidates that could be used as multiomic biomarkers for the development of specific diagnostic tools and treatments against cancer.

2 Materials and methods

2.1 Data selection, quality control, and construction of gene expression matrices

An advanced search was conducted on the National Center for Biotechnology Information (NCBI) GEO database (http://www.ncbi.nlm.nih.gov/geo/) to identify studies analyzing global gene expression in lung cancer, colon cancer, and gastric cancer. The search tool was used with the keywords "lung cancer," "colon cancer," and "gastric cancer". Studies were limited to *Homo sapiens* as the organism, with expression profiling by array or RNA sequencing as the dataset type. The inclusion criteria encompassed studies that: (1) utilized any version of microarrays or any chemical of next generation sequencing; (2) analyzed at least three samples of each cancer type and at least three normal tissue samples for comparison; (3) provided raw data availability; and (4) passed quality control measures. All datasets underwent a quality control (QC) process to ensure their suitability for analysis. The initial step involved assessing signal comparability across different samples in each dataset to verify technical consistency. We then conducted a thorough examination of transcriptome correlations between samples to identify any significant deviations that might indicate poor quality samples. Principal component analysis (PCA) was employed as an additional tool for detecting low-quality samples. PCA helps visualize the variance within the dataset and allows for the identification of samples that significantly deviate from the main group. Samples exhibiting extreme variance or those that were outliers in the PCA plot were flagged as low quality. These low-quality samples, along with any datasets that did not meet our quality standards, were subsequently excluded from further analysis. Additionally, after processing and cleaning the datasets, we conducted an over-representation pathway analysis using the DAVID (Database for Annotation, Visualization, and Integrated Discovery) tool. This analysis was performed on the lists of DEGs obtained from each dataset individually. The aim was to confirm that the genes identified as differentially expressed were associated with known biological pathways relevant to cancer. This additional validation provided an extra layer of confidence in our results, ensuring that the selected genes were not only significantly different in expression but also implicated in critical biological processes related to the disease.

Of the total number of datasets analyzed, ten lung cancer datasets, five colon cancer datasets, and ten gastric cancer datasets (Table 1), passed the quality control phase and were used to obtain a gene expression matrix with Limma library in R (Ritchie et al., 2015), or DESeq2 (Love et al., 2014). For Affymetrix data, processing was conducted using the Limma R/Bioconductor software package (Ritchie et al., 2015). Data normalization and log2 transformation were carried out using the Robust Multi-array Average (RMA) algorithm. Owing to the presence of multiple probes for the same gene on Affymetrix chips, only the most informative probe, demonstrating the highest variability across experimental groups, was retained, whereas redundant probes were discarded. As noted in Table 1, some datasets have differences in the number of cases and controls. We have this in account by using Limma. Limma's strength lies in its ability to fit linear models and adjust for varying group sizes. It employs an empirical Bayes approach that stabilizes the variance estimates by shrinking them toward a common value. This method enhances the accuracy of variance estimates, allowing Limma to efficiently handle datasets with unequal sample sizes. Consequently, Limma provides reliable and precise results even when there are significant differences in the sizes of the experimental groups. For RNA-Seq data analysis, preprocessing began directly with the gene count table available in GEO. Normalization of these count tables was performed using the method implemented in DESeq2 (Love et al., 2014) to address differences in library size and composition across samples. Subsequently, differential expression analysis was carried out using DESeq2 to identify genes exhibiting significant expression changes between experimental conditions. For both Affymetrix and RNA-Seq data, a gene was considered differentially expressed if the fold change in expression exceeded 1.5 or was less than −1.5, and the adjusted p-value was less than 0.05.

2.2 Gene functional annotation and gene networks analysis

The DEG lists of every dataset in every type of cancer were compared to identify the common overregulated and

10.3389/fcimb.2024.1425388

TABLE 1 Cancer datasets and number of samples. .

Cancer Datasets	Number of samples
GSE19804	Normal (60) vs. cancer NSCLC (60)
E-MTAB-3950	Normal (30) vs. early squamous lung carcinoma (30)
GSE108055	Normal (9) vs. small-cell lung cancer (54)
GSE10072	Normal (49) vs. lung adenocarcinoma (58)
GSE3268	Normal (5) vs. squamous lung cancer cells (5)
GSE52248	Normal (6) vs. lung adenocarcinoma (12)
GSE70089	Normal (3) vs. lung carcinoma (3)
GSE81089	Normal (19) vs. cancer NSCLC (199)
GSE84776	Normal (9) vs. squamous lung cancer (9)
E-MTAB-5231	Normal (18) vs. cancer NSCLC (22)
GSE9348	Normal (12) vs. colon cancer (70)
GSE23878	Normal (24) vs. colon cancer (35)
GSE24514	Normal (15) vs. colon cancer (34)
GSE35279	Normal (5) vs. colon cancer (74)
GSE4107	Normal (10) vs. colon cancer (12)
GSE113255	Normal gastric tissues (n = 10), gastric cancer diffuse mucinous (n = 10)
GSE113255	Normal gastric tissues (n = 10), gastric cancer diffuse differentiated (n = 42)
GSE63089	Normal gastric tissues (n = 45), gastric cancer (n = 45)
GSE54129	Normal gastric tissues (n = 21), gastric cancer (n = 111)
GSE33335	Normal gastric tissues (n = 25), gastric cancer (n = 25)
GSE26899	Normal gastric tissues (n = 12), gastric cancer intestinal (n = 8)
GSE26899	Normal gastric tissues (n = 12), gastric cancer diffuse (n = 7)
GSE13911	Normal gastric tissues (n = 31), gastric cancer (n = 38)
GSE13195	Normal gastric tissues (n = 25), gastric cancer (n = 23)
GSE2685	Normal gastric tissues (n = 8), gastric cancer (n = 22)

downregulated genes, highlighting membrane receptors, and TFs in at least seven datasets of lung and gastric cancer, and at least three datasets of colon cancer (Supplementary Tables 1-3). DAVID´s annotation tool was used to identify the related biological functions and signaling pathways associated with the common overregulated DEGs and deregulated TFs in every type of cancer (Sherman et al., 2022). The TRNs were constructed with the expression matrix of common TFs in every type of cancer in the Reconstruction of Transcriptional regulatory Networks and analysis of regulons (RTN) library (Groenevelt et al., 2024). The GRNs and CRNs were constructed with the expression matrix of common overexpressed DEGs, and deregulated TFs in every type of cancer with the CoRegNet library (Nicolle et al., 2015). The regulatory interactions between common deregulated TFs were analyzed based on TRNs and CRNs, and the regulators (TFs) of key receptors were identified through the analysis of the GRNs. All libraries were used under our own bioinformatic pipeline (Supplementary Methods 2).

2.3 Global transcriptomic network analysis of gut and lung cancer

Common DEGs of membrane receptors, TFs, and DEGs involved in signaling pathways associated with the interaction of cancer-related cells and microorganisms were highlighted by DAVID´s annotation analysis of all common DEGs in each type of cancer. The Results section focuses on the main TFs of every cancer type according to the TRN analysis and features their regulatory function according to the biological processes and signaling pathways that might control them during the tumorigenic process. The Discussion section considers the experimental evidence related to the TFs and signaling pathways involved in the host cell and microbiota interactions directly or through microbiota expressed proteins, with specific membrane receptors, identified as common DEGs in every cancer type. BioRender was used to show, in one image, all the knowledge generated by scientific research in the field of host-microbiome crosstalk, through cancer transcriptomic studies. Lung, colon, and gastric cancer TRNs represent intricate gene regulatory programs involved in tumorigenesis, whereas the co-regulatory analysis of TFs assesses the formation of key protein-protein interaction complexes that might be important for unlocking the phenotypic plasticity of cancer-related cells through the control of key regulatory programs in a specific spatial, temporal, and sequential manner, probably according to their communication with the characteristic microbiome network. Consequently, a global transcriptomic analysis was carried out based on a bioinformatic analysis to organize and present all the scientific evidence present in several publications in the field of microbiome and cancer, in an image. This image features the best known microorganisms and their proteins that interact with key membrane receptors deregulated in every cancer type, the actual evidence of the signaling pathways that they might activate, and the following control of gene expression programs through the activation of cancer TRNs that might be related to the unlocking of phenotypic plasticity and acquisition of the hallmarks of cancer, as well as the control of the gene expression of key TFs over the gene expression of the main membrane receptors that interact with the microbiome network, representing the impact of the TRN in the communication with the microbiome network during the tumorigenic process. In the Conclusion, we summarize for every cancer type, the key TFs and their regulatory interactions, the membrane receptors and the best-known microorganisms that interact with them, and the signaling pathways, with experimental evidence that might be used to establish the current state of microbiome and cancer research, which can be used as the guiding core and starting point for future multiomic studies in this field.

3 Results

3.1 Differentially expressed genes and transcription factors in tumorigenic processes of the gut-lung axis

Ten gene expression datasets of lung cancer were analyzed; 417 common overregulated genes and 438 downregulated genes were identified in at least seven of the datasets (Supplementary Table 1) (Otálora-Otálora et al., 2023a). Five gene expression datasets of colon cancer were analyzed; 474 common overregulated genes and 640 downregulated genes were identified in at least three of the datasets (Supplementary Table 2). Ten gene expression datasets of gastric cancer were analyzed; 195 common overregulated genes and 309 downregulated were identified in at least seven of the datasets (Supplementary Table 3). Eighteen overregulated and 16 downregulated TFs were identified in the lung cancer common genes list, 37 overregulated and seven downregulated TFs were identified in the colon cancer common DEGs list, and 10 overregulated and 12 downregulated TFs were identified in the gastric cancer common DEGs list. There were seven overregulated and four downregulated TFs in common between lung and colon cancer, three overregulated and three downregulated TFs in common between lung and gastric cancer, five overregulated and three downregulated TFs in common between colon and gastric cancer, and two overregulated and two downregulated TFs in common between the three types of cancer (Figure 2).

Lung cancer common overregulated DEGs are related to epigenetic reprogramming (phosphorylation, acetylation, methylation, hydroxylation, and ubiquitin-like conjugations [Ubls]), the formation of extracellular exosomes, cell division, apoptosis, adhesion, proliferation, and junctions, the regulation of transcription, the epigenetic regulation of gene expression, DNA damage, repair, recombination, and replication, the formation of TF complexes, the regulation of stem cell population maintenance, and signaling pathways involved in DNA replication, cellular senescence, base excision repair, viral carcinogenesis, the biosynthesis of co-factors, mismatch repair, the cell cycle, purines, and metabolism, Wnt, hepatitis B (HBV), Epstein–Barr (EBV), human papillomavirus (HPV), and human T-cell leukemia virus 1 infection (HTLV-I) (Supplementary Table 1). Colon cancer common overregulated DEGs are related to epigenetics reprogramming (phosphorylation, acetylation, methylation, and ubl conjugation), the formation of extracellular exosomes, cell adhesion, proliferation, apoptosis, junctions, migration, and division, the regulation of transcription, DNA damage, repair, and replication, the formation of TF complexes, and stem cell proliferation, as well as signaling involved in the cell cycle, proteoglycans in cancer, cellular senescence, amoebiasis, malaria, and hepatitis C virus (HCV), EBV, HPV, and HTLV-I infection (Supplementary Table 2). Gastric cancer overregulated common DEGs are related to epigenetic reprogramming (hydroxylation, phosphorylation, and ubl conjugation), the formation of extracellular exosomes, cell adhesion, proliferation, migration, division, apoptosis, junctions, and growth, DNA replication, angiogenesis, the regulation of telomerase activity, the regulation of the epithelial to mesenchymal transition (EMT), inflammatory response, angiogenesis, gene expression regulation, cellular response to TNF, innate immunity, and host-virus

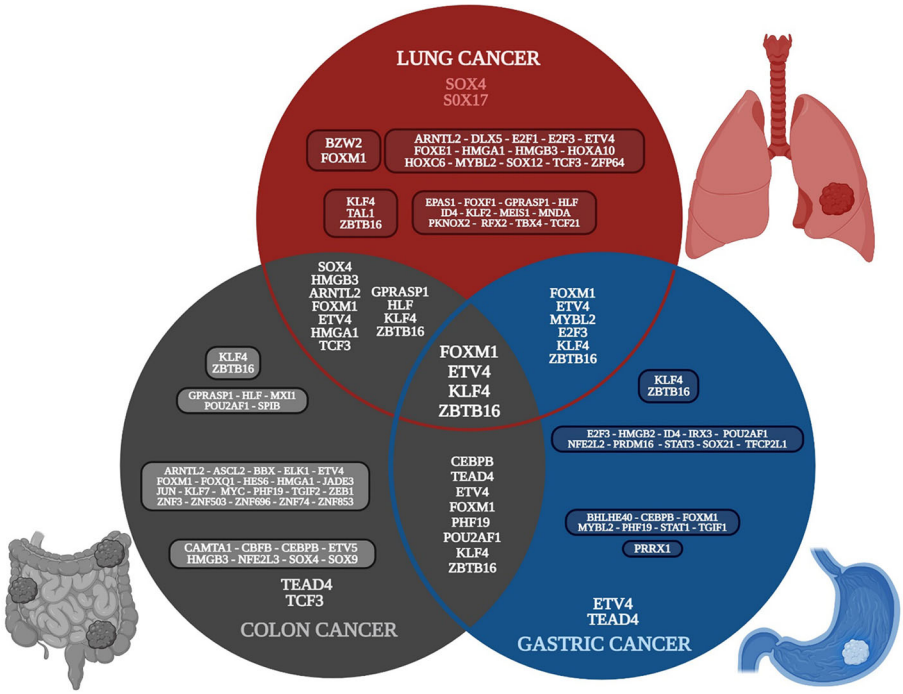

FIGURE 2
Venn diagram of the transcriptomic metafirm of gut-lung axis tumorigenic processes, with the common and unique deregulated transcription factors of each type of cancer. Created with BioRender.com.

interaction, as well as signaling involved in malaria, amoebiasis, pertussis, Kaposi sarcoma-associated herpesvirus, and HPV (Supplementary Table 3).

3.2 Transcriptional and gene regulatory network analysis

3.2.1 Lung cancer

SOX4 is overregulated in all ten lung cancer datasets and is related to: 1) apoptosis along with E2F1; 2) cell proliferation along with FOXM1, DLX5, and E2F3; 3) the formation of TF complexes along with E2F3, ARNTL2, HMGA1, HOXA10, and TCF3; 4) the positive regulation of transcription along with E2F1, FOXM1, ETV4, DLX5, FOXE1, HMGA1, and TCF3; and 5) the positive regulation of the Wnt signaling pathway along with DLX5 (Supplementary Table 1). FOXM1 is overregulated in nine lung cancer datasets and is related to: 1) the negative regulation of transcription along with E2F1, FOXE1, and HMGA1; 2) cellular senescence along with E2F1, E2F3, and MYBL2; and 3) DNA repair and damage. E2F1 is overregulated in seven lung cancer datasets and is related to: 1) HPV infection; 2) HBV and EBV virus infection along with E2F3; 3) the cell cycle and pathways in cancer along with E2F3; and 4) HTVL-I infection along with E2F3 and TCF3. According to the TRN of lung cancer (Figure 3), SOX4, FOXM1, ETV4, HOXC6, and E2F3 are the main positive regulators, whereas SOX17, KLF4, and ZBTB16 are the main negative regulators of transcription, controlling the expression of other TFs and target genes in lung cancer. Additionally, the TFs are capable of forming co-regulatory complexes in NSCLC (DLX5, BZW2, E2F3, FOXM1, HMGA1, HMGB3, HOXC6, MYBL2, and SOX4) and SCLC (DLX5, E2F1, E2F3, FOXM1, HOXC6, SOX4, and TCF3). According to DAVID analysis, SOX4 is regulated by acetylation, whereas DLX5 is regulated by phosphorylation; both positively regulate transcription and the canonical Wnt signaling pathway (Supplementary Table 1). SOX4 has 140 target genes in the GRN, which are in the nucleus, cytoplasm, cytoskeleton, and membrane, and are related to epigenetic reprogramming (phosphorylation and acetylation), host-virus interactions, five membrane receptors (HMMR, LRP8, PTPRF, SRPRB, and TNFRSF21), and signaling pathways related to HTLV-I and HBV infection. According to the TRN analysis, SOX4 can be regulated by HOXC6, whereas DLX5 can be regulated by SOX4, FOXM1, and ETV4 (Figure 3), and according to the co-regulatory network analysis, they both participate in the formation of TF complexes in both subtypes of lung cancer (NSCLC and SCLC) (Supplementary Table 1).

3.2.2 Colon cancer

TCF3 is overregulated in four of the five datasets and is related to: 1) the positive regulation of transcription along with SOX4, SOX9, CEBPB, FOXM1, ETV4, JUN, ELK1, ARNTL2, and HMGA1; 2) the formation of a transcription regulatory complex along with TEAD4, JUN, SOX4, SOX9, ARNTL2, HES6, and HMGA1; 3) the positive regulation of transcription from the RNA polymerase II promoter along with TEAD4, ELK1, ETV4, ARNTL2, CAMTA1, HMGA1, CEBPB, ETV5, JUN, KLF7, MYC, SOX4, SOX9, ASCL2, CBFB, FOXM1, and ZEB1; 4) the negative regulation of transcription from the RNA polymerase II promoter along with CEBPB, ETV5, JUN, KLF7, MYC, NFE2L3, PHF19, SOX4, SOX9, ASCL2, CBFB, FOXM1, FOXQ1, HES6, TCFL5, ZEB1, and ZNF3; and 5) HTLV-I infection along with ELK1, JUN, and MYC. SOX4 is overregulated in four of the five datasets and is related to: 1) the positive regulation of proliferation along with SOX9, FOXM1, and MYC; 2) the regulation of apoptosis along

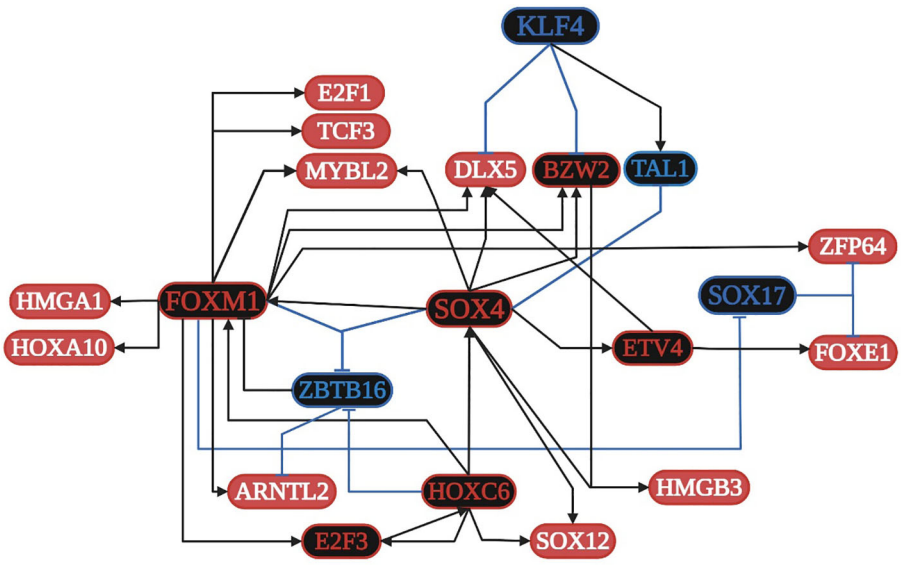

FIGURE 3
Transcriptional regulatory network (TRN) of common transcription factors (TFs) in lung cancer. Downregulated TFs are in blue, upregulated TFs are in red, and the key overregulated and downregulated TFs are in black. The black pointed arrows represent overregulation and the blue flat arrows represent downregulation. Created with BioRender.com.

10.3389/fcimb.2024.1425388

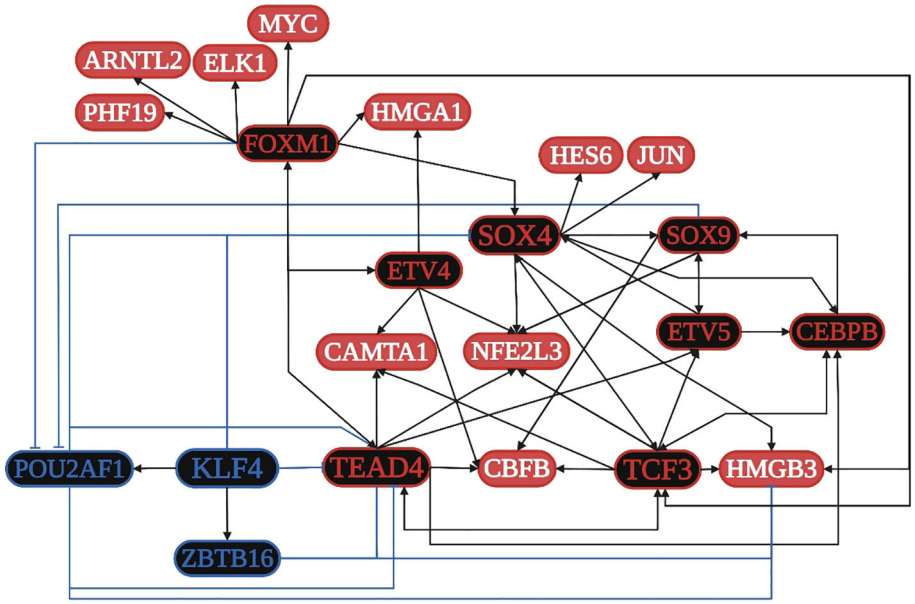

FIGURE 4
Transcriptional regulatory network (TRN) of common transcription factors (TFs) in colon cancer. Downregulated TFs are in blue, upregulated TFs are in red, and the key overregulated and downregulated TFs are in black. The black pointed arrows represent overregulation, and the blue flat arrows represent downregulation. Created with BioRender.com.

with JUN, SOX9, and MYC; 3) the regulation of translation along with MYC; and 4) the regulation of the Wnt signaling pathway along with SOX9. JUN is overregulated in three of the five datasets and is related to: 1) colon cancer signaling pathways along with MYC; 2) the focal adhesion pathway along with ELK1; 3) pathways in cancer along with ELK1 and MYC; 4) EBV infection along with MYC; and 5) angiogenesis. MYC is overregulated in three of the five datasets and is related to: 1) cellular senescence along with FOXM1; 2) proteoglycans in cancer along with ELK1; and 3) HCV infection (Supplementary Table 2). According to the TRN analysis (Figure 4), TCF3 is related to the upregulation of TEAD4, SOX4, ETV5, CEBPB, CBFB, HMGB3, and NFE2L3; TEAD4 is related to the upregulation of TCF3, ETV5, FOXM1, CAMTA1, CEBPB, CBFB, and NFE2L3; SOX4 is related to the overregulation of TCF3, SOX9, CEBPB, NFE2L3, HMGB3, JUN, and HES6; and FOXM1 is related to the overregulation of TCF3, TEAD4, SOX4, ETV4, MYC, ELK1, ARNTL2, HMGA1, and PHF19. The co-regulatory analysis suggests the formation of protein integration complexes between overregulated TFs (CAMTA1, CBFB, CEBPB, ETV4, FOXM1, HES6, JUN, MYC, NFE2L3, PHF19, SOX4, SOX9, and TEAD4) controls transcriptional regulatory function during the acquisition of the hallmarks of cancer.

3.2.3 Gastric cancer

STAT1 is overregulated in seven datasets and is related to: 1) angiogenesis; 2) the formation of the macromolecular complex; 3) type I interferon, cytokine-mediated signaling, and pathways in cancer; and 4) Kaposi sarcoma-associated herpes (KSH) and HPV infection. CEBPB is overregulated in seven datasets and is related to 1) the regulation of the inflammatory response, 2) the cellular response to amino acid stimulus, and 3) the TNF and IL-17 signaling pathways. TGIF1 is overregulated in seven datasets and is related to 1) the cellular response to growth factor stimulus and 2) the TGF-beta signaling pathway. FOXM1 is overregulated in seven datasets and is related to 1) the regulation of cell proliferation and 2) the cellular senescence along with MYBL2. TEAD4, ETV4, and PRRX1 are overexpressed in nine and seven of the ten datasets analyzed, but they are not in DAVID´s annotation analysis (Supplementary Table 3). According to the TRN analysis (Figure 5), TEAD4 and ETV4 are related to the overregulation of STAT1, MYBL2, CEBPB, PHF19, BHLHE40, TGIF1, and FOXM1. PRRX1 is related to the overregulation of STAT1 and CEBPB. FOXM1 is related to the overregulation of TEAD4 and MYBL2. STAT1 is related to the overregulation of PRRX1 and CEBPB. MYBL2 is related to the overregulation of ETV4 and FOXM1. CEBPB is related to the overregulation of STAT1 and BHLHE40. TEAD4 is also related to the downregulation of KLF4, whereas FOXM1 and MYBL2 are related to the downregulation of ZBTB16. The co-regulatory analysis suggests that the formation of protein-protein interaction complexes between eight overregulated TFs (BHLHE40, ETV4, FOXM1, MYBL2, PHF19, PRRX1, STAT1, and TEAD4) controls transcriptional regulatory function.

4 Discussion

Bioinformatic analysis of high-throughput sequencing methodologies, such as microarrays and RNA sequencing, allows the identification of all the transcriptionally deregulated genes (DEGs) involved in the modulation of biological processes and signaling pathways related to tumor cells grade, differentiation status, metastatic potential, and patients' survival (Otálora-

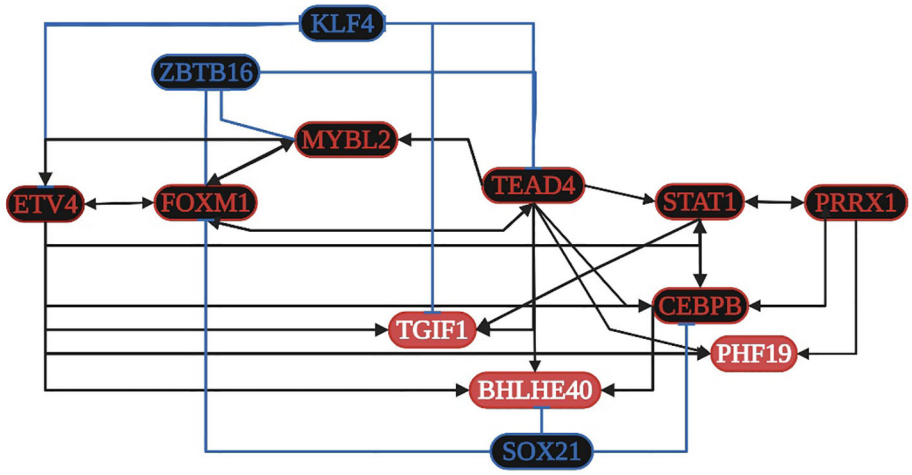

FIGURE 5
Transcriptional regulatory network (TRN) of common transcription factors (TFs) in gastric cancer. Downregulated TFs are in blue, upregulated TFs are in red, and the key overregulated and downregulated TFs are in black. The black pointed arrows represent overregulation, and the blue flat arrows represent downregulation. Created with BioRender.com.

Otálora et al., 2019, Otálora-Otálora et al., 2023a). The human genome has information for approximately 1,400 regulatory genes known as TFs, representing approximately 6% of all human protein coding genes. DNA-binding TFs recognize cis-regulatory elements of target genes, which make them the most direct regulators of gene transcription during cellular differentiation, development, and the response to external factors through the activation and/or inhibition of specific signaling pathways (Weidemüller et al., 2021). In normal cells and tumor cells, TF coding genes can be regulated positively or negatively by genetic and epigenetic mechanisms (Figure 1) that control protein localization on the binding site, resulting in a loss or gain of function (Whiteside and Goodbourn, 1993; Filtz et al., 2014).

The global transcriptomic network analysis highlighted the impact of five TFs, SOX4, TCF3, TEAD4, ETV4, and FOXM1, in gut and lung cancer (Figure 2). SOX4 is an important developmental TF known to regulate stemness, differentiation, progenitor development, and signaling pathways, including the TGF-β, p53, PI3K-Akt, and Wnt pathways, which strengthen its expression (Moreno, 2020). SOX4 shows increased expression in NSCLC tissues, which is specifically correlated with differentiated degree status, the clinical stage, T classification, N classification, M classification, and poor overall patient survival (Wang et al., 2015). *SOX4* is a known target gene of the TGF-β signaling pathway, via the direct binding of SMAD2/3 in complex with SMAD4 to the *SOX4* gene promoter region, and has been shown to be related to the regulation of neural-related nature target genes in SCLC lung tumors with neuroendocrine characteristics (Castillo et al., 2012). In lung cancer, *BMP5* is a common gene but it is downregulated, as are TGF-β receptors and SMADs; therefore, none of them may be involved in the regulation of SOX4 and DLX5 expression. However, according to the TRN analysis, SOX4 can be regulated by HOXC6, whereas DLX5 can be regulated by SOX4, FOXM1, and ETV4 (Figure 3); therefore, its regulation might be controlled by the pathways related to these TFs. In colon cancer, *BMP7* is common overregulated gene, as are *TGFB2*, *TGFBI*, and *TGIF2*, which might be involved in the regulation of SOX4 (Supplementary Table 2). Junction plakoglobin (*JUP*), also known as γ-catenin, a major component of the submembrane of adherens junctions and desmosomes in mammalian cells, can interact with cadherin 3 in adherens junctions in the cytoplasmic component; both are common overregulated genes in lung cancer (Supplementary Table 1) and bind to SOX4 via two trypsinized fragments (Figure 6), while Wnt signaling induces the nuclear colocalization of SOX4 and JUP (Lai et al., 2011). In lung cancer, SOX4 expression is probably related to the overregulation of WNT5A; then, SOX4, FOXM1, TCF3, and JUP might form a stable protein complex with other factors and co-factors for the regulation of transcriptional targets (Figure 6). SOX4 overexpression promotes sphere formation and the self-renewal of colorectal cancer cells (Figure 2), which directly bind to the HDAC1 promoter, encouraging HDAC1 transcription and thereby stem cell maintenance, Wnt, Notch, the cell cycle, and transcriptional misregulation pathways in cancer (Liu et al., 2021b). Forkhead box protein M1 (FOXM1) is overexpressed in NSCLC and SCLC, is related to the regulation tumorigenesis, cell cycle progression,cancer therapy resistance, and metastasis, as it can translocate to the nucleus and bind to the regulatory regions of several target genes crucial for the survival of cancer cells (Zhang et al., 2015; Liang et al., 2021). FOXM1 is a key cell cycle regulator that plays a key role in embryogenesis and cell proliferation and has been strongly linked to solid tumors like colon cancer, where it is linked to reduced disease-free survival, which suggests it is an important prognostic marker (Rather et al., 2023). Furthermore, in gastric cancer, FOXM1 is related to proliferation and invasion, and when it is co-expressed with hTERT it might be involved in cell-cycle-related pathways and positively related to advanced stages and poor outcomes (Tang et al., 2023). In the transcriptomic analysis, there were three other common DEGs (*NEK2*, *GREM1*, and *HSP90AB1*) related to polymerase activity (Supplementary Table 3) that might be related to the process.

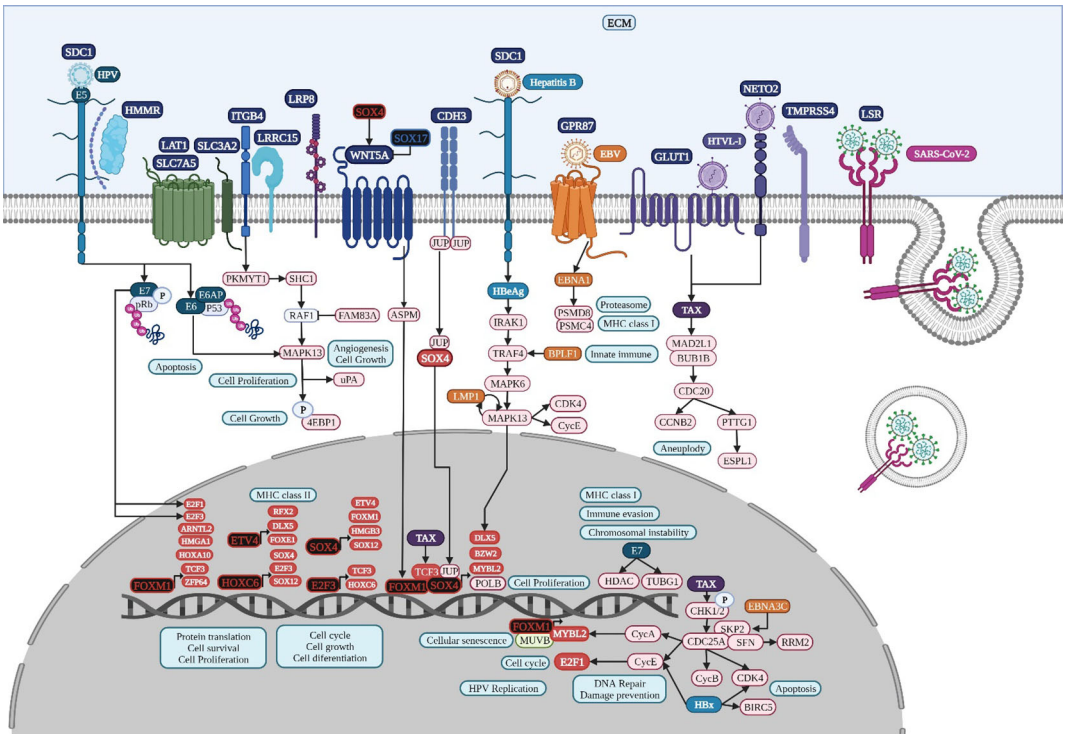

FIGURE 6
Microbiome interaction with the membrane receptors of lung cancer-related cells, activating signaling pathways involved in transcriptional regulation during lung tumorigenesis. Upregulated genes and TFs are in red and the key upregulated TFs are in black. Created with BioRender.com.

The transcription factor 3 gene (*TCF3*) is a key TF overexpressed in lung cancer (Figure 2) and is mainly involved in the cell cycle, cell division, and proliferation (Zhang et al., 2018). TCF3 is primarily a transcriptional repressor (Gregorieff and Clevers, 2005) and is not expressed in adult intestine (Wong et al., 2002). Non-canonical WNT signaling could be related to TCF3 upregulation in colon cancer (Figure 4), along with other key overregulated TFs, and the formation of transcriptional regulatory complexes according to DAVID´s analysis (Supplementary Table 2); therefore, it might be involved in the control of gene expression for the acquisition of the hallmarks of cancer (Figure 1). TCF3 (E2A immunoglobulin enhancer-binding factors E12/E47) E12 forms heterodimers with other basic helix-loop-helix proteins during cell differentiation, whereas E47 can homo and heterodimerize, promoting tumor angiogenesis and proliferation (Peinado et al., 2004); both act as transcriptional repressors of E-cadherin during EMT, which is linked to tumor aggressiveness (Perez-Moreno et al., 2001). TCF3 upregulation is caused by promoter hypomethylation during development, colon cancer progression (Li et al., 2014), and the transcriptional upregulation of multiple cyclin-dependent kinase inhibitors like CDKN1A, p15INK4B, and p16INK4B (Pagliuca et al., 2000), and probably CDKN3 in colon cancer (Supplementary Table 2). According to the RTN analysis, the overregulation of TCF3 might be controlled by TEAD4, SOX4, CEBPB, and FOXM1 (Figure 4).

TEAD4 belongs to a transcriptional enhancer activator domain family of TFs, has a profound impact on physiological and pathological processes through gene expression regulation during cell survival, cell proliferation, tissue regeneration, and stem cell maintenance (Gu et al., 2020), controls chemoresistance, promotes EMT, ECM remodeling, the secretion of paracrine factors, and heterotypic cellular communication, and is related to several signaling pathways (Liu et al., 2024). According to the RTN analysis, the overregulation of TEAD4 might be controlled by TCF3 and FOXM1 (Figure 4). In colon cancer, TEAD4 may also form a complex with TCF3 under the regulation of Wnt (Jiao et al., 2017). The non-canonical Wnt signaling pathway might be involved in colon cancer progression (Figure 7), specifically in planar cell polarity (PCP), in which WNT2 binds to FZD3, a frizzled transmembrane receptor, to activate ankyrin repeat domain 16 (ANKRD16), ras homolog gene family members B and Q (*RHOB* and *RHOQ*), and a mitogen-activated protein kinase, MAP3K20, modifying JUN phosphorylation and its transcriptional regulatory function, which affects cell polarity and cytoskeleton organization (Gómez-Orte et al., 2013). In colon cancer, WNT2 might bind to FZD3 to upregulate AXIN2, as well as RNF43 for its negative feedback regulation (Jho et al., 2002), in which the modification and degradation of β-catenin are key pathway events in tumor progression (Zhao et al., 2022).

TEAD4 stimulates the glycolysis and proliferation of gastric cancer cells (Zhan et al., 2023). The TNF-α-ERK-VGLL1-TEAD4 pathway upregulates integrin αV expression, increasing the adhesion and invasive ability of gastric cancer cells (Hwang et al., 2022). ETV4 is a TF of the E26 transformation-specific (ETS) family and plays an important role in tissue development, promoting the growth and metastasis of gastric cancer (Lu et al., 2019). ETV4 is

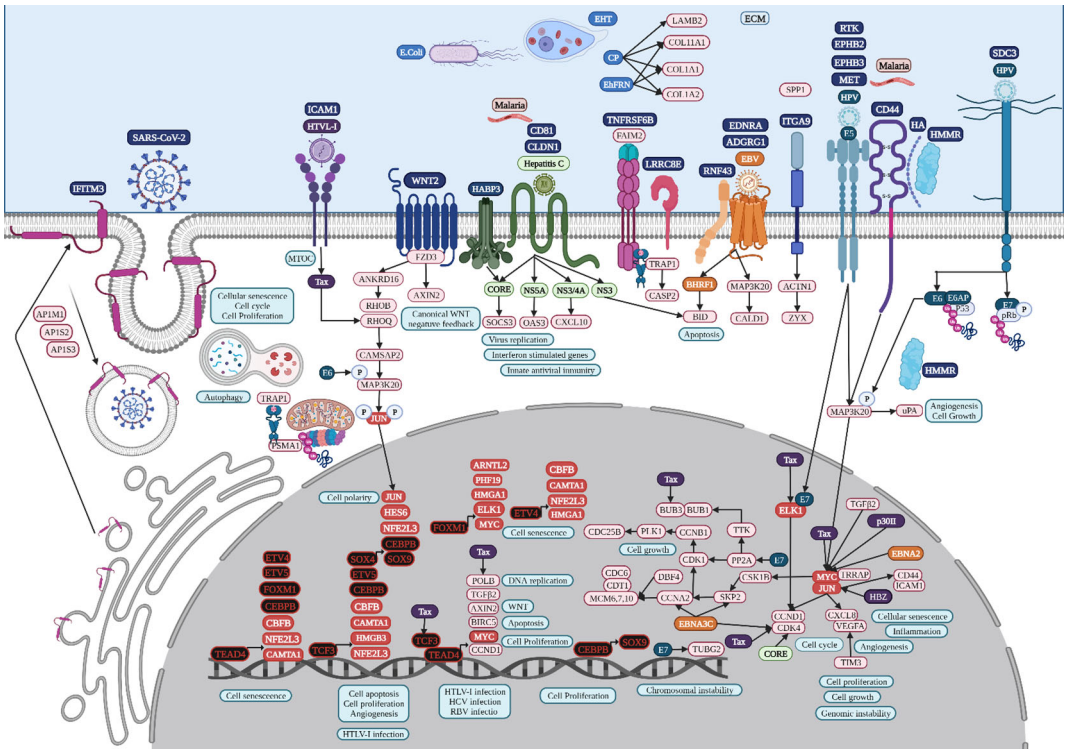

FIGURE 7
Microbiome interaction with the membrane receptors of colon cancer-related cells, activating signaling pathways involved in transcriptional regulation during colon tumorigenesis. Upregulated genes and TFs are in red and the key upregulated TFs are in black. Created with BioRender.com.

also significantly related to growth at the advanced stage, lymph node metastasis, and the poor prognosis of NSCLCs, with a direct regulatory effect on matrix metalloproteinase 1 (*MMP1*), which is a common overregulated gene (Supplementary Table 1) related to cell proliferation and migration, and its co-overexpression is associated with a poor prognosis in human NSCLCs, suggesting that it could be a useful biomarker of tumor progression and worse outcomes in NSCLCs (Wang et al., 2020). Moreover, ETV4 is one of the most expressed genes in colon adenocarcinoma, and it is related to cell proliferation, colony formation, and cell migration (Fonseca et al., 2021). ETV4 is a transcription activator of TNF-α, promoting hepatic inflammation in hepatocellular carcinoma (Qi et al., 2023). Several hallmark pathways are significantly enriched in patients with high PRRX1, including IFN-γ response, IL6-Jak-Stat3 signaling, TNF-α signaling via NF-kB, and IFN-α response in uveal melanoma cancer patients (Meng et al., 2022b). There is evidence that suggests an important role of TEAD4, ETV4, and PRRX1 regulatory activity, the main TFs identified in the TRN analysis (Figure 2), during the TNF and IFN singling pathway in gastric tumorigenesis (Figure 8), along with STAT1 and CEBPB, that might be validated experimentally, to establish their importance during the acquisition of the hallmarks of cancer. Signal transducer and activator of transcription 1 (STAT1) has been linked to anti-tumor immune responses, and *H. pylori* might be involved in the regulation of its expression (Li et al., 2022). In gastric cancer, elevated alpha-inducible protein 6 (IFI6) and FKBP prolyl isomerase 10 (FKBP10) (Supplementary Table 3) could be responsible for the activation of STAT1 expression, diminishing antiviral responses (James et al., 2020).

Transcriptomic studies of gut and lung cancer have been performed and analyzed by several scientific groups around the world. In colon cancer, there are transcriptomic analyses comparing tumor cases and healthy controls, identifying the differences in global transcriptional regulatory programs, showing a large reduction of transcriptional interactions in tumor networks, TFs, and target genes, while the average gene expression is conserved and some TFs increased their connectivity (Cordero et al., 2014). One study analyzed the signatures of co-deregulated genes and their transcriptional regulators in five datasets, highlighting 17 hub co-upregulated genes and 18 hub co-downregulated genes, including three well-known TFs and three kinases, as critical genes in colon cancer (Mastrogamvraki and Zaravinos, 2020). In gastric cancer, there are transcriptomic analyses comparing tumor cases and healthy controls, in which microarray datasets were analyzed to make a protein-protein interaction network with the retrieval of an interacting genes database and TCGA-STAD datasets, identifying the top TFs according to the calculation of the regulatory impact factor (Wang, 2017) (Zhao et al., 2021). An algorithm named mRBioM was even developed for the identification of potential mRNA biomarkers from the complete transcriptomic RNA profiles of gastric adenocarcinoma (Dong et al., 2021), of which some were TFs and cell receptors; however, it did not identify the main regulators of transcription related to the acquisition of the hallmarks of cancer or suggest any other biological processes in

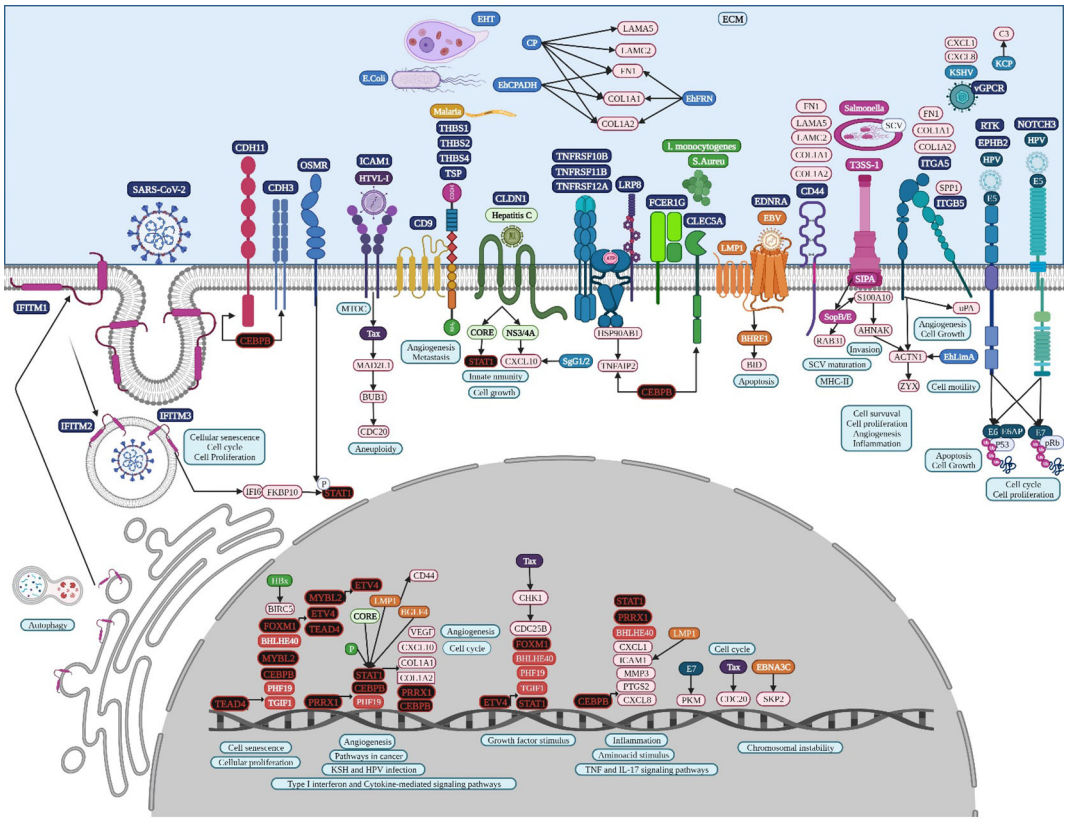

FIGURE 8
Microbiome interaction with the membrane receptors of gastric cancer-related cells, activating signaling pathways involved in transcriptional regulation during gastric tumorigenesis. Upregulated genes and TFs are in red and the key upregulated TFs are in black. Created with BioRender.com.

which all might be involved during the tumorigenic process. In our lung cancer bioinformatic analysis of TF RUNX2 (Otálora-Otálora et al., 2022a), we analyzed and compared our pipeline and results (Otálora-Otálora et al., 2019, Otálora-Otálora et al., 2022b) with previous studies, finding eleven publications assessing the lung cancer TRN with different microarray and RNA-Seq studies, and performing direct and very different bioinformatics analyses on datasets created or selected from the databases. None attempted to perform a global analysis of lung cancer, and most conducted the analysis with a reduced number of datasets for each subtype of lung cancer independently. None of them tried to select deregulated genes unique to lung cancer that are not deregulated in other lung diseases or other types of cancer, and none performed a joint co-regulatory analysis to study the cooperative and coordinated regulatory functions of TFs. However, TFs identified using our bioinformatic pipelines are also in some of the other studies but their regulatory functions during tumor processes were not deeply analyzed. Therefore, regardless of the cell types, the detection methodology of gene expression, and the bioinformatics methodology used, there is a group of regulatory genes or TFs (Otálora-Otálora et al., 2023a).

DAVID´s gene enrichment analyses in lung, colon, and gastric cancer highlights the activation of tumorigenic signaling pathways through the interaction of specific cancer-cell membrane receptors with several microorganisms, including HTLV-1, HPV, EBV, and SARS–CoV–2, which might be related to the establishment of the TRN of TFs in lung cancer (Figure 3), colon cancer (Figure 4), and gastric cancer (Figure 5), and these may be related to the formation of the microbiome network, controlling the gene expression regulation of the specific cancer-cell membrane receptors (Table 2). HTLV-1 is an enveloped single stranded RNA human deltaretrovirus that causes lifelong infection of CD4+ and CD8+ T-cells, monocytes, and other lymphoid and non-lymphoid cells via the ubiquitous glucose transporter-1 (GLUT1) and neuropilin (Einsiedel et al., 2021). *GLUT1*, also known as solute carrier family 2 (*SLC2A1*), is a common overregulated gene in lung cancer that might also function as a receptor for HTLV-1 (Manel et al., 2003). GLUT1 is a transmembrane protein involved in passive glucose transport and has a high glucose affinity compared with other transporters; therefore, it might be key in tissues where glucose is the main energy source (Kokeza et al., 2023). GLUT1 is overexpressed in various solid and hematological malignancies, such as colorectal carcinomas, gastrointestinal stromal tumors, and lung cancers (Zhang et al., 2019), but the correlation with the grade and stage of the tumor and the clinical outcome has not been defined yet (Schuurbiers et al., 2014). The HTLV-1 transactivator protein Tax is a potent activator of a variety of transcription pathways and interacts with cell cycle components dysregulating normal cell cycle controls, leading to several cellular abnormalities, including aneuploidy, the regulation of TCF3 (Figure 6), and the

10.3389/fcimb.2024.1425388

TABLE 2 Cancer-cell membrane receptors related to the interaction of key microorganisms according to KEGG signaling pathways and DAVID´s annotation analysis, and the regulation of their gene expression by key transcription factors.

cancer-cell membrane receptor	Expression regulated by Transcription factorS	Microorganism	Type of cancer
Glucose transporter-1 (GLUT1) solute carrier family 2 (SLC2A1)	SOX4, BZW2, FOXM1, HOXC6, HMGA1, and HMGB3	HTLV-1	Lung
Neuropilin and tolloid-like 2 (NETO2)	DLX5 and HMGB3	HTLV-1	Lung
Intercellular adhesion molecule-1 (ICAM-1)	TEAD4, TCF3, ETV4, ETV5, FOXM1, SOX4, and SOX9	HTLV-1	Colon
	TEAD4, PHF19, PRRX1, BHLHE40, MYBL2, FOXM1, ETV4, and STAT1	HTLV-1	Gastric
Syndecan 1 (SDC1)	DLX5, ETV4, FOXM1, and HMGB3	HPV	Lung
Syndecan 3 (SDC3)	TEAD4, TCF3, ETV4, ETV5, FOXM1, SOX4, and SOX9	HPV	Colon
MET proto-oncogene, receptor tyrosine kinase (MET)	TEAD4, TCF3, ETV4, ETV5, FOXM1, SOX4, and SOX9	HPV	Colon
EPH receptor B2 (EPHB2)	PRRX1, TEAD4, ETV4, and FOXM1	HPV	Gastric
G Protein-Coupled Receptor 87 (GPR87)	FOXM1, HOXC6, HMGB3, and E2F3	EBV	Lung
Endothelin Receptor Type A (EDNRA)	TEAD4, TCF3, ETV4, ETV5, FOXM1, SOX4, and SOX9	EBV	Colon
	PRRX1, BHLHE40, ETV4, and STAT1	EBV	Gastric
Adhesion G protein-coupled receptor G1 (ADGRG1)	TEAD4, TCF3, ETV4, ETV5, FOXM1, SOX4, and SOX9	EBV	Colon
Lipolysis-stimulated lipoprotein receptor (LSR)	ETV4, FOXM1, HOXC6, and HMGB3	CD	Lung
		SARS–CoV–2	Lung
Interferon-induced transmembrane protein 3 (IFITM3)	TEAD4, TCF3, ETV4, ETV5, FOXM1, SOX4, and SOX9	SARS–CoV–2	Colon
Interferon-induced transmembrane protein 1,2,3 (IFITM1,2,3)	TEAD4, ETV4, PRRX1, and FOXM1	SARS–CoV–2	Gastric
Integrin beta 4 (ITGB4)	FOXM1, HOXC6, HMGB3, and HMGA1	HCV	Lung
Claudin-1 (CLDN1)	TEAD4, TCF3, ETV4, ETV5, FOXM1, SOX4, and SOX9	HCV	Colon
Integrin-α9 (ITGA9)	TEAD4, TCF3, ETV4, ETV5, FOXM1, SOX4, and SOX9	EHT	Colon
Integrin subunit alpha 5 (ITGA5)	PRRX1, PHF19, TEAD4, FOXM1, and ETV4	EHT	Gastric
Integrin subunit beta 5 (ITGB5)	PRRX1, PHF19, TEAD4, FOXM1, and MYBL2	EHT	Gastric
Integrin subunit beta like 1 (ITGBL1)	PRRX1	EHT	Gastric
Hyaluronan-mediated motility receptor (HMMR)	SOX4, FOXM1, HOXC6, HMGB3, E2F3, HOXA10, E2F1, and DLX5	HBV	Lung
Large amino acid transporter 1 (LAT1 or SLC7A5)	SOX4, DLX5, BZW2, FOXM1, HMGB3, and HMGA1	HBV	Lung
S100 calcium binding protein A10 (S100A10)	PRRX1, PHF19, TEAD4, FOXM1, and MYBL2	SEST	Gastric

(Continued)

immortalization of T-cells, all of which play key roles in oncogenesis (Currer et al., 2012). Increased CHK1/2 activity by Tax during S phase restricts the CDK-dependent phosphorylation of FOXM1, preventing the premature expression of G2/M genes, including those encoding cyclin-dependent kinase 4, cyclin B1, and cyclin A2 (Branigan et al., 2021), all common DEGs in lung cancer (Supplementary Table 1). In lung cancer, cyclin-dependent kinase 3 may inactivate retinoblastoma and DREAM through phosphorylation for the temporal control of expression of two gene sets: the expression of the first gene set peaks in G1/S for DNA synthesis, and it might be activated by E2F1; the second set reaches maximum expression during G2/M for mitosis, coordinated by MuvB, MYBL2, and FOXM1 (Fischer et al., 2022), a complex that regulates cell cycle progression and entry into senescence (Figure 6). *NETO2* (Neuropilin and tolloid-like 2) is a common overexpressed gene in lung cancer that encodes a transmembrane protein containing two extracellular CUB domains followed by a low-density lipoprotein class A domain (Figure 6), which may also be related to HTLV-1 infection, as it has been associated with clinical stage and lymph node metastasis, cell proliferation, apoptosis, tumor growth, migration, and EMT, increasing the phosphorylation of ERK (Xu et al., 2021a).

HTLV-1 spreads directly between lymphocytes and other cells via a specialized cell-cell contact, named the virological synapse, which is accompanied by the orientation of the microtubule-organizing center in the infected T cell toward the cell contact region with the non-infected target cell, followed by intracellular Tax protein expression and the stimulation of intercellular adhesion molecule-1 (ICAM-1) on the cell surface to trigger microtubule organization center polarization in the HTLV-1–infected colon cell (Figure 7), key in the migration and activation of signaling pathways (Nejmeddine et al., 2009). HTLV-1 Tax acts on genes indirectly by binding several TFs, such as TCF3, ELK1, and MYC in

colon cancer, as well as POLB, BUB3, and CDK4, according to the HTLV-1 infection signaling pathway (Figure 7). HTLV-1 HBZ might bind to JunD, possibly to mediate the activation of ICAM-1 expression, which increases the efficiency of HTLV-1 infection (Fazio et al., 2019). HTLV-1 pX ORF II encodes two proteins, p13II and p30II, multifunctional regulators that modulate Tax-responsive element-mediated transcription and repress cell and viral gene expression to favor cell survival (Green, 2004), which deregulates host signaling pathways involved in aberrant cell growth and proliferation through the induction of lysine-acetylation of c-MYC oncoprotein (Figure 7) and the inhibition of apoptosis, contributing to HTLV-1-induced carcinogenesis (Romeo et al., 2015).

HTLV-1 may spread between gastric cancer cells, followed by the combination of intracellular Tax protein expression and the stimulation of ICAM-1 on the cell surface to trigger microtubule organization center polarization (Nejmeddine et al., 2009) (Figure 8). HTLV-1 Tax directly targets G2 and mitotic regulator hsMAD1, activates mitotic spindle checkpoint function following chromosomal mis-segregation, and controls the G1/S check point, resulting in aberrant anaphase progression, chromosomal instability, DNA aneuploidy, and continuous cellular proliferation (de la Fuente et al., 2006). Tax promotes activation of the anaphase promoting complex (APC)-APCCdc20p, leading to a reduction in Pds1p/securin and Clb2p/cyclin B levels (Liu et al., 2003). Tax represses cellular DNA repair by binding to Chk2 and Chk1, impairing kinase activities *in vitro* and *in vivo*, silencing cellular checkpoints, which guard against DNA structural damage and chromosomal mis-segregation, thus increasing the appearance of a mutant phenotype and perturbing dynamic complexes that coordinate the processes of cell cycle regulation and DNA repair (Park et al., 2004).

HPV is a family of more than 200 small non-enveloped double-stranded circular DNA viruses that can be subdivided in two main groups: high risk and low risk, based on their ability to induce several types of cancers, including lung carcinomas in smoker and non-smoker subjects (Osorio et al., 2022b). HPV infects the basal cells of the mucosal epithelium through capsid proteins L1 and L2, which induce internalization of the virus, probably through the attachment to syndecan 1 (SDC1) (Ozbun and Campos, 2021). Early genomic regions E1 and E2 are the first transcribed for HPV genome amplification; E2 protein is a TF, containing viral DNA binding and transactivation domains (McBride, 2013), E5 is a multipass protein that activates receptors and induces proliferation, E6 inhibits apoptosis by interacting with p53, inducing its degradation and increasing telomerase activity, and E7 binds to protein phosphatase 2A subunits, releasing and activating TFs like E2F involved in cell cycle progression (Figure 6). Then, E6 and E7 induce genome amplification and uncontrolled proliferation in growth arrested differentiated cells, increasing the infected area to finally package HPV genome into L1 and L2 capsid protein and exit cells, which have lost nuclear and cytoplasmic integrity, aided by the E4 protein, which disrupts cytokeratin filaments (Medda et al., 2021). E7 oncoprotein rapidly induces centrosome abnormalities thereby causing the formation of supernumerary mitotic spindle poles and increasing the risk of chromosome mis-segregation (Figure 6) through a process that involves an increase in PLK4 mRNA steady-state levels (Korzeniewski et al., 2011) and tubulin gamma 1 (Starita et al., 2004), which are both overregulated common genes in lung cancer (Supplementary Table 1). HPV16 E7 recruits histone deacetylase HDAC1 and histone demethylase JARID1B or KDM5B to the regulatory region upstream of the TLR9 transcriptional start site and reduces H4 acetylation and H3K4me3, leading to the downregulation of TLR9 expression and the evasion of innate immune responses (Hasan et al., 2013). The treatment of HPV-positive tumor cells with an HDAC inhibitor increases the surface expression of the major histocompatibility complex class I (MHC-I) molecules, increasing the susceptibility of tumor cells to E7-specific CD8+ T cells (Lee et al., 2013). HPV oncoprotein E7 interacts with the DNA methyltransferase DNMT1, an overregulated common gene in lung cancer (Supplementary Table 1), stimulating its methyltransferase activity (Burgers et al., 2007) to induce epigenetic reprogramming in tumor cells.

HPV capsid proteins L1 and L2 may induce virus internalization, probably through the attachment to syndecan 3 (*SDC3*) (Figure 7), a known HPV-binding receptor during colon tumorigenic processes (Mukherjee et al., 2023) and a common overregulated gene in colon cancer. *SDC3* could also be a WNT2 receptor in colon cancer and a potential regulator for the development of chronic inflammation (Chen et al., 2022). Early HPV genomic regions E1, E2, E5, E6, and E7 might be fulfilling some of the same functions as lung cancer (Medda et al., 2021). Furthermore, E6 can selectively upregulate WNT4, JIP1, and JIP2 translation, resulting in the activation of the non-canonical WNT-PCP-JNK pathway through the phosphorylation of mitogen-activated protein kinase (Figure 7) to promote cell proliferation and tumor growth (Zhao et al., 2019). HPV may also bypass IFITM restriction and use certain IFN-inducible proteins to facilitate virus infection (Westrich et al., 2017). HPV16 E5 may increase MET levels, a growth factor receptor critical for tumor cell invasion, motility, and cancer metastasis (Scott et al., 2018). Furthermore, MET induction by E5 requires EGFR, which is also increased by E5 at the mRNA level. Crosstalk between c-MET and various membrane protein partners, including the EGFR, α6β4 integrin, and CD44, results in additional signaling response modulation (Raj et al., 2022). CD44 upregulation enables cell self-renewal, inflammation, and migration at multiple stages and is related to a poor prognosis (Wang et al., 2019). Cell surface interaction between HMMR, CD44, HA, and tyrosine kinases activates MAP kinase cascade, which, in absence of intracellular HMMR, can regulate a mitogenic response involved in cell proliferation and random motility, and in the presence of intracellular HMMR, MAPKs bind to protein partners, which allows HMMR to enter the nucleus to regulate the expression of MYC, controlling its stabilization via AURKA (Otto et al., 2009), microtubule dynamics via the centrosome, and cell cycle progression also via AURKA, a targeting protein for TPX2, hence controlling the expression of genes involved in cell motility, such as matrix metallopeptidases (Raj et al., 2022). HPV capsid proteins L1 and L2 may induce virus internalization, probably through the attachment to neurogenic locus notch homolog protein 3

(NOTCH3) or EPH receptor B2 (EPHB2) in gastric cancer (Figure 8). HPV E7 may regulate the formation of TF complexes to control cell cycle progression and promote aberrant cellular proliferation (Das et al., 2021), as suggested by the intersect of HPV and the NOTCH signaling pathway in gastric cancer (Xie and Yan, 2023). NOTCH3 is associated with more aggressive disease and poor prognosis, acting as a molecular switch in angiogenesis and the release from tumor dormancy (Inder et al., 2017). In cancer cells, EPHB2 may promote EMT (Gao et al., 2014), and in small extracellular vesicles, EPHB2 may promote angiogenesis, inducing ephrin-B reverse signaling, and STAT phosphorylation (Sato et al., 2019).

EBV is a ubiquitous gamma herpesvirus that causes persistent infections and some lymphoid and epithelial tumors (Osorio et al., 2022a) and might use G protein-coupled receptor (GPCR) signaling (Zhang et al., 2016), like GPR87, a common overregulated DEG in lung cancer (Figure 6). Viral GPCRs are composed of seven membrane-spanning helices and intracellular and extracellular domains and have a ligand-independent signaling capacity or constitutive activation, but behave like human chemokine receptors, but behave like human chemokine receptors to guide immune cells to the site of inflammation and participate in tumor cells survival, growth, and metastasis (Zhang et al., 2016). The EBV open reading frame (BILF1) evades the host immune system by downregulating MHC class I and is capable of inducing signaling-mediated tumorigenesis (Fares et al., 2019). The N-terminal part of the large BPLF1 protein contains the catalytic site for ubiquitin ligase and deubiquitinase activity and suppresses TLR-mediated activation as a mechanism to counteract the innate antiviral immunity of infected hosts (van Gent et al., 2014). EBV nuclear antigen 1 (EBNA1) is required for the replication and maintenance of the EBV's extrachromosomal genome in the host cell, with a GAr signal (glycine and alanine rich segment) that interferes with a protein's degradation and allows the virus to escape host immunity via the MHC class I pathway (Finley, 2009). The EBV-encoded *LMP1* oncogene is involved in the transformation, proliferation, and metastasis of several EBV-associated tumors, which are related to its ability to upregulate anti-apoptotic proteins and growth signals and the expression of p38 (MAPK13) in response to stimuli such as stress or primary infection that lead to an increase in LMP1 promoter activity, and may allow the cells to escape apoptosis, suggesting the presence of a positive autoregulatory loop in LMP1 upregulation (Johansson et al., 2010). EBV nuclear antigen (EBNA)3C functions as a transcriptional regulator by interacting with several well-known cellular and viral TFs (Kumar et al., 2009). EBNA3C recruits SKP2 E3 ligase activity to facilitate the degradation of p27KIP1 and pRb, and interacts with cyclin A, cyclin D1, p53, E2F1, and CHK2 (Bhattacharjee et al., 2016). EBV might use G protein-coupled receptor (GPCR) signaling (Zhang et al., 2016), like EDNRA and ADGRG1, which are common DEGs in colon cancer. EBV Bam HI fragment H rightward open reading frame (BHRF1) is a viral homolog of cellular BCL-2 pro-survival proteins (vBCL-2s) and confers strong resistance to diverse apoptotic stimuli and interacts with the cellular pro-apoptotic BCL-2 protein BID in colon cancer (Figure 7) to inhibit DNA-damage-induced apoptosis (Fitzsimmons et al., 2020). EBV EBNA2 induces transcription of the MYC oncogene and decreases lytic EBV replication (Münz, 2019). EBNA3C stabilizes c-Myc and recruits c-Myc and its co-factor Skp2 to c-Myc-dependent promoters, which result in increased c-Myc-dependent transcription (Kumar et al., 2009). Cyclin A, an activator of S phase progression, binds tightly to EBNA3C to stimulate cyclin A-dependent kinase activity and cell cycle progression (Knight and Robertson, 2004). EBNA3C increases the activity of the cyclin D1-CDK4 complex toward histone H1 and a truncated mutant of pRb, increasing pRb poly-ubiquitination and thereby increasing its degradation and abolishing its growth suppressive function (Saha et al., 2011).

EBV also uses GPCR signaling (Zhang et al., 2016), such as *EDNRA*, a common DEG in gastric cancer. BHRF1 also interacts with the cellular pro-apoptotic BCL-2 protein BID (Figure 8) to inhibit DNA-damage-induced apoptosis (Fitzsimmons et al., 2020). EBNA3C may also function in gastric cancer as a transcriptional regulator by interacting with several well-known cellular and viral TFs (Kumar et al., 2009), and recruits SKP2 to facilitate the degradation of p27KIP1 and pRb (Bhattacharjee et al., 2016). EBV LMP1 expression in gastric carcinomas may lead to tumor growth avoiding its apoptotic effects and immunologically mediated elimination (Sheu et al., 1998). LMP1 induces STAT1 expression, which probably induces tyrosine phosphorylation depending on the secretion of IFNs (Najjar et al., 2005), and transcriptional activity mediated by the specialized C-terminal activating region 1 or 2 cytoplasmic domains of LMP-1 (Richardson et al., 2003). LMP1 induces the expression of CD44 on the cell surface, a molecule implicated in increased tumor growth and dissemination (Zhu et al., 2021). EBV BGLF4 protein kinase may have a similar function as cellular cyclin-dependent kinase, regulating multiple cellular and viral substrates, which represses the poly(I:C)-stimulated expression of endogenous IFN-beta mRNA and the phosphorylation of STAT1 at Tyr701, which promotes the expression of downstream genes, suppressing host innate immune responses and facilitating virus replication (Wang et al., 2009). The C-terminal activator region 1 of LMP1 delivers a cooperating signal to induce ICAM1 mRNA in response to various inflammatory mediators, including bacterial lipopolysaccharide, phorbol esters, oxidant stress, and pro-inflammatory cytokines, such as TNFα, IL-1β, and γ-IFN (Mehl et al., 2001).

The lipolysis-stimulated lipoprotein receptor (LSR) is the target molecule for cell binding and the internalization of *Clostridium difficile* and might cooperate with the LDL receptors (Yen et al., 2008) to regulate cell proliferation, invasion, and migration (Zhang and Ma, 2021), probably via MAPK signaling (Nagase et al., 2022). LSR may also activate the SARS−CoV−2 S proteins and increase the viral infection of lung cancer cells (Gong et al., 2023), along with host co-receptors that might be involved in cell infection, such as NETO2, GRP87, and transmembrane protease serine 4 (TMPRSS4) (Avdonin et al., 2023) (Figure 6). Interferon-induced transmembrane protein 3 (*IFITM3*) is a common overregulated gene in all five datasets of colon cancer and is an immune-related protein involved in tumor transformation, with protein turnover controlled by autophagy (Friedlová et al., 2022). Y20 phosphorylation of IFITM3 hinders adaptor complex AP-2 recognizing its YEML motif, which is responsible for IFITM3

endocytosis (Chesarino et al., 2014). In colon cancer, adaptor related protein complex 1 subunit mu 1 (AP1M1), subunit sigma 2 (AP1S2), and subunit sigma 3 (AP1S3) are common overregulated genes and might be related to the accumulation of IFITM3 protein on the cell surface (Figure 7). IFITM3 mutation within its endocytosis-promoting YXXΦ motif converts IFITM3 into an enhancer of SARS-CoV-2 infection by promoting virus-cell fusion (Shi et al., 2021). Krüppel-like factor 4 (KLF4) is a common downregulated TF in cancer (Figure 2) that would inhibit IFITM3 (Li et al., 2011) and SOX4 expression (Figure 4). IFITM3 might be related to CCND1 and CDK4 upregulation (Figure 7) during cell growth (Gan et al., 2019). The IFITM family may also be mutated in gastric cancer, regulating the entry of viruses into host cells (Prelli Bozzo et al., 2021), activating IFI6 and FKBP10 (Figure 8) and leading to TF phosphorylation like STAT1 (DeDiego et al., 2019). IFITM1 overexpression is related to the migration and invasiveness of gastric cancer cells (Lee et al., 2012). IFITM2 promotes gastric cancer progression by promoting cell migration and invasion, and inducing EMT (Xu et al., 2017), and interacts with the SARS-CoV-2 S at the cell surface and virus-cell fusion in early endosomes (Prelli Bozzo et al., 2021). IFTIM3 promotes gastric cancer progression, metastasis, stemness, and chemoresistance through the crosstalk between signaling pathways (Chu et al., 2022) and the activation of integrin signaling pathways (Friedlová et al., 2022). IFITM2 and IFITM3 promote human coronavirus OC43 infection, as three distinct mutations in tyrosine phosphorylation convert IFITM1 and IFITM3 from inhibitors to enhancers of SARS-CoV and MERS-CoV spike protein-mediated entry, challenging the "rigid-membrane" hypothesis (Table 1) (Zhao et al., 2018).

HCV might be involved in the activation of important tumorigenic signaling pathways of lung (Figure 6) and colon cancer (Figure 7), interacting with several membrane receptors (Table 2). HCV upregulates mRNA and protein expression levels of SLC3A2 through NS3/4A-mediated oxidative stress, as well as SLC3A2/LAT1 complex levels, contributing to HCV-mediated pathogenesis (Nguyen et al., 2018). Solute carrier family 3 member 2 (SLC3A2) can associate with integrin-β chains like Integrin beta 4 (ITGB4) in lung cancer, thereby influencing integrin signaling, cell survival, and cell migration (Fort et al., 2007). In lung cancer, protein kinase membrane-associated tyrosine/threonine 1 (PKMYT1) might be related to the activation of the MAPK signaling pathway and 4EBP1 phosphorylation (Figure 6) (Fuchs and Bode, 2005), promoting cell proliferation and apoptosis resistance (Zhang et al., 2020). ITGB4 is a heterodimer that is a non-covalently associated transmembrane glycoprotein receptor that forms complexes that vary in their ligand-binding specificities. It is an important component of the ECM that affects cell adhesion, migration, invasion, proliferation, and apoptosis during viral infection, and its phosphorylation at Y1510 is involved in the regulation of the MAPK-MEK1-ERK1/2 signaling pathway (Meng et al., 2020). In lung cancer, ITGB4 might be related to leucine-rich repeat-containing protein 15 (LRRC15), which is involved in cell-cell and cell-matrix interactions and overexpressed in mesenchymal-derived tumors (Ray et al., 2022), exerting a metastatic invasion role in lung cancer (Ruan et al., 2022). *ITGB4* and urokinase-type plasminogen activator (uPA) encoded by *PLAU*, two common overregulated genes in lung cancer, promote angiogenesis via ERK1/2 phosphorylation, leading to cell growth (LaRusch et al., 2010; Breuss and Uhrin, 2012). The overexpression of eukaryotic translation initiation factor 4E (eIF4E)-binding protein 1 (4EBP1) in NSCLC patients has been related to a lower survival (Tang et al., 2022). 4EBP1 is a usual phosphorylation target of the mTOR and MAPK-ERK signaling pathways (Figure 6), with HPV-E6 as intermediary, causing its release from eIF4E to allow cap-dependent translation, protein synthesis, and cell growth to meet the increased metabolic demand (She et al., 2010). Low-density lipoprotein receptor-related (LDLR) protein 8 (*LRP8*) is a common overexpressed gene in lung cancer tissues and cell lines and is correlated with poor clinicopathological characteristics and prognosis by modulating the Wnt signaling pathway (Fang et al., 2022). LDLRs are highly conserved receptors for multiple alphaviruses, which infect vertebrate species and insect vectors separated by hundreds of millions of years of evolutionary history (Clark et al., 2022). HCV core protein directly binds to STAT1 to induce its hetero- or homodimerization, resulting in HCV resistance to IFN therapy (Anjum et al., 2013). HCV-1b core protein also induces miR-93-5p upregulation and inhibits the IFN signaling pathway by directly targeting IFNAR1, whereas the miR-93-5p-IFNAR1 axis regulates STAT1 phosphorylation, which plays a crucial role in cancer development (He et al., 2018). The multi-step process of HCV entry might be facilitated by various host factors, including the tight junction protein claudin-1 (CLDN1), which is required for efficient HCV virion accumulation at the tight junction from the basolateral membrane (So et al., 2023). BID contains a specific cleavage site recognized by HCV NS3/NS4A proteases, downstream apoptotic molecules of the mitochondrial pathway (Hsu et al., 2003). Chemokine (C-X-C motif) ligand (CXCL)10 belongs to the ELR-CXC family and is a pro-inflammatory cytokine secreted upon IFN-γ stimulation by different cell types. It is involved in a wide variety of processes such as chemotaxis, differentiation, innate defense following viral infection with the activation of peripheral immune cells, and the regulation of cell growth (Liu et al., 2011), and is induced by HCV NS3/4A (Schaefer et al., 2011). HCV core is the first synthesized protein upon viral infection, regulates viral and cell expression, induces tumorigenesis, modulates apoptosis, and suppresses host immunity (Ray and Ray, 2001). HCV core protein has a pro-proliferative role through the increase of c-myc stability (Park et al., 2011). IFN-γ production and T-cell responses are negatively regulated by suppressors of cytokine signaling (SOCS) family members SOCS1 and SOCS3 through the inhibition of the Jak-STAT pathway (Bode et al., 2003). HCV core protein inhibits T-cell responses by interacting with gC1qR (complement component 1 Q subcomponent-binding protein, mitochondrial [C1QBP] or hyaluronan-binding protein 1 [HABP1]), and SOCS1/3, suppressing STAT1/3 (Kittlesen et al., 2000). In colon cancer, *HABP3* is a common overregulated gene that might be involved in the interaction with SOCS3 and the expression of IFN-stimulated genes (Figure 7). HCV NS5A confers innate immune evasion by interacting with 2′,5′-oligoadenylate synthetase (2′,5′-OAS) and inhibiting IFN antiviral activity (Taguchi et al., 2004). Human monoclonal transbodies that

interfere with HCV NS5A activities have led to HCV replication inhibition and host immunity restoration (Glab-ampai et al., 2017).

Entamoeba histolytica trophozoites (EHT) might be involved in the activation of important tumorigenic signaling pathways in colon (Figure 7) and gastric cancer (Figure 8), interacting with several membrane receptors (Table 2). EHT causes substantial damage to the colonic epithelial cells that detach from the substrate to eventually be phagocytosed by the parasite (Cornick and Chadee, 2017), causing amoebiasis in 50 million people and killing 100.000 individuals around the world (Shirley et al., 2020). EHT Fibronectin (FN)-binding molecule (EhFNR) is like human β1 integrin (Talamás-Rohana et al., 1998) and is involved in adhesion, migration, and the invasion process, as well as the mobilization of the receptor molecule from internal vesicles to the plasma membrane, playing an important role during tumor development (Hernández-Ramírez et al., 2007). FN is a major host ECM component that induces actin remodeling in the parasite in a RAB21-dependent manner, forming invadosomes that promote the chemotactic migration of the metastatic cancer cells and non-transformed cells by remodeling the ECM (Emmanuel et al., 2015). RAB31 may be involved in the formation of invadosomes in colon cancer, promoting actin dot formation under an FN-induced signal in EHT, invasion, and pathogen virulence (Figure 7). The interaction with enteropathogenic *Escherichia coli* could modify the virulence of EH to cause amebiasis, resulting in a marked upregulation of EH cysteine proteinase (CP) virulence factors, which are critical in tumor pathogenesis and progression (Fernández-López et al., 2019). The overexpression of the EHT cysteine protease EhCP112 provokes major epithelial injury, increasing intestinal epithelial permeability, likely due to apical erosion and claudin-1 and claudin-2 degradation (Cuellar et al., 2017). The key EHT virulence factor that elicits the fast release of mucin by goblet cells as cysteine protease 5 (EhCP5) couples with goblet cell αvβ3 receptors and degrades the colonic mucus layer at the site of invasion (Cornick et al., 2016), suggesting that integrin-α9 (ITGA9) might be related to amoebiasis infection. ITGA9 is expressed in colonic glandular epithelial cells at the fetal stage and in colon adenocarcinoma, but not in normal adults (Xu et al., 2021b). ACTN1 may positively interact with ITGA9 to promote proliferation, invasion, and EMT in colon cancer (Wang et al., 2023).

The initial epithelial damage produced by EHT is characterized by the opening of tight junctions, followed by a dramatic drop in transepithelial electrical resistance with the participation of EhCPADH complex that affects claudin-1 and occludin (Betanzos et al., 2013), and damages adherens junctions and desmosomes (Hernández-Nava et al., 2017). EhFNR may also be involved in adhesion, migration, and the invasion process, as well as the mobilization of the receptor molecule from internal vesicles to the plasma membrane, playing an important role during gastric tumor development (Hernández-Ramírez et al., 2007). RAB31 may also be involved in the formation of invadosomes in gastric cancer by promoting actin dot formation under the fibronectin-induced signal in EHT and thus playing an important role during invasion and modulating pathogen virulence (Figure 8). The interaction with enteropathogenic *E. coli* could modify the virulence of EH to cause amebiasis, resulting in a marked upregulation of EH CP during tumor pathogenesis and progression (Fernández-López et al., 2019). Integrin subunit alpha 5 (ITGA5) and integrin subunit beta 5 (ITGB5) may form a heterodimer in gastric cancer that positively interacts with ACTN1 (Figure 8) to promote proliferation, invasion, and EMT (Wang et al., 2023). Both integrins participate in the integrin-mediated signaling pathway, viral entry into the host, HPV infection, the phagosome, focal adhesion, ECM-receptor interaction, and the cell junction (Supplementary Table 3). ITGA5 participates in the positive regulation of cell migration, along with CLDN1 and Ephrin type-B receptor 2 (EPHB2), and angiogenesis, along with EPHB2, TNFAIP2, and TNFRSF12A. ITGB5 expression contributes to a poor prognosis and is significantly associated with ECM organization, cell-substrate adhesion, focal adhesion, ECM-receptor interaction, and the phagosome (Liu et al., 2021a). The key virulence factor in live EHT may also elicit the fast release of mucin by goblet cells as EhCP5 couples with goblet cell αvβ3 receptors and degrades the colonic mucus layer at the site of invasion (Cornick et al., 2016), suggesting that ITGA5, ITGB5, and integrin subunit beta like 1 (ITGBL1) might be related to amoebiasis infection in gastric cancer.

HBV might be involved in the activation of important tumorigenic signaling pathways of lung cancer (Figure 6), interacting with several membrane receptors (Table 2). HBV is a small single-strand circular DNA virus that may be able to attach to heparan sulfate (HS) molecules and cell-free HS or SDC1, a transmembrane (type I) HS proteoglycan (HSPG), which occurs within clusters of integrins of the extracellular matrix (ECM) (Shi et al., 2013), which are receptors encoded by a common DEG in lung cancer (Supplementary Table 1). HBV may also attach to members of the solute carrier family (Somiya et al., 2016), such as *SLC7A5*, another common overregulated gene in lung cancer (Supplementary Table 1). The interaction between SDC1 and HMMR, the hyaluronan-mediated motility receptor overregulated in lung cancer, is related to tumor cell motility and differentiation (Yeh et al., 2018), as well as the pathological stage, T classification, lymph node metastasis, and distant metastasis (Li et al., 2021). The interaction of HMMR with SLC7A11 activates ferroptosis, enhances the cytotoxic effect of CD8 +T cells, and regulates the tumor immune microenvironment (Shan et al., 2023), suggesting an interaction with SLC7A5 in lung cancer. SLC7A5 or large amino acid transporter 1 (LAT1) is a heterodimeric transmembrane protein complex that catalyzes amino acid transport. It belongs to the SLC7-APC (amino acid-polyamine-organocation) superfamily (Scalise et al., 2018), participates in the immunosuppressive lung tumor microenvironment, and is associated with a low response to immunotherapy (Liu et al., 2022), high cancer stem cell (CSC) activity, and shorter overall survival (Liu et al., 2021c). Solute carrier family 3 member 2 (SLC3A2), or CD98hc, encodes another subunit of heterodimeric amino acid transporter that is overregulated in six lung cancer datasets and establishes a heterodimeric transmembrane protein complex with SLC7A5 to catalyze amino acid transport (Chiduza et al., 2019). HBV has evolved strategies to counter Toll-like receptor responses by suppressing their expression, regulating downstream signaling pathways related to adaptive immunity, and facilitating viral persistence (Du et al.,

2022), like the non-canonical p38 mitogen-activated protein kinase (MAPK13) pathways, and probably the following phosphorylation and activation of DLX5 (Figure 6). HBV X protein (HBx) affects transcription and HBV replication, and it seems to be implicated in the regulation of BIRC5, cyclin E, and CDK4, and induces p16 hypermethylation, retinoblastoma phosphorylation, and E2F and DNMT1 activity (Tavakolian et al., 2020).

Salmonella enterica serovar Typhimurium (SEST) might be involved in the activation of important tumorigenic signaling pathways in gastric cancer (Figure 8), interacting with membrane receptors (Table 2). SEST resides in a membrane-bound compartment called the *Salmonella*-containing vacuole (SCV), which interacts with early endosomes to acquire a subset of late endosomal/lysosomal proteins through four characterized regulators of endocytic recycling, present on the SCV after invasion (Smith et al., 2005), from where they deliver effector proteins to the host cell via the *Salmonella* pathogenesis island 2 (SPI-2) type III secretion system (T3SS), inhibiting the process of antigen presentation by mature MHCII molecules (Azimi et al., 2020). SPI-5 encodes Salmonella outer protein B, which is involved in neutrophil recurrence (Wallis and Galyov, 2000), the interaction with the chloride channel, ion balance in the host cell, the management of SVC to inhibit lysosome vacuole fusion (Jantsch et al., 2011), and the returning of Rab5 to the SCV, causing the aggregation of phosphatidylinositide-3-phosphate (Mallo et al., 2008). ARF6 and Rab4 associate immediately but their presence diminishes 60 min post-infection, whereas syntaxin13 association peaks at 60 min to regulate the recycling of MHC class I. RAB11 association also peaks at 60 min to regulate the recycling of CD44 (Smith et al., 2005). *RAB31* is a common overregulated gene in gastric cancer and it might be able to distinguish the intracellular vacuole of human-adapted and broad-host SEST, which may have implications for the understanding of the marked differences between SEST's biology and the fine-tuning of T3SSs activity to adapt their function to the unique requirements of each SEST because differences in a single type III secretion effector protein result in fundamental changes to *Salmonella*'s intracellular niche (Spanò et al., 2011). Annexin A2 (phosphatidylinositol (4,5)-bisphosphate binding protein), p11 (S100 calcium binding protein A10 (S100A10)), and AHNAK nucleoprotein are required for the T3SS-mediated *Salmonella* invasion of cultured epithelial cells, and T3SS effector SopB is required for the recruitment of AnxA2 and AHNAK to *Salmonella* invasion sites; *Salmonella* can then intersect the host cell actin pathway via AnxA2 (Jolly et al., 2014). In gastric cancer, S100A10 and AHNAK2 are common DEGs that might be involved in *Salmonella* infection; however, annexin A2 is not (Supplementary Table 3), suggesting that the pathway might be actin independent or another protein is recruited to actin assembly sites at cellular membranes (Figure 8).

The study of the specific mechanisms by which the TRN and microbiome networks related to viral, bacterial, fungal, and parasite infections influence cancer establishment and progression in the oral-gut-lung axis will continue with: (1) single-cell transcriptomics and epigenomics in circulating extracellular vesicles (host-cells and microbially derived extracellular vesicles) and tissue tumoral cells in gastric, colon, and lung cancer patients to validate the TRN and analyze its relationship with the microbiome network; (2) proteomic and metabolomic analyses in circulating extracellular vesicles (host-cells and microbially derived extracellular vesicles) and tissue tumoral cells in gastric, colon, and lung cancer, in the same cohort, to study the formation of protein-protein interaction networks by TFs and transcription co-factors, the binding of gene expression regulatory complexes to their specific target genes, and the posttranslational regulation mediated by these regulatory complexes; (3) metaproteomic and metabolomic analyses of the microbiome network, which can activate or repress certain signal transduction pathways involved in inflammatory and tumorigenic processes; (4) multiomic analyses of inflammatory diseases, such as periodontitis, pulmonary arterial hypertension, and inflammatory bowel disease, in the development of tumorigenic processes in our population; (5) the development of three-dimensional cell organoid models of healthy individuals and cancer patients to study the response to microbiome and epidrugs controlling regulatory and epigenomics mechanisms related to the transcriptional and posttranslational regulation of host-microbiome TF networks in the treatment of tumorigenic processes within the framework of personalized medicine; and (6) exploring exosomes as new generation vehicles for cancer treatment, drug delivery, the control of signaling pathways, and genomic expression through the regulation of transcriptomic and epigenomic mechanisms. All steps are crucial for developing targeted advanced therapies against lung and gut cancer.

5 Conclusion

The global transcriptomic network analysis of gut and lung cancer highlights the impact of five TFs (SOX4, TCF3, TEAD4, ETV4, and FOXM1) that might be related to stem cell programing and cancer progression through the regulation of the expression of an important number of common deregulated genes, such as cancer-cell membrane receptors that interact with several microorganisms, including HTLV-1, HPV, EBV, and SARS–CoV–2. The regulatory function of SOX4, FOXM1, and ETV4, over other key TFs (Figure 3) and common DEGs, was highlighted in lung cancer, establishing key co-regulatory complexes in NSCLC and SCLC. The regulatory function of TEAD4, TCF3, ETV4, SOX4, and FOXM1, over other key TFs (Figure 4) and common DEGs, was highlighted in colon cancer, establishing key co-regulatory complexes. The regulatory function of TEAD4, ETV4, PRRX1, and FOXM1, over other key TFs (Figure 5) and common DEGs, was highlighted in gastric cancer, establishing key co-regulatory complexes. ETV4 and FOXM1 are the two common overregulated TFs in the three types of cancer and are important in the regulation of other key TFs and DEGs, as well as the formation of co-regulatory complexes, during the tumorigenic process in the gut-lung axis. KLF4 and ZBTB16 are the two common downregulated TFs in the three types of cancer that might control key overregulated TFs and DEGs, and therefore, their expression must be controlled by key overregulated TFs during the tumorigenic process. There are specific overregulated cancer-cell membrane receptors crucial for the interaction with HTVL-1, HPV,

EBV, and SARS–CoV–2 in every type of cancer, which are regulated by the key TFs (Table 2) and might be involved in the regulation of the MAPK signaling pathway (Figure 6), the non-canonical Wnt signaling pathway (Figure 7), and the regulation of the IFN signaling pathway (Figure 8) during the lung and gut tumorigenic process.

Our global transcriptomic analysis suggests a complex crosstalk between the microbiome and cancer TRN, as shown by the co-expression of common DEGs that codify for membrane receptors and TFs, and consequently, the possible participation in the same biological process, along with all experimental studies that have demonstrated that the interaction of the microbiome and specific receptors identified as common DEGs in cancer might be able to activate signaling pathways that regulate gene expression. The actual evidence in the field highlighted receptors that might be involved in the crosstalk between the microbiome network and the host cell TRN in a spatial, temporal, and sequential manner during the tumorigenic process in the gut-lung axis. Additionally, the evidence identified signaling pathways activated downstream that might be implicated in the regulation of the host cancer cell TRN, the regulation of gene expression during the establishment and progression of cancer, and in turn in the regulation of the communication with the microbiome network.

The regulatory function of key TFs over all common DEGs must be validated experimentally to fully understand how they are involved in the interaction of host cancer cells and microbiome gene expression networks that might be able to unlock cell phenotypic plasticity for the acquisition of the hallmarks of cancer in the gut-lung axis. All our findings must be experimentally validated with proper methodologies to specifically prove how, when, and where: 1) the microbiome network is interacting with the membrane receptors of cancer-related cells; 2) the host-microbiome interaction activates the signaling pathways related to gene expression; and 3) the cancer TRN is regulating the crosstalk with the microbiome network. *In vitro* studies of single and multiple microorganism infection are necessary to gain insight into general entry mechanisms and the activation and/or silencing of specific signaling pathways, as are studies involving patient cohorts that aim to identify the clinical relevance of molecular host-virus interactions, which are essential in the development of novel diagnostic and treatment approaches that control the formation of microorganism-host protein complexes. Then, it will be necessary to identify which signaling pathway is regulating the expression of which TFs and which DEGs are being controlled by which TFs, and highlighting between those, the genes that codify for membrane receptors that interact with the microbiome network; only then will the regulation circle of the tumorigenic processes between the microbiome and cancer TRNs be fully complete.

Data availability statement

The original contributions presented in the study are included in the article/Supplementary Material. Further inquiries can be directed to the corresponding author.

Ethics statement

Ethical approval was not required for the study involving humans in accordance with the local legislation and institutional requirements. Written informed consent to participate in this study was not required from the participants or the participants' legal guardians/next of kin in accordance with the national legislation and the institutional requirements.

Author contributions

BO-O: Conceptualization, Formal analysis, Investigation, Methodology, Writing – original draft, Writing – review & editing. CP-G: Data curation, Formal analysis, Methodology, Software, Writing – review & editing. JL-R: Investigation, Writing – review & editing. NP-A: Data curation, Formal analysis, Methodology, Software, Writing – review & editing. CA-G: Writing – review & editing. MI-R: Writing – review & editing. CÁ-M: Conceptualization, Investigation, Writing – review & editing.

Funding

The author(s) declare that no financial support was received for the research, authorship, and/or publication of this article.

Conflict of interest

Authors JL-R and CÁ-M were employed by the company Clínica Colsanitas S.A.

The remaining authors declare that the research was conducted in the absence of any commercial or financial relationships that could be construed as a potential conflict of interest.

Publisher's note

Supplementary material

The Supplementary Material for this article can be found online at: https://www.frontiersin.org/articles/10.3389/fcimb.2024.1425388/full#supplementary-material

SUPPLEMENTARY METHODS 1
Bioinformatic pipeline.

SUPPLEMENTARY TABLE 1
Lung cancer common DEGs selection, annotation, and gene regulatory networks.

SUPPLEMENTARY TABLE 2
Colon cancer common DEGs selection, annotation, and gene regulatory networks.

SUPPLEMENTARY TABLE 3
Gastric cancer common DEGs selection, annotation, and gene regulatory networks.

References

Ackermann, C. J., Guller, U., Jochum, W., Schmied, B. M., and Warschkow, R. (2018). The prognostic value of signet ring cell histology in stage I/II colon cancer—a population-based, propensity score-matched analysis. *Int. J. Colorectal Dis.* 33, 1183–1193. doi: 10.1007/s00384-018-3096-5

Anjum, S., Afzal Sohail, M., Ahmad, T., Aslam, B., Waheed, Y., Shafi, T., et al. (2013). Mutations in the STAT1-interacting domain of the hepatitis C virus core protein modulate the response to antiviral therapy. *Mol. Med. Rep.* 8, 487–492. doi: 10.3892/mmr.2013.1541

Avdonin, P. P., Rybakova, E. Y., Trufanov, S. K., and Avdonin, P. V. (2023). SARS-CoV-2 receptors and their involvement in cell infection. *Biochem. (Mosc) Suppl. Ser. A Membr Cell Biol.* 17, 1–11. doi: 10.1134/S1990747822060034

Azimi, T., Zamirnasta, M., Sani, M. A., Soltan Dallal, M. M., and Nasser, A. (2020). Molecular mechanisms of salmonella effector proteins: A comprehensive review. *Infect. Drug Resist.* 13, 11–26. doi: 10.2147/IDR.S230604

Betanzos, A., Javier-Reyna, R., García-Rivera, G., Bañuelos, C., González-Mariscal, L., Schnoor, M., et al. (2013). The EhCPADH112 complex of Entamoeba histolytica interacts with tight junction proteins occludin and claudin-1 to produce epithelial damage. *PloS One* 8, e65100. doi: 10.1371/journal.pone.0065100

Bhattacharjee, S., Ghosh Roy, S., Bose, P., and Saha, A. (2016). Role of EBNA-3 family proteins in EBV associated B-cell lymphomagenesis. *Front. Microbiol.* 7. doi: 10.3389/fmicb.2016.00457

Bode, J. G., Ludwig, S., Ehrhardt, C., Albrecht, U., Erhardt, A., Schaper, F., et al. (2003). IFN-alpha antagonistic activity of HCV core protein involves induction of suppressor of cytokine signaling-3. *FASEB J.* 17, 488–490. doi: 10.1096/fj.02-0664fje

Branigan, T. B., Kozono, D., SChade, A. E., Deraska, P., Rivas, H. G., Sambel, L., et al. (2021). MMB-FOXM1-driven premature mitosis is required for CHK1 inhibitor sensitivity. *Cell Rep.* 34, 108808. doi: 10.1016/j.celrep.2021.108808

Breuss, J. M., and Uhrin, P. (2012). VEGF-initiated angiogenesis and the uPA/uPAR system. *Cell Adh Migr* 6, 535–615. doi: 10.4161/cam.22243

Burgers, W. A., Blanchon, L., Pradhan, S., Launoit, Y.d., Kouzarides, T., and Fuks, F. (2007). Viral oncoproteins target the DNA methyltransferases. *Oncogene* 26, 1650–1655. doi: 10.1038/sj.onc.1209950

Castillo, S. D., Matheu, A., Mariani, N., Carretero, J., Lopez-Rios, F., Lovell-Badge, R., et al. (2012). Novel transcriptional targets of the SRY-HMG box transcription factor SOX4 link its expression to the development of small cell lung cancer. *Cancer Res.* 72, 176–186. doi: 10.1158/0008-5472.CAN-11-3506

Chen, C., Luo, L., Xu, C., Yang, X., Liu, T., Luo, J., et al. (2022). Tumor specificity of WNT ligands and receptors reveals universal squamous cell carcinoma oncogenes. *BMC Cancer* 22, 790. doi: 10.1186/s12885-022-09898-2

Chen, S., Cao, Z., Prettner, K., Kuhn, M., Yang, J., Jiao, L., et al. (2023). Estimates and projections of the global economic cost of 29 cancers in 204 countries and territories from 2020 to 2050. *JAMA Oncol.* 9, 465–472. doi: 10.1001/jamaoncol.2022.7826

Chesarino, N. M., McMichael, T. M., Hach, J. C., and Yount, J. S. (2014). Phosphorylation of the antiviral protein interferon-inducible transmembrane protein 3 (IFITM3) dually regulates its endocytosis and ubiquitination. *J. Biol. Chem.* 289, 11986–11992. doi: 10.1074/jbc.M114.557694

Chiduza, G. N., Johnson, R. M., Wright, G. S. A., Antonyuk, S. V., Muench, S. P., and Hasnain, S. S. (2019). LAT1 (SLC7A5) and CD98hc (SLC3A2) complex dynamics revealed by single-particle cryo-EM. *Acta Crystallogr. D Struct. Biol.* 75, 660–669. doi: 10.1107/S2059798319009094

Chow, R. D., Bradley, E. H., and Gross, C. P. (2022). Comparison of cancer-related spending and mortality rates in the US vs 21 high-income countries. *JAMA Health Forum* 3, e221229–e221229. doi: 10.1001/jamahealthforum.2022.1229

Chu, P.-Y., Huang, W.-C., Tung, S.-L., Tsai, C.-Y., Chen, C. J., Liu, Y.-C., et al. (2022). IFITM3 promotes Malignant progression, cancer stemness and chemoresistance of gastric cancer by targeting MET/AKT/FOXO3/c-MYC axis. *Cell Biosci.* 12, 124. doi: 10.1186/s13578-022-00858-8

Clark, L. E., Clark, S. A., Lin, C., Liu, J., Coscia, A., Nabel, K. G., et al. (2022). VLDLR and ApoER2 are receptors for multiple alphaviruses. *Nature* 602, 475–480. doi: 10.1038/s41586-021-04326-0

Cordero, D., Solé, X., Crous-Bou, M., Sanz-Pamplona, R., Paré-Brunet, L., Guinó, E., et al. (2014). Large differences in global transcriptional regulatory programs of normal and tumor colon cells. *BMC Cancer* 14. doi: 10.1186/1471-2407-14-708

Cornick, S., and Chadee, K. (2017). Entamoeba histolytica: Host parasite interactions at the colonic epithelium. *Tissue Barriers* 5, e1283386. doi: 10.1080/21688370.2017.1283386

Cornick, S., Moreau, F., and Chadee, K. (2016). Entamoeba histolytica Cysteine Proteinase 5 Evokes Mucin Exocytosis from Colonic Goblet Cells via αvβ3 Integrin. *PloS Pathog.* 12, e1005579. doi: 10.1371/journal.ppat.1005579

Cuellar, P., Hernández-Nava, E., García-Rivera, G., Chávez-Munguía, B., Schnoor, M., Betanzos, A., et al. (2017). Entamoeba histolytica EhCP112 Dislocates and Degrades Claudin-1 and Claudin-2 at Tight Junctions of the Intestinal Epithelium. *Front. Cell Infect. Microbiol.* 7. doi: 10.3389/fcimb.2017.00372

Currer, R., Van Duyne, R., Jaworski, E., Guendel, I., Sampey, G., Das, R., et al. (2012). HTLV tax: a fascinating multifunctional co-regulator of viral and cellular pathways. *Front. Microbiol.* 3. doi: 10.3389/fmicb.2012.00406

Das, T., Zhong, R., and Spiotto, M. T. (2021). Notch signaling and human papillomavirus-associated oral tumorigenesis. *Adv. Exp. Med. Biol.* 1287, 105–122. doi: 10.1007/978-3-030-55031-8_8

DeDiego, M. L., Nogales, A., Martinez-Sobrido, L., and Topham, D. J. (2019). Interferon-induced protein 44 interacts with cellular FK506-binding protein 5, negatively regulates host antiviral responses, and supports virus replication. *mBio* 10. doi: 10.1128/mBio.01839-19

de la Fuente, C., Gupta, M. V., Klase, Z., Strouss, K., Cahan, P., McCaffery, T., et al. (2006). Involvement of HTLV-I Tax and CREB in aneuploidy: a bioinformatics approach. *Retrovirology* 3, 43. doi: 10.1186/1742-4690-3-43

Dong, C., Rao, N., Du, W., Gao, F., Lv, X., Wang, G., et al. (2021). mRBioM: an algorithm for the identification of potential mRNA biomarkers from complete transcriptomic profiles of gastric adenocarcinoma. *Front. Genet.* 12. doi: 10.3389/fgene.2021.679612

Du, Y., Wu, J., Liu, J., Zheng, X., Yang, D., and Lu, M. (2022). Toll-like receptor-mediated innate immunity orchestrates adaptive immune responses in HBV infection. *Front. Immunol.* 13. doi: 10.3389/fimmu.2022.965018

Einsiedel, L., Chiong, F., Jersmann, H., and Taylor, G. P. (2021). Human T-cell leukaemia virus type 1 associated pulmonary disease: clinical and pathological features of an under-recognised complication of HTLV-1 infection. *Retrovirology* 18, 1. doi: 10.1186/s12977-020-00543-z

Emmanuel, M., Nakano, Y. S., Nozaki, T., and Datta, S. (2015). Small GTPase Rab21 mediates fibronectin induced actin reorganization in Entamoeba histolytica: implications in pathogen invasion. *PloS Pathog.* 11, e1004666. doi: 10.1371/journal.ppat.1004666

Fang, Z., Zhong, M., Zhou, L., Le, Y., Wang, H., and Fang, Z. (2022). Low-density lipoprotein receptor-related protein 8 facilitates the proliferation and invasion of non-small cell lung cancer cells by regulating the Wnt/β-catenin signaling pathway. *Bioengineered* 13, 6807–6818. doi: 10.1080/21655979.2022.2036917

Fares, S., Spiess, K., Olesen, E. T. B., Zuo, J., Jackson, S., Kledal, T. N., et al. (2019). Distinct roles of extracellular domains in the epstein-barr virus-encoded BILF1 receptor for signaling and major histocompatibility complex class I downregulation. *mBio* 10. doi: 10.1128/mBio.01707-18

Fazio, A. L., Kendle, W., Hoang, K., Korleski, E., Lemasson, I., and Polakowski, N. (2019). Human T-cell leukemia virus type 1 (HTLV-1) bZIP factor upregulates the expression of ICAM-1 to facilitate HTLV-1 infection. *J. Virol.* 93. doi: 10.1128/JVI.00608-19

Fernández-López, L. A., Gil-Becerril, K., Galindo-Gómez, S., Estrada-García, T., Ximénez, C., Leon-Coria, A., et al. (2019). Entamoeba histolytica Interaction with Enteropathogenic Escherichia coli Increases Parasite Virulence and Inflammation in Amebiasis. *Infect. Immun.* 87. doi: 10.1128/IAI.00279-19

Filtz, T. M., Vogel, W. K., and Leid, M. (2014). Regulation of transcription factor activity by interconnected post-translational modifications. *Trends Pharmacol. Sci.* 35, 76–85. doi: 10.1016/j.tips.2013.11.005

Finley, D. (2009). Recognition and processing of ubiquitin-protein conjugates by the proteasome. *Annu. Rev. Biochem.* 78, 477–513. doi: 10.1146/annurev.biochem.78.081507.101607

Fischer, M., SChade, A. E., Branigan, T. B., Müller, G. A., and DeCaprio, J. A. (2022). Coordinating gene expression during the cell cycle. *Trends Biochem. Sci.* 47, 1009–1022. doi: 10.1016/j.tibs.2022.06.007

Fitzsimmons, L., Cartlidge, R., Chang, C., Sejic, N., Galbraith, L. C. A., Suraweera, C. D., et al. (2020). EBV BCL-2 homologue BHRF1 drives chemoresistance and lymphomagenesis by inhibiting multiple cellular pro-apoptotic proteins. *Cell Death Differ* 27, 1554–1568. doi: 10.1038/s41418-019-0435-1

Fleming, M., Ravula, S., Tatishchev, S. F., and Wang, H. L. (2012). Colorectal carcinoma: Pathologic aspects. *J. Gastrointest Oncol.* 3, 153–173. doi: 10.3978/j.issn.2078-6891.2012.030

Fonseca, A. S., Ramão, A., Bürger, M. C., de Souza, J. E. S., Zanette, D. L., de Molfetta, G. A., et al. (2021). ETV4 plays a role on the primary events during the adenoma-adenocarcinoma progression in colorectal cancer. *BMC Cancer* 21. doi: 10.1186/s12885-021-07857-x

Fort, J., de la Ballina, L. R., Burghardt, H. E., Ferrer-Costa, C., Turnay, J., Ferrer-Orta, C., et al. (2007). The structure of human 4F2hc ectodomain provides a model for homodimerization and electrostatic interaction with plasma membrane. *J. Biol. Chem.* 282, 31444–31452. doi: 10.1074/jbc.M704524200

Franzin, R., Netti, G. S., Spadaccino, F., Porta, C., Gesualdo, L., Stallone, G., et al. (2020). The use of immune checkpoint inhibitors in oncology and the occurrence of AKI: where do we stand? *Front. Immunol.* 11. doi: 10.3389/fimmu.2020.574271

Friedlová, N., Zavadil Kokáš, F., Hupp, T. R., Vojtěšek, B., and Nekulová, M. (2022). IFITM protein regulation and functions: Far beyond the fight against viruses. *Front. Immunol.* 13. doi: 10.3389/fimmu.2022.1042368

Fuchs, B. C., and Bode, B. P. (2005). Amino acid transporters ASCT2 and LAT1 in cancer: Partners in crime? *Semin. Cancer Biol.* 15, 254–266. doi: 10.1016/j.semcancer.2005.04.005

Galli, G., and Rossi, G. (2021). Lung cancer histology-driven strategic therapeutic approaches. *Shanghai Chest* 4, 1–16. doi: 10.21037/shc.2020.01.03

Gan, C. P., Sam, K. K., Yee, P. S., Zainal, N. S., Lee, B. K. B., Abdul Rahman, Z. A., et al. (2019). IFITM3 knockdown reduces the expression of CCND1 and CDK4 and suppresses the growth of oral squamous cell carcinoma cells. *Cell Oncol. (Dordr)* 42, 477–490. doi: 10.1007/s13402-019-00437-z

Gao, Q., Liu, W., Cai, J., Li, M., Gao, Y., Lin, W., et al. (2014). EphB2 promotes cervical cancer progression by inducing epithelial-mesenchymal transition. *Hum. Pathol.* 45, 372–381. doi: 10.1016/j.humpath.2013.10.001

Glab-ampai, K., Chulanetra, M., Malik, A. A., Juntadech, T., Thanongsaksrikul, J., Srimanote, P., et al. (2017). Human single chain-transbodies that bound to domain-I of non-structural protein 5A (NS5A) of hepatitis C virus. *Sci. Rep.* 7, 15042. doi: 10.1038/s41598-017-14886-9

Gómez-Orte, E., Sáenz-Narciso, B., Moreno, S., and Cabello, J. (2013). Multiple functions of the noncanonical Wnt pathway. *Trends Genet.* 29, 545–553. doi: 10.1016/j.tig.2013.06.003

Gong, Y., An, Y., Wang, C., Wang, Z., Kong, F., Jiang, M., et al. (2023). LSR is a cell-intrinsic defence factor against SARS-CoV-2 infection in small intestine. doi: 10.21203/rs.3.rs-3579436/v1

Green, P. L. (2004). HTLV-1 p30II: selective repressor of gene expression. *Retrovirology* 1, 40. doi: 10.1186/1742-4690-1-40

Gregorieff, A., and Clevers, H. (2005). Wnt signaling in the intestinal epithelium: from endoderm to cancer. *Genes Dev.* 19, 877–890. doi: 10.1101/gad.1295405

Groenevelt, C., Gordon, R., Wang, X., Fletcher, M., Markowetz, F., Meyer, K., et al. (2024). *Package ' RTN.'*. 1–70. Available at: https://bioconductor.org/packages/release/bioc/html/RTN.html.

Gu, C., Huang, Z., Chen, X., Liu, C., Rocco, G., Zhao, S., et al. (2020). TEAD4 promotes tumor development in patients with lung adenocarcinoma via ERK signaling pathway. *Biochim. Biophys. Acta (BBA) - Mol. Basis Dis.* 1866, 165921. doi: 10.1016/j.bbadis.2020.165921

Guilford, P., Hopkins, J., Harraway, J., McLeod, M., McLeod, N., Harawira, P., et al. (1998). E-cadherin germline mutations in familial gastric cancer. *Nature* 392, 402–405. doi: 10.1038/32918

Hanahan, D. (2022). Hallmarks of cancer: new dimensions. *Cancer Discovery* 12, 31–46. doi: 10.1158/2159-8290.CD-21-1059

Hasan, U. A., Zannetti, C., Parroche, P., Goutagny, N., Malfroy, M., Roblot, G., et al. (2013). The human papillomavirus type 16 E7 oncoprotein induces a transcriptional repressor complex on the Toll-like receptor 9 promoter. *J. Exp. Med.* 210, 1369–1387. doi: 10.1084/jem.20122394

He, C.-L., Liu, M., Tan, Z.-X., Hu, Y.-J., Zhang, Q.-Y., Kuang, X.-M., et al. (2018). Hepatitis C virus core protein-induced miR-93-5p up-regulation inhibits interferon signaling pathway by targeting IFNAR1. *World J. Gastroenterol.* 24, 226–236. doi: 10.3748/wjg.v24.i2.226

Hernández-Nava, E., Cuellar, P., Nava, P., Chávez-Munguía, B., Schnoor, M., Orozco, E., et al. (2017). Adherens junctions and desmosomes are damaged by Entamoeba histolytica: Participation of EhCPADH complex and EhCP112 protease. *Cell Microbiol.* 19. doi: 10.1111/cmi.12761

Hernández-Ramírez, V. I., Rios, A., Angel, A., Magos, M. A., Pérez-Castillo, L., Rosales-Encina, J. L., et al. (2007). Subcellular distribution of the Entamoeba histolytica 140 kDa FN-binding molecule during host-parasite interaction. *Parasitology* 134, 169–177. doi: 10.1017/S0031182006001260

Hsu, E. C., Hsi, B., Hirota-Tsuchihara, M., Ruland, J., Iorio, C., Sarangi, F., et al. (2003). Modified apoptotic molecule (BID) reduces hepatitis C virus infection in mice with chimeric human livers. *Nat. Biotechnol.* 21, 519–525. doi: 10.1038/nbt817

Hwang, M.-A., Won, M., Im, J.-Y., Kang, M.-J., Kweon, D.-H., and Kim, B.-K. (2022). TNF-α Secreted from macrophages increases the expression of prometastatic integrin αV in gastric cancer. *Int. J. Mol. Sci.* 24. doi: 10.3390/ijms24010376

Inder, S., O'Rourke, S., McDermott, N., Manecksha, R., Finn, S., Lynch, T., et al. (2017). The Notch-3 receptor: A molecular switch to tumorigenesis? *Cancer Treat Rev.* 60, 69–76. doi: 10.1016/j.ctrv.2017.08.011

James, C. D., Fontan, C. T., Otoa, R., Das, D., Prabhakar, A. T., Wang, X., et al. (2020). Human papillomavirus 16 E6 and E7 synergistically repress innate immune gene transcription. *mSphere* 5. doi: 10.1128/mSphere.00828-19

Jantsch, J., Chikkaballi, D., and Hensel, M. (2011). Cellular aspects of immunity to intracellular Salmonella enterica. *Immunol. Rev.* 240, 185–195. doi: 10.1111/j.1600-065X.2010.00981.x

Jho, E., Zhang, T., Domon, C., Joo, C.-K., Freund, J.-N., and Costantini, F. (2002). Wnt/beta-catenin/Tcf signaling induces the transcription of Axin2, a negative regulator of the signaling pathway. *Mol. Cell Biol.* 22, 1172–1183. doi: 10.1128/MCB.22.4.1172-1183.2002

Jiao, S., Li, C., Hao, Q., Miao, H., Zhang, L., Li, L., et al. (2017). VGLL4 targets a TCF4-TEAD4 complex to coregulate Wnt and Hippo signalling in colorectal cancer. *Nat. Commun.* 8, 14058. doi: 10.1038/ncomms14058

Johansson, P., Jansson, A., Rüetschi, U., and Rymo, L. (2010). The p38 signaling pathway upregulates expression of the Epstein-Barr virus LMP1 oncogene. *J. Virol.* 84, 2787–2797. doi: 10.1128/JVI.01052-09

Jolly, C., Winfree, S., Hansen, B., and Steele-Mortimer, O. (2014). The Annexin A2/p11 complex is required for efficient invasion of Salmonella Typhimurium in epithelial cells. *Cell Microbiol.* 16, 64–77. doi: 10.1111/cmi.2014.16.issue-1

Kim, S. T., Cristescu, R., Bass, A. J., Kim, K.-M., Odegaard, J. I., Kim, K., et al. (2018). Comprehensive molecular characterization of clinical responses to PD-1 inhibition in metastatic gastric cancer. *Nat. Med.* 24, 1449–1458. doi: 10.1038/s41591-018-0101-z

Kittlesen, D. J., Chianese-Bullock, K. A., Yao, Z. Q., Braciale, T. J., and Hahn, Y. S. (2000). Interaction between complement receptor gC1qR and hepatitis C virus core protein inhibits T-lymphocyte proliferation. *J. Clin. Invest.* 106, 1239–1249. doi: 10.1172/JCI10323

Knight, J. S., and Robertson, E. S. (2004). Epstein-Barr virus nuclear antigen 3C regulates cyclin A/p27 complexes and enhances cyclin A-dependent kinase activity. *J. Virol.* 78, 1981–1991. doi: 10.1128/JVI.78.4.1981-1991.2004

Kokeza, J., Strikic, A., Ogorevc, M., Kelam, N., Vukoja, M., Dilber, I., et al. (2023). The effect of GLUT1 and HIF-1α Expressions on glucose uptake and patient survival in non-small-cell lung carcinoma. *Int. J. Mol. Sci.* 24. doi: 10.3390/ijms241310575

Korzeniewski, N., Treat, B., and Duensing, S. (2011). The HPV-16 E7 oncoprotein induces centriole multiplication through deregulation of Polo-like kinase 4 expression. *Mol. Cancer* 10, 61. doi: 10.1186/1476-4598-10-61

Kumar, P., Murakami, M., Kaul, R., Saha, A., Cai, Q., and Robertson, E. S. (2009). Deregulation of the cell cycle machinery by Epstein-Barr virus nuclear antigen 3C. *Future Virol.* 4, 79–91. doi: 10.2217/17460794.4.1.79

Kushima, R. (2022). The updated WHO classification of digestive system tumours-gastric adenocarcinoma and dysplasia. *Pathologe* 43, 8–15. doi: 10.1007/s00292-021-01023-7

Lai, Y.-H., Cheng, J., Cheng, D., Feasel, M. E., Beste, K. D., Peng, J., et al. (2011). SOX4 interacts with plakoglobin in a Wnt3a-dependent manner in prostate cancer cells. *BMC Cell Biol.* 12, 50. doi: 10.1186/1471-2121-12-50

LaRusch, G. A., Mahdi, F., Shariat-Madar, Z., Adams, G., Sitrin, R. G., Zhang, W. M., et al. (2010). Factor XII stimulates ERK1/2 and Akt through uPAR, integrins, and the EGFR to initiate angiogenesis. *Blood* 115, 5111–5120. doi: 10.1182/blood-2009-08-236430

Lauren, P. (1965). The two histological main types of gastric carcinoma: diffuse and so-called intestinal-type carcinoma. An attempt at a histo-clinical classification. *Acta Pathol. Microbiol. Scand.* 64, 31–49. doi: 10.1111/apm.1965.64.1.31

Lee, J., Goh, S.-H., Song, N., Hwang, J.-A., Nam, S., Choi, I. J., et al. (2012). Overexpression of IFITM1 has clinicopathologic effects on gastric cancer and is regulated by an epigenetic mechanism. *Am. J. Pathol.* 181, 43–52. doi: 10.1016/j.ajpath.2012.03.027

Lee, S. Y., Huang, Z., Kang, T. H., Soong, R.-S., Knoff, J., Axenfeld, E., et al. (2013). Histone deacetylase inhibitor AR-42 enhances E7-specific CD8+ T cell-mediated antitumor immunity induced by therapeutic HPV DNA vaccination. *J. Mol. Med.* 91, 1221–1231. doi: 10.1007/s00109-013-1054-9

Li, C., Cai, S., Wang, X., and Jiang, Z. (2014). Hypomethylation-associated up-regulation of TCF3 expression and recurrence in stage II and III colorectal cancer. *PloS One* 9, 1–10. doi: 10.1371/journal.pone.0112005

Li, X., Pan, K., Vieth, M., Gerhard, M., Li, W., and Mejías-Luque, R. (2022). JAK-STAT1 signaling pathway is an early response to helicobacter pylori infection and contributes to immune escape and gastric carcinogenesis. *Int. J. Mol. Sci.* 23. doi: 10.3390/ijms23084147

Li, D., Peng, Z., Tang, H., Wei, P., Kong, X., Yan, D., et al. (2011). KLF4-mediated negative regulation of IFITM3 expression plays a critical role in colon cancer pathogenesis. *Clin. Cancer Res.* 17, 3558–3568. doi: 10.1158/1078-0432.CCR-10-2729

Li, X., Zuo, H., Zhang, L., Sun, Q., Xin, Y., and Zhang, L. (2021). Validating HMMR expression and its prognostic significance in lung adenocarcinoma based on data mining and bioinformatics methods. *Front. Oncol.* 11. doi: 10.3389/fonc.2021.720302

Liang, S.-K., Hsu, C.-C., Song, H.-L., Huang, Y.-C., Kuo, C.-W., Yao, X., et al. (2021). FOXM1 is required for small cell lung cancer tumorigenesis and associated with poor clinical prognosis. *Oncogene* 40, 4847–4858. doi: 10.1038/s41388-021-01895-2

Liu, M., Guo, S., and Stiles, J. K. (2011). The emerging role of CXCL10 in cancer (Review). *Oncol. Lett.* 2, 583–589. doi: 10.3892/ol.2011.300

Liu, M., Hu, W., Meng, X., and Wang, B. (2024). TEAD4: A key regulator of tumor metastasis and chemoresistance - Mechanisms and therapeutic implications. *Biochim. Biophys. Acta (BBA) - Rev. Cancer* 1879, 189050. doi: 10.1016/j.bbcan.2023.189050

Liu, Y.-H., Li, Y.-L., Shen, H.-T., Chien, P.-J., Sheu, G.-T., Wang, B.-Y., et al. (2021c). L-type amino acid transporter 1 regulates cancer stemness and the expression of programmed cell death 1 ligand 1 in lung cancer cells. *Int. J. Mol. Sci.* 22. doi: 10.3390/ijms222010955

Liu, B., Liang, M.-H., Kuo, Y., Liao, W., Boros, I., Kleinberger, T., et al. (2003). Human T-lymphotropic virus type 1 oncoprotein tax promotes unscheduled degradation of Pds1p/securin and Clb2p/cyclin B1 and causes chromosomal instability. *Mol. Cell Biol.* 23, 5269–5281. doi: 10.1128/MCB.23.15.5269-5281.2003

Liu, D., Liu, S., Fang, Y., Liu, L., and Hu, K. (2021a). Comprehensive analysis of the expression and prognosis for ITGBs: identification of ITGB5 as a biomarker of poor prognosis and correlated with immune infiltrates in gastric cancer. *Front. Cell Dev. Biol.* 9. doi: 10.3389/fcell.2021.816230

Liu, Y., Ma, G., Liu, J., Zheng, H., Huang, G., Song, Q., et al. (2022). SLC7A5 is a lung adenocarcinoma-specific prognostic biomarker and participates in forming immunosuppressive tumor microenvironment. *Heliyon* 8, e10866. doi: 10.1016/j.heliyon.2022.e10866

Liu, J., Qiu, J., Zhang, Z., Zhou, L., Li, Y., Ding, D., et al. (2021b). SOX4 maintains the stemness of cancer cells via transcriptionally enhancing HDAC1 revealed by comparative proteomics study. *Cell Biosci.* 11, 23. doi: 10.1186/s13578-021-00539-y

Love, M. I., Huber, W., and Anders, S. (2014). Moderated estimation of fold change and dispersion for RNA-seq data with DESeq2. *Genome Biol.* 15, 550. doi: 10.1186/s13059-014-0550-8

Lu, Y.-X., Ju, H.-Q., Liu, Z.-X., Chen, D.-L., Wang, Y., Zhao, Q., et al. (2019). Correction: ME1 regulates NADPH homeostasis to promote gastric cancer growth and metastasis. *Cancer Res.* 79, 3789. doi: 10.1158/0008-5472.CAN-19-1611

Mallo, G. V., Espina, M., Smith, A. C., Terebiznik, M. R., Alemán, A., Finlay, B. B., et al. (2008). SopB promotes phosphatidylinositol 3-phosphate formation on Salmonella vacuoles by recruiting Rab5 and Vps34. *J. Cell Biol.* 182, 741–752. doi: 10.1083/jcb.200804131

Manel, N., Kim, F. J., Kinet, S., Taylor, N., Sitbon, M., and Battini, J.-L. (2003). The ubiquitous glucose transporter GLUT-1 is a receptor for HTLV. *Cell* 115, 449–459. doi: 10.1016/S0092-8674(03)00881-X

Mastrogamvraki, N., and Zaravinos, A. (2020). Signatures of co-deregulated genes and their transcriptional regulators in colorectal cancer. *NPJ Syst. Biol. Appl.* 6, 1–16. doi: 10.1038/s41540-020-00144-8

McBride, A. A. (2013). The papillomavirus E2 proteins. *Virology* 445, 57–79. doi: 10.1016/j.virol.2013.06.006

Medda, A., Duca, D., and Chiocca, S. (2021). Human papillomavirus and cellular pathways: hits and targets. *Pathogens* 10. doi: 10.3390/pathogens10030262

Mehl, A. M., Floettmann, J. E., Jones, M., Brennan, P., and Rowe, M. (2001). Characterization of intercellular adhesion molecule-1 regulation by epstein-barr virus-encoded latent membrane protein-1 identifies pathways that cooperate with nuclear factor κB to activate transcription*. *J. Biol. Chem.* 276, 984–992. doi: 10.1074/jbc.M003758200

Meng, Z., Chen, Y., Wu, W., Yan, B., Zhang, L., Chen, H., et al. (2022b). PRRX1 is a novel prognostic biomarker and facilitates tumor progression through epithelial-mesenchymal transition in uveal melanoma. *Front. Immunol.* 13. doi: 10.3389/fimmu.2022.754645

Meng, X., Liu, P., Wu, Y., Liu, X., Huang, Y., Yu, B., et al. (2020). Integrin beta 4 (ITGB4) and its tyrosine-1510 phosphorylation promote pancreatic tumorigenesis and regulate the MEK1-ERK1/2 signaling pathway. *Bosn J. Basic Med. Sci.* 20, 106–116. doi: 10.17305/bjbms.2019.4255

Meng, N.-L., Wang, Y., Wang, H.-L., Zhou, J.-L., and Wang, S. (2022a). Research on the histological features and pathological types of gastric adenocarcinoma with mucinous differentiation. *Front. Med.* 9. doi: 10.3389/fmed.2022.829702

Moreno, C. S. (2020). SOX4: The unappreciated oncogene. *Semin. Cancer Biol.* 67, 57–64. doi: 10.1016/j.semcancer.2019.08.027

Mukherjee, A., Ye, Y., Wiener, H. W., Kuniholm, M. H., Minkoff, H., Michel, K., et al. (2023). Variations in genes encoding human papillomavirus binding receptors and susceptibility to cervical precancer. *Cancer Epidemiol. Biomarkers Prev.* 32, 1190–1197. doi: 10.1158/1055-9965.EPI-23-0300

Münz, C. (2019). Latency and lytic replication in Epstein-Barr virus-associated oncogenesis. *Nat. Rev. Microbiol.* 17, 691–700. doi: 10.1038/s41579-019-0249-7

Nagase, Y., Hiramatsu, K., Funauchi, M., Shiomi, M., Masuda, T., Kakuda, M., et al. (2022). Anti-lipolysis-stimulated lipoprotein receptor monoclonal antibody as a novel therapeutic agent for endometrial cancer. *BMC Cancer* 22, 679. doi: 10.1186/s12885-022-09789-6

Najjar, I., Baran-Marszak, F., Le Clorennec, C., Laguillier, C., Schischmanoff, O., Youlyouz-Marfak, I., et al. (2005). Latent membrane protein 1 regulates STAT1 through NF-kappaB-dependent interferon secretion in Epstein-Barr virus-immortalized B cells. *J. Virol.* 79, 4936–4943. doi: 10.1128/JVI.79.8.4936-4943.2005

Nejmeddine, M., Negi, V. S., Mukherjee, S., Tanaka, Y., Orth, K., Taylor, G. P., et al. (2009). HTLV-1–Tax and ICAM-1 act on T-cell signal pathways to polarize the microtubule-organizing center at the virological synapse. *Blood* 114, 1016–1025. doi: 10.1182/blood-2008-03-136770

Nguyen, N. N. T., Lim, Y.-S., Nguyen, L. P., Tran, S. C., Luong, T. T. D., Nguyen, T. T. T., et al. (2018). Hepatitis C Virus Modulates Solute carrier family 3 member 2 for Viral Propagation. *Sci. Rep.* 8, 15486. doi: 10.1038/s41598-018-33861-6

Nicolle, R., Radvanyi, F., and Elati, M. (2015). CoRegNet: Reconstruction and integrated analysis of co-regulatory networks. *Bioinformatics* 31, 3066–3068. doi: 10.1093/bioinformatics/btv305

Osorio, J. C., Blanco, R., Corvalán, A. H., Muñoz, J. P., Calaf, G. M., and Aguayo, F. (2022a). Epstein-barr virus infection in lung cancer: insights and perspectives. *Pathogens* 11. doi: 10.3390/pathogens11020132

Osorio, J. C., Candia-Escobar, F., Corvalán, A. H., Calaf, G. M., and Aguayo, F. (2022b). High-risk human papillomavirus infection in lung cancer: mechanisms and perspectives. *Biol. (Basel)* 11. doi: 10.3390/biology11121691

Otálora-Otálora, B. A., Florez, M., López-Kleine, L., Canas Arboleda, A., Grajales Urrego, D. M., and Rojas, A. (2019). Joint transcriptomic analysis of lung cancer and other lung diseases. *Front. Genet.* 10. doi: 10.3389/fgene.2019.01260

Otálora-Otálora, B. A., González Prieto, C., Guerrero, L., Bernal-Forigua, C., Montecino, M., Cañas, A., et al. (2022a). Identification of the transcriptional regulatory role of RUNX2 by network analysis in lung cancer cells. *Biomedicines* 10, 1–18. doi: 10.3390/biomedicines10123122

Otálora-Otálora, B. A., López-Kleine, L., and Rojas, A. (2023a). Lung cancer gene regulatory network of transcription factors related to the hallmarks of cancer. *Curr. Issues Mol. Biol.* 45, 434–464. doi: 10.3390/cimb45010029

Otálora-Otálora, B. A., López-Rivera, J. J., Aristizábal-Guzmán, C., Isaza-Ruget, M. A., and Álvarez-Moreno, C. A. (2023b). Host transcriptional regulatory genes and microbiome networks crosstalk through immune receptors establishing normal and tumor multiomics metafirm of the oral-gut-lung axis. *Int. J. Mol. Sci.* 24. doi: 10.3390/ijms242316638

Otálora-Otálora, B. A., Osuna-Garzón, D. A., Carvajal-Parra, M. S., Cañas, A., Montecino, M., López-Kleine, L., et al. (2022b). Identifying general tumor and specific lung cancer biomarkers by transcriptomic analysis. *Biol. (Basel)* 11. doi: 10.3390/biology11071082

Otto, T., Horn, S., Brockmann, M., Eilers, U., Schüttrumpf, L., Popov, N., et al. (2009). Stabilization of N-Myc is a critical function of Aurora A in human neuroblastoma. *Cancer Cell* 15, 67–78. doi: 10.1016/j.ccr.2008.12.005

Ozbun, M. A., and Campos, S. K. (2021). The long and winding road: human papillomavirus entry and subcellular trafficking. *Curr. Opin. Virol.* 50, 76–86. doi: 10.1016/j.coviro.2021.07.010

Pagliuca, A., Gallo, P., De Luca, P., and Lania, L. (2000). Class A helix-loop-helix proteins are positive regulators of several cyclin-dependent kinase inhibitors' promoter activity and negatively affect cell growth. *Cancer Res.* 60, 1376–1382.

Park, H. U., Jeong, J.-H., Chung, J. H., and Brady, J. N. (2004). Human T-cell leukemia virus type 1 Tax interacts with Chk1 and attenuates DNA-damage induced G2 arrest mediated by Chk1. *Oncogene* 23, 4966–4974. doi: 10.1038/sj.onc.1207644

Park, S.-H., Lim, J. S., Lim, S.-Y., Tiwari, I., and Jang, K. L. (2011). Hepatitis C virus Core protein stimulates cell growth by down-regulating p16 expression via DNA methylation. *Cancer Lett.* 310, 61–68. doi: 10.1016/j.canlet.2011.06.012

Peinado, H., Marin, F., Cubillo, E., Stark, H.-J., Fusenig, N., Nieto, M. A., et al. (2004). Snail and E47 repressors of E-cadherin induce distinct invasive and angiogenic properties in *vivo*. *J. Cell Sci.* 117, 2827–2839. doi: 10.1242/jcs.01145

Perez-Moreno, M. A., Locascio, A., Rodrigo, I., Dhondt, G., Portillo, F., Nieto, M. A., et al. (2001). A new role for E12/E47 in the repression of E-cadherin expression and epithelial-mesenchymal transitions. *J. Biol. Chem.* 276, 27424–27431. doi: 10.1074/jbc.M100827200

Prelli Bozzo, C., Nchioua, R., Volcic, M., Koepke, L., Krüger, J., Schütz, D., et al. (2021). IFITM proteins promote SARS-CoV-2 infection and are targets for virus inhibition in *vitro*. *Nat. Commun.* 12, 4584. doi: 10.1038/s41467-021-24817-y

Qi, D., Lu, M., Xu, P., Yao, X., Chen, Y., Gan, L., et al. (2023). Transcription factor ETV4 promotes the development of hepatocellular carcinoma by driving hepatic TNF-α signaling. *Cancer Commun. (Lond)* 43, 1354–1372. doi: 10.1002/cac2.12482

Raj, S., Kesari, K. K., Kumar, A., Rathi, B., Sharma, A., Gupta, P. K., et al. (2022). Molecular mechanism(s) of regulation(s) of c-MET/HGF signaling in head and neck cancer. *Mol. Cancer* 21, 31. doi: 10.1186/s12943-022-01503-1

Rather, T. B., Parveiz, I., Bhat, G. A., Rashid, G., Wani, R. A., Khan, I. Y., et al. (2023). Evaluation of Forkhead BOX M1 (FOXM1) gene expression in colorectal cancer. *Clin. Exp. Med.* 23, 2385–2405. doi: 10.1007/s10238-022-00929-7

Rawla, P., Sunkara, T., and Barsouk, A. (2019). Epidemiology of colorectal cancer: incidence, mortality, survival, and risk factors. *Prz Gastroenterol.* 14, 89–103. doi: 10.5114/pg.2018.81072

Ray, U., Pathoulas, C. L., Thirusangu, P., Purcell, J. W., Kannan, N., and Shridhar, V. (2022). Exploiting LRRC15 as a novel therapeutic target in cancer. *Cancer Res.* 82, 1675–1681. doi: 10.1158/0008-5472.CAN-21-3734

Ray, R. B., and Ray, R. (2001). Hepatitis C virus core protein: intriguing properties and functional relevance. *FEMS Microbiol. Lett.* 202, 149–156. doi: 10.1111/fml.2001.202.issue-2

Richardson, C., Fielding, C., Rowe, M., and Brennan, P. (2003). Epstein-Barr virus regulates STAT1 through latent membrane protein 1. *J. Virol.* 77, 4439–4443. doi: 10.1128/JVI.77.7.4439-4443.2003

Ritchie, M. E., Phipson, B., Wu, D., Hu, Y., Law, C. W., Shi, W., et al. (2015). limma powers differential expression analyses for RNA-sequencing and microarray studies. *Nucleic Acids Res.* 43, e47–e47. doi: 10.1093/nar/gkv007

Romeo, M. M., Ko, B., Kim, J., Brady, R., Heatley, H. C., He, J., et al. (2015). Acetylation of the c-MYC oncoprotein is required for cooperation with the HTLV-1 p30(II) accessory protein and the induction of oncogenic cellular transformation by p30(II)/c-MYC. *Virology* 476, 271–288. doi: 10.1016/j.virol.2014.12.008

Ruan, Y., Chen, L., Xie, D., Luo, T., Xu, Y., Ye, T., et al. (2022). Mechanisms of cell adhesion molecules in endocrine-related cancers: A concise outlook. *Front. Endocrinol.* 13. doi: 10.3389/fendo.2022.865436

Saha, A., Halder, S., Upadhyay, S. K., Lu, J., Kumar, P., Murakami, M., et al. (2011). Epstein-barr virus nuclear antigen 3C facilitates G1-S transition by stabilizing and enhancing the function of cyclin D1. *PloS Pathog.* 7, e1001275. doi: 10.1371/journal.ppat.1001275

Salmani-Javan, E., Jadid, M. F. S., and Zarghami, N. (2024). Recent advances in molecular targeted therapy of lung cancer: Possible application in translation medicine. *Iran J. Basic Med. Sci.* 27, 122–133. doi: 10.22038/IJBMS.2023.72407.15749

Sato, S., Vasaikar, S., Eskaros, A., Kim, Y., Lewis, J. S., Zhang, B., et al. (2019). EPHB2 carried on small extracellular vesicles induces tumor angiogenesis via activation of ephrin reverse signaling. *JCI Insight* 4. doi: 10.1172/jci.insight.132447

Scalise, M., Galluccio, M., Console, L., Pochini, L., and Indiveri, C. (2018). The human SLC7A5 (LAT1): the intriguing histidine/large neutral amino acid transporter and its relevance to human health. *Front. Chem.* 6. doi: 10.3389/fchem.2018.00243

Schaefer, C. J., Kossen, K., Lim, S. R., Lin, J.-H., Pan, L., Bradford, W., et al. (2011). Danoprevir monotherapy decreases inflammatory markers in patients with chronic hepatitis C virus infection. *Antimicrob. Agents Chemother.* 55, 3125–3132. doi: 10.1128/AAC.00131-11

Schuurbiers, O. C. J., Meijer, T. W. H., Kaanders, J. H. A. M., Looijen-Salamon, M. G., de Geus-Oei, L.-F., van der Drift, M. A., et al. (2014). Glucose metabolism in NSCLC is histology-specific and diverges the prognostic potential of 18FDG-PET for adenocarcinoma and squamous cell carcinoma. *J. Thorac. Oncol.* 9, 1485–1493. doi: 10.1097/JTO.0000000000000286

Scott, M. L., Coleman, D. T., Kelly, K. C., Carroll, J. L., Woodby, B., Songock, W. K., et al. (2018). Human papillomavirus type 16 E5-mediated upregulation of Met in human keratinocytes. *Virology* 519, 1–11. doi: 10.1016/j.virol.2018.03.021

Shan, G., Minchao, K., Jizhao, W., Rui, Z., Guangjian, Z., Jin, Z., et al. (2023). Resveratrol improves the cytotoxic effect of CD8 +T cells in the tumor microenvironment by regulating HMMR/Ferroptosis in lung squamous cell carcinoma. *J. Pharm. BioMed. Anal.* 229, 115346. doi: 10.1016/j.jpba.2023.115346

She, Q.-B., Halilovic, E., Ye, Q., Zhen, W., Shirasawa, S., Sasazuki, T., et al. (2010). 4E-BP1 is a key effector of the oncogenic activation of the AKT and ERK signaling pathways that integrates their function in tumors. *Cancer Cell* 18, 39–51. doi: 10.1016/j.ccr.2010.05.023

Sherman, B. T., Hao, M., Qiu, J., Jiao, X., Baseler, M. W., Lane, H. C., et al. (2022). DAVID: a web server for functional enrichment analysis and functional annotation of gene list, (2021 update). *Nucleic Acids Res.* 50, W216–W221. doi: 10.1093/nar/gkac194

Sheu, L. F., Chen, A., Wei, Y. H., Ho, K. C., Cheng, J. Y., Meng, C. L., et al. (1998). Epstein-Barr virus LMP1 modulates the Malignant potential of gastric carcinoma cells involving apoptosis. *Am. J. Pathol.* 152, 63–74.

Shi, Q., Jiang, J., and Luo, G. (2013). Syndecan-1 serves as the major receptor for attachment of hepatitis C virus to the surfaces of hepatocytes. *J. Virol.* 87, 6866–6875. doi: 10.1128/JVI.03475-12

Shi, G., Kenney, A. D., Kudryashova, E., Zani, A., Zhang, L., Lai, K. K., et al. (2021). Opposing activities of IFITM proteins in SARS-CoV-2 infection. *EMBO J.* 40, e106501. doi: 10.15252/embj.2020106501

Shirley, D.-A., Hung, C.-C., and Moonah, S. (2020). "94 - entamoeba histolytica (Amebiasis),". Eds. E. T. Ryan, D. R. Hill, T. Solomon, N. E. Aronson, P. B. T.-H. T. M. T. and I. D. E. *Hunter's tropical medicine and emerging infectious diseases* (Elsevier, London), 699–706. doi: 10.1016/B978-0-323-55512-8.00094-6

Siegel, R. L., Miller, K. D., Wagle, N. S., and Jemal, A. (2023). Cancer statistic. *CA Cancer J. Clin.* 73, 17–48. doi: 10.3322/caac.21763

Smith, A. C., Cirulis, J. T., Casanova, J. E., Scidmore, M. A., and Brumell, J. H. (2005). Interaction of the Salmonella-containing vacuole with the endocytic recycling system. *J. Biol. Chem.* 280, 24634–24641. doi: 10.1074/jbc.M500358200

So, C.-W., Sourisseau, M., Sarwar, S., Evans, M. J., and Randall, G. (2023). Roles of epidermal growth factor receptor, claudin-1 and occludin in multi-step entry of hepatitis C virus into polarized hepatoma spheroids. *PloS Pathog.* 19, e1011887. doi: 10.1371/journal.ppat.1011887

Somiya, M., Liu, Q., Yoshimoto, N., Iijima, M., Tatematsu, K., Nakai, T., et al. (2016). Cellular uptake of hepatitis B virus envelope L particles is independent of sodium taurocholate cotransporting polypeptide, but dependent on heparan sulfate proteoglycan. *Virology* 497, 23–32. doi: 10.1016/j.virol.2016.06.024

Spanò, S., Liu, X., and Galán, J. E. (2011). Proteolytic targeting of Rab29 by an effector protein distinguishes the intracellular compartments of human-adapted and broad-host Salmonella. *Proc. Natl. Acad. Sci. U.S.A.* 108, 18418–18423. doi: 10.1073/pnas.1111959108

Starita, L. M., Machida, Y., Sankaran, S., Elias, J. E., Griffin, K., Schlegel, B. P., et al. (2004). BRCA1-dependent ubiquitination of γ-tubulin regulates centrosome number. *Mol. Cell Biol.* 24, 8457–8466. doi: 10.1128/MCB.24.19.8457-8466.2004

Taguchi, T., Nagano-Fujii, M., Akutsu, M., Kadoya, H., Ohgimoto, S., Ishido, S., et al. (2004). Hepatitis C virus NS5A protein interacts with 2',5'-oligoadenylate synthetase and inhibits antiviral activity of IFN in an IFN sensitivity-determining region-independent manner. *J. Gen. Virol.* 85, 959–969. doi: 10.1099/vir.0.19513-0

Takenaka, R., Okada, H., Kato, J., Makidono, C., Hori, S., Kawahara, Y., et al. (2007). Helicobacter pylori eradication reduced the incidence of gastric cancer, especially of the intestinal type. *Aliment Pharmacol. Ther.* 25, 805–812. doi: 10.1111/j.1365-2036.2007.03268.x

Talamás-Rohana, P., Hernández-Ramirez, V. I., Perez-García, J. N., and Ventura-Juárez, J. (1998). Entamoeba histolytica contains a beta 1 integrin-like molecule similar to fibronectin receptors from eukaryotic cells. *J. Eukaryot Microbiol.* 45, 356–360. doi: 10.1111/j.1550-7408.1998.tb04549.x

Tang, Q., Liu, C., Zhang, S., He, L., Liu, Y., Wang, J., et al. (2023). FOXM1 increases hTERT protein stability and indicates poor prognosis in gastric cancer. *Neoplasia (United States)* 36. doi: 10.1016/j.neo.2022.100863

Tang, Y., Luo, J., Yang, Y., Liu, S., Zheng, H., Zhan, Y., et al. (2022). Overexpression of p-4EBP1 associates with p-eIF4E and predicts poor prognosis for non-small cell lung cancer patients with resection. *PloS One* 17, e0265465. doi: 10.1371/journal.pone.0265465

Tavakolian, S., Goudarzi, H., and Faghihloo, E. (2020). Cyclin-dependent kinases and CDK inhibitors in virus-associated cancers. *Infect. Agent Cancer* 15, 27. doi: 10.1186/s13027-020-00295-7

van Gent, M., Braem, S. G. E., de Jong, A., Delagic, N., Peeters, J. G. C., Boer, I. G. J., et al. (2014). Epstein-Barr virus large tegument protein BPLF1 contributes to innate immune evasion through interference with toll-like receptor signaling. *PloS Pathog.* 10, e1003960. doi: 10.1371/journal.ppat.1003960

Wallis, T. S., and Galyov, E. E. (2000). Molecular basis of Salmonella-induced enteritis. *Mol. Microbiol.* 36, 997–1005. doi: 10.1046/j.1365-2958.2000.01892.x

Wang, Y. (2017). Transcriptional regulatory network analysis for gastric cancer based on mRNA microarray. *Pathol. Oncol. Res.* 23, 785–791. doi: 10.1007/s12253-016-0159-1

Wang, Y., Ding, X., Liu, B., Li, M., Chang, Y., Shen, H., et al. (2020). ETV4 overexpression promotes progression of non–small cell lung cancer by upregulating PXN and MMP1 transcriptionally. *Mol. Carcinog* 59, 73–86. doi: 10.1002/mc.23130

Wang, J.-T., Doong, S.-L., Teng, S.-C., Lee, C.-P., Tsai, C.-H., and Chen, M.-R. (2009). Epstein-Barr virus BGLF4 kinase suppresses the interferon regulatory factor 3 signaling pathway. *J. Virol.* 83, 1856–1869. doi: 10.1128/JVI.01099-08

Wang, R., Gao, Y., and Zhang, H. (2023). ACTN1 interacts with ITGA5 to promote cell proliferation, invasion and epithelial-mesenchymal transformation in head and neck squamous cell carcinoma. *Iran J. Basic Med. Sci.* 26, 200–207. doi: 10.22038/IJBMS.2022.67056.14703

Wang, D., Hao, T., Pan, Y., Qian, X., and Zhou, D. (2015). Increased expression of SOX4 is a biomarker for Malignant status and poor prognosis in patients with non-small cell lung cancer. *Mol. Cell Biochem.* 402, 75–82. doi: 10.1007/s11010-014-2315-9

Wang, Z., Tang, Y., Xie, L., Huang, A., Xue, C., Gu, Z., et al. (2019). The prognostic and clinical value of CD44 in colorectal cancer: A meta-analysis. *Front. Oncol.* 9. doi: 10.3389/fonc.2019.00309

Weidemüller, P., Kholmatov, M., Petsalaki, E., and Zaugg, J. B. (2021). Transcription factors: Bridge between cell signaling and gene regulation. *Proteomics* 21, 1–14. doi: 10.1002/pmic.202000034

Westrich, J. A., Warren, C. J., and Pyeon, D. (2017). Evasion of host immune defenses by human papillomavirus. *Virus Res.* 231, 21–33. doi: 10.1016/j.virusres.2016.11.023

Whiteside, S. T., and Goodbourn, S. (1993). Signal transduction and nuclear targeting: regulation of transcription factor activity by subcellular localisation. *J. Cell Sci.* 104, 949–955. doi: 10.1242/jcs.104.4.949

Wong, M. H., Huelsken, J., Birchmeier, W., and Gordon, J. I. (2002). Selection of multipotent stem cells during morphogenesis of small intestinal crypts of Lieberkuhn is perturbed by stimulation of Lef-1/beta-catenin signaling. *J. Biol. Chem.* 277, 15843–15850. doi: 10.1074/jbc.M200184200

Wu, X., Lin, H., and Li, S. (2019). Prognoses of different pathological subtypes of colorectal cancer at different stages: A population-based retrospective cohort study. *BMC Gastroenterol.* 19, 1–8. doi: 10.1186/s12876-019-1083-0

Xie, L., and Yan, J. (2023). γ-tocotrienol regulates gastric cancer by targeting notch signaling pathway. *Hereditas* 160, 15. doi: 10.1186/s41065-023-00277-w

Xu, J., Chen, T., Liao, L., Chen, T., Li, Q., Xu, J., et al. (2021a). NETO2 promotes esophageal cancer progression by inducing proliferation and metastasis via PI3K/AKT and ERK pathway. *Int. J. Biol. Sci.* 17, 259–270. doi: 10.7150/ijbs.53795

Xu, S., Zhang, T., Cao, Z., Zhong, W., Zhang, C., Li, H., et al. (2021b). Integrin-α9β1 as a novel therapeutic target for refractory diseases: recent progress and insights. *Front. Immunol.* 12. doi: 10.3389/fimmu.2021.638400

Xu, L., Zhou, R., Yuan, L., Wang, S., Li, X., Ma, H., et al. (2017). IGF1/IGF1R/STAT3 signaling-inducible IFITM2 promotes gastric cancer growth and metastasis. *Cancer Lett.* 393, 76–85. doi: 10.1016/j.canlet.2017.02.014

Yang, D., Hendifar, A., Lenz, C., Togawa, K., Lenz, F., Lurje, G., et al. (2011). Survival of metastatic gastric cancer: Significance of age, sex and race/ethnicity. *J. Gastrointest Oncol.* 2, 77–84. doi: 10.3978/j.issn.2078-6891.2010.025

Yeh, M.-H., Tzeng, Y.-J., Fu, T.-Y., You, J.-J., Chang, H.-T., Ger, L.-P., et al. (2018). Extracellular matrix–receptor interaction signaling genes associated with inferior breast cancer survival. *Anticancer Res.* 38, 4593 LP–4605. doi: 10.21873/anticanres.12764

Yen, F. T., Roitel, O., Bonnard, L., Notet, V., Pratte, D., Stenger, C., et al. (2008). Lipolysis stimulated lipoprotein receptor: A NOVEL MOLECULAR LINK BETWEEN HYPERLIPIDEMIA, WEIGHT GAIN, AND ATHEROSCLEROSIS IN MICE *. *J. Biol. Chem.* 283, 25650–25659. doi: 10.1074/jbc.M801027200

Zhan, L., Wu, W., Yang, Q., Shen, H., Liu, L., and Kang, R. (2023). Transcription factor TEAD4 facilitates glycolysis and proliferation of gastric cancer cells by activating PKMYT1. *Mol. Cell Probes* 72, 101932. doi: 10.1016/j.mcp.2023.101932

Zhang, Q.-Y., Chen, X.-Q., Liu, X.-C., and Wu, D.-M. (2020). PKMYT1 promotes gastric cancer cell proliferation and apoptosis resistance. *Onco Targets Ther.* 13, 7747–7757. doi: 10.2147/OTT.S255746

Zhang, J., Feng, H., Xu, S., and Feng, P. (2016). Hijacking GPCRs by viral pathogens and tumor. *Biochem. Pharmacol.* 114, 69–81. doi: 10.1016/j.bcp.2016.03.021

Zhang, S., Li, M., Ji, H., and Fang, Z. (2018). Landscape of transcriptional deregulation in lung cancer. *BMC Genomics* 19. doi: 10.1186/s12864-018-4828-1

Zhang, M., and Ma, C. (2021). LSR promotes cell proliferation and invasion in lung cancer. *Comput. Math Methods Med.* 2021, 6651907. doi: 10.1155/2021/6651907

Zhang, Y., Vaccarella, S., Morgan, E., Li, M., Etxeberria, J., Chokunonga, E., et al. (2023). Global variations in lung cancer incidence by histological subtype in 2020: a population-based study. *Lancet Oncol.* 24, 1206–1218. doi: 10.1016/S1470-2045(23)00444-8

Zhang, B., Xie, Z., and Li, B. (2019). The clinicopathologic impacts and prognostic significance of GLUT1 expression in patients with lung cancer: A meta-analysis. *Gene* 689, 76–83. doi: 10.1016/j.gene.2018.12.006

Zhang, J., Zhang, J., Cui, X., Yang, Y., Li, M., Qu, J., et al. (2015). *FoxM1: a novel tumor biomarker of lung cancer*. Available online at: www.ijcem.com/.

Zhao, H., Ming, T., Tang, S., Ren, S., Yang, H., Liu, M., et al. (2022). Wnt signaling in colorectal cancer: pathogenic role and therapeutic target. *Mol. Cancer* 21, 144. doi: 10.1186/s12943-022-01616-7

Zhao, X., Sehgal, M., Hou, Z., Cheng, J., Shu, S., Wu, S., et al. (2018). Identification of residues controlling restriction versus enhancing activities of IFITM proteins on entry of human coronaviruses. *J. Virol.* 92. doi: 10.1128/JVI.01535-17

Zhao, L., Wang, L., Zhang, C., Liu, Z., Piao, Y., Yan, J., et al. (2019). E6-induced selective translation of WNT4 and JIP2 promotes the progression of cervical cancer via a noncanonical WNT signaling pathway. *Signal Transduct Target Ther.* 4, 32. doi: 10.1038/s41392-019-0060-y

Zhao, X., Wu, S., and Jing, J. (2021). Identifying diagnostic and prognostic biomarkers and candidate therapeutic drugs of gastric cancer based on transcriptomics and single-cell sequencing. *Pathol. Oncol. Res.* 27. doi: 10.3389/pore.2021.1609955

Zhou, X. H., Chu, X. Y., Xue, G., Xiong, J. H., and Zhang, H. Y. (2019). Identifying cancer prognostic modules by module network analysis. *BMC Bioinf.* 20. doi: 10.1186/s12859-019-2674-z

Zhu, N., Xu, X., Wang, Y., Zeng, M.-S., and Yuan, Y. (2021). EBV latent membrane proteins promote hybrid epithelial-mesenchymal and extreme mesenchymal states of nasopharyngeal carcinoma cells for tumorigenicity. *PloS Pathog.* 17, e1009873. doi: 10.1371/journal.ppat.1009873

frontiers | Frontiers in Cellular and Infection Microbiology

TYPE Original Research
PUBLISHED 02 September 2024
DOI 10.3389/fcimb.2024.1417946

OPEN ACCESS

EDITED BY
Maurizio Sanguinetti,
Catholic University of the Sacred Heart, Italy

REVIEWED BY
Abhiram Maddi,
Medical University of South Carolina, United States
Dominic Augustine,
M S Ramaiah University of Applied Sciences, India

*CORRESPONDENCE
Gary P. Moran
gmoran@tcd.ie

RECEIVED 15 April 2024
ACCEPTED 13 August 2024
PUBLISHED 02 September 2024

CITATION
Selvaraj A, McManus G, Healy CM and Moran GP (2024) *Fusobacterium nucleatum* induces invasive growth and angiogenic responses in malignant oral keratinocytes that are cell line- and bacterial strain-specific. *Front. Cell. Infect. Microbiol.* 14:1417946. doi: 10.3389/fcimb.2024.1417946

Fusobacterium nucleatum induces invasive growth and angiogenic responses in malignant oral keratinocytes that are cell line- and bacterial strain-specific

Ajith Selvaraj[1], Gavin McManus[2], Claire M. Healy[3] and Gary P. Moran[1]*

[1]Division of Oral Biosciences, Dublin Dental University Hospital and School of Dental Science, Trinity College Dublin, Dublin, Ireland, [2]School of Biochemistry and Immunology, Trinity Biomedical Sciences Institute, Trinity College Dublin, Dublin, Ireland, [3]Division of Oral and Maxillofacial Surgery, Oral Medicine and Oral Pathology, Dublin Dental University Hospital and School of Dental Science, Trinity College Dublin, Dublin, Ireland

Fusobacterium nucleatum is an anaerobic commensal of the oral cavity recently reported to be associated with cancers of the gastrointestinal tract and oral squamous cell carcinoma (OSCC). In this study, we investigate the impact on oral keratinocytes of infection with a genetically diverse set of strains of *F. nucleatum* subsp. *polymorphum* recovered from patients with oral dysplasia (n=6). We employed H357 oral keratinocytes derived from a stage 1 OSCC and H376 cells derived from a stage 3 OSCC. Adhesion phenotypes were strain specific, with 3/6 clinical isolates examined exhibiting higher adherence to the stage 3 H376 cell line. Conversely, intracellular invasion was greatest in the H357 cells and was associated with specific transcriptional responses including autophagy and keratinization. Infection of both H357 and H376 cell lines induced transcriptional and cytokine responses linked to cancer cell migration and angiogenesis. *F. nucleatum* infection induced greater levels of MMP9 secretion in the H376 cell line which was associated with enhanced motility and invasion phenotypes. Additionally, the degree of *F. nucleatum* induced invasive growth by H376 cells varied between different clinical isolates of *F. nucleatum* subsp. *polymorphum*. Blockage of CCL5 signalling using the inhibitor metCCL5 resulted in reduced keratinocyte invasion. *F. nucleatum* infection also induced expression of the pro-angiogenic chemokine MCP-1 and the angiogenic growth factor VEGF-A resulting in increased capillary-like tube formation in HUVEC cells, most significantly in H376 cells. Treatment of HUVEC cells with resveratrol, a VEGF-A signalling inhibitor, significantly attenuated *F. nucleatum* induced tube formation. Our data indicate that the outcomes of *F. nucleatum*-oral cell interactions can vary greatly depending on the bacterial genotype and the malignant phenotype of the host cell.

KEYWORDS

***Fusobacterium nucleatum*, oral cancer, invasion, angiogenesis, inflammation**

Introduction

Fusobacterium species are Gram-negative obligate anaerobes belonging to the phylum Fusobacteria (Han, 2015; Brennan and Garrett, 2019). There are four subspecies of *F. nucleatum*, namely *animalis, nucleatum, polymorphum* and *vincentii*, each of which have been shown to exhibit different adhesive and biofilm forming capabilities (Gharbia et al., 1990; Muchova et al., 2022). Within the last decade, *F. nucleatum* has come under increased scrutiny due to its association with cancers of the gastrointestinal tract, particularly colorectal carcinoma (CRC) (Castellarin et al., 2012; Kostic et al., 2012). The presence of *F. nucleatum* within CRC tissue has been associated with increased tumor staging, chemoresistance and poor patient outcomes (Mima et al., 2016; Yu et al., 2017; Kunzmann et al., 2019). Recent research has suggested that *F. nucleatum* promotes a proinflammatory microenvironment in CRC that promotes cell proliferation, cell migration and metastases (Rubinstein et al., 2013, 2019; Coppenhagen-Glazer et al., 2015; Gur et al., 2015; Umana et al., 2019). In CRC, *F. nucleatum* has been proposed to modulate cellular properties due to the interaction of two well characterised adhesins, namely Fap2 and FadA with host cells (Gur et al., 2015, 2019; Bullman et al., 2017; Casasanta et al., 2020; Niño et al., 2022). The Fap2 adhesin targets D-galactose-β(1–3)-*N*-acetyl-D-galactosamine (Gal-GalNAc) residues which are upregulated in CRC tissues and in breast tumors and this enhanced presentation of Gal-GalNAc has been suggested as the reason for enrichment of *F. nucleatum* in these tumors (Abed et al., 2016; Parhi et al., 2020). Deletion of Fap2 in *F. nucleatum* has shown that this protein is required for IL-8 and CXCL1 induction which are involved in host cell migration phenotypes (Casasanta et al., 2020). Additionally, the FadA adhesin has been demonstrated to bind to E-cadherin on host epithelial cells and has been reported to activate β-catenin signalling and activation of pro-oncogenic and inflammatory responses (Rubinstein et al., 2013, 2019).

The role of *F. nucleatum* in the progression of oral squamous cell carcinoma is less well defined. *F. nucleatum* has been identified as a major component of the intratumoral microbiome in OSCC where it has been shown to be metabolically active (Yost et al., 2018). Using FISH, Galeano Niño et al. showed that *F. nucleatum* can be found in localised micro-niches within OSCC tissues and that these areas exhibited localised immunosuppressive effects including increased expression of ARG1 (arginase 1) the T-cell-inhibitory receptor PD-1 and decreased expression of wild-type p53 (Niño et al., 2022). Clinically, it has been reported that the abundance of *Fusobacterium* present in the mouth increases with tumor staging, from 4.35% in stage 1 OSCC to 7.92% in stage 4 OSCC (Yang et al., 2018).

Infection of oral malignant cell lines with *F. nucleatum in vitro* was shown to induce epithelial-mesenchymal transition (EMT), oncogene expression and promote invasive growth (Harrandah et al., 2020; Shao et al., 2021). *F. nucleatum* has also been shown to accelerate carcinogenesis in chemically induced OSCC murine models (Gallimidi et al., 2015; Harrandah et al., 2020). We have recently shown that oral mucosal surfaces, including dysplastic tissue and OSCC are primarily colonised by *F. nucleatum* subsp. *polymorphum* and that these isolates exhibit a high degree of genetic variation, including a high degree of variability in the copy number of fadA- and fap2-related adhesin encoding genes (Crowley et al., 2024). In this study, we attempt to determine if these clinically relevant and genetically diverse strains of *F. nucleatum* subsp. *polymorphum* have different interactions with host cells. In addition, we also examine the impact of host cell phenotype on this interaction using two different OSCC cell lines, namely a stage 1 tumor derived cell line (H357) and a stage 3 derived cell line (H376). Our data indicate that the outcomes of *F. nucleatum*-host cell interactions can vary greatly depending on the bacterial genotype and the nature of the host cell.

Materials and methods

Microbial growth conditions

F. nucleatum was routinely cultured on BHI agar supplemented with 5% defibrinated horse blood (TCS Biosciences Ltd, UK). Cultures were maintained in anaerobic jars supplemented with AnaeroGen 3.5L sachets (Thermo Fisher Scientific, UK) in 37˚C incubators. For isolation of *F. nucleatum* from clinical swab samples, swabs were cultured on Fastidious Anaerobe Agar (FAA) (Neogen, Lansing, MI, USA), supplemented with 5% (vol/vol) defibrinated horse blood and the antibiotics josamycin (3 μg/mL), vancomycin (4 μg/mL) and norfloxacin (1 μg/mL) [JVN medium; (Brazier et al., 1991)]. For liquid culture, *F. nucleatum* was grown in BHI broth (Sigma-Aldrich, St. Louis, USA) supplemented with 2.5 g yeast extract, 0.3 g L-Cysteine, 5 μg/ml haemin and 1 μg/ml Menadione (Sigma-Aldrich). Overnight broth cultures of *F. nucleatum* were grown to exponential phase, centrifuged (4000 rpm for 5 minutes) and washed three times with sterile PBS before standardising the bacterial suspension at OD_{600} of 0.7 which was diluted in PBS to yield a suspension of $1x10^7$ cfu/ml.

The type strain *Fusobacterium nucleatum* subsp. *polymorphum* NCTC10562 (equivalent to ATCC 10953) was obtained from the National Collection of Type Cultures (NCTC, Porton Down, UK). All clinical isolates of *F. nucleatum* used in this study were obtained from mucosal swabs recovered with ethical approval granted by the Joint Hospitals Research Ethics Committee (JREC; reference no. 2017-11-Chairman's Actions-7). *F. nucleatum* was recovered from patients with oral epithelial dysplasia attending the Dublin Dental University Hospital by gentle swabbing of the affected mucosal location (see Table 1) followed by anaerobic culture on JVN medium as described (Crowley et al., 2024). Isolates used in the analysis (Table 1) included strains from mild (60A2), moderate (40A2) and severe dysplasia (41A, 43A3) as well as isolates recovered from contralateral healthy mucosa in the same patients (41B2, 43B1). These strains were subjected to whole genome sequencing (Crowley et al., 2024) and the estimated copy numbers of the major *F. nucleatum* adhesins encoded in each strain are detailed in Table 1. *Escherichia coli* strain DH5α was obtained from the Dublin Dental University Hospital microbiological strain collection.

10.3389/fcimb.2024.1417946

TABLE 1 Details of *F. nucleatum* subsp. *polymorphum* isolates used in this study including copy number of major adhesins from whole genome sequences.

Strain	Patient ID	Nationality	Location	Disease*	Adhesin Copy Number**							
					Fap2	CmpA	RadD	Aim1	FN868	FN1003	FadA1	FadA2	FadA3
NCTC10562	NA	USA	Inflamed gingiva	Inflamed gingiva	2	0	1	2	0	0	1	1	2
40A2	40	Irish	Ventral Tongue	OLK (Moderate dysplasia)	1	0	0	0	0	0	1	0	3
41A	41	Irish	Ventral Tongue	OLK (Severe dysplasia)	2	1	0	0	0	0	1	0	2
41B2	41	Irish	Lateral Border Tongue	Healthy mucosa	2	1	0	0	0	0	1	0	2
43A3	43	Irish	Floor of Mouth	OLK (Severe dysplasia)	2	1	0	0	0	1	1	0	1
43B1	43	Irish	Lateral Border Tongue	Healthy mucosa	2	1	0	0	0	1	1	0	1
60A2	60	Irish	Floor of Mouth	OLK (Mild Dysplasia)	2	0	0	0	0	0	1	0	4

*OLK=Oral Leukoplakia

**Estimated number of putative adhesin encoding genes in each genome identified by whole genome sequencing. Green = no copies of the gene; Orange = 1 to 4 copies as indicated. Data from Crowley et al. (Crowley et al., 2024).

Cell lines and cell culture

Two malignant oral keratinocyte cell lines were used in this study; H357 cells originated from a SCC of the tongue (stage 1) and H376 cells originated from a SCC of the floor of mouth (stage 3) (Prime et al., 2005). Both malignant cell lines were a gift of Dr. Simon Whawell (Dental School, Plymouth, UK) and were grown and maintained in 75 cm^2 tissue culture flasks with vented caps (Corning, NY, USA) in Keratinocyte Growth Media (KGM) consisting of Dulbecco's Modified Eagle Medium (DMEM) containing 2 mM L-glutamine (Gibco, Thermo Fisher Scientific, UK), 10% foetal bovine serum (Thermo Fisher Scientific), 2.6 g/l F-12 Ham nutrient mixture (Sigma-Aldrich), 0.5 µg/ml hydrocortisone (Sigma Aldrich), 10 ng/ml cholera toxin (Thermo Fisher Scientific), 5 µg/ml insulin (Roche Life Sciences, Switzerland), 10 ng/ml epidermal growth factor (R&D Systems, MN, USA), 25 ng/ml adenine, 200 IU/ml penicillin and 200 µg/ml streptomycin (Sigma-Aldrich). Media was replaced every third day and cells were harvested every 5-6 days after reaching 80% confluence and sub-cultured in fresh sterile tissue culture flasks.

TERT-1/OKF6 telomerase immortalized cells (Dickson et al., 2000) were a gift from Dr Antonio Amelio (Department of Oral and Craniofacial health Science, University of North Carolina at Chapel Hill, USA). TERT-1/OKF6 cells (Dickson et al., 2000) were grown using keratinocyte serum free media (SFM) including 5 ng/ml epidermal growth factor and 50 µg/ml bovine pituitary extract (Gibco Thermo Fisher Scientific, UK) supplemented with 200 IU/ml penicillin, 200 µg/ml streptomycin and 0.3 mM $CaCl_2$ (Sigma Aldrich). HUVEC cells were cultured in MCDB medium (Thermo Fisher Scientific) supplemented with 8 mM L-glutamine (Thermo Fisher Scientific), 1 mg/ml hydrocortisone (Thermo Fisher Scientific), 10 µg/ml epidermal growth factor (R&D Systems), 200 IU/ml penicillin, 200 µg/ml streptomycin (Sigma Aldrich) and 15% heat inactivated foetal calf serum (Thermo Fisher Scientific).

Cell culture supernatants recovered following *F. nucleatum* infection (MOI 10:1 in DMEM unless stated otherwise) are referred to henceforth as conditioned media (CM) and were used in ELISA and transwell invasion assays. ELISA assays for CCL5/RANTES and CCL2/MCP-1 were performed using Quantikine sandwich ELISA kits (R&D Systems) according to the manufacturer's instructions. Multiplex analyte assays were performed by Eve Technologies Ltd. (AB, Canada) using the Human Cytokine/Chemokine Discovery Assay (HD48A) and the Human MMP and TIMP 13-Plex Discovery Assay (HMMP/TIMP-C,O). Cytokine assays were performed with a minimum of 3 biological replicates.

Fluorescent staining

Coverslips coated with epithelial cells were fixed with 3.7% paraformaldehyde, then washed 3 times in 1 ml PBS for 3 minutes. Cells were then permeabilized in 1 ml 0.1% triton X100 buffer for 5 minutes then washed 3 times in 1 ml PBS for 3 minutes. The cells were then treated with a primary anti-E-cadherin antibody (polyclonal goat IgG) followed by a secondary antibody (donkey anti-goat Ig). The cells were then treated with DAPI to stain the nuclei and mounted on glass slides using Mowiol (Sigma-Aldrich)

and images were captured using a Leica SP8 Scanning Confocal microscope. To detect the presence of Gal-GalNAc residues on cell surfaces, cells were fixed using 3.7% paraformaldehyde, washed with PBS and incubated with 50 µl of FITC-labelled peanut agglutinin (PNA, Sigma-Aldrich) at a concentration of 100 µg/ml for 30 min and mounted on glass slides using Mowiol (Sigma-Aldrich).

Bacterial adhesion and invasion assays

For adhesion assays, H357 and H376 cells were grown in 6-well plates to 80% confluency (~1 x 10^6 cells). Cells were infected with *F. nucleatum* subsp. *polymorphum* (MOI 10:1) in the absence of antibiotics. The plate was spun at 800 x g for five minutes and incubated with 5% CO_2 at 37˚C for two hours. The infected cells were then washed three times using PBS to remove non-adherent bacteria and then lysed using sterile water. The cell lysate was cultured anaerobically for 4-5 days when bacterial CFUs were counted. Adhesion was determined the number of CFUs recovered from lysates expressed as a percentage of total CFUs recovered from the inoculum. To examine invasion, H357 and H376 cells (5x10^4) were seeded in 8-well µ-slides (Ibidi, Munich, Germany) to obtain a confluency of 60-70%. *F. nucleatum* suspensions were added (MOI 10:1) for four hours under controlled conditions of 5% CO_2 and 37˚C. The cells were then treated with 1 mg/ml Hoescht stain, 5 µl of 1 mg/ml propidium iodide (PI) to stain the bacteria and 1 µl of 1 mg/ml fluorescein to stain the extracellular space. Slides were examined using a Leica SP8 Scanning Confocal microscope. 3-D images of epithelial cell invasion were created and the surface area of intracellular PI stained bacteria was quantified in at least 3 fields of view using the Oxford Bitplane Imaris Software (version 9.2.1). Invasion was expressed as μm^2 of bacteria per cell. To compare invasion levels between cell lines, data were normalised for differences in typical cell size. We quantified the level of intracellular bacteria in at least three independent infection experiments for each strain in H357 and H376 cells.

Scratch wound assay

Confluent layers of epithelial cells were grown in 6-well plates (Greiner Bio-One GmbH, Austria) and a clear linear scratch was produced in the centre of the well using a sterile micropipette tip. The cells were then infected with *F. nucleatum* subsp. *polymorphum* (MOI 10:1) and incubated in a 37˚C with 5% CO_2 for 24 hours. The wound healing was calculated measuring the width of the wound at time 0 and time 24 h using a Zoe fluorescent cell imager (BioRad, CA, USA). Data were recorded from three biological replicate experiments.

Trans-well cell invasion assay

ECM gel (Sigma-Aldrich) was diluted to a final concentration of 1 mg/ml and stored at -20˚C and thawed overnight at 4˚C prior to use. Millicell cell culture inserts (8.0 µm pore, 12 mm well diameter; Millipore, Sigma-Aldrich) were placed in 24-well plates (Greiner Bio-One GmbH, Austria) and chilled to 4˚C before 40 µl of ECM gel was added into the upper compartment. The plate was immediately placed in a 37˚C incubator with circulating 5% CO_2 for 2-3 hours for the ECM gel to set. Conditioned media (400 µl) obtained from 24 h *F. nucleatum* infections of epithelial cells were added to the wells, ensuring contact with the base of the inserts. Epithelial cells (1 x 10^5) in 200 µl serum free DMEM were added to the upper compartment of the inserts and incubated at 37˚C with 5% CO_2 for 48 h. The inserts were removed and the insert membrane was fixed with 3.7% formalin for 10 minutes, followed by staining with 1% crystal violet in 2% ethanol for 20 minutes. The cells were washed thoroughly to remove excess stain and successfully migrated cells were counted using a light microscope. All experiments were performed with three biological replicates.

HUVEC tube formation assay

Tube formation assays were carried out as described by Fromm et al (Fromm et al., 2019). HUVEC cell culture medium was used to prepare bacterial suspensions for infections of H357 and H376 cells (MOI 10:1) and after 24 h this conditioned medium (CM) was recovered. Matrigel matrix (Corning, USA) was defrosted just before the commencement of the assay and chilled on ice. 50 µl of Matrigel was pipetted into each of the experimental wells of the 96-wells plate and incubated at 37˚C and 5% CO2 for 30 min to solidify the gel matrix. Once set, 8 x 10^4 HUVEC cells in 80 µl were added to each well along with 120 µl CM. Positive control wells contained 50 ng/ml recombinant human VEGF-A (rVEGF-A; R&D Systems) in HUVEC cell culture media. Experiments were incubated at 37˚C and 5% CO2 for 12 hours to promote tube formation. Tube formation was quantified at 200x magnification by counting the number of capillary-like branches formed. Capillary counts from three fields per well were considered and an average tube formation of the three fields was reported.

RNA sequencing

H357 and H376 cells were infected with *F. nucleatum* 23726 (MOI 10:1) for 3 h and then RNA was extracted using the RNeasy minikit (Qiagen). Strand-specific, polyA mRNA libraries were sequenced using the Illumina NovaSeq 6000, generating paired end 150 bp reads, by Novogene (Cambridge, UK). Samples were sequenced in triplicate with a minimum of 45 m reads (>6.0 Gb data) per sample with Q30 >90%. At least 94% of reads mapped to the human genome (*Homo sapiens* GRCh38/hg38). Biological replicate samples exhibited Pearson correlation R^2 values >0.95. DESeq2 was used for analysis of differential expression between infected and uninfected samples (3 biological replicates each) and these gene sets were subjected to Gene Ontology (GO) enrichment analysis to identify processes induced or repressed by *F. nucleatum* infection (Love et al., 2014).

Results

Phenotype of malignant oral cells

We wished to examine the interaction of *F. nucleatum* with two malignant oral keratinocyte cell lines, H357 and H376 (Connolly et al., 2016). We first examined the phenotypes of these cells, initially characterising expression of the cell adhesion molecule E-cadherin. We included the telomerase immortalised oral cell line TERT-1/OKF6 as a control for E-cadherin expression and as expected, these cells stained positively for E-cadherin (Figure 1). H357 cells, which originated from a stage 1 tumor, also exhibited E-cadherin expression at cell-cell junctions whereas the H376 cells, originating from a stage 3 tumor, were negative (Figure 1). Conversely, the E-cadherin negative H376 cells stained extensively with peanut agglutinin lectin, recognising Gal-GalNAc residues, whereas the E-cadherin positive H357 cells and TERT-1/OKF6 cells exhibited weaker expression of Gal-GalNAc (Figure 1). We next examined whether *F. nucleatum* exhibited adhesion to these cell lines using the type strain *F. nucleatum* subsp. *polymorphum* NCTC10562 (equivalent to ATCC10953). This strain exhibited significantly greater adhesion to the H357 cells (~25% adhesion) compared to the H376 cells (~11% adhesion) and the OKF6 cell line (Figure 1B).

Adhesion to oral keratinocytes

We have previously shown that *F. nucleatum* subsp. *polymorphum* is the most frequently cultured subspecies of *F. nucleatum* recovered from oral mucosal surfaces (both normal and potentially malignant oral leukoplakia [OLK]) (Crowley et al., 2024). In the current study, we wished to determine if adhesion of *F. nucleatum* subsp. *polymorphum* varied with bacterial strain and keratinocyte phenotype. For this, we examined adhesion to H357 and H376 cells by a panel of *F. nucleatum* subsp. *polymorphum* isolates recovered from OLK or normal mucosa (Table 1). As reported by Crowley et al. (Crowley et al., 2024) genome sequencing of these isolates revealed variation in copy number of encoded FadA-like and Type V autotransporter adhesins (Table 1). As noted in Figure 1, the type strain NCTC10562 exhibited greater adherence to the H357 cells relative to H376 cells. Two different patterns of adhesion were observed in the clinical strains; 40A2, 41A and 41B2 exhibited similar adhesion to both cell lines, whereas isolates 43A3, 43B1 and 60A2 exhibited greater adhesion to the stage 3 tumor-derived H376 cells (Figure 2A). Comparisons between the isolates showed that the adhesion of NCTC10562 to stage 1 tumor-derived H357 cells was greater than any of the clinical isolates tested (Figure 2B) whereas its adhesion to the H376 cells was significantly lower compared to isolates 43A3, 43B1 and 60A2 (Figure 2C).

In order to determine if adhesion involved lectin interactions with galactose residues on oral keratinocytes, we pre-treated the bacterial strains with 60 mM galactose for 30 minutes before performing the assays. We found that 60 mM galactose pre-treatment significantly reduced adhesion of NCTC10562 to both cell lines (Figures 2D, E). We also examined if lectin interactions were involved in the high level adhesion exhibited by strain 43A3 to the H376 cell line and found that adhesion of 43A3 was very significantly reduced by galactose (Figure 2E).

Invasion of oral keratinocytes

In order to determine if *F. nucleatum* subsp. *polymorphum* could invade these cell lines, we carried out confocal microscopy. Staining of *F. nucleatum* subsp. *polymorphum* with propidium iodide (PI) clearly showed adhesion to and penetration of the plasma membrane by Fusobacteria (Figure 3A) and also showed the presence bacteria in the intracellular compartment (Figure 3B), which was confirmed in sagittal sections of infected cells (Figure 3C) and z-stacked images (Figure 3D). Quantification of intracellular bacterial fluorescence

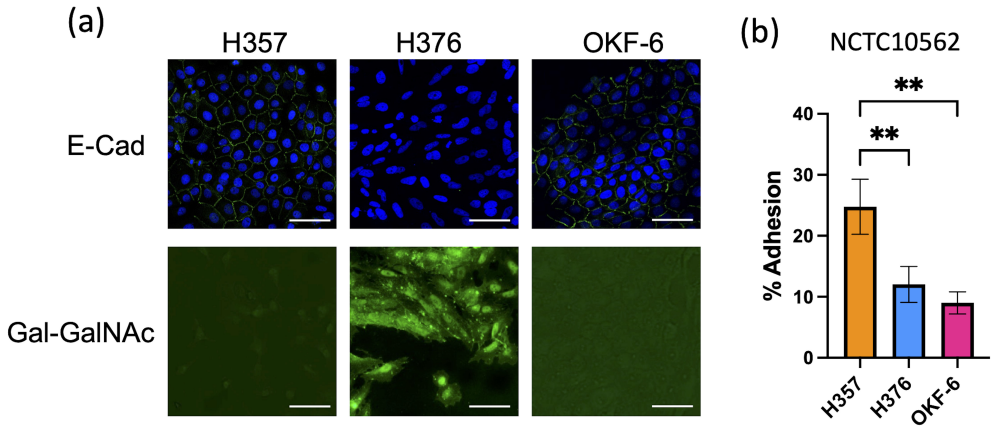

FIGURE 1
Characterisation of oral keratinocyte cell lines. **(A)** Top row shows immuno-staining of H357, H376 and TERT-1/OKF6 cells for E-cadherin expression using anti-E-cadherin antibody (staining green fluorescent junctions) and DAPI stained nuclei in blue. Bottom row shows staining of H357, H376 and TERT-1/OKF6 cells with FITC labelled peanut agglutinin. The scale bar represents 75 μm in length. **(B)** Adhesion of *F. nucleatum* subsp *polymorphum* strain NCTC10562 to H357, H376 and TERT-1/OKF6 cells (** = ANOVA p <0.001).

10.3389/fcimb.2024.1417946

(a)

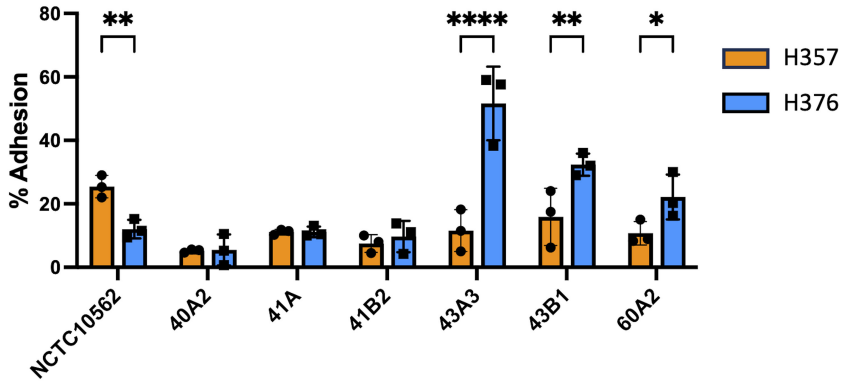

(b)

H357 Cells	NCTC 10562	40A2	41A	41B2	43A3	43B1	60A2
Mean adhesion (%)	25.4	5.2	11.1	7.5	11.5	15.9	10.7
Significantly different from NCTC10562	-	***	*	**	*	NS	*
Adjusted *p* value	-	0.007	0.014	0.002	0.018	0.14	0.012

(c)

H376 Cells	NCTC 10562	40A2	41A	41B2	43A3	43B1	60A2
Mean adhesion (%)	12.0	5.4	11.2	9.7	51.6	32.3	22.2
Significantly different from NCTC10562	-	NS	NS	NS	****	***	*
Adjusted *p* value	-	0.19	0.859	0.63	<0.0001	0.0007	0.05

(d)

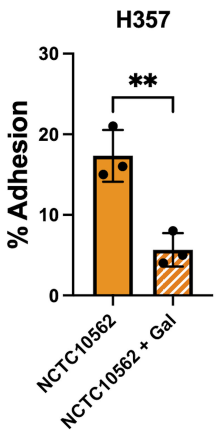

(e)

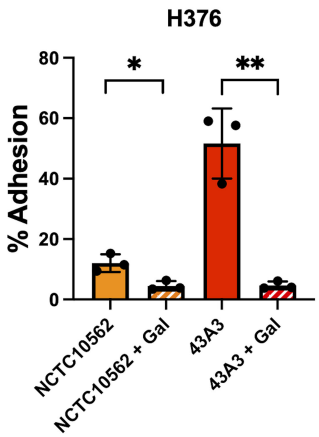

FIGURE 2
Adhesion of *F. nucleatum* subsp. *polymorphum* clinical strains to oral keratinocytes. **(A)** Adhesion of *F. nucleatum* subsp. *polymorphum* strains to E-cadherin positive H357 and E-cadherin negative H376 cells. Significant differences between cell lines indicate by asterisks (adjusted *p*= *<0.05, **<0.01, *** < 0.001, **** < 0.0001). **(B, C)** Comparisons of adhesion of NCTC10562 and the indicated clinical isolates of *F. nucleatum* subsp. *polymorphum* to **(B)** H357 and **(C)** H376 cells using ANOVA with Dunnett's multiple comparison test. **(D)** Impact of galactose (60 mM) on the adhesion of NCTC10562 to H357 cells (t-test *p*= **<0.01). **(E)** Impact of galactose (60 mM) on the adhesion of strains NCTC10562 and 43A3 to H376 cells (t-test *p*= *<0.05, **<0.01).

facilitated measurement of the surface area of bacteria per cell (μm^2/cell). With the exception of strain 43A3, all *F. nucleatum* isolates examined exhibited significantly greater invasion of H357 cells compared to H376 cells (Figure 3E). Some variation was observed in the ability of strains to invade H357 cells, with strain 41B2 exhibiting significantly greater invasion than NCTC10562, and strains 40A2 and 43A3 exhibiting significantly weaker invasion (Supplementary Figure S1). Similarly strain variation was observed in relation to invasion of H376 cells with strains 41A and 41B2 both showing significantly greater invasion than NCTC10562 (Supplementary Figure S1).

We also investigated if invasion was dependent on lectin interactions with galactose residues on oral keratinocytes. We

10.3389/fcimb.2024.1417946

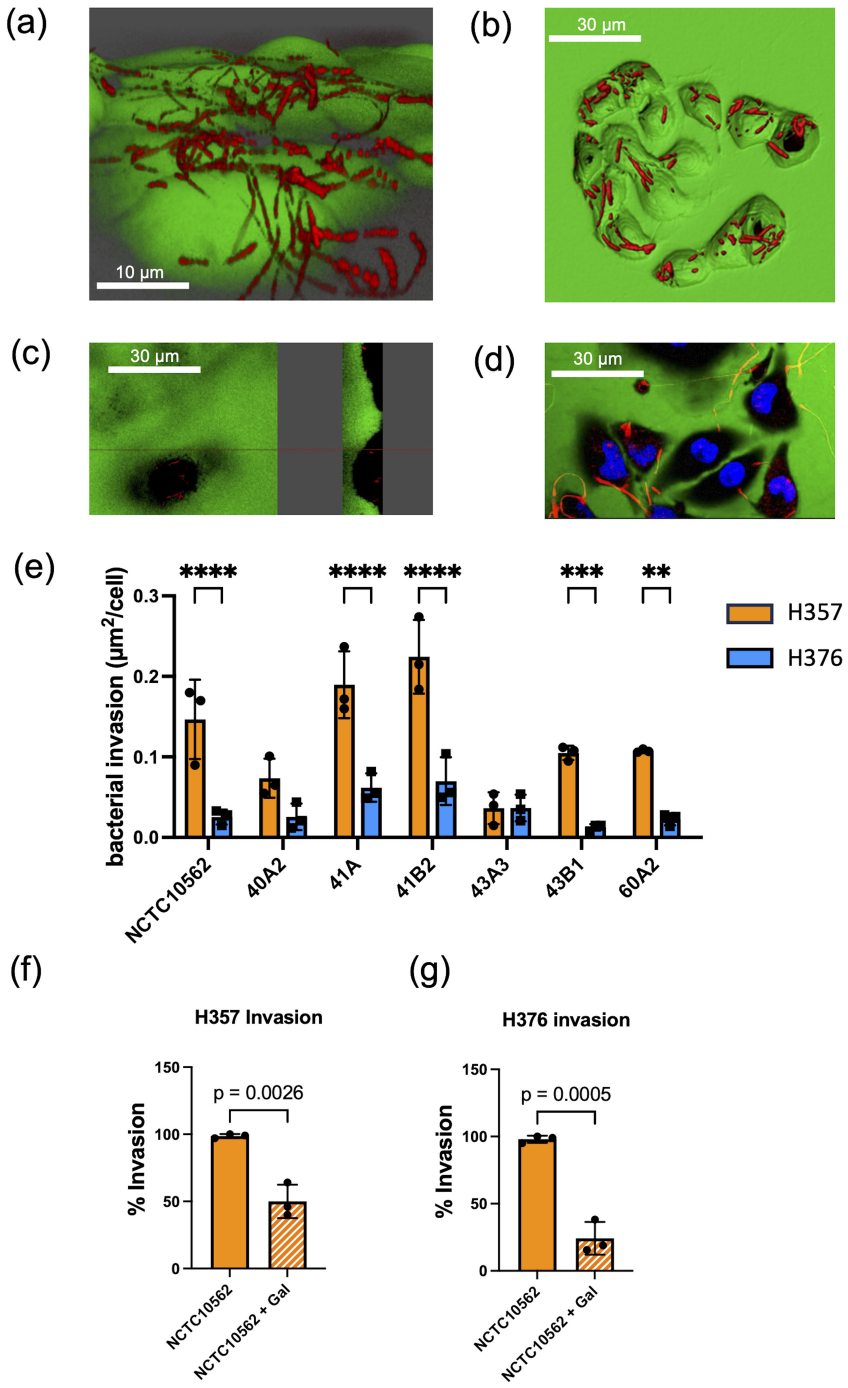

FIGURE 3
Invasion of oral keratinocytes by *F. nucleatum* subsp. *polymorphum*. **(A)** Propidium iodide (PI) stained cells of *F. nucleatum* subsp. *polymorphum* NCTC10562 interacting with H357 oral keratinocytes. **(B)** 3D confocal image of H376 oral keratinocytes with internalised cells of *F. nucleatum* subsp. *polymorphum* NCTC10562 stained with PI. **(C)** Saggital-section of H357 epithelial cells showing internalised bacteria of strain NCTC10562. **(D)** Confocal Z stack image of invasion assay of H357 cells (nuclei stained using Hoescht) being invaded by strain NCTC10562. **(E)** Bacterial invasion of H357 and H376 oral keratinocytes quantified using Imaris software as μm^2 of bacteria per cell. Significant differences in the invasion of H357 and H376 cells indicated by asterisks (ANOVA adjusted p = ** < 0.01, *** <0.001, **** <0.0001). **(F)** Impact of galactose (60 mM) on the invasion of H357 cells by strain NCTC10562 with t-test *p* value. **(G)** Impact of galactose (60 mM) the invasion of H376 cells by strain NCTC10562 with t-test *p* value.

pre-treated strain NCTC10562 with 60 mM galactose for 30 minutes before performing the assays. We observed that galactose pre-treatment significantly reduced invasion both H357 and H376 cells by strain NCTC10562 (Figures 3F, G).

Analysis of cellular responses to infection

We next analysed the cytokine response of the H357 and H376 cells to infection with NCTC10652 and clinical strains of *F. nucleatum* subsp. *polymorphum*. In the absence of infecting bacteria, both cell-lines secreted baseline levels of IL-8, which were greatest in the E-cadherin negative H376 cells (Figure 4A). Infection with NCTC10562 was seen to induce a variety of inflammatory cytokines and chemokines including IP-10, RANTES/CCL5 and MCP-1/CCL2 (Figure 4A). These responses were also induced by *E. coli* DH5α (MOI 50:1), indicating that this may be a general response to Gram-negative bacterial infection. As RANTES/CCL5 has been previously linked to MMP9 expression and tumor cell migration, we confirmed induction of CCL5 expression using ELISA. CCL5 was induced in both cell lines by NCTC10562 and the clinical strains 40A2 and 43A3. Differences in induction could be discerned, with the low adhesion isolate 40A2 inducing significantly less secretion than NCTC10562 in H357 and H376 cells and the high adhesion isolate 43A3 inducing significantly higher secretion compared to NCTC10562 in H376 cells. In this case, inhibition of adhesion of 43A3 to H376 cells with galactose (60mM) could significantly reduce secretion of CCL5 (Figure 4D).

Multiplex analysis of MMP expression also indicated that *F. nucleatum* infection induces secretion of MMP9 in both cell lines. As MMP9 has been linked to tumor cell invasion and migration we examined MMP9 expression using ELISA (Figures 4E, F). H376 cells expressed higher levels of MMP9 following *F. nucleatum* infection and these were significantly higher in cells infected with the high adhesion isolate 43A3 (Figures 4E, F).

Transcriptional responses to *F. nucleatum*

In order to support the findings of the cytokine data, we analysed transcriptomic data from H357 and H376 oral keratinocytes infected with *F. nucleatum* in order to determine if transcriptional responses related to motility and invasion are activated. Although this analysis was performed with *F. nucleatum* subsp. *nucleatum* ATCC23726, the data are likely to reflect responses activated by *F. nucleatum* in general. Infection of both cell lines activated transcriptional responses, with the H357 cell line exhibiting a greater number of significantly regulated genes compared to uninfected cells (1423 up and 669 down genes; $p < 0.05$) compared to the H376 cells (543 up and 363 down genes, $p < 0.05$) (Supplementary Figure S2; Supplementary Tables S1, S2). As expected, both cell lines activated a response to Gram-negative infection, with significant enrichments in expression of genes within the GO terms "response to lipopolysaccharide", "positive regulation of cytokine activity" and "NF-κB signalling" (Figure 5; Supplementary Tables S3, S4). Both cell lines also activated angiogenic responses and responses involved in cellular mobility and migration (Figure 5). Uniquely, the H357 cell line underwent a transcriptional response that suggests a major shift in metabolism, involving reduced aerobic respiration, ribosome biogenesis and increased catabolism and autophagy (Figure 5). The H357 cells also activated responses involved in keratinization and epidermis development (Figure 5). Uniquely, the H357 cells also activated a response termed "entry into host cell" including genes that may be induced upon pathogen entry. Fewer specific responses were identified in the E-cadherin negative H376 cell line, however some responses such as the response to lipopolysaccharide and cell migration categories exhibited more highly significant adjusted *p* values due to the smaller size of the total gene set.

F. nucleatum subsp. *polymorphum* induces migration and invasion by H357 and H376 keratinocytes

To assess the impact of *F. nucleatum* subsp. *polymorphum* infection on the motility and invasiveness of oral keratinocytes, we assessed the responses of H357 and H376 cells using a scratch wound assay and trans-well invasion assay. For the scratch wound assay (Figure 6A), keratinocytes were infected by *F. nucleatum* subsp. *polymorphum* (MOI 10:1) for 24 hours. Infection of keratinocytes (both H357 and H376) by strains NCTC10562 or 43A3 resulted in significantly greater migration in a scratch wound assay (Figures 6B, C). Next, we examined keratinocyte invasiveness in response to CM by measuring keratinocyte migration across matrix coated filters (Figure 7A). In general, we observed that H376 cells exhibited greater migration in response to CM compared to H357 cells (Figure 7B). However the response of H376 cells varied between strains with significantly greater invasion of H376 cells observed with CM from strain 43A3 and significantly less with CM from strain 40A2 compared to strain NCTC10562. Recombinant CCL5 could also enhance migration of both cell lines (Figures 7C, D). Compared to DMEM alone, CM from strains NCTC10562 and 43A3 induced the most significant increases in migration (Figures 7C, D). Next, we examined whether blockage of CCL5 signalling using the inhibitor metCCL5 (3 ng/ml pre-treatment for 30 min) could reduce the migration response to CM. We observed a significant reduction in migration of both H357 and H376 cells in response to NCTC10562 CM following metCCL5 treatment (Figures 7C, D). We also observed a significant reduction in the migration of H376 cells in response to CM from 43A3 following metCCL5 treatment (Figure 7D).

F. nucleatum subsp. *polymorphum* induces angiogenic responses in H357 and H376 keratinocytes

Based on the pro-angiogenic transcriptional responses (Figure 4) and the observed induction of CCL2/MCP-1 in our multiplex assays (Figure 5), we investigated whether *F. nucleatum*

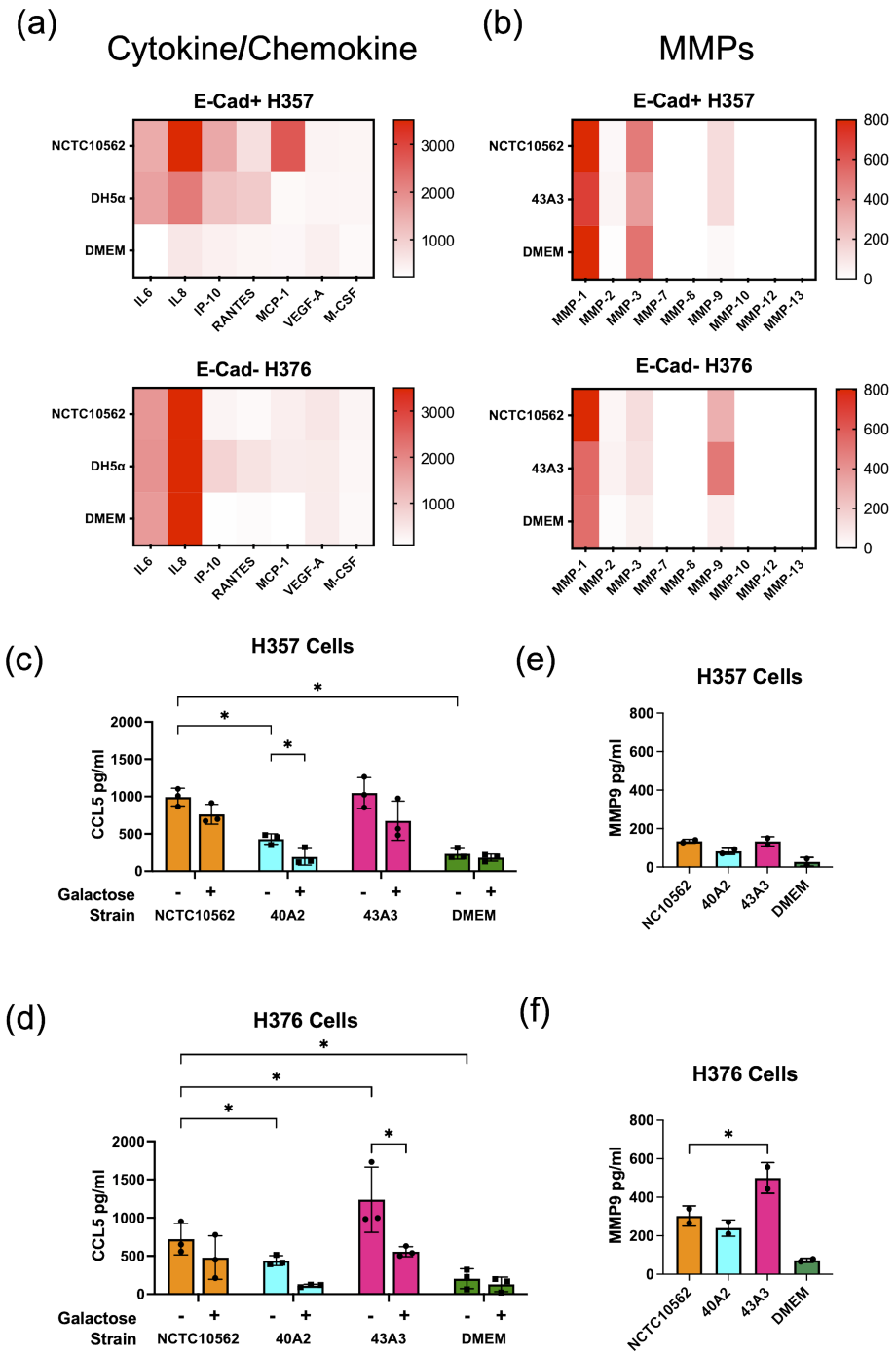

FIGURE 4
Response of H357 and H376 oral keratinocytes to *F. nucleatum* infection. **(A)** Expression of selected cytokines and chemokines (pg/ml) detected in a multiplex assay (Eve Technologies, Canada) in cell culture media (DMEM) recovered from H357 and H376 cells infected with *F. nucleatum* subsp. *polymorphum* NCTC10562 (MOI 10:1) or *E. coli* DH5α (MOI 50:1). **(B)** Expression of MMPs (pg/ml) detected in a multiplex assay (Eve Technologies, Canada) in cell culture media (DMEM) recovered from H357 and H376 cells infected with *F. nucleatum* subsp. *polymorphum* NCTC10562 or 43A3. **(C)** ELISA of CCL5 expression in H357 cells and **(D)** H376 cells uninfected (DMEM only) and infected with the indicated strains of *F. nucleatum* subsp. *polymorphum* in the presence or absence of galactose. Asterisk indicates significant differences identified in 2-way ANOVA corrected for multiple comparisons (adjusted p= *<0.05). **(E)** ELISA results of MMP9 expression in H357 and **(F)** H376 cells uninfected (DMEM only) and infected with the indicated strains of *F. nucleatum* subsp. *polymorphum*. Asterisk indicates significant difference from NCTC10562 in ANOVA with Dunnett's test for multiple (adjusted p= *<0.05).

subsp. *polymorphum* infection could induce the angiogenic factor VEGF-A or angiogenic responses in HUVEC cells. CCL2/MCP-1 is known to induce VEGF-A expression in malignant cells via stimulation of its cognate receptor CCR2. Using ELISA we found that clinical strains 40A2, 43A3 and the type strain NCTC10562 could induce significantly increased secretion of CCL2 in both H357 and H376 cells (Figure 8A). We next investigated the impact of *F. nucleatum* subsp. *polymorphum* infection on VEGF-A secretion.

10.3389/fcimb.2024.1417946

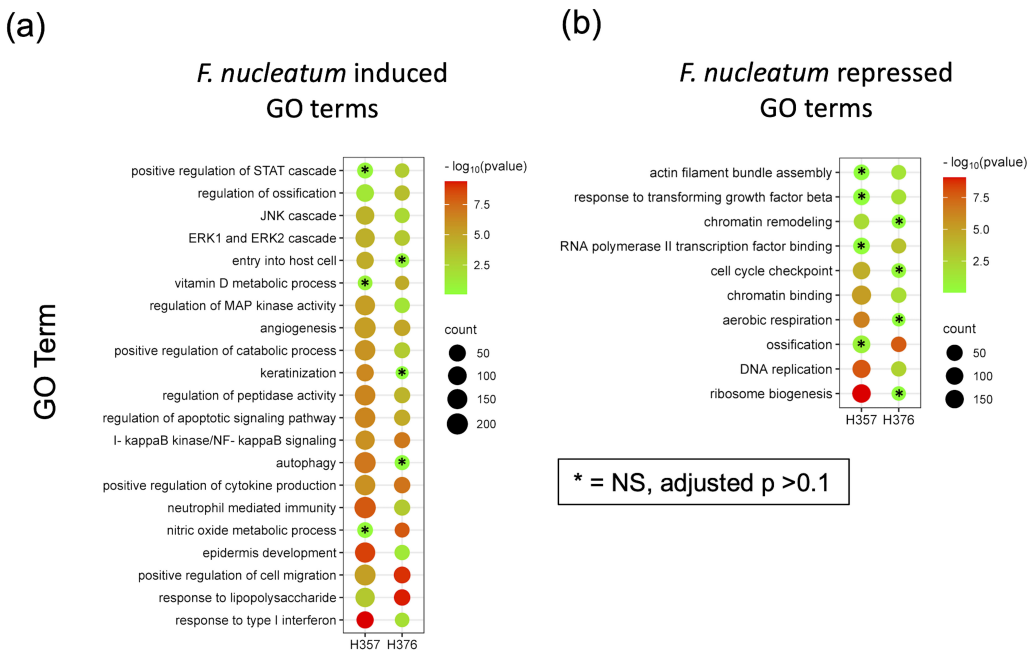

FIGURE 5
RNA-Seq analysis of the response of H357 and H376 oral keratinocytes to infection with *F. nucleatum* 23726. Oral keratinocytes were infected with *F. nucleatum* for 3 h at an MOI of 10:1. Plot shows the results of Gene Ontology (GO) term enrichment analysis in the **(A)** upregulated and **(B)** down regulated gene sets in both cell lines. Adjusted *p* values were generated using the Benjamini-Hochberg FDR method. The most significant non-redundant GO terms were selected for display. Cell lines with adjusted p values >0.1 are indicated by asterisks. A full list can be seen in Supplementary Tables S3, S4.

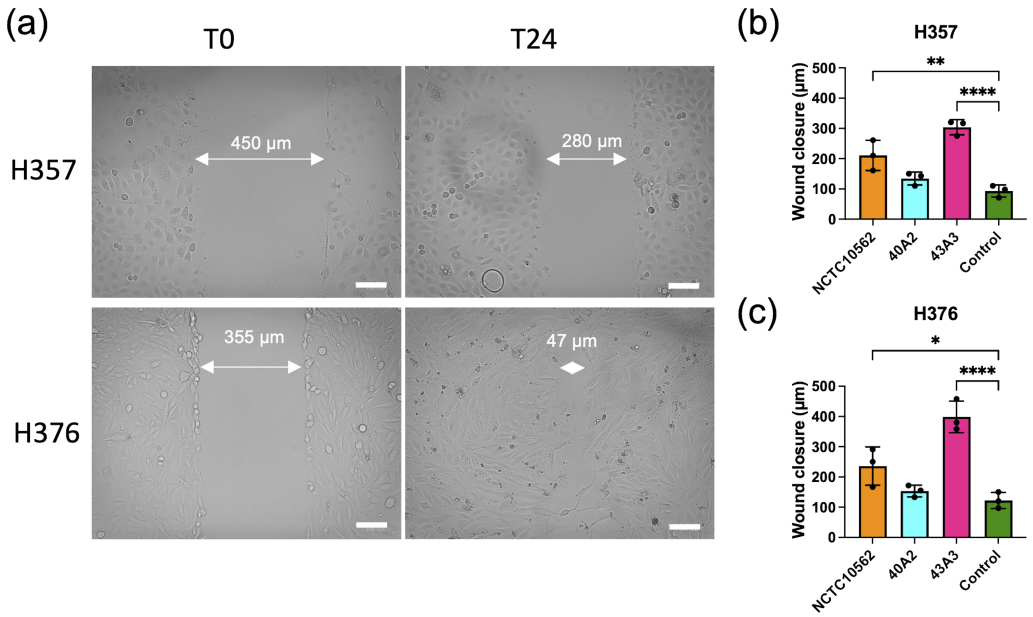

FIGURE 6
Scratch wound assay. **(A)** Representative images of scratch wounds in H357 cells (top row) and H376 cells (bottom row). Left panel shows cell at time 0 and right panel after 24 h infections with strain NCTC10562. Arrows indicate scratch wound width (µM). Scale bar=100 µm. **(B)** Wound closure measurements in H357 cells and **(C)** H376 cells following incubation with DMEM (control) or infections with the indicated strains. Cell migration was assessed by calculating the amount of wound closure after 24 h infection. Treatments significantly different from the control (DMEM) are indicated by asterisks (ANOVA adjusted p = * <0.05, ** < 0.01, **** <0.0001).

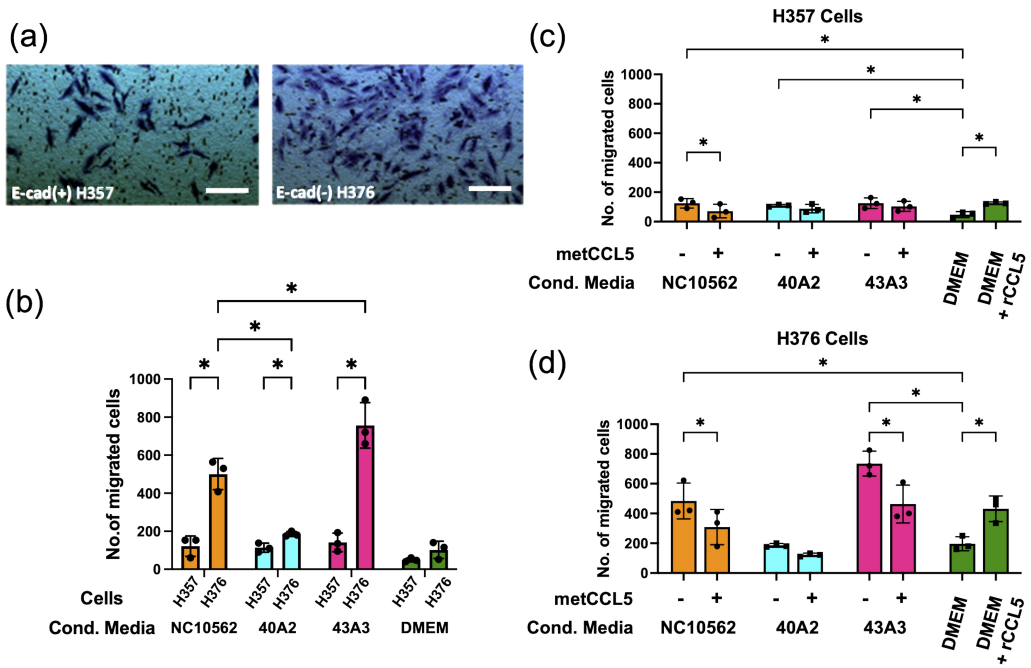

FIGURE 7
Analysis of invasive phenotypes in H357 and H376 cells in response to CM from cells infected with *F. nucleatum* subsp. *polymorphum*. **(A)** Representative image showing stained oral keratinocytes following migration across the matrix coated filter. The white lines represent scale bar=100 µm **(B)** Comparison of migration of H357 and H376 keratinocytes following treatment with CM from the indicated strains. Asterisks indicate results of 2-way ANOVA (adjusted p= *<0.05). **(C)** Analysis of H357 and **(D)** H376 cell invasion following treatment with CM from the indicated strains with and without pre-treatment with the inhibitor metCCL5. Asterisks indicates CM treatments significantly different from DMEM and significant reductions in invasion following metCCL5 treatment (2-way ANOVA adjusted p= *<0.05).

Without *F. nucleatum* stimulation, the H376 cells were found to secrete significantly higher baseline levels of VEGF-A compared to H357 cells (t-test p <0.001). However, in the case of both cell lines, exposure to *F. nucleatum* subsp. *polymorphum* increased VEGF-A secretion (Figure 8B).

We next examined if CM from infected cells could enhance angiogenesis in HUVEC cells by measuring tube formation. Supplementation of sterile HUVEC medium with recombinant human VEGF-A (rVEGF) resulted in a significant increase in tube formation (Figure 9A). Tube formation was also induced by conditioned HUVEC media recovered from both uninfected cell lines, with medium from the high VEGF-A secreting H376 cells inducing greater tube formation than H357 cells (Figure 9A). Next we examined if exposure to conditioned HUVEC media produced following infection of the cells lines with *F. nucleatum* subsp. *polymorphum* could enhance tube formation to a similar extent. In

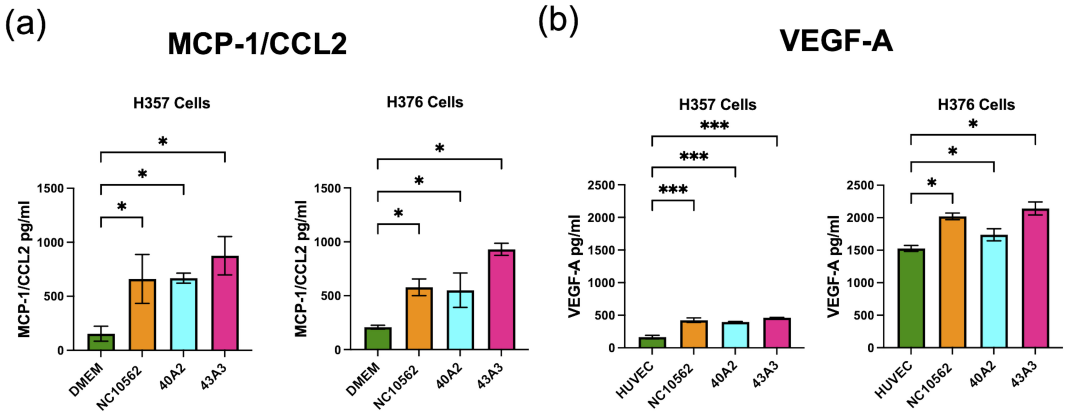

FIGURE 8
Analysis of secretion of **(A)** MCP-1/CCL2 and **(B)** VEGF-A by H357 and H376 oral keratinocytes following *F. nucleatum* infection. ELISA quantification was carried out on culture medium (DMEM or HUVEC) following 24 h infection with the indicated strains of *F. nucleatum* subsp, *polymorphum* (MOI 10:1). Significant differences from uninfected cells was calculated using ANOVA with Dunnett's test for multiple comparisons (adjusted p = *<0.05, ***<0.001).

the case of both H357 and H376 cells, CM from infections with all three *F. nucleatum* subsp. *polymorphum* strains, NCTC10562, 40A2 and 43A3, resulted in significantly increased tube formation compared to HUVEC medium from uninfected cells (Figures 9A, B). In order to confirm whether these phenotypes were VEGF-A specific, we treated cells with resveratrol, which has been shown to inhibit VEGF receptor 2 phosphorylation and signalling. Exposure of HUVEC cells to 1.5 µM resveratrol could reduce tube formation in all preparations of conditioned media (Figure 9C).

Discussion

Our previous studies identified *F. nucleatum* subsp. *polymorphum* as the most common subspecies recovered from healthy and diseased oral mucosa (including OLK and OSCC) (Crowley et al., 2024). These data concur with Krieger et al. (Krieger et al., 2024) who show that subsp. *polymorphum* is the *F. nucleatum* subspecies with the highest abundance in the oral microbiome (Krieger et al., 2024). One of the most surprising aspects of our genetic analysis of these strains was the level of heterogeneity in the accessory genome, especially in copy number of Fap2-like autotransporter adhesins and copy number of FadA-like adhesins. The overarching goal of the current study was to determine if this genetic heterogeneity manifested in phenotypic differences in host-cell interaction. The clinical isolates selected were previously shown to differ in adherence to oral keratinocytes and to vary in their repertoire of adhesin genes (Crowley et al., 2024). In addition, we evaluated the interaction with two different malignant cell lines which differed in origin in terms of tumor stage (stage 1 v stage 3). The H376 cells had lost expression of E-cadherin and showed increased expression of Gal-GalNAc, properties typical of a more advanced tumor, whereas the H357 cells from a stage 1 tumor still expressed E-cadherin and were morphologically more similar to the immortalized OKF-6 cells (Fardini et al., 2011; Coppenhagen-Glazer et al., 2015).

We could detect considerable variation in adhesion to these oral keratinocytes, with the type strain NCTC10562 exhibiting a strong preference for adhesion to the H357 cells, whereas 3 of the 6 clinical isolates examined exhibited a preference to the H376 cells. Galactose was shown to inhibit the interaction of bacteria with both cell lines, indicating the importance of lectin binding in these interactions. Strain 43A3, which exhibited extremely high levels of adhesion to the Gal-GalNAc expressing H376 cell line was very significantly inhibited by galactose (~85%). These data also suggest that as epithelial dysplasia advances and Gal-GalNAc expression

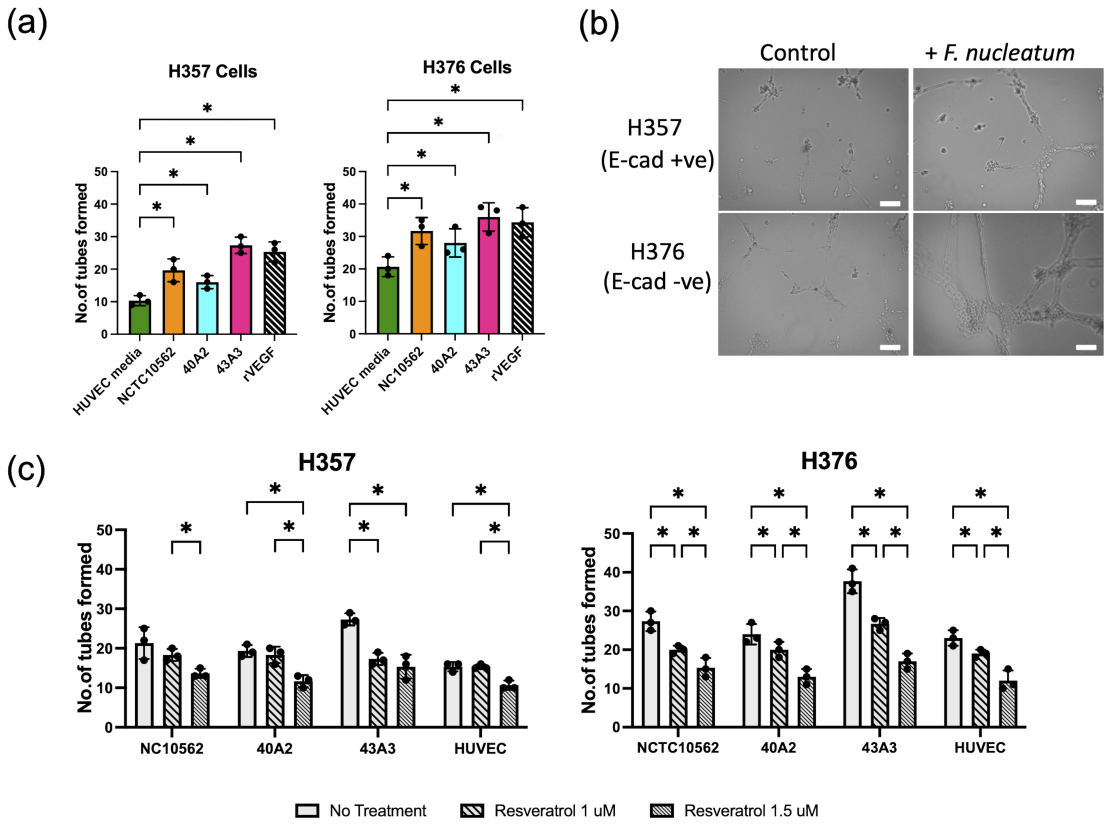

FIGURE 9
Analysis tube formation by HUVEC cells. **(A)** Quantification of tube formation in HUVEC cells exposed to conditioned HUVEC medium from H357 and H376 oral keratinocytes following *F. nucleatum* infection (24 h infection, MOI 10:1). Recombinant VEGF-A (rVEGF; 50 ng/ml) is included as a positive control. Significant differences from uninfected control (HUVEC medium) was calculated using ANOVA with Dunnett's test for multiple comparisons (adjusted p = *<0.05). **(B)** Representative images of HUVEC cells after 12 h exposure to conditioned HUVEC medium obtained from H357 cells (top row) or H376 cells (bottom row) that were uninfected (control) or infected with *F. nucleatum* strain 43A3 (+ *F. nucleatum*). The white lines represent scale bar=100 µm. **(C)** Inhibition of HUVEC tube formation by resveratrol (1 µM and 1.5 µM). Significant differences between treatments were identified using 2-way ANOVA (q = *<0.05).

increases (Abdalla et al., 2017) strains of *F. nucleatum* that adhere strongly to Gal-GalNAc residues may be selected. The identification of clinical isolates here exhibiting high adhesion to Gal-GalNAc expressing cells could be the result of *in vivo* selection for dysplasia adapted genotypes. In the absence of efficient gene deletion tools for *F. nucleatum* subsp. *polymorphum* it is impossible to dissect the adhesin-receptor interactions at play. However what these data illustrate is the heterogeneity in adhesive phenotypes among clinical isolates of subspecies *polymorphum* that possess different repertoires of adhesins. *F. nucleatum* is highly recombinogenic which may facilitate the generation of variants that can adhere to different surfaces (Mira et al., 2004).

Keratinocyte invasion by *F. nucleatum* was greatest in the H357 cell line. We observed lower levels of invasion of H376 cells, even by isolates which exhibited strong adherence to these cells. The H357 cell line was shown to express E-cadherin, which could be involved in receptor mediated internalization via the FadA adhesin on the surface of *F. nucleatum* (Ikegami et al., 2009). All of the isolates under investigation possess FadA and FadA-related adhesins (FadA2, FadA3) which may mediate these interactions. Although the role of E-cadherin in this phenotype may require knock-down experiments to confirm, our data show that invasion of keratinocytes by clinical strains of *F. nucleatum* is highly cell-line dependent and is likely influenced by the expression of different receptors on the epithelial cells. H357 cells, which permitted higher levels of bacterial internalization, also exhibited a stronger transcriptional response to *F. nucleatum*. Specific responses of the H357 cells included a keratinization response, which may be a defensive response to invasion, and a metabolic response that included induction of autophagy, a process previously linked with infection induced chemoresistance in tumor cells (Yu et al., 2017). Both cell lines exhibited induction of transcriptional responses linked to cellular motility and angiogenesis, processes strongly associated with tumor development and metastases (Claffey and Robinson, 1996; Lien et al., 2020; Ralli et al., 2020). Analysis of secreted factors induced following *F. nucleatum* infection supported this association with significant induction of the chemokine CCL5/RANTES and MMP-9 detected in conditioned medium. CCL5/RANTES is a known inducer of MMP9 expression which has been shown to facilitate cellular invasion (Woodhouse et al., 1997; Chuang et al., 2009). Lectin interactions have previously been shown to play a role in chemokine induction by *F. nucleatum* and our data show that disruption of adhesion with galactose can partly attenuate CCL5 induction (Casasanta et al., 2020). We also observed that the highly adherent isolate 43A3 induced higher responses compared to the low adhesion isolate 40A2. However, although lectins such as Fap2 may play significant roles in mediating host cell interaction, the finding that a high MOI infection with *E. coli* (MOI 50:1) could stimulate a somewhat similar cytokine response suggests that this may be a general response to a Gram-negative infection.

Examination of the response of oral keratinocytes to infection also revealed cell line-specific and bacterial strain-specific responses. The E-cadherin negative H376 cell line generally exhibited greater motility and invasion across ECM gel relative to E-cadherin positive cells in our assays. This may be related to the loss of intercellular adhesion afforded by E-cadherins and the greater basal expression of MMP9 (Chuang et al., 2009; Mohamet et al., 2011). Loss of E-cadherins have been associated with aggressiveness, advanced stage and poor prognosis of cancers (Abdalla et al., 2017). Cellular invasion and migration of H376 cells were significantly increased by strains NCTC10562 and 43A3, both of which were stronger inducers of CCL5/RANTES and MMP9 compared to strain 40A2. The involvement of the CCL5 axis in this phenotype could be inferred from the inhibitory effects of metCCL5, a competitor inhibitor for CCR5 receptors, on cell migration (Chuang et al., 2009).

Our transcriptional and chemokine expression data indicate that *F. nucleatum* induces pro-angiogenic responses, which to our knowledge have not been previously reported. VEGF-A, which is essential for the formation of new blood vessels in the body, including those in growing tumors, is regulated by multiple factors, including oncogenes, pro-inflammatory cytokines and chemokines such as MCP-1/CCL2, WNT1-inducible signaling pathway protein-1 (WISP-1/CCN-4), hormonal modulators and hypoxia (Claffey and Robinson, 1996; Lien et al., 2020). Infection of both cell lines with *F. nucleatum* resulted in induction of the chemokine MCP-1/CCL2 which has been shown to induce VEGF-A in OSCC (Lien et al., 2020). We could also demonstrate induction of VEGF-A following *F. nucleatum* infection in both cell lines and this was reflected in the enhanced capillary-like tube formation induced in HUVEC cells. The tube formations were reduced when an increasing concentration of resveratrol, a selective VEGFR inhibitor was used (Igura et al., 2001). Induction of angiogenesis indicates that *F. nucleatum* may exacerbate tumor growth and metastases by stimulating blood vessel formation required for provision of nutrients and oxygen to the growing tumor.

Further studies using animal models of angiogenesis or chorioallantoic membrane (CAM) assays would be needed to confirm these responses. In addition, a larger panel of *F. nucleatum* isolates would be required to determine of any of these phenotypes are stronger in isolates recovered from severe epithelial dysplasia or OSCC.

Conclusion

In conclusion, our study has uncovered a high degree of phenotypic variability in *F. nucleatum* subsp. *polymorphum*, the most common *F. nucleatum* subspecies associated with healthy and dysplastic oral mucosa. The variability in adhesin gene complement shows that specific strains of subspecies *polymorphum* may be better adapted to adhere to certain cell types, suggesting that tumor development may select for certain *F. nucleatum* genotypes that can bind to tumor-specific markers such as Gal-GalNAc. Crowley et al. have shown that recombination among adhesin-encoding genes occurs in other subspecies of *F. nucleatum* suggesting that inter-strain variability is not likely to be unique to subspecies *polymorphum*. Host cell phenotype also appears to be an important variable in influencing the outcome of *F. nucleatum*-keratinocyte interactions. The E-cadherin expressing H357 cell line examined here, despite harboring more intracellular bacteria and activating stronger transcriptional responses, was generally less motile and less invasive in response to *F. nucleatum* infection compared to the E-cadherin negative H376 cell line. This could

suggest that the detrimental effects *F. nucleatum* infection are most pronounced in higher stage tumors where loss of E-cadherin and EMT phenotypes are more advanced, acting as a driver of metastatic phenotypes.

Data availability statement

The datasets presented in this study can be found in online repositories. The names of the repository/repositories and accession number(s) can be found below: https://www.ncbi.nlm.nih.gov/, PRJNA1071052.

Ethics statement

The studies involving humans were approved by the joint Hospital Research Ethics Committee (JREC) Dublin. The studies were conducted in accordance with the local legislation and institutional requirements. The participants provided their written informed consent to participate in this study.

Author contributions

GM: Conceptualization, Formal analysis, Funding acquisition, Methodology, Project administration, Supervision, Visualization, Writing – review & editing. AS: Data curation, Formal analysis, Investigation, Methodology, Project administration, Visualization, Writing – original draft. GM: Formal analysis, Methodology, Visualization, Writing – review & editing. CH: Conceptualization, Funding acquisition, Project administration, Supervision, Writing – review & editing.

Funding

The author(s) declare financial support was received for the research, authorship, and/or publication of this article. GM and CH are funded to carry out this work by the Irish Health Research Board (Grant no. ILP-POR-2019-030). AS was funded by a Provost's Award PhD Scholarship from Trinity College Dublin.

Acknowledgments

The authors would like to thank Dr. Simon Whawell (Dental School, Plymouth, UK) for the gift of H357 and H376 cell lines, Dr Antonio Amelio (Department of Oral and Craniofacial health Science, University of North Carolina at Chapel Hill, USA) for the gift of OKF-6 cells and Prof. Daniel Slade (Virginia Tech, USA) for the gift of *F. nucleatum* 23726. We would also like to thank Dr. Ursula Fearon (Department of Molecular Rheumatology, Trinity College Dublin, Ireland) for advice on tube formation assays.

Conflict of interest

The authors declare that the research was conducted in the absence of any commercial or financial relationships that could be construed as a potential conflict of interest.

Publisher's note

Supplementary material

The Supplementary Material for this article can be found online at: https://www.frontiersin.org/articles/10.3389/fcimb.2024.1417946/full#supplementary-material

SUPPLEMENTARY FIGURE S1
Comparisons of invasion of NCTC10562 and the indicated clinical isolates of *F. nucleatum* subsp. *polymorphum* to H357 and H376 cells.

SUPPLEMENTARY FIGURE S2
Volcano plots showing differentially expressed genes (p <0.05) in H357 and H376 cells following infection with *F. nucleatum* 23726, identified using DeSeq2.

SUPPLEMENTARY TABLE S1
Differentially expressed genes in *F. nucleatum* infected H357 cells compared to uninfected cells identified using DeSeq2 (p <0.05).

SUPPLEMENTARY TABLE S2
Differentially expressed genes in *F. nucleatum* infected H376 cells compared to uninfected cells identified using DeSeq2 (p <0.05).

SUPPLEMENTARY TABLE S3
Significant GO term enrichments in *F. nucleatum* infected H357 cells compared to uninfected cells (padj <0.05).

SUPPLEMENTARY TABLE S4
Significant GO term enrichments in *F. nucleatum* infected H376 cells compared to uninfected cells (padj <0.05).

References

Abdalla, Z., Walsh, T., Thakker, N., and Ward, C. M. (2017). Loss of epithelial markers is an early event in oral dysplasia and is observed within the safety margin of dysplastic and T1 OSCC biopsies. *PloS One* 12, 17. doi: 10.1371/journal.pone.0187449

Abed, J., Emgård, J. E. M., Zamir, G., Faroja, M., Almogy, G., Grenov, A., et al. (2016). Fap2 mediates *fusobacterium nucleatum* colorectal adenocarcinoma enrichment by binding to tumor- expressed gal-galNAc. *Cell Host Microbe* 20, 215–225. doi: 10.1016/j.chom.2016.07.006

Brazier, J. S., Citron, D. M., and Goldstein, E. J. C. (1991). A selective medium for *Fusobacterium* spp. *J. Appl. Bacteriol.* 71, 343–346. doi: 10.1111/j.1365-2672.1991.tb03798.x

Brennan, C. A., and Garrett, W. S. (2019). *Fusobacterium nucleatum* — symbiont, opportunist and oncobacterium. *Nat. Rev. Microbiol.* 17, 156–166. doi: 10.1038/s41579-018-0129-6

Bullman, S., Pedamallu, C. S., Sicinska, E., Clancy, T. E., Zhang, X., Cai, D., et al. (2017). Analysis of *Fusobacterium* persistence and antibiotic response in colorectal cancer. *Science* 358, 1443–1448. doi: 10.1126/science.aal5240

Casasanta, M. A., Yoo, C. C., Udayasuryan, B., Sanders, B. E., Umaña, A., Zhang, Y., et al. (2020). *Fusobacterium nucleatum* host-cell binding and invasion induces IL-8 and CXCL1 secretion that drives colorectal cancer cell migration. *Sci. Signal* 13, eaba9157. doi: 10.1126/scisignal.aba9157

Castellarin, M., Warren, R. L., Freeman, J. D., Dreolini, L., Krzywinski, M., Strauss, J., et al. (2012). *Fusobacterium nucleatum* infection is prevalent in human colorectal carcinoma. *Genome Res.* 22, 299–306. doi: 10.1101/gr.126516.111

Chuang, J., Yang, W., Chen, H., Huang, C., Tan, T., Lin, Y., et al. (2009). CCL5/CCR5 axis promotes the motility of human oral cancer cells. *J. Cell. Physiol.* 220, 418–426. doi: 10.1002/jcp.21783

Claffey, K. P., and Robinson, G. S. (1996). Regulation of VEGF/VPF expression in tumor cells: Consequences for tumor growth and metastasis. *Cancer Metastasis. Rev.* 15, 165–176. doi: 10.1007/bf00437469

Connolly, E., Millhouse, E., Doyle, R., Culshaw, S., Ramage, G., and Moran, G. P. (2016). The *Porphyromonas gingivalis* hemagglutinins HagB and HagC are major mediators of adhesion and biofilm formation. *Mol. Oral. Microbiol.* 32, 35–47. doi: 10.1111/omi.12151

Coppenhagen-Glazer, S., Sol, A., Abed, J., Naor, R., Zhang, X., Han, Y. W., et al. (2015). Fap2 of *fusobacterium nucleatum* is a galactose-inhibitable adhesin involved in coaggregation, cell adhesion, and preterm birth. *Infect. Immun.* 83, 1104–1113. doi: 10.1128/iai.02838-14

Crowley, C., Selvaraj, A., Hariharan, A., Healy, C. M., and Moran, G. P. (2024). Fusobacterium nucleatum subsp. *polymorphum* recovered from Malignant and potentially Malignant oral disease exhibit heterogeneity in adhesion phenotypes and adhesin gene copy number, shaped by inter-subspecies HGT and recombination-derived mosaicism. *Microbial. Genomics* 10, 1217. doi: 10.1099/mgen.0.001217

Dickson, M. A., Hahn, W. C., Ino, Y., Ronfard, V., Wu, J. Y., Weinberg, R. A., et al. (2000). Human Keratinocytes That Express hTERT and Also Bypass a p16INK4a-Enforced Mechanism That Limits Life Span Become Immortal yet Retain Normal Growth and Differentiation Characteristics. *Mol. Cell. Biol.* 20, 1436–1447. doi: 10.1128/mcb.20.4.1436-1447.2000

Fardini, Y., Wang, X., Témoin, S., Nithianantham, S., Lee, D., Shoham, M., et al. (2011). *Fusobacterium nucleatum* adhesin FadA binds vascular endothelial cadherin and alters endothelial integrity. *Mol. Microbiol.* 82, 1468–1480. doi: 10.1111/j.1365-2958.2011.07905.x

Fromm, S., Cunningham, C. C., Dunne, M. R., Veale, D. J., Fearon, U., and Wade, S. M. (2019). Enhanced angiogenic function in response to fibroblasts from psoriatic arthritis synovium compared to rheumatoid arthritis. *Arthritis Res. Ther.* 21, 297. doi: 10.1186/s13075-019-2088-3

Gallimidi, A. B., Fischman, S., Revach, B., Bulvik, R., Maliutina, A., Rubinstein, A. M., et al. (2015). Periodontal pathogens *Porphyromonas gingivalis* and *Fusobacterium nucleatum* promote tumor progression in an oral-specific chemical carcinogenesis model. *Oncotarget* 6, 22613–22623. doi: 10.18632/oncotarget.4209

Gharbia, S. E., Shah, H. N., Lawson, P. A., and Haapasalo, M. (1990). The distribution and frequency of *Fusobacterium nucleatum* subspecies in the human oral cavity. *Oral. Microbiol. Immun.* 5, 324–327. doi: 10.1111/j.1399-302x.1990.tb00434.x

Gur, C., Ibrahim, Y., Isaacson, B., Yamin, R., Abed, J., Gamliel, M., et al. (2015). Binding of the fap2 protein of *fusobacterium nucleatum* to human inhibitory receptor TIGIT protects tumors from immune cell attack. *Immunity* 42, 344–355. doi: 10.1016/j.immuni.2015.01.010

Gur, C., Maalouf, N., Shhadeh, A., Berhani, O., Singer, B. B., Bachrach, G., et al. (2019). *Fusobacterium nucleatum* supresses anti-tumor immunity by activating CEACAM1. *OncoImmunology* 8, e1581531. doi: 10.1080/2162402x.2019.1581531

Han, Y. W. (2015). *Fusobacterium nucleatum*: a commensal-turned pathogen. *Curr. Opin. Microbiol.* 23, 141–147. doi: 10.1016/j.mib.2014.11.013

Harrandah, A. M., Chukkapalli, S. S., Bhattacharyya, I., Progulske-Fox, A., and Chan, E. K. L. (2020). Fusobacteria modulate oral carcinogenesis and promote cancer progression. *J. Oral. Microbiol.* 13, 1849493. doi: 10.1080/20002297.2020.1849493

Igura, K., Ohta, T., Kuroda, Y., and Kaji, K. (2001). Resveratrol and quercetin inhibit angiogenesis in *vitro*. *Cancer Lett.* 171, 11–16. doi: 10.1016/s0304-3835(01)00443-8

Ikegami, A., Chung, P., and Han, Y. W. (2009). Complementation of the fadA Mutation in *Fusobacterium nucleatum* Demonstrates that the Surface-Exposed Adhesin Promotes Cellular Invasion and Placental Colonization. *Infect. Immun.* 77, 3075–3079. doi: 10.1128/iai.00209-09

Kostic, A. D., Gevers, D., Pedamallu, C. S., Michaud, M., Duke, F., Earl, A. M., et al. (2012). Genomic analysis identifies association of *Fusobacterium* with colorectal carcinoma. *Genome Res.* 22, 292–298. doi: 10.1101/gr.126573.111

Krieger, M., AbdelRahman, Y. M., Choi, D., Palmer, E. A., Yoo, A., McGuire, S., et al. (2024). Stratification of *Fusobacterium nucleatum* by local health status in the oral cavity defines its subspecies disease association. *Cell Host Microbe* 32, 479–488. doi: 10.1016/j.chom.2024.02.010

Kunzmann, A. T., Proença, M. A., Jordao, H. W., Jiraskova, K., Schneiderova, M., Levy, M., et al. (2019). *Fusobacterium nucleatum* tumor DNA levels are associated with survival in colorectal cancer patients. *Eur. J. Clin. Microbiol. Infect. Dis.* 38, 1891–1899. doi: 10.1007/s10096-019-03649-1

Lien, M.-Y., Chang, A.-C., Tsai, H.-C., Tsai, M.-H., Hua, C.-H., Cheng, S.-P., et al. (2020). Monocyte chemoattractant protein 1 promotes VEGF-A expression in OSCC by activating ILK and MEK1/2 signaling and downregulating miR-29c. *Front. Oncol.* 10. doi: 10.3389/fonc.2020.592415

Love, M. I., Huber, W., and Anders, S. (2014). Moderated estimation of fold change and dispersion for RNA-seq data with DESeq2. *Genome Biol.* 15, 550. doi: 10.1186/s13059-014-0550-8

Mima, K., Nishihara, R., Qian, Z. R., Cao, Y., Sukawa, Y., Nowak, J. A., et al. (2016). *Fusobacterium nucleatum* in colorectal carcinoma tissue and patient prognosis. *Gut* 65, gutjnl–2015-310101. doi: 10.1136/gutjnl-2015-310101

Mira, A., Pushker, R., Legault, B. A., Moreira, D., and Rodríguez-Valera, F. (2004). Evolutionary relationships of *Fusobacterium nucleatum* based on phylogenetic analysis and comparative genomics. *BMC Evol. Biol.* 4, 50. doi: 10.1186/1471-2148-4-50

Mohamet, L., Hawkins, K., and Ward, C. M. (2011). Loss of function of E-cadherin in embryonic stem cells and the relevance to models of tumorigenesis. *J. Oncol.* 2011, 352616. doi: 10.1155/2011/352616

Muchova, M., Balacco, D. L., Grant, M. M., Chapple, I. L. C., Kuehne, S. A., and Hirschfeld, J. (2022). *Fusobacterium nucleatum* Subspecies Differ in Biofilm Forming Ability in *vitro*. *Front. Oral. Heal.* 3. doi: 10.3389/froh.2022.853618

Niño, J. L. G., Wu, H., LaCourse, K. D., Kempchinsky, A. G., Baryiames, A., Barber, B., et al. (2022). Effect of the intratumoral microbiota on spatial and cellular heterogeneity in cancer. *Nature* 611, 810–817. doi: 10.1038/s41586-022-05435-0

Parhi, L., Alon-Maimon, T., Sol, A., Nejman, D., Shhadeh, A., Fainsod-Levi, T., et al. (2020). Breast cancer colonization by Fusobacterium nucleatum accelerates tumor growth and metastatic progression. *Nat. Commun.* 11, 3259. doi: 10.1038/s41467-020-16967-2

Prime, S. S., Nixon, S. V. R., Crane, I. J., Stone, A., Matthews, J. B., Maitland, N. J., et al. (2005). The behaviour of human oral squamous cell carcinoma in cell culture. *J. Pathol.* 160, 259–269. doi: 10.1002/path.1711600313

Ralli, M., Grasso, M., Gilardi, A., Ceccanti, M., Messina, M. P., Tirassa, P., et al. (2020). The role of cytokines in head and neck squamous cell carcinoma: A review. *La. Clin. Terapeutica.* 171, e268–e274. doi: 10.7417/ct.2020.2225

Rubinstein, M. R., Baik, J. E., Lagana, S. M., Han, R. P., Raab, W. J., Sahoo, D., et al. (2019). *Fusobacterium nucleatum* promotes colorectal cancer by inducing Wnt/β-catenin modulator Annexin A1. *EMBO Rep.* 20, e47638. doi: 10.15252/embr.201847638

Rubinstein, M. R., Wang, X., Liu, W., Hao, Y., Cai, G., and Han, Y. W. (2013). *Fusobacterium nucleatum* Promotes Colorectal Carcinogenesis by Modulating E-Cadherin/β-Catenin Signaling via its FadA Adhesin. *Cell Host Microbe* 14, 195–206. doi: 10.1016/j.chom.2013.07.012

Shao, W., Fujiwara, N., Mouri, Y., Kisoda, S., Yoshida, K., Yoshida, K., et al. (2021). Conversion from epithelial to partial-EMT phenotype by *Fusobacterium nucleatum* infection promotes invasion of oral cancer cells. *Sci. Rep-uk.* 11, 14943. doi: 10.1038/s41598-021-94384-1

Umana, A., Sanders, B. E., Yoo, C. C., Casasanta, M. A., Udayasuryan, B., Verbridge, S. S., et al. (2019). Reevaluating the *fusobacterium* virulence factor landscape. *Biorxiv*, 534297. doi: 10.1101/534297

Woodhouse, E. C., Chuaqui, R. F., and Liotta, L. A. (1997). General mechanisms of metastasis. *Cancer* 80, 1529–1537. doi: 10.1002/(sici)1097-0142(19971015)80:8<1529::aid-cncr2>3.0.co;2-f

Yang, C.-Y., Yeh, Y.-M., Yu, H.-Y., Chin, C.-Y., Hsu, C.-W., Liu, H., et al. (2018). Oral microbiota community dynamics associated with oral squamous cell carcinoma staging. *Front. Microbiol.* 9. doi: 10.3389/fmicb.2018.00862

Yost, S., Stashenko, P., Choi, Y., Kukuruzinska, M., Genco, C. A., Salama, A., et al. (2018). Increased virulence of the oral microbiome in oral squamous cell carcinoma revealed by metatranscriptome analyses. *Int. J. Oral. Sci.* 10, 32. doi: 10.1038/s41368-018-0037-7

Yu, T., Guo, F., Yu, Y., Sun, T., Ma, D., Han, J., et al. (2017). *Fusobacterium nucleatum* promotes chemoresistance to colorectal cancer by modulating autophagy. *Cell* 170, 548–552.e16. doi: 10.1016/j.cell.2017.07.008

frontiers | Frontiers in Cellular and Infection Microbiology

TYPE Original Research
PUBLISHED 17 January 2025
DOI 10.3389/fcimb.2024.1483544

OPEN ACCESS

EDITED BY
Maurizio Sanguinetti,
Catholic University of the Sacred Heart, Italy

REVIEWED BY
Ilaria Cuccu,
Sapienza University of Rome, Italy
Gianluca Quaranta,
Agostino Gemelli University Polyclinic (IRCCS), Italy

*CORRESPONDENCE
Xiaomei Wu
w_xiaomei@163.com

RECEIVED 20 August 2024
ACCEPTED 11 December 2024
PUBLISHED 17 January 2025

CITATION
Li Y and Wu X (2025) Vaginal microbiome distinction in women with HPV+, cervical intraepithelial neoplasia, and cervical cancer, a retrospective study.
Front. Cell. Infect. Microbiol. 14:1483544.
doi: 10.3389/fcimb.2024.1483544

Vaginal microbiome distinction in women with HPV+, cervical intraepithelial neoplasia, and cervical cancer, a retrospective study

Yuanyue Li[1,2] and Xiaomei Wu*[,1,2]

[1]Department of Gynecology, The First People's Hospital of Yunnan Province, Kunming, China, [2]The Affiliated Hospital of Kunming University of Science and Technology, Kunming, Yunnan, China

Introduction: The vaginal microbiota is a complex and dynamic micro-ecosystem that plays a pivotal role in protecting the host from various pathogens. Previous studies have investigated the diversity of the vaginal microbiome and its association with health outcomes, particularly the development of HPV-related disorders. This study aimed to investigate the correlation between the vaginal microbiota, HPV infection, cervical intraepithelial neoplasias (CINs), and cervical cancers in 69 women.

Methods: DNA was extracted from vaginal samples, followed by HPV genotyping through PCR and sequenced of the16S rRNA gene.

Results: Our results revealed that *Lactobacillus* was the predominant bacterium across all groups, with prevalence rates of 60.2% in women with HPV+, 63.9% in CINI, 97.7% in CINII, 52.0% in CINIII, 36.9% in cervical cancer, and 70.9% in NILM (normal cytology). Additionally, an elevated proportion of Gardnerella was identified as a high-risk bacterium associated with HPV infection, potentially contributing to the progression of cervical lesions. High-risk HPV genotypes, particularly HPV16, 52, and 33, were found to be more prevalent among women with HPV+, CIN, and cervical cancer. We also observed significantly higher alpha diversity in the vaginal microbiome of women with HPV+ and CIN, as indicated by increased Sobs, Shannon, Ace, and Chao indices, compared to the NILM group.

Conclusion: These findings suggest that HPV infection and its associated pathological conditions are closely linked to alterations in the vaginal microbiome. This underscores the need for further research to unravel the intricate relationship between HPV genotype infections and vaginal microbiota, which could pave the way for new diagnostic and therapeutic approaches.

KEYWORDS

human papillomavirus, HPV genotypes, vaginal microbiome, cervical intraepithelial neoplasia, cervical cancer

Introduction

Human papillomavirus (HPV) is a dsDNA, non-enveloped virus that commonly infects the genital tract. It is a major causative agent of cervical intraepithelial neoplasia (CIN) which has the potential to progress to cervical cancer (Gheit, 2019). Cervical carcinoma remains a significant public health concern, particularly in underdeveloped regions, such as Africa where mortality rates are disproportionately high. Cervical cancer ranked among the top three cancers affecting women aged 45-yearsin 146 out of 185 assessed countries. Eswatini reports the highest incidence, with a rate of approximately 6.5%. Notably, China and India together account for over one-third of the global cervical cancer burden, with 106,000 and 97,000 cases reported annually, respectively. Their mortality rates are equally alarming, with approximately 48,000 deaths in China and 60,000 in India each year (Arbyn et al., 2020). The global average age for cervical cancer diagnosis is 53 years, while the average age at death from the disease is59 years (Arbyn et al., 2020). HPV is commonly transmitted to women during sexual intercourse. However, most infections resolve within 2.5 years, depending on factors such as the HPV genotype, viral load, and the host's immune response (Kombe Kombe et al., 2020). Women who achieve viral clearance and maintain normal cervical cytology are at a significantly lower risk of developing cervical intraepithelial neoplasia (CIN) (Gilham et al., 2019; Borgogna et al., 2020). In the case of HPV latency and reactivation, the persistent infection may lead to CINI, CINII, CINIII, or cervical cancer (Gilham et al., 2019).

HPV genotypes have been grouped into high-risk (HR-HPVs) and low-risk (LR-HPVs) depending on their carcinogenicity. For example, HR-HPVs are responsible for persistent cervical infections, lesions, cervical cancers, oropharyngeal cancers, and anogenital cancers, whereas LR-HPVs cause anogenital and cutaneous warts in infected individuals (Kombe Kombe et al., 2020; Usyk et al., 2020). In the case of persistent HPV infections, the viral genome is integrated into the host genome to cause cervical cancer (Usyk et al., 2020). Previous findings show that HPV16 and 18 are the most frequent genotypes responsible for approximately 75% of cervical cancers globally. While HPV31, 33, 35, 45, 52, and 58 vary among different countries and regions, causing 20% of cervical cancers (de Sanjose et al., 2010; Li et al., 2011). HPV31 and 33 are more common in Europe and America, while genotypes 35,45 are more common in Africa, and HPV 58 and 52 in Asia (de Sanjose et al., 2010). Our recent study reported that HPV16, 52, 18, 58, and 53 were the most prevalent genotypes responsible for cervical cancer and other gynecological-related problems in different regions of Yunnan, China (Baloch et al., 2015) (unpublished data). Therefore, regional data on HPV prevalence and its various genotype distributions are important for estimating the impact of vaccines on cervical cancer. In addition to the HPV genotypes, risk factors, such as sexual practices, smoking, contraceptives, etc., were reportedly linked with the HPV infection and its progression to cervical carcinomas (Kombe Kombe et al., 2020).

The vaginal microbiota is a complex community of microorganisms, including bacteria, fungi, protozoa, and viruses. Under normal conditions, these microorganisms maintain a delicate balance, both among themselves and with the host, playing a vital role in maintaining vaginal health (Avitabile et al., 2024). However, when this balance is disrupted, it can lead to the development of various gynecological conditions. In healthy women, the vaginal microbiota is primarily dominated by Lactobacillus species, including L. crispatus, L. gasseri, L. iners, and L. jensenii (Smith and Ravel, 2017). These bacteria produce bacteriocins, hydrogen peroxide, and lactic acid, which help inhibit the growth of pathogenic microbes, regulate the immune response, and enhance the vagina's resistance to infections (Aldunate et al., 2015). Research has found that dysbiosis of the vaginal microbiome in HPV-infected women is linked to several gynecological disorders, with bacterial imbalances playing a key role. One study revealed a significant relationship between HPV infection and variations in the vaginal microbiota's composition (Kombe Kombe et al., 2020).

The vaginal microbiota abundance characterized five microbial community state types (CST) in asymptomatic female cases using 16S rRNA gene sequencing (Ravel et al., 2011). *Lactobacillus* dominated four (CST-I, II, III, and V). A lower abundance of *Lactobacillus* and higher levels of *Gardnerella*, *Mobiluncus*, *Mycoplasma*, and *Prevotella* were characterized in CST-IV cases (Ravel et al., 2011). However, the vaginal microbiome's function and pathophysiological role in HPV infections are largely unknown. It has been suggested that the vaginal microbiome influences HR-HPV persistence infection and the occurrence of CINI, CINII, CINIII, and cervical cancers (Brusselaers et al., 2019). Despite growing evidence, the role of diverse vaginal microbial communities in HPV genotype infections, CIN I, CIN II, CIN III, and cervical cancer remains insufficiently explored. Therefore, this study aimed to investigate whether HPV genotype infections and associated cervical conditions influence the composition and diversity of vaginal microbiome communities in women from Yunnan Province, China.

Methods

Study design

In this study, 69 women, including 16 healthy controls, were recruited from the Out-Patient Department of the First People's Hospital of Yunnan Province between December 2018 and September 2020. Participants were excluded if they met any of the following criteria: vaginal washing within 24 hours prior to sampling, use of vaginal medications within two weeks, sexual activity within three days, oral antibiotic use within two weeks, or a history of cervical therapy. A standardized questionnaire was administered to collect detailed participant information, including ethnicity, education level, age, marital status, smoking and drinking habits, sexual activity, occupation, and other relevant factors.

Ethical statement

This study was approved by the Ethics Committee of the Faculty of Life Science and Technology at Kunming University of Science and Technology, as well as the Center for Disease Control and Prevention (CDC) in Yunnan Province, China. Written informed consent was obtained from all participants, and all experiments were conducted in accordance with the regulations and guidelines of the Ethics Committee.

Sample collection

For sample collection, a cotton swab (Santai, Jiangsu, China) was inserted 2–3 cm into the vagina, gently rotated for 15–20 seconds, and then placed into the 1.5 ml tube with 1.0 ml 0.9% physiological saline. The swab samples containing microbial content were transported to the laboratory in 30 minutes on ice. There, each specimen was centrifuged at 10000× g for 10 min at room temperature. After centrifugation, the supernatant was discarded, and the bacterial sediment was preserved at −80°C for further analysis.

Histopathological analysis

During colposcopy, the cervix was divided into four quadrants, and each was carefully examined individually. Biopsies were taken from areas with visible abnormalities, while a random biopsy was collected from the squamocolumnar junction in quadrants that appeared normal. Endocervical curettage was also performed. Cervical biopsies were obtained using standard 2 mm POI biopsy forceps, which facilitate quick healing and reduce patient discomfort. Histological slides were reviewed by two senior pathologists from Yunnan First People's Hospital. Diagnoses of cervical intraepithelial neoplasia (CIN I–III) and cervical cancer were made based on the World Health Organization's classification system.

HPV genotyping

HPV genomic DNA was extracted from each sample using the TIANamp DNA Extraction Kit (TIANgen Biotech, Co., Hong Kong), following manufacturer instructions. The extracted DNA was amplified through PCR using consensus primers (MY09/11) targeting the HPV L1 region, employing the GenoArray Test Kit (Hybribio, Chaozhou, China). The HPV L1 consensus primer was used to amplify twenty-three HPV genotypes, including thirteen HR-HPVs (HPV16, 18, 31, 33, 35, 39, 45, 51, 52, 56, 58, 59, 68, 53, 66, and 81), and seven LR-HPVs (HPV6, 11, 42, 43, 44, and 61), following manufacturer protocol. Positive controls consisted of PCR-amplified DNA from the HeLa and Caski cell lines, while negative controls included PCR mixture without sample DNA.

16S rRNA gene sequencing and analysis

Genomic DNA from each vaginal sample was extracted using the TIANamp DNA Extraction Kit (TIANgen Biotech, Co., Hong Kong) according to the manufacturer's instructions. After extraction and purification, DNA concentration was quantified with the Qubit v2.0 Fluorometer (Thermo Fisher Sci., USA), and its integrity was confirmed via agarose gel electrophoresis. The KAPA HTP/LTP Library Preparation Kits (Kapa Bio-systems, USA) were used to construct the DNA library for sequencing on the Agilent 2100 (Agilent, US) sequencer. The libraries from each sample were then sequenced on the MiSeq Illumina benchtop System (Illumina, California, USA) at Shanghai Majorbio Bio-Pharm Technology, China. The 16S rRNA gene V4 region was amplified using consensus primers, 5′CCTACGGGNGGC WGCAG3′, and 5′GACTACHVGGGTATCTAATCC3′, targeting the vaginal microbiome. Raw reads were processed by trimming low-quality bases, removing sequences with unknown N bases, adapters, and bases with Phred scores below 20. The resulting paired-end clean reads were aligned against the known microbial genomes in the NCBI using SOAP aligner v2.21 (Li et al., 2008). The sequences mapped to the host genome were abandoned while the subsequent sequences were subjected to downstream analysis.

Taxonomic profiling

Taxonomic profiling was conducted at the family, genus, and species levels. After *de novo* assembling into contigs, all clean reads were clustered into operational taxonomic units (OTUs) with a 97% similarity threshold. Mothur v1.30.1 was used to determine alpha microbial diversity, while beta diversity was determined using Quantitative Insights Into Microbial Ecology (QIIME). Microbial diversity indicators, such as Chao and ACE, were calculated using the Calypso tools (http://www.mothur.org/wiki/Chao; http://www.mothur.org/wiki/Ace). Bacterial abundance was assessed using Shannon and Simpson's indices (http://www.mothur.org/wiki/Shann; http://www.mothur.org/wiki/Simps). Principal coordinates analysis (PCoA) was performed using Bray-Curtis dissimilarity matrices. Linear discriminant analysis (LDA) with effect size (LEfSe) was carried out using the LEfSe program to identify significant differences in microbial communities (Segata et al., 2011). Moreover, Tax4Fun2, a powerful open-source R package, predicts the functional capabilities of microbiomes. Further, we compared the coverage of the pipelines in terms of reads classified and mapped to KEGG and COG databases.

Statistical analysis

The significance of each taxon (phylum, family, genus, and species, between women with HPV+, HPV genotype, CINI, CINII, CINIII, cervical cancer, and NILM) was then determined using a non-parametric unpaired two-sample Wilcoxon test. P-values were FDR-corrected using the Benjamini-Hochberg method. Enriched

features of each group with an adjusted $P < 0.05$ were identified based on the Wilcox rank-sum value. KEGG, COG, and KO were used to determine the organism's features among the HPV+, CINI, CINII, CINIII, cervical cancers, and NILM. The LEfSe analysis explained the differences between the microbiomes (White et al., 2009). To compare the relationships between HPV+, ethnicity, married status, age, smoking, drinking, and the number of sexual partners, Fisher's exact test was used.

Results

Demographic characteristics

The socio-demographic characteristics of the 69 participants are summarized in Table 1. The mean age ± SD of women diagnosed with HPV+, CIN I, CIN II, CIN III, and cervical cancer was 37.14 ± 10.02, 37.17 ± 5.08, 42.93 ± 9.28, and 46.5 ± 4.50 years, respectively. Among the ethnic groups, the majority of participants were of Han ethnicity, comprising 81.2% of HPV+ cases, 71.4% of CIN I, 83.3% of CIN II, and 80% of CIN III cases. In contrast, other ethnicities accounted for 18.8% of HPV+ cases, 28.6% of CIN I, 16.7% of CIN II, and 20% of CIN III cases. Notably, no cervical cancer cases were reported among women from non-Han ethnic groups. The educational background of HPV+ participants revealed that 18.8% had completed primary school or below, 50% had a middle school education, and 31.2% had attained a college education or higher.

Distribution of HR-HPV and LR-HPV

The overall high-risk HPV (HR-HPV) infection rates were 88.46% in HPV+ cases, 28.99% in CIN I, 13.04% in CIN II, and 24.64% in CIN III. In contrast, low-risk HPV (LR-HPV) infection rates were 7.25% in CIN I, 4.35% in CIN II, and 4.35% in CIN III. Notably, no LR-HPV infections were detected in cervical cancer cases (Table 2). Among the HR-HPV types, HPV52 showed the highest prevalence at 23.08%, followed by HPV16, which was found in 20% of CIN I cases and 25% of CIN III cases. In cervical cancer cases, two HR-HPV genotypes—HPV16 and HPV52—were identified, while no LR-HPV types were reported.

TABLE 1 Socio–demographic characteristics of the 69 participant.

Parameter	HPV+ (n=16)	CINI (n=14)	CINII (n=6)	CINIII (n=15)	Cervical cancer (n=2)	NILM (n=16)
Age						
Mean age ± SD	36.13 ± 9.40	37.14 ± 10.02	37.17 ± 5.08	42.93 ± 9.28	46.5 ± 4.50	35.75 ± 7.94
Age range (years)	22 ~ 55	22 ~ 53	29 ~ 45	28 ~ 59	42 ~ 51	23 ~ 49
Ethnic, n (%)						
Han	13 (81.2)	10 (71.4)	5 (83.3)	12 (80)	2 (100)	11 (68.8)
Others	3 (18.8)	4 (28.6)	1 (16.7)	3 (20)	0 (0)	5 (31.2)
Education level						
Primary/below	3 (18.8)	2 (14.3)	2 (33.3)	3 (20)	1 (50)	4 (25)
Middle	8 (50)	8 (57.1)	3 (50)	6 (40)	1 (50)	7 (43.8)
College/above	5 (31.2)	4 (28.6)	1 (16.7)	6 (40)	0 (0)	5 (31.2)
Marriage status						
Married	14 (87.5)	12 (85.7)	6 (100)	14 (93.3)	2 (100)	16 (100)
Unmarried	2 (12.5)	1 (7.1)	0 (0)	1 (6.7)	0 (0)	0 (0)
Smoking						
Yes	0 (0)	0 (0)	0 (0)	1 (6.7)	0 (0)	1 (6.2)
No	16 (100)	14 (100)	6 (100)	14 (93.3)	2 (100)	15 (93.8)
Drinking						
Yes	0 (0)	1 (7.1)	0 (0)	2 (13.3)	0 (0)	1 (6.2)
No	16 (100)	13 (92.9)	6 (100)	13 (86.7)	2 (100)	15 (93.8)
Sexual partner						
1	13 (81.3)	11 (78.6)	4 (66.7)	12 (80)	2 (100)	15 (93.8)
2 or more	3 (18.7)	3 (21.4)	2 (33.3)	3 (20)	0 (0)	1 (6.2)

All the data is represented as mean ± standard deviation (± SD) and the p-value < 0.05 was considered significant.

TABLE 2 Distribution of HR-HPV and LR-HPV genotypes in women diagnosed with various CIN, and cervical cancer.

HPV type	HPV+ 26 (%)	CINI, 25 (%)	CINII, 12 (%)	CINIII, 20 (%)	Cervical cancer, 2 (%)	Overall 85 (%)
HR-HPV						
HPV-16	3 (11.54)	5 (20)	1 (8.33)	5 (25)	1 (50)	15
HPV-18	1 (3.85)	1 (4)	0 (0)	1 (5)	0 (0)	3
HPV-31	0 (0)	0 (0)	0 (0)	1 (5)	0 (0)	1
HPV-33	3 (11.54)	2 (8)	1 (8.33)	4 (20)	0 (0)	10
HPV-34	1 (3.85)	0 (0)	0 (0)	0 (0)	0 (0)	1
HPV-35	1 (3.85)	2 (8)	0 (0)	0 (0)	0 (0)	3
HPV-51	1 (3.85)	3 (12)	1 (8.33)	0 (0)	0 (0)	5
HPV-52	6 (23.08)	2 (8)	1 (8.33)	2 (10)	1 (50)	12
HPV-53	2 (7.69)	2 (8)	0 (0)	0 (0)	0 (0)	4
HPV-58	1 (3.85)	1 (4)	2 (16.66)	4 (20)	0 (0)	8
HPV-59	1 (3.85)	1 (4)	1 (8.33)	0 (0)	0 (0)	3
HPV-66	1 (3.85)	0 (0)	2 (16.66)	0 (0)	0 (0)	3
HPV-68	2 (7.69)	1 (4)	0 (0)	0 (0)	0 (0)	3
LR-HPV						
HPV-6	0 (0)	1 (4)	0 (0)	0 (0)	0 (0)	1
HPV-11	0 (0)	0 (0)	1 (8.33)	0 (0)	0 (0)	1
HPV-43	1 (3.85)	0 (0)	0 (0)	0 (0)	0 (0)	1
HPV-55	0 (0)	0 (0)	1 (8.33)	0 (0)	0 (0)	1
HPV-61	1 (3.85)	0 (0)	1 (8.33)	0 (0)	0 (0)	2
HPV-72	0 (0)	0 (0)	0 (0)	2 (10)	0 (0)	2
HPV-81	1 (3.85)	1 (4)	0 (0)	1 (5)	0 (0)	3
HPV-82	0 (0)	1 (4)	0 (0)	0 (0)	0 (0)	1
HPV-83	0 (0)	1 (4)	0 (0)	0 (0)	0 (0)	1
HPV-84	0 (0)	1 (4)	0 (0)	0 (0)	0 (0)	1

HR-HPV, high-risk HPV genotypes; LR-HPV, low-risk HPV genotypes.

In this study, the overall HR-HPV infection rate was 83.53%, while 16.47% of infections were attributed to LR-HPV. Among the HR-HPV genotypes, HPV16 was the most prevalent, detected in 15 cases across women with HPV+, CIN I, CIN II, CIN III, and cervical cancer. This was followed by HPV52 and HPV33, which were identified in twelve and ten cases, respectively. Specifically, six cases of HR-HPV52 were found in the HPV+ group, while five cases of HPV16 were detected in both CIN I and CIN III groups.

Vaginal microbiota

A 16S rRNA-targeted metagenomics analysis was performed to determine bacterial abundance of each participant. A heatmap diagram depicts different bacterial communities in women with HPV+, CINI, CINII, CINIII, cervical cancers, and control. According to the heatmap diagram, the bacteria with the highest abundance belonged to the species unclassified of the genus *Lactobacillus*. The bar color represents the richness of bacterial communities ranging from bottom to top (Figure 1). The details of the bacterial abundance at species and genus levels are shown in Figure 2.

The details of the α-diversity indicators (i.e., Sobs, Shannon, Simpson, Ace, Chao, Coverage, Shannon, and Simpson) of the women with HPV+, CINI, CINII, CINIII, cervical cancers, and NILM at the species level are shown in Supplementary Table S1. In HPV+ cases, the Sobs index was significantly higher (62.63 ± 36.49) than those in CINI (42.64 ± 23.62), CINII (28.17 ± 13.41), and the control (40.25 ± 19.39) (p = 0.001), indicating diverse bacterial communities. In contrast, the Sobs index was higher (70.80 ± 41.08) in CINIII and cervical cancer (76.50 ± 13.50) than in the rest of the groups. The Shannon index (0.68 ± 0.51) in HPV+ women was significantly higher than CINII (0.13 ± 0.07) and control (0.67 ± 0.56), but less than CINI (0.72 ± 0.86), CINIII (0.88 ± 0.71), and cervical cancer (1.82 ± 0.67) (p = <0.001), suggesting increased vaginal microbiota in HPV+ cases and decreased in NILM. In brief,

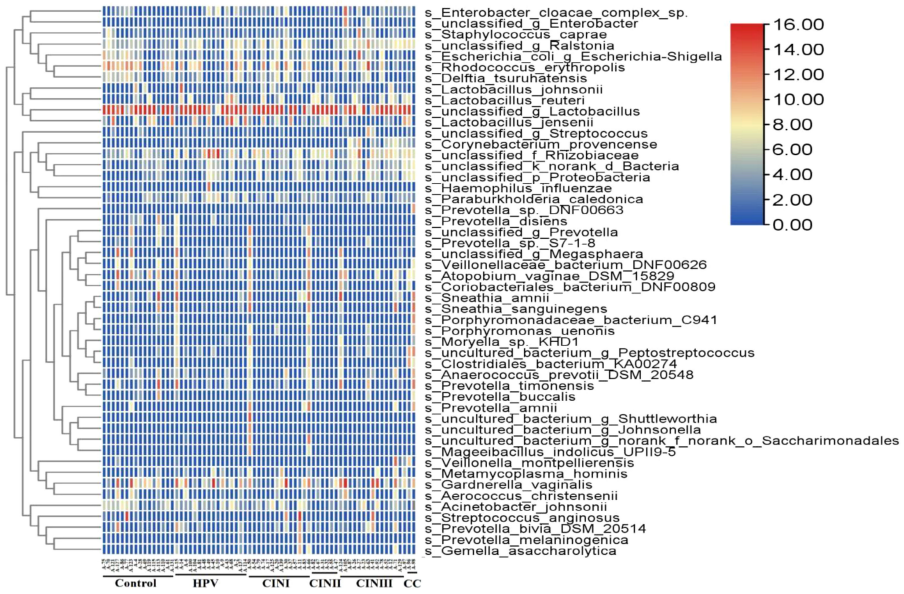

FIGURE 1
Heatmap shows diverse microbial communities in women with HPV+, CINI, CINII, CINIII, cervical cancers, and NILM (control). The color bar from red to blue represents the relative abundance of bacterial species from high to low.

diversity indicators, Ace, Chao, and Coverage, showed significantly different (p = <0.001) bacterial communities among the women with different pathological conditions. Moreover, the details of the alpha-microbial diversity indicators at the genus level are shown in Supplementary Table S2. Furthermore, the bacterial β-diversity profile (PCoA) among HPV+, CINs, cervical cancer cases, and NILM is shown in Figure 3A.

Taxon identity and abundance were also established based on OTU levels. Identical OTU, species abundance, and sobs index was found in the vaginal microbiome of women with HPV+, CINI, CINII, CINIII, cervical cancer, and NILM (Figure 3B). The highest identical bacterial abundance was found in women with CINIII (1531), followed by HPV+ (1139), CINI (701), cervical cancer (223), and CINII (215).

Understanding microbial alteration in different groups

To investigate the correlation in vaginal microbiota in HPV+, CINI, CINII, CINIII, cervical cancers, and NILM, LEfSe analysis was performed (Figure 3C). The LDA scores showed that unclassified species within the genus *Lactobacillus* were the most dominant bacteria in CINI, whereas uncultured species within the genus *Paenochrobactrum* were distinct among all groups. In the HPV+, *Lactobacillus reuteri* was predominant, followed by Burkholderia caballeronia paraburkholderia, *Tepidiphilus*, and unclassified species in the genus Norank. Interestingly, *Lactobacillus fermentum* was the only species present in the CINI. In the CINII, only two taxa were identified: unclassified species within the genus *Lactobacillus* and *Capnocytophaga*. For CINIII, the family *Burkholderiaceae* and unclassified species within the genus *Ralstonia* were the most common, followed by the family *Corynebacteriaceae* and the genus *Corynebacterium*.

Discussion

The vaginal microbiome has garnered growing interest for its potential influence on the genital tract environment, its critical role in female reproductive health, and its association with HPV infection (Anahtar et al., 2018). HPV infection is widespread, with its prevalence and impact varying significantly across and within regions. These differences are influenced by factors such as age, gender, geographical location, lifestyle, and socio-economic conditions (LeConte et al., 2018). Aside from cervical cancer and its precursors, growing evidence suggests that HPV infection plays a crucial role in diseases of the lower genital tract, particularly in the development of vaginal and vulvar precancerous conditions (Bogani et al., 2023). In our study, the mean age (46.5 ± 4.50 years), ranging from 42–51 years of participants for cervical cancer diagnosis, was lower when compared to other life-threatening cancers (Yang et al., 2004).

The management of HPV-related lesions continues to be a global challenge, with significant implications for patient prognosis. Recent studies, such as the work by Golia D'Augè et al. (2024), highlight the growing importance of a personalized, tailored approach to managing HPV-related cervical lesions. Advances in our understanding of HPV pathogenesis, combined with improved diagnostic tools, now allow for more precise management strategies. These strategies consider factors such as lesion severity, HPV type, vaccination status, and the patient's immune profile, all of which contribute to the optimal approach for treatment. Tailored management not only improves the prognosis of patients with

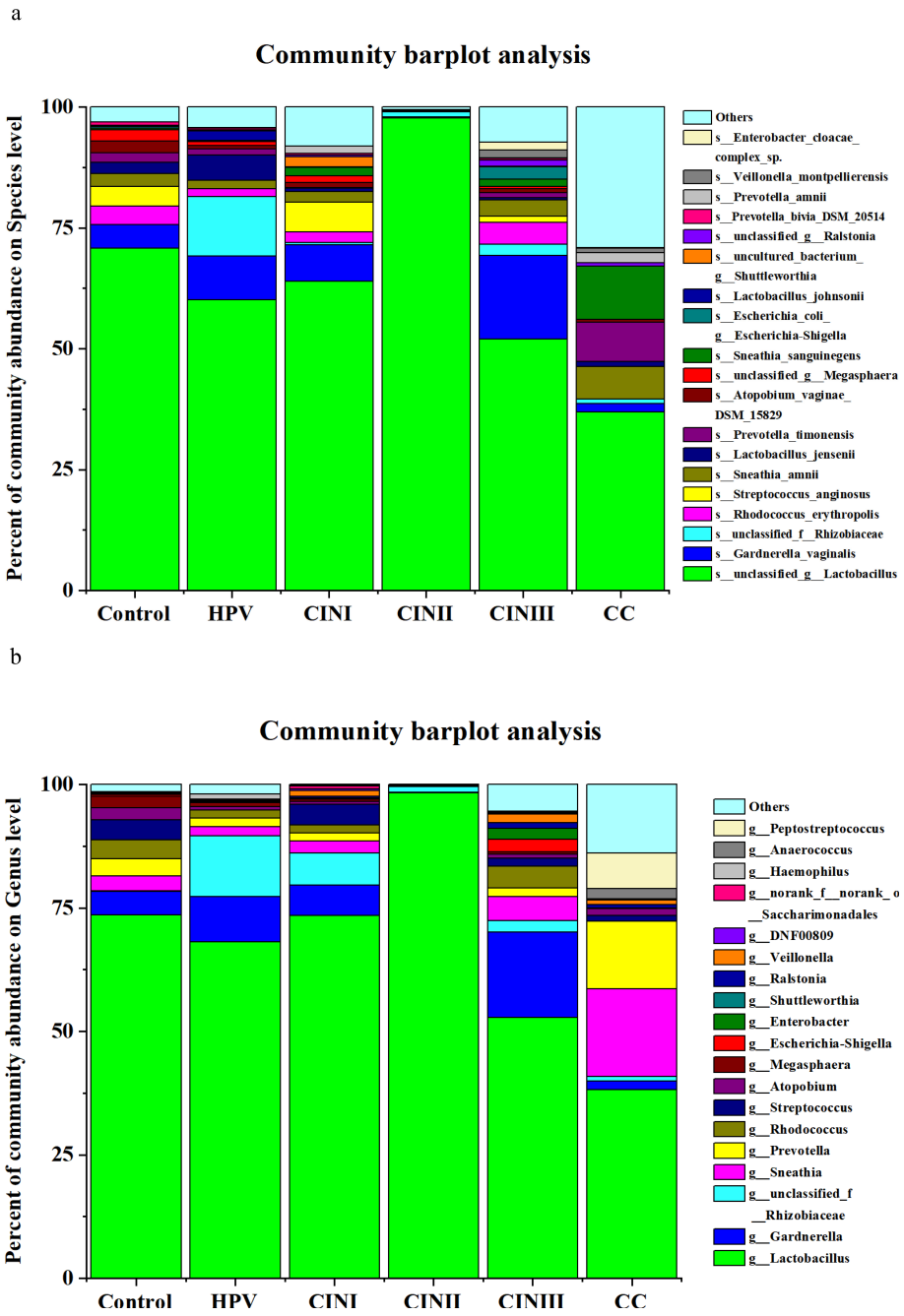

FIGURE 2
The vaginal microbiota in women with HPV+, CINI, CINII, CINIII, cervical cancers, and NILM (control) at species **(A)** and genus levels **(B)**. (the participants received no treatment till sample collection).

HPV-related lesions but also has the potential to prevent the progression of lesions to cervical cancer. In light of these developments, our study aims to contribute to the ongoing conversation by further elucidating the role of the vaginal microbiota in influencing the persistence and progression of HPV infections.

According to the predictions, the dynamics of HPV transmission and the consequences of HPV infection in developing and underdeveloped countries would be similar to those in developed countries (WHO, 2022). It is worth mentioning that there was only one CINI woman with LR-HPV6 infection. According to our findings, HPV16 genotype infection was much less than that reported in Beijing in 2014 and 2015 (Shen et al., 2018). A study identified 396 HPV genotypes in infected people using metagenomic sequencing (Bzhalava et al., 2014). Among them, 14 genotypes were HR-HPV due to their oncogenic potential, with HPV16 being the most prevalent genotype, in line with previous findings (Crow, 2012).

In this cohort, we explored the diverse vaginal microbiome in women with HPV+, CINI, CINII, CINIII, cervical cancers, and

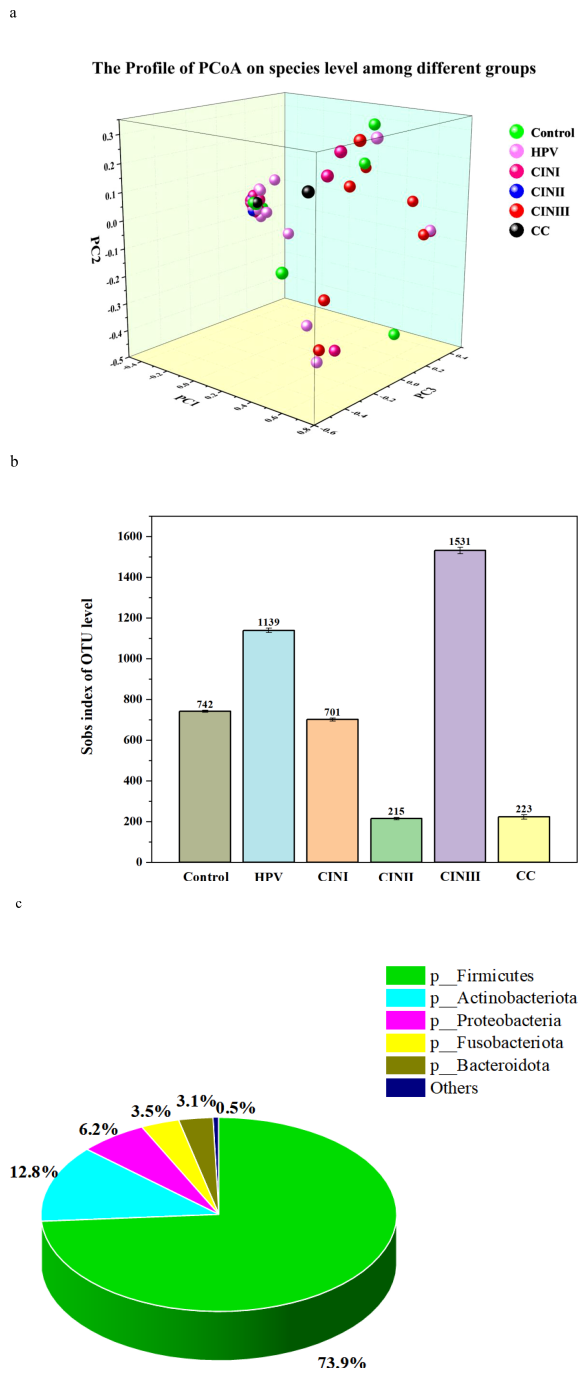

FIGURE 3
PCoA profile, Sobs index of OUT level, and taxonomic biomarkers LEfSe analysis of the cohort associated with HPV+, CINI, CINII, CINIII, cervical cancers, and NILM (control). **(A)** PCoA profile of the cohort associated with HPV infection status. Each dot presented a sample, and the color was according to each group, i.e., HPV+, CINI, CINII, CINIII, cervical cancers, and NILM (control). **(B)** The alpha-diversity (Sobs index of OUT level) between HPV+, CINI, CINII, CINIII, cervical cancers, and NILM (control). **(C)** Taxonomic biomarkers: the LEfSe analysis among HPV+, CINI, CINII, CINIII, cervical cancers, and NILM (control).

NILM through high-throughput sequencing. Our findings were consistent with another study that found *Lactobacillus* to be the dominant genus (Anahtar et al., 2018), creating an acidic environment via lactic acid production to protect women from opportunistic pathogens and HPV infection. The increased *Gardnerella vaginalis*, *Rhizobiaceae*, and decreased *Peptostreptococcus* and *Enterobacter cloacae complex* were closely associated with HPV-associated gynecological disorders. The vaginal microbiome is primarily dominated by certain *Lactobacillus* species like *L. crispatus*, *L. gasseri*, *L. jensenii*, and *L. iners* (Borgogna et al., 2020), which maintain an acidic environment through lactic acid production. In contrast, Lee and Collogue reported a lower proportion of *Lactobacillus* in HPV-infected women (Lee et al., 2013). Studies also reported that *Lactobacillus* could inhibit the growth of other opportunistic pathogens by protecting the lower reproductive tract from infection (Martin and Marrazzo, 2016; Nunn and Forney, 2016). In consistent with our study, *Lactobacillus* abundance was lower in HPV16-infected individuals than in NILM. *Lactobacillus* normally adheres to the genital tract epithelial cells and secretes lactic acid via glycogen decomposition, maintaining a mild acidic vaginal environment to prevent pathogenic microbes from colonizing. These bacteria also produce antimicrobial secondary metabolites such as bacteriocins to prevent and inhibit pathogenic microbes from colonization, thereby maintaining a normal environment (Boris and Barbés, 2000; Tachedjian et al., 2017). In contrast, reduced *Lactobacillus* promotes opportunistic bacterial growth such as *Fusobacterium*, *Gardnerella*, *Mobiluncus*, *Parvimonas*, *Peptostreptococcus*, and *Prevotella* in HPV16-infected women. It has been shown that *Gardnerella* may produce virulence factors, adhesion, and cytotoxin (Nowak et al., 2018) that inhibit the growth of pathogens, further suggesting its potential role in vaginal dysbiosis.

Generally, less diversity in microbial communities signifies good health (Turnbaugh et al., 2007). The sob, Ace, and Chao indexes of α-diversity of the vaginal microbiome at the species and genus levels showed an increasing trend among women with HPV+, CINI, CINII, CINIII, and cervical cancers and NILM. The sobs, Shannon, Ace, and Chao coverage α-diversity identified at the species level among the women with various gynecological disorders and NILM significantly increased estimated OTUs compared with those in NILM. On the other hand, the Simpson, Shannoneven, and Simpsoneven indexes of α-microbial diversity at the species level showed no significant difference (p = 0.094; p = 0.096; p = 0.106). In contrast, we did not observe any significant difference in Shannon, Simpson, Shannoneven, and Simpsoneven indicators at the genus level. We further analyzed β-diversity to evaluate species complexity among HPV+, CINI, CINII, CINIII, cervical cancers, and NILM. Thus, our findings suggest that maintaining a stable vaginal microbiome may potentially prevent HPV infection. Globally, managing HPV-related lesions remains a significant challenge. In the future, modulating the vaginal microbiome could offer a promising strategy for this patient group, providing a novel approach to overcoming current therapeutic limitations.

Conclusions

This study revealed significant alterations in the vaginal microbiota of women with HPV infection, CIN I, CIN II, CIN III,

and cervical cancer. Specifically, an increased presence of Lactobacillus and a reduced abundance of the Enterobacter cloacae complex, Peptostreptococcus, and other microorganisms were observed. These findings suggest that disruptions in the vaginal microbiota may contribute to persistent HPV infection, progression to cervical intraepithelial neoplasia (CIN), and the development of cervical cancer. Moreover, infections with multiple HPV genotypes appear to influence the composition of the vaginal microbiome, notably affecting organisms such as Gardnerella vaginalis and members of the Rhizobiaceae family. Further research is essential to elucidate the complex interplay between persistent HPV infection and vaginal microbiota diversity, paving the way for the discovery of affordable therapeutic interventions in the future.

Data availability statement

The data presented in the study are deposited in the https://www.ncbi.nlm.nih.gov/, accession number PRJNA799456.

Ethics statement

The studies involving humans were approved by The Ethics Committee of the Faculty of Life Science and Technology, Kunming University of Science and Technology, and the Center for Disease Control and Prevention (CDC), Yunnan Province, China, approved this cohort. Written consent was obtained from each participant. All the experiments were completed per the regulations of the Ethics Committee. The studies were conducted in accordance with the local legislation and institutional requirements. The participants provided their written informed consent to participate in this study.

Author contributions

YL: Writing – original draft. XW: Writing – review & editing.

Funding

The author(s) declare financial support was received for the research, authorship, and/or publication of this article. This study was supported by a grant from Projects: KHBS-2022-008, 2022-KHRCBZ-C03, 2023YJZX-FC17, 202302AA310044, 82360489, Yunnan Provincial Key Laboratory of Clinical Virology 14 (202205AG070053-10), and Central Government Guidance Fund for Local Science and Technology Development(202407AB110013). All funders have been credited.

Acknowledgments

We thank Dr. Songmei Shan, Dr. Mei Yang, and Dr. Lu Xu from the Department of gynecology, the First People's First Hospital of Yunnan Province, for helping with sample collection.

Conflict of interest

The authors declare that the research was conducted in the absence of any commercial or financial relationships that could be construed as a potential conflict of interest.

Publisher's note

Supplementary material

The Supplementary Material for this article can be found online at: https://www.frontiersin.org/articles/10.3389/fcimb.2024.1483544/full#supplementary-material

References

Aldunate, M., Srbinovski, D., Hearps, A. C., Latham, C. F., Ramsland, P. A., Gugasyan, R., et al. (2015). Antimicrobial and immune modulatory effects of lactic acid and short chain fatty acids produced by vaginal microbiota associated with eubiosis and bacterial vaginosis. *Front. Physiol.* 6, 164. doi: 10.3389/fphys.2015.00164

Anahtar, M. N., Gootenberg, D. B., Mitchell, C. M., and Kwon, D. S. (2018). Cervicovaginal microbiota and reproductive health: the virtue of simplicity. *Cell Host Microbe* 23, 159–168. doi: 10.1016/j.chom.2018.01.013

Arbyn, M., Weiderpass, E., Bruni, L., de Sanjose, S., Saraiya, M., Ferlay, J., et al. (2020). Estimates of incidence and mortality of cervical cancer in 2018: a worldwide analysis. *Lancet Glob Health* 8, e191–e203. doi: 10.1016/S2214-109X(19)30482-6

Avitabile, E., Menotti, L., Croatti, V., Giordani, B., Parolin, C., and Vitali, B. (2024). Protective mechanisms of vaginal lactobacilli against sexually transmitted viral infections. *Int. J. Mol. Sci.* 25 (17), 9168. doi: 10.3390/ijms25179168

Baloch, Z., Yue, L., Yuan, T., Feng, Y., Tai, W., Liu, Y., et al. (2015). Zhang AM et al: Status of Human Papillomavirus Infection in the Ethnic Population in Yunnan Province, China. *BioMed. Res. Int.* 2015, 314815. doi: 10.1155/2015/314815

Bogani, G., Sopracordevole, F., Ciavattini, A., Ghelardi, A., Vizza, E., Vercellini, P., et al. (2023). De Vincenzo R et al: HPV-related lesions after hysterectomy for high-grade cervical intraepithelial neoplasia and early-stage cervical cancer: A focus on the potential role of vaccination. *Tumori J.* 110, 139–145. doi: 10.1177/03008916231208344

Borgogna, J. C., Shardell, M. D., Santori, E. K., Nelson, T. M., Rath, J. M., Glover, E. D., et al. (2020). The vaginal metabolome and microbiota of cervical HPV-positive and HPV-negative women: a cross-sectional analysis. *Bjog* 127, 182–192. doi: 10.1111/1471-0528.15981

Boris, S., and Barbés, C. (2000). Role played by lactobacilli in controlling the population of vaginal pathogens. *Microbes Infect.* 2, 543–546. doi: 10.1016/S1286-4579(00)00313-0

Brusselaers, N., Shrestha, S., van de Wijgert, J., and Verstraelen, H. (2019). Vaginal dysbiosis and the risk of human papillomavirus and cervical cancer: systematic review and meta-analysis. *Am. J. Obstet Gynecol* 221, 9–18.e18. doi: 10.1016/j.ajog.2018.12.011

Bzhalava, D., Muhr, L. S., Lagheden, C., Ekstrom, J., Forslund, O., Dillner, J., et al. (2014). Deep sequencing extends the diversity of human papillomaviruses in human skin. *Sci. Rep.* 4, 5807. doi: 10.1038/srep05807

Crow, J. (2012). HPV: The global burden. *Nature* 488, S2–S3. doi: 10.1038/488S2a

de Sanjose, S., Quint, W. G., Alemany, L., Geraets, D. T., Klaustermeier, J. E., Lloveras, B., et al. (2010). Human papillomavirus genotype attribution in invasive cervical cancer: a retrospective cross-sectional worldwide study. *Lancet Oncol.* 11, 1048–1056. doi: 10.1016/S1470-2045(10)70230-8

Gheit, T. (2019). Mucosal and cutaneous human papillomavirus infections and cancer biology. *Front. Oncol.* 9, 355. doi: 10.3389/fonc.2019.00355

Gilham, C., Sargent, A., Kitchener, H. C., and Peto, J. (2019). HPV testing compared with routine cytology in cervical screening: long-term follow-up of ARTISTIC RCT. *Health Technol. Assess.* 23, 1–44. doi: 10.3310/hta23280

Golia D'Augè, T., Cuccu, I., Etrusco, A., D'Amato, A., Laganà, A. S., D'Oria, O., et al. (2024). State of the art on HPV-related cervical lesions. *Ital. J. Gynaecology Obstet.* 36 (2), 135-137. doi: 10.36129/jog.2024.161

Kombe Kombe, A. J., Li, B., Zahid, A., Mengist, H. M., Bounda, G. A., Zhou, Y., et al. (2020). Epidemiology and burden of human papillomavirus and related diseases, molecular pathogenesis, and vaccine evaluation. *Front. Public Health* 8, 552028. doi: 10.3389/fpubh.2020.552028

LeConte, B. A., Szaniszlo, P., Fennewald, S. M., Lou, D. I., Qiu, S., Chen, N. W., et al. (2018). Differences in the viral genome between HPV-positive cervical and oropharyngeal cancer. *PLoS One* 13, e0203403. doi: 10.1371/journal.pone.0203403

Lee, J. E., Lee, S., Lee, H., Song, Y. M., Lee, K., Han, M. J., et al. (2013). Association of the vaginal microbiota with human papillomavirus infection in a Korean twin cohort. *PLoS One* 8, e63514. doi: 10.1371/journal.pone.0063514

Li, N., Franceschi, S., Howell-Jones, R., Snijders, P. J., and Clifford, G. M. (2011). Human papillomavirus type distribution in 30,848 invasive cervical cancers worldwide: Variation by geographical region, histological type and year of publication. *Int. J. Cancer* 128, 927–935. doi: 10.1002/ijc.v128.4

Li, R., Li, Y., Kristiansen, K., and Wang, J. (2008). SOAP: short oligonucleotide alignment program. *Bioinformatics* 24, 713–714. doi: 10.1093/bioinformatics/btn025

Martin, D. H., and Marrazzo, J. M. (2016). The vaginal microbiome: current understanding and future directions. *J. Infect. Dis.* 214 Suppl 1, S36–S41. doi: 10.1093/infdis/jiw184

Nowak, R. G., Randis, T. M., Desai, P., He, X., Robinson, C. K., Rath, J. M., et al. (2018). Higher levels of a cytotoxic protein, vaginolysin, in lactobacillus-deficient community state types at the vaginal mucosa. *Sex Transm Dis.* 45, e14–e17. doi: 10.1097/OLQ.0000000000000774

Nunn, K. L., and Forney, L. J. (2016). Unraveling the dynamics of the human vaginal microbiome. *Yale J. Biol. Med.* 89, 331–337.

Ravel, J., Gajer, P., Abdo, Z., Schneider, G. M., Koenig, S. S., McCulle, S. L., et al. (2011). Tacket CO et al: Vaginal microbiome of reproductive-age women. *Proc. Natl. Acad. Sci. U. S. A.* 108 Suppl 1, 4680–4687. doi: 10.1073/pnas.1002611107

Segata, N., Izard, J., Waldron, L., Gevers, D., Miropolsky, L., Garrett, W. S., et al. (2011). Metagenomic biomarker discovery and explanation. *Genome Biol.* 12, R60. doi: 10.1186/gb-2011-12-6-r60

Shen, J., Gao, L. L., Zhang, Y., Han, L. L., and Wang, J. D. (2018). Prevalence of high-risk HPV and its distribution in cervical precancerous lesions among 35-64 years old women who received cervical cancer screening in Beijing. *Zhonghua Yu Fang Yi Xue Za Zhi* 52, 493–497. doi: 10.3760/cma.j.issn.0253-9624.2018.05.008

Smith, S. B., and Ravel, J. (2017). The vaginal microbiota, host defence and reproductive physiology. *J. Physiol.* 595, 451–463. doi: 10.1113/tjp.2017.595.issue-2

Tachedjian, G., Aldunate, M., Bradshaw, C. S., and Cone, R. A. (2017). The role of lactic acid production by probiotic Lactobacillus species in vaginal health. *Res. Microbiol.* 168, 782–792. doi: 10.1016/j.resmic.2017.04.001

Turnbaugh, P. J., Ley, R. E., Hamady, M., Fraser-Liggett, C. M., Knight, R., and Gordon, J. I. (2007). The human microbiome project. *Nature* 449, 804–810. doi: 10.1038/nature06244

Usyk, M., Zolnik, C. P., Castle, P. E., Porras, C., Herrero, R., Gradissimo, A., et al. (2020). Cervicovaginal microbiome and natural history of HPV in a longitudinal study. *PLoS Pathog.* 16, e1008376. doi: 10.1371/journal.ppat.1008376

White, J. R., Nagarajan, N., and Pop, M. (2009). Statistical methods for detecting differentially abundant features in clinical metagenomic samples. *PLoS Comput. Biol.* 5, e1000352. doi: 10.1371/journal.pcbi.1000352

WHO (2022). *WHO Cervical cancer: Key facts*. Available online at: https://www.who.int/news-room/fact-sheets/detail/cervical-cancer (Accessed June 7, 2022).

Yang, B. H., Bray, F. I., Parkin, D. M., Sellors, J. W., and Zhang, Z. F. (2004). Cervical cancer as a priority for prevention in different world regions: an evaluation using years of life lost. *Int. J. Cancer* 109, 418–424. doi: 10.1002/ijc.v109:3

frontiers | Frontiers in Cellular and Infection Microbiology

TYPE Review
PUBLISHED 21 January 2025
DOI 10.3389/fcimb.2024.1529441

OPEN ACCESS

EDITED BY
Maurizio Sanguinetti,
Catholic University of the Sacred Heart, Italy

REVIEWED BY
Nadine Laure Samara,
National Institutes of Health (NIH),
United States
Peng Li,
Westlake University, China

*CORRESPONDENCE
Dawit Kidane
dawit.kidane-mulat@howard.edu

RECEIVED 16 November 2024
ACCEPTED 19 December 2024
PUBLISHED 21 January 2025

CITATION
Shahi A and Kidane D (2025) Decoding mitochondrial DNA damage and repair associated with *H. pylori* infection. *Front. Cell. Infect. Microbiol.* 14:1529441. doi: 10.3389/fcimb.2024.1529441

Decoding mitochondrial DNA damage and repair associated with *H. pylori* infection

Aashirwad Shahi and Dawit Kidane*

Department of Physiology and Biophysics, College of Medicine, Howard University, Washington, DC, United States

Mitochondrial genomic stability is critical to prevent various human inflammatory diseases. Bacterial infection significantly increases oxidative stress, driving mitochondrial genomic instability and initiating inflammatory human disease. Oxidative DNA base damage is predominantly repaired by base excision repair (BER) in the nucleus (nBER) as well as in the mitochondria (mtBER). In this review, we summarize the molecular mechanisms of spontaneous and *H. pylori* infection-associated oxidative mtDNA damage, mtDNA replication stress, and its impact on innate immune signaling. Additionally, we discuss how mutations located on mitochondria targeting sequence (MTS) of BER genes may contribute to mtDNA genome instability and innate immune signaling activation. Overall, the review summarizes evidence to understand the dynamics of mitochondria genome and the impact of mtBER in innate immune response during *H. pylori*-associated pathological outcomes.

KEYWORDS

mitochondrial DNA damage and repair, *H. pylori*, genomic instability, cytosolic DNA, innate immune signaling, Type I interferon response, base excision DNA repair, cGAS-STING

Introduction

Mitochondria are essential organelles responsible for energy production and maintaining calcium homeostasis, lipid, and amino acid metabolism (Casanova et al., 2023). The human mitochondria DNA (mtDNA) is present in multiple copies per cell (Filograna et al., 2021). Targeting mitochondria has emerged as a key strategy for bacteria to hijack host cell physiology and promote infection (Blanke, 2005; Fielden et al., 2017). Numerous pathogenic bacteria have evolved strategies to subvert the mitochondrial functions of host cells to support their own proliferation and dissemination (Galmiche et al., 2000; Fischer et al., 2004; Stavru et al., 2011). In addition, bacteria can modulate mitochondrial functions to access nutrients and/or evade the host's immune system (Spier et al., 2019). Infection by extracellular pathogens including *H. pylori* is able to change the mitochondrial metabolic and oxidative profile of infected cells (Andrieux et al., 2021). Furthermore, a study has shown that *H. pylori* infection induces genetic dysfunction in both nDNA and mtDNA (Hiyama et al., 2003).

Notably, mtDNA is a hotspot for constant insult from both exogenous and endogenous stresses (Alexeyev et al., 2013). Cellular and biochemical evidence suggests that mtDNA is more susceptible to oxidized DNA damages than nuclear DNA due to its proximity to the sites of oxidative phosphorylation and lack of protection by histones (Yakes and Van Houten, 1997; Druzhyna et al., 2008). Excessive accumulation of mtDNA damages leads to mitochondrial dysfunction and provokes the pathogenesis of many human diseases, including neurodegeneration, cancer, and diabetes (Wallace, 2005; Nakabeppu et al., 2007; Llanos-Gonzalez et al., 2019). Oxidative DNA damage lesions in mtDNA and/or mtDNA replication blocks are removed by different types of DNA damage repair enzymes (LeDoux et al., 1992; Zhao and Sumberaz, 2020). Most of the repair proteins and/or enzymes are imported from the nucleus, where they process oxidative mtDNA lesions and promote repair (Bohr, 2002; de Souza-Pinto et al., 2009; Gredilla, 2010). However, the loss of these nuclear and mitochondria-encoded repair proteins significantly impairs repair efficiency in mitochondria (Lia et al., 2018). Therefore, the role and function of mitochondrial oxidative DNA damage repair are not expected to be independent of nuclear BER.

In eukaryotic cells, mtDNA molecules are organized into several hundred nucleoids (Legros et al., 2004; Wang and Bogenhagen, 2006; Bogenhagen, 2012; Prachar, 2016), which function as units of mtDNA propagation for replication, segregation, and gene expression (Spelbrink, 2010; Ban-Ishihara et al., 2013; Kolesnikov, 2016). Several proteins are involved in maintaining the integrity of mitochondrial genome replication, including DNA polymerase γ (POLG), TWINKLE (DNA helicase), mitochondrial RNA polymerase (POLRMT), mitochondrial single-stranded DNA-binding protein (mtSSB), RNASEH1, DNA ligase III, mitochondrial genome maintenance exonuclease1 (MGME1), flap endonuclease 1 (FEN1), and topoisomerase (Sharma and Sampath, 2019; Fontana and Gahlon, 2020). POLG plays a significant role in maintaining mtDNA replication integrity and participates in base excision repair. Moreover, POLG has 3′–5′ exonuclease and 5′-deoxyribose phosphate (dRP) activities associated with its catalytic subunit (Kaguni, 2004; Graziewicz et al., 2006). POLG's polymerase activity is critical to synthesize DNA, and it also has a weak dRP lyase function that is complemented by DNA polymerase beta (POLB) dRP lyase activity (Longley et al., 1998; Sykora et al., 2017). Furthermore, the primase activity of PrimPol initiates *de novo* DNA synthesis using deoxynucleotide while discriminating against ribonucleotides (Martinez-Jimenez et al., 2018; Diaz-Talavera et al., 2022). Other DNA repair factors, such as mitochondrial single-stranded binding protein 1 (SSBP1), protect the active replicative DNA regions (Guilliam et al., 2015). Based on several studies, three different models have been proposed for mtDNA replication (Robberson et al., 1972; McKinney and Oliveira, 2013). Among these three models, the strand-displacement model (SDM) is the most accepted model because it best explains the dynamics of mtDNA replication. According to this model, replication starts at the oriH site and proceeds unidirectionally until it reaches the origin of light strand (oriL). At this point, the synthesis of light strand begins in the opposite direction, continuing until the replication of both strands is complete. Importantly, mutations in the mitochondrial replisome's proteins POLG, TFAM, and MGME1 genes are associated with the accumulation of mtDNA deletions that may also increase susceptibility for infection-induced chronic-inflammation-associated disease (Spelbrink et al., 2001; Longley et al., 2006; Nicholls et al., 2014; Fontana and Gahlon, 2020). In the next section of this manuscript, we will address key questions such as (i) how do host cells handle oxidative stress-associated mtDNA damage via BER in the presence and absence of bacterial infection, (ii) how do oxidative-stress-induced base lesions or repair intermediates impact mtDNA replication dynamics, and (iii) does infection by extracellular bacteria, such as *H. pylori*, induce mtDNA-mediated innate immune signaling?

mtDNA damage and BER in mitochondria

Upon bacterial infection, a major challenge for host cells is the maintenance of genomic integrity. Pathogenic bacteria can cause DNA damage in host cells, often resulting in DNA double-strand breaks (DSBs) (Cancer Genome Atlas Research N, 2014; Song and Bent, 2014). Numerous studies have reported that *H. pylori* infection induces DNA damage and alter the DNA repair capacity (Dorer et al., 2010; Lieber, 2010; Toller et al., 2011; Chaturvedi et al., 2014; Koeppel et al., 2015). *H. pylori* has been found to cause several types of DNA damage, including single-strand breaks (SSBs) and DSBs in nuclear genome (Fox and Wang, 2007; Lieber, 2010). High-throughput genomic analyses have shown that *H. pylori* causes a specific pattern of DNA damage in the transcribed and telomere-proximal regions of the genome (Chaturvedi et al., 2014). Furthermore, *H. pylori* infection induces mtDNA damage that includes oxidative damage, adducts formation, base mismatch, and DNA strand breaks (Babbar et al., 2020). Given its proximity to ROS-generating electron transport chain and the absence of histones, mtDNA is more vulnerable to oxidative DNA damage than nDNA (Maynard et al., 2009). Oxidative damage to mtDNA can manifest as base modifications, abasic sites, and various other types of lesions (Cooke et al., 2003). One of the most studied lesions in mtDNA is 8-oxoguanine (8-oxoG), which is a mutagenic lesion (Kurosaka et al., 1991). Mispairing of 8-oxoG with adenine results in a G–C to T–A transversion during subsequent rounds of replication. Early studies showed that 8-oxoG lesions are 16 times more frequent in mtDNA than in nDNA (Richter et al., 1988). In more definitive studies, Yakes and Van Houten showed that mtDNA damage is more extensive and persists longer than nDNA damage in human cells following oxidative stress (Yakes and Van Houten, 1997). In addition, unrepaired mtDNA base damage intermediates, such as single-stranded strand breaks (SSBs), arise as a result of the erroneous or abortive activity of DNA topoisomerase I (Hudson et al., 2012), contributing to mitochondrial genome instability (Zhang et al., 2001). In addition, *H. pylori* infection may also lead to replication stress in mtDNA that may eventually alter the

expression and function of mitochondrial genes and transcription factors that contribute to the accumulation of mtDNA damage (Chatre et al., 2017). It is also possible that the enhanced oxidative stress due to *H. pylori* infection might be a possible cause of unfit mitochondria for replication in infected host cells. Another important factor for increased mitochondrial DNA damage is mtDNA mutations that occur during replication by insertion/deletion of the wrong nucleotide. Although the POLG has 3′–5′ exonuclease proofreading activity that corrects the mis-incorporation of the nucleotide, the error rate of mDNA replication, however, exceeds the repair capacity, potentially increasing the mutation frequency (Kaguni, 2004). Moreover, *H. pylori* induces genomic instability in nuclear CA repeats in mice and in mtDNA (MaChado et al., 2009).

Although various DNA repair pathways have been documented including direct reversal, BER, NER, and MMR in cells (Jalal et al., 2011; Chatterjee and Walker, 2017), the BER pathway is the predominant pathway for repairing mtDNA damage (Bohr and Anson, 1999; Druzhyna et al., 2008). Like nDNA, an efficient mtDNA repair pathway, especially the BER pathway, may play an important role in repairing oxidative mtDNA damage (Figure 1). Mitochondria BER (mtBER) proteins are localized in the inner membrane and co-exist with the TFAM nucleoid structure protein (Stuart et al., 2005). The first step of mtBER involves DNA base damage recognition by seven different DNA glycosylases. These glycosylases contain a mitochondria translocation signaling (MTS) leader sequence, which facilitates their transport into the mitochondria. Once inside, these DNA glycosylases remove damaged mtDNA nucleotide lesions. The second step involves cleaving the sugar–phosphate backbone of the mtDNA using AP endonuclease that processes the abasic site (AP). This is followed by the action of POLG, which re-synthesizes missing DNA patches. Finally, DNA ligase (LIG3) seals the DNA fragments (Szczepanowska and Trifunovic, 2015). The alternative mechanism is that mtDNA repair machinery engages in end processing using distinct gap-tailoring enzymes, including aprataxin (Ahel et al., 2006) and TDP1 (Das et al., 2010). However, if aprataxin proteins are unable to repair the 5′-AMP group, it can block DNA ligase repair activity and generate SSBs (Sykora et al., 2011). The mtDNA damage induced by *H. pylori* infection may lead to mtDNA single-strand breaks (mtSSBs), mtDNA double-strand breaks (mtDSBs), and base mismatches which are potentially processed via different types of repair machinery (Figure 1). Due to the types of oxidative DNA damage substrate specificity, the preference of DNA glycosylase may vary, and it is possible that they might influence each other's activity (MaChado et al., 2009). The DNA glycosylases OGG1, UDG1, and MYH (Ohtsubo et al., 2000) are all associated with the particulate fraction of the mitochondria as are POLG, DNA ligase III, and a minor portion of AP endonuclease activity (Stuart et al., 2005). The mitochondria harbor bifunctional 8-oxoguanine, DNA glycosylase-1 (OGG1), and monofunctional uracil–DNA glycosylase (UNG1) to process different mtDNA base lesions (Jacobs and Schar, 2012). These glycosylases are discussed below.

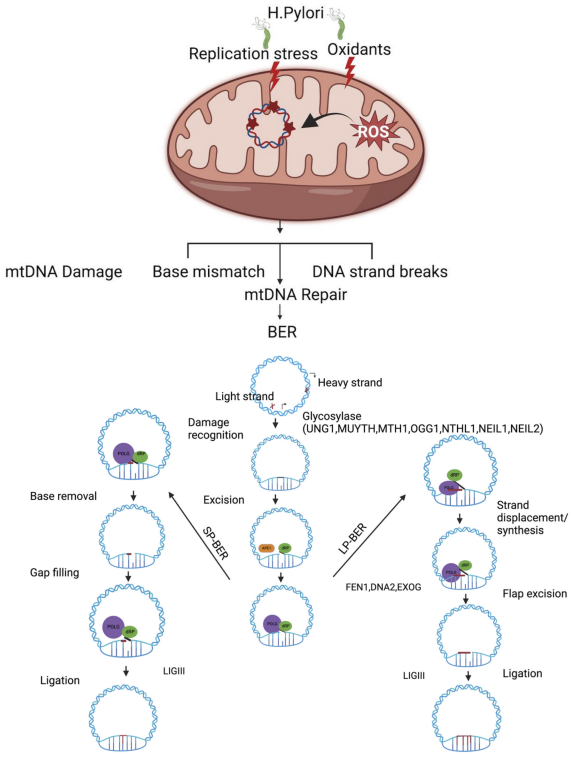

FIGURE 1
Oxidative stress induced by *H. pylori* infection leads to damage in mitochondrial DNA (mtDNA), which is primarily repaired through the base excision repair (BER) pathway. The BER pathway operates through two different mechanisms to maintain the mitochondrial genome: short-patch BER (SP-BER) removes a single damaged nucleotide, while long-patch BER (LP-BER) removes between two and eight damaged nucleotides during the repair process. *H. pylori* infection induces genotoxin-mediated mtDNA and increases oxidative-stress-associated mtDNA damage and mtDNA replication stress. A single-base damage or single-strand break on mtDNA is likely processed via BER. mtDNA single-base damage is potentially recognized and removed by one of the DNA glycosylases (UNG1, OGG1, MUTHY MTH1, NTHL1 NEIL1, and NEIL2), followed by end processing via the dRP lyase activity of POLB and gap filling with POLG inserts in the correct base, and LIGII seals the mtDNA nick. In long-patch BER, strand displacement DNA synthesis is processed by POLG and displaces 5′ DNA flap downstream of the repair site, which must be removed by flap endonuclease (FEN1) and other partner/DNA2/EXOG involved to process the 5′ end of the DNA. Once tailoring of the 5′ and 3′ ends of mtDNA is complete, LIGIII seals the mtDNA nick. Figure created with BioRender.com.

DNA glycosylase in mitochondria

Several studies have identified five bifunctional and two monofunctional DNA glycosylases in the mitochondria (Prakash and Doublie, 2015). Uracil–DNA glycosylase 1 (UDG1 or uracil-*N*-glycosylase1 [UNG1]) (Anderson and Friedberg, 1980) and MUTYH (MYH), a homolog of the *Escherichia coli* MutY glycosylase (Ohtsubo et al., 2000), are classified as monofunctional DNA glycosylases. The substrate specificities of UNG1 and MUTYH have been recently reviewed (Svilar et al., 2011). MUTYH is an adenine–DNA glycosylase that preferentially excise adenine when paired with 8-oxoG, initiating a round of base excision repair that restores the 8-

oxoG:C pair and protects the DNA from mutagenic 8-oxoG lesions (Michaels et al., 1992). In addition, several studies have shown that mitochondria can repair alkylation lesions using monofunctional glycosylase, MPG (Chakravarti et al., 1991; Pirsel and Bohr, 1993; Ledoux et al., 1998). The UNG1 enzymes cleave substrates from both single-stranded (ss) DNA and double-stranded (ds) DNA with a slight preference for ss over ds substrates. Importantly, UNG1 has a MTS comprising a 30-amino-acid leader sequence at the N-terminal end of the enzyme that likely facilitates entry into the inner mitochondrial membrane (Neupert, 1997). Amino acid substitution (Y147A or N204D) in the catalytic domain of UNG1 switches the substrate specificity of the enzyme and is able to remove thymine and uracil from mtDNA (Kavli et al., 1996). Removing mtDNA base lesions in this manner leaves excess apyrimidinic sites, which are highly genotoxic to the cells (Glassner et al., 1998; Lindahl and Wood, 1999). mtDNA has been shown to accumulate high levels of mutagenic lesions of 8-hydroxy-2′-deoxyguanosine, which is the byproduct of guanine hydroxylation (Nakabeppu, 2014). Previous work has shown that 8-oxodG, the most prominent oxidative DNA base lesion, is repaired more efficiently in the mitochondria than in the nucleus (Thorslund et al., 2002). These 8oxoG lesions are recognized and processed by OGG1 glycosylase (Mandal et al., 2012) which localizes to both the nucleus and mitochondria (Klungland et al., 1999; Nishioka et al., 1999; Klungland and Bjelland, 2007). However, the loss of OGG1 compromises the metabolic function of mitochondria, indicating an additional role in maintaining the bioenergetic homeostasis of the cell (Lia et al., 2018). Notably, other DNA glycosylases such as NTHL1 are found in both the nucleus and mitochondria and only active with duplex DNA. NTHL1 is a bifunctional glycosylase involved in the excision of oxidized DNA bases such as Tg, 5-hydroxycytosine (5-hC), 5-hydroxyuracil (5-hU), and the ring-opened 2,6-diamino-4-hydroxy-5-formamidopyrimidine (Fapy) lesions (Prakash and Doublie, 2015). Previously, we have shown that the single-nucleotide variant of NTHL1 promotes genomic instability in cells (Galick et al., 2013). However, the biological significance of this mutant variant in mitochondria is unclear and requires further investigation. Additionally, chromatin immunoprecipitation analysis demonstrated that DNA glycosylases, including *NEIL1* and *NEIL2*, form a complex with mitochondrial genes MT-CO2 and MT-CO3 (cytochrome c oxidase subunit 2 and 3) and mitochondrion-specific POLG (Mandal et al., 2012). NEIL2 interacts with PNK to maintain the mammalian mitochondrial genome (Mandal et al., 2012). NEIL2 shows a unique preference for excising lesions from a DNA bubble. In contrast, NEIL1 efficiently excises 5-hydroxyuracil, an oxidation product of cytosine, from the bubble and single-stranded DNA but does not have strong activity toward 8-oxoguanine in the bubble (Dou et al., 2003). Furthermore, MTH1 DNA glycosylase, which is localized in both the mitochondria and nucleus, plays a significant role in repairing oxidized dATP and ATP, such as 2-OH-dATP and 2-OH-ATP, as well as 8-oxo-dGTP (Bialkowski and Kasprzak, 1998; Fujikawa et al., 1999; Fujikawa et al., 2001; Nakabeppu et al., 2006). The function of those nuclear-encoded DNA glycosylases likely depends on their ability to pass through the mitochondrial membrane via MTS signals. However, there are single-nucleotide polymorphisms (SNPs) on the MTS of these glycosylases that may impact their function and cause mitochondrion-associated human diseases (Table 1). Uncovering the biological significance of these SNPs will likely shed mechanistic insights on the impact of DNA glycosylase in mitochondrial genome integrity and its biological outcomes.

APE1 endonuclease

APE1 is a multifunctional protein that plays a central role in the maintenance of nuclear and mitochondrial genomes. APE1 translocates into the mitochondria in response to oxidative stress and increases mitochondrial DNA (mtDNA) repair rate and cell survival (Barchiesi et al., 2020). Protein sequence analysis suggests that APE1 harbors MTS signal sequence within residues 289–318 in the C terminus, which is normally masked by the intact N-terminal structure (Li et al., 2010). Once APE1 is translocated in the mitochondria, it is able to remove the AP sites and hand over the reaction to the next repair factors. In contrast, genetic ablation of APE1 results in the accumulation of damaged mitochondrial mRNA species, impairment in protein translation, and reduced expression of mitochondrial encoded proteins, leading to less efficient mitochondrial respiration (Barchiesi et al., 2020). It is possible that loss of APE1 may increase the number of AP sites, potentially driving mtDNA instability. A few studies suggested that APE1 depletion in cells leads to increased mtDNA copy number (Barchiesi et al., 2021).

DNA polymerase enzymes

The ability to effectively repair various types of DNA damage is achieved through multiple, often overlapping, DNA repair pathways. DNA POLB and POLG are involved in mtDNA repair process (Copeland, 2010). Once the AP site is processed by APE1, the gap is filled by POLG with correct nucleotides. The Wilson study estimated that ~30% of POLB localize to the mitochondria, as shown through the colocalization studies of TOM20 (Prasad et al., 2017). Additional high-quality immunogold electron microscopy (EM) localization studies demonstrated that 20% of POLB localize to the mitochondrial matrix and 60% to the nucleus (Prasad et al., 2017). POLG has DNA polymerase activity to fill DNA gaps but lacks efficient dRP lyase activity to process the 5′dRP groups (Kaufman and Van Houten, 2017). Bohr's and Wilson's groups identified a robust dRP lyase activity in the mitochondria belonging to POLB (Sykora et al., 2017). Biochemical characterization indicates that the 5′dRP lyase activity of DNA polymerase beta plays a primary role in complementing POLG by removing the 5′ dRP group, thus promoting short-patch-BER in mtDNA. Both POLB and POLG support gap filling in single nucleotide gaps (Kaufman and Van Houten, 2017). POLG is known for its high replication fidelity, which allows it to support both replication and repair functions in the mitochondria. This high fidelity, however,

TABLE 1 Variants associated with mutation on mitochondrial targeting sequence (MTS) of base excision repair (BER) genes and its clinical significance.

Gene	MTS location	Position changed	Variation	Variant id	Mutation description	Clinical significance	References
OGG1	8-21	9	p.Arg9Ser	rs769947581	Missense, Benign (uniprot)	Unknown	PMID:29848661
		12	p.Gly12Glu	rs772520254	Missense, Benign (Uniprot)	Unknown	MTSviewer
MTH1	1-18	2	pGly2Asp	rs144573336	Missense (Uniprot)	Unknown	PMID: 16607562
		17	pArg17Gln	rs372407158	Somatic, Missense (Uniprot)	Unknown	MTSviewer
UNG	1-35	11	p.Phe11Ser	947219	Germline, Missense (ClinVar)	Hyper IgM syndrome type 5	PMID: 9776759
		21	p.Ala21Thr	643750	Germline, Missense (ClinVar)	Hyper IgM syndrome type 5	MTSviewer
MUYTH	1-14	1	p.Met1Val	230848	Germline, Missense, Pathogenic (ClinVar)	Familial adenomatous polyposis 2/ Hereditary cancer- predisposing syndrome/Gastric cancer Familial adenomatous polyposis 2.	PMID:21235684
		12	p.Trp12Ter	483936	Germline, Nonsense, pathogenic (ClinVar)	Familial adenomatous polyposis 2	MTSviewer
NTHL1	1-95	18	p.Thr10Ser	657414	Germline, Missense, likely Benign (ClinVar)	Familial adenomatous polyposis 3/ Hereditary cancer-predisposing syndrome	PMID:9611236
		62	p.Gln54Ter	662775	Germline, Missense, pathogenic (ClinVar)	Familial adenomatous polyposis 3/ Hereditary cancer-predisposing syndrome	MTSviewer
NEIL1	1-89	68	p.Pro68His	rs187873972	Missense (Uniprot)	Unknown	PMID:2575473
		24	p.Gly24Cys	rs761525934	Missense (Uniport)	Unknown	MTSviewer
NEIL2	No canonical MTS	N/A	N/A	N/A	N/A	N/A	PMID:22130663, PMID: 25754732 MTSviewer
APEX1	289-318	291	p.L291Vfs*6	rs747329195	Somatic, Frameshift (Uniprot)	Unknown	PMID:20231292
		307	p.Ser307Asn	rs1183577581	Missense (Uniport)	Unknown	MTSviewer
POLG	1-25	10	p.Ala10Val	458708	Germline, Missense, Benign (ClinVar)	Progressive sclerosing poliodystrophy	PMID 8884268 PMID: 18546365
		11	p.Gly11Ser	619334	Germline, Missense,	Progressive sclerosing poliodystrophy	MTSviewer

(Continued)

TABLE 1 Continued

Gene	MTS location	Position changed	Variation	Variant id	Mutation description	Clinical significance	References
					Benign (ClinVar)		
POLB	1-17	8	p.Gln8Arg	Rs200636493	Missense, Benign (Uniprot)	Unknown	PMID:28559431
		7	p.Pro7ser	Rs1463614564	Missense, Benign (Uniprot)	Unknown	MTSviewer
LIG3	73-333	224	p.Arg224Trp	782153	Germline, Missense, Benign (ClinVar)	Unknown	PMID:10207110
		241	p.Ser241Leu	987864	Germline, Missense, Benign (ClinVar)	Unknown	MTSviewer

This table summarizes the mutations within the mitochondrial targeting sequence (MTS) of various base excision repair (BER) genes, along with the positions of the amino acid changes, corresponding variant IDs, and their clinical significance based on databases ClinVar and UniPort as well as software MTSviewer and existing published literature.

may be detrimental in situations that require the polymerase to bypass a lesion.

DNA ligase

DNA LIG III is a key factor of the BER pathway which is shared between the mitochondria and the nucleus compartment, where it is involved in sealing DNA nicks to complete mtDNA repair processes. LIG3 is the only vertebral mitochondrial DNA ligase identified so far and is essential for mitochondrial DNA maintenance (Gao et al., 2011; Simsek et al., 2011). In the mitochondria, LIG3 interacts with tyrosyl-DNA phosphodiesterase 1 (TDP1), NEIL1/2 glycosylases, and POLG (Simsek and Jasin, 2011). *In vitro* work shows that downregulation of LIG3 in human fibroblastoma cell lines decreased the mtDNA copy number, reduces respiration, and leads to the accumulation of DNA SSBs in mtDNA. In contrast, the complete lack of LIG3 in murine cells leads to the full depletion of mtDNA, underlying the essential role of LIG3 in mitochondrial genome integrity (Lakshmipathy and Campbell, 2001; Shokolenko et al., 2013). The somatic and germline variants of LIG3 may contribute to the loss of function and accumulation of mtDNA damage which likely drives mitochondrion-associated human pathologies.

Impact of aberrant BER repair on mitochondrial genomic integrity

Loss of BER results in the accumulation of mutation [(C:G→T transversions] (Whitaker et al., 2017) or DNA single-strand (Lindahl, 1993) or double-strand breaks (DSBs)] (Woodbine et al., 2011; Fridlich et al., 2015), which are principal sources of genomic instability (Khanna and Jackson, 2001; Caldecott, 2008). Dysfunctional mtBER leads to the accumulation of mtDNA D-loop mutation in gastrointestinal cancer (Wang et al., 2018). DNA-repair-deficient mitochondria are more susceptible to oxidative DNA damage agents (Shokolenko et al., 2003). It is possible that loss or mutation in MTS signaling sequence contributes to the lack of mtBER in the mitochondrial compartment. Mutations in MTS of BER genes may prevent the import of the nuclear encoded BER proteins into the mitochondria, resulting in the loss of their biological functions in the mitochondria. Germline and somatic variants of BER genes that harbor MTS mutations likely cause deficiency in mtBER repair pathways, contributing to mitochondrial genome instability and human diseases (Table 1). Germline BER variants with non-synonymous mutations in the MTS sequence likely increase the risk factor for different pathophysiological outcomes. Similarly, mutations in BER genes within tumors may contribute to tumor initiation and progression. It is important to note that the genetic mutations in MTS, analyzed using the MTSViewer platform, suggested MTS mutation sites, and clinical variant scores likely suggest the potential impact of these mutations on protein structure and function in the mitochondria.

Impact of *H. pylori* infection on mitochondrial genome transactions

H. pylori infection causes chronic gastric inflammation (Peek and Blaser, 2002), and patients with a previous history of *H. pylori* infection are at a higher risk to develop gastric cancers (Aoi et al., 2006). Furthermore infection with *H. pylori* suppresses stomach acidity and may result in a more permissive milieu for colonization with other bacteria (Dicksved et al., 2009). Mitochondrial dynamics play important roles in bacterial pathogenesis, with multiple mitochondrial functions mechanistically linked to their morphology, which is defined by ongoing events of fission and fusion of the outer and inner membranes (Cogliati et al., 2016). *H.*

pylori infection dysregulates the delicate balance of mitochondrial fission and fusion networks (Scott and Youle, 2010). Mitochondrial fusion allows the mitochondria with normal mtDNA to compensate for defects in the mitochondria with damaged mtDNA (Nakada et al., 2001; Ono et al., 2001; Yang and Gao, 2018). These processes are governed by a complex molecular machinery and finely tuned by regulatory proteins (Tilokani et al., 2018). *H. pylori*-induced mtDNA damage may contribute to trigger this event via genomic instability such as mutations and deletions in mitochondrial DNA that yield a heteroplasmic mixture of wild-type and mutant mitochondrial genomes within one cell (Taylor and Turnbull, 2005). As shown in Figure 2, the mtDNA that harbor extensive damage likely removed from the cellular system via mitochondria fission process to minimize the carryover of undesirable genetic traits to next cell cycle. Furthermore, mitochondrial fission is needed to create not only new mitochondria, but also contributes to quality control by enabling the removal of damaged mitochondria and can facilitate apoptosis during high levels of cellular stress. Therefore, mitochondrial fission is an important element to eliminate infected cells and reduce cell-to-cell-spreading, thus modulating apoptosis and bacterial dissemination (Spier et al., 2019). In contrast mitochondria harboring different genetic lesions likely compensate for their defects by relying on the genetic content from other mitochondria through the fusion process. Damaged and undamaged mtDNAs yield a heteroplasmic mixture of normal and mutant mitochondrial genomes within the same cell (Wonnapinij et al., 2008; Aryaman et al., 2018). The mitochondria fusion scenario likely maintained if the mutation rate in the mitochondria remain below ~ 80% per cell, the mitochondria in heteroplasmic cells complement one another to compensate their defects (Yoneda et al., 1994; Nakada et al., 2001). Mitochondrial Fusion can rescue two mitochondria with mutations in different genes through cross-complementation to one another, and it can mitigate the effects of *H. pylori* infection induced DNA damage by the exchange of repair proteins and other factors with other mitochondria. It is also important that mitochondrial fusion can therefore maximize oxidative capacity in response to toxic stress and use alternative resource or repair factors to fix the damaged region of mtDNA.

H. pylori toxin-induced mitochondria dysfunction

Mitochondria play a central role in the innate immune response. It is at the center of the inflammatory response in the case of a viral or bacterial infection or spontaneous cellular damage. Because of their structural similarity to their bacterial ancestor, extracellular mitochondria and their components may operate as a danger signal by means of their interaction with pattern recognition receptors (PRRs). PRRs are a group of receptors that can specifically detect molecular patterns found on the surfaces of pathogens, apoptotic cells and damaged senescent cells. In the case of an infection by a pathogenic agent, the microorganisms will be detected by PRR that recognize pathogen-associated molecular patterns (PAMPs), such as flagellins, lipopolysaccharide, mannose, nucleic acids and proteins and the danger-associated molecular motifs (DAMPs) molecules. In addition, the presence of

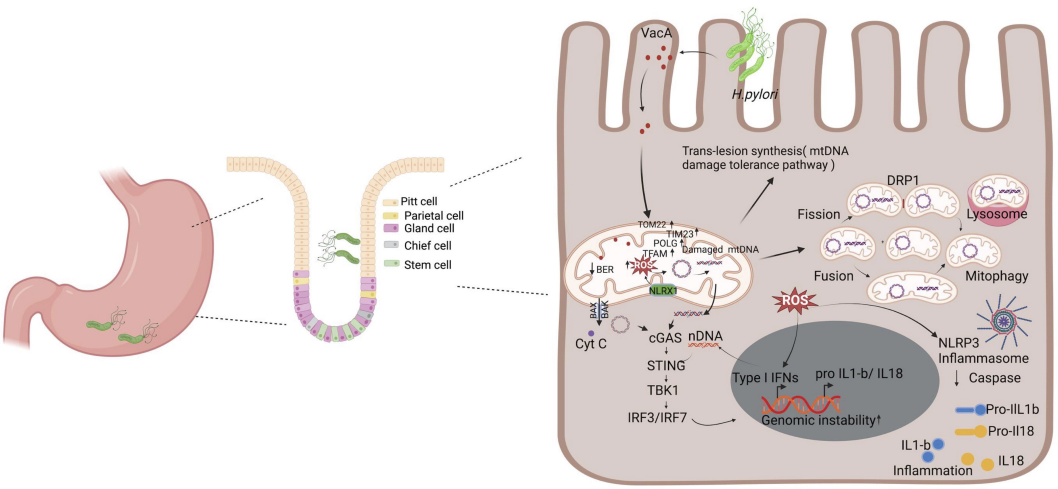

FIGURE 2
H. pylori-mediated mitochondrial dysfunction and inflammation. Upon infection, *H. pylori* secretes toxins such as VacA, which interacts with the mitochondria, leading to the modulation of its function and ultimately promoting pathogenesis. It decreases the mitochondrial membrane potential, leading to reduced ATP production and an increase in cytochrome c release that triggers autophagy. Additionally, VacA enhances the mtDNA damage and the generation of ROS. This triggers a series of stress responses, including the upregulation of mitochondrial DNA repair mechanism factors (e.g., POLG and TFAM) and the activation of the cGAS/STING pathway due to the release of damaged mtDNA and nDNA in the cytosol. Cells have a mechanism to respond to unrepaired mtDNA damages that includes trans-lesion synthesis, fusion, fission, and mitophagy that degrades severely damaged mitochondria. The accumulation of ROS and the release of mitochondrial contents also activate the NLRP3 inflammasome, leading to the processing and release of pro-inflammatory cytokines IL-1β and IL-18. Collectively, these processes contribute to chronic inflammation and genomic instability, which are key factors in the pathogenesis of *H. pylori*-related diseases, including gastritis and gastric cancer. Figure created with BioRender.com.

the bacterial virulence factors such as type IV secretion system (T4SS), the bacterial protein CagA and the vacuolating cytotoxin (VacA) is associated with chronic inflammation and increased risk of gastric cancer development (Peek and Blaser, 2002). *H. pylori* strains are categorized into *cagA*-positive and *cagA*-negative strains based on the presence or absence of the *cag* pathogenicity island (*cag*PAI). The *cag*PAI, is an ~40-kb DNA segment containing around 30 genes (open reading frames), which include *cagA* and several genes encoding components of a bacterial Type IV secretion system (T4SS), that delivers CagA into attached gastric epithelial cells (Covacci and Rappuoli, 2000). Cag A is capable to induce cytosolic Ca^{2+} influx, leading to mitochondria ROS production. In addition, Cag A can upregulate the expression level of spermine oxidase (SMO), which can convert spermine to spermidine and simultaneously releases hydrogen peroxide (Chaturvedi et al., 2011; Cindrilla et al., 2016).

H. pylori is known to target mitochondria through its vacuolating cytotoxin (VacA), which triggers mitochondria-dependent apoptosis in mammalian cells (Calore et al., 2010). In gastric epithelial cells, VacA localizes to endosomal compartments and reaches the mitochondrial inner membrane where it forms anion-conductive channels (Calore et al., 2010; Domanska et al., 2010). VacA reduces mitochondrial membrane potential leading to decreased ATP production and cytochrome c release (Galmiche and Rassow, 2010). The pore-forming VacA toxin of the *H. pylori*, recruits and activates Drp1 resulting in mitochondrial fission, Bax activation, MOMP and cytochrome *c* release (Jain et al., 2011). VacA is also an efficient inducer of autophagy (Terebiznik et al., 2009). It is possible that *H. pylori* deregulate host cell mitochondria at early and late stage of infection with different dynamics. At the early stage of infection, *H. pylori* induce VacA dependent dysregulation of mitochondria hemostasis, which promotes transient increase in mitochondrial translocases, mitochondrial DNA replication maintenance factors such as POLG and TFAM. In contrast, at late infection stage the mechanism of dysregulation is VacA independent alteration in mitochondrial replication and import components, suggesting the involvement of additional H. *pylori* activities in mitochondrion-mediated effects (Figure 2).

mtDNA modulates *H. pylori* infection-associated inflammation

Mitochondria have been reported as modulators of cellular antibacterial immunity and inflammatory response (Andrieux et al., 2021). Abundant lines of research implicate the mitochondria as a key immune modulator in mouse models and human materials. Components of mtDNA such as TFAM, extracellular ATP, and numerous others have the capacity to elicit strong immune responses and, as such, and are thus considered mitochondrial damage-associated molecular patterns (DAMPs) (Galluzzi et al., 2012; West et al., 2015; De Gaetano et al., 2021). Mitochondrial DNA (mtDNA) encodes essential subunits of the oxidative phosphorylation system and is also a major damage-associated molecular pattern (DAMP) that engages innate immune sensors when released into the cytoplasm, outside of cells or into the circulation. As a DAMP, mtDNA not only contributes to anti-viral resistance but also causes pathogenic inflammation in many disease contexts. Several studies also report that when mtDNA is discharged outside the cell, whether intact or damaged, it shows considerable pro- or anti-inflammatory effects in different models, thus highlighting the paradoxical interactions between these organelles and immune cells (Boudreau et al., 2014; Torralba et al., 2016). Mitochondrial DNA released into the cytosol is recognized by a DNA sensor cGAS, a cGAMP/STING which activates a pathway leading to the enhanced expression of type I interferons (Figure 2). Additionally, mtDNA activates NLRP3 inflammasome, which promotes the activation of pro-inflammatory cytokines interleukin-1 beta and interleukin-18 (West et al., 2015; Zhong et al., 2018; Swanson et al., 2019). In the endosome, mtDNA can also bind to Toll-like receptor-9, triggering a pathway that results in the expression of pro-inflammatory cytokines (De Gaetano et al., 2021). Stress-induced release of mtDNA or mtRNA into the cytoplasm can activate a type I IFN-I response that confers resistance to viral infection (West et al., 2015; Dhir et al., 2018; Sprenger et al., 2021). Inflammation caused by infection leads to the production of ROS and subsequent oxidative DNA damage (Sahan et al., 2018). ROS partially derives from active immune systems and host cells (Cindrilla et al., 2016). During infection, the stimulation of phagocytic cells, such as neutrophils, eosinophils, monocytes, and macrophages, activates the NADPH oxidase (Nox) pathway, which catalyzes the reduction of oxygen using NADPH and generates superoxide (Brown and Griendling, 2009). In infected cells, the production of ROS is further amplified in the mitochondria via a mechanism involving NLRX1, a member of the intracellular Nod-like receptor (NLR) family that is localized in the mitochondria (Abdul-Sater et al., 2010). The resulting ROS can enter the nucleus and attack the DNA, generating oxidative DNA damage, such as 8-oxo-G, AP sites, and single-strand breaks (SSBs) (Kidane et al., 2014). Overall, further work is needed to uncover whether mtDNA and/or nuclear DNA damage continuously provides the fuel to exacerbate *H. pylori* infection-mediated inflammation.

Future perspective

Mitochondrial DNA integrity is critical to keep cellular homeostasis and prevent undesirable immune activation. Spontaneous or exogenous-stress-mediated mtDNA damage triggers different types of mitochondrial responses including fission or fusion to restore normal function and physiology. In addition, mtDNA damage activates DNA repair pathways such as BER to process the oxidative- or alkylating-agent-induced mtDNA damage and resolve some of the repair intermediates. Furthermore, unrepaired mtDNA base damage has an ability to deregulate the mtDNA replication dynamics leading to replication stress or blockage. mtDNA damage has been implicated in a variety of

bacterial pathogens to drive inflammation and disease—for example, intracellular pathogenic bacteria such as *Salmonella typhimurium* induces typhoid-toxin-dependent mtDNA damage, promotes the release of mtDNA into the cytosol, and triggers the cGAS-STING pathway (Xu et al., 2022; Chen et al., 2024). *Mycobaterium abscessus* and *Mycobacterium tuberculosis* also cause mtDNA damage, leading to inflammation via inflammasome activation or cGAS-STING signaling (Wiens and Ernst, 2016; Kim et al., 2020). *H. pylori* infection potentially impacts the mtDNA integrity and transitory alteration of mitochondrial import translocases and a dramatic upregulation of POLG and TFAM. Spontaneous as well as chronic infection induces excessive accumulation of mtDNA damage which leads to the release of mtDNA into the cytoplasm and activates cGAS/STING-dependent type I interferon response or activate other additional signaling pathways to promote inflammation- and infection-associated pathogenicity. Future risk assessment of patients may look for the potential link between a mutation in the MTS sequence of BER genes and the biological consequence of insufficient mt BER repair factors. In the future, the clinical relevance and the mechanism underlying the altered mtDNA dynamics with or without *H. pylori* infection probably will provide a new insight for cancer risk assessments and therapeutic planning across different stages of gastric cancer.

Author contributions

DK: Conceptualization, Funding acquisition, Investigation, Project administration, Supervision, Validation, Writing – original draft, Writing – review & editing. AS: Data curation, Formal Analysis, Investigation, Methodology, Validation, Writing – original draft, Writing – review & editing.

Funding

The author(s) declare that financial support was received for the research, authorship, and/or publication of this article. Research reported in this publication was supported by the National Institute of Allergy and Infectious Diseases of the National Institutes of Health under Award Number R01AI179899.

Conflict of interest

The authors declare that the research was conducted in the absence of any commercial or financial relationships that could be construed as a potential conflict of interest.

The author(s) declared that they were an editorial board member of Frontiers, at the time of submission. This had no impact on the peer review process and the final decision.

Generative AI statement

The author(s) declare that no Generative AI was used in the creation of this manuscript.

Publisher's note

References

Abdul-Sater, A. A., Saïd-Sadier, N., Lam, V. M., Singh, B., Pettengill, M. A., Soares, F., et al. (2010). Enhancement of reactive oxygen species production and chlamydial infection by the mitochondrial Nod-like family member NLRX1. *J. Biol. Chem.* 285, 41637–41645. doi: 10.1074/jbc.M110.137885

Ahel, I., Rass, U., El-Khamisy, S. F., Katyal, S., Clements, P. M., McKinnon, P. J., et al. (2006). The neurodegenerative disease protein aprataxin resolves abortive DNA ligation intermediates. *Nature* 443, 713–716. doi: 10.1038/nature05164

Alexeyev, M., Shokolenko, I., Wilson, G., and LeDoux, S. (2013). The maintenance of mitochondrial DNA integrity–critical analysis and update. *Cold Spring Harb. Perspect. Biol.* 5, a012641. doi: 10.1101/cshperspect.a012641

Anderson, C. T., and Friedberg, E. C. (1980). The presence of nuclear and mitochondrial uracil-DNA glycosylase in extracts of human KB cells. *Nucleic Acids Res.* 8, 875–888.

Andrieux, P., Chevillard, C., Cunha-Neto, E., and Nunes, J. P. S. (2021). Mitochondria as a cellular hub in infection and inflammation. *Int. J. Mol. Sci.* 22. doi: 10.3390/ijms222111338

Aoi, T., Marusawa, H., Sato, T., Chiba, T., and Maruyama, M. (2006). Risk of subsequent development of gastric cancer in patients with previous gastric epithelial neoplasia. *Gut* 55, 588–589. doi: 10.1136/gut.2005.086884

Aryaman, J., Johnston, I. G., and Jones, N. S. (2018). Mitochondrial heterogeneity. *Front. Genet.* 9, 718. doi: 10.3389/fgene.2018.00718

Babbar, M., Basu, S., Yang, B., Croteau, D. L., and Bohr, V. A. (2020). Mitophagy and DNA damage signaling in human aging. *Mech. Ageing Dev.* 186, 111207. doi: 10.1016/j.mad.2020.111207

Ban-Ishihara, R., Ishihara, T., Sasaki, N., Mihara, K., and Ishihara, N. (2013). Dynamics of nucleoid structure regulated by mitochondrial fission contributes to cristae reformation and release of cytochrome c. *Proc. Natl. Acad. Sci. U.S.A.* 110, 11863–11868. doi: 10.1073/pnas.1301951110

Barchiesi, A., Bazzani, V., Jabczynska, A., Borowski, L. S., Oeljeklaus, S., Warscheid, B., et al. (2021). DNA repair protein APE1 degrades dysfunctional abasic mRNA in mitochondria affecting oxidative phosphorylation. *J. Mol. Biol.* 433, 167125. doi: 10.1016/j.jmb.2021.167125

Barchiesi, A., Bazzani, V., Tolotto, V., Elancheliyan, P., Wasilewski, M., Chacinska, A., et al. (2020). Mitochondrial oxidative stress induces rapid intermembrane space/matrix translocation of Apurinic/Apyrimidinic endonuclease 1 protein through TIM23 complex. *J. Mol. Biol.* 432, 166713. doi: 10.1016/j.jmb.2020.11.012

Bialkowski, K., and Kasprzak, K. S. (1998). A novel assay of 8-oxo-2'-deoxyguanosine 5'-triphosphate pyrophosphohydrolase (8-oxo-dGTPase) activity in cultured cells and its use for evaluation of cadmium(II) inhibition of this activity. *Nucleic Acids Res.* 26, 3194–3201. doi: 10.1093/nar/26.13.3194

Blanke, S. R. (2005). Micro-managing the executioner: pathogen targeting of mitochondria. *Trends Microbiol.* 13, 64–71. doi: 10.1016/j.tim.2004.12.007

Bogenhagen, D. F. (2012). Mitochondrial DNA nucleoid structure. *Biochim. Biophys. Acta* 1819, 914–920. doi: 10.1016/j.bbagrm.2011.11.005

Bohr, V. A. (2002). Repair of oxidative DNA damage in nuclear and mitochondrial DNA, and some changes with aging in mammalian cells. *Free Radic. Biol. Med.* 32, 804–812. doi: 10.1016/S0891-5849(02)00787-6

Bohr, V. A., and Anson, R. M. (1999). Mitochondrial DNA repair pathways. *J. Bioenerg Biomembr.* 31, 391–398. doi: 10.1023/A:1005484004167

Boudreau, L. H., Duchez, A. C., Cloutier, N., Soulet, D., Martin, N., Bollinger, J., et al. (2014). Platelets release mitochondria serving as substrate for bactericidal group IIA-secreted phospholipase A2 to promote inflammation. *Blood* 124, 2173–2183. doi: 10.1182/blood-2014-05-573543

Brown, D. I., and Griendling, K. K. (2009). Nox proteins in signal transduction. *Free Radical Biol. Med.* 47, 1239–1253. doi: 10.1016/j.freeradbiomed.2009.07.023

Caldecott, K. W. (2008). Single-strand break repair and genetic disease. *Nat. Rev. Genet.* 9, 619–631. doi: 10.1038/nrg2380

Calore, F., Genisset, C., Casellato, A., Rossato, M., Codolo, G., Esposti, M. D., et al. (2010). Endosome-mitochondria juxtaposition during apoptosis induced by *H. pylori* VacA. *Cell Death Differ.* 17, 1707–1716. doi: 10.1038/cdd.2010.42

Cancer Genome Atlas Research N (2014). Comprehensive molecular characterization of gastric adenocarcinoma. *Nature* 513, 202–209. doi: 10.1038/nature13480

Casanova, A., Wevers, A., Navarro-Ledesma, S., and Pruimboom, L. (2023). Mitochondria: It is all about energy. *Front. Physiol.* 14, 1114231. doi: 10.3389/fphys.2023.1114231

Chakravarti, D., Ibeanu, G. C., Tano, K., and Mitra, S. (1991). Cloning and expression in Escherichia coli of a human cDNA encoding the DNA repair protein N-methylpurine-DNA glycosylase. *J. Biol. Chem.* 266, 15710–15715. doi: 10.1016/S0021-9258(18)98467-X

Chatre, L., Fernandes, J., Michel, V., Fiette, L., Ave, P., Arena, G., et al. (2017). *Helicobacter pylori* targets mitochondrial import and components of mitochondrial DNA replication machinery through an alternative VacA-dependent and a VacA-independent mechanisms. *Sci. Rep.* 7, 15901. doi: 10.1038/s41598-017-15567-3

Chatterjee, N., and Walker, G. C. (2017). Mechanisms of DNA damage, repair, and mutagenesis. *Environ. Mol. Mutagen.* 58, 235–263. doi: 10.1002/em.22087

Chaturvedi, R., Asim, M., Piazuelo, M. B., Yan, F., Barry, D. P., Sierra, J. C., et al. (2014). Activation of EGFR and ERBB2 by *Helicobacter pylori* results in survival of gastric epithelial cells with DNA damage. *Gastroenterology* 146, 1739–51.e14. doi: 10.1053/j.gastro.2014.02.005

Chaturvedi, R., Asim, M., Romero–Gallo, J., Barry, D. P., Hoge, S., de Sablet, T., et al. (2011). Spermine oxidase mediates the gastric cancer risk associated with *helicobacter pylori* CagA. *Gastroenterology* 141, 1696–708.e2. doi: 10.1053/j.gastro.2011.07.045

Chen, H. Y., Hsieh, W. C., Liu, Y. C., Li, H. Y., Liu, P. Y., Hsu, Y. T., et al. (2024). Mitochondrial injury induced by a *Salmonella* genotoxin triggers the proinflammatory senescence-associated secretory phenotype. *Nat. Commun.* 15, 2778. doi: 10.1038/s41467-024-47190-y

Cindrilla, C., Rajendra Kumar, G., Rike, Z., and Thomas, F. M. (2016). Subversion of host genome integrity by bacterial pathogens. *Nat. Rev. Mol. Cell Biol.* 17. 10.1038/nrm.2016.100

Cogliati, S., Enriquez, J. A., and Scorrano, L. (2016). Mitochondrial cristae: where beauty meets functionality. *Trends Biochem. Sci.* 41, 261–273. doi: 10.1016/j.tibs.2016.01.001

Cooke, M. S., Evans, M. D., Dizdaroglu, M., and Lunec, J. (2003). Oxidative DNA damage: mechanisms, mutation, and disease. *FASEB J.* 17, 1195–1214. doi: 10.1096/fj.02-0752rev

Copeland, W. C. (2010). The mitochondrial DNA polymerase in health and disease. *Subcell Biochem.* 50, 211–222. doi: 10.1007/978-90-481-3471-7 11

Covacci, A., and Rappuoli, R. (2000). Tyrosine-phosphorylated bacterial proteins: Trojan horses for the host cell. *J. Exp. Med.* 191, 587–592. doi: 10.1084/jem.191.4.587

Das, B. B., Dexheimer, T. S., Maddali, K., and Pommier, Y. (2010). Role of tyrosyl-DNA phosphodiesterase (TDP1) in mitochondria. *Proc. Natl. Acad. Sci. U.S.A.* 107, 19790–19795. doi: 10.1073/pnas.1009814107

De Gaetano, A., Solodka, K., Zanini, G., Selleri, V., Mattioli, A. V., Nasi, M., et al. (2021). Molecular mechanisms of mtDNA-mediated inflammation. *Cells* 10. doi: 10.3390/cells10112898

de Souza-Pinto, N. C., Mason, P. A., Hashiguchi, K., Weissman, L., Tian, J., Guay, D., et al. (2009). Novel DNA mismatch-repair activity involving YB-1 in human mitochondria. *DNA Repair (Amst).* 8, 704–719. doi: 10.1016/j.dnarep.2009.01.021

Dhir, A., Dhir, S., Borowski, L. S., Jimenez, L., Teitell, M., Rotig, A., et al. (2018). Mitochondrial double-stranded RNA triggers antiviral signalling in humans. *Nature* 560, 238–242. doi: 10.1038/s41586-018-0363-0

Diaz-Talavera, A., Montero-Conde, C., Leandro-Garcia, L. J., and Robledo, M. (2022). PrimPol: A breakthrough among DNA replication enzymes and a potential new target for cancer therapy. *Biomolecules* 12. doi: 10.3390/biom12020248

Dicksved, J., Lindberg, M., Rosenquist, M., Enroth, H., Jansson, J. K., and Engstrand, L. (2009). Molecular characterization of the stomach microbiota in patients with gastric cancer and in controls. *J. Med. Microbiol.* 58, 509–516. doi: 10.1099/jmm.0.007302-0

Domanska, G., Motz, C., Meinecke, M., Harsman, A., Papatheodorou, P., Reljic, B., et al. (2010). *Helicobacter pylori* VacA toxin/subunit p34: targeting of an anion channel to the inner mitochondrial membrane. *PloS Pathog.* 6, e1000878. doi: 10.1371/journal.ppat.1000878

Dorer, M. S., Fero, J., and Salama, N. R. (2010). DNA damage triggers genetic exchange in *Helicobacter pylori*. *PloS Pathog.* 6, e1001026. doi: 10.1371/journal.ppat.1001026

Dou, H., Mitra, S., and Hazra, T. K. (2003). Repair of oxidized bases in DNA bubble structures by human DNA glycosylases NEIL1 and NEIL2. *J. Biol. Chem.* 278, 49679–49684. doi: 10.1074/jbc.M308658200

Druzhyna, N. M., Wilson, G. L., and LeDoux, S. P. (2008). Mitochondrial DNA repair in aging and disease. *Mech. Ageing Dev.* 129, 383–390. doi: 10.1016/j.mad.2008.03.002

Fielden, L. F., Kang, Y., Newton, H. J., and Stojanovski, D. (2017). Targeting mitochondria: how intravacuolar bacterial pathogens manipulate mitochondria. *Cell Tissue Res.* 367, 141–154. doi: 10.1007/s00441-016-2475-x

Filograna, R., Mennuni, M., Alsina, D., and Larsson, N. G. (2021). Mitochondrial DNA copy number in human disease: the more the better? *FEBS Lett.* 595, 976–1002. doi: 10.1002/1873-3468.14021

Fischer, S. F., Vier, J., Kirschnek, S., Klos, A., Hess, S., Ying, S., et al. (2004). Chlamydia inhibit host cell apoptosis by degradation of proapoptotic BH3-only proteins. *J. Exp. Med.* 200, 905–916. doi: 10.1084/jem.20040402

Fontana, G. A., and Gahlon, H. L. (2020). Mechanisms of replication and repair in mitochondrial DNA deletion formation. *Nucleic Acids Res.* 48, 11244–11258. doi: 10.1093/nar/gkaa804

Fox, J. G., and Wang, T. C. (2007). Inflammation, atrophy, and gastric cancer. *J. Clin. Invest.* 117, 60–69. doi: 10.1172/JCI30111

Fridlich, R., Annamalai, D., Roy, R., Bernheim, G., and Powell, S. N. (2015). BRCA1 and BRCA2 protect against oxidative DNA damage converted into double-strand breaks during DNA replication. *DNA Repair (Amst).* 30, 11–20. doi: 10.1016/j.dnarep.2015.03.002

Fujikawa, K., Kamiya, H., Yakushiji, H., Fujii, Y., Nakabeppu, Y., and Kasai, H. (1999). The oxidized forms of dATP are substrates for the human MutT homologue, the hMTH1 protein. *J. Biol. Chem.* 274, 18201–18205. doi: 10.1074/jbc.274.26.18201

Fujikawa, K., Kamiya, H., Yakushiji, H., Nakabeppu, Y., and Kasai, H. (2001). Human MTH1 protein hydrolyzes the oxidized ribonucleotide, 2-hydroxy-ATP. *Nucleic Acids Res.* 29, 449–454. doi: 10.1093/nar/29.2.449

Galick, H. A., Kathe, S., Liu, M., Robey-Bond, S., Kidane, D., Wallace, S. S., et al. (2013). Germ-line variant of human NTH1 DNA glycosylase induces genomic instability and cellular transformation. *Proc. Natl. Acad. Sci. U.S.A.* 110, 14314–14319. doi: 10.1073/pnas.1306752110

Galluzzi, L., Kepp, O., and Kroemer, G. (2012). Mitochondria: master regulators of danger signalling. *Nat. Rev. Mol. Cell Biol.* 13, 780–788. doi: 10.1038/nrm3479

Galmiche, A., and Rassow, J. (2010). Targeting of Helicobacter pylori VacA to mitochondria. *Gut Microbes* 1, 392–395. doi: 10.4161/gmic.1.6.13894

Galmiche, A., Rassow, J., Doye, A., Cagnol, S., Chambard, J. C., Contamin, S., et al. (2000). The N-terminal 34 kDa fragment of *Helicobacter pylori* vacuolating cytotoxin targets mitochondria and induces cytochrome c release. *EMBO J.* 19, 6361–6370. doi: 10.1093/emboj/19.23.6361

Gao, Y., Katyal, S., Lee, Y., Zhao, J., Rehg, J. E., Russell, H. R., et al. (2011). DNA ligase III is critical for mtDNA integrity but not Xrcc1-mediated nuclear DNA repair. *Nature* 471, 240–244. doi: 10.1038/nature09773

Glassner, B. J., Rasmussen, L. J., Najarian, M. T., Posnick, L. M., and Samson, L. D. (1998). Generation of a strong mutator phenotype in yeast by imbalanced base excision repair. *Proc. Natl. Acad. Sci. U.S.A.* 95, 9997–10002. doi: 10.1073/pnas.95.17.9997

Graziewicz, M. A., Longley, M. J., and Copeland, W. C. (2006). DNA polymerase gamma in mitochondrial DNA replication and repair. *Chem. Rev.* 106, 383–405. doi: 10.1021/cr040463d

Gredilla, R. (2010). DNA damage and base excision repair in mitochondria and their role in aging. *J. Aging Res.* 2011, 257093. doi: 10.4061/2011/257093

Guilliam, T. A., Jozwiakowski, S. K., Ehlinger, A., Barnes, R. P., Rudd, S. G., Bailey, L. J., et al. (2015). Human PrimPol is a highly error-prone polymerase regulated by single-stranded DNA binding proteins. *Nucleic Acids Res.* 43, 1056–1068. doi: 10.1093/nar/gku1321

Hiyama, T., Tanaka, S., Shima, H., Kose, K., Kitadai, Y., Ito, M., et al. (2003). Somatic mutation of mitochondrial DNA in Helicobacter pylori-associated chronic gastritis in patients with and without gastric cancer. *Int. J. Mol. Med.* 12, 169–174. doi: 10.3892/ijmm.12.2.169

Hudson, J. J., Chiang, S. C., Wells, O. S., Rookyard, C., and El-Khamisy, S. F. (2012). SUMO modification of the neuroprotective protein TDP1 facilitates chromosomal single-strand break repair. *Nat. Commun.* 3, 733. doi: 10.1038/ncomms1739

Jacobs, A. L., and Schar, P. (2012). DNA glycosylases: in DNA repair and beyond. *Chromosoma* 121, 1–20. doi: 10.1007/s00412-011-0347-4

Jain, P., Luo, Z. Q., and Blanke, S. R. (2011). *Helicobacter pylori* vacuolating cytotoxin A (VacA) engages the mitochondrial fission machinery to induce host cell death. *Proc. Natl. Acad. Sci. U.S.A.* 108, 16032–16037. doi: 10.1073/pnas.1105175108

Jalal, S., Earley, J. N., and Turchi, J. J. (2011). DNA repair: from genome maintenance to biomarker and therapeutic target. *Clin. Cancer Res.* 17, 6973–6984. doi: 10.1158/1078-0432.CCR-11-0761

Kaguni, L. S. (2004). DNA polymerase gamma, the mitochondrial replicase. *Annu. Rev. Biochem.* 73, 293–320. doi: 10.1146/annurev.biochem.72.121801.161455

Kaufman, B. A., and Van Houten, B. (2017). POLB: A new role of DNA polymerase beta in mitochondrial base excision repair. *DNA Repair (Amst).* 60, A1–A5. doi: 10.1016/j.dnarep.2017.11.002

Kavli, B., Slupphaug, G., Mol, C. D., Arvai, A. S., Peterson, S. B., Tainer, J. A., et al. (1996). Excision of cytosine and thymine from DNA by mutants of human uracil-DNA glycosylase. *EMBO J.* 15, 3442–3447. doi: 10.1002/j.1460-2075.1996.tb00710.x

Khanna, K. K., and Jackson, S. P. (2001). DNA double-strand breaks: signaling, repair and the cancer connection. *Nat. Genet.* 27, 247–254. doi: 10.1038/85798

Kidane, D., Murphy, D. L., and Sweasy, J. B. (2014). Accumulation of abasic sites induces genomic instability in normal human gastric epithelial cells during *Helicobacter pylori* infection. *Oncogenesis* 3, e128–e12e. doi: 10.1038/oncsis.2014.42

Kim, B. R., Kim, B. J., Kook, Y. H., and Kim, B. J. (2020). Mycobacterium abscessus infection leads to enhanced production of type 1 interferon and NLRP3 inflammasome activation in murine macrophages via mitochondrial oxidative stress. *PloS Pathog.* 16, e1008294. doi: 10.1371/journal.ppat.1008294

Klungland, A., and Bjelland, S. (2007). Oxidative damage to purines in DNA: role of mammalian Ogg1. *DNA Repair (Amst).* 6, 481–488. doi: 10.1016/j.dnarep.2006.10.012

Klungland, A., Rosewell, I., Hollenbach, S., Larsen, E., Daly, G., Epe, B., et al. (1999). Accumulation of premutagenic DNA lesions in mice defective in removal of oxidative base damage. *Proc. Natl. Acad. Sci. U.S.A.* 96, 13300–13305. doi: 10.1073/pnas.96.23.13300

Koeppel, M., Garcia-Alcalde, F., Glowinski, F., Schlaermann, P., and Meyer, T. F. (2015). *Helicobacter pylori* infection causes characteristic DNA damage patterns in human cells. *Cell Rep.* 11, 1703–1713. doi: 10.1016/j.celrep.2015.05.030

Kolesnikov, A. A. (2016). The mitochondrial genome. *Nucleoid. Biochem. (Mosc).* 81, 1057–1065. doi: 10.1134/S0006297916100047

Kurosaka, M., Ohno, O., and Hirohata, K. (1991). Arthroscopic evaluation of synovitis in the knee joints. *Arthroscopy* 7, 162–170. doi: 10.1016/0749-8063(91)90104-6

Lakshmipathy, U., and Campbell, C. (2001). Antisense-mediated decrease in DNA ligase III expression results in reduced mitochondrial DNA integrity. *Nucleic Acids Res.* 29, 668–676. doi: 10.1093/nar/29.3.668

Ledoux, S. P., Shen, C. C., Grishko, V. I., Fields, P. A., Gard, A. L., and Wilson, G. L. (1998). Glial cell-specific differences in response to alkylation damage. *Glia* 24, 304–312. doi: 10.1002/(SICI)1098-1136(199811)24:3<304::AID-GLIA4>3.0.CO;2-1

LeDoux, S. P., Wilson, G. L., Beecham, E. J., Stevnsner, T., Wassermann, K., and Bohr, V. A. (1992). Repair of mitochondrial DNA after various types of DNA damage in Chinese hamster ovary cells. *Carcinogenesis* 13, 1967–1973. doi: 10.1093/carcin/13.11.1967

Legros, F., Malka, F., Frachon, P., Lombes, A., and Rojo, M. (2004). Organization and dynamics of human mitochondrial DNA. *J. Cell Sci.* 117, 2653–2662. doi: 10.1242/jcs.01134

Li, M., Zhong, Z., Zhu, J., Xiang, D., Dai, N., Cao, X., et al. (2010). Identification and characterization of mitochondrial targeting sequence of human apurinic/apyrimidinic endonuclease 1. *J. Biol. Chem.* 285, 14871–14881. doi: 10.1074/jbc.M109.069591

Lia, D., Reyes, A., de Melo Campos, J. T. A., Piolot, T., Baijer, J., Radicella, J. P., et al. (2018). Mitochondrial maintenance under oxidative stress depends on mitochondrially localised alpha-OGG1. *J. Cell Sci.* 131. doi: 10.1242/jcs.213538

Lieber, M. R. (2010). The mechanism of double-strand DNA break repair by the nonhomologous DNA end-joining pathway. *Annu. Rev. Biochem.* 79, 181–211. doi: 10.1146/annurev.biochem.052308.093131

Lindahl, T. (1993). Instability and decay of the primary structure of DNA. *Nature* 362, 709–715. doi: 10.1038/362709a0

Lindahl, T., and Wood, R. D. (1999). Quality control by DNA repair. *Science* 286, 1897–1905. doi: 10.1126/science.286.5446.1897

Llanos-Gonzalez, E., Henares-Chavarino, A. A., Pedrero-Prieto, C. M., Garcia-Carpintero, S., Frontinan-Rubio, J., Sancho-Bielsa, F. J., et al. (2019). Interplay between mitochondrial oxidative disorders and proteostasis in Alzheimer's disease. *Front. Neurosci.* 13, 1444. doi: 10.3389/fnins.2019.01444

Longley, M. J., Clark, S., Yu Wai Man, C., Hudson, G., Durham, S. E., Taylor, R. W., et al. (2006). Mutant POLG2 disrupts DNA polymerase gamma subunits and causes progressive external ophthalmoplegia. *Am. J. Hum. Genet.* 78, 1026–1034. doi: 10.1086/504303

Longley, M. J., Prasad, R., Srivastava, D. K., Wilson, S. H., and Copeland, W. C. (1998). Identification of 5'-deoxyribose phosphate lyase activity in human DNA polymerase gamma and its role in mitochondrial base excision repair *in vitro*. *Proc. Natl. Acad. Sci. U.S.A.* 95, 12244–12248. doi: 10.1073/pnas.95.21.12244

MaChado, A. M., Figueiredo, C., Touati, E., Maximo, V., Sousa, S., Michel, V., et al. (2009). *Helicobacter pylori* infection induces genetic instability of nuclear and mitochondrial DNA in gastric cells. *Clin. Cancer Res.* 15, 2995–3002. doi: 10.1158/1078-0432.CCR-08-2686

Mandal, S. M., Hegde, M. L., Chatterjee, A., Hegde, P. M., Szczesny, B., Banerjee, D., et al. (2012). Role of human DNA glycosylase Nei-like 2 (NEIL2) and single strand break repair protein polynucleotide kinase 3'-phosphatase in maintenance of mitochondrial genome. *J. Biol. Chem.* 287, 2819–2829. doi: 10.1074/jbc.M111.272179

Martinez-Jimenez, M. I., Calvo, P. A., Garcia-Gomez, S., Guerra-Gonzalez, S., and Blanco, L. (2018). The Zn-finger domain of human PrimPol is required to stabilize the initiating nucleotide during DNA priming. *Nucleic Acids Res.* 46, 4138–4151. doi: 10.1093/nar/gky230

Maynard, S., Schurman, S. H., Harboe, C., de Souza-Pinto, N. C., and Bohr, V. A. (2009). Base excision repair of oxidative DNA damage and association with cancer and aging. *Carcinogenesis* 30, 2–10. doi: 10.1093/carcin/bgn250

McKinney, E. A., and Oliveira, M. T. (2013). Replicating animal mitochondrial DNA. *Genet. Mol. Biol.* 36, 308–315. doi: 10.1590/S1415-47572013000300002

Michaels, M. L., Tchou, J., Grollman, A. P., and Miller, J. H. (1992). A repair system for 8-oxo-7,8-dihydrodeoxyguanine. *Biochemistry* 31, 10964–10968. doi: 10.1021/bi00160a004

Nakabeppu, Y. (2014). Cellular levels of 8-oxoguanine in either DNA or the nucleotide pool play pivotal roles in carcinogenesis and survival of cancer cells. *Int. J. Mol. Sci.* 15, 12543–12557. doi: 10.3390/ijms150712543

Nakabeppu, Y., Kajitani, K., Sakamoto, K., Yamaguchi, H., and Tsuchimoto, D. (2006). MTH1, an oxidized purine nucleoside triphosphatase, prevents the cytotoxicity and neurotoxicity of oxidized purine nucleotides. *DNA Repair (Amst).* 5, 761–772. doi: 10.1016/j.dnarep.2006.03.003

Nakabeppu, Y., Tsuchimoto, D., Yamaguchi, H., and Sakumi, K. (2007). Oxidative damage in nucleic acids and Parkinson's disease. *J. Neurosci. Res.* 85, 919–934. doi: 10.1002/jnr.21191

Nakada, K., Inoue, K., Ono, T., Isobe, K., Ogura, A., Goto, Y. I., et al. (2001). Inter-mitochondrial complementation: Mitochondria-specific system preventing mice from expression of disease phenotypes by mutant mtDNA. *Nat. Med.* 7, 934–940. doi: 10.1038/90976

Neupert, W. (1997). Protein import into mitochondria. *Annu. Rev. Biochem.* 66, 863–917. doi: 10.1146/annurev.biochem.66.1.863

Nicholls, T. J., Zsurka, G., Peeva, V., Scholer, S., Szczesny, R. J., Cysewski, D., et al. (2014). Linear mtDNA fragments and unusual mtDNA rearrangements associated with pathological deficiency of MGME1 exonuclease. *Hum. Mol. Genet.* 23, 6147–6162. doi: 10.1093/hmg/ddu336

Nishioka, K., Ohtsubo, T., Oda, H., Fujiwara, T., Kang, D., Sugimachi, K., et al. (1999). Expression and differential intracellular localization of two major forms of human 8-oxoguanine DNA glycosylase encoded by alternatively spliced OGG1 mRNAs. *Mol. Biol. Cell.* 10, 1637–1652. doi: 10.1091/mbc.10.5.1637

Ohtsubo, T., Nishioka, K., Imaiso, Y., Iwai, S., Shimokawa, H., Oda, H., et al. (2000). Identification of human MutY homolog (hMYH) as a repair enzyme for 2-hydroxyadenine in DNA and detection of multiple forms of hMYH located in nuclei and mitochondria. *Nucleic Acids Res.* 28, 1355–1364. doi: 10.1093/nar/28.6.1355

Ono, T., Isobe, K., Nakada, K., and Hayashi, J. I. (2001). Human cells are protected from mitochondrial dysfunction by complementation of DNA products in fused mitochondria. *Nat. Genet.* 28, 272–275. doi: 10.1038/90116

Peek, R. M. Jr., and Blaser, M. J. (2002). *Helicobacter pylori* and gastrointestinal tract adenocarcinomas. *Nat. Rev. Cancer.* 2, 28–37. doi: 10.1038/nrc703

Pirsel, M., and Bohr, V. A. (1993). Methyl methanesulfonate adduct formation and repair in the DHFR gene and in mitochondrial DNA in hamster cells. *Carcinogenesis* 14, 2105–2108. doi: 10.1093/carcin/14.10.2105

Prachar, J. (2016). Ultrastructure of mitochondrial nucleoid and its surroundings. *Gen. Physiol. Biophys.* 35, 273–286. doi: 10.4149/gpb_2016008

Prakash, A., and Doublie, S. (2015). Base excision repair in the mitochondria. *J. Cell Biochem.* 116, 1490–1499. doi: 10.1002/jcb.v116.8

Prasad, R., Caglayan, M., Dai, D. P., Nadalutti, C. A., Zhao, M. L., Gassman, N. R., et al. (2017). DNA polymerase beta: A missing link of the base excision repair machinery in mammalian mitochondria. *DNA Repair (Amst).* 60, 77–88. doi: 10.1016/j.dnarep.2017.10.011

Richter, C., Park, J. W., and Ames, B. N. (1988). Normal oxidative damage to mitochondrial and nuclear DNA is extensive. *Proc. Natl. Acad. Sci. U.S.A.* 85, 6465–6467. doi: 10.1073/pnas.85.17.6465

Robberson, D. L., Kasamatsu, H., and Vinograd, J. (1972). Replication of mitochondrial DNA. Circular replicative intermediates in mouse L cells. *Proc. Natl. Acad. Sci. U.S.A.* 69, 737–741. doi: 10.1073/pnas.69.3.737

Sahan, A. Z., Hazra, T. K., and Das, S. (2018). The pivotal role of DNA repair in infection mediated-inflammation and cancer.(Report)(Brief article). *Front. Microbiol.* 9. doi: 10.3389/fmicb.2018.00663

Scott, I., and Youle, R. J. (2010). Mitochondrial fission and fusion. *Essays Biochem.* 47, 85–98. doi: 10.1042/bse0470085

Sharma, P., and Sampath, H. (2019). Mitochondrial DNA integrity: role in health and disease. *Cells* 8. doi: 10.3390/cells8020100

Shokolenko, I. N., Alexeyev, M. F., Robertson, F. M., LeDoux, S. P., and Wilson, G. L. (2003). The expression of Exonuclease III from E. coli in mitochondria of breast cancer cells diminishes mitochondrial DNA repair capacity and cell survival after oxidative stress. *DNA Repair (Amst).* 2, 471–482. doi: 10.1016/S1568-7864(03)00019-3

Shokolenko, I. N., Fayzulin, R. Z., Katyal, S., McKinnon, P. J., Wilson, G. L., and Alexeyev, M. F. (2013). Mitochondrial DNA ligase is dispensable for the viability of cultured cells but essential for mtDNA maintenance. *J. Biol. Chem.* 288, 26594–26605. doi: 10.1074/jbc.M113.472977

Simsek, D., Furda, A., Gao, Y., Artus, J., Brunet, E., Hadjantonakis, A. K., et al. (2011). Crucial role for DNA ligase III in mitochondria but not in Xrcc1-dependent repair. *Nature* 471, 245–248. doi: 10.1038/nature09794

Simsek, D., and Jasin, M. (2011). DNA ligase III: a spotty presence in eukaryotes, but an essential function where tested. *Cell Cycle* 10, 3636–3644. doi: 10.4161/cc.10.21.18094

Song, J., and Bent, A. F. (2014). Microbial pathogens trigger host DNA double-strand breaks whose abundance is reduced by plant defense responses. *PloS Pathog.* 10, e1004030. doi: 10.1371/journal.ppat.1004030

Spelbrink, J. N. (2010). Functional organization of mammalian mitochondrial DNA in nucleoids: history, recent developments, and future challenges. *IUBMB Life.* 62, 19–32. doi: 10.1002/iub.v62:1

Spelbrink, J. N., Li, F. Y., Tiranti, V., Nikali, K., Yuan, Q. P., Tariq, M., et al. (2001). Human mitochondrial DNA deletions associated with mutations in the gene encoding Twinkle, a phage T7 gene 4-like protein localized in mitochondria. *Nat. Genet.* 28, 223–231. doi: 10.1038/90058

Spier, A., Stavru, F., and Cossart, P. (2019). Interaction between intracellular bacterial pathogens and host cell mitochondria. *Microbiol. Spectr.* 7. doi: 10.1128/microbiolspec.BAI-0016-2019

Sprenger, H. G., MacVicar, T., Bahat, A., Fiedler, K. U., Hermans, S., Ehrentraut, D., et al. (2021). Cellular pyrimidine imbalance triggers mitochondrial DNA-dependent innate immunity. *Nat. Metab.* 3, 636–650. doi: 10.1038/s42255-021-00385-9

Stavru, F., Bouillaud, F., Sartori, A., Ricquier, D., and Cossart, P. (2011). Listeria monocytogenes transiently alters mitochondrial dynamics during infection. *Proc. Natl. Acad. Sci. U.S.A.* 108, 3612–3617. doi: 10.1073/pnas.1100126108

Stuart, J. A., Mayard, S., Hashiguchi, K., Souza-Pinto, N. C., and Bohr, V. A. (2005). Localization of mitochondrial DNA base excision repair to an inner membrane-associated particulate fraction. *Nucleic Acids Res.* 33, 3722–3732. doi: 10.1093/nar/gki683

Svilar, D., Goellner, E. M., Almeida, K. H., and Sobol, R. W. (2011). Base excision repair and lesion-dependent subpathways for repair of oxidative DNA damage. *Antioxid Redox Signal.* 14, 2491–2507. doi: 10.1089/ars.2010.3466

Swanson, K. V., Deng, M., and Ting, J. P. (2019). The NLRP3 inflammasome: molecular activation and regulation to therapeutics. *Nat. Rev. Immunol.* 19, 477–489. doi: 10.1038/s41577-019-0165-0

Sykora, P., Croteau, D. L., Bohr, V. A., and Wilson, D. M. 3rd (2011). Aprataxin localizes to mitochondria and preserves mitochondrial function. *Proc. Natl. Acad. Sci. U.S.A.* 108, 7437–7442. doi: 10.1073/pnas.1100084108

Sykora, P., Kanno, S., Akbari, M., Kulikowicz, T., Baptiste, B. A., Leandro, G. S., et al. (2017). DNA polymerase beta participates in mitochondrial DNA repair. *Mol. Cell Biol.* 37. doi: 10.1128/MCB.00237-17

Szczepanowska, K., and Trifunovic, A. (2015). Different faces of mitochondrial DNA mutators. *Biochim. Biophys. Acta* 1847, 1362–1372. doi: 10.1016/j.bbabio.2015.05.016

Taylor, R. W., and Turnbull, D. M. (2005). Mitochondrial DNA mutations in human disease. *Nat. Rev. Genet.* 6, 389–402. doi: 10.1038/nrg1606

Terebiznik, M. R., Raju, D., Vazquez, C. L., Torbricki, K., Kulkarni, R., Blanke, S. R., et al. (2009). Effect of Helicobacter pylori's vacuolating cytotoxin on the autophagy pathway in gastric epithelial cells. *Autophagy* 5, 370–379. doi: 10.4161/auto.5.3.7663

Thorslund, T., Sunesen, M., Bohr, V. A., and Stevnsner, T. (2002). Repair of 8-oxoG is slower in endogenous nuclear genes than in mitochondrial DNA and is without strand bias. *DNA Repair (Amst).* 1, 261–273. doi: 10.1016/S1568-7864(02)00003-4

Tilokani, L., Nagashima, S., Paupe, V., and Prudent, J. (2018). Mitochondrial dynamics: overview of molecular mechanisms. *Essays Biochem.* 62, 341–360. doi: 10.1042/EBC20170104

Toller, I. M., Neelsen, K. J., Steger, M., Hartung, M. L., Hottiger, M. O., Stucki, M., et al. (2011). Carcinogenic bacterial pathogen *Helicobacter pylori* triggers DNA double-strand breaks and a DNA damage response in its host cells. *Proc. Natl. Acad. Sci. U.S.A.* 108, 14944–14949. doi: 10.1073/pnas.1100959108

Torralba, D., Baixauli, F., and Sanchez-Madrid, F. (2016). Mitochondria know no boundaries: mechanisms and functions of intercellular mitochondrial transfer. *Front. Cell Dev. Biol.* 4, 107. doi: 10.3389/fcell.2016.00107

Wallace, D. C. (2005). A mitochondrial paradigm of metabolic and degenerative diseases, aging, and cancer: a dawn for evolutionary medicine. *Annu. Rev. Genet.* 39, 359–407. doi: 10.1146/annurev.genet.39.110304.095751

Wang, Y., and Bogenhagen, D. F. (2006). Human mitochondrial DNA nucleoids are linked to protein folding machinery and metabolic enzymes at the mitochondrial inner membrane. *J. Biol. Chem.* 281, 25791–25802. doi: 10.1074/jbc.M604501200

Wang, Y., Xu, H., Liu, T., Huang, M., Butter, P. P., Li, C., et al. (2018). Temporal DNA-PK activation drives genomic instability and therapy resistance in glioma stem cells. *JCI Insight* 3. doi: 10.1172/jci.insight.98096

West, A. P., Khoury-Hanold, W., Staron, M., Tal, M. C., Pineda, C. M., Lang, S. M., et al. (2015). Mitochondrial DNA stress primes the antiviral innate immune response. *Nature* 520, 553–557. doi: 10.1038/nature14156

Whitaker, A. M., Schaich, M. A., Smith, M. R., Flynn, T. S., and Freudenthal, B. D. (2017). Base excision repair of oxidative DNA damage: from mechanism to disease. *Front. Biosci. (Landmark Ed).* 22, 1493–1522. doi: 10.2741/4555

Wiens, K. E., and Ernst, J. D. (2016). The mechanism for type I interferon induction by mycobacterium tuberculosis is bacterial strain-dependent. *PloS Pathog.* 12, e1005809. doi: 10.1371/journal.ppat.1005809

Wonnapinij, P., Chinnery, P. F., and Samuels, D. C. (2008). The distribution of mitochondrial DNA heteroplasmy due to random genetic drift. *Am. J. Hum. Genet.* 83, 582–593. doi: 10.1016/j.ajhg.2008.10.007

Woodbine, L., Brunton, H., Goodarzi, A. A., Shibata, A., and Jeggo, P. A. (2011). Endogenously induced DNA double strand breaks arise in heterochromatic DNA regions and require ataxia telangiectasia mutated and Artemis for their repair. *Nucleic Acids Res.* 39, 6986–6997. doi: 10.1093/nar/gkr331

Xu, L., Li, M., Yang, Y., Zhang, C., Xie, Z., Tang, J., et al. (2022). Salmonella Induces the cGAS-STING-Dependent Type I Interferon Response in Murine Macrophages by Triggering mtDNA Release. *mBio* 13, e0363221. doi: 10.1128/mbio.03632-21

Yakes, F. M., and Van Houten, B. (1997). Mitochondrial DNA damage is more extensive and persists longer than nuclear DNA damage in human cells following oxidative stress. *Proc. Natl. Acad. Sci. U.S.A.* 94, 514–519. doi: 10.1073/pnas.94.2.514

Yang, W., and Gao, Y. (2018). Translesion and repair DNA polymerases: diverse structure and mechanism. *Annu. Rev. Biochem.* 87, 239–261. doi: 10.1146/annurev-biochem-062917-012405

Yoneda, M., Miyatake, T., and Attardi, G. (1994). Complementation of mutant and wild-type human mitochondrial DNAs coexisting since the mutation event and lack of complementation of DNAs introduced separately into a cell within distinct organelles. *Mol. Cell Biol.* 14, 2699–2712. doi: 10.1128/mcb.14.4.2699-2712.1994

Zhang, H., Barcelo, J. M., Lee, B., Kohlhagen, G., Zimonjic, D. B., Popescu, N. C., et al. (2001). Human mitochondrial topoisomerase I. *Proc. Natl. Acad. Sci. U.S.A.* 98, 10608–10613. doi: 10.1073/pnas.191321998

Zhao, L., and Sumberaz, P. (2020). Mitochondrial DNA damage: prevalence, biological consequence, and emerging pathways. *Chem. Res. Toxicol.* 33, 2491–2502. doi: 10.1021/acs.chemrestox.0c00083

Zhong, Z., Liang, S., Sanchez-Lopez, E., He, F., Shalapour, S., Lin, X. J., et al. (2018). New mitochondrial DNA synthesis enables NLRP3 inflammasome activation. *Nature* 560, 198–203. doi: 10.1038/s41586-018-0372-z

frontiers | Frontiers in Cellular and Infection Microbiology

TYPE Original Research
PUBLISHED 29 January 2025
DOI 10.3389/fcimb.2025.1511625

OPEN ACCESS

EDITED BY
Maurizio Sanguinetti,
Catholic University of the Sacred Heart, Italy

REVIEWED BY
Shintaro Nakajima,
California Institute of Technology,
United States
Izabela Korona-Glowniak,
Medical University of Lublin, Poland
Meghan Lynne Ruebel,
United States Department of Agriculture,
United States

*CORRESPONDENCE
Aleksandra Kowalczyk
aleksandra.strzelczyk@biol.uni.lodz.pl

RECEIVED 15 October 2024
ACCEPTED 02 January 2025
PUBLISHED 29 January 2025

CITATION
Kuźmycz O, Kowalczyk A, Bolanowska A, Drozdzowska A, Lach J, Wierzbińska W, Kluz T and Stączek P (2025) A comprehensive analysis of the uterine microbiome in endometrial cancer patients - identification of *Anaerococcus* as a potential biomarker and carcinogenic cofactor.
Front. Cell. Infect. Microbiol. 15:1511625.
doi: 10.3389/fcimb.2025.1511625

A comprehensive analysis of the uterine microbiome in endometrial cancer patients - identification of *Anaerococcus* as a potential biomarker and carcinogenic cofactor

Olga Kuźmycz[1], Aleksandra Kowalczyk[1]*, Aleksandra Bolanowska[2], Anna Drozdzowska[2], Jakub Lach[1,3], Wiktoria Wierzbińska[1,4], Tomasz Kluz[2,5] and Paweł Stączek[1]

[1]Department of Molecular Microbiology, Institute of Microbiology, Biotechnology and Immunology, University of Lodz, Faculty of Biology and Environmental, Protection, Lodz, Poland, [2]Department of Gynecology and Obstetrics, Fryderyk Chopin University Hospital No. 1, Rzeszow, Poland, [3]Biobank Lab, Department of Cancer Biology and Epigenetics, University of Lodz, Faculty of Biology and Environmental Protection, Lodz, Poland, [4]BioMedChem Doctoral School of the University of Lodz and Lodz Institutes of the Polish Academy of Sciences, Lodz, Poland, [5]Department of Gynecology, Gynecology Oncology and Obstetrics, Institute of Medical Sciences, Medical College of Rzeszow University, Rzeszow, Poland

Introduction: Endometrial cancer (EC) is a significant gynecological malignancy with increasing incidence worldwide. Emerging evidence highlights the role of the uterine microbiome in the pathogenesis of EC. This study aims to characterize the uterine microbiome in EC patients and identify potential microbial biomarkers, with a focus on *Anaerococcus* as a differentiating taxon.

Methods: The endocervical canal swabs from patients with EC (n=16) and non-cancerous patients (EM, n=13) were collected. The V3-V4 region of the 16S rRNA gene was sequenced using the Illumina platform. Bioinformatic analyses were performed with QIIME2, and statistical comparisons were conducted to assess differences in microbial composition and diversity. *In vitro* experiments were conducted to assess the functional impact of *Anaerococcus* on human uterine fibroblasts, including its ability to adhere to the human cells and induce oxidative stress.

Results: The α-diversity metrics, including Shannon entropy and observed amplicon sequence variants (ASVs), revealed significantly higher microbial diversity in EC samples compared to EM. *Anaerococcus* was identified as a key taxon differentiating EC from EM groups, showing a higher relative abundance in EC samples. Functional predictions and *in vitro* assays indicated that *Anaerococcus* may contribute to carcinogenesis by inducing reactive oxygen species (ROS) production, and has the high ability to adhere to the human endometrial fibroblasts.

Discussion: The study provides evidence of distinct microbial signatures in EC, with *Anaerococcus* emerging as a potential biomarker. The *in vitro* findings suggest its role in endometrial carcinogenesis, underscoring its potential as a target for future diagnostic and therapeutic applications.

KEYWORDS

endometrial cancer, microbiome, *Anaerococcus vaginalis*, 16S rRNA metagenomics, ANCOM analysis

1 Introduction

Endometrial cancer (EC) is one of the most common female reproductive tract malignancies in developed countries. According to the International Agency for Research on Cancer, the incidence rate of EC is increasing rapidly compared with 2018 and is estimated to increase by more than 50% worldwide by 2040. In 2020, Poland had the highest rate of EC in the world, which corresponded to 9,869 diagnosed new cases (Chen et al., 2017; Morice et al., 2016; World Cancer Research Fund International, 2023). Only several factors, including host genetic alterations and hereditary factors, have been shown to play important roles in endometrial carcinogenesis. But still, this can only explain 10–20% of EC cases. A woman's lifetime risk of EC is approximately 3%, with a median age at diagnosis of 61 years. Environmental factors, such as hormones, obesity, inflammation, as well as menopausal status and microbiome composition, were found to be related to EC initiation and progression (Kuźmycz and Stączek, 2020; Morice et al., 2016). The Human Microbiome Project has revealed that about 9% of the total human microbiome was found in the female reproductive tract. Historically, the cervix was considered to be the barrier which protected the upper genital tract from bacteria. Thus, the uterus, in its physiological state, was suggested to be a bacteria-free zone. However, the studies with the use of metagenome sequencing techniques demonstrated a diversity of bacterial populations in the uterus, which additionally can undergo significant changes in pathological states (Moreno et al., 2022). Interestingly, a risk factor for EC is postmenopause since, in this period, an increase of uterine bacterial diversity is observed, which is associated with disorders and pathologies in the female reproductive tract. The endometrial microbiota in postmenopausal women may create conditions that allow the bacterial community correlated to EC to emerge. It was suggested that EC-related bacteria are probably associated with chronic inflammation and disruption of host cellular functions, leading to a carcinogenic process (Medina-Bastidas et al., 2022; Walsh et al., 2019). In the presented study, the endocervical canal microbiomes of women with EC or endometrial myoma (EM) were examined to reveal the differences in microbial composition. Some pathological taxa were identified, which may play a crucial role in EC development and progression. Previous studies have linked species such as *Prevotella* and *Gardnerella* to uterine dysbiosis in endometrial cancer (EC). However, their association with other gynecological and systemic diseases, such as bacterial vaginosis (BV) and pelvic inflammatory disease (PID) (Gilbert et al., 2019; Qing et al., 2024), challenges their utility as specific diagnostic markers for EC. In contrast, the role of *Anaerococcus* in the uterine microenvironment and EC pathogenesis remains unexplored. This study provides a preliminary evaluation of *A. vaginalis*'s capacity to induce reactive oxygen species (ROS) production and adhere to endometrial cells—two critical processes that may underlie its involvement in cancer progression. By focusing on these initial interactions, we aim to position *Anaerococcus* as a potential microbiological biomarker specific to EC, distinguishing it from previously studied genera. Importantly, our work represents a novel perspective on this microorganism and highlights its potential diagnostic relevance.

2 Materials and methods

2.1 Participant enrollment

In this study, we analyzed the endocervical canal microbiomes of the 29 participants. The endocervical canal swabs were prepared and supplied by the Fryderyk Chopin Clinic no 1 of Rzeszow, Poland. The procedure of material identification and collection was supported with all necessary protocols and procedures and obtained the Regional Bioethics Committee approval number 24/B/2019 with further updates. Participants were patients of the Gynecology Department of Fryderyk Chopin Clinical Hospital no 1 in Rzeszow who were qualified for surgical treatment due to diagnosed EC or EM. The mainstay of treatment for EC is total hysterectomy with bilateral salpingo-oophorectomy. Hysterectomy and adnexectomy can be done with minimally invasive techniques (laparoscopy or robotassisted surgery), vaginally, or laparotomically (Braun et al., 2016; Morice et al., 2016). Removal of the uterus is also recommended for women with symptomatic EM, for whom medical treatments have failed, and who have completed childbearing (Thubert et al., 2016). The main criteria for the selection of participants were as follows: women aged 18 years or older, with EC or EM, who had not been treated with antibacterial

agents for more than one month before collecting the samples. Participants also completed the additional questionnaires, the data of which are presented in Table 1. Continuous variables were compared using the Mann-Whitney U test, and categorical variables were analyzed using Fisher's exact test. A p-value < 0.05 was considered statistically significant.

The study was approved by the Bioethics Committee of the Regional Medical Council in Rzeszow City (Protocol number 24/B/2019, update 54/B/2020, date of approval 21.05.2020).

TABLE 1 Patient demographics.

Variables	Endometrial myoma (n= 13)	Endometrial cancer (n=16)	P-value
Age (years) - median, IQR	48.6 (42-53)	63.6 (51-78)	**0,002**
Caucasian ethnicity (%)	13 (100)	16 (100)	–
Age of the first menstruation (years) – median, IQR	13,8 (10-17)	13,8 (11-17)	–
Postmenopausal status	100%	100%	–
Number of births – median, IQR	2.1 (0-4)	2.1 (0-5)	0,765
Miscarriages	2	0	0,474
Antibiotics for last month	0	0	0,043
Antibiotics for last year	2	2	1,000
HRT **Yes** **No**	0 13	1 15	1,000
PCOS **Yes** **No**	0 13	1 15	1,000
Endometriosis **Yes** **No**	1 12	1 15	1,000
Wight – median, IQR	72.44 (55-82)	80.92 (57-115)	0,098
BMI – median, IQR	26 (20-31)	30 (24-38)	0,051
Diabetes **Yes** **No**	1 12	4 12	0,324
Smoking status **Yes** **No**	1 12	1 15	1,000
Thyroid abnormalities **Yes** **No**	0 13	5 11	**0,043**
Breast cancer **Yes** **No**	0 13	1 13	1,000

IQR – interquartile range; HRT, hormone replacement therapy; PCOS, polycystic ovary syndrome; BMI, body mass index.
Statistical analyses were performed using Mann-Whitney U for nonparametric data categorical variables were analyzed using Fisher's exact test. The significant differences are marked in bold ($p < 0.05$)."

2.2 Endocervical canal swabs collection

Swabs were collected by the surgeon from the endocervical canal (after visualization in a speculum) before the hysterectomy using sterile Dacron swabs and then placed in sterile Falcon tubes. The smear material prepared in this way was stored on dry ice. For long-term storage, -80°C was used. No additional buffer was added to the swabs.

2.3 Sample preparation and processing

1 ml of the sterile Dulbecco's Phosphate Buffered Saline (DPBS) was added to the swabs and then vortexed three times for 15 seconds. Samples were then centrifuged at 10,000 x g for 15 minutes to collect all bacterial cells in the supernatant. All genomic DNA extractions were performed using the DNeasy Power Soil Kit (Qiagen, Hilden, Germany) with minor modifications. For lysis, Lysis Solution was used, which was a part of the kit supplemented with Lysozyme (10 mg/ml), Mutanolyzin (10 U/µl), and Lizostaphin (0.4 U/µl) (AandA Biotechnology, Gdańsk, Poland). Lysis was performed overnight at 37°C with gentle shaking. Subsequent DNA extraction steps were performed according to the manufacturer's instructions. The amount of eluted DNA was measured on BioDrop (BioDrop Ltd, Harvard Bioscience, Hollistone, USA. MA). The 5 ng of extracted DNA was used for polymerase chain reaction (PCR) amplification of the V3-V4 region of 16S rDNA. The reaction was prepared according to the instructions for 16S Metagenomic Sequencing Library Preparation (Illumina, San Diego, USA. CA) and the Nextera XT DNA Library Preparation Kit (Illumina, San Diego, USA. CA). 16S rDNA sequencing was performed by the University of Lodz Biobank Lab using the Illumina MiSeq next generation sequencing platform (Illumina, San Diego, USA. CA) (Figure 1).

2.4 Bioinformatic sequence analysis

In this study, 16S metagenomics targeting the V3-V4 region was employed rather than full metagenomic sequencing. This approach was chosen for its high resolution in analyzing microbial communities and cost-effectiveness for exploratory studies. At the first stage of analysis, the quality of reads was checked using FastQC. In the next step, adaptors and low-quality sequences were removed from the reads with trim galore v. 0.6.4 set on default parameters. Further analysis was performed with QIIME2 2021.4. DADA2 was used for denoising data and ASVs (amplicon sequence variants) table generation with parameters –p-trim-left-f 25 –p-trunclen-f 240 –p-trim-left-r 25 –p-trunc-len-r 240. Alpha and beta diversity metrics were generated with the core-metrics-phylogenetic plugin with a sampling depth of 27 132. Alpha diversity, which presents the evenness and richness of bacterial population within samples, was investigated with the Shannon index, Pielou's evenness and ASVs number. Between groups, a comparison of α-diversity was performed with the Kruskal-Wallis test. Beta diversity was measured by three methods: Bray-Curtis dissimilarity, Unweighted UniFrac distance and Weighted UniFrac distance. These indexes were calculated for analysis of the shared diversity between bacterial communities in

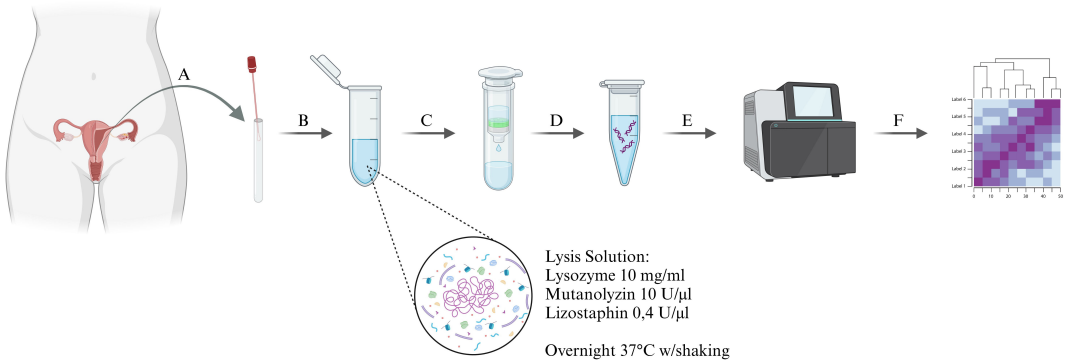

FIGURE 1
Diagram of the experimental procedure, **(A)** – sample collection, **(B)** – primary lysis in Lysis Solution, containing the specific bacterial enzymes cocktail, **(C)** - bacterial DNA extraction, **(D)** – bacterial DNA amplification, **(E)** – sequencing using the Illumina MiSeq next-generation sequencing platform, **(F)** – bioinformatic analysis of the samples.

terms of ecological distance between samples. Differences in β-diversity between groups were tested by the PERMANOVA procedure, which is a multivariate analysis of variance based on distance matrices and permutation. Principal coordinate analysis (PCoA) of β-diversity was also performed and plotted with QIIME2. The Analysis of Compositions of Microbiomes (ANCOM) was performed using the standard QIIME2 pipeline.

The purpose of alpha and beta diversity analyses was to assess variability and composition of the microbiome in EC and EM patient samples. The Shannon index was used to evaluate the evenness and richness of bacterial populations, while beta diversity was analyzed using Unweighted and Weighted UniFrac metrics and Bray-Curtis distances. The results indicate significant differences in microbiota composition between groups, potentially reflecting the pathological role of the microbiome in EC.

2.5 Human uterine fibroblasts cell culture

Human uterine fibroblasts (HUF; C12385) were purchased from PromoCell and cultured in Fibroblast Growth Medium 2 (23020 PromoCell, Heidelberg, Germany) supplemented with 2% fetal bovine serum (FBS, PromoCell, Heidelberg, Germany) and 1x streptomycin/penicillin solution (Cytogen, Zgierz, Poland). The culture was performed at 37°C, 5% CO_2. Prior to the experiment, subculture was performed in Basal Medium Eagle (BME, Cytogen, Zgierz, Poland) supplemented with 2% FBS without antibiotics. Subculture was performed under normoglycemic conditions by adding 5 mM D-(+)-glucose solution (Merck, Darmstadt, Germany) to the culture medium.

2.6 Bacterial culture and MOI determination

Anaerococcus vaginalis (DSM no. 7457, Leibniz Institute DSMZ-German Collection of Microorganisms and Cell Cultures GmbH, Braunschweig, Germany) was anaerobically cultured in tryptic soy broth (TSB; BioMaxima S.A., Lublin, Poland) complemented with 5% defibrinated horse blood (BioMaxima S.A., Lublin, Poland), vitamin K1 (ThermoFisher Scientific, Waltham, USA. MA), and HAEMIN (ThermoFisher Scientific, Waltham, USA. MA)), solutions. *Lactobacillus jensenii* (DSM no. 20557, Leibniz Institute DSMZ-German Collection of Microorganisms and Cell Cultures GmbH, Braunschweig, Germany), used as a physiological control, was cultured in TSB containing 10% FBS at 37°C and 5% CO_2. The multiplicity of infection (MOI) was determined by direct infection of human uterine fibroblasts (10,000 cells/well) with bacteria from each double-dilution. Subsequently, the viability of human uterine cells was analyzed 24 hours after infection by microscopic observation and staining with a 5% crystal violet solution. The viable and death cells ratio was calculated. The MOI at which only 30% of cells were dead was considered suitable.

2.7 Adhesion assay

HUF cells were precultured overnight in a BME medium containing 2% FBS at a density of 500,000 cells/well. Bacterial cells were centrifuged at 10,000 rpm/10 min, and the culture medium residue was discarded. The pellets were resuspended in fresh BME w/2% FBS medium, and the HUF cells were infected at the calculated MOI. At 24 hours post-infection, HUF cells were washed with DPBS and stained for 15 minutes with BacLight Green fluorescent dye (Invitrogen, Waltham, USA. MA), prepared according to the manufacturer's instructions. Cells were then trypsinized and collected by centrifugation (5,000 rpm/5min). The supernatant was discarded, and the pellet was suspended in DPBS. Samples prepared in this manner were placed on a flat-bottomed black culture plate. The measurement was performed at a wavelength of Ex/Em = 480/561 nm using the SpectraMax i3 plate reader (Molecular Devices, San Jose, USA. CA).

2.8 ROS level measurement

HUF cells were precultured, as described above. Bacterial cells were centrifuged at 10,000 rpm/10 min, and the culture medium residue was discarded. Microbial cells were suspended in fresh BME w/2% FBS medium. Next, HUF cells were infected with bacterial inoculum at calculated MOI and cocultured for 24 hours. Then, the cell monolayer was washed with DPBS, and H_2DCF-DA dye (ThermoFisher Scientific, Waltham, USA. MA) in BME medium w/o FBS was added. Incubation with the dye was performed for 40 min at 37°C. After incubation, cells were trypsinized, collected by centrifugation (5,000 rpm/5min), and placed on a flat-bottomed black culture plate. The measurement was performed at Ex/Em = 492/527 nm using the SpectraMax i3 plate reader (Molecular Devices, San Jose, USA. CA)

2.9 Statistics

The bioinformatics analysis pathway for data obtained from 16S rRNA amplicon sequencing was described in detail in section 2.4 Bioinformatic sequence analysis, where it was indicated that the analyses were carried out based on the QIIME2 2021.4 platform. The statistics related with *in vitro* examination were performed by using GraphPad Prism 8.

3 Results

3.1 Participants characteristics

Twenty-nine patients were included in this study. The patients were divided into two major groups: 13 participants with endometrial EM and 16 with EC. The characteristics of cohorts are described in Table 1. Material examination and diagnoses were made by a pathologist at the Fryderyk Chopin Clinic no 1 (Rzeszow, Poland). The material from healthy women was not considered in this study because the hysterectomy is not provided in healthy patients. Endometrial myoma was chosen instead because these cells are non-tumorigenic in nature, and at the molecular level, they have qualities closer to normal cells on molecular bases. Significant differences were observed for age (p = 0.002) and thyroid abnormalities (p = 0.043) between the EM and EC groups, with endometrial cancer patients being older and more likely to report thyroid abnormalities.

3.2 Statistical comparison of uterus lesions microbiome

The α-diversity comparison based on the Shannon index revealed statistically significant differences between EM and EC samples (p = 0.028, p < 0.01) (Figure 2). It can be noticed that samples collected from the EC patients were characterized by greater biodiversity than samples from the EM patients, which may suggest the appearance of dysbiosis. The observed amplicon sequence variants (ASVs) number is included in Figure 3. It was shown that EM and EC differ statistically significantly in terms of the ASVs number (p = 0.039), wherein a higher number of ASVs is observed in the EC group. In addition to Shannon index and ASVs number, statistical comparison was also performed in an analogous way for Pielou's evenness and showed a statistically significant difference between the EM and EC groups (p = 0.02).

To provide a comprehensive overview of alpha diversity metrics, a detailed summary of the results, including mean, standard deviation (SD), median, and interquartile range (IQR), is presented in Table 2. The table further illustrates the observed differences in Shannon entropy, ASVs number, and Pielou's evenness between the EM and EC groups. These results indicate that the EC group demonstrates greater richness and variability in the microbiota, consistent across all alpha diversity metrics analyzed.

The α-diversity results collectively indicate significant differences in the richness, balance, and evenness of the microbiota between the groups, underscoring a potential role of dysbiosis in endometrial cancer pathogenesis.

Principal Coordinate Analysis (PCoA), based on Bray-Curtis distance (Table 3, Figure 4A), showed the significant sample separation according to the pathology type. Moreover, the sequencing results revealed that EM samples were colonized by a homogeneous microbiome dominated by *Lactobacillus* spp. (Figure 4B, blue dots). The comparison between the EM and EC groups based on Bray-Curtis distance showed statistically significant differences (p = 0.001).

These observations were also confirmed by β-diversity analysis with the use of the Unweighted UniFrac (p = 0.014), as well as with Weighted UniFrac methods (p = 0.005) (Figure 5), and the results are presented in Table 4.

ANCOM analysis of the samples was performed using the model in which taxa that were identified in less than five samples were removed. The results of taxon analysis were associated with the differentiating effect of d:Bacteria; p:*Firmicutes*; c:*Clostridia*; o:*PeptostreptococcalesTissierellales*; f:*Peptostreptococcales-Tissierellales*; g:*Anaerococcus*, which were predominant in the samples from EC. Possibly, the *Anaerococcus* representatives could be the indicators of dysbiosis, and their presence correlates with EC incidence. Detailed data on detection thresholds and prevalence are presented in Table 5.

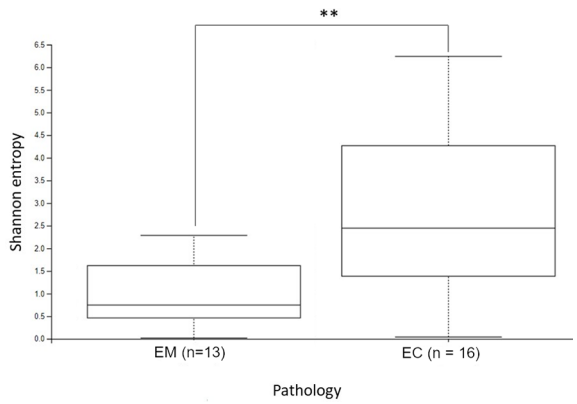

FIGURE 2
The alpha diversity comparison of EM and EC microbiome, based on the Shannon index. **p < 0.01.

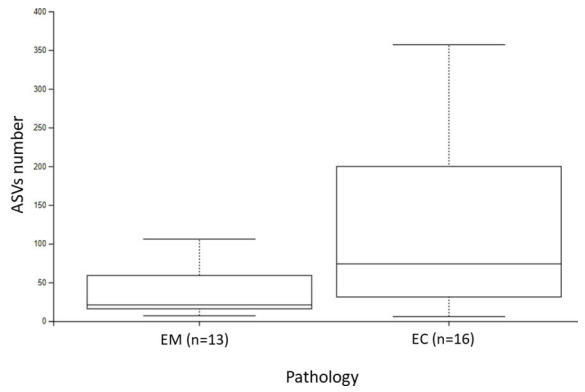

FIGURE 3
The ASVs number of endometrial myoma (EM) and endometrial cancer (EC) samples.

Additionally, quantitative analysis revealed significant differences in the average abundance and median presence of *Anaerococcus* between EC and EM groups, as shown in Table 6.

In this analytical model, the sample types differed significantly in the abundance of *Firmicutes* and *Cyanobacteria* in EM. Moreover, the analysis showed the predomination of pathogenic taxons such as *Streptococcus*, *Anaerococcus*, *Prevotella*, *Gardnerella*, *Peptoniphilus*, and *Porphyromonas* to predominate in EC samples (Figure 6A). The main types of bacteria in the pathologies studied and their percentage distribution in the form of pie chart are presented in Figure 6B.

3.3 The adhesion level of *Anaerococcus vaginalis* to human uterus fibroblasts

Based on the above taxonomic analysis of the uterine microbiota, revealing genus *Anaerococcus* as a differentiating taxon between EC and EM, the strain *A. vaginalis* DSM 7457 was selected for the next experimental steps. This strain was originally isolated from an ovarian abscess (Ezaki et al., 2001). Adhesion assays were conducted to assess *A. vaginalis* ability to bind to endometrial cells. Cells were cultured and incubated with *A. vaginalis* for 24-hours, and non-adherent bacteria were washed off. Adhesion was quantified via BacLight Green dye fluorescence measurement. Appropriate control, such as physiological vaginal flora representative *L. jensenii*, was included to validate the results.

The results of the test showed a high adhesion rate for both *L. jensenii* and *A. vaginalis* strains (Figure 7). However, the tendency of a higher adhesion rate of *A. vaginalis* to HUF cells compared to *L. jensenii* was observed. The percentage of adhesion of the studied pathogenic strain was almost 50% after 24 hours of infection. The MOI of 0.5 was found to be suitable for testing, as the result of calculations described in methodology.

3.4 The ROS level changes in HUF cells after *Anaerococcus vaginalis* infection

The increase in reactive oxygen species (ROS) level is one of the indicators of the inflammatory process that could be associated with infections caused by pathogens. It is one of the responses of the host's innate immunity to microbial invaders and is aimed at eliminating pathogens. However, long-term exposure to bacterial infection could lead to repercussions - the accumulation of damage in the human cellular apparatus. These abnormalities could lead to the development of cancer (Kennel and Greten, 2021; Spooner and Yilmaz, 2011). We performed ROS production assays using non-malignant human endometrial cells (HUF) exposed to *A. vaginalis*. ROS levels were quantified using DCFH-DA fluorescence measurement, following describe previously protocol. Controls included untreated cells and cells exposed to L. jenseni, as well as

TABLE 2 Summary of alpha diversity metrics for EM and EC groups, including Shannon entropy, ASVs number, and Pielou's evenness.

Metric	Group	Mean	SD	Median	IQ	IIIQ	IQR
Shannon entropy	EM	1.17	1.06	0.75	0.46	1.63	1.17
	EC	2.85	1.92	2.45	0.94	4.75	3.81
ASVs number	EM	41.92	35.07	21.00	16.00	77.00	61.00
	EC	121.25	107.51	74.00	27.75	203.25	175.50
Pielou evenness	EM	0.33	0.22	0.28	0.18	0.57	0.38
	EC	0.37	0.22	0.36	0.17	0.53	0.36

EC – samples from patients diagnosed with endometrial cancer; EM – samples from the endometrial microbiota of non-cancer patients; SD – Standard Deviation; IQ – interquartile (The first quartile, Q1, which represents the 25th percentile of the data); IIIQ – interquartile (The third quartile, Q3, which represents the 75th percentile of the data); IQR – interquartile Range (The difference between Q3 and Q1, indicating the spread of the central 50% of the data). Data are presented as mean ± SD, median, and interquartile ranges (IQ, IIIQ, IQR).

TABLE 3 The Bray-Curtis distance comparison of endometrial myoma (EM) and endometrial cancer (EC) samples.

Group 1	Group 2	Sample size	Permutations	pseudo-F	*p*-value	*q*-value
EM	EC	29	999	2.647731	0.001	0.0030

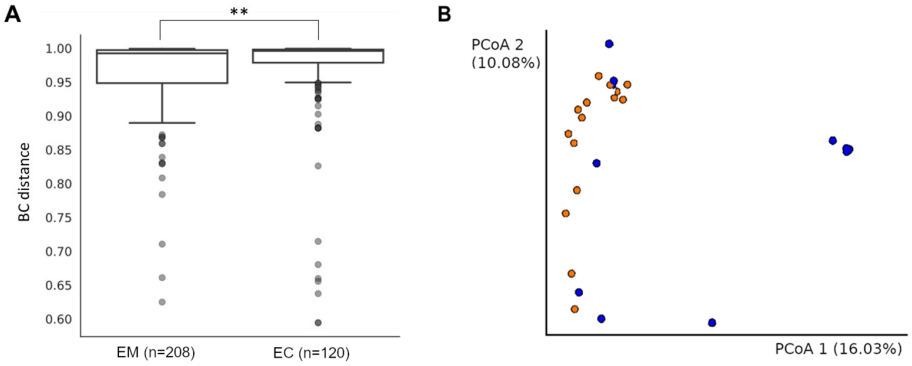

FIGURE 4
The Bray-Curtis distance comparison of endometrial myoma (EM) and endometrial cancer (EC) samples. ** = $p < 0.001$ **(A)**. The Bray-Curtis distance mapping of samples. EM – blue; EC – orange **(B)**.

0,5% H2O2. The level of ROS in HUF cells 24 h after infection with *A. vaginalis* are shown in Figure 8.

The results of ROS level measurement in HUF cells after 24 hours of infection with *A. vaginalis* show a statistically significant increase. This level was statistically similar to the one induced by 0.5% H_2O_2. Such effect was not observed when HUF cells were infected with the *L. jensenii*, indicating a reduced impact on oxidative stress induction in human cells. The observed increase in ROS levels in uterine fibroblasts in response to *Anaerococcus vaginalis* infection indicates early inflammatory changes. However, this study is limited to an acute infection model. Future research should incorporate inflammatory markers analysis such as IL-6 and TNF-α, which could provide valuable insights into the role of inflammation in EC progression.

4 Discussion

Since the progress of sequencing techniques, microbiome studies found practical applications in cancer research. It has been shown that microbial pathogens have a tumorigenic effect in 15-20% of reported cancer cases and are referred to as "oncomicrobes." The risk of pathogen influence on carcinogenesis and progression is also present in the so-called "complicit" microbes, whose functions are broad and yet not well understood (Menati Rashno et al., 2021; Sepich-Poore et al., 2021). The pathogenic changes of microbiota can promote resistance to host cell death, which is one of the cancer hallmarks, and induce cancer-promoting inflammation. The composition of the bacterial microbiome modulates the specific alternative responses, one of which depends on the inflammasome complex and the second on the inflammasome independent secretion of pro-inflammatory cytokines, highlighting the key role in activating different degrees of inflammation (De Seta et al., 2019). In addition, the microbiota influences carcinogenesis by releasing carcinogenic molecules (e.g., genotoxins) and producing tumor-promoting metabolites. It is undeniable that the microbiome has serious implications for human health and the progression of disease (Menati Rashno et al., 2021; Schwabe and Jobin, 2013).

Endometrial cancer is one of the most common cancers among women in high-income countries. There are many known risk factors: the excessive, uncontrolled exposure of the endometrium to estrogens, including uncontrolled estrogen therapy, early

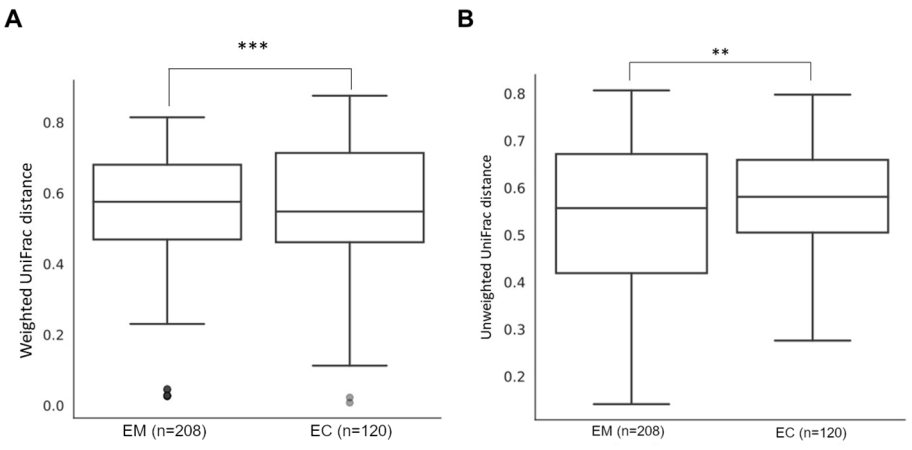

FIGURE 5
Weighted **(A)** and unweighted **(B)** UniFrac comparison of endometrial myoma (EM) and endometrial cancer (EC) samples. ** = $p < 0.01$, *** = $p < 0.001$.

TABLE 4 Unweighted and weighted UniFrac method comparison of endometrial myoma (EM) and endometrial cancer (EC) samples.

Group 1	Group 2	Sample size	Permutations	pseudo-F	*p*-value	*q*-value
Unweighted UniFrac						
EM	EC	29	999	2.999545	0.014	0.042
Weighted UniFrac						
EM	EC	29	999	4.624288	0.005	0.0150

menarche, late menopause, tamoxifen therapy, nulliparity, infertility or failure to ovulate, polycystic ovary syndrome, diet, and general lifestyle. Other risk factors include increasing age, obesity, hypertension, diabetes mellitus, and hereditary nonpolyposis colon cancer. It was found that menopausal age was positively associated with EC, and the risk increased for women of age above 46.5 years (Braun et al., 2016; Wu et al., 2019). Until the second half of the 20th century, the uterine cavity was considered free of microbes. Then it was assumed that colonization of the uterine cavity occurs from the intestine, oral cavity, bloodstream and vaginal mucosa. However, there is increasing evidence of the unique microbial composition of the female reproductive tract (Benner et al., 2018; Toson et al., 2022).

The upper genital tract of healthy women is dominated by *Lactobacillus* species. Studies by De Seta et al. showed the relationship between the presence of lactobacilli and the level of immunological mediators in the vagina (De Seta et al., 2019). This scheme could also be possible in the upper parts of the genital tract. The samples were grouped according to community state types (CSTI-IV), where CSTI was characterized by the presence of *L. crispatus*, CSTII - *L. gasseri*, CSTIII - *L. iners*, and CSTIV by a low number of lactobacilli. Several cross-sectional studies have revealed the interplay between lactobacilli dysbiosis and the changes in microbial composition in the EC (Lu et al., 2021; Walsh et al., 2019; Walther-António et al., 2016).

In our study, we identified the endocervical canal microbiomes of the 29 participants with EC or EM. The inclusion of additional alpha diversity metrics (Table 2), such as ASVs number and Pielou's evenness, allowed for a more nuanced understanding of microbial diversity and distribution in EC and EM samples. The significantly higher ASVs number observed in EC samples aligns with the hypothesis of a more diverse and potentially pathogenic microbiota in cancerous environments. The endometrial communities of women in both groups markedly differed from one another in terms of bacterial species composition. We observed that EM samples had homogeneous microbiomes dominated by *Lactobacillus*, while the EC group featured a higher diversity of microorganisms. Our results are consistent with the findings of Mitchell et al (Mitchell et al., 2015), who reported that the most commonly detected taxon in the group of 58 women undergoing hysterectomy for noncancer indications was the genus *Lactobacillus*. Moreover, the recent study conducted by Kaakous et al (Kaakoush et al., 2022). indicated that EC was associated with decreased abundance of *Lactobacillus* genus in the group of 70 postmenopausal women undergoing hysterectomy due to the benign pathology or EC. So far, several studies have indicated that disruption of microbial homeostasis may promote many gynecological malignancies and inflammation, eventually leading to carcinogenesis. When the microbial load is too rich in representatives of certain taxa, excessive tissue destruction or immune stimulation can occur, being the stimulus of gynecological diseases. Indeed, our study confirmed that the samples taken from patients with EC were enriched in certain pathogenic taxa such as *Streptococcus*, *Anaerococcus*, *Prevotella*, *Gardnerella*, *Peptoniphilus* and *Porphyromonas*, which is also consistent with the existent literature of endometrial microbiota composition among patients with EC. In a recent study conducted on a group of 28 postmenopausal women undergoing hysterectomy, Wang et al (Wang et al., 2022). proved that although *Lactobacillus* and *Gardnerella* were the dominant bacterial taxa in both EC and adjacent non-EC tissue samples, only the EC samples were enriched in such genera as *Prevotella*, *Atopobium*, *Anaerococcus*, *Dialister*, *Porphyromonas* and *Peptoniphilus*.

Nowadays, more and more studies point to the presence of specific strains as potential indicators of EC. Microorganisms in the stage of dysbiosis, especially some certain pathogenic taxa, may stimulate the immunopathological processes and promote destabilization of the host genome by releasing bacterial secondary metabolites, which can damage human genetic material. In a recent study, Li et al (Li et al., 2021). confirmed that the increasing abundance of *Prevotella* in endometrial tissue, especially

TABLE 5 Prevalence of *Anaerococcus* in EC and EM samples at different detection thresholds.

	Present > 0	%	Present > 0.1%	%	Present > 1%	%
EM	6	46,154	1	7,692	0	0,000
EC	14	87,500	10	62,500	8	50,000

EC – samples from patients diagnosed with endometrial cancer; EM – samples from the endometrial microbiota of non-cancer patients; Present > 0% – detection of *Anaerococcus* in samples at an abundance higher than 0%; Present > 0.1% – detection of *Anaerococcus* in samples at an abundance higher than 0.1%; Present > 1% – detection of *Anaerococcus* in samples at an abundance higher than 1%. The table shows the percentage of samples with *Anaerococcus* detected above thresholds of >0%, >0.1%, and >1% in EC (endometrial cancer) and EM (endometrial microbiota) groups. These data illustrate the significantly higher prevalence of *Anaerococcus* in EC samples.

10.3389/fcimb.2025.1511625

TABLE 6 Quantitative analysis of *Anaerococcus* abundance in EC and EM samples.

	Mean	SD	Median	IQ	IIIQ	IQR
EM	0,016	0,045	0,000	0,000	0,003	0,003
EC	3,943	5,753	1,184	0,016	5,887	5,872

SD – Standard Deviation; IQ – interquartile (The first quartile, Q1, which represents the 25th percentile of the data); IIIQ – interquartile (The third quartile, Q3, which represents the 75th percentile of the data); IQR – interquartile Range (The difference between Q3 and Q1, indicating the spread of the central 50% of the data). The table presents the mean percentage abundance, standard deviation (SD), median, and interquartile range (IQR) of *Anaerococcus* in EC and EM groups, highlighting the significantly higher abundance in EC samples.

when correlated with the elevated level of serum D-dimer (DD) and fibrin degradation products (FDPs), may be an important factor associated with carcinogenesis. A study conducted by Lu et al (Lu et al., 2021). indicated a correlation between an increased abundance of *Micrococcus* and IL-6 and IL-17 mRNA levels in EC patients, which suggests the pro-inflammatory role of these microorganisms in tumor genesis. In another study, Walter-Antonio et al (Walther-António et al., 2016). revealed that the simultaneous presence of *Atopobium vaginae* and *Porphyromonas somerae*, especially if combined with an increased vaginal pH (>4,5), was associated with EC in a group of 31 patients with EC, endometrial hyperplasia or benign uterine conditions. In a study of 148 women undergoing hysterectomy due to benign disease, endometrial hyperplasia or EC, Walsh et al (Walsh et al., 2019). also identified *P. somerae* as the most predictive microbial marker of EC. Moreover, Caselli et al (Caselli et al., 2019). revealed that *P. somerae* and *A. vaginae* induced the release of proinflammatory cytokines by human endometrial cells after 24 hours of co-culturing. As indicated by the above studies, enrichment in certain taxa was observed among patients suffering from hyperplasia and cancer, suggesting an inflammatory role of specific microorganisms in carcinogenesis.

The presence of certain bacterial species may contribute to altering the expression of genes encoding proteins involved in the inflammatory response, proliferation or apoptosis. Consequently, these events may ultimately disrupt physiological processes and promote the development of disease states, such as endometritis and endometriosis, which are associated with the development of cancer. In the study described herein, using ANCOM analysis of the 16S rRNA metagenomics data, we identified *Anaerococcus* as the taxon differentiating between EC and EM microbiomes. The increased prevalence and abundance of *Anaerococcus* in EC samples, as demonstrated in Tables 5 and 6, supports its potential involvement in the pathogenesis of endometrial cancer. While correlation does not

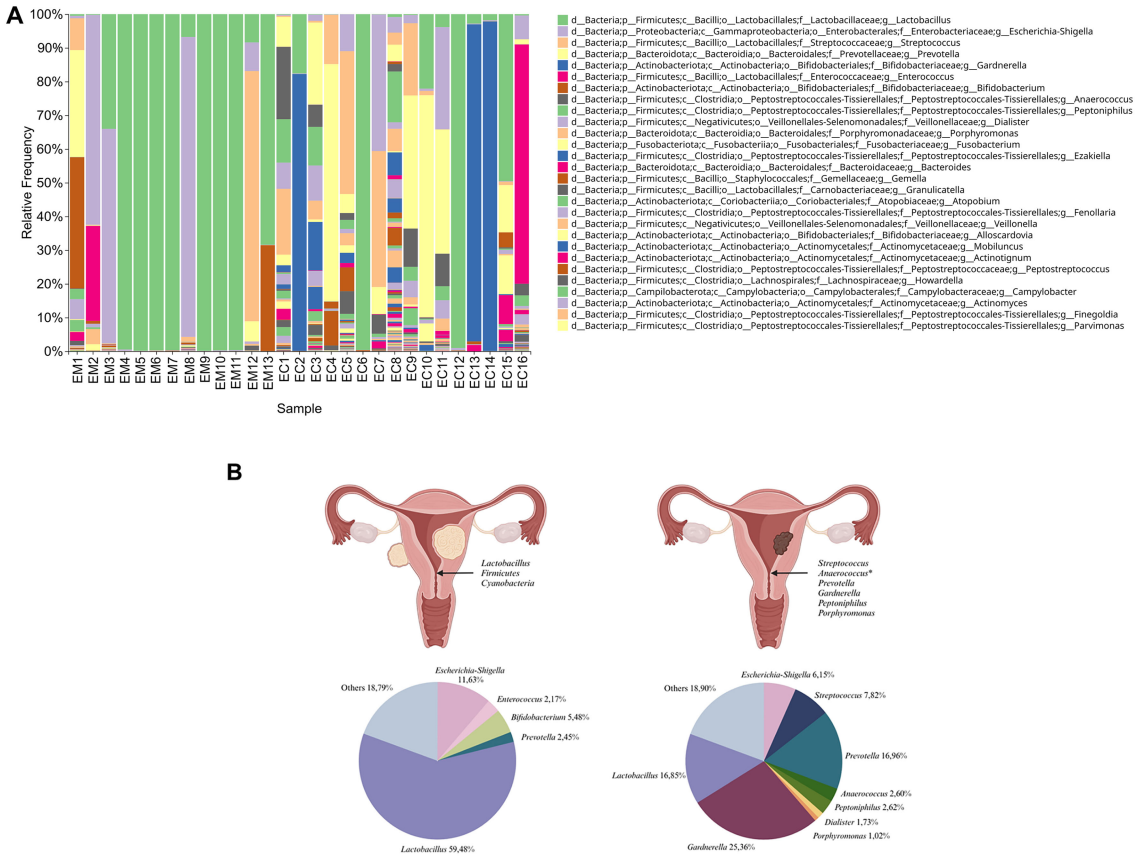

FIGURE 6
Taxonomic composition of the samples' microbiota at the genus level. Samples were sorted by groups of endometrial myoma (EM1-EM13) and endometrial cancer (EC1 -EC16) cohorts **(A)**. The main taxons of bacteria identified in the samples from women with endometrial myoma (left) and endometrial cancer (right) and their corresponding percentage distribution in the form of a pie chart **(B)**.

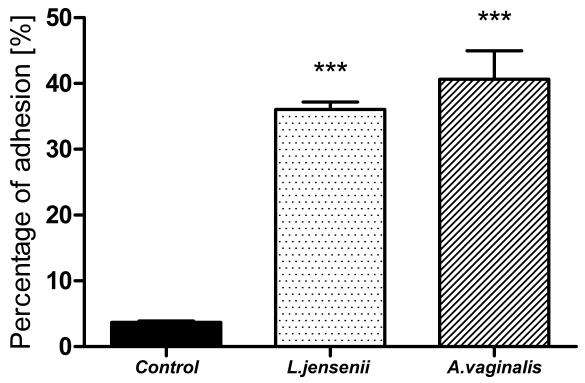

FIGURE 7
Percentage of *L. jensenii* and *A. vaginalis* adhesion to HUF cells at 0.5 MOI of *L. jensenii* and *A. vaginalis*. Data were obtained by measuring fluorescence at Ex/Em = 480/561 nm in three independent experiments. Results were statistically compared with the control using One-way ANOVA with Bonferroni multiple comparison test. ***p < 0.001.

imply causation, these data strengthen its candidacy as a biomarker and underline the need for further functional studies. In the study conducted by Tsementzi et al (Tsementzi et al., 2020), samples of vaginal swabs from women suffering from gynecological cancer who were undergoing pre-radiation therapy (N=65), post-radiation therapy (N=25) and from a control group of healthy volunteers (N=67) were sequenced. Results from 16S rRNA V4 region sequencing revealed that the swabs taken from the cancer group were enriched in 16 phylogroups associated with BV and inflammation, including *Sneathia*, *Prevotella*, *Peptoniphilus*, *Fusobacterium*, *Anaerococcus*, *Dialister*, *Moryella* and *Peptostreptococcus*, comparing to the healthy group. In another study, Liu et al (Liu et al., 2019). collected and sequenced endometrial biopsy tissue and fluid from 130 infertile women with chronic endometritis, revealing that this malignancy is associated with the abundance of

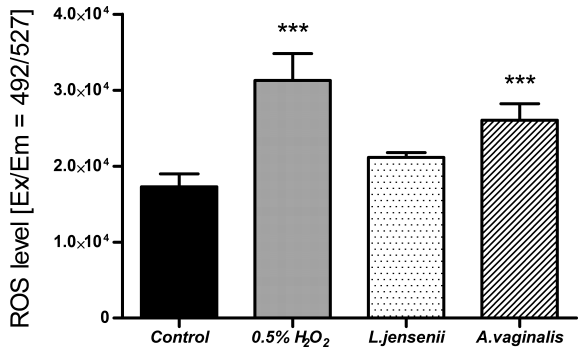

FIGURE 8
ROS level in HUF cells, after 24-hour co-incubation at 0.5 MOI of *L. jensenii* and *A. vaginalis*. Data were obtained by measuring fluorescence after H2DCFDA staining at Ex/Em = 492/527 nm in three independent experiments. Results were statistically compared with the control using a One-way ANOVA with Bonferroni multiple comparison test; *** = p < 0.001; *L. jensenii* was used as a representative of the physiological state, and the 0,5% H_2O_2 as the positive control (ROS inducer).

bacterial taxa including *Dialister*, *Bifidobacterium*, *Prevotella*, *Gardnerella* and *Anaerococcus*. Another study conducted by Perrotta et al (Perrotta et al., 2020). revealed that in a group of 59 patients with different types of endometriosis, the amount of *Lactobacillus* species was decreased while the vaginal pathogenic bacteria, including *Anaerococcus*, was increased, compared to 24 control samples from healthy volunteers' group. Moreover, in a recent study, Semertzidou et al (Semertzidou et al., 2024). compared the microbiota composition from 24 benign diseases and 37 EC patients from different anatomical sites (vagina, cervix, endometrium) and observed a high diversity and *Lactobacillus* depletion in the EC group. EC samples were also enriched in several pathogenic species, including *Porphyromonas*, *Prevotella*, *Peptoniphilus*, and *Anaerococcus*.

Based on our sequencing data, we have selected *A. vaginalis* as a representative of the taxon differentiating between EC and EM. While previous studies have identified *Prevotella* and *Gardnerella* as components of dysbiotic uterine microbiomes in EC, these microorganisms are also frequently associated with bacterial vaginosis, a condition prevalent among non-cancerous cohorts. Their presence may therefore reflect generalized microbial dysbiosis rather than EC-specific pathogenesis. In contrast, our study is the first to explore *Anaerococcus* as a first-placed potential contributor to endometrial carcinogenesis. By demonstrating its ability to adhere to endometrial cells and elevate ROS levels *in vitro*, *A. vaginalis* emerges as a unique candidate for further investigation. *Lactobacillus jensenii* was used as a member of the genus *Lactobacillus*, found in the physiological microflora of the uterus. Both strains showed a high adhesion rate, which means they can efficiently colonize endometrium, and the imbalance between lactobacilli and pathogenic species such as *A. vaginalis* may lead to dysbiosis. There is a significant gap in *in vitro* studies investigating the direct effects of *Anaerococcus* on human endometrial cells. Current knowledge is limited to initial observations, such as ROS production and bacterial adhesion, as demonstrated in this study. These findings underscore the need for comprehensive investigations into the molecular mechanisms underlying *A. vaginalis* interactions with host cells, particularly in the context of inflammation or dysbiosis.

Bacterial infections can promote genetic instability of nearby host cells through bacterial genotoxins or tumor promoting metabolite secretion, and the relationship between chronic infections and cancer has already been demonstrated, e.g. in the case of *Helicobacter pylori* and *Fusobacterium nucleatum* in gastric and colorectal cancers, respectively (Kostic et al., 2012; Lofgren et al., 2011; McCoy et al., 2013; Touati et al., 2003). Moreover, bacterial infections usually lead to inflammation, causing ROS induction, dysregulation of the innate immune system and cell damage. However, the association between inflammation and cancer is not fully understood (Coussens and Werb, 2002; Hussain et al., 2003; Lin and Karin, 2007). Dossus et al. conducted a case-control study which comprised 305 incident cases of EC and 574 matched controls, where they observed a significant increase in the risk of EC with elevated levels of three inflammatory markers: C-reactive protein (CRP), interleukin 6 (IL6), and IL1 receptor antagonist (IL1Ra) (Dossus et al., 2010). In addition to inflammatory markers, free radicals are generated during the inflammation response to eliminate invading photogenes (Spooner

and Yilmaz, 2011). However, elevated levels of ROS can also damage healthy human cells and trigger carcinogenesis (Hussain et al., 2003). It has been estimated that infections and associated inflammation contribute to about 15% of all cancer cases worldwide (Coussens and Werb, 2002). In our research, we have demonstrated that *A. vaginalis* induced a significant increase of ROS inside human uterine fibroblasts, and the levels were much higher than in the presence of *L. jensenii*. High levels of ROS may damage proteins, lipids, membranes, and organelles. The oncogenic role of ROS is associated with the induction of oxidative DNA damage involving double-stranded breaks and the formation of 8-oxo-7,8-dihydro-2′-deoxyguanosine (8-oxodG). This oxidized guanine induces transversion of guanine to thymine and is a major cause of spontaneous mutagenesis, leading to carcinogenesis (Nakamura and Takada, 2021; Valavanidis et al., 2009). Moreover, ROS as the one of the inflammation inducers, could be a key contributor to carcinogenesis (Coussens and Werb, 2002). Inflammatory markers such as interleukins (e.g., IL-6, IL-8), TNF-α, and other chemokines could also provide additional evidence of the inflammatory environment in EC patients. Future studies incorporating measurements of these markers in serum or conditioned media from *in vitro* models could help establish a more comprehensive understanding of the interplay between inflammation, ROS levels, and microbial dysbiosis.

The literature data and the results of 16S rRNA metagenomics presented in this study indicated significant differences in the composition of the uterine microbiome between cases of EC and benign lesions of this organ. Our results are not only in agreement with data indicating the pathological involvement of the genus *Anaerococcus* in the development of the most common gynecological diseases but also shed new light on our previous understanding regarding the possibility of induction of neoplastic processes by this microorganism. This knowledge may lead to new diagnostic and preventive strategies for EC, but clarifying the role of *A. vaginalis* in EC requires further research. If confirmed in the larger cohorts, examination of the microbiome of cervical swabs concerning the presence of *A. vaginalis* as an EC indicator could form the basis of microbiological diagnosis of EC, which would be of great importance in detecting the early stages of the disease.

5 Conclusions

In conclusion, our study indicated that microbial composition significantly differs between patients with endometrial cancer and benign lesions such as myoma. Furthermore, some pathogenic taxa, such as *Streptococcus*, *Anaerococcus*, *Prevotella*, *Gardnerella*, *Peptoniphilus*, and *Porphyromonas*, may play a key role in endometrial cancer development and progression. Understanding the functional interactions between the endometrial microbiome and the immune system could provide new insights into the pathogenesis of endometrial cancer. Despite the limitations, such as the limited sample size, our study provides two key contributions to the field. First, it introduces *Anaerococcus* as a novel genus associated with EC, offering a new avenue for biomarker research. The presence of specific microbial signatures, including *Anaerococcus*, could serve as early indicators of endometrial cancer, aiding in timely diagnosis. Second, by evaluating *A. vaginalis* potential to drive ROS production and adhere to non-malignant endometrial cells, we establish a foundation for understanding its functional role in EC pathogenesis. These findings distinguish *A. vaginalis* from previously studied genera and emphasize its diagnostic potential. Understanding the role of *Anaerococcus* in EC may lead to novel therapeutic interventions aimed at modifying the uterine microbiome to prevent or treat cancer. While further research is required to validate these findings, this study marks an important step toward identifying microbial signatures that may enhance the early diagnosis of EC.

Data availability statement

The data presented in the study are deposited in the NCBI Sequence Read Archive (BioProjects), accession number PRJNA1203774. The repository can be accessed at the following link: https://www.ncbi.nlm.nih.gov/bioproject/?term=PRJNA1203774. Additionally the key raw data has been validated onto The University of Lodz Repository: http://hdl.handle.net/11089/52937.

Ethics statement

The studies involving humans were approved by Bioethics Committee of the Regional Medical Council in Rzeszow City (Protocol number 24/B/2019, update 54/B/2020, date of approval 21.05.2020). The studies were conducted in accordance with the local legislation and institutional requirements. The participants provided their written informed consent to participate in this study.

Author contributions

OK: Conceptualization, Data curation, Investigation, Validation, Visualization, Writing – original draft. AK: Conceptualization, Data curation, Formal analysis, Funding acquisition, Investigation, Methodology, Project administration, Resources, Supervision, Visualization, Writing – original draft, Writing – review & editing. AB: Data curation, Investigation, Methodology, Resources, Writing – original draft. AD: Data curation, Investigation, Methodology, Resources, Writing – original draft. JL: Data curation, Investigation, Methodology, Software, Validation, Writing – original draft. WW: Investigation, Writing – original draft. TK: Conceptualization, Formal analysis, Supervision, Writing – review & editing. PS: Conceptualization, Formal analysis, Funding acquisition, Project administration, Supervision, Writing – review & editing.

Funding

The author(s) declare that financial support was received for theresearch, authorship, and/or publication of this article. This research was funded in part by the National Science Centre,

Poland (grant number 2021/43/D/NZ7/01386), 1st edition of the Doctoral Fellowship Programme of University of Lodz (No. 26/DGB/IDUB/2022), and by a subsidy for scientific activity provided to the Department of Molecular Microbiology by the University of Lodz (B2211000000038.01). For the purpose of Open Access, the author has applied a CC-BY public copyright licence to any Author Accepted Manuscript (AAM) version arising from this submission.

Conflict of interest

The authors declare that the research was conducted in the absence of any commercial or financial relationships that could be construed as a potential conflict of interest.

Generative AI statement

The author(s) declare that no Generative AI was used in the creation of this manuscript.

Publisher's note

All claims expressed in this article are solely those of the authors and do not necessarily represent those of their affiliated organizations, or those of the publisher, the editors and the reviewers. Any product that may be evaluated in this article, or claim that may be made by its manufacturer, is not guaranteed or endorsed by the publisher.

References

Benner, M., Ferwerda, G., Joosten, I., and van der Molen, R. G. (2018). How uterine microbiota might be responsible for a receptive, fertile endometrium. *Hum. Reprod. Update* 24, 393–415. doi: 10.1093/humupd/dmy012

Braun, M. M., Overbeek-Wager, E. A., and Grumbo, R. J. (2016). Diagnosis and management of endometrial cancer. *Am. Family Physician* 93, 468–474.

Caselli, E., Soffritti, I., D'Accolti, M., Piva, I., Greco, P., and Bonaccorsi, G. (2019). Atopobium vaginae And Porphyromonas somerae Induce Proinflammatory Cytokines Expression In Endometrial Cells: A Possible Implication For Endometrial Cancer? *Cancer Manage. Research Volume* 11, 8571–8575. doi: 10.2147/CMAR.S217362

Chen, C., Song, X., Wei, W., Zhong, H., Dai, J., Lan, Z., et al. (2017). The microbiota continuum along the female reproductive tract and its relation to uterine-related diseases. *Nat. Commun.* 8, 875. doi: 10.1038/s41467-017-00901-0

Coussens, L. M., and Werb, Z. (2002). Inflammation and cancer. *Nature* 420, 860–867. doi: 10.1038/nature01322

De Seta, F., Campisciano, G., Zanotta, N., Ricci, G., and Comar, M. (2019). The vaginal community state types microbiome-immune network as key factor for bacterial vaginosis and aerobic vaginitis. *Front. Microbiol.* 10 (2451). doi: 10.3389/fmicb.2019.02451

Dossus, L., Rinaldi, S., Becker, S., Lukanova, A., Tjonneland, A., Olsen, A., et al. (2010). Obesity, inflammatory markers, and endometrial cancer risk: a prospective case–control study. *Endocrine-Related Cancer* 17, 1007–1019. doi: 10.1677/ERC-10-0053

Ezaki, T., Kawamura, Y., Li, N., Li, Z. Y., Zhao, L., and Shu, S. (2001).). Proposal of the genera Anaerococcus gen. nov., Peptoniphilus gen. nov. and Gallicola gen. nov. for members of the genus Peptostreptococcus. *Int. J. Systematic Evolutionary Microbiol.* 51, 1521–1528. doi: 10.1099/00207713-51-4-1521

Gilbert, N. M., Lewis, W. G., Li, G., Sojka, D. K., Lubin, J. B., and Lewis, A. L. (2019). Gardnerella vaginalis and Prevotella bivia Trigger Distinct and Overlapping Phenotypes in a Mouse Model of Bacterial Vaginosis. *J. Infect. Dis.* 220, 1099–1108. doi: 10.1093/infdis/jiy704

Hussain, S. P., Hofseth, L. J., and Harris, C. C. (2003). Radical causes of cancer. *Nat. Rev. Cancer* 3, 276–285. doi: 10.1038/nrc1046

Kaakoush, N. O., Olzomer, E. M., Kosasih, M., Martin, A. R., Fargah, F., Lambie, N., et al. (2022). Differences in the active endometrial microbiota across body weight and cancer in humans and mice. *Cancers* 14, 2141. doi: 10.3390/cancers14092141

Kennel, K. B., and Greten, F. R. (2021). Immune cell - produced ROS and their impact on tumor growth and metastasis. *Redox Biol.* 42, 101891. doi: 10.1016/j.redox.2021.101891

Kostic, A. D., Gevers, D., Pedamallu, C. S., Michaud, M., Duke, F., Earl, A. M., et al. (2012). Genomic analysis identifies association of Fusobacterium with colorectal carcinoma. *Genome Res.* 22, 292–298. doi: 10.1101/gr.126573.111

Kuźmycz, O., and Stączek, P. (2020). Prospects of NSAIDs administration as double-edged agents against endometrial cancer and pathological species of the uterine microbiome. *Cancer Biol. Ther.* 21, 486–494. doi: 10.1080/15384047.2020.1736483

Li, C., Gu, Y., He, Q., Huang, J., Song, Y., Wan, X., et al. (2021). Integrated analysis of microbiome and transcriptome data reveals the interplay between commensal bacteria and fibrin degradation in endometrial cancer. *Front. Cell. Infection Microbiol.* 11. doi: 10.3389/fcimb.2021.748558

Lin, W.-W., and Karin, M. (2007). A cytokine-mediated link between innate immunity, inflammation, and cancer. *J. Clin. Invest.* 117, 1175–1183. doi: 10.1172/JCI31537

Liu, Y., Ko, E. Y.-L., Wong, K. K.-W., Chen, X., Cheung, W.-C., Law, T. S.-M., et al. (2019). Endometrial microbiota in infertile women with and without chronic endometritis as diagnosed using a quantitative and reference range-based method. *Fertility Sterility* 112, 707–717.e1. doi: 10.1016/j.fertnstert.2019.05.015

Lofgren, J. L., Whary, M. T., Ge, Z., Muthupalani, S., Taylor, N. S., Mobley, M., et al. (2011). Lack of commensal flora in helicobacter pylori–infected INS-GAS mice reduces gastritis and delays intraepithelial neoplasia. *Gastroenterology* 140, 210–220.e4. doi: 10.1053/j.gastro.2010.09.048

Lu, W., He, F., Lin, Z., Liu, S., Tang, L., Huang, Y., et al. (2021). Dysbiosis of the endometrial microbiota and its association with inflammatory cytokines in endometrial cancer. *Int. J. Cancer* 148, 1708–1716. doi: 10.1002/ijc.33428

McCoy, A. N., Araújo-Pérez, F., Azcárate-Peril, A., Yeh, J. J., Sandler, R. S., and Keku, T. O. (2013). Fusobacterium is associated with colorectal adenomas. *PloS One* 8, e53653. doi: 10.1371/journal.pone.0053653

Medina-Bastidas, D., Camacho-Arroyo, I., and García-Gómez, E. (2022). Current findings in endometrial microbiome: impact on uterine diseases. *Reproduction* 163, R81–R96. doi: 10.1530/REP-21-0120

Menati Rashno, M., Mehraban, H., Naji, B., and Radmehr, M. (2021). Microbiome in human cancers. *Access Microbiol.* 3 (8), 000247. doi: 10.1099/acmi.0.000247

Mitchell, C. M., Haick, A., Nkwopara, E., Garcia, R., Rendi, M., Agnew, K., et al. (2015). Colonization of the upper genital tract by vaginal bacterial species in nonpregnant women. *Am. J. Obstetrics Gynecology* 212, 611.e1–611.e9. doi: 10.1016/j.ajog.2014.11.043

Moreno, I., Garcia-Grau, I., Perez-Villaroya, D., Gonzalez-Monfort, M., Bahçeci, M., Barrionuevo, M. J., et al. (2022). Endometrial microbiota composition is associated with reproductive outcome in infertile patients. *Microbiome* 10, 1. doi: 10.1186/s40168-021-01184-w

Morice, P., Leary, A., Creutzberg, C., Abu-Rustum, N., and Darai, E. (2016). Endometrial cancer. *Lancet* 387, 1094–1108. doi: 10.1016/S0140-6736(15)00130-0

Nakamura, H., and Takada, K. (2021). Reactive oxygen species in cancer: Current findings and future directions. *Cancer Sci.* 112, 3945–3952. doi: 10.1111/cas.15068

Perrotta, A. R., Borrelli, G. M., Martins, C. O., Kallas, E. G., Sanabani, S. S., Griffith, L. G., et al. (2020). The vaginal microbiome as a tool to predict rASRM stage of disease in endometriosis: a pilot study. *Reprod. Sci.* 27, 1064–1073. doi: 10.1007/s43032-019-00113-5

Qing, X., Xie, M., Liu, P., Feng, O., Leng, H., Guo, H., et al. (2024). Correlation between dysbiosis of vaginal microecology and endometriosis: A systematic review and meta-analysis. *PloS One* 19, e0306780. doi: 10.1371/journal.pone.0306780

Schwabe, R. F., and Jobin, C. (2013). The microbiome and cancer. *Nat. Rev. Cancer* 13, 800–812. doi: 10.1038/nrc3610

Semertzidou, A., Whelan, E., Smith, A., Ng, S., Roberts, L., Brosens, J. J., et al. (2024). Microbial signatures and continuum in endometrial cancer and benign patients. *Microbiome* 12, 118. doi: 10.1186/s40168-024-01821-0

Sepich-Poore, G. D., Zitvogel, L., Straussman, R., Hasty, J., Wargo, J. A., and Knight, R. (2021). The microbiome and human cancer. *Science* 371 (6536), eabc4552. doi: 10.1126/science.abc4552

Spooner, R., and Yilmaz, Ö. (2011). The role of reactive-oxygen-species in microbial persistence and inflammation. *Int. J. Mol. Sci.* 12, 334–352. doi: 10.3390/ijms12010334

Thubert, T., Foulot, H., Vinchant, M., Santulli, P., Marzouk, P., Borghese, B., et al. (2016). Surgical treatment: Myomectomy and hysterectomy; Endoscopy: A major advancement. *Best Pract. Res. Clin. Obstetrics Gynaecology* 34, 104–121. doi: 10.1016/j.bpobgyn.2015.11.021

Toson, B., Simon, C., and Moreno, I. (2022). The endometrial microbiome and its impact on human conception. *Int. J. Mol. Sci.* 23, 485. doi: 10.3390/ijms23010485

Touati, E., Michel, V., Thiberge, J.-M., Wuscher, N., Huerre, M., and Labigne, A. (2003). Chronic Helicobacter pylori infections induce gastric mutations in mice1 1This report is dedicated to the memory of Prof. *Maurice Hofnung. Gastroenterol.* 124, 1408–1419. doi: 10.1016/S0016-5085(03)00266-X

Tsementzi, D., Pena-Gonzalez, A., Bai, J., Hu, Y., Patel, P., Shelton, J., et al. (2020). Comparison of vaginal microbiota in gynecologic cancer patients pre- and post-radiation therapy and healthy women. *Cancer Med.* 9, 3714–3724. doi: 10.1002/cam4.3027

Valavanidis, A., Vlachogianni, T., and Fiotakis, C. (2009). 8-hydroxy-2′ -deoxyguanosine (8-OHdG): A critical biomarker of oxidative stress and carcinogenesis. *J. Environ. Sci. Health* 27, 120–139. doi: 10.1080/10590500902885684

Walsh, D. M., Hokenstad, A. N., Chen, J., Sung, J., Jenkins, G. D., Chia, N., et al. (2019). Postmenopause as a key factor in the composition of the Endometrial Cancer Microbiome (ECbiome). *Sci. Rep.* 9, 19213. doi: 10.1038/s41598-019-55720-8

Walther-António, M. R. S., Chen, J., Multinu, F., Hokenstad, A., Distad, T. J., Cheek, E. H., et al. (2016). Potential contribution of the uterine microbiome in the development of endometrial cancer. *Genome Med.* 8, 122. doi: 10.1186/s13073-016-0368-y

Wang, L., Yang, J., Su, H., Shi, L., Chen, B., and Zhang, S. (2022). Endometrial microbiota from endometrial cancer and paired pericancer tissues in postmenopausal women: differences and clinical relevance. *Menopause* 29, 1168–1175. doi: 10.1097/GME.0000000000002053

World Cancer Research Fund International. Available online at: https://www.wcrf.org/cancertrends/endometrial-cancer-statistics (Accessed April 15, 2023).

Wu, Y., Sun, W., Liu, H., and Zhang, D. (2019). Age at menopause and risk of developing endometrial cancer: A meta-analysis. *BioMed. Res. Int.* 2019, 1–13. doi: 10.1155/2019/8584130

frontiers | Frontiers in Cellular and Infection Microbiology

TYPE Review
PUBLISHED 14 February 2025
DOI 10.3389/fcimb.2025.1539847

OPEN ACCESS

EDITED BY
Marco Antonio Hernández-Luna,
University of Guanajuato, Mexico

REVIEWED BY
Madhur Sachan,
Brigham and Women's Hospital and Harvard Medical School, United States
Damien F. Meyer,
Institut National de la Recherche Agronomique (INRA), France

*CORRESPONDENCE
Jere W. McBride
jemcbrid@utmb.edu

RECEIVED 04 December 2024
ACCEPTED 27 January 2025
PUBLISHED 14 February 2025

CITATION
Solomon RN, Pittner NA, McCoy JR, Warwick PA and McBride JW (2025) Cell signaling in *Ehrlichia* infection and cancer: Parallels in pathogenesis.
Front. Cell. Infect. Microbiol. 15:1539847.
doi: 10.3389/fcimb.2025.1539847

Cell signaling in *Ehrlichia* infection and cancer: Parallels in pathogenesis

Regina N. Solomon[1], Nicholas A. Pittner[1], Jaclyn R. McCoy[1], Paityn A. Warwick[1] and Jere W. McBride[1,2,3,4,5]*

[1]Department of Pathology, University of Texas Medical Branch, Galveston, TX, United States, [2]Department of Microbiology and Immunology, University of Texas Medical Branch, Galveston, TX, United States, [3]Center for Biodefense and Emerging Infectious Diseases, University of Texas Medical Branch, Galveston, TX, United States, [4]Sealy Institute for Vaccine Sciences, University of Texas Medical Branch, Galveston, TX, United States, [5]Institute for Human Infections and Immunity, University of Texas Medical Branch, Galveston, TX, United States

Ehrlichia chaffeensis (*E. chaffeensis*) has recently emerged as an intracellular bacterial pathogen with sophisticated survival mechanisms that include repurposing evolutionarily conserved eukaryotic cell signaling pathways for immune evasion. *E. chaffeensis* exploits four major developmental signaling pathways (Wnt, Notch, Hedgehog, and Hippo) using short linear motif (SLiM) ligand mimicry to initiate signaling cascades. Dysregulation of these major signaling pathways leading to unchecked cell survival is implicated in various diseases, most notably cancer. *E. chaffeensis* exploits Wnt, Notch, Hedgehog and Hippo signaling pathways to inhibit apoptosis and co-opt other cellular functions to promote infection. This review will explore the signaling pathways exploited during *Ehrlichia* infection and the new discoveries that have illuminated this interesting example of the cell signaling convergence in cellular infection and cancer biology.

KEYWORDS

***Ehrlichia*, apoptosis, cancer, short linear motif, notch, Wnt, hedgehog, hippo**

Introduction

Ehrlichia chaffeensis is a gram-negative, obligately intracellular rickettsial pathogen and the etiologic agent of human monocytotropic ehrlichiosis (HME), an emerging life-threatening tick-borne zoonosis of increasing public health importance (Paddock and Childs, 2003). *E. chaffeensis* preferentially replicates in mononuclear phagocytes by effectively reprogramming the host cell through secreted tandem repeat effectors, most notably the 120 kDa tandem repeat protein (TRP120). Over the past decade, TRP120 has become recognized as a multifunctional "moonlighting" effector acting as a transcription factor, invasin, HECT E3 ubiquitin ligase, and most remarkably, a ligand mimic for multiple signaling pathways (Figure 1) (Zhu et al., 2011; Wang et al., 2020; Pittner et al., 2023). In fact, TRP120 is the first bacterial effector described capable of complex multi-pathway ligand mimicry driven by short linear motifs (SLiMs). SLiMs are small, functionally diverse protein interaction modules involved in regulatory interactions within the cell (Van Roey et al., 2014). While classical protein-protein interactions often depend on complex tertiary structures,

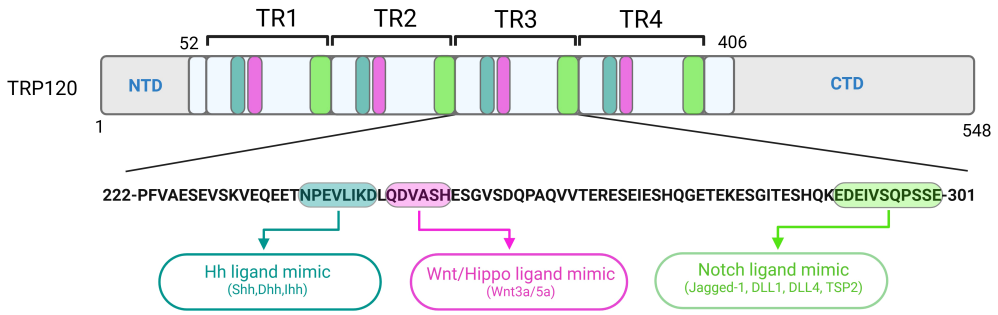

FIGURE 1
Localization of functionally characterized *E. chaffeensis* TRP120 SLiMs. Repetitive Hh, Wnt, Hippo and Notch SLiMs located within each tandem repeat (TR) domain of TRP120 have been experimentally validated and shown to activate respective pathways during infection.

recent advances have shown that interactions also occur via SLiM-globular and intrinsically disordered domain (IDD)-globular interfaces (Van Roey et al., 2014).

Over the past two decades, structural studies have revealed that a significant proportion of eukaryotic proteins are intrinsically disordered (Tompa, 2011, 2012). While they lack a well-defined tertiary structure, intrinsically disordered regions exhibit various cellular functions encoded within short sequences, now recognized as SLiMs (Davey et al., 2012). SLiMs have been identified as an *ex-nihilo* evolutionary adaptation, introducing functional interfaces to previously non-functional regions of proteins (Davey et al., 2015). Driving protein-protein interactions, SLiMs have been shown to regulate immune and inflammatory responses, cell proliferation, differentiation, and apoptosis, as well as control protein stability, recruit substrates, direct cellular trafficking and pose as sites for post-translational modifications (PTMs) and proteolytic cleavage (Davey et al., 2015; Sologova et al., 2022). The recognition of SLiMs has reshaped our understanding of cell biology with insurmountable evidence demonstrating SLiMs are reframing the paradigms of cellular regulation through eukaryotic protein interactions as well as pathogen-host interactions during infection (Neduva and Russell, 2005; Stein and Aloy, 2008; Van Roey et al., 2014).

The Eukaryotic Linear Motif (ELM) database is a computational biology resource with an expanding catalog of 4,277 experimentally validated SLiMs. According to an ELM prediction, *E. chaffeensis* TRP120 has 45 unique SLiM classes and 189 total SLiM instances (Kumar et al., 2024). This SLiM inventory does not include the recently described Wnt, Notch, Hedgehog (Hh) and Hippo mimics, suggesting that many TRP120 SLiMs remain to be identified and that most of the predicted TRP120 SLiMs have not been functionally validated. To date, the most definitive studies of *E. chaffeensis* TRP120 SLiM function are related to PTMs that affect pathogen-host interactions and those involved in cell signaling which impacts bacterial entry and innate immune defenses including autophagy and TLR expression, and perhaps most importantly apoptosis, to create a suitable niche for intracellular survival (Lina et al., 2016, 2017; Luo et al., 2016; Wang et al., 2020; Patterson et al., 2023). In the context of *Ehrlichia* infection, SLiM ligand mimicry (SLiM-icry) is used to engage host cell receptors and activate evolutionarily conserved signaling pathways (Pittner et al., 2023). Multiple instances of unique SLiM-icry are present in the tandem repeat domain of TRP120, capable of directly activating/deactivating Notch, Wnt, Hh and Hippo signaling pathways during ehrlichial infection (Figure 1) (Pittner et al., 2023). The Wnt pathway was the first evolutionarily conserved signaling pathway shown to be co-opted by *E. chaffeensis* SLiM-icry (Rogan et al., 2021). The revelation of this sophisticated survival strategy led to the discovery that *E. chaffeensis* also uses SLiM-icry to exploit Notch, Hh and Hippo (Byerly et al., 2022, 2023; Patterson et al., 2022).

Considering what is known about Wnt, Notch, Hh, and Hippo signaling pathways, the intersection between immune evasion strategies employed by *E. chaffeensis* and the hallmarks of cancer biology is intriguing. Dysfunction of these pathways has been appreciated in cancer biology as well as in other developmental diseases for decades (Kling and Blumenthal, 2017; Zheng and Pan, 2019; Kumar et al., 2021; Fu et al., 2022; Sharma et al., 2022), however, understanding the dysregulation of evolutionarily conserved cellular signaling pathways in cancer biology and its resistance to anticancer therapies is a major hurdle for improving therapeutic approaches to cancer treatment (Liang et al., 1999; Hanahan and Weinberg, 2011; Kumar et al., 2021). Interestingly, there are similarities in the molecular survival strategies employed by *E. chaffeensis* and the oncogenic mechanisms in malignant cancer cells that may provide synergistic insight to both areas of research. This is further supported by various TRP120 SLiMs identified by the ELM database that are implicated in carcinogenesis such as Src homology 2 (SH2) interaction motif (LIG_SH2_STAT3), BRCA1 tumor suppressor binding domain (LIG_BRCT_BRCA1_1), retinoblastoma protein interaction motif (LIG_RB_LxCxE_1) and MAP kinase docking site (DOC_MAPK_MEF2A_6) (Pittner et al., 2023; Kumar et al., 2024). While numerous pathogens utilize similar mechanisms to reprogram host cellular pathways (Holla et al., 2016; Konstantinou et al., 2016; Smelkinson, 2017; Smelkinson et al., 2017; Iriana et al., 2021), *E. chaffeensis* has emerged as a model pathogen adept at modulating molecular mechanisms involved in signaling pathway activation and regulation that may be useful in understanding cancer biology. This review will summarize key cellular and molecular insights and implications for advancing our knowledge of *E. chaffeensis* immune evasion as well as cancer biology.

Wnt pathway

Wnt signaling is an evolutionarily conserved pathway first discovered in 1982 as proto-oncogene "Int-1" in mice and was later revealed as the homolog of the "wingless" gene in *Drosophila*. Wnt pathway components are comprised of more than sixteen, mammalian, cysteine-rich secreted ligands necessary for canonical and noncanonical Wnt pathway activation. Wnt pathway activation is initiated when Wnt ligands bind the extracellular domain of Frizzled (Fzd) receptors which dimerize with coreceptors lipoprotein receptor-related protein (Lrp) 5, -6, or tyrosine kinase-like orphan receptor (Ror) 2 to subsequently activate disheveled (Dvl). Canonical Wnt is defined as β-catenin-dependent, whereas noncanonical Wnt is β-catenin-independent. Two distinct noncanonical pathways have been described: Calcium (Ca^{2+}) and Planar Cell Polarity (PCP). Canonical Wnt/β-catenin signaling controls cellular proliferation and differentiation, and is important in embryogenesis, organogenesis, and homeostasis. Conversely, activation of non-canonical Wnt pathways primarily results in regulation of cell motility and polarity (Di Bartolomeo et al., 2023). Wnt signaling is essential for embryonic development, cellular differentiation, polarization, as well as the control and growth of stem cells. Therefore, it is unsurprising that aberrant signaling has been implicated in various diseases including neurodegenerative, metabolic, and inflammatory diseases, as well as various cancers (Duchartre et al., 2016). Furthermore, Wnt signaling is involved in regulation of innate immune responses making it an important target for infectious agents (Silva-García et al., 2014; Jati et al., 2019; Mukherjee and Balaji, 2019; Rogan et al., 2019).

Wnt signaling in cancer

Wnt signaling has been linked to various types of cancers including colon, cutaneous melanoma, hepatocellular carcinoma (HCC) and breast cancer. It is also involved in metastasis as Wnt regulates cell morphology and motility. Increased Wnt ligand 5a (Wnt5a) in melanoma was correlated with increased invasiveness, cell motility and changes in morphology through changes in calcium signaling. Wnt5a has been extensively associated with proto-oncogenic cellular phenotypes. Wnt5a has been shown to act as a proto-oncogene in melanoma, breast cancer, prostate and pancreatic cancer, and a tumor suppressor in breast cancer, colon, thyroid and esophageal squamous cell carcinoma, acute lymphoblastic lymphoma, acute myeloid lymphoma, and neuroblastoma (Taciak et al., 2018).

In canonical Wnt signaling, binding of nuclear β-catenin to TCF/LEF transcription factors stimulate expression of cyclin D1 and c-MYC which alters cell cycle progression and promotes tumorigenesis in cutaneous melanoma (Taciak et al., 2018). β-catenin/TCF2 is a negative regulator of IFIT1 and IFIT2, host antiviral defense mediators through apoptosis. In colorectal cancer, IFIT2 expression is decreased which creates a pro-survival environment for cancer cells through inhibition of apoptosis. The β-catenin/TCF2 complex and down regulation of IFIT1/2 is commonly seen in colorectal cancer compared to normal tissue (Table 1) (Taciak et al., 2018).

The non-canonical Wnt/PCP pathway plays an important role in tumor development through its influence on cancer metastasis. Downstream signaling of the PCP pathway induces cytoskeletal rearrangement which facilitates cellular motility (Humphries and Mlodzik, 2018; Di Bartolomeo et al., 2023). In breast cancer, fibroblast-derived exosomes promote autocrine Wnt11/PCP signaling to enhance invasiveness. The invasive breast cancer cells displayed asymmetric localization of core PCP complexes like that found in development (Humphries and Mlodzik, 2018). In addition, there is a correlation between non-canonical Wnt, proinflammatory cytokines, and epithelial-mesenchymal transition (EMT). EMT induces metastasis in various cancer types and non-canonical Wnt signaling is commonly associated with EMT due to its role in cellular differentiation (Taciak et al., 2018). Likewise, proinflammatory cytokine interleukin (IL)-8 was found to induce EMT through Wnt signaling. Macrophages can limit cancer cell division through inhibition of canonical Wnt, but this increases non-canonical pathways. In cancer cells, increased non-canonical Wnt promotes differentiation, polarization, and separation from the tumor by EMT resulting in metastasis.

Wnt signaling in *Ehrlichia*

E. chaffeensis repurposes Wnt signaling to evade host immune responses and promote survival. Silencing of Wnt pathway components significantly reduces *E. chaffeensis* bacterial load, indicating the importance of Wnt signaling during infection. TRP120 contains a repetitive Wnt SLiM mimic (QDVASH) within the tandem repeat domain (TRD) (Rogan et al., 2021; Byerly et al., 2023). *E. chaffeensis* TRP120 Wnt SLiM mimic binds Fzd5 and induces nuclear translocation of β-catenin to modulate transcription of downstream Wnt target genes (Figure 2; Table 1) (Luo et al., 2016; Rogan et al., 2021). In this context, Wnt pathway activation results in cytoskeletal rearrangement and the induction of phagocytosis which contributes to ehrlichial host cell entry (Luo et al., 2016). Moreover, TRP120 has been shown to exploit the Wnt pathway to prevent autolysosome formation and allow *E. chaffeensis* to evade oxidative killing (Lina et al., 2017). Specifically, TRP120 binds to Wnt receptor and activates Dvl which subsequently activates the PI3K/AKT pathway and inhibits GSK3. PI3K/AKT activation inhibits negative regulator TSC2, which activates mTORC1. Activated mTOR phosphorylates TFEB, preventing nuclear translocation and subsequent upregulation of lysosomal target genes which prevents autolysosome formation (Lina et al., 2017). Additionally, canonical Wnt/β-catenin activation represses p62, an autophagy protein, as a mechanism for intracellular survival (Petherick et al., 2013). Interestingly, *E. chaffeensis* also activates the transcription factor nuclear factor of activated T-cells (NFAT) and initiates nuclear translocation of NFAT through the non-canonical Wnt/Ca2+ pathway. While knockdown of NFAT has been shown to significantly reduce *E. chaffeensis* bacterial load, the function of NFAT during infection has not been elucidated (Table 1) (Luo et al., 2016; Rogan et al., 2019).

TABLE 1 Parallels in cell signaling across *Ehrlichia* infection and cancer.

Pathway	Protein	Function in *Ehrlichia*	Function in cancer	References
Wnt	FZD5	TRP120 SLiM-activated receptor of Wnt and Hippo signaling during infection	Initiates Wnt signaling in triple negative breast cancer (TNBC) to promote DNA damage repair and enhance chemoresistance.	(Sun et al., 2020; Rogan et al., 2021; Byerly et al., 2023)
	β-catenin	Canonical Wnt transcription factor, increased nuclear localization during infection associated with enhanced bacterial entry.	Inhibits apoptosis in colorectal cancer cells via negative regulation of host defense mediators, (IFIT1/2).	(Luo et al., 2016; Taciak et al., 2018; Rogan et al., 2021)
	NFAT	Non-canonical Wnt transcription factor activated during infection; function unknown.	Downstream target of α4β6 integrin signaling enhancing cell migration and carcinoma invasion.	(Jauliac et al., 2002; Luo et al., 2016)
Notch	Notch1	TRP120 SLiM-activated receptor of Notch signaling during infection.	Promotes proliferation and inhibits apoptosis in pancreatic cancer via APOL-mediated activation.	(Lin et al., 2021; Patterson et al., 2022)
	NICD	Canonical Notch transcription factor, binds and sequesters XIAP and shown to delay host cell apoptosis.	Initiates lung tumorigenesis in conjunction with MYC activity in knock-in mouse models.	(Allen et al., 2011; Patterson et al., 2022, 2023)
	ADAM17	Metalloprotease associated with Notch activation, shown to interact with TRP120 during infection.	Promotes EMT transition via TGF-β/Smad pathway contributing to gastric cancer progression.	(Lina et al., 2016; Ni et al., 2020; Patterson et al., 2022)
	XIAP	Interaction with NICD stabilizes expression and promotes delayed host cell apoptosis during infection.	Downregulation via small molecule inhibitor decreased cell viability and induced apoptosis in breast cancer cells.	(Hussain et al., 2017; Patterson et al., 2023)
	FBW7	TRP120-mediated degradation leads to upregulation of oncoproteins (c-MYC, NICD,c-Jun and MCL1) during infection.	Decreased expression via ERK-mediated degradation disrupts tumor-suppressive activity in pancreatic cancer.	(Ji et al., 2015; Wang et al., 2020)
	PU.1	Transcription factor responsible for TLR2/4 expression, downregulated during infection to disrupt immune response.	Exhibits tumor-suppressive effects by inhibiting cell migration and promoting apoptosis via BCL-2 inhibition, downregulated in lung adenocarcinoma tissues.	(Lina et al., 2016; Liu et al., 2023b)
Hedgehog	PTCH2	TRP120 SLiM-activated receptor of Hh signaling during infection	Enhanced tumor growth observed in transcription activator-like effector nuclease (TALEN)-mediated Ptch2 gene-edited mice models	(Veenstra et al., 2018; Byerly et al., 2022)
	GLI1	Hh transcription factor, increased nuclear localization during infection associated with delayed apoptosis.	RNA silencing attenuated stem-like properties in lung-adenocarcinoma cells and increased susceptibility to apoptosis.	(Po et al., 2017; Byerly et al., 2022)
	BCL-2	Anti-apoptotic protein, increased expression associated with delayed apoptosis during infection	High expression shown to confer growth advantage to human Epstein Barr Virus (EBV)-lymphoblastoid B cells.	(Warren et al., 2019; Byerly et al., 2022)
Hippo	YAP/TAZ	Hippo transcription factors, increased nuclear localization correlates with delayed host cell apoptosis during infection	Overexpression induces malignant transformation of human mammary epithelial cells	(Byerly et al., 2023; Luo et al., 2023)
	BCL-xL	Anti-apoptotic protein, increased expression associated with delayed apoptosis during infection	Promotes stemness and tumor progression in melanoma and glioblastomas	(Trisciuoglio et al., 2017; Byerly et al., 2023)
	GLUT1	Regulates glucose metabolism and BCL2 family of proteins (BCL-xL and BAX) to delay apoptosis during infection	Expression correlated with tumor proliferation in epithelial ovarian carcinoma	(Semaan et al., 2011; Byerly et al., 2023)
	APC	Degraded during infection to inhibit negative regulation of β-catenin and YAP.	C-terminal loss of function mutation disrupts tumor suppressive activity and promotes tumorigenesis in colorectal cancer.	(Zhang and Shay, 2017; Byerly et al., 2024)

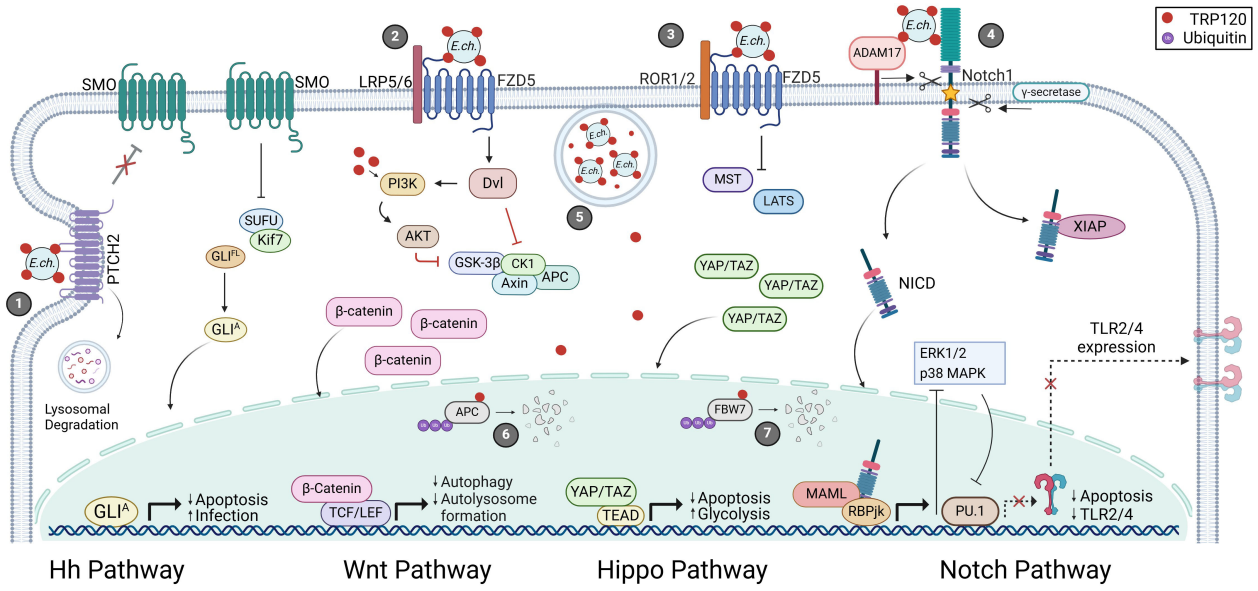

FIGURE 2
E. chaffeensis TRP120-mediated activation and functional outcomes of Hh, Wnt, Hippo and Notch signaling pathways. 1) Surface expressed TRP120 interacts with PTCH2 resulting in receptor internalization and lysosomal degradation. Active SMO accumulates and inhibits the SUFU protein complex releasing GLI to translocate to the nucleus and activate Hh target genes. 2) TRP120 binds FZD5 leading to the recruitment of co-receptor LRP5/6 and activation Wnt signaling activation. Active Dvl inhibits the β-catenin destruction complex (GSK3β, CK1, Axin, and APC) resulting in cytoplasmic accumulation of β-catenin and subsequent nuclear localization. 3) Additionally, TRP120 utilizes FZD5 to modulate Hippo signaling by inhibiting MST/LATS-mediated YAP/TAZ degradation. 4) Notch signaling is activated upon TRP120 interaction with Notch1 followed by receptor cleavage by ADAM17 and γ-secretase. Once cleaved, NICD stabilizes XIAP to inhibit apoptosis and translocates to the nucleus to regulate gene transcription. 5) *E. chaffeensis* enters host monocytes by receptor-mediated phagocytosis and reside in cytoplasmic vacuoles. TRP120 is secreted by the type-1 secretion system (T1SS) and translocates to the nucleus to mediate proteasomal degradation of 6) APC and 7) FBW7 to promote infection.

Notch pathway

Over a century ago, the Notch gene was discovered in *Drosophila melanogaster* (Zhou et al., 2022a). Genetic studies of *D. melanogaster* demonstrated that knockdown of the Notch gene was lethal (Zhou et al., 2022a). Since its discovery, Notch has been linked to developmental and cellular pathways including cell fate, proliferation, differentiation, adhesion, apoptosis, inflammation, and angiogenesis (Kumar et al., 2021). Furthermore, Notch dysregulation promotes cancer and infectious disease (Zhou et al., 2022a; Aster et al., 2017; Kumar et al., 2021). As a highly conserved and common target in disease, the Notch pathway is a prevalent area of research, as determining its interactions and roles in disease could lead to new therapeutic strategies (Aster et al., 2017; Kumar et al., 2021; Zhou et al., 2022a). Notch pathway activation is initiated by the interaction of Notch ligands (DLL1, -3, -4 and Jagged-1, -2) expressed on signal-sending cells and mature Notch receptors (Notch1, -2, -3 and -4) on signal-receiving cells that are glycosylated and cleaved in the Golgi by a Furin-like protease followed by receptor cleavage via ADAM17 and γ-secretase (Zhou et al., 2022a). The Notch intracellular domain (NICD) promotes transcription of Notch target gene families, including Hairy/Enhancer of Split (HES) and Hairy/Enhancer of Split related to YRPW motif (HEY), NF-κB, c-MYC, p21, through nuclear interactions with repressor CBF-1/suppressor of hairless/Lag1 (CSL/RBPJ) and transcriptional co-activator Mastermind-like protein (MAML) (Figure 2) (Capaccione and Pine, 2013; Zhou et al., 2022a). Notch, through nuclear and cytoplasmic interactions, modulates pathways associated with cell fate, proliferation, differentiation, adhesion, apoptosis, inflammation, and angiogenesis (Kumar et al., 2021).

Notch signaling in cancer

As a key regulator of the immune response and cell fate, Notch associated genes are commonly mutated in several cancers. In breast cancer, genetic mutations upregulate Notch through gain-of-function mutations in *Notch1* (5-10%) and loss-of-function mutations in Numb (50%), a negative regulator of Notch (Stylianou et al., 2006; Aster et al., 2017). In T-cell acute lymphoblastic leukemia (T-ALL), loss-of-function mutations in F-Box and WD domain repeating containing 7 (FBW7) (20%) and gain-of-function mutation in *Notch1* (50-60%) also result in upregulated Notch signaling (Aster et al., 2017; Sanchez-Martin and Ferrando, 2017).

In both T-ALL and breast cancer, aberrant expression of Notch promotes cell proliferation and inhibits apoptosis (Stylianou et al., 2006; Palomero et al., 2007; Aster et al., 2017; Sanchez-Martin and Ferrando, 2017; Baker et al., 2018). Downstream effects include the inhibition of the JNK and p53 pathways resulting in decreased levels of pro-apoptotic factors, Puma and Noxa (Stylianou et al., 2006).

Furthermore, Notch modulates the PI3K/AKT pathway through transcriptional downregulation of PTEN, a negative regulator of the PI3K/AKT pathway, in both T-ALL and breast cancer (Palomero et al., 2007; Baker et al., 2018).

Intriguingly, downregulation of PTEN and inhibition of FBW7 have both been associated with chemotherapeutic resistance. Both PTEN and FBW7 inhibition in cancer are associated with resistance to γ-secretase inhibitors (GSI) which are used to treat breast cancer and are known to downregulate Notch (Palomero et al., 2007; Thompson et al., 2007; Baker et al., 2018; Fan et al., 2022; Chen et al., 2023). In these cancers, upregulation of Notch promotes a tumorigenic environment through inhibition of apoptosis and regulation of cell growth and proliferation which encourages further resistance to chemotherapeutics.

Notch signaling in *Ehrlichia*

During *E. chaffeensis* infection the Notch pathway is activated by TRP120 to inhibit apoptosis and promote infection. TRP120 promotes Notch activation through three mechanisms: direct activation of Notch, degradation of negative regulators, and transcriptional upregulation of Notch genes (Lina et al., 2016; Wang et al., 2020; Patterson et al., 2022, 2023). TRP120 contains an 11 amino acid SLiM (EDEIVSQPSSE) that mimics Notch ligands thereby activating Notch signaling during infection (Patterson et al., 2022). Moreover, TRP120 contains a HECT E3 ubiquitin ligase which ubiquitinates host FBW7, a negative regulator of NICD to maintain Notch activation (Figure 2) (Wang et al., 2020). FBW7 negatively regulates several oncoproteins (NICD, MCL-1, c-Jun, and c-MYC) through ubiquitination and subsequent proteasomal degradation (Wang et al., 2020). To further promote Notch activation, TRP120 binds the promoter regions of *Notch1* and *ADAM17* to promote transcription during infection (Lina et al., 2016). Upregulation of *Notch1* promotes generation of the Notch-1 receptor while *ADAM17* increases NICD S2 cleavage of the Notch receptors (Lina et al., 2016). *E. chaffeensis* activation of Notch inhibits PU.1, Toll-like receptor 2 and 4 (TLR2/4) expression through manipulation of ERK1/2 and p38 pathways (Lina et al., 2016). Further, X-linked inhibitor of apoptosis protein (XIAP) is sequestered and stabilized during infection due to increased cytoplasmic NICD (Patterson et al., 2023). Equally important, Notch activation leads to transcription of Notch target genes that modulate cell fate and proliferation to promote infection (Table 1) (Patterson et al., 2022).

Hedgehog pathway

The Hedgehog (Hh) pathway is among a primary group of signaling pathways indispensable for embryonic development (Iriana et al., 2021; Zhou et al., 2022b). Hh signaling was first discovered in 1980 through mutagenesis screenings in *Drosophila* (Sari et al., 2018) and was found to be critical for embryogenesis, cell differentiation and tissue polarity (Iriana et al., 2021). Not surprisingly, aberrant Hh signaling results in developmental disorders and birth defects and has been shown to suppress host immune responses during tumorigenesis and pathogenic infections (Konstantinou et al., 2016; Smelkinson, 2017; Shi et al., 2018; Iriana et al., 2021). The Hh pathway is evolutionarily conserved among invertebrates and vertebrates, with pathway redundancy observed in the latter. In mammals, there are three Hh ligands, Sonic hedgehog (Shh), Dessert hedgehog (Dhh) and Indian hedgehog (Ihh) that bind to Patched1 (PTCH1) or Patched2 (PTCH2) receptors and activate glioma-associated oncogene (GLI) transcriptions factors, GLI-1, -2, or -3. Hh signaling has essential functions for cell-fate, pattern formation, proliferation and cell survival during development therefore dysregulated Hh signaling is associated with diseases such as Parkinsons's, autism, epilepsy, osteoarthritis (OA), basal cell carcinoma (BCC), and pancreatic cancer (Li et al., 2021; Smith et al., 2022).

Hedgehog signaling in cancer

Hh signaling is involved in numerous developmental processes, and thus is implicated in various genetic diseases, including cancer. The Hh signaling pathway is known to promote tumor formation via ligand-independent or ligand-dependent mechanisms. Hh ligand-independent cancers include basal cell carcinoma, medulloblastoma (MB) and pediatric brain tumors. Mechanisms required for ligand-independent cancers involve mutations in Hh pathway components that lead to constitutive activation of smoothened (SMO) and GLI and repression of PTCH and the suppressor of fused (SUFU) (Sari et al., 2018). Hh ligand-dependent cancers such as colorectal, ovarian, breast, prostate, pancreatic and liver cancers utilize either autocrine or paracrine signaling to promote tumorigenesis whereby endogenous ligands are copiously secreted, facilitating feed-forward pathway activation. Paracrine ligand-dependent Hh signaling requires endogenous ligands to bind stromal cell PTCH receptors thereby initiating the release of growth signals such as interleukin-6 (IL-6), vascular endothelial growth factor (VEGF), platelet derived growth factor (PDGF), bone morphogenetic protein (BMP), and insulin-like growth factor (IGF) to promote tumor progression (Sari et al., 2018).

Hedgehog signaling in *Ehrlichia*

E. chaffeensis TRP120 engages the PTCH2 receptor through a repeated SLiM ligand mimic (NPEVLIKD) to activate Hh signaling. This activation results in nuclear translocation of GLI-1 in THP-1 cells and primary human monocytes (PHM) (Figure 2) (Byerly et al., 2022). Informational spectrum method (ISM) predicted the TRP120 Hh SLiM shares sequence and functional similarity with endogenous Hh ligands. This prediction was supported by protein interaction assays which demonstrated the tandem repeat domain of TRP120 co-localizes and directly interacts with the PTCH2 receptor. Furthermore, TRP120-mediated GLI-1 nuclear translocation resulted in upregulation of key target genes that were consistent with classical Hh ligands (Table 1) (Byerly et al., 2022).

During *E. chaffeensis* infection, Hh activation has been shown to significantly increase the expression of anti-apoptotic protein, BCL-

2, thus preventing Bax-mediated cytochrome c release to maintain mitochondrial membrane integrity (Table 1) (Byerly et al., 2022). This ehrlichial survival strategy blocks intrinsic cell death signals and appropriates host cell nutrients for survival and dissemination. Further, knockdown of pathway components including GLI-1, PTCH2 and SMO decreases *E. chaffeensis* infection. In addition, THP-1 cell treatment with an antibody against the TRP120 Hh SLiM or treatment with a TRP120 Hh SLiM mutant prevented GLI-1 nuclear translocation and subsequent pathway activation. Moreover, *E. chaffeensis*-infected THP-1 cells showed decreased GLI-1 nuclear translocation and increased cell death after treatment with a Hh pathway inhibitor (Vismodegib/GDC-0449), suggesting that Hh signaling plays a significant role in *E. chaffeensis* infection by inhibiting apoptosis (Byerly et al., 2022). This study was the first to show *E. chaffeensis* TRP120 SLiM-mediated Hh activation, highlighting the necessity to understand the nuances of Hh signaling which will be fundamental in defining distinct mechanisms of pathway regulation in various diseases.

Hippo pathway

Discovered in 2003, the Hippo signaling pathway is conserved in metazoans and essential in processes including regulation of organ size, organ homeostasis, and embryologic development (Liu et al., 2021; Xiao and Dong, 2021; Wang et al., 2021; Cox et al., 2018; Jiang et al., 2020). This pathway largely accomplishes its functions via control over cell survival and differentiation, and is generally influenced by signals including mechanical cues, stress, cell polarity, cell density, and soluble factors (Yu et al., 2012; Harvey et al., 2013; Misra and Irvine, 2018; Fu et al., 2022). Given the important cellular and developmental roles of Hippo signaling, it is not surprising that aberrant Hippo signaling results in many human diseases. Notably, the association of Hippo with cell proliferation, apoptosis, and survival is responsible for the high prevalence of abnormal Hippo signaling in malignancy.

Hippo signaling in cancer

Although the role of Hippo signaling in cancer is context-dependent, the pathway is typically considered tumor suppressing. Thus, inactivation of Hippo signaling and downstream activation of Yes-associated protein 1 (YAP) and WW-domain-containing transcription regulator 1 (TAZ) is common in a variety of malignancies such as breast, gastric, renal, hepatic, and hematologic cancers (Xu et al., 2019; Kyriazoglou et al., 2021; Ma et al., 2021; Noorbakhsh et al., 2021; Song et al., 2022; Wu et al., 2022; Liu et al., 2023a; Messina et al., 2023; Li et al., 2024; Yang et al., 2024). Elevated activation of YAP/TAZ is implicated in tumor initiation, metastasis, and drug resistance through mechanisms including inhibition of apoptosis and reprogramming of metabolic pathways in tumor cells (Liu et al., 2021; Fu et al., 2022). Additionally, Hippo signaling engages in crosstalk with other pathways, such as Wnt signaling (discussed above), further mediating cancer cell survival and tumor progression (Jiang et al., 2020; Noorbakhsh et al., 2021; Li et al., 2019b).

When bound to transcriptional enhanced associated domain family of proteins (TEAD 1-4), YAP/TAZ may upregulate the expression of anti-apoptotic factors such as members of the BCL-2 and inhibitor of apoptosis protein (IAP) families (Cheng et al., 2022; Zhang et al., 2022). These proteins directly inhibit apoptosis by preventing apoptotic signals such as Bax/Bak-mediated mitochondrial outer membrane permeabilization or caspase cleavage, respectively (Cetraro et al., 2022; Czabotar and Garcia-Saez, 2023). Such mechanisms have been observed in malignancies including colorectal cancer and adenocarcinoma, amongst others (Zhang et al., 2015, 2022; Jin et al., 2021). YAP/TAZ activation can also contribute to metabolic reprograming in cancer cells, specifically in the upregulation of proteins that facilitate increased glucose uptake and glycolytic flux such as GLUT1-3, phosphofructokinase and others (Liu et al., 2021). These proteins not only support cancer cell growth by elevating energy acquisition but may also contribute to maintaining an anti-apoptotic profile by positive regulation of BCL-2 family proteins (Coloff et al., 2011; Liu et al., 2014; Fang et al., 2015; Lin and Xu, 2017; Li et al., 2019a). For example, GLUT1 upregulation is a consequence of YAP activation in both breast and gastric cancer and has been correlated with BCL-xL expression in colorectal and gastric cancer (Wincewicz et al., 2007; Lin and Xu, 2017; Li et al., 2019a). Interestingly, Hippo signaling also interacts with other signaling pathways and modulates cell survival through crosstalk (Jiang et al., 2020).

A key example of Hippo pathway crosstalk is that with the Wnt pathway. Activation of Hippo signaling impedes Wnt signaling, as phosphorylated, cytoplasmic YAP/TAZ sequesters β-catenin outside the nucleus, preventing its translocation and subsequent upregulation of Wnt target genes (Imajo et al., 2012). Therefore, it is unsurprising that some Wnt ligands, notably Wnt3a and Wnt5a, can inactivate Hippo signaling through Fzd5 to ensure successful β-catenin nuclear translocation (Park et al., 2015). The crosstalk between these pathways is particularly relevant in cancer, as Hippo inactivation and Wnt activation are common mechanisms of cancer cell survival (Jiang et al., 2020; Noorbakhsh et al., 2021; Li et al., 2019b; Andl and Zhang, 2017). YAP activation is essential for β-catenin function in a variety of cancers including melanoma, hepatoblastoma, colon cancer, and breast cancer, and a screen of 85 cancer cell lines determined that those driven by β-catenin were dependent on YAP (Rosenbluh et al., 2012; Tao et al., 2014; Liu et al., 2019; Quinn et al., 2021). Additionally, the latter study also concluded that β-catenin and YAP act as transcriptional coregulators, forming a complex that upregulates gene expression of anti-apoptotic proteins, survivin and BCL2L1 (Rosenbluh et al., 2012). Hippo and Wnt signaling are therefore inextricably linked and possess a great deal of influence over cell proliferation and survival. Intriguingly, co-option of the crosstalk between these two pathways has been observed during infection of host cells by *E. chaffeensis*, one of the few bacterial pathogens associated with Hippo signaling (Byerly et al., 2023).

Hippo signaling in *Ehrlichia*

The role of Hippo signaling in bacterial infection is critically understudied for such a ubiquitous and influential signaling

pathway. Interestingly, one of the best examples of Hippo pathway involvement in bacterial infection is *E. chaffeensis*, which is extensively demonstrated to inactivate Hippo through SLiM-icry. In fact, *E. chaffeensis* uses the same SLiM to both activate Wnt signaling and inactivate Hippo signaling, taking advantage of the crosstalk between these pathways. By inactivating Hippo signaling, *E. chaffeensis* ensures the efficacy of Wnt signaling activation while promoting YAP-mediated anti-apoptotic gene expression in host cells (Figure 2) (Byerly et al., 2023).

Motivated by the role of Wnt in *E. chaffeensis* pathology, and the existence of Wnt/Hippo crosstalk, YAP activation was investigated in a cell culture model of *E. chaffeensis* infection. In *E. chaffeensis*-infected cells, YAP is activated and translocates to the nucleus, where it upregulates a diverse panel of target genes. YAP activation during *E. chaffeensis* infection was attributed to the TRP120 Wnt SLiM, suggesting this sequence is responsible for Hippo inactivation in addition to activation of Wnt signaling. Furthermore, in Fzd5 knockout cells, YAP is not activated by *E. chaffeensis* or the TRP120 Wnt SLiM (Byerly et al., 2023). Finally, TRP120 ubiquitinates adenomatous polyposis coli (APC), a negative regulator of YAP and β-catenin, targeting it for degradation (Figure 2; Table 1) (Byerly et al., 2024). Taken together, these findings demonstrate that *E. chaffeensis* inactivates Hippo signaling through the same mechanism as Wnt signaling activation (Byerly et al., 2023).

As described above, inactivation of Hippo signaling may contribute to excessive cellular survival and metabolic reprogramming through YAP-mediated genetic regulation. Notably, this phenomenon is also observed in *E. chaffeensis*-infected cells. Hippo inactivation by *E. chaffeensis* is critical for pathogen survival as knockdown of YAP and TEAD family transcription factors significantly decreases infection (Byerly et al., 2023). Both *E. chaffeensis* and TRP120 Wnt SLiM significantly increase expression of GLUT1, while GLUT1 knockdown significantly decreases infection, suggesting this metabolic protein is crucial for maintaining infection (Table 1). Further investigation revealed that BCL-xL levels increase while Bax levels decrease in response to infection and the TRP120 Wnt SLiM, and this result is abrogated by treatment with Verteporfin, a YAP inhibitor (Liu-Chittenden et al., 2012; Byerly et al., 2023). Verteporfin also significantly decreases bacterial load and cell viability in infected cells, and significantly increases caspase activation, indicating an increase in apoptosis. Collectively, these results illustrate that *E. chaffeensis* inactivates Hippo signaling to engage the YAP-GLUT1-BCL-xL axis and establishes an anti-apoptotic profile in host cells, a mechanism like that observed in multiple cancers (Byerly et al., 2023).

Conclusion and future perspectives

Cell death resistance and immune evasion are common survival strategies among various cancers and host-dependent pathogens. Given what is known about aberrant Wnt, Notch, Hh and Hippo signaling during oncogenesis and ehrlichial pathogenesis, it is important to understand pathway regulation in both contexts. Modulation of evolutionarily conserved embryonic pathways during *E. chaffeensis* infection is gaining attention as *E. chaffeensis* has proved a powerful model for investigating complex signal transduction pathways (Rogan et al., 2021; Byerly et al., 2022, 2023; Patterson et al., 2022; Pittner et al., 2023). Most importantly, *E. chaffeensis* has restructured our understanding of ligand binding requirements, challenging the long-accepted dogma of a tertiary ligand structure required for receptor interactions. It is important to understand SLiMs, not only as a biochemical phenomenon but as a means to broaden investigations of various diseases with the potential for SLiM-driven interactions, thereby improving the likelihood of SLiM-targeted therapies. The SLiM-mediated cellular interactions employed by *E. chaffeensis* have taught scientists the power of revisiting what was previously understood and has allowed appreciation of novel molecular strategies employed by a single bacterium.

SLiM-mediated pathway activation is not exclusive to *E. chaffeensis* (Van Roey et al., 2014; Elde and Malik, 2009; Pha et al., 2024; Giménez et al., 2024; Simonetti et al., 2023); however, unlike other infectious agents, *E. chaffeensis* has advanced our understanding of distinct mechanisms regulated by a single pathogen effector protein. Therefore, the use of *E. chaffeensis* to further study this phenomenon will undoubtably yield an even greater understanding of signaling pathways and their control over cell survival in cancer and intracellular infection. The balance of Wnt, Notch, Hh and Hippo signaling is crucial for stem cell development, cellular polarization, and differentiation. Consequently, aberrant signaling of these pathways have been heavily implicated in cancer and infectious diseases. Therapeutics targeting different components of these signaling pathways may be useful for treating cancer and infectious diseases. For example, the SMO inhibitor, Vismodegib, is an FDA approved cancer therapeutic used to treat basal cell carcinoma and while clinical trials are still ongoing to evaluate the efficacy of this drug in other tumors, the use of Vismodegib on *E. chaffeensis*-infected THP-1 cells to ameliorate cell death resistance associated with infection is a promising example of how understanding signaling mechanisms in cancer and pathogenic infections could improve standard clinical interventions for both diseases (Iriana et al., 2021; Byerly et al., 2022). Additionally, OMP-18R5 (vantictumab) interacts with Fzd5 to block Wnt activation and PKF115-584 inhibits the interaction between β-catenin and TCF/LEF, preventing gene activation (Tai et al., 2015). GSI inhibitors that prevent the cleavage and release of the NICD into the cytoplasm are promising therapeutics for aberrant Notch activation (Palomero et al., 2007; Baker et al., 2018). Furthermore, Verteporfin, a YAP inhibitor effective in preclinical studies of Hippo-implicated malignancies, was also demonstrated to significantly enhance apoptosis and decrease bacterial load in a cell culture model of *E. chaffeensis* infection (Wei and Li, 2020; Byerly et al., 2023).

Studies of *E. chaffeensis* have uncovered multiple SLiMs capable of modulating numerous signaling pathways, information useful as a tool in advancing general cellular and molecular approaches, design of pathway-modulating molecules, and detection of novel mechanisms in anomalous Wnt, Notch, Hh and Hippo signaling. There is growing evidence that several cancers are mediated by SLiMs including Burkitt's lymphoma, prostate cancer, ovarian cancer and colorectal cancer (Vitari et al., 2011; Uyar et al., 2014; Kumar et al., 2024). The recognition of SLiM-mediated cancers has improved drug development efforts by exhibiting non-classical targets for therapeutics such as, Nutlins and Cilengitide. These drugs entered

clinical trials as they have been shown to specifically target SLiM-mediated protein interactions in retinoblastoma, liposarcoma and glioblastoma (Uyar et al., 2014) signifying the possibility of targeting additional SLiM-mediated cancers in the near future. Not only is there opportunity to investigate SLiM-mediated pathway activation in cancers and other diseases, but researchers can now extend studies of *E. chaffeensis* as a tool to understand the signaling cascades reprogrammed in certain cancers, potentially improving therapeutic targets beyond globular protein-protein interactions. Due to the parallels of Wnt, Notch, Hh and Hippo signaling in cancer and *E. chaffeensis* infection, utilizing *E. chaffeensis* as a model to study aberrant signaling as it relates to cancer, intracellular pathogens, and production of novel therapeutics is essential.

Author contributions

RNS: Writing – original draft, Writing – review & editing. NAP: Writing – original draft, Writing – review & editing. JRM: Writing – original draft, Writing – review & editing. PAW: Writing – original draft, Writing – review & editing. JWM: Conceptualization, Funding acquisition, Supervision, Writing – review & editing.

Funding

The author(s) declare financial support was received for the research, authorship, and/or publication of this article. This work was supported by the National Institute of Allergy and Infectious Disease grants AI158422, AI146637, AI149136, and AI137779 awarded to JWM, NIH T32AI007526-22 biodefense training fellowship awarded to RS, and UTMB McLaughlin Endowment Predoctoral Fellowship awarded to NP.

Conflict of interest

The authors declare that the research was conducted in the absence of any commercial or financial relationships that could be construed as a potential conflict of interest.

Generative AI statement

The author(s) declare that no Generative AI was used in the creation of this manuscript.

Publisher's note

References

Allen, T. D., Rodriguez, E. M., Jones, K. D., and Bishop, J. M. (2011). Activated Notch1 induces lung adenomas in mice and cooperates with Myc in the generation of lung adenocarcinoma. *Cancer Res.* 71. doi: 10.1158/0008-5472.CAN-11-0595

Andl, T., and Zhang, Y. (2017). Reaping Wnt after calming Hippo: Wnt and Hippo signaling cross paths in lung cancer. *J. Thorac. Dis.* 9. doi: 10.21037/jtd.2017.10.29

Aster, J. C., Pear, W. S., and Blacklow, S. C. (2017). The varied roles of notch in cancer. *Annu. Rev. Pathology: Mech. Dis.* 12. doi: 10.1146/annurev-pathol-052016-100127

Baker, A., Wyatt, D., Bocchetta, M., Li, J., Filipovic, A., Green, A., et al. (2018). Notch-1-PTEN-ERK1/2 signaling axis promotes HER2+ breast cancer cell proliferation and stem cell survival. *Oncogene* 37. doi: 10.1038/s41388-018-0251-y

Byerly, C. D., Mitra, S., Patterson, L. N. L., Pittner, N. A., Velayutham, T. S., Paessler, S., et al. (2022). Ehrlichia SLiM ligand mimetic activates Hedgehog signaling to engage a BCL-2 antiapoptotic cellular program. *PloS Pathog.* 18. doi: 10.1371/journal.ppat.1010345

Byerly, C. D., Patterson, L. N. L., Pittner, N. A., Solomon, R. N., Patel, J. G., Rogan, M. R., et al. (2023). Ehrlichia Wnt SLiM ligand mimic deactivates the Hippo pathway to engage the anti-apoptotic Yap-GLUT1-BCL-xL axis. *Infect. Immun.* 91. doi: 10.1128/iai.00085-23

Byerly, C. D., Zhu, B., Warwick, P. A., Patterson, L. L., Pittner, N. A., and McBride, J. W. (2024). Ehrlichia chaffeensis TRP120 ubiquitinates tumor suppressor APC to modulate Hippo and Wnt signaling. *Front. Cell Dev. Biol.* 12. doi: 10.3389/fcell.2024.1327418

Capaccione, K. M., and Pine, S. R. (2013). The Notch signaling pathway as a mediator of tumor survival. *Carcinogenesis* 34. doi: 10.1093/carcin/bgt127

Cetraro, P., Plaza-Diaz, J., Mackenzie, A., and Abadía-Molina, F. (2022). A review of the current impact of inhibitors of apoptosis proteins and their repression in cancer. *Cancers (Basel)* 14. doi: 10.3390/cancers14071671

Chen, S., Leng, P., Guo, J., and Zhou, H. (2023). FBXW7 in breast cancer: mechanism of action and therapeutic potential. *J. Exp. Clin. Cancer Res.* 42. doi: 10.1186/s13046-023-02767-1

Cheng, Y., Mao, M., and Lu, Y. (2022). The biology of YAP in programmed cell death. *biomark. Res.* 10. doi: 10.1186/s40364-022-00365-5

Coloff, J. L., Mason, E. F., Altman, B. J., Gerriets, V. A., Liu, T., Nichols, A. N., et al. (2011). Akt requires glucose metabolism to suppress Puma expression and prevent apoptosis of leukemic T cells. *J. Biol. Chem.* 286. doi: 10.1074/jbc.M110.179101

Cox, A. G., Tsomides, A., Yimlamai, D., Hwang, K. L., Miesfeld, J., Galli, G. G., et al. (2018). Yap regulates glucose utilization and sustains nucleotide synthesis to enable organ growth. *EMBO J.* 37. doi: 10.15252/embj.2018100294

Czabotar, P. E., and Garcia-Saez, A. J. (2023). Mechanisms of BCL-2 family proteins in mitochondrial apoptosis. *Nat. Rev. Mol. Cell Biol.* 24. doi: 10.1038/s41580-023-00629-4

Davey, N. E., Cyert, M. S., and Moses, A. M. (2015). Short linear motifs – ex nihilo evolution of protein regulation. *Cell Communication Signaling* 13. doi: 10.1186/s12964-015-0120-z

Davey, N. E., Van Roey, K., Weatheritt, R. J., Toedt, G., Uyar, B., Altenberg, B., et al. (2012). Attributes of short linear motifs. *Mol. Biosyst.* 8. doi: 10.1039/c1mb05231d

Di Bartolomeo, L., Vaccaro, F., Irrera, N., Borgia, F., Li Pomi, F., Squadrito, F., et al. (2023). Wnt signaling pathways: from inflammation to non-melanoma skin cancers. *Int. J. Mol. Sci.* 24. doi: 10.3390/ijms24021575

Duchartre, Y., Kim, Y. M., and Kahn, M. (2016). The Wnt signaling pathway in cancer. *Crit. Rev. Oncol. Hematol.* 99. doi: 10.1016/j.critrevonc.2015.12.005

Elde, N. C., and Malik, H. S. (2009). The evolutionary conundrum of pathogen mimicry. *Nat. Rev. Microbiol.* 7. doi: 10.1038/nrmicro2222

Fan, J., Bellon, M., Ju, M., Zhao, L., Wei, M., Fu, L., et al. (2022). Clinical significance of FBXW7 loss of function in human cancers. *Mol. Cancer* 21. doi: 10.1186/s12943-022-01548-2

Fang, J., Zhou, S. H., Fan, J., and Yan, S. X. (2015). Roles of glucose transporter-1 and the phosphatidylinositol 3-kinase/protein kinase B pathway in cancer radioresistance (Review). *Mol. Med. Rep.* 11. doi: 10.3892/mmr.2014.2888

Fu, M., Hu, Y., Lan, T., Guan, K. L., Luo, T., and Luo, M. (2022). The Hippo signalling pathway and its implications in human health and diseases. *Signal Transduct Target Ther.* 7. doi: 10.1038/s41392-022-01191-9

Giménez, A., Del Giudice, M. G., López, P. V., Guaimas, F., Sámano-Sánchez, H., Gibson, T. J., et al. (2024). Brucella NpeA is a secreted Type IV effector containing an N-WASP-binding short linear motif that promotes niche formation. *mBio* 15, e0072624. doi: 10.1128/mbio.00726-24

Hanahan, D., and Weinberg, R. A. (2011). Hallmarks of cancer: The next generation. *Cell* 144. doi: 10.1016/j.cell.2011.02.013

Harvey, K. F., Zhang, X., and Thomas, D. M. (2013). The Hippo pathway and human cancer. *Nat. Rev. Cancer* 13. doi: 10.1038/nrc3458

Holla, S., Stephen-Victor, E., Prakhar, P., Sharma, M., Saha, C., Udupa, V., et al. (2016). Mycobacteria-responsive sonic hedgehog signaling mediates programmed death-ligand 1-and prostaglandin e 2-induced regulatory T cell expansion. *Sci. Rep.* 6. doi: 10.1038/srep24193

Humphries, A. C., and Mlodzik, M. (2018). From instruction to output: Wnt/PCP signaling in development and cancer. *Curr. Opin. Cell Biol.* 51. doi: 10.1016/j.ceb.2017.12.005

Hussain, A. R., Siraj, A. K., Ahmed, M., Bu, R., Pratheeshkumar, P., Alrashed, A. M., et al. (2017). XIAP over-expression is an independent poor prognostic marker in Middle Eastern breast cancer and can be targeted to induce efficient apoptosis. *BMC Cancer* 17. doi: 10.1186/s12885-017-3627-4

Imajo, M., Miyatake, K., Iimura, A., Miyamoto, A., and Nishida, E. (2012). A molecular mechanism that links Hippo signalling to the inhibition of Wnt/β-catenin signalling. *EMBO J.* 31. doi: 10.1038/emboj.2011.487

Iriana, S., Asha, K., Repak, M., and Sharma-Walia, N. (2021). Hedgehog signaling: Implications in cancers and viral infections. *Int. J. Mol. Sci.* 22. doi: 10.3390/ijms22031042

Jati, S., Sarraf, T. R., Naskar, D., and Sen, M. (2019). Wnt signaling: Pathogen incursion and immune defense. *Front. Immunol.* 10. doi: 10.3389/fimmu.2019.02551

Jauliac, S., López-Rodriguez, C., Shaw, L. M., Brown, L. F., Rao, A., and Toker, A. (2002). The role of NFAT transcription factors in integrin-mediated carcinoma invasion. *Nat. Cell Biol.* 4. doi: 10.1038/ncb816

Ji, S., Qin, Y., Shi, S., Liu, X., Hu, H., Zhou, H., et al. (2015). ERK kinase phosphorylates and destabilizes the tumor suppressor FBW7 in pancreatic cancer. *Cell Res.* 25. doi: 10.1038/cr.2015.30

Jiang, L., Li, J., Zhang, C., Shang, Y., and Lin, J. (2020). YAP-mediated crosstalk between the Wnt and Hippo signaling pathways (Review). *Mol. Med. Rep.* 22. doi: 10.3892/mmr.2020.11529

Jin, L., Chen, Y., Cheng, D., He, Z., Shi, X., Du, B., et al. (2021). YAP inhibits autophagy and promotes progression of colorectal cancer via upregulating Bcl-2 expression. *Cell Death Dis.* 12. doi: 10.1038/s41419-021-03722-8

Kling, J. C., and Blumenthal, A. (2017). Roles of WNT, NOTCH, and Hedgehog signaling in the differentiation and function of innate and innate-like lymphocytes. *J. Leukoc. Biol.* 101. doi: 10.1189/jlb.1mr0616-272r

Konstantinou, D., Bertaux-Skeirik, N., and Zavros, Y. (2016). Hedgehog signaling in the stomach. *Curr. Opin. Pharmacol.* 31. doi: 10.1016/j.coph.2016.09.003

Kumar, M., Michael, S., Alvarado-Valverde, J., Zeke, A., Lazar, T., Glavina, J., et al. (2024). ELM-the Eukaryotic Linear Motif resource-2024 update. *Nucleic Acids Res.* 52. doi: 10.1093/nar/gkad1058

Kumar, V., Vashishta, M., Kong, L., Wu, X., Lu, J. J., Guha, C., et al. (2021). The role of notch, hedgehog, and wnt signaling pathways in the resistance of tumors to anticancer therapies. *Front. Cell Dev. Biol.* 9. doi: 10.3389/fcell.2021.650772

Kyriazoglou, A., Liontos, M., Zakopoulou, R., Kaparelou, M., Tsiara, A., Papatheodoridi, A. M., et al. (2021). The role of the hippo pathway in breast cancer carcinogenesis, prognosis, and treatment: A systematic review. *Breast Care* 16. doi: 10.1159/000507538

Li, H., Fu, L., Liu, B., Lin, X., Dong, Q., and Wang, E. (2019a). Ajuba overexpression regulates mitochondrial potential and glucose uptake through YAP/Bcl-xL/GLUT1 in human gastric cancer. *Gene* 693. doi: 10.1016/j.gene.2019.01.018

Li, L., Tang, J., Cao, B., Xu, Q., Xu, S., Lin, C., et al. (2024). GPR137 inactivates Hippo signaling to promote gastric cancer cell Malignancy. *Biol. Direct* 19. doi: 10.1186/s13062-023-00449-8

Li, N., Lu, N., and Xie, C. (2019b). The Hippo and Wnt signalling pathways: crosstalk during neoplastic progression in gastrointestinal tissue. *FEBS J.* 286. doi: 10.1111/febs.15017

Li, X., Li, Y., Li, S., Li, H., Yang, C., and Lin, J. (2021). The role of Shh signalling pathway in central nervous system development and related diseases. *Cell Biochem. Funct.* 39. doi: 10.1002/cbf.3582

Liang, X. H., Jackson, S., Seaman, M., Brown, K., Kempkes, B., Hibshoosh, H., et al. (1999). Induction of autophagy and inhibition of tumorigenesis by beclin 1. *Nature* 402. doi: 10.1038/45257

Lin, C., and Xu, X. (2017). YAP1-TEAD1-Glut1 axis dictates the oncogenic phenotypes of breast cancer cells by modulating glycolysis. *Biomedicine Pharmacotherapy* 95. doi: 10.1016/j.biopha.2017.08.091

Lin, J., Xu, Z., Xie, J., Deng, X., Jiang, L., Chen, H., et al. (2021). Oncogene APOL1 promotes proliferation and inhibits apoptosis via activating NOTCH1 signaling pathway in pancreatic cancer. *Cell Death Dis.* 12. doi: 10.1038/s41419-021-03985-1

Lina, T. T., Dunphy, P. S., Luo, T., and McBride, J. W. (2016). Ehrlichia chaffeensis TRP120 activates canonical notch signaling to downregulate TLR2/4 expression and promote intracellular survival. *mBio* 7. doi: 10.1128/mBio.00672-16

Lina, T. T., Luo, T., Velayutham, T. S., Das, S., and McBridea, J. W. (2017). Ehrlichia activation of Wnt-PI3K-mTOR signaling inhibits autolysosome generation and autophagic destruction by the mononuclear phagocyte. *Infect. Immun.* 85. doi: 10.1128/IAI.00690-17

Liu, T., Kishton, R. J., Macintyre, A. N., Gerriets, V. A., Xiang, H., Liu, X., et al. (2014). Glucose transporter 1-mediated glucose uptake is limiting for B-cell acute lymphoblastic leukemia anabolic metabolism and resistance to apoptosis. *Cell Death Dis.* 5. doi: 10.1038/cddis.2014.431

Liu, D., Li, Q., Zang, Y., Li, X., Li, Z., Zhang, P., et al. (2023a). USP1 modulates hepatocellular carcinoma progression via the Hippo/TAZ axis. *Cell Death Dis.* 14. doi: 10.1038/s41419-023-05777-1

Liu, Q., Liu, X., and Song, G. (2021). The hippo pathway: A master regulatory network important in cancer. *Cells* 10. doi: 10.3390/cells10061416

Liu, X., Xu, M., Jia, W., Duan, Y., Ma, J., and Tai, W. (2023b). PU.1 negatively regulates tumorigenesis in non-small-cell lung cancer. *Med. Oncol.* 40. doi: 10.1007/s12032-023-01946-6

Liu, T., Zhou, L., Yang, K., Iwasawa, K., Kadekaro, A. L., Takebe, T., et al. (2019). The β-catenin/YAP signaling axis is a key regulator of melanoma-associated fibroblasts. *Signal Transduct Target Ther.* 4. doi: 10.1038/s41392-019-0100-7

Liu-Chittenden, Y., Huang, B., Shim, J. S., Chen, Q., Lee, S. J., Anders, R. A., et al. (2012). Genetic and pharmacological disruption of the TEAD-YAP complex suppresses the oncogenic activity of YAP. *Genes Dev.* 26. doi: 10.1101/gad.192856.112

Luo, J., Deng, L., Zou, H., Guo, Y., Tong, T., Huang, M., et al. (2023). New insights into the ambivalent role of YAP/TAZ in human cancers. *J. Exp. Clin. Cancer Res.* 42. doi: 10.1186/s13046-023-02704-2

Luo, T., Dunphy, P. S., Lina, T. T., and McBride, J. W. (2016). Ehrlichia chaffeensis exploits canonical and noncanonical host Wnt signaling pathways to stimulate phagocytosis and promote intracellular survival. *Infect. Immun.* 84. doi: 10.1128/IAI.01289-15

Ma, S., Wu, Z., Yang, F., Zhang, J., Johnson, R. L., Rosenfeld, M. G., et al. (2021). Hippo signalling maintains ER expression and ER+ breast cancer growth. *Nature* 591. doi: 10.1038/s41586-020-03131-5

Messina, B., Lo Sardo, F., Scalera, S., Memeo, L., Colarossi, C., Mare, M., et al. (2023). Hippo pathway dysregulation in gastric cancer: from Helicobacter pylori infection to tumor promotion and progression. *Cell Death Dis.* 14. doi: 10.1038/s41419-023-05568-8

Misra, J. R., and Irvine, K. D. (2018). The hippo signaling network and its biological functions. *Annu. Rev. Genet.* 52. doi: 10.1146/annurev-genet-120417-031621

Mukherjee, T., and Balaji, K. N. (2019). The WNT framework in shaping immune cell responses during bacterial infections. *Front. Immunol.* 10. doi: 10.3389/fimmu.2019.01985

Neduva, V., and Russell, R. B. (2005). Linear motifs: Evolutionary interaction switches. *FEBS Lett.* 579. doi: 10.1016/j.febslet.2005.04.005

Ni, P., Yu, M., Zhang, R., He, M., Wang, H., Chen, S., et al. (2020). Prognostic significance of adam17 for gastric cancer survival: A meta-analysis. *Medicina (Lithuania)* 56. doi: 10.3390/medicina56070322

Noorbakhsh, N., Hayatmoghadam, B., Jamali, M., Golmohammadi, M., and Kavianpour, M. (2021). The Hippo signaling pathway in leukemia: function, interaction, and carcinogenesis. *Cancer Cell Int.* 21. doi: 10.1186/s12935-021-02408-7

Paddock, C. D., and Childs, J. E. (2003). Ehrlichia chaffeensis: a prototypical emerging pathogen. *Clin. Microbiol. Rev.* 16. doi: 10.1128/cmr.16.2.355.2003

Palomero, T., Sulis, M. L., Cortina, M., Real, P. J., Barnes, K., Ciofani, M., et al. (2007). Mutational loss of PTEN induces resistance to NOTCH1 inhibition in T-cell leukemia. *Nat. Med.* 13. doi: 10.1038/nm1636

Park, H. W., Kim, Y. C., Yu, B., Moroishi, T., Mo, J. S., Plouffe, S. W., et al. (2015). Alternative wnt signaling activates YAP/TAZ. *Cell* 162. doi: 10.1016/j.cell.2015.07.013

Patterson, L. N. L., Byerly, C. D., Solomon, R., Pittner, N., Bui, D. C., Patel, J., et al. (2023). Ehrlichia Notch signaling induction promotes XIAP stability and inhibits apoptosis. *Infect. Immun.* 91. doi: 10.1128/iai.00002-23

Patterson, L. L., Velayutham, T. S., Byerly, C. D., Bui, D. C., Patel, J., Veljkovic, V., et al. (2022). Ehrlichia SLiM ligand mimetic activates notch signaling in human monocytes. *mBio* 13. doi: 10.1128/mbio.00076-22

Petherick, K. J., Williams, A. C., Lane, J. D., Ordóñez-Morán, P., Huelsken, J., Collard, T. J., et al. (2013). Autolysosomal β-catenin degradation regulates Wnt-autophagy-p62 crosstalk. *EMBO J.* 32. doi: 10.1038/emboj.2013.123

Pha, K., Mirrashidi, K., Sherry, J., Tran, C. J., Herrera, C. M., McMahon, E., et al. (2024). The Chlamydia effector IncE employs two short linear motifs to reprogram host vesicle trafficking. *Cell Rep.* 43, 114624. doi: 10.1016/j.celrep.2024.114624

Pittner, N. A., Solomon, R. N., Bui, D. C., and McBride, J. W. (2023). Ehrlichia effector SLiM-icry: Artifice of cellular subversion. *Front. Cell Infect. Microbiol.* 13. doi: 10.3389/fcimb.2023.1150758

Po, A., Silvano, M., Miele, E., Capalbo, C., Eramo, A., Salvati, V., et al. (2017). Noncanonical GLI1 signaling promotes stemness features and *in vivo* growth in lung adenocarcinoma. *Oncogene* 36. doi: 10.1038/onc.2017.91

Quinn, H. M., Vogel, R., Popp, O., Mertins, P., Lan, L., Messerschmidt, C., et al. (2021). YAP and β;-Catenin cooperate to drive oncogenesis in basal breast cancer. *Cancer Res.* 81. doi: 10.1158/0008-5472.CAN-20-2801

Rogan, M. R., Patterson, L. L., Byerly, C. D., Luo, T., Paessler, S., Veljkovic, V., et al. (2021). Ehrlichia chaffeensis TRP120 is a wnt ligand mimetic that interacts with wnt receptors and contains a novel repetitive short linear motif that activates wnt signaling. *mSphere* 6. doi: 10.1128/msphere.00216-21

Rogan, M. R., Patterson, L. L., Wang, J. Y., and McBride, J. W. (2019). Bacterial manipulation of wnt signaling: A host-pathogen tug-of-wnt. *Front. Immunol.* 10. doi: 10.3389/fimmu.2019.02390

Rosenbluh, J., Nijhawan, D., Cox, A. G., Li, X., Neal, J. T., Schafer, E. J., et al. (2012). [amp]]beta;-Catenin-driven cancers require a YAP1 transcriptional complex for survival and tumorigenesis. *Cell* 151. doi: 10.1016/j.cell.2012.11.026

Sanchez-Martin, M., and Ferrando, A. (2017). The NOTCH1-MYC highway toward T-cell acute lymphoblastic leukemia. *Blood* 129. doi: 10.1182/blood-2016-09-692582

Sari, I. N., Phi, L. T. H., Jun, N., Wijaya, Y. T., Lee, S., and Kwon, H. Y. (2018). Hedgehog signaling in cancer: A prospective therapeutic target for eradicating cancer stem cells. *Cells* 7. doi: 10.3390/cells7110208

Semaan, A., Munkarah, A. R., Arabi, H., Bandyopadhyay, S., Seward, S., Kumar, S., et al. (2011). Expression of GLUT-1 in epithelial ovarian carcinoma: Correlation with tumor cell proliferation, angiogenesis, survival and ability to predict optimal cytoreduction. *Gynecol Oncol.* 121. doi: 10.1016/j.ygyno.2010.11.019

Sharma, U., Tuli, H. S., Uttam, V., Choudhary, R., Sharma, B., Sharma, U., et al. (2022). Role of Hedgehog and Hippo signaling pathways in cancer: A special focus on non-coding RNAs. *Pharmacol. Res.* 186. doi: 10.1016/j.phrs.2022.106523

Shi, X., Wei, S., Simms, K. J., Cumpston, D. N., Ewing, T. J., and Zhang, P. (2018). Sonic hedgehog signaling regulates hematopoietic stem/progenitor cell activation during the granulopoietic response to systemic bacterial infection. *Front. Immunol.* 9. doi: 10.3389/fimmu.2018.00349

Silva-García, O., Valdez-Alarcón, J. J., and Baizabal-Aguirre, V. M. (2014). The Wnt/β -catenin signaling pathway controls the inflammatory response in infections caused by pathogenic bacteria. *Mediators Inflammation* 2014. doi: 10.1155/2014/310183

Simonetti, L., Nilsson, J., McInerney, G., Ivarsson, Y., and Davey, N. E. (2023). SLiM-binding pockets: an attractive target for broad-spectrum antivirals. *Trends Biochem. Sci.* 48. doi: 10.1016/j.tibs.2022.12.004

Smelkinson, M. G. (2017). The Hedgehog signaling pathway emerges as a pathogenic target. *J. Dev. Biol.* 5. doi: 10.3390/jdb5040014

Smelkinson, M. G., Guichard, A., Teijaro, J. R., Malur, M., Loureiro, M. E., Jain, P., et al. (2017). Influenza NS1 directly modulates Hedgehog signaling during infection. *PloS Pathog.* 13. doi: 10.1371/journal.ppat.1006588

Smith, A. E., Sigurbjörnsdóttir, E. S., Steingrímsson, E., and Sigurbjörnsdóttir, S. (2022). Hedgehog signalling in bone and osteoarthritis: the role of Smoothened and cholesterol. *FEBS J.* doi: 10.1111/febs.16440

Sologova, S. S., Zavadskiy, S. P., Mokhosoev, I. M., and Moldogazieva, N. T. (2022). Short linear motifs orchestrate functioning of human proteins during embryonic development, redox regulation, and cancer. *Metabolites* 12. doi: 10.3390/metabo12050464

Song, Y., Chen, X., Huang, R., and Liu, J. (2022). Dysregulated YAP1/hippo pathway contributes to doxorubicin (ADM) resistance in acute myeloid leukemia (AML). *Curr. Pharm. Biotechnol.* 24. doi: 10.2174/1389201023666220617150346

Stein, A., and Aloy, P. (2008). Contextual specificity in peptide-mediated protein interactions. *PloS One* 3. doi: 10.1371/journal.pone.0002524

Stylianou, S., Clarke, R. B., and Brennan, K. (2006). Aberrant activation of Notch signaling in human breast cancer. *Cancer Res.* 66. doi: 10.1158/0008-5472.CAN-05-3054

Sun, Y., Wang, Z., Na, L., Dong, D., Wang, W., and Zhao, C. (2020). FZD5 contributes to TNBC proliferation, DNA damage repair and stemness. *Cell Death Dis.* 11. doi: 10.1038/s41419-020-03282-3

Taciak, B., Pruszynska, I., Kiraga, L., Bialasek, M., and Krol, M. (2018). Wnt signaling pathway in development and cancer. *J. Physiol. Pharmacol.* 69. doi: 10.26402/JPP.2018.2.07

Tai, D., Wells, K., Arcaroli, J., Vanderbilt, C., Aisner, D. L., Messersmith, W. A., et al. (2015). Targeting the WNT signaling pathway in cancer therapeutics. *Oncologist* 20. doi: 10.1634/theoncologist.2015-0057

Tao, J., Calvisi, D. F., Ranganathan, S., Cigliano, A., Zhou, L., Singh, S., et al. (2014). Activation of β-catenin and Yap1 in human hepatoblastoma and induction of hepatocarcinogenesis in mice. *Gastroenterology* 147. doi: 10.1053/j.gastro.2014.05.004

Thompson, B. J., Buonamici, S., Sulis, M. L., Palomero, T., Vilimas, T., Basso, G., et al. (2007). The SCFFBW7 ubiquitin ligase complex as a tumor suppressor in T cell leukemia. *J. Exp. Med.* 204. doi: 10.1084/jem.20070872

Tompa, P. (2011). Unstructural biology coming of age. *Curr. Opin. Struct. Biol.* 21. doi: 10.1016/j.sbi.2011.03.012

Tompa, P. (2012). Intrinsically disordered proteins: A 10-year recap. *Trends Biochem. Sci.* 37. doi: 10.1016/j.tibs.2012.08.004

Trisciuoglio, D., Tupone, M. G., Desideri, M., Di Martile, M., Gabellini, C., Buglioni, S., et al. (2017). BCL-XL overexpression promotes tumor progression-associated properties article. *Cell Death Dis.* 8. doi: 10.1038/s41419-017-0055-y

Uyar, B., Weatheritt, R. J., Dinkel, H., Davey, N. E., and Gibson, T. J. (2014). Proteome-wide analysis of human disease mutations in short linear motifs: Neglected players in cancer? *Mol. Biosyst.* 10. doi: 10.1039/c4mb00290c

Van Roey, K., Uyar, B., Weatheritt, R. J., Dinkel, H., Seiler, M., Budd, A., et al. (2014). Short linear motifs: Ubiquitous and functionally diverse protein interaction modules directing cell regulation. *Chem. Rev.* 114. doi: 10.1021/cr400585q

Veenstra, V. L., Dingjan, I., Waasdorp, C., Damhofer, H., van der Wal, A. C., van Laarhoven, H. W., et al. (2018). Patched-2 functions to limit Patched-1 deficient skin cancer growth. *Cell. Oncol.* 41. doi: 10.1007/s13402-018-0381-9

Vitari, A. C., Leong, K. G., Newton, K., Yee, C., Oǧrourke, K., Liu, J., et al. (2011). COP1 is a tumour suppressor that causes degradation of ETS transcription factors. *Nature* 474. doi: 10.1038/nature10005

Wang, M., Dai, M., Wang, D., Xiong, W., Zeng, Z., and Guo, C. (2021). The regulatory networks of the Hippo signaling pathway in cancer development. *J. Cancer* 12. doi: 10.7150/jca.62402

Wang, J. Y., Zhu, B., Patterson, L. N. L., Rogan, M. R., Kibler, C. E., and McBride, J. W. (2020). Ehrlichia chaffeensis TRP120-mediated ubiquitination and proteasomal degradation of tumor suppressor FBW7 increases oncoprotein stability and promotes infection. *PloS Pathog.* 16. doi: 10.1371/journal.ppat.1008541

Warren, C. F. A., Wong-Brown, M. W., and Bowden, N. A. (2019). BCL-2 family isoforms in apoptosis and cancer. *Cell Death Dis.* 10. doi: 10.1038/s41419-019-1407-6

Wei, C., and Li, X. (2020). Verteporfin inhibits cell proliferation and induces apoptosis in different subtypes of breast cancer cell lines without light activation. *BMC Cancer* 20. doi: 10.1186/s12885-020-07555-0

Wincewicz, A., Sulkowska, M., Koda, M., Kanczuga-Koda, L., Witkowska, E., and Sulkowski, S. (2007). Significant coexpression of GLUT-1, Bcl-xL, and Bax in colorectal cancer. *Ann. New York Acad. Sci.* doi: 10.1196/annals.1397.007

Wu, H., Liu, Y., Liao, Z., Mo, J., Zhang, Q., Zhang, B., et al. (2022). The role of YAP1 in liver cancer stem cells: proven and potential mechanisms. *biomark. Res.* 10. doi: 10.1186/s40364-022-00387-z

Xiao, Y., and Dong, J. (2021). The hippo signaling pathway in cancer: A cell cycle perspective. *Cancers (Basel)* 13. doi: 10.3390/cancers13246214

Xu, S., Zhang, H., Chong, Y., Guan, B., and Guo, P. (2019). YAP promotes VEGFA expression and tumor angiogenesis though gli2 in human renal cell carcinoma. *Arch. Med. Res.* 50. doi: 10.1016/j.arcmed.2019.08.010

Yang, Y., Gan, X., Zhang, W., Zhu, B., Huangfu, Z., Shi, X., et al. (2024). Research progress of Hippo signaling pathway in renal cell carcinoma. *Asian J. Urol.* doi: 10.1016/j.ajur.2024.02.005

Yu, F. X., Zhao, B., Panupinthu, N., Jewell, J. L., Lian, I., Wang, L. H., et al. (2012). Regulation of the Hippo-YAP pathway by G-protein-coupled receptor signaling. *Cell* 150. doi: 10.1016/j.cell.2012.06.037

Zhang, W., Gao, Y., Li, F., Tong, X., Ren, Y., Han, X., et al. (2015). YAP promotes Malignant progression of Lkb1-deficient lung adenocarcinoma through downstream regulation of survivin. *Cancer Res.* 75. doi: 10.1158/0008-5472.CAN-14-3396

Zhang, L., and Shay, J. W. (2017). Multiple roles of APC and its therapeutic implications in colorectal cancer. *J. Natl. Cancer Inst* 109. doi: 10.1093/jnci/djw332

Zhang, Y., Wang, X., and Zhou, X. (2022). Functions of Yes-association protein (YAP) in cancer progression and anticancer therapy resistance. *Brain Sci. Adv.* 8. doi: 10.26599/bsa.2022.9050008

Zheng, Y., and Pan, D. (2019). The hippo signaling pathway in development and disease. *Dev. Cell* 50. doi: 10.1016/j.devcel.2019.06.003

Zhou, Y., Huang, J., Jin, B., He, S., Dang, Y., Zhao, T., et al. (2022b). The emerging role of hedgehog signaling in viral infections. *Front. Microbiol.* 13. doi: 10.3389/fmicb.2022.870316

Zhou, B., Lin, W., Long, Y., Yang, Y., Zhang, H., Wu, K., et al. (2022a). Notch signaling pathway: architecture, disease, and therapeutics. *Signal Transduct Target Ther.* 7. doi: 10.1038/s41392-022-00934-y

Zhu, B., Kuriakose, J. A., Luo, T., Ballesteros, E., Gupta, S., Fofanov, Y., et al. (2011). Ehrlichia chaffeensis TRP120 binds a G+C-rich motif in host cell DNA and exhibits eukaryotic transcriptional activator function. *Infect. Immun.* 79. doi: 10.1128/IAI.05422-11

frontiers | Frontiers in Cellular and Infection Microbiology

TYPE Original Research
PUBLISHED 18 February 2025
DOI 10.3389/fcimb.2025.1511900

OPEN ACCESS

EDITED BY
Maurizio Sanguinetti,
Catholic University of the Sacred Heart, Italy

REVIEWED BY
Brunella Posteraro,
Catholic University of the Sacred Heart, Italy
Marco Antonio Hernández-Luna,
University of Guanajuato, Mexico

*CORRESPONDENCE
Zhengchen Jiang
medicaljzc@163.com
Bo Zhang
zhangbo1705@zjcc.org.cn
Shi Wang
wangshi@zjcc.org.cn

†These authors have contributed equally to this work

RECEIVED 15 October 2024
ACCEPTED 24 January 2025
PUBLISHED 18 February 2025

CITATION
Liu K, Jiang Z, Ma Y, Xia R, Zheng Y, Yin K, Pang C, Yuan L, Cheng X, Liu Z, Zhang B and Wang S (2025) Multiomics insights into BMI-related intratumoral microbiota in gastric cancer. *Front. Cell. Infect. Microbiol.* 15:1511900. doi: 10.3389/fcimb.2025.1511900

Multiomics insights into BMI-related intratumoral microbiota in gastric cancer

Kang Liu[1†], Zhengchen Jiang[2,3*†], Yubo Ma[1], Ruihong Xia[1], Yingsong Zheng[4], Kailai Yin[4], Chuhong Pang[4], Li Yuan[3,5], Xiangdong Cheng[2,6], Zhuo Liu[2], Bo Zhang[5*] and Shi Wang[7*]

[1]The Second Clinical Medical College of Zhejiang Chinese Medical University, Hangzhou, Zhejiang, China, [2]Department of Gastric Surgery, Zhejiang Cancer Hospital, Hangzhou Institute of Medicine (HIM), Chinese Academy of Sciences, Hangzhou, Zhejiang, China, [3]Zhejiang Key Lab of Prevention, Diagnosis and Therapy of Upper Gastrointestinal Cancer, Zhejiang Cancer Hospital, Hangzhou, Zhejiang, China, [4]Postgraduate training base Alliance of Wenzhou Medical University (Zhejiang Cancer Hospital), Hangzhou, Zhejiang, China, [5]Department of Integrated Chinese and Western Medicine, Zhejiang Cancer Hospital, Hangzhou Institute of Medicine (HIM), Chinese Academy of Sciences, Hangzhou, Zhejiang, China, [6]Zhejiang Provincial Research Center for Upper Gastrointestinal Tract Cancer, Zhejiang Cancer Hospital, Hangzhou, Zhejiang, China, [7]Endoscopy Division, Zhejiang Cancer Hospital, Hangzhou Institute of Medicine (HIM), Chinese Academy of Sciences, Hangzhou, Zhejiang, China

Introduction: Body mass index (BMI) is considered an important factor in tumor prognosis, but its role in gastric cancer (GC) remains controversial. There is a lack of studies exploring the effect of BMI on gastric cancer from the perspective of intratumoral microbiota. This study aimed to compare and analyze the differences in and functions of intratumoral microbiota among GC patients with varying BMIs, aiming to ascertain whether specific microbial features are associated with prognosis in low-BMI (LBMI) gastric cancer patients.

Methods: A retrospective analysis of the clinicopathological features and prognosis of 5567 patients with different BMIs was performed between January 2010 and December 2019. Tumor tissues from 189 GC patients were collected for 16S rRNA sequencing, 64 samples were selected for transcriptome sequencing, and 57 samples were selected for untargeted metabolomic analysis.

Results: Clinical cohort analysis revealed that GC patients with a low BMI presented poorer clinical and pathological characteristics than those with a non-low-BMI (NLBMI). LBMI was identified as a significant independent risk factor for adverse prognosis, potentially exerting immunosuppressive effects on postoperative adjuvant chemotherapy. 16S rRNA sequencing revealed no significant differences in the alpha and beta diversity of the intratumoral microbiota between the two groups of GC patients. However, LEfSe analysis revealed 32 differential intratumoral microbiota between the LBMI and NLBMI groups. Notably, the genus Abiotrophia was significantly enriched in the LBMI group. Further in-depth analysis indicated that the genus Abiotrophia was inversely associated with eosinophils, P2RY12, and SCN4B genes, and positively linked with LGR6 in LBMI gastric cancer patients. Metabolomic assessments revealed that LBMI was positively associated with purine metabolites, specifically guanine and inosine diphosphate (IDP).

Discussion: In conclusion, LBMI is an independent risk factor for poor prognosis in gastric cancer patients and may have an inhibitory effect on postoperative adjuvant chemotherapy. Intratumor flora of gastric cancer patients with different BMI levels differed, with different immune cell infiltration and metabolic characteristics. The genus Abiotrophia may promote gastric cancer development and progression by regulating eosinophils and the purine metabolism pathway, which provides a new idea for the precise treatment of gastric cancer.

KEYWORDS

GC, BMI, intratumoral microbiota, immune cells, metabolome

Introduction

Gastric cancer (GC) is the fifth most common malignancy globally and the fifth leading cause of cancer-related deaths (Bray et al., 2024). Over the past two decades, the 5-year survival rate of patients with GC has significantly improved due to various factors such as early detection, improvement in surgical techniques, improvement in nutritional care, and widespread use of systemic chemotherapy and immune-targeted therapy (Ahn et al., 2011). However, in China, most GC patients are diagnosed at an advanced or even late stage, with a higher proportion of patients experiencing significant weight loss and worse prognosis (Li et al., 2022).

BMI is a measure of body weight. It is an important prognostic factor for various tumors, such as colorectal cancer, breast cancer, and pancreatic cancer (Chen et al., 2024). However, its role in regulating the prognosis of patients with tumors including those with GC, is still controversial (Schooling et al., 2015; Feng et al., 2018; Ma et al., 2021; Zhao et al., 2021). Ma et al. (2021) demonstrated that GC patients with LBMI had a poor long-term prognosis, while Feng et al. (2018) found that GC patients with a high BMI had a better long-term prognosis. Interestingly, Schooling et al. (2015) found that obese patients had a high risk of death and poor prognosis. However, Zhao et al. (2021) showed no association between BMI and GC prognosis.

Previous studies have shown that intratumoral microbiota may contribute to tumorigenesis and progression and impact prognosis by inducing genomic instability and mutations affecting epigenetic modifications, promoting inflammatory responses, averting immune destruction, regulating metabolism, and activating invasion and metastasis (Wang et al., 2023; Cao et al., 2024; Liu et al., 2024). For example, *Fusobacterium nucleatum* is more abundant in various tumors such as colorectal cancer(CRC), oral cancer, and gastric cancers and affects long-term prognosis (Mitsuhashi et al., 2015; Mima et al., 2016; Hsieh et al., 2022), A novel virulence protein of *Fusobacterium nucleatum*, Fn-Dps, has been found to promote invasion and metastasis of CRC cells by inducing EMT through upregulation of the chemokine CCL2/CCL7 (Mima et al., 2016). Interestingly, two recent studies have demonstrated the heterogeneity of microorganisms at different BMI states (Huang et al., 2024; Li et al., 2024). In one of them, Huang et al (Huang et al., 2024). Similarly, in their study of CRC patients with different BMIs states similarly found the same significant enrichment at the portal level was detected in hyper-reorganized CRC patients, with significant enrichment of *Actinobacteria* spp,*Desulfovibrio* spp, and *Mycobacterium* spp at the genus level. Another study found that Peptostreptococcus stomatis was elevated in obese patients and that there were differential changes in metabolites between the two BMI groups, particularly in fatty acid and phospholipid dysregulation (Li et al., 2024). A study on intratumoral microbiota and GC revealed that *Methylobacterium tumefaciens* was significantly associated with poor prognosis in gastric cancer patients and was negatively correlated with CD8+ tissue-resident memory T (TRM) cells and TGF-β in the tumor immune microenvironment (TIME).Experimental methods verified that *Methylobacterium* could reduce TGF-β expression and the number of $CD8^+$ TRM cells in tumors. These findings suggest that intratumoral microbiota may regulate the development of GC by influencing the tumor immune microenvironment (Peng et al., 2022).

Therefore, intratumoral microbiota have attracted increasing attention as influencing factors of the TIME. However, few studies have been conducted on GC, especially on LBMI GC patients with associated immunosuppression or intolerance (Indini et al., 2021). Therefore, in this study, we performed a multiomics analysis based on intratumoral microbiotas combined with transcriptomics and metabolomics to analyze intratumoral microbes and their functions in GC patients with different BMIs to understand the characteristics of the differential intratumoral microbes of LBMI GC patients, i.e., the mechanism of potential modulation of GC, and to provide a new solution for the precision treatment of GC.

Abbreviations: 16S rRNA-seq, 16S ribosomal RNA sequencing; BMI, Body mass index; GC, gastric cancer; CRC, colorectal cancer; APCs, antigen-presenting cells; TIME, tumor immune microenvironment; DEGs, differentially expressed genes; KEGG, kyoto encyclopedia of genes and genomes; GO, Gene Ontology; PCoA, principal coordinates analysis; PC, Polymerase Chain Reaction; QC, Quality control; PSM, Propensity score matching; RNA-seq, RNA sequencing; TRM, tissue-resident memory T; TIME, tumor immune microenvironment; TNM, tumor-node-metastasis; COX, Cox regression model; OS, overall survival.

Material and methods

Clinical cohort data collection and definitions

A retrospective analysis was conducted on 7,192 patients who underwent gastrectomy at Zhejiang Cancer Hospital from January 2010 to December 2019. Among them, 5,567 patients met the following inclusion criteria: 1.Preoperative pathological biopsy confirmed primary gastric cancer; 2.Underwent radical or palliative gastrectomy; 3.No concomitant severe diseases such as acute cardiovascular and cerebrovascular diseases, liver cirrhosis, and chronic renal failure. Exclusion criteria: 1.Received neoadjuvant treatments such as preoperative radiotherapy, chemotherapy, or immunotherapy; 2.Number of dissected lymph nodes<16; 3.Presence of other heterogeneous tumors; 4.Other types of gastric cancer (e.g.,neuroendocrine carcinoma, squamous cell carcinoma, adenosquamous carcinoma); 5.Patients with missing critical clinical data. The median follow-up time was 85 months (interquartile range:71 months). All eligible patients underwent radical gastrectomy according to the Japanese gastric cancer treatment guidelines (Association JGC, 2020). Surgical methods included proximal, total, and distal gastrectomy. Postoperatively, specimens were reviewed by pathology experts at the Cancer Hospital of the Chinese Academy of Sciences. Pathological tumor-lymph node metastasis (pTNM) staging was based on the 8th edition of the American Joint Committee on Cancer (AJCC) TNM staging system (Amin et al., 2017). Potential curative resection was defined as R0 resection. Survival time was calculated from the date of surgery to the date of GC-related death or the most recent follow-up. The follow-up cut-off date was August 1, 2023. Perioperative management followed routine procedures, with no differences between groups. Patients meeting the above criteria were divided into two groups according to the Preoperative BMI standards set by WHO: the low BMI group (BMI<18.5 kg/m^2) and the non-low BMI group (BMI≥18.5 kg/m^2). Various clinicopathological characteristics, surgery-related indicators, and postoperative outcome factors were collected for analysis, including gender, height, and weight. BMI was calculated based on the patients' height and weight. Tumor location was classified according to the center of the lesion as Upper 1/3 (cardia, fundus), Middle 1/3 (body), Lower 1/3 (antrum, including the angular incisure and pylorus), or involving the entire stomach (Total) (tumor involving more than 2/3 of the stomach wall). Tumor size was determined by the maximum diameter of the tumor. The positive levels of tumor markers were defined as CA199 ≥ 37 U/ml and CEA ≥ 5 ng/ml.

Clinical specimen collection and preparation

Samples were collected from 335 patients between January 2013 and December 2018 from Zhejiang Cancer Hospital. After screening according to the above clinical cohort criteria and ensuring that no antibiotics or intestinal microecological agents had been used in the previous month, 198 eligible GC patients were included in the final analysis. All patients were followed up by telephone and outpatient clinics with a follow-up cut-off date of 1 August 2023.The study was conducted by the Zhejiang Cancer Hospital (ZCH). The study was approved by the Ethics Committee of Zhejiang Cancer Hospital (approval number: IRB-2023-791) and written informed consent was obtained from all participants. Gastric samples were collected from patients who underwent gastrectomy, with peritumoral tissue 2-5 cm from the tumor margin. Notably, for metabolomics analysis, tissue specimens were subjected to cold ischemia for less than 30 minutes before freezing at -80 degrees Celsius. For 16S rRNA sequencing and transcriptome analyses, tissue specimens were immersed in an RNA-protecting solution at 4°C overnight, and then frozen at -80°C. Specimens for each histology were collected simultaneously. All tissue samples were collected at the time of surgical specimen removal. Histological sections at the top and bottom of each specimen were reviewed by a senior board-certified pathologist to confirm whether the tissue was tumor tissue or adjacent non-tumor tissue. For the purposes of this study, tumor samples had to have an average of 60% tumor cell nuclei and less than 20% necrosis to qualify.

16S rRNA sequencing

Microbial DNA was extracted using an E.Z.N.A. Tissue DNA Kit (D3396-01; Omega, Norcross, Georgia, USA) following the manufacturer's instructions as described previously. The DNAs were quantified using a Qubit 2.0 Fluorometer (Invitrogen, Carlsbad, CA, USA), and molecular size was estimated using agarose gel electrophoresis. Primers targeting the hypervariable V3-V4 region of the 16S rRNA gene were used to amplify the extracted DNA samples. The forward primer was 5'-CCTACGGGNGGCWGCAG-3' and the reverse primer was 5'-GACTACHVGGGTATCTAATCC-3'. AxyPrep PCR Clean-up Kit (AP-PCR-500G; Corning, NY, USA) was used to separate, extract and purify the PCR products, and the products were quantified using a Quant-iT PicoGreen dsDNA Reagent (P7581, Thermo Scientific, Waltham, MA, USA). After quality determination, libraries passing quality control were sequenced with Novaseq sequencer for 2 x Two terminal sequencing of 250 bp at LC-Bio Co., Ltd.

Species annotation of the colonies was performed using the Greengene database v13.8, and then the ASV/OUT data of the colonies were extracted using the phyloseq package v1.26.1. We used the α-diversity index to characterize the diversity of the flora, where Shannon and Simpson indices were used to characterize species richness, homogeneity, and concentration reflecting species diversity, respectively. Beta diversity was calculated based on weighted Unifrac distances, and principal coordinate analysis (PCoA) was used in order to assess differences in microbial community composition. Linear discriminant analysis (LDA) was performed using the Mann-Whitney U test, and linear discriminant analysis effect size (LEfSe) analysis was performed using lefse software v1.0.0 to screen for species most likely to explain

differences between groups, while LDA scores were used to assess effect sizes for species with significant differences between groups, with |LDA |> 2 and P < 0.05 as the thresholds of difference to screen for differences between species, and ggplot 2 software was used to assess differences in the composition of microbial communities. The results were also analyzed as bar graphs using the ggplot 2 software package v3.4.0. The results were presented as bar graphs. The α-diversity, β-diversity indices between the two groups were compared using Mann-Whitney U rank sum test through vegan software package v2.5.6. All the above analyses were carried out in R software v4.3.1, and the above P-values were two-tailed tests, and differences were considered statistically significant when P<0.05.

Transcriptome sequencing

Paired tumor tissues from 108 GCs were subjected to mRNA sequencing (RNA-seq).In the end, 64 samples met the screening criteria. Total RNA was isolated from tumor tissues and NATs using TRIzol reagent (Invitrogen, Carlsbad, CA, USA) in an RNA protection solution. the amount and purity of RNA from each sample was quantified using a NanoDrop ND-1000 (NanoDrop, Wilmington, DE, USA). RNA integrity was assessed using an Agilent 2100 with a RIN>7.0. For mRNA sequencing, libraries were prepared on 1 μg of DNase I-treated total RNA using the TruSeq kit (Illumina) and processed for 150 bpb on the Illumina HiSeq X Ten instrument at LC-Bio Technology Co. (Hangzhou, China) on an Illumina HiSeq X Ten instrument with 150-bp paired-end sequencing. (Hangzhou, China) performed 150-bp paired-end sequencing on an Illumina HiSeq X Ten machine according to the protocol recommended by the vendor.

We aligned reads of all samples to the < research species > reference genome using HISAT2 (https://daehwankimlab.github.io/hisat2/, version:hisat2-2.0.4) package, which initially remove a portion of the reads based on quality information accompanying each read and then maps the reads to the reference genome. HISAT2 allows multiple alignments per read (up to 20 by default) and a maximum of two mismatch when mapping the reads to the reference. HISAT2 build a database of potential splice junctions and confirms these by comparing the previously unmapped reads against the database of putative junctions. The mapped reads of each sample were assembled using StringTie (http://ccb.jhu.edu/software/stringtie/, version:stringtie- 1.3.4d) with default parameters. Then, all transcriptomes from all samples were merged to reconstruct a comprehensive transcriptome using gffcompare software (http://ccb.jhu.edu/software/stringtie/gffcompare.shtml, version: gffcompare-0.9.8). After the final transcriptome was generated, StringTie and ballgown (http://www.bioconductor.org/packages/release/bioc/html/ballgown.html) were used to estimate the expression levels of all transcripts and perform expression abundance for mRNAs by calculating FPKM (fragment per kilobase of transcript per million mapped reads) value.

Differentially expressed genes (DEGs) were screened by DESeq261. genes with P< 0.05 and FC ≥ 2 or FC ≤ 0.5 were considered statistically significant DEGs. enriched functional pathways and modules were analyzed by using KEGG and CO databases. The Mann-Whitney U test was used to compare differences between groups.

GC tumor immune microenvironment analysis

CIBERSORT is a computational method for analyzing the composition of immune cells from RNA sequencing data based on the expression profiles of immune cell-specific genes and uses machine learning algorithms to analyze and classify the expression patterns of these genes. We use the CIBERSORT R-script v1.03 to construct a support vector regression-based model using the known expression data of the reference genes and to-be-estimated gene expression data of the mixed samples, constructed the optimization problem by the correlation matrix consisting of the cellular composition, and solved it in the form of a sparse solution. Thus, the cellular composition ratio of the mixed samples is estimated. The FPKM matrix obtained by transcriptome sequencing was transformed into a matrix of relative content of 22 different types and functional states of immune cells. The flora matrix was combined with the immune cell abundance matrix and the correlation coefficients between the columns in the combined matrix were calculated by calling the rcorr function. The type of correlation coefficient was Spearman's correlation coefficient.

Metabolome assays

The samples were taken out of the -80°C freezer and thawed on ice, and metabolite were extracted with 80% methanol buffer. Briefly, 50 mg of sample was extracted with 0.5 ml of precooled 80% methanol. The extraction mixture was then stored in 30 min at -20°C. After centrifugation at 20,000 g for 15 min, the supernatants were transferred into new tube to and vacuum dried. The samples were redissolved with 100 μL 80% methanol and stored at -80°C prior to the LC-MS analysis. In addition, pooled QC samples were also prepared by combining 10 μL of each extraction mixture. The extracted samples were then sorted for machine analysis with randomization. QC samples were inserted before, in the middle, and after the samples to evaluate experimental technical replicates. The samples underwent mass spectrometry positive and negative ion scans. All samples were acquired by the LC-MS system followed machine orders. Firstly, all chromatographic separations were performed using an UltiMate 3000 UPLC System (Thermo Fisher Scientific, Bremen, Germany). An ACQUITY UPLC T3 column (100mm×2.1mm,1.8μm, Waters, Milford, USA) was used for the reversed phase separation. The column oven was maintained at 40° C. A high-resolution tandem mass spectrometer TripleTOF 6600 (SCIEX, Framingham, MA, USA) was used to detect metabolites eluted form the column. The Q-TOF was operated in both positive and negative ion modes. The curtain gas was set 30 PSl,lon source gas1 was set 60 PSI,lon source gas2 was set 60 PSI, and an interface heater temperature was 500°C. For positive ion mode, the lonspray voltage floating were set at 5000 V, respectively. For negative ion

mode, the lonspray voltage floating were set at -4500V, respectively. The mass spectrometry data were acquired in IDA mode. The TOF mass range was from 60 to 1200 Da. The survey scans were acquired in 150 ms and as many as 12 production scans were collected if exceeding a threshold of 100 counts per second (counts/s) and with a 1^+charge-state. Dynamic exclusion was set for 4s. During the acquisition, the mass accuracy was calibrated every 20 samples. Furthermore, in order to evaluate the stability of the LC-MS during the whole acquisition, a quality control sample (Pool of all samples) was acquired after every 10 samples.

The raw data from mass spectrometry were converted into readable data mzXML format using Proteowizard's MSConvert software. XCMS software was utilized for peak extraction, and peak extraction quality control was conducted. Subsequently, substances extracted were annotated using CAMERA for adduct and ion annotation, followed by primary identification using the metaX software. Identification was performed separately using the mass spectrometry first-level information and matching the mass spectrometry second-level information with an in-house standard compound database. Differential metabolites were identified by Mann-Whitney U test and partial least squares discriminant analysis (PLS-DA).Metabolites with variable importance in projection (VIP) > 1 and $p < 0.05$ and FC ≥ 2 or FC ≤ 0.5 were considered differential metabolites. The functions of these metabolites and metabolic pathways were analyzed using the KEGG database.

Statistical method

Continuous variables with normal distribution are expressed as mean ± standard deviation (x ± s) or Mean ± SD and analyzed using t-test or Mann-Whitney U test. Categorical variables are presented as counts (n, %) and analyzed using Chi-square test or Fisher's exact test. Propensity score matching (PSM) was used to account for differences in patient backgrounds, with a 1:4 ratio set to minimize selection bias between the two groups. Survival rates were calculated using the Kaplan-Meier method and survival curves were compared using the log-rank test. A Cox proportional hazards model with forward stepwise regression was employed to identify independent prognostic factors. Spearman correlation was used for the joint analysis of microbiome with transcriptome and metabolome. All data were analyzed using SPSS software version 26.0 (IBM USA), the Medsta statistical platform (www.medsta.cn/software), OmicStudio tools (https://www.omicstudio.cn/tool), and R version 4.3.1. All statistical tests were two-sided, and a p-value < 0.05 was considered statistically significant.

Results

LBMI is an independent prognostic risk factor for poor prognosis in patients with GC

In this study, data from 5567 patients who met the criteria and had complete follow-up information were collected from 7192 hospitalized patients with GC (Figure 1A). There were no statistically significant differences between the two groups of BMI patients in terms of smoking history, alcohol consumption history, extent of resection, type of pathology, pM stage or recurrent metastasis (all P > 0.05). Analysis revealed that relative to NLBMI patients, LBMI patients had a smaller percentage of family history of GC; more tumors were located in the lower 1/3 and the whole stomach and less in the upper 1/3, and there was a greater percentage of larger and more poorly differentiated tumors, and a greater percentage of open surgeries (all P < 0.05); the level of pre-CA199 positivity was significantly greater (P=0.039), and the pre-CEA positivity level was similar; and the percentage of nerve invasion was greater (P=0.011), while there was no significant difference in vascular invasion. Moreover, in the LBMI group, the percentage of female patients aged ≥60 years, incidence of complications, deep tumor infiltration, high number of lymph node metastases, late pathological stage and low percentage of receiving postoperative adjuvant chemotherapy were significantly greater than that those in the NLBMI group (P<0.001). (Supplementary Table S1).

Univariate and multivariate COX analysis revealed that LBMI is an independent poor prognostic factor for overall survival (OS) in GC patients (HR=1.28, 95%CI: 1.13-1.45, P<0.001) (Table 1). Kaplan-Meier survival analysis based on BMI classification showed that LBMI patients had worse prognosis compared to NLBMI patients before PSM (5-yr OS: 50.8% vs. 66.2%, P<0.001) (Figure 1B). After adjusting for clinicopathological characteristics that influence prognosis (P<0.05) using PSM (ratio 1:4), the clinical characteristics of the two groups were comparable (P>0.05, Supplementary Table S2). Similarly, LBMI patients had worse prognosis (5-yr OS: 50.8% vs. 60.5%, P<0.001) (Figure 1C). Stratified analysis by TNM stage show no significant difference in OS between the two BMI groups in stage I and IV disease (Figures 1D, G); however, in stage II and III patients, LBMI disease have worse OS compared to NLBMI patients (Figures 1E, F). Subgroup analysis based on receiving postoperative chemotherapy set the PSM ratio to 1:4, and included clinicopathological data that influence prognosis. After PSM, the clinicopathological characteristics of the two BMI groups were comparable (Supplementary Table S3), and LBMI patients had worse OS both before and after PSM (Figures 1H, I).

Intratumoral microbiome landscape in LBMI and NLBMI gastric cancer patients

To evaluate whether there were differences in microbial diversity, abundance, and composition between LBMI and NLBMI gastric cancer patients, we included 189 eligible gastric cancer patients, including 27 in the LBMI cohort and 162 in the NLBMI cohort (Supplementary Figure S1). As shown in Supplementary Table S4, the clinicopathologic data were balanced and comparable between the two cohorts. On the basis of the species sparsity curves (Supplementary Figures S2B, C), we found that the curves of the four groups in both metrics flattened out. The Venn diagram (Supplementary Figure S2A) revealed that there are

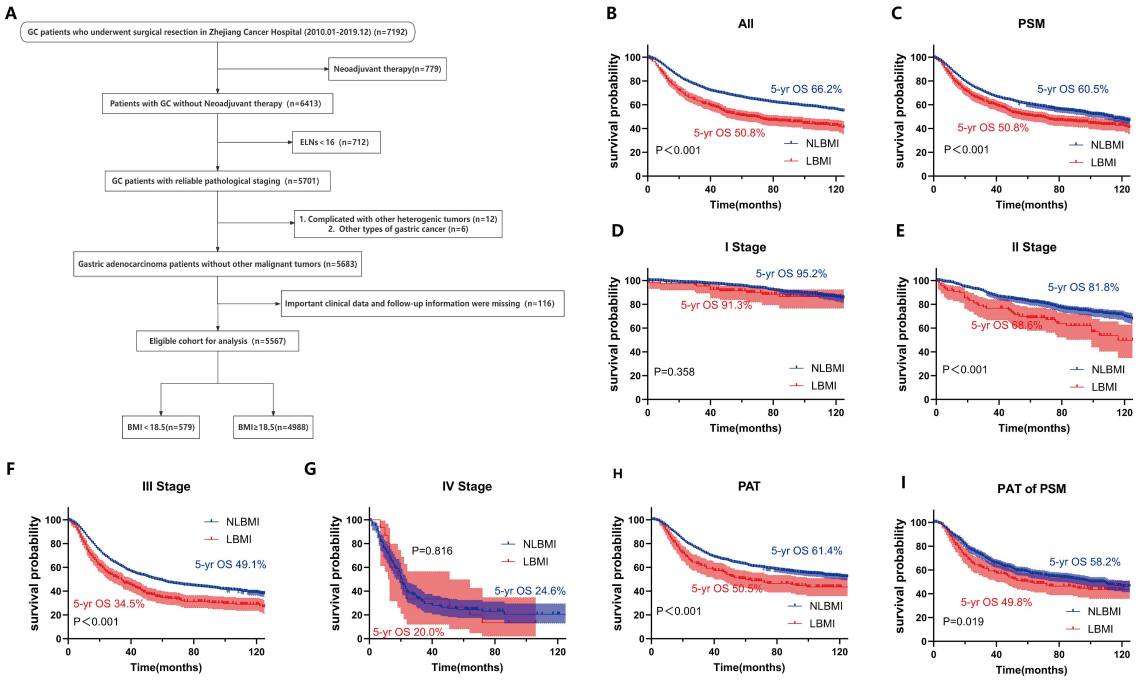

FIGURE 1
LBMI is an independent risk factor for poor prognosis in GC. **(A)** Clinical cohort screening flowchart. Kaplan-Meier survival curve analysis for different cohorts classified by BMI. **(B)** All patients. **(C)** All matched patients. **(D)** Stage I **(E)** Stage II. **(F)** Stage III. **(G)** Stage IV. **(H)** PAT. **(I)** PAT of PSM. BMI, Body Mass Index. ELNs, Number of dissected lymph nodes. PSM, Propensity Score Matching. PAT, Postoperative Adjuvant Therapy. LBMI, Low Body Mass Index (BMI < 18.5). NLBMI, Non-Low Body Mass Index (BMI ≥ 18.5).All P values for survival curves were corrected for multiplicity by the BH method.

many overlaps in the microbial environments among the four groups. The diversity within the cancer tissues was significantly greater in both LBMI and NLBMI carcinomas than in the LBMI and NLBMI paracarcinomas, whereas there was no significant difference between the two cohorts of LBMI and NLBMI cancer tissues (Figures 2A, B). Principal coordinate analysis (PCoA) revealed significant differences in both BMI carcinomas and paracancers in both groups; however, there was no significant difference between LBMI-CT and NLBMI-CT (P=0.855) (Figure 2C). PLS-DA analysis, revealed that the intratumoral microbiome of two groups of BMI carcinomas could be divided into two different clusters (Figure 2D). Regarding species composition, the differences were a smaller between the tumor tissues of different BMI groups, while the differences were a greater between tumor and peritumoral tissues of the same BMI group (Figures 2E, F).

LBMI intratumor *g_Abiotrophia* was significantly elevated

To determine the differentially dominant flora in GC patients with different BMIs, LEfSe analysis was performed (LDA> 2.0, P<0.05), which revealed 59 (Supplementary Figure S3) and 230 (Supplementary Figure S4) differentially dominant flora in the LBMI group and the NLBMI group, respectively, compared with the paracancerous tissues. There were 32 differentially dominant flora in the LBMI-CT group compared with the NLBMI-CT group. At the phylum level only *p_Nitrospinae* dominated the flora in LBMI, whereas at the genus level *g_Lachnoanaerobaculum, g_Brevundimonas* and *g_Stomatobaculum* dominated the flora in the NLBMI group, whereas *g_Acidiphilium,g_Thiobacillus* and *g_Abiotrophia* and 9 other genera were the dominant flora in the LBMI group. At the species level, *s_Knoelia_sp_BA2_2011* and 15 other species were dominant flora in the LBMI group (Figure 3A; Supplementary Figure S5). At the genus level, the abundances of two groups of differentially bacteria, *g_Abiotrophia* and *g_Lachnoanaerobaculum*, significantly differed (Figures 3B-J). Spearman correlation analysis revealed that g_Abiotrophia was positively correlated with *g_Lachnoanaerobaculum* and *g_Stomatobaculum* and that *g_Brevundimonas* was negatively correlated. These findings suggest a possible complementary relationship between the dominant differential flora between the two BMI groups (Supplementary Figure S2D).

LBMI intratumoral *g_Abiotrophia* negatively correlates with P2RY12

RNA sequencing analysis was performed on 64 tumor tissues from both groups, and PCA revealed that there was no significant difference in BMI the between the two groups (P=0.136) (Figure 4A). Compared with NLBMI, 343 genes were significantly upregulated and 320 genes in LBMI were significantly downregulated (Figure 4B). KEGG and GO analyses were performed on the BMI differential

TABLE 1 Single factor and multi-factors Cox analysis risk factor for gastric cancer OS.

Parameters	Univariate	P value	Multivariate	P value
	HR (95%CI)		HR (95%CI)	
Gender(Male vs Female)	1.21 (1.10 ~ 1.34)	<0.001		
Age (≥60years vs<60years)	1.65 (1.51 ~ 1.80)	<0.001	1.37 (1.25 ~ 1.51)	<0.001
BMI(<18.5 vs ≥18.5)	1.60 (1.41 ~ 1.80)	<0.001	1.28 (1.13 ~ 1.45)	<0.001
Family.history	0.91 (0.83 ~ 0.99)	0.041		
Smoking.history	1.06 (0.97 ~ 1.15)	0.171		
Drinking.history	1.03 (0.94 ~ 1.13)	0.531		
Surgery.methods(Laparoscopy vs Open)	0.50 (0.43 - 0.58)	<0.001	0.78 (0.68 - 0.91)	<0.001
Tumor location		<0.001		0.002
Upper1/3	Ref		Ref	
Middle1/3	0.53 (0.46 ~ 0.61)	<0.001	0.88 (0.76 ~ 1.02)	0.097
Lower1/3	0.61 (0.55 ~ 0.67)	<0.001	0.90 (0.82 ~ 0.99)	0.039
Total	2.26 (1.84 ~ 2.77)	<0.001	1.46 (1.18 ~ 1.80)	<0.001
Pathological type		0.042		<0.001
Adenocarcinoma	Ref		Ref	
MGC	0.87 (0.66 ~ 1.13)	0.296	0.62 (0.47 ~ 0.81)	<0.001
SRCC	1.23 (1.05 ~ 1.43)	0.010	1.34 (1.14 ~ 1.57)	<0.001
Differentiation		<0.001		
Poorly	Ref			
Moderately	0.37 (0.23 ~ 0.59)	<0.001		
Well	0.79 (0.70 ~ 0.89)	<0.001		
Vascular.tumor.thrombus	2.45 (2.25 ~ 2.68)	<0.001	1.38 (1.26 ~ 1.52)	<0.001
Nerve.invasion	2.95 (2.68 ~ 3.24)	<0.001	1.42 (1.28 ~ 1.58)	<0.001
Maximum tumor diameter(≥5cm vs <5cm)	2.92 (2.68 ~ 3.18)	<0.001	1.57 (1.43 ~ 1.72)	<0.001
pTNM Satge		<0.001		<0.001
I	Ref		Ref	
II	3.14 (2.53 ~ 3.91)	<0.001	2.23 (1.77 ~ 2.79)	<0.001
III	9.31 (7.72 ~ 11.23)	<0.001	4.90 (3.95 ~ 6.07)	<0.001
IV	18.67 (14.43 ~ 24.15)	<0.001	10.59 (8.00 ~ 14.02)	<0.001
Pre-CEA	1.89 (1.72 ~ 2.08)	<0.001	1.31 (1.19 ~ 1.45)	<0.001
Pre-CA199	2.13 (1.93 ~ 2.34)	<0.001	1.26 (1.14 ~ 1.39)	<0.001
Postoperative adjuvant therapy	1.14 (1.05 ~ 1.24)	0.002	0.71 (0.65 ~ 0.78)	<0.001

BMI: Body Mass Index,MGC: Mucinous adenocarcinoma,SRCC:signet-ring cell carcinoma,Pre-:Pre-operation.P < 0.05 was considered significant. All P values were corrected by BH method.

genes of the two groups, and KEGG analysis revealed that the LBMI group was enriched mainly in the Wnt signaling pathway, gastric cancer, and African trypanosomiasis (Figure 4C); similarly GO enrichment analysis was performed mainly in the extracellular region, extracellular space, plasma membrane and Wnt signaling pathway (Figure 4D). Correlation analysis of the DEGs associated with the dominant flora at the genus level revealed that *g_Abiotrophia* was significantly positively correlated with 11 genes, such as LGR6, and significantly negatively correlated with 30 genes, such as P2RY12 and SCN4B,in the LBMI group (Figure 4E; for details, see Additional File S1). The above results revealed that GC patients with different BMIs presented different transcriptomic landscapes and that many of these genes were closely related to differential intratumoral microbiota, suggesting that differential intratumoral microbiota may regulate the progression of GC by influencing the genes of the host.

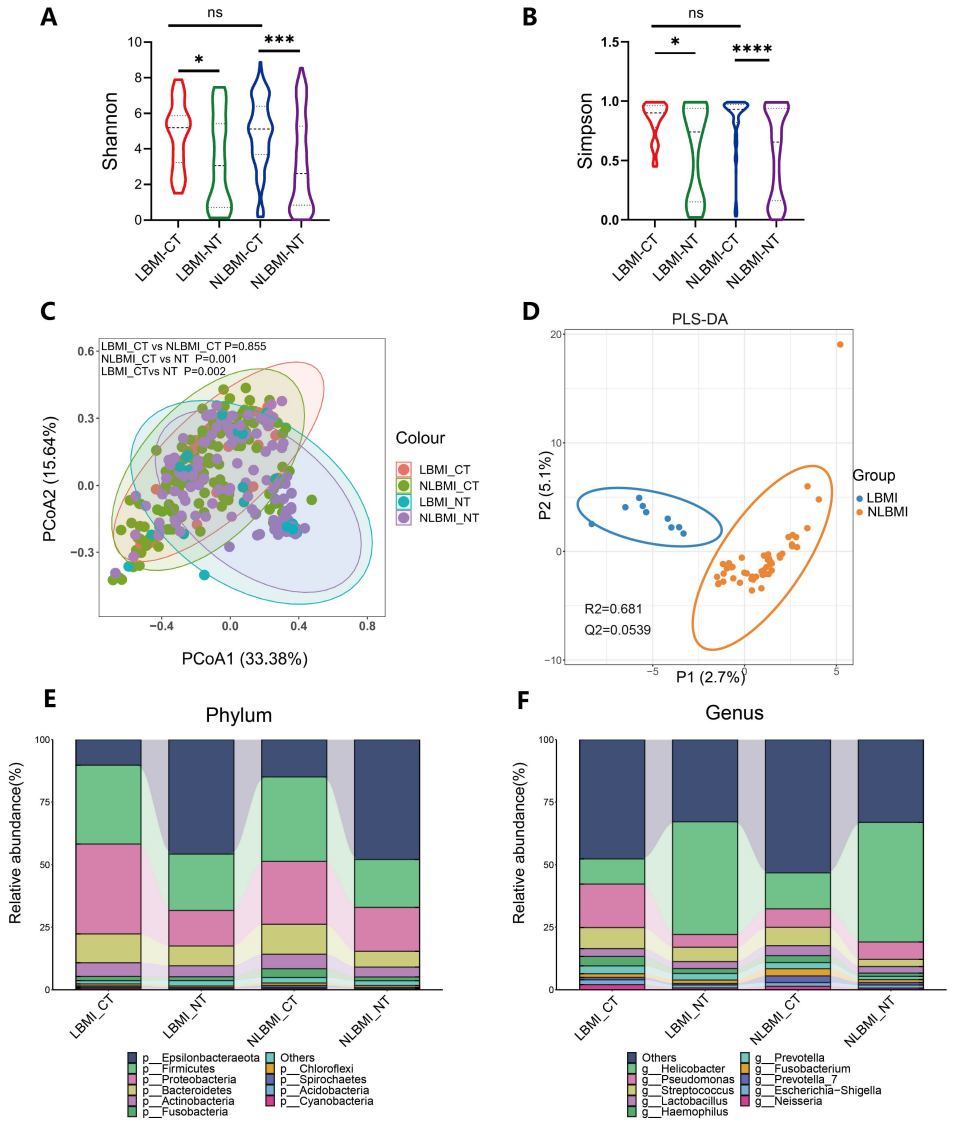

FIGURE 2
Tumor microbiome landscape of LBMI and NLBMI gastric cancer patients. Alpha diversity analysis of the LBMI and NLBMI groups. **(A)** Shannon index and **(B)** Simpson index in gastric cancer samples of each group. **(C)** Beta diversity analysis using UniFrac distance-weighted PCoA shows differences between cancerous and adjacent tissues in low BMI and non-low BMI groups. **(D)** PLS-DA analysis shows that the tumor microbiome composition of GC patients in the LBMI group and NLBMI group can be clearly divided into two different clusters. Stacked bar charts showing the species composition at **(E)** phylum level and **(F)** genus level for LBMI and NLBMI groups. LBMI-CT, Low BMI tumor tissue; LBMI-NT, Low BMI adjacent normal tissue; NLBMI-CT, Non-Low BMI tumor tissue; NLBMI-NT, Non-Low BMI adjacent normal tissue. PLS-DA, Partial Least Squares Discriminant Analysis. PCoA, Principal Coordinate Analysis. $P < 0.05$ is considered statistically significant. no * indicates P value $\geq$ 0.05, * indicates $0.01 \leq P < 0.05$, ** indicates $0.001 \leq P < 0.01$, *** indicates $P < 0.001$. ns, No sense.

LBMI intratumoral *g_Abiotrophia* negatively correlates with eosinophils

To explore the associations between BMI-associated intratumoral microbiota and tumor-infiltrating immune cells, we analyzed the composition of immune cells in 64 GC patients via transcriptome sequencing information and BMI data and plotted bar graphs of immune cell abundance (Figures 5A, B) to discover the unique features of the TIME of GC patients with different BMIs.

Correlation analysis revealed that in the NLBMI group, *g_Lachnoanaerobaculum* showed a significant positive correlation with T cell follicular helper, while Mast cells resting exhibited a significant negative correlation. *g_Stomatobaculum* demonstrated a significant positive correlation with T cell follicular helper, whereas T cells CD4 memory resting showed a significant negative correlation. In the LBMI group, *g_Enterobacter* displayed a significant positive correlation with B cells naive, while Dendritic cells activated and T cells CD4 memory resting showed significant negative correlations.*g_Abiotrophia* showed a significant negative correlation with eosinophils (Figure 5C). The above results indicated that the BMI-related dominant intratumoral microbiota of GC patients were significantly associated with various tumor-

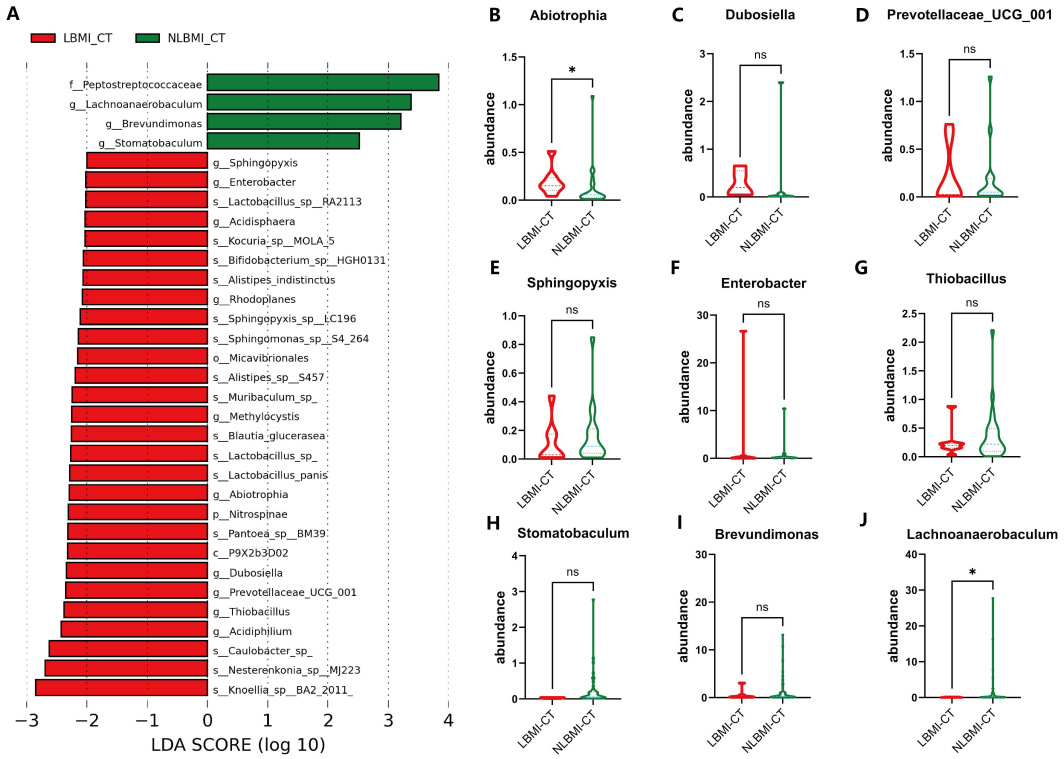

FIGURE 3
Significantly increased intratumoral *g_Abiotrophia* in LBMI. **(A)** Lefse analysis of LBM-CT and NLBMI-CT groups. The criterion for feature selection is an LDA score >2.0. The color of the bars represents the group, and the length of the bars represents the size of the LDA score. LDA score indicates the influence of the microbiota on LBMI and NLBMI groups. **(B-J)** Box plots of differential genus-level dominant bacteria abundance in GC patients between LBMI and NLBMI groups. P < 0.05 is considered statistically significant. The "*" in the figure indicates the significance level: no * indicates P value ≥ 0.05, * indicates 0.01 ≤ P < 0.05, ** indicates 0.001 ≤ P < 0.01, *** indicates P < 0.001. ns, No sense. LBMI-CT, Low BMI tumor tissue; NLBMI-CT, Non-Low BMI tumor tissue.

infiltrating immune cells, suggesting that they may play a role in regulating the immune microenvironment of GC.

High purine metabolism in LBMI tumors

Untargeted metabolomic analysis was performed on 57 tumor tissues in the transcriptome(Supplementary Table S5), and a total of 2688 metabolites were identified, of which 122 metabolites were significantly different between the LBMI and NLBMI groups (P<0.05, FC ≥2 or FC ≤0.5) (Figure 6A), and the PLS-DA scoring plot revealed that the different metabolites in the LBMI versus NLBMI tumors could be classified into two different clusters (R2Y = 0.432,Q2Y = 0.368) (Figure 6B). Tests of the PLS-DA model revealed that R2 > Q2 and the Q2 regression line had a negative intercept (R2 = [0.0, 0.354],Q2 = [0.0, -0.421]) (Figure 6C). The heatmap revealed that compared to the NLBMI group, the LBMI group had higher abundance of intratumoral purine metabolites, such as idp (Supplementary Figure S6).Differentially abundant metabolite KEGG enrichment analysis revealed that the LBMI group was enriched mainly in pathways such as purine metabolism and the caffeine metabolism pathway(Figure 6D). Genus-level differential dominant bacteria and differentially abundant metabolite correlation analysis, as shown in Figure 6E, revealed that the differential dominant bacteria in the NLBMI group, *g_Lachnoanaerobaculum*, were significantly negatively correlated with 12 differentially abundant metabolites, such as 8-methoxykynurenate; *g_Stomatobaculum* was significantly negatively correlated; *g_Brevundimonas* was significantly positively correlated with eleutheroside b1 and 2-dodecylbenzenesulfonic acid and significantly negatively correlated with mimosine and latamoxef. *g_Abiotrophia* in the LBMI group presented a significant negative correlation with demethoxyfumitremorgin c, whereas it presented a significant positive correlation with guanine and idp; *g_Dubosiella* presented a significant positive correlation with caffeine and four others; *g_Enterobacter* presented a significant positive correlation with cyclic n-acetylserotonin glucuronide and 8-methoxykynurenate presented a significant positive correlation; *g_Sphingopyxis* showed significant negative correlation with 2-piperidinone;*g_Prevotellaceae_UCG-001* and *g_Methylocystis* demonstrated a significant negative correlation with differentially abundant metabolites that were not significantly correlated(see Additional File S2). The above results revealed significant correlations between the two groups of intratumoral microbiota and metabolites, suggesting that they may further affect the biological process of gastric cancer by influencing metabolites.

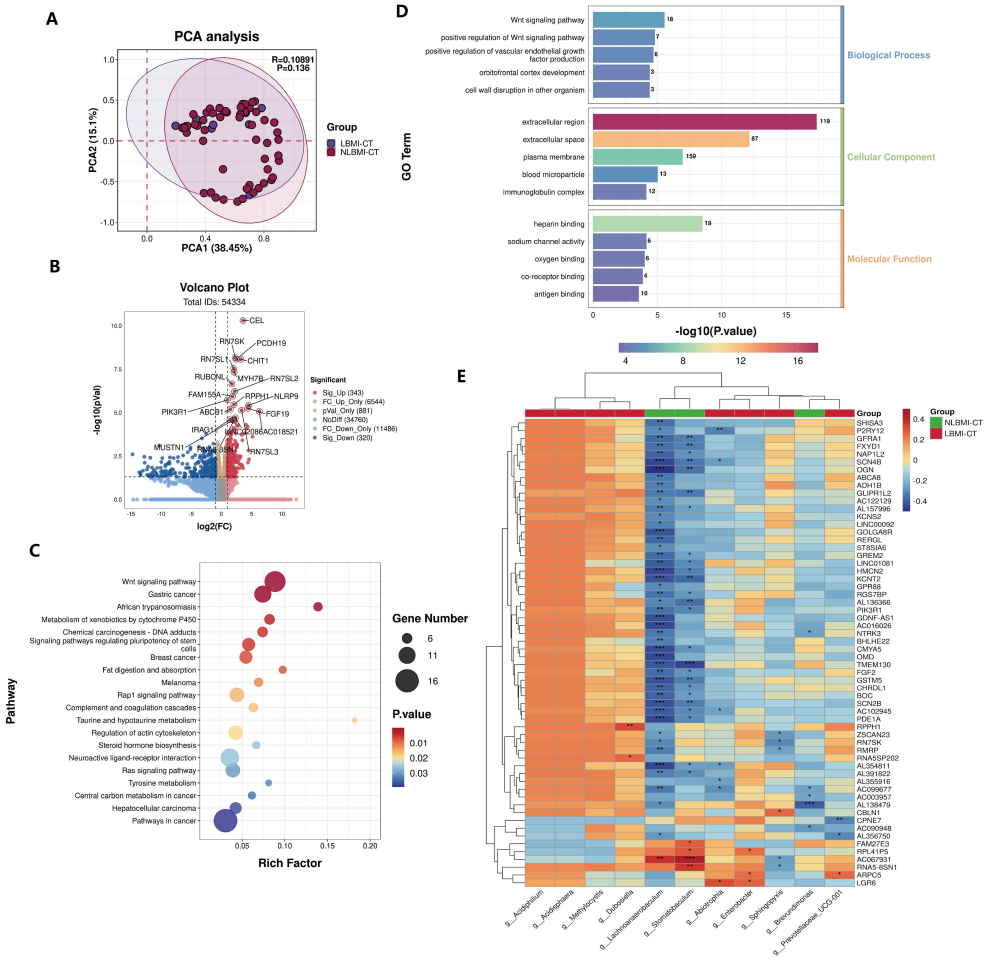

FIGURE 4
Negative correlation between intratumoral *g_Abiotrophia* and P2RY12 in LBMI. **(A)** Principal Component Analysis (PCA) of transcriptome samples from GC patients in the LBM-CT and NLBMI-CT groups. **(B)** Volcano plot of GC patients in the LBM-CT and NLBMI-CT groups, with selection criteria (|log2FC| ≥ 1, P < 0.05). **(C, D)** The function of these genes and transcription pathways was investigated using the KEGG and GO databases, and the TOP20 KEGG pathways were displayed in a bubble chart and the TOP15 GO pathways were shown in a bar chart. **(E)** Correlation heatmap showing the spearman analysis of the TOP60 differential genes and genus-level intratumoral bacteria. Red indicates positive correlation; blue indicates negative correlation. The color depth represents the magnitude of the correlation coefficient, with color ranging from light to dark indicating increasing correlation value. P < 0.05 is considered statistically significant. The "*" in the figure indicates the significance level: no * indicates P value ≥ 0.05, * indicates 0.01 ≤ P < 0.05, ** indicates 0.001 ≤ P < 0.01, *** indicates P < 0.001. LBMI-CT, Low BMI tumor tissue; NLBMI-CT, Non-Low BMI tumor tissue.

Discussion

In recent years, the relationship between GC and BMI has been studied with varying results (Schooling et al., 2015; Feng et al., 2018; Ma et al., 2021; Zhao et al., 2021). The long-term prognosis of patients with different BMIs remains unclear. Therefore, the present study was conducted to investigate BMI and GC in a large cohort. In this study, LBMI was found to be an independent risk predictor of poor prognosis, and when PSM was used to adjust for confounders and K–M survival curve analysis, it was observed that the LBMI group had a worse long-term prognosis in all patients than did the NLBMI group. This result is consistent with the findings of Feng et al (Feng et al., 2018). Several other studies have concluded that patients with LBMI have a poor prognosis (Indini et al., 2021; Ma et al., 2021; Spyrou et al., 2021). When specific subgroups, such as stage I versus stage IV patients, were analyzed, there was no significant difference in prognosis between the two groups. In contrary in stage II and III patients, LBMI patients had a significantly worse prognosis than NLBMI patients did. This finding is consistent with those of Spyrou et al. (2021) and may be because BMI has little effect on long-term prognosis in stage I versus stage IV patients. Moreover, among patients receiving postoperative adjuvant therapy, LBMI patients had worse overall survival rates and fewer benefits than NLBMI patients did, possibly because preoperative cancer-related malignancies are almost always associated with some degree of weight loss, which makes patients intolerant of postoperative adjuvant therapy side effects (Indini et al., 2021; Ma et al., 2021). Therefore, special perioperative nutritional support therapy and meticulous follow-up treatment for this special population with LBMI may improve the clinical outcome of patients.

Intratumoral microbiota are microorganisms present in tumor tissues and are now considered important regulators of many

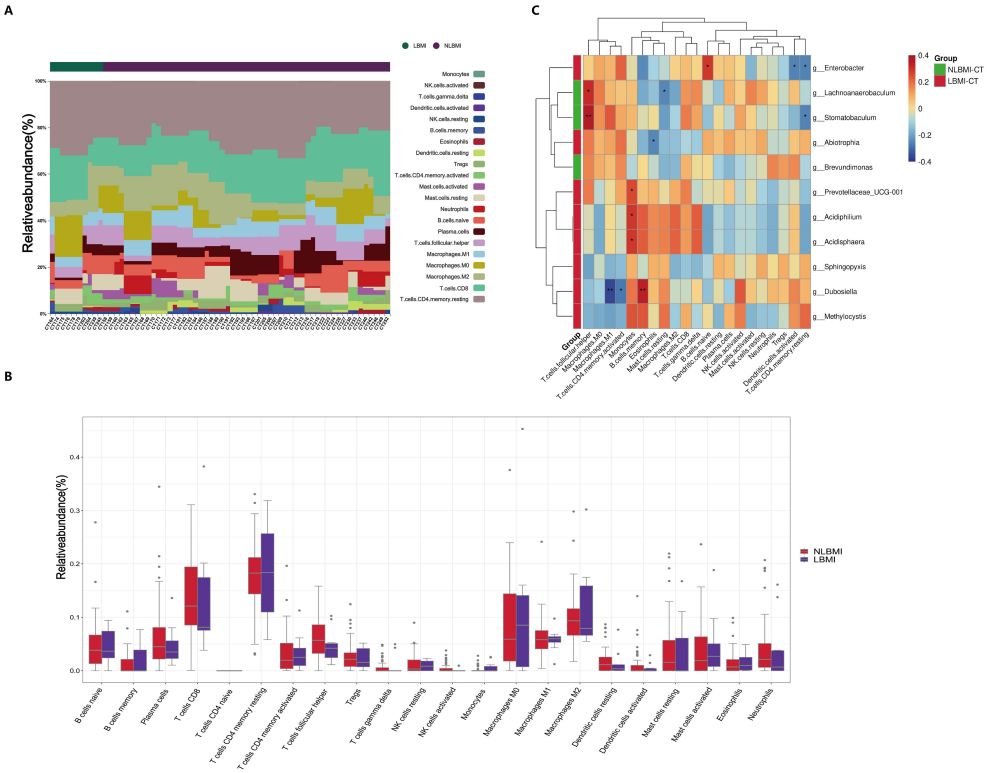

FIGURE 5
Negative correlation between intratumoral *g_Abiotrophia* and eosinophils in LBMI. **(A)** Bar chart of the relative abundance of 22 immune cells in GC patients grouped by BMI status. Each bar represents a sample, with each color corresponding to a different immune cell type. The y-axis represents the relative abundance values of the immune cells, with the sum of the relative abundance of all immune cells in a single sample equal to 1. **(B)** Box plot showing differences in the abundance of tumor-infiltrating immune cells between LBMI and NLBMI groups. **(C)** Correlation heatmap showing spearman analysis between tumor-infiltrating immune cells and genus-level intratumoral bacteria. The x-axis represents immune cells, and the y-axis represents bacteria. Red indicates positive correlation; blue indicates negative correlation. The color depth represents the magnitude of the spearman correlation coefficient, with color ranging from light to dark indicating increasing correlation value. The "*" in the figure indicates the significance level: no * indicates P value ≥ 0.05, * indicates 0.01 ≤ P < 0.05, ** indicates 0.001 ≤ P < 0.01, *** indicates P < 0.001. LBMI-CT, Low BMI tumor tissue; NLBMI-CT, Non-Low BMI tumor tissue.

tumors, especially those of the gastrointestinal tract (Galeano Niño et al., 2022). Two recent studies have shown heterogeneity among microorganisms at different BMI states (Huang et al., 2024; Li et al., 2024). In the present study, we found significant differences in the alpha and beta diversity of the microbiota between tumor tissue and peritumoral tissue in the two groups, whereas there were no differences between intratumoral microbiota (Figures 2A-C). A 16S rRNA study evaluating the differences in gastric flora between 229 tumor tissues and 247 peritumoral tissues revealed that the Shannon and Simpson indices of the alpha and beta diversity of gastric intratumoral microbiota in patients with GC were significantly greater than those in paraneoplastic tissues, which is in line with the results of the present study (Liu et al., 2019). In addition, Huang et al (Li et al., 2024), There was no difference in the alpha and beta diversity of intratumoral flora between the two groups, which was consistent with the results of this study. Moreover analysis (Figures 3A, B) revealed a greater abundance of the differentially dominant bacterium *g_Abiotrophia* in LBMI than in NLBMI.*g_Abiotrophia* is a nutrient-variant Streptococcus species that is most commonly found in the oral cavity, frequently observed in nutritionally deficient states, and results in infective endocarditis (Mosca et al., 2021). *g_Abiotrophia* can promote fibronectin-mediated adhesion of HUVECs via DnaK and induce a proinflammatory response, leading to infective endocarditis in patients (Sasaki et al., 2021). Two studies have shown that this bacterium is highly abundant in patients with oral cancer (Mäkinen et al., 2023) and gastric cancer (Wu et al., 2018) and promotes tumor development and metastasis.

To further explore the intratumoral transcriptomic differences between the different BMI groups, a gene correlation analysis (Figure 4E) was performed, and the present findings revealed a significant negative correlation between *g_Abiotrophia* and P2RY12. P2RY12 was initially identified on platelets and plays an important role in platelet activation, which is also important in inflammation through the regulation of the innate and adaptive immune response (Ferrari et al., 2020). Indeed, following ADP-induced activation of P2RY12, platelets release mediators from their granules, including a variety of cytokines and chemokines, which recruit and activate leukocytes (Gómez Morillas et al., 2021). Widespread expression is also now present in many immune cells (Li et al., 2021) and it has been shown that activation of this P2RY12 receptor on dendritic cells promotes specific T- cell activation by increasing antigen endocytosis (Ben Addi et al., 2010), whereas P2RY12 inhibition induces immunosuppressive effects by

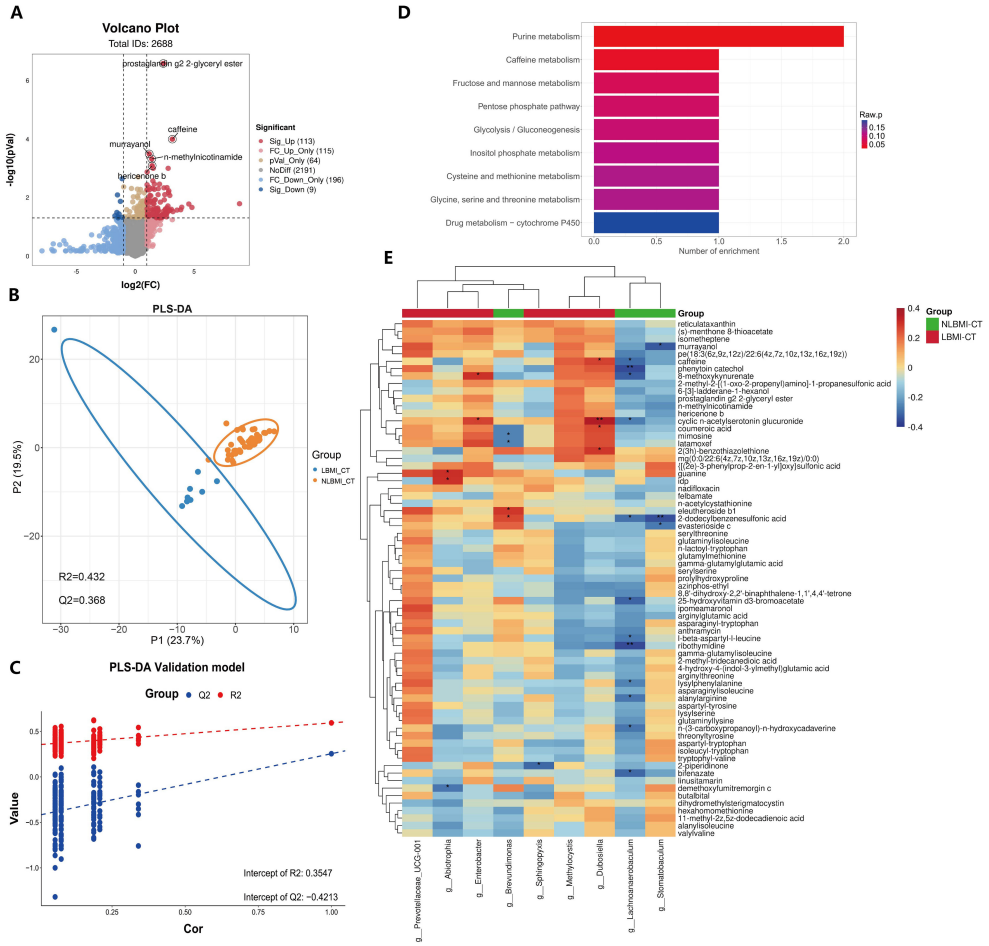

FIGURE 6
Increased purine metabolism in LBMI intratumoral environment. **(A)** Volcano plot of GC patients' tumor tissues comparing LBM-CT and NLBMI-CT groups, with screening criteria (|log2FC|≥1, P < 0.05). **(B)** PLS-DA analysis of differential metabolites between LBM-CT and NLBMI-CT groups, with screening criteria (VIP>1, |log2FC|≥1, P < 0.05). **(C)** Validation of the PLS-DA model indicating that the model established in this study is effective. **(D)** Bar chart of enriched pathways using the KEGG database to investigate the functions of these metabolites and metabolic pathways. **(E)** Correlation heatmap showing spearman analysis between differential metabolites and genus-level intratumoral bacteria. Red indicates positive correlation; blue indicates negative correlation. The color depth represents the magnitude of the correlation coefficient, with color ranging from light to dark indicating increasing correlation value. The "*" in the figure indicates the significance level: no * indicates P value ≥ 0.05, * indicates 0.01 ≤ P < 0.05, ** indicates 0.001 ≤ P < 0.01, *** indicates P < 0.001. LBMI-CT, Low BMI tumor tissue; NLBMI-CT, Non-Low BMI tumor tissue.

decreasing antigen uptake (Mansour et al., 2020). Several recent studies have demonstrated that P2RY12 is a favorable factor for long-term prognosis in brain gliomas (Noorani et al., 2023), lung cancer (Yu et al., 2021), and hepatocellular carcinoma (Ma et al., 2022). In conclusion, we hypothesize that the inhibition of P2RY12 expression by *g_Abiotrophia* leads to the development of immunosuppression in GC patients, which leads to a poor prognosis in patients with LBMI.

As an important influence on the TIME, intratumoral microbiota can also play important roles in tumor development and metastasis by influencing immune cells (Zhou et al., 2023). In this study, *g_Abiotrophia* in the LBMI group was negatively correlated with eosinophils (Figure 5C). Eosinophils were first identified in peripheral blood, and it is commonly believed that eosinophils and their mediators are usually associated with deleterious effects in allergic diseases but can also induce a protective host immune response against microbial pathogens (Yousefi et al., 2008). Interestingly, a review reported that eosinophils have a beneficial effect on probiotics and may respond to local immunity by modulating homeostasis between pro- and anti-inflammatory effects (Rosenberg et al., 2016). Many studies have investigated the role of eosinophils in tumor growth control, and a review (Varricchi et al., 2017) summarizing these studies reported that the presence of eosinophils at the tumor site or in the peripheral blood is a favorable prognostic factor for most cancers. Although there is evidence that eosinophils are tumorigenic, this review demonstrated that eosinophils have an antitumor effect on patients with gastric cancer with a better prognosis via the GEO database. Two reports also reached the same conclusion (Iwasaki et al., 1986; Cuschieri et al., 2002). In addition, eosinophils can act as nonspecialized antigen-presenting cells (APCs), and upon activation by certain cytokines or other inflammatory stimuli, eosinophils can upregulate MHC class II or costimulatory markers and stimulate an initiated CD4+T-cell

response *in vitro* and *in vivo* (Farhan et al., 2016). These findings suggest that eosinophils may act as helper cells in cancer and play an antitumor role. Taken together, these findings indicate that *g_Abiotrophia* may lead to tumor development and metastasis by affecting eosinophils, thus contributing to the poor prognosis of patients with LBMI gastric cancer.

Intratumoral microbiota can modulate tumor cell function by producing specific metabolites such as polyamines and short-chain fatty acids (SCFAs) (Natarajan and Pluznick, 2014). In this study, we found that LBMI-CT purine metabolism was enriched (Figure 6D) and that *g_Abiotrophia* was positively correlated with guanine and idp (Figure 6E). Purine nucleotides, such as RNA and DNA, are critical for synthesis, signaling, metabolism and energy homeostasis (Xie et al., 2024). Nutrients are required for the proliferation and differentiation of tumor cells, and guanine and idp are purine metabolites that can be synthesized into purine nucleotides through the purine metabolic pathway, which further provides nutrients for the proliferation and differentiation of tumor tissues and their development and metastasis (Yin et al., 2018). Two recent studies reported elevated nucleoside levels in GC tumor tissues (Kaji et al., 2020; Dai et al., 2021). One study, Kaji et al. (2020) reported that nucleoside concentrations were higher in GC patients with peritoneal recurrence than in GC patients without peritoneal recurrence. It is possible that increased levels of nucleosides, especially adenosine, lead to shorter survival in gastric cancer patients. Notably, a recent study (Tran et al., 2024) reported that feeding nucleosides to mice accelerated tumor growth, whereas inhibition of purine remediation slowed tumor progression, revealing a critical role of the purine remediation pathway in tumor metabolism. Interestingly, this study revealed that *g_Abiotrophia* was negatively correlated with P2RY12 (Figure 4E). The P2RY12 gene expresses a receptor that is a purinergic receptor and the gene is coupled to a Gi protein, resulting in reduced cAMP production (Borea et al., 2018). A recent study reported that decreased expression of P2RY12 resulted in decreased ligand production and increased cAMP production, which further led to increased synthesis of purine nucleotides or other purine metabolites within tumor tissues, thereby providing energy for tumor growth and development and promoting tumor development (Burnstock and Di Virgilio, 2013). Therefore, *g_Abiotrophia* may provide nutrients to tumor tissues by affecting P2RY12, which in turn affects on the conversion of guanine and IDP to purine nucleotides through the purine metabolic pathway.

There are several limitations to this study. First, weight loss is a common symptom in patients with GC, leading to significant differences in the distribution of BMI compared with healthy controls. This difference introduces a potential source of analytic inaccuracy and is unavoidable given the high degree of heterogeneity among GC patients. Second, the limited sample size of this study and the fact that it was a single-center retrospective analysis and that some of the missing data were not included in this study may have resulted in some selection bias. Third, compared with macrogenome sequencing, 16S rRNA gene sequencing was unable to annotate certain species at the species level, and the depth of species identification by 16S rRNA gene sequencing was relatively shallow. Lastly, basic experimental validation was not performed to draw relevant conclusions from the analysis of the histological data. Therefore, to overcome these limitations, further data validation of large-scale and prospective multicenter studies, which are combined with basic experimental validation, are needed to further validate the findings. The aforementioned limitations also offer valuable insights for future research aimed at enhancing treatment strategies for these patients.

Conclusion

LBMI is an important independent risk factor for poor prognosis and possible immunosuppression or intolerance to postoperative adjuvant chemotherapy. *g_Abiotrophia*, a high-abundance dominant bacterium in LBMI with a negative correlation between LBMI and eosinophils, may inhibit P2RY12 to promote purine metabolism, modulate the TIME and thus contribute to gastric cancer development. Further validation in a separate cohort may be needed.

Data availability statement

The raw reads of 16S rDNA and the raw data of transcriptomewere deposited into the NCBI SRA database (Accession Number: Bioproject PRJNA1061213). The raw data of metabolome deposited into the MetaboLights database (Accession Number: MTBLS9211). The sample groupings used for the microbiome, transcriptome, and metabolome in this study are detailed in Supplementary File 3. The code used in this study and all supporting data are available upon request..

Ethics statement

The studies involving humans were approved by The Research Ethics Committees of Zhejiang Cancer Hospital. The studies were conducted in accordance with the local legislation and institutional requirements. The participants provided their written informed consent to participate in this study. The manuscript presents research on animals that do not require ethical approval for their study. Written informed consent was obtained from the individual (s) for the publication of any potentially identifiable images or data included in this article.

Author contributions

KL: Conceptualization, Data curation, Formal Analysis, Funding acquisition, Investigation, Methodology, Project administration, Resources, Software, Supervision, Validation, Visualization, Writing – original draft, Writing – review & editing. ZJ: Conceptualization, Data curation, Formal Analysis, Funding acquisition, Investigation, Methodology, Project administration, Resources, Software, Supervision, Validation,

Visualization, Writing – original draft, Writing – review & editing. YM: Data curation, Formal Analysis, Writing – review & editing. RX: Data curation, Writing – review & editing. YZ: Data curation, Writing – review & editing. KY: Data curation, Writing –review & editing. CP: Data curation, Writing – review & editing. LY: Conceptualization, Funding acquisition, Project administration, Resources, Supervision, Writing – review & editing. XC: Conceptualization, Funding acquisition, Project administration, Resources, Supervision, Writing – review & editing. ZL: Conceptualization, Funding acquisition, Project administration, Resources, Writing – review & editing. BZ: Conceptualization, Writing – review & editing. SW: Conceptualization, Writing – review & editing.

Funding

The author(s) declare financial support was received for the research, authorship, and/or publication of this article. The National Key R&D Program of China (2021YFA0910100), Medical Science and Technology Project of Zhejiang Province (2022KY114, WKJ-ZJ-2104), Natural Science Foundation of Zhejiang Province (HDMY22H160008), National Natural Science Foundation of China (82074245, 81973634, 82204828), Innovation Team and Talents Cultivation Program of National Administration of Traditional Chinese Medicine (No: ZYYCXTD-C-202208), Medical Science and Technology Project of Zhejiang Province (2018KY305, 2021KY582), National Natural Science Foundation of China (82404084), China Postdoctoral Science Foundation (2024M763328).

Acknowledgments

The authors would like to thank all of the participants who recruited patients in this study and the colleagues at Zhejiang Cancer Hospital.

Conflict of interest

The authors declare that the research was conducted in the absence of any commercial or financial relationships that could be construed as a potential conflict of interest.

Generative AI statement

The author(s) declare that no Generative AI was used in the creation of this manuscript.

Publisher's note

Supplementary material

The Supplementary Material for this article can be found online at: https://www.frontiersin.org/articles/10.3389/fcimb.2025.1511900/full#supplementary-material

SUPPLEMENTARY FIGURE 1
Bioinformatics Pipeline Flowchart. This flowchart illustrates the bioinformatics pipeline used in the study, detailing the steps involved in data collection, processing, and analysis for the gastric cancer patient cohorts. Each step is visually represented to show the flow of data from initial patient selection through various analyses, including microbiota assessment, transcriptome analysis, and metabolomics evaluation. The figure provides an overview of how the different aspects of the research are integrated to assess the impact of BMI on gastric cancer outcomes and microbiota interactions.

SUPPLEMENTARY FIGURE 2
Correlation Analysis of Gastric Microbiota Samples in LBMI and NLBMI Groups and Rarefaction Curve Analysis. **(A)** Venn diagram representing the distribution of gastric microbiota and showing intersections across multiple microhabitats. **(B)** Shannon diversity measurement. **(C)** Simpson diversity measurement. **(D)** Correlation heatmap of the differential dominant genera at the genus level in tumor tissues of LBMI and NLBMI groups. The x-axis and y-axis represent bacteria. Red indicates a positive correlation, while blue indicates a negative correlation. The depth of color represents the magnitude of the Spearman correlation coefficient, with lighter colors indicating smaller values and darker colors indicating larger values. The "*" in the figure indicates the significance of the p-value: no * indicates p-value $\geq$ 0.05, * indicates 0.01 $\leq$ p < 0.05, ** indicates 0.001 $\leq$ p < 0.01, *** indicates p < 0.001.LBMI-CT, Low BMI tumor tissue; LBMI-NT, Low BMI adjacent normal tissue; NLBMI-CT, Non-low BMI tumor tissue; NLBMI-NT, Non-low BMI adjacent normal tissue.

SUPPLEMENTARY FIGURE 3
Differential Analysis of Microbiota in Different Tissue Sites of GC Patients in the LBMI Group. **(A)** Positive and negative bar graphs of Lefse analysis of gastric cancer microbiota in tumor and adjacent tissues of the LBMI group. The characteristic selection criterion is LDA score > 2.0. The color of the bar represents the group, and the length of the bar represents the LDA score. The LDA score indicates the influence level of the microbiota. **(B)** Evolutionary branch diagram of Lefse analysis of gastric cancer microbiota in tumor and adjacent tissues of the LBMI group. The node size represents the abundance of the species, proportional to their abundance. The color of the nodes indicates the group, with yellow nodes representing species with no significant difference between groups. Red nodes represent species significantly more abundant in the LBMI-CT group, while green nodes represent species significantly more abundant in the LBMI-NT group. The nodes within each layer, from inside to outside, represent phylum/class/order/family/genus/species, with the species annotations in each layer marking from outside to inside as phylum/class/order/family/genus/species. LBMI-CT, Low BMI tumor tissue; LBMI-NT, Low BMI adjacent tissue.

SUPPLEMENTARY FIGURE 4
Differential Analysis of Microbiota in Different Tissue Sites of GC Patients in the NLBMI Group. (A) Positive and negative bar graphs of Lefse analysis of gastric cancer microbiota in tumor and adjacent tissues of the NLBMI group. The characteristic selection criterion is LDA score > 2.0. The color of the bar represents the group, and the length of the bar represents the LDA score. The LDA score indicates the influence level of the microbiota. **(B)** Evolutionary branch diagram of Lefse analysis of gastric cancer microbiota in tumor and adjacent tissues of the NLBMI group. The node size represents the abundance of the species, proportional to their abundance. The color of the nodes indicates the group, with yellow nodes representing species with no significant difference between groups. Red nodes represent species significantly more abundant in the NLBMI-CT group, while green nodes represent species significantly more abundant in the NLBMI-NT group. The

nodes within each layer, from inside to outside, represent phylum/class/order/family/genus/species, with the species annotations in each layer marking from outside to inside as phylum/class/order/family/genus/species. NLBMI-CT, Non-Low BMI tumor tissue; NLBMI-NT, Non-Low BMI adjacent tissue.

SUPPLEMENTARY FIGURE 5
Evolutionary Branch Diagram of Lefse Differential Analysis of Intratumoral Microbiota in LBMI and NLBMI Groups of GC Patients. The size of the nodes represents the abundance of the species, proportional to their abundance. The color of the nodes indicates the group, with yellow nodes representing species with no significant difference between groups. Red nodes represent species significantly more abundant in the NLBMI-CT group, while green nodes represent species significantly more abundant in the NLBMI-NT group. The nodes within each layer, from inside to outside, represent phylum/class/order/family/genus/species, with the species annotations in each layer marking from outside to inside as phylum/class/order/family/genus/species. LBMI-CT, Low BMI tumor tissue; NLBMI-CT, Non-Low BMI tumor tissue.

SUPPLEMENTARY FIGURE 6
Heatmap showing the correlation between metabolites and BMI. The heatmap displays the differential abundance of metabolites between LBMI-CT (n = 37) and NLBMI-CT (n = 16). It illustrates the relative abundance (Log) of 69 metabolites. Red indicates positive correlation; blue indicates negative correlation. The depth of the color represents the magnitude of abundance, with color ranging from light to dark indicating increasing abundance value. LBMI-CT, Low BMI tumor tissue; NLBMI-CT, Non-Low BMI tumor tissue.

References

Ahn, H. S., Lee, H. J., Yoo, M. W., Jeong, S. H., Park, D. J., Kim, H. H., et al. (2011). Changes in clinicopathological features and survival after gastrectomy for gastric cancer over a 20-year period. *Br. J. Surg.* 98, 255–260. doi: 10.1002/bjs.7310

Amin, M. B., Greene, F. L., Edge, S. B., Compton, C. C., Gershenwald, J. E., Brookland, R. K., et al. (2017). The Eighth Edition AJCC Cancer Staging Manual: Continuing to build a bridge from a population-based to a more "personalized" approach to cancer staging. *CA: A Cancer J. Clin.* 67, 93–99. doi: 10.3322/caac.21388

Association JGC (2020). Japanese gastric cancer treatment guidelines 2018 (5th edition). *Gastric Cancer.* 24, 1–21.

Ben Addi, A., Cammarata, D., Conley, P. B., Boeynaems, J.-M., and Robaye, B. (2010). Role of the P2Y12 receptor in the modulation of murine dendritic cell function by ADP. *J. Immunol.* 185, 5900–5906. doi: 10.4049/jimmunol.0901799

Borea, P. A., Gessi, S., Merighi, S., Vincenzi, F., and Varani, K. (2018). Pharmacology of adenosine receptors: the state of the art. *Physiol. Rev.* 98, 1591–1625. doi: 10.1152/physrev.00049.2017

Bray, F., Laversanne, M., Sung, H., Ferlay, J., Siegel, R. L., Soerjomataram, I., et al. (2024). Global cancer statistics 2022: GLOBOCAN estimates of incidence and mortality worldwide for 36 cancers in 185 countries. *CA: A Cancer J. Clin.* 74, 229–263. doi: 10.3322/caac.21834

Burnstock, G., and Di Virgilio, F. (2013). Purinergic signalling and cancer. *Purinergic Signalling.* 9, 491–540. doi: 10.1007/s11302-013-9372-5

Cao, Y., Xia, H., Tan, X., Shi, C., Ma, Y., Meng, D., et al. (2024). Intratumoural microbiota: a new frontier in cancer development and therapy. *Signal Transduction Targeted Ther.* 9. doi: 10.1038/s41392-023-01693-0

Chen, Y., Zheng, X., Liu, C., Liu, T., Lin, S., Xie, H., et al. (2024). Anthropometrics and cancer prognosis: a multicenter cohort study. *Am. J. Clin. Nutr.* 120, 47–55. doi: 10.1016/j.ajcnut.2024.05.016

Cuschieri, A., Talbot, I. C., and Weeden, S. (2002). Influence of pathological tumour variables on long-term survival in resectable gastric cancer. *Br. J. Cancer.* 86, 674–679. doi: 10.1038/sj.bjc.6600161

Dai, D., Yang, Y., Yu, J., Dang, T., Qin, W., Teng, L., et al. (2021). Interactions between gastric microbiota and metabolites in gastric cancer. *Cell Death Dis.* 12. doi: 10.1038/s41419-021-04396-y

Farhan, R. K., Vickers, M. A., Ghaemmaghami, A. M., Hall, A. M., Barker, R. N., and Walsh, G. M. (2016). Effective antigen presentation to helper T cells by human eosinophils. *Immunology* 149, 413–422. doi: 10.1111/imm.2016.149.issue-4

Feng, F., Zheng, G., Guo, X., Liu, Z., Xu, G., Wang, F., et al. (2018). Impact of body mass index on surgical outcomes of gastric cancer. *BMC Cancer* 18. doi: 10.1186/s12885-018-4063-9

Ferrari, D., Vuerich, M., Casciano, F., Longhi, M. S., Melloni, E., Secchiero, P., et al. (2020). Eosinophils and purinergic signaling in health and disease. *Front. Immunol.* 11. doi: 10.3389/fimmu.2020.01339

Galeano Niño, J. L., Wu, H., LaCourse, K. D., Kempchinsky, A. G., Baryiames, A., Barber, B., et al. (2022). Effect of the intratumoral microbiota on spatial and cellular heterogeneity in cancer. *Nature* 611, 810–817. doi: 10.1038/s41586-022-05435-0

Gómez Morillas, A., Besson, V. C., and Lerouet, D. (2021). Microglia and neuroinflammation: what place for P2RY12? *Int. J. Mol. Sci.* 22. doi: 10.3390/ijms22041636

Hsieh, Y.-Y., Kuo, W.-L., Hsu, W.-T., Tung, S.-Y., and Li, C. (2022). Fusobacterium nucleatum-induced tumor mutation burden predicts poor survival of gastric cancer patients. *Cancers* 15. doi: 10.3390/cancers15010269

Huang, Y., Huang, X., Wang, Z., He, F., Huang, Z., Chen, C., et al. (2024). Analysis of differences in intestinal flora associated with different BMI status in colorectal cancer patients. *J. Trans. Med.* 22. doi: 10.1186/s12967-024-04903-7

Indini, A., Rijavec, E., Ghidini, M., Tomasello, G., Cattaneo, M., Barbin, F., et al. (2021). Impact of BMI on survival outcomes of immunotherapy in solid tumors: A systematic review. *Int. J. Mol. Sci.* 22. doi: 10.3390/ijms22052628

Iwasaki, K., Torisu, M., and Fujimura, T. (1986). Malignant tumor and eosinophils: I. Prognostic significance in gastric cancer. *Cancer* 58, 1321–1327. doi: 10.1002/1097-0142(19860915)58:6<1321::AID-CNCR2820580623>3.0.CO;2-O

Kaji, S., Irino, T., Kusuhara, M., Makuuchi, R., Yamakawa, Y., Tokunaga, M., et al. (2020). Metabolomic profiling of gastric cancer tissues identified potential biomarkers for predicting peritoneal recurrence. *Gastric Cancer.* 23, 874–883. doi: 10.1007/s10120-020-01065-5

Li, J., Chen, Z., Wang, Q., Du, L., Yang, Y., Guo, F., et al. (2024). Microbial and metabolic profiles unveil mutualistic microbe-microbe interaction in obesity-related colorectal cancer. *Cell Rep. Med.* 5. doi: 10.1016/j.xcrm.2024.101429

Li, X., Zhang, G., and Cao, X. (2021). The function and regulation of platelet P2Y12 receptor. *Cardiovasc. Drugs Ther.* 37, 199–216. doi: 10.1007/s10557-021-07229-4

Liu, X., Shao, L., Liu, X., Ji, F., Mei, Y., Cheng, Y., et al. (2019). Alterations of gastric mucosal microbiota across different stomach microhabitats in a cohort of 276 patients with gastric cancer. *EBioMedicine* 40, 336–348. doi: 10.1016/j.ebiom.2018.12.034

Li, Y., Ren, N., Zhang, B., Yang, C., Li, A., Li, X., et al. (2022). Gastric cancer incidence trends in China and Japan from 1990 to 2019: Disentangling age–period–cohort patterns. *Cancer* 129, 98–106.

Liu, Z., Zhang, D., and Chen, S. (2024). Unveiling the gastric microbiota: implications for gastric carcinogenesis, immune responses, and clinical prospects. *J. Exp. Clin. Cancer Res.* 43. doi: 10.1186/s13046-024-03034-7

Ma, C., Fu, Q., Diggs, L. P., McVey, J. C., McCallen, J., Wabitsch, S., et al. (2022). Platelets control liver tumor growth through P2Y12-dependent CD40L release in NAFLD. *Cancer Cell.* 40, 986–98.e5. doi: 10.1016/j.ccell.2022.08.004

Ma, S., Liu, H., Ma, F.-H., Li, Y., Jin, P., Hu, H.-T., et al. (2021). Low body mass index is an independent predictor of poor long-term prognosis among patients with resectable gastric cancer. *World J. Gastrointestinal Oncol.* 13, 161–173. doi: 10.4251/wjgo.v13.i3.161

Mäkinen, A. I., Pappalardo, V. Y., Buijs, M. J., Brandt, B. W., Mäkitie, A. A., Meurman, J. H., et al. (2023). Salivary microbiome profiles of oral cancer patients analyzed before and after treatment. *Microbiome* 11. doi: 10.1186/s40168-023-01613-y

Mansour, A., Bachelot-Loza, C., Nesseler, N., Gaussem, P., and Gouin-Thibault, I. (2020). P2Y12 inhibition beyond thrombosis: effects on inflammation. *Int. J. Mol. Sci.* 21. doi: 10.3390/ijms21041391

Mima, K., Nishihara, R., Qian, Z. R., Cao, Y., Sukawa, Y., Nowak, J. A., et al. (2016). Fusobacterium nucleatumin colorectal carcinoma tissue and patient prognosis. *Gut* 65, 1973–1980. doi: 10.1136/gutjnl-2015-310101

Mitsuhashi, K., Nosho, K., Sukawa, Y., Matsunaga, Y., Ito, M., Kurihara, H., et al. (2015). Association ofFusobacteriumspecies in pancreatic cancer tissues with molecular features and prognosis. *Oncotarget* 6, 7209–7220. doi: 10.18632/oncotarget.3109

Mosca, A. M., Mané, F., Marques Pires, C., and Medeiros, P. (2021). Infective endocarditis by a rare and fastidious agent:Abiotrophia defectiva. *BMJ Case Rep.* 14. doi: 10.1136/bcr-2021-241964

Natarajan, N., and Pluznick, J. L. (2014). From microbe to man: the role of microbial short chain fatty acid metabolites in host cell biology. *Am. J. Physiology-Cell Physiol.* 307, C979–CC85. doi: 10.1152/ajpcell.00228.2014

Noorani, I., Sidlauskas, K., Pellow, S., Savage, R., Norman, J. L., Chatelet, D. S., et al. (2023). Clinical impact of anti-inflammatory microglia and macrophage phenotypes at glioblastoma margins. *Brain Commun.* 5. doi: 10.1093/braincomms/fcad176

Peng, R., Liu, S., You, W., Huang, Y., Hu, C., Gao, Y., et al. (2022). Gastric microbiome alterations are associated with decreased CD8+ Tissue-resident memory T cells in the tumor microenvironment of gastric cancer. *Cancer Immunol. Res.* 10, 1224–1240. doi: 10.1158/2326-6066.CIR-22-0107

Rosenberg, H. F., Masterson, J. C., and Furuta, G. T. (2016). Eosinophils, probiotics, and the microbiome. *J. Leukocyte Biol.* 100, 881–888. doi: 10.1189/jlb.3RI0416-202R

Sasaki, M., Shimoyama, Y., Kodama, Y., and Ishikawa, T. (2021). Abiotrophia defectiva dnaK promotes fibronectin-mediated adherence to HUVECs and induces a proinflammatory response. *Int. J. Mol. Sci.* 22. doi: 10.3390/ijms22168528

Schooling, C. M., Taghizadeh, N., Boezen, H. M., Schouten, J. P., Schröder, C. P., Vries, E. G. E. d., et al. (2015). BMI and lifetime changes in BMI and cancer mortality risk. *PloS One* 10 (4).

Spyrou, N., Vallianou, N., Kadillari, J., and Dalamaga, M. (2021). The interplay of obesity, gut microbiome and diet in the immune check point inhibitors therapy era. *Semin. Cancer Biol.* 73, 356–376. doi: 10.1016/j.semcancer.2021.05.008

Tran, D. H., Kim, D., Kesavan, R., Brown, H., Dey, T., Soflaee, M. H., et al. (2024). *De novo* and salvage purine synthesis pathways across tissues and tumors. *Cell* 187, 3602–18.e20. doi: 10.1016/j.cell.2024.05.011

Varricchi, G., Galdiero, M. R., Loffredo, S., Lucarini, V., Marone, G., Mattei, F., et al. (2017). Eosinophils: The unsung heroes in cancer? *OncoImmunology* 7. doi: 10.1080/2162402X.2017.1393134

Wang, G., He, X., and Wang, Q. (2023). Intratumoral bacteria are an important "accomplice" in tumor development and metastasis. *Biochim. Biophys. Acta (BBA) - Rev. Cancer* 1878. doi: 10.1016/j.bbcan.2022.188846

Wu, J., Xu, S., Xiang, C., Cao, Q., Li, Q., Huang, J., et al. (2018). Tongue coating microbiota community and risk effect on gastric cancer. *J. Cancer.* 9, 4039–4048. doi: 10.7150/jca.25280

Xie, J., Liu, J., Chen, X., and Zeng, C. (2024). Purinosomes involved in the regulation of tumor metabolism: current progress and potential application targets. *Front. Oncol.* 14. doi: 10.3389/fonc.2024.1333822

Yin, J., Ren, W., Huang, X., Deng, J., Li, T., and Yin, Y. (2018). Potential mechanisms connecting purine metabolism and cancer therapy. *Front. Immunol.* 9. doi: 10.3389/fimmu.2018.01697

Yousefi, S., Gold, J. A., Andina, N., Lee, J. J., Kelly, A. M., Kozlowski, E., et al. (2008). Catapult-like release of mitochondrial DNA by eosinophils contributes to antibacterial defense. *Nat. Med.* 14, 949–953. doi: 10.1038/nm.1855

Yu, L., Cao, S., Li, J., Han, B., Zhong, H., and Zhong, R. (2021). Prognostic value and immune infiltration of a novel stromal/immune score-related P2RY12 in lung adenocarcinoma microenvironment. *Int. Immunopharmacology.* 98. doi: 10.1016/j.intimp.2021.107734

Zhao, W., Wang, P., Sun, W., Gu, P., Wang, X., Wu, Z., et al. (2021). Effects of a high body mass index on the short-term outcomes and prognosis after radical gastrectomy. *Surg. Today* 51, 1169–1178. doi: 10.1007/s00595-021-02259-9

Zhou, Y., Cheng, L., Liu, L., and Li, X. (2023). NK cells are never alone: crosstalk and communication in tumour microenvironments. *Mol. Cancer.* 22. doi: 10.1186/s12943-023-01737-7

frontiers | Frontiers in Cellular and Infection Microbiology

TYPE Original Research
PUBLISHED 21 February 2025
DOI 10.3389/fcimb.2025.1543186

OPEN ACCESS

EDITED BY
Maurizio Sanguinetti,
Catholic University of the Sacred Heart, Italy

REVIEWED BY
Irina Miralda,
Emory University, United States
Mukulika Bose,
University of Texas MD Anderson Cancer Center, United States

*CORRESPONDENCE
Dae-Kyun Chung
dkchung@khu.ac.kr
Soojin Jang
soojin.jang@ip-korea.org

†These authors have contributed equally to this work

RECEIVED 11 December 2024
ACCEPTED 03 February 2025
PUBLISHED 21 February 2025

CITATION
Jang K, Kim H, Choi D, Jang S and Chung D-K (2025) *Staphylococcus aureus* utilizes vimentin to internalize human keratinocytes.
Front. Cell. Infect. Microbiol. 15:1543186.
doi: 10.3389/fcimb.2025.1543186

Staphylococcus aureus utilizes vimentin to internalize human keratinocytes

Kyoungok Jang[1†], Hangeun Kim[2†], Dobin Choi[3], Soojin Jang[1*] and Dae-Kyun Chung[2,3*]

[1]Therapeutic Research Group, Antibacterial Resistance Laboratory, Institute Pasteur Korea, Seongnam-si, Gyeonggi-do, Republic of Korea, [2]Research and Development Center, Skin Biotechnology Center Co. Ltd., Yongin, Republic of Korea, [3]Graduate School of Biotechnology, Kyung Hee University, Yongin, Republic of Korea

Introduction: Vimentin is an intermediate filamentous cytoskeletal protein involved in cell migration, adhesion, and division. Recent studies have demonstrated that several bacteria and viruses interact with vimentin to facilitate entry and trafficking within eukaryotic cells. However, the relationship between *Staphylococcus aureus* and vimentin remains unclear.

Methods: In the current study, we elucidated vimentin expression mechanism in human keratinocytes infected with *S. aureus* using Western blot (WB), Flow cytometry, Immunofluorescence (IF) staining, utilizing neutralizing antibodies, and small interference (si) RNA, and a vimentin overexpression vector. The physical interaction between vimentin and *S. aureus* was shown by IF on cell surface, intra- and intercellular space.

Results: HaCaT cells increased vimentin expression through physical interaction with live *S. aureus*, and not by heat-killed bacteria or bacterial culture supernatants. The Toll-like receptor (TLR) 2 signaling pathway, which includes interleukin 1 receptor-associated kinase (IRAK) and nuclear factor kappa B (NF-κB)/c-Jun N-terminal kinase (JNK) signaling activation, was involved in *S. aureus*-mediated vimentin expression. The vimentin protein induced by *S. aureus* was secreted extracellularly and bound to *S. aureus* in the culture media. The binding of vimentin to *S. aureus* accelerated the intracellular infection of HaCaT cells.

Discussion: Thus, these experiments elucidated the mechanism of vimentin protein expression during *S. aureus* infection in human skin keratinocytes and revealed the role of vimentin in this process. These findings suggest that vimentin could serve as a potential target for the prevention or treatment of *S. aureus* infections.

KEYWORDS

vimentin, *Staphylococcus aureus*, keratinocytes, HaCaT cells, skin infection, TLR signaling

1 Introduction

Vimentin is an intermediate filament protein whose expression is specifically increased in cells undergoing epithelial-mesenchymal transition (EMT). It is overexpressed in a variety of epithelial cancers, including lung cancer, breast cancer, gastrointestinal cancer, prostate cancer, malignant melanoma, and central nervous system cancers. The overexpression of vimentin in cancer cells is closely linked to tumor growth, invasion, and poor prognosis (Ivaska, 2011; Satelli and Li, 2011). Although vimentin was initially described in a limited number of physiological and pathophysiological contexts, recent findings have revealed that it plays diverse roles across a wide range of cellular and tissue functions. Additionally, vimentin is associated with various human diseases, including cataracts, cancer, Crohn's disease, and HIV (Muller et al., 2009; Satelli and Li, 2011; Henderson et al., 2014). It is a crucial component of the cytoplasmic intermediate filaments (IFs) of astrocytes, which play vital roles in the organization of the central nervous system (CNS) and control many functions of the brain, spinal cord, and retina in both health and disease (Ridge et al., 2022).

On the other hand, vimentin plays a significant role in bacterial transport and the subsequent immune-inflammatory responses (Murli et al., 2001; Guignot and Servin, 2008; Su et al., 2019). When expressed on the cell surface, vimentin can exhibit both pro- and anti-bacterial properties, promoting bacterial invasion in certain contexts while limiting bacterial survival in others (Zou et al., 2006). Additionally, vimentin is secreted and found extracellularly, where it primarily regulates inflammation induced by bacterial infections (Mor-Vaknin et al., 2003). Vimentin has been shown to play important roles in virus attachment and entry of severe acute respiratory syndrome-related coronavirus (SARS-CoV), dengue and encephalitis viruses, among others. Moreover, the presence of vimentin in specific virus-targeted cells and its induction by proinflammatory cytokines and tissue damage contribute to its implication in viral infection (Ramos et al., 2020). Since vimentin is involved in bacterial and viral infections, and consequently induces inflammatory responses, which in severe cases can be life-threatening, developing drugs targeting vimentin could have the effect of controlling bacterial and viral infections (Miao et al., 2023). Although vimentin is thought to be involved in bacterial infection, evidence for infection mechanism through the interaction of vimentin and *S. aureus* in skin keratinocytes is unclear.

S. aureus is a species of gram-positive staphylococcus commonly found in the nasal cavity, respiratory tract, and on the skin. While it can lead to various infections, including skin infections, respiratory infections, sinusitis, and food poisoning, it may also exist as part of the normal bacterial flora without causing disease (Gehrke et al., 2023). On the skin, *S. aureus* is responsible for conditions such as folliculitis, boils, and impetigo, primarily through the infection of keratinocytes. Additionally, it can exacerbate atopic dermatitis and, although infrequently, may lead to necrotizing fasciitis as a result of severe soft tissue infections. Systemic infections caused by *S. aureus* can result in toxic shock syndrome. Despite being a component of the normal skin flora, *S. aureus* can pose significant health risks when the integrity of the skin barrier is compromised or when immune function is diminished. Furthermore, this bacterium frequently exhibits antibiotic resistance, complicating treatment efforts (David and Daum, 2017; Clebak and Malone, 2018; Geoghegan et al., 2018).

S. aureus can survive within human skin keratinocytes at concentrations 20 times higher than the standard minimal inhibitory concentration of commonly utilized anti-staphylococcal antibiotics, including flucloxacillin, teicoplanin, clindamycin, and linezolid, with the exception of rifampicin. Consequently, the internalization of *S. aureus* by human skin keratinocytes enables the bacteria to evade elimination by the majority of anti-staphylococcal antibiotics. This underscores the necessity for antimicrobial strategies that incorporate combinations of antibiotics capable of effectively penetrating animal cells to treat *S. aureus* infections (Al Kindi et al., 2019; Ngo et al., 2022).

Although cell surface receptors, such as fibronectin and integrins, are known to play a role in the intracellular infection of *S. aureus*, the function of vimentin has not yet been reported. Therefore, elucidating the role of vimentin in the infection of keratinocytes by *S. aureus* may enhance our understanding of immune evasion strategies and the pathogenesis of skin commensals, including *S. aureus*. The human skin serves as a primary defense mechanism and is frequently exposed to various pathogens, including *S. aureus*. Abnormal skin conditions, such as atopic dermatitis, create an environment conducive to *S. aureus* infection, allowing the bacteria to penetrate the stratum corneum, where it can proliferate and disseminate. Consequently, this study aims to elucidate the role of vimentin in the infection of keratinocytes by *S. aureus*, as well as the expression mechanisms triggered by the interaction between TLR2 present on the surface of HaCaT cells and *S. aureus*.

2 Results

2.1 *S. aureus* increased vimentin expression in HaCaT cells

To analyze gene variation in *S. aureus*-infected HaCaT cells, transcriptome analysis was performed (Supplementary Figure 1). Four genes—vimentin, SERPINE1, SPN, and PRELP—known to have a strong correlation with *S. aureus* infection, were selected from those whose expression increased more than fivefold in response to *S. aureus* in the quantitative RNA sequencing. In the following experiment, real-time PCR demonstrated that vimentin mRNA levels increased in a time-dependent manner, reaching approximately a nine-fold increase at 6 h post-infection, while the expression pattern of the other genes were atypical. Given that vimentin plays a crucial role in intracellular infections caused by viruses and bacteria (Ramos et al., 2020), we chose to further investigate vimentin, which was shown to be statistically and dose-dependently elevated by *S. aureus*, to evaluate its impact on *S. aureus* infection in HaCaT cells. Vimentin expression was

observed not only in HaCaT cells, which are keratinocytes of the skin, but also in colonic epithelial cells. We observed that vimentin expression increased following *S. aureus* infection in HT-29, HCT-116, and CT-26 cells (Supplementary Figure 2). While vimentin demonstrates a response to *S. aureus* infection in various cell types, this study specifically focused on elucidating its expression mechanism in skin keratinocytes.

It appears that HaCaT cells do not express detectable levels of vimentin protein under normal conditions. However, upon infection with *S. aureus*, vimentin levels increased for up to 6 h before declining (Figure 1A, upper panel). The relative quantities of protein bands from the Western blot are displayed in the lower panel of Figure 1A. In contrast to intracellular expression, the cell surface expression of vimentin remained unchanged up to 3 h post-infection but increased by 21% after 6 h (Figure 1B). The expression of vimentin in HaCaT cells was mediated by live *S. aureus*, as neither heat-killed *S. aureus* nor soluble factors in the culture supernatants influenced vimentin expression (Figure 1C, left panel). In experiments utilizing a transwell chamber, separate incubation of *S. aureus* and HaCaT cells did not induce vimentin expression. In contrast, vimentin expression was induced in the co-culture of *S. aureus* and HaCaT cells within a non-isolated chamber. The relative quantities of protein bands obtained from Western blots are presented in the right panel of Figure 1C. These results suggest that vimentin expression necessitates physical interaction between live *S. aureus* and HaCaT cells, and that an intact cell surface factor on *S. aureus* may play a crucial role in its interaction with host cells.

Vimentin expression was differentially regulated in HaCaT cells treated with probiotics and pathogens. As shown in Figure 1D, *Lactiplantibacillus plantarum* K8 did not induce vimentin expression in HaCaT cells, whereas it increased in a dose-dependent manner in *S. aureus*-treated HaCaT cells (Figure 1D, upper panel). The relative quantities of protein bands are displayed in the lower panel. This finding suggests that probiotics and non-pathogenic bacteria do not stimulate vimentin expression in HaCaT cells, which may influence bacterial infection. Vimentin expression increased in both the cytoplasm and on the cell surface in a time-dependent manner following *S. aureus* infection (Figures 1E, F). The relative quantities of fluorescence intensities are illustrated in Figure 1G, clearly demonstrating that the expression of total

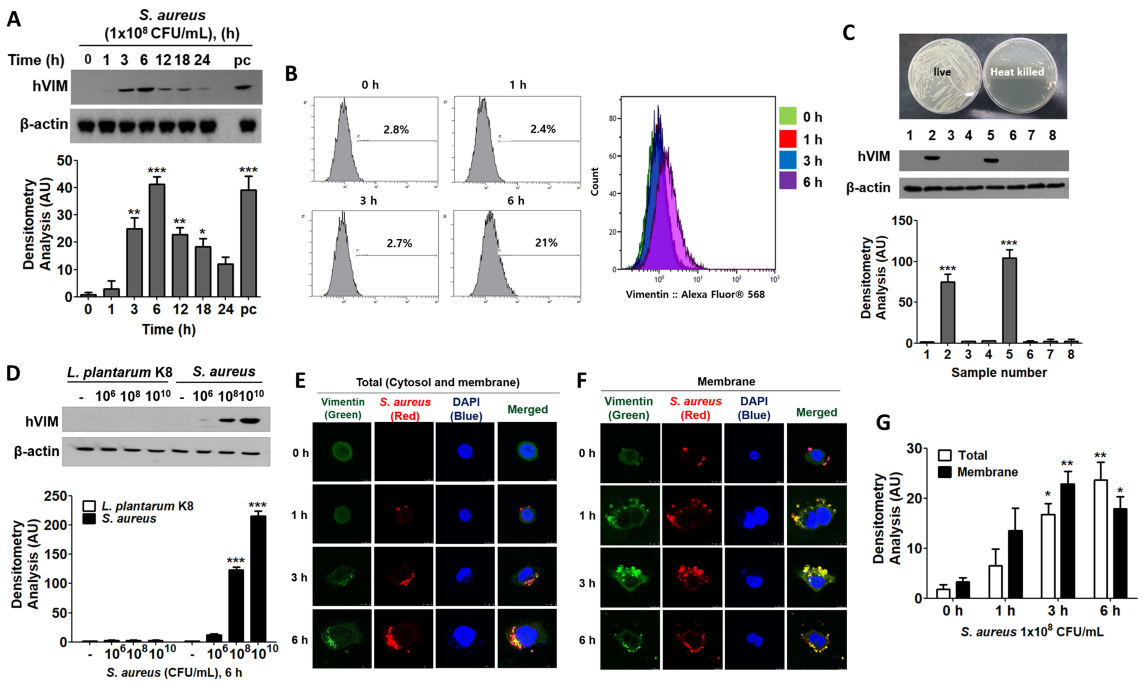

FIGURE 1
Vimentin expression in HaCaT cells treated with *S. aureus*. **(A)** HaCaT cells were treated with $1x10^8$ CFU/mL of *S. aureus* for the indicated times and cells were washed, lysed, and the protein levels were analyzed using Western blot (WB). **(B)** The cell surface expression of vimentin was assessed through fluorescence-activated cell sorting (FACS) analysis after treatment with $1x10^8$ CFU/mL of *S. aureus* for the indicated times. **(C)** HaCaT cells were treated with live and heat-killed *S. aureus* (1×10^8 CFU/mL) and culture medium for 6 h. A transwell chamber was employed to separate the HaCaT cells from *S. aureus*. Following the harvesting of HaCaT cells, vimentin protein expression was evaluated using WB. Lane 1: Untreated; lane 2: Treatment with live *S. aureus*; lane 3: Treatment with heat-killed *S. aureus*; lane 4: Separate culture of *S. aureus* and HaCaT cells in a transwell chamber; lane 5: Non-isolated co-culture of *S. aureus* and HaCaT cells in a transwell chamber; lane 6: Treated with brain heart infusion (BHI) medium; lane 7: Treatment with culture supernatant from *S. aureus* cultured in BHI; lane 8: Treatment with culture supernatant from HaCaT cells treated with *S. aureus*. **(D)** HaCaT cells were treated with the specified doses of *L. plantarum* K8 and *S. aureus* for 6 h, after which intracellular vimentin was analyzed by WB. **(E, F)** Immunofluorescence staining was conducted on *S. aureus*-infected HaCaT cells. Cells were permeabilized prior to staining to assess cytoplasmic vimentin expression **(E)**, while intact cells were stained to evaluate membrane-bound vimentin expression **(F)**. **(G)** Densitometric image analysis of fluorescence intensities in panels **(E, F)** was conducted using ImageJ software. For panels **(A, C, D)**, densitometric image analysis of band intensities was also performed using ImageJ software. The data are presented as the mean ± SD and were statistically analyzed using a one-way ANOVA followed by Tukey's multiple comparison test (for panels **A, C, G**) and a two-way ANOVA (for panel **D**). Statistical significance was defined as *p < 0.05, **p < 0.01, and ***p < 0.001.

vimentin (both cytosolic and membrane-bound) and the expression of membrane-bound vimentin increased in a time-dependent manner. Immunofluorescence (IF) images demonstrated that vimentin was associated with *S. aureus* in the cytoplasm and on the cell surface, indicating that the binding of *S. aureus* to vimentin may impact the intracellular infection of *S. aureus* in HaCaT cells.

2.2 *S. aureus* internalized into HaCaT cells via vimentin

When HaCaT cells were treated with $1x10^8$ CFU/mL of *S. aureus* for the indicated times, intracellular *S. aureus* was increased up to 6 h and subsequently decreased (Figure 2A). This trend in *S. aureus* infection parallels the pattern of vimentin expression in HaCaT cells exposed to *S. aureus*, as shown in Figure 1A. HaCaT cell viability began to decline at 6 h post-infection with *S. aureus* and was significantly reduced by 12 h post-infection (Figure 2B). This decline in cell viability accounts for the decrease in intracellular CFU observed at 12 h post-infection in Figure 2A. Experiments utilizing CRISPR-Cas9 to knock down vimentin demonstrated that not only was cytoplasmic vimentin expression diminished, but intracellular *S. aureus* infection was also reduced (Figures 2C, D). The densitometric analysis of the Western blot presented in Figure 2C demonstrated a significant reduction in vimentin levels due to CRISPR-Cas9 treatment (Figure 2C, lower panel). Overexpression of vimentin in HaCaT cells via a transgenic vimentin expression vector resulted in a dose-dependent increase

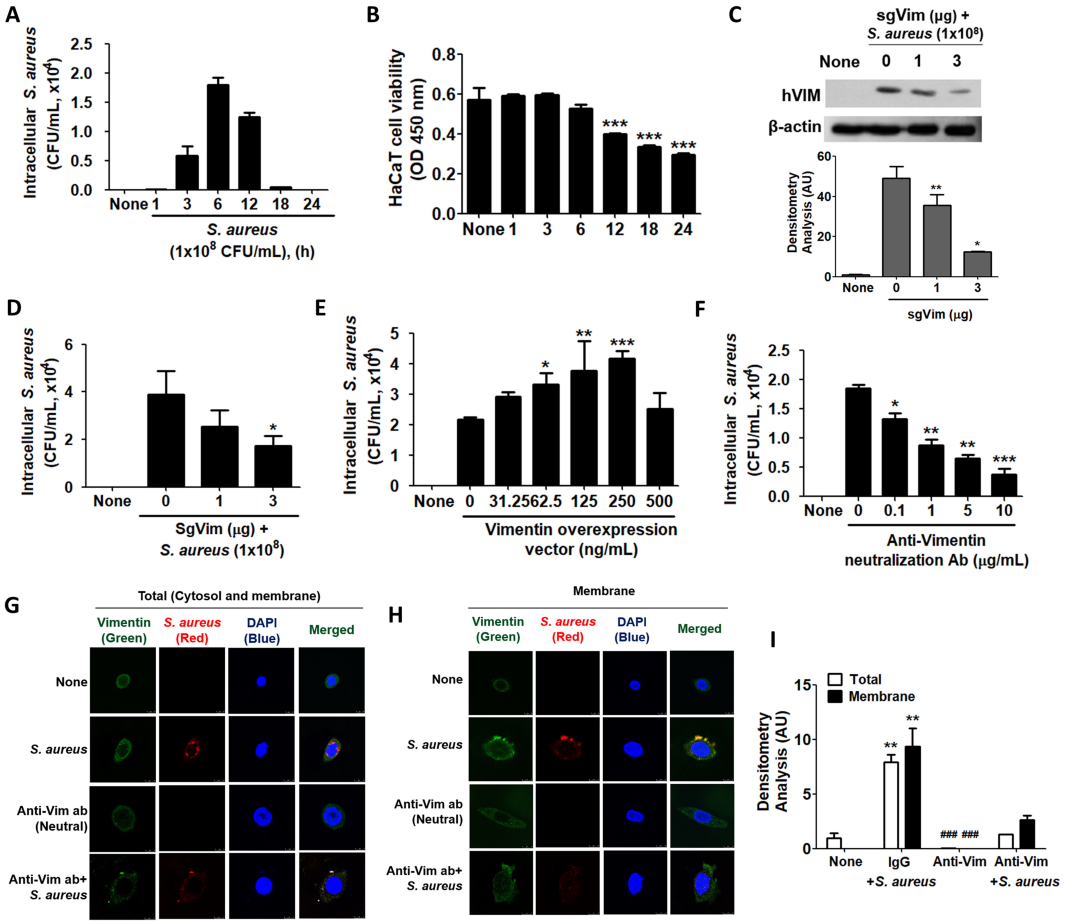

FIGURE 2
Intracellular infection of *S. aureus* using vimentin. **(A)** HaCaT cells were treated with $1x10^8$ CFU/mL of *S. aureus* for the indicated times, and cell lysates were plated on BHI agar to quantify colony-forming units (CFU). **(B)** Following infection with $1x10^8$ CFU/mL of *S. aureus* for the indicated time periods, a cell viability assay was conducted using WST-1 reagent. **(C, D)** Vimentin-specific sgRNA (sgVim) was transfected into HaCaT cells, which were subsequently treated with $1x10^8$ CFU/mL of *S. aureus* for 6 h Vimentin expression was evaluated using WB, and densitometric analysis of band intensities was conducted with ImageJ software. **(C)**. Intracellular *S. aureus* infection was evaluated by BHI agar plating of cell lysates **(D)**. **(E)** HaCaT cells were transiently transfected with the indicated dose of a vimentin overexpression vector and subsequently treated with $1x10^8$ CFU/mL of *S. aureus* for 6 h. The intracellular *S. aureus* infection was assessed by BHI agar plating of cell lysates. **(F)** HaCaT cells were pre-treated with control immunoglobulin (IgG) or with the indicated dose of an anti-vimentin neutralizing antibody for 30 min, followed by treatment with $1x10^8$ CFU/mL of *S. aureus* for 6 h. The intracellular *S. aureus* infection was evaluated through BHI agar plating of cell lysates. **(G, H)** HaCaT cells were pre-treated with control IgG or 10 μg/mL of an anti-vimentin neutralizing antibody for 30 min, followed by treatment with $1x10^8$ CFU/mL of *S. aureus* for 6 h. IF staining was performed to detect intracellular *S. aureus* **(G)** and cell surface-bound *S. aureus* **(H)**. **(I)** Densitometric image analysis of fluorescence intensities in images G and H was conducted using ImageJ software. Data were expressed as the mean ± SD and were statistically analyzed using a paired, one-tailed t-test **(A)** and one-way ANOVA followed by Tukey's multiple comparison test in the other cases. *$p < 0.05$, **$p < 0.01$, and ***$p < 0.001$.

in intracellular *S. aureus* infection, with the exception of a high vector dose of 500 ng/mL (Figure 2E). Similar results were obtained in experiments employing an anti-vimentin neutralizing antibody. As shown in Figure 2F, intracellular *S. aureus* levels in HaCaT cells were significantly reduced in a dose-dependent manner with the neutralizing antibody. In IF images, intracellular *S. aureus* levels increased and were associated with vimentin protein, whereas *S. aureus* was barely detectable in cells treated with the anti-vimentin neutralizing antibody (Figure 2G). In control experiments, *S. aureus* bound to vimentin on the cell membrane; however, no binding between *S. aureus* and vimentin was observed in cells treated with the anti-vimentin neutralizing antibodies (Figure 2H). Notably, *S. aureus* was undetectable in the neutralizing antibody experiments, indicating that the anti-vimentin antibody effectively blocked *S. aureus* binding to cell surface vimentin (Figure 2H). Densitometric analysis of fluorescence intensities in the merged images presented in Figures 2G, H revealed consistent results: neutralizing antibodies against vimentin decreased both intracellular infection and membrane association of *S. aureus* when compared to control IgG treatment (Figure 2I).

Unlike *S. aureus*, probiotics such as *L. plantarum* and *Enterococcus faecium* rarely cause intracellular infections in HaCaT cells. When HaCaT cells were treated with $1x10^8$ CFU/mL of bacteria for 6 h, *L. plantarum* was infected 400 times less frequently, and *E. faecium* was infected approximately 50 times less frequently than *S. aureus* (Supplementary Figure 3). These probiotics did not induce vimentin expression in HaCaT cells, suggesting a close association between vimentin and the intracellular infection of bacteria. In contrast, *Escherichia coli* and *Shigella flexneri*, which are classified as pathogens, induced less vimentin expression in HaCaT cells compared to *S. aureus* and caused approximately 40 to 80 times less intracellular infection (Supplementary Figure 4). These results further imply a strong correlation between vimentin expression and infection in HaCaT cells.

2.3 Secreted vimentin binds to *S. aureus* and facilitates intracellular infection

It is known that vimentin is secreted into the extracellular space and plays a role in bacterial killing and the generation of oxidative metabolites in activated macrophages (Mor-Vaknin et al., 2003). In this study, we investigated whether vimentin levels increase in HaCaT cells treated with *S. aureus* and whether it is secreted extracellularly to interact with the bacteria. Notably, only live *S. aureus* induced vimentin expression in HaCaT cells, and vimentin was detected in the extracellular space (Figure 3A, left panel). The relative quantities of protein bands obtained from Western blots are shown in the right panel of Figure 3A. Vimentin expression was significantly increased both intracellularly and extracellularly by live *S. aureus*. To investigate the interaction between *S. aureus* and vimentin, IF analysis was performed. As shown in Figure 3B, when *S. aureus* was added to conditioned media (CM) derived from unstimulated HaCaT cells, only *S. aureus* was detected, while vimentin was absent. Conversely, when *S. aureus* was added to CM obtained from HaCaT cells previously treated with *S. aureus*, both vimentin and *S. aureus* were detected, and binding between vimentin and *S. aureus* was observed. The relative quantities of fluorescence intensity are displayed in the lower panel of Figure 3B, indicating that the intensity decreased proportionally with dilution. Similar results were obtained when *S. aureus* was added to diluted CMs or media containing recombinant vimentin. The binding of vimentin to *S. aureus* was observed in both the intracellular (cytoplasmic and membrane) regions and at the cell surface (Figure 3C). The relative quantities of fluorescence intensities are presented in the lower panel of Figure 3C, indicating that *S. aureus* infection enhances vimentin expression and its binding. Additionally, vimentin binding to *S. aureus* was observed at locations distant from the cell (see enlarged box), suggesting that vimentin may interact with *S. aureus* in the extracellular space rather than solely at the cell surface, potentially facilitating the intracellular infection of *S. aureus*.

2.4 TLR2 was primarily involved in the induction of vimentin in HaCaT cells treated with *S. aureus*

S. aureus is known to interact with Toll-like receptors (TLRs), fibronectin (FN), and integrins (Kielian et al., 2005; Stenzel et al., 2008; Josse et al., 2017). We investigated which receptor is involved in the initiation of vimentin expression by *S. aureus* in HaCaT cells. First, small interfering RNA (siRNA) targeting TLR2 and TLR4 was applied, and a decrease in the expression of TLR2 and TLR4 was observed by WB (Figures 4A, B). siTLR2 RNA inhibited vimentin expression in a dose-dependent manner, whereas siTLR4 had no effect. Densitometric analysis of protein bands yielded similar results (Lower panels in Figures 4A, B). Vimentin expression was significantly decreased in TLR2 knockdown cells, while it remained significantly increased in TLR4 knockdown cells. Neutralizing antibody against CD36 also showed no inhibitory effect on vimentin expression in HaCaT cells treated with *S. aureus* (Figure 4C). siRNA targeting fibronectin 1 (FN1) significantly reduced vimentin expression in cells treated with 10 nM and 20 nM of FN1 siRNA (Figure 4D). Additionally, vimentin expression was decreased by the ATN161 inhibitor, an antagonist of integrin $\alpha5\beta1$, suggesting that $\alpha5\beta1$ may play a role in *S. aureus*-mediated vimentin expression (Figure 4E). The results of the densitometric analysis of protein bands are presented in the lower panel of each figure. Collectively, these findings indicate that TLR2 is primarily involved in vimentin expression in HaCaT cells treated with *S. aureus*, while fibronectin and integrin also contribute to vimentin expression. Notably, when HaCaT cells were transiently transfected with siTLR2 RNA, intracellular *S. aureus* infection was significantly reduced in a dose-dependent manner (Figure 4F).

2.5 NF-κB and JNK signaling pathways are implicated in the regulation of vimentin expression in HaCaT cells exposed to *S. aureus*

Signaling initiation through TLR2 recruits interleukin-1 receptor-associated kinase (IRAK) proteins, with IRAK4 forming

10.3389/fcimb.2025.1543186

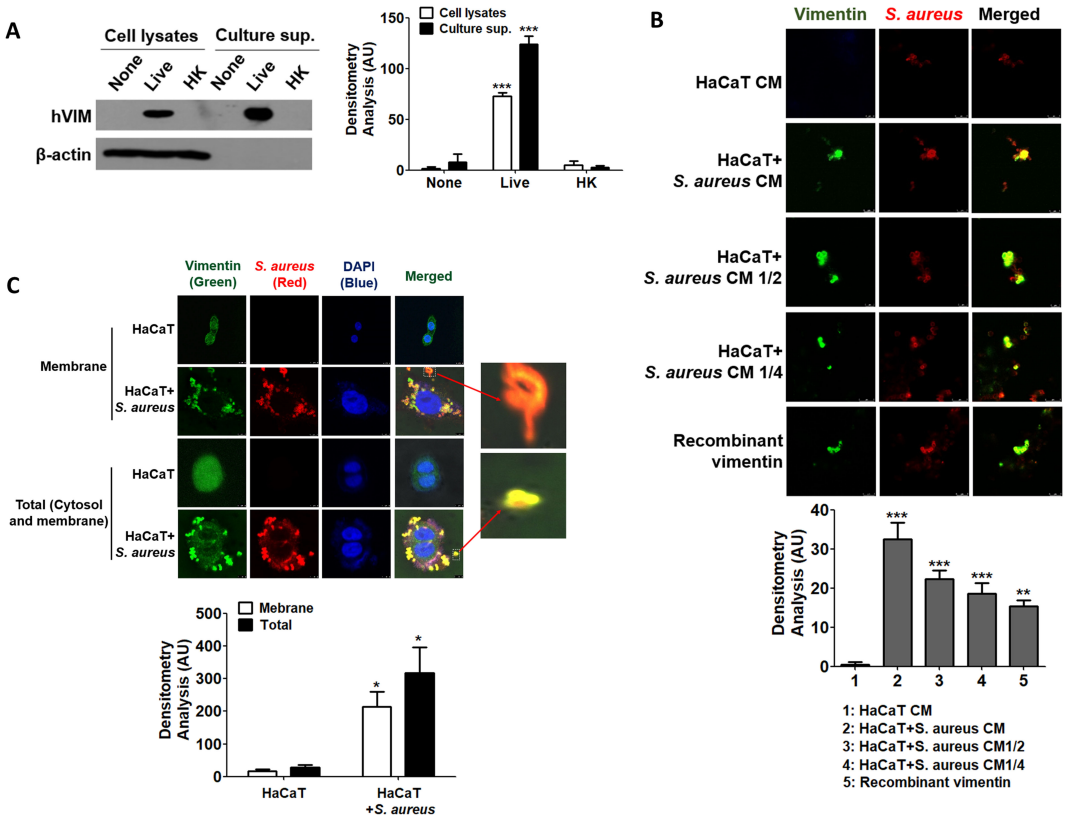

FIGURE 3
Binding of secreted vimentin to *S. aureus*. **(A)** HaCaT cells were treated with 1x10^8 CFU/mL of live *S. aureus* or heat-killed *S. aureus* for 6 h, and vimentin was detected by WB in both cell lysates and culture supernatants. **(B)** CM were prepared from untreated HaCaT cells and from HaCaT cells treated with 1x10^8 CFU/mL of *S. aureus* for 6 h. CM, diluted CMs, and recombinant vimentin were incubated with 2x10^6 CFU/mL of live *S. aureus* for 1 h, followed by IF analysis. **(C)** HaCaT cells were treated with 1x10^8 CFU/mL of *S. aureus* for 6 h, and IF was performed to observe the interaction between vimentin and *S. aureus* in the cytoplasm and on the cell surface. The binding of *S. aureus* to vimentin, which detached from HaCaT cells, is shown enlarged in the box. Densitometric image analysis of band intensities **(A)** and fluorescence intensities **(B, C)** was conducted using ImageJ software. The data are expressed as the mean ± SD and were statistically analyzed using a one-way ANOVA followed by Tukey's multiple comparison test in the other instances. *p < 0.05 and ***p < 0.001.

a heterodimer with either IRAK1 or IRAK2 (Pereira and Gazzinelli, 2023). The expression of IRAK family proteins was found to increase in a time-dependent manner in HaCaT cells treated with 1x10^8 CFU/mL of *S. aureus* (Figure 5A). Additionally, the protein levels of downstream signaling molecules, such as tumor necrosis factor receptor-associated factor 6 (TRAF6) and transforming growth factor-β-activated kinase 1 (TAK1), also exhibited a time-dependent increase, indicating that the TLR2 signaling pathway was activated by *S. aureus*. Notably, the protein expression of IRAK-M was also elevated, which may play a role in inhibiting *S. aureus*-mediated signaling initiated at TLR2 at some stage. The TLR2-mediated signaling pathway initiated by *S. aureus* led to the activation of p38, c-Jun N-terminal kinases (JNK)1/2, NF-kappa-B inhibitor alpha (IκBα), and transcription factors such as c-Jun and nuclear factor kappa B (NF-κB) (Figure 5B). The results of the densitometric analysis of protein bands are presented in the lower panels of each figure. Furthermore, when HaCaT cells were treated with inhibitors targeting specific signaling molecules prior to *S. aureus* exposure, the inhibitors for NF-κB and JNK resulted in a reduction of vimentin expression, suggesting that these signaling pathways are primarily implicated in *S. aureus*-mediated vimentin expression in HaCaT cells (Figure 5C, upper panel). Densitometric analysis indicated that the Akt and p38 signaling pathways were also implicated in vimentin expression (Figure 5C, lower panel).

3 Discussion

Through this experiment, we discovered that vimentin, which is expressed following the binding of *S. aureus* to TLR2 on skin keratinocytes, facilitates the internalization of *S. aureus* into HaCaT cells. Notably, heat-killed *S. aureus* did not induce vimentin expression in HaCaT cells, nor did it result in internalization. Only live *S. aureus* was found to induce vimentin expression in HaCaT cells and influence the internalization process. This observation suggests that a component on the surface of *S. aureus* interacts with TLR2, and this protein appears to be particularly sensitive to heat. Generally, ligands that bind to TLR2 in bacteria include lipoteichoic acid (LTA), lipoproteins, and peptidoglycan (Fournier, 2013). Among these, LTA is relatively heat-stable (Grunfeld et al., 1999). Conversely, peptidoglycan and lipoproteins are susceptible to heat, leading to the expectation that

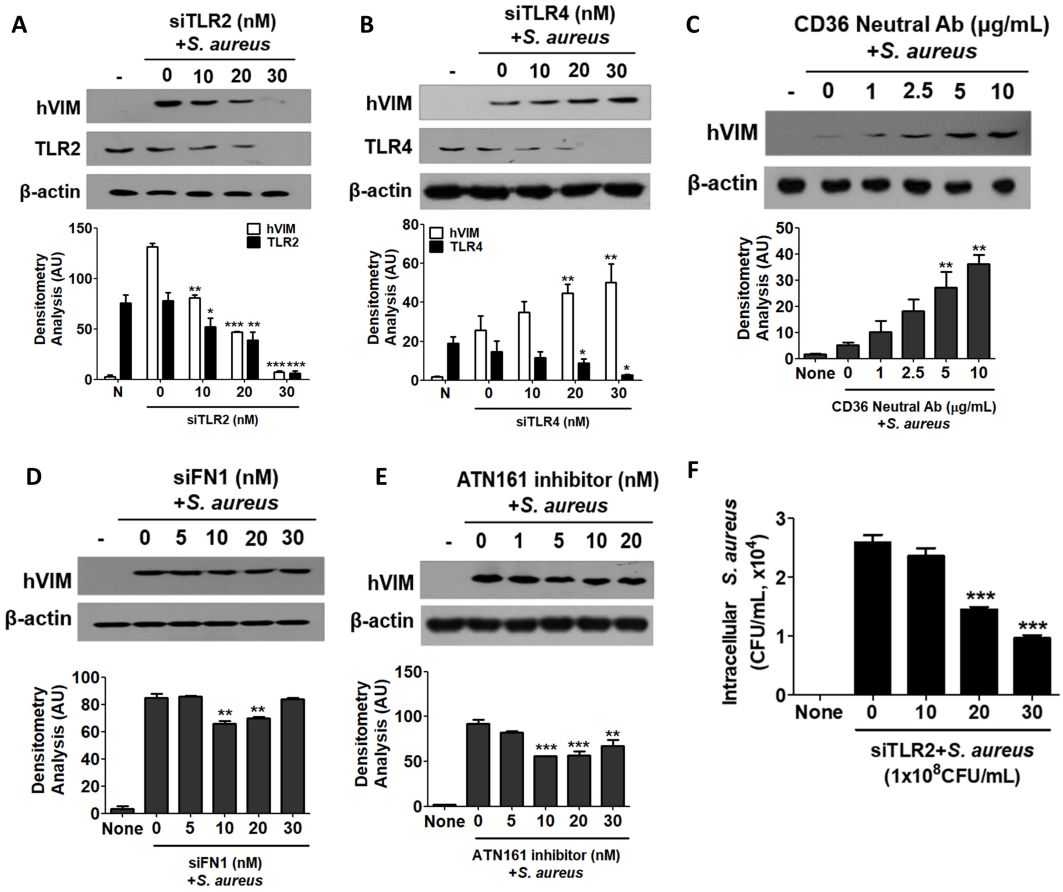

FIGURE 4
Cell surface receptors involved in signaling initiation. **(A-E)** HaCaT cells were pre-treated for 30 min with small interfering RNA targeting TLR2 **(A)**, TLR4 **(B)**, neutralizing antibodies against CD36 **(C)**, FN1 **(D)**, or an inhibitor of ATN161 **(E)**. Subsequently, the cells were exposed to 1 x 10^8 CFU/mL of *S. aureus* for 6 h. Cell lysates were analyzed using Western blotting to assess intracellular vimentin expression. **(F)** HaCaT cells were transiently transfected with siTLR2 RNA and subsequently treated with 1x10^8 CFU/mL of *S. aureus* for 6 h. Following lysis, the cells were plated onto BHI agar plates, and CFU were counted after overnight incubation. Densitometric image analysis of band intensities was conducted using ImageJ software **(A-E)**. The data are presented as the mean ± SD and were statistically analyzed using one-way ANOVA followed by Tukey's multiple comparison test. A significance level of *p < 0.05, **p < 0.01, and ***p < 0.001 was observed.

these substances would bind to TLR2 in HaCaT cells and induce vimentin expression (Cebrián et al., 2017; Jiang et al., 2023). Previous research has indicated that the transcription factors AP-1 and NF-kB are crucial for vimentin expression (Paulin et al., 2022). In this study, we demonstrated that the JNK and NF-kB signaling pathways are significant in vimentin expression in HaCaT cells treated with *S. aureus*, as evidenced by experiments utilizing specific inhibitors. The activation of the JNK and NF-kB pathways occurs via IRAK proteins following the binding of *S. aureus* to TLR2. Vimentin expressed in response to *S. aureus* was detected not only in the cytoplasm of skin keratinocytes but was also secreted onto the cell surface and into the culture medium. Intracytoplasmic vimentin contributes to the mechanical integrity of cells and aids in the localization of intracellular components (Guo et al., 2013). Cell surface vimentin may function as a receptor or ligand for endogenous proteins, such as von Willebrand factor (vWF), as well as for exogenous proteins, including those derived from bacteria and viruses (Paulin et al., 2022). However, the role of vimentin that is secreted into the intercellular space, particularly in the context of bacterial intracellular infection, remains poorly understood. In this study, we demonstrated that vimentin secreted into the intercellular space binds to *S. aureus* and facilitates its entry into the cell. These findings contribute to a better understanding of the role of secreted vimentin in bacterial infection.

Secreted vimentin has been shown to bind to *S. aureus*, facilitating intracellular infection. Notably, findings from our experiments suggest a correlation between vimentin expression and *S. aureus* infection. Specifically, probiotics did not induce vimentin expression, which consequently resulted in a lack of intracellular internalization. In contrast, *E. faecium*, *E. coli*, and *S. flexneri* exhibited significantly lower levels of intracellular internalization compared to *S. aureus*, and these bacteria also did not induce high levels of vimentin expression relative to *S. aureus*. This indicates a strong relationship between vimentin expression and the intracellular infection process of *S. aureus*. Probiotics, such as *L. plantarum* K8, did not promote vimentin expression, leading to the conclusion that intracellular infection did not occur in these cases. Conversely, while *E. coli* and *S. flexneri* were not expressed in this experiment, they demonstrated higher rates of intracellular internalization into HaCaT

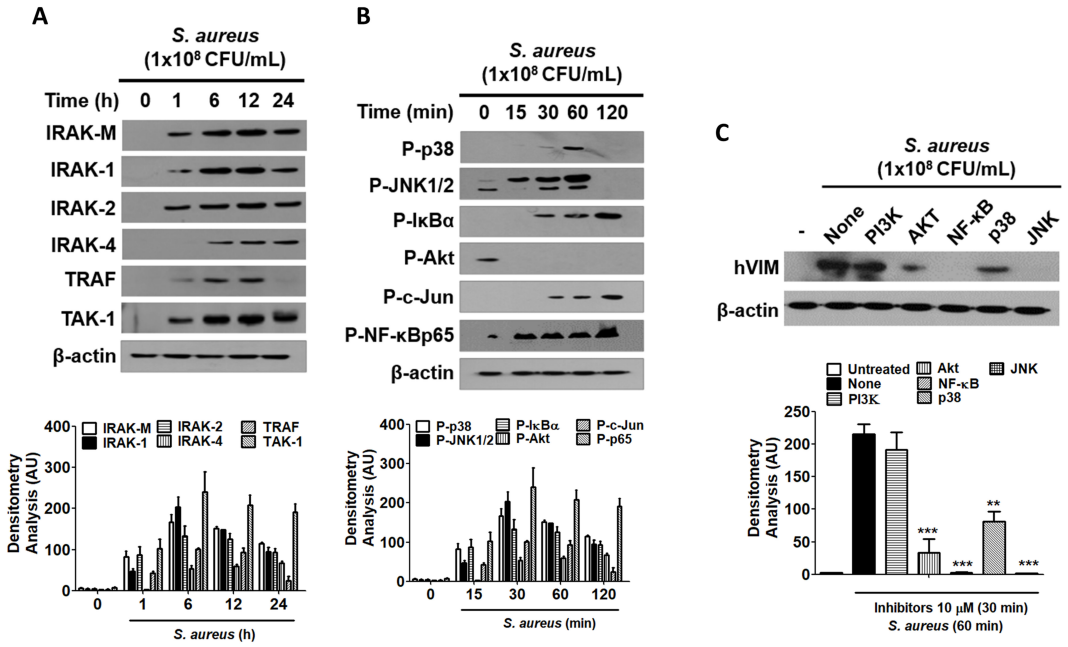

FIGURE 5
The role of NF-κB and JNK in vimentin expression. **(A, B)** HaCaT cells were treated with 1x10^8 CFU/mL *S. aureus* for the indicated times. TLR2 associated protein levels were examined by WB **(A)** and the activation of signaling molecules were detected by WB **(B)**. **(C)** HaCaT cells were pre-treated with 10 μM inhibitors for 30 min, followed by exposure to 1 x 10^8 CFU/mL *S. aureus* for 60 min. Vimentin expression was analyzed via WB using cell lysates. Densitometric image analysis of band intensities was conducted using ImageJ software and is presented in the lower panels (**A-C**). The data are presented as the mean ± SD and were statistically analyzed using one-way ANOVA followed by Tukey's multiple comparison test. A significance level of **p < 0.01 and ***p < 0.001 was observed.

cells compared to probiotics. This difference can be attributed to the ability of gram-negative pathogens to utilize various infection routes, as noted in previous studies (Gophna et al., 2001; Schroeder and Hilbi, 2008). However, some literature indicates that *E. coli* can enhance vimentin expression and interact with it during the process of intracellular internalization (Chi et al., 2010). The absence of this phenomenon in our experiment may be attributed to the specific characteristics of the HaCaT cells utilized or the possibility that vimentin expression in *S. aureus* was sufficiently robust to remain relatively undetectable.

Current knowledge identifies several factors that mediate the binding of pathogens to vimentin, including IbeA and MBP-1. Additionally, various bacterial factors, such as SptP, SpyA, CPAF, and AptA, have been reported to interfere with vimentin's function, potentially through mechanisms involving proteolysis or post-translational modifications (Chi et al., 2010; Humphreys et al., 2009; Icenogle et al., 2012; Snavely et al., 2014; Babrak et al., 2015; Zhao et al., 2024). To date, there has been no investigation into the relationship between vimentin and the intracellular infection of *S. aureus*. In the present study, we confirmed the binding of vimentin to *S. aureus* through IF and neutralizing antibody assays. However, the specific factor of *S. aureus* that interacts with vimentin remains unidentified. The attachment and internalization of *S. aureus* may be modulated by Staphylococcal protein A (spa) and coagulation factor B (clfB), which are produced by the regulatory factor SpoVG, a known general regulatory element in *S. aureus* (Zhu et al., 2019). The pathogenesis of invasive *S. aureus* infections is attributed to various virulence factors, including protein A and alpha-hemolysin (Hla), which engage host signaling pathways to induce pathological effects. *S. aureus* exploits the inflammatory predisposition of human keratinocytes to trigger pyroptosis, a form of inflammatory cell death that is dependent on caspase 1, which is essential for the bacterium's ability to penetrate the keratinocyte barrier (Soong et al., 2012). The infection of skin keratinocytes by *S. aureus* can involve several mechanisms, including the utilization of sphingosine 1-phosphate and its receptor, integrin-linked kinase, Rac1, the Chemerin-CMKLR1 axis, fibronectin-binding protein, and multiple high-affinity fibronectin-binding repeats within fibronectin-binding protein A (Edwards et al., 2011; Bur et al., 2013; Nguyen et al., 2018; Igawa et al., 2019; Chen et al., 2024). From the perspective of a host cell, TLR2 and lipoprotein-like lipoproteins have been implicated in the infection process of *S. aureus* (Sayedyahossein et al., 2015). In addition, actin filaments, microtubules, receptor-mediated endocytosis, and protein tyrosine kinases are critical for the uptake of *S. aureus*. Furthermore, fibronectin-binding protein and β1-integrin have been identified as essential cell surface molecules that facilitate the internalization of *S. aureus* by non-phagocytic cells (Alexander and Hudson, 2001). Future research should focus on a comprehensive examination of the interactions between the surface proteins of *S. aureus* and the receptors present on the surface of eukaryotic cells.

It can be challenging to recognize bacterial infections as a significant contributor to cancer. Nevertheless, studies have demonstrated two primary mechanisms by which bacteria are associated with cancer: the production of carcinogenic metabolites and the induction of chronic inflammation. For

example, certain species of Bacteroides can generate phenocarpentaene, a potent mutagen, in substantial quantities under laboratory conditions. *Helicobacter pylori* has a lifelong propensity to induce inflammation and is epidemiologically linked to adenocarcinoma of the distal stomach (Parsonnet, 1995). *H. pylori* infection is recognized as a contributing factor to stomach cancer, while persistent chlamydial infection is a risk factor for the development of cervical cancer, particularly in patients who are concurrently infected with human papillomavirus (HPV) (Yusuf et al., 2023). Among survivors of *S. aureus* bacteremia (SAB), the risk of developing primary cancer was found to be 65% higher than in a randomized control group, suggesting that susceptibility to infectious diseases may serve as a marker of immunodeficiency related to cancer (Gotland et al., 2020). Indeed, chronic *S. aureus* infection has been associated with an increased risk of certain cancers, including skin and oral cancers. Chronic inflammation resulting from persistent *S. aureus* infection may lead to DNA damage, disrupt cell signaling pathways, and create an immunosuppressive microenvironment that promotes cancer progression (Odunitan et al., 2024). Vimentin is known to be overexpressed in various epithelial malignancies, including breast, gastrointestinal, prostate, central nervous system, lung cancers, and malignant melanoma (Satelli and Li, 2011). For example, patients diagnosed with vimentin-positive gastric cancer exhibit a significantly poorer prognosis compared to those with vimentin-negative gastric cancer (Fuyuhiro et al., 2010). The presence of vimentin in cancer cells, particularly its secretion into the extracellular environment, is believed to facilitate infections by *S. aureus*. Given vimentin's role in both the metastasis of cancer cells and susceptibility to bacterial infections, exploring the modulation of vimentin may be a viable strategy for achieving both anticancer and antibacterial therapeutic effects.

In conclusion, *S. aureus* enhances the expression of vimentin protein via TLR2 signaling in keratinocytes. Vimentin is secreted intracellularly, presented on the cell surface, and released into the extracellular medium, where it binds to *S. aureus*, facilitating the internalization of the bacteria into HaCaT cells. Infected *S. aureus* has the ability to evade the host immune response, allowing for its proliferation and subsequent release. Given the critical role of vimentin in the life cycle of *S. aureus*, there is potential for the development of therapeutics that target vimentin to manage intracellular infections caused by this pathogen.

4 Materials and methods

4.1 Reagents

Neutralizing antibodies, including anti-TLR2 (Cat# MA5-14112) and anti-CD36 (Cat# MA5-11883), were purchased from Invitrogen (MA, USA). siRNAs targeting TLR2 (FlexiTube Genesolution GS7097), TLR4 (GS7044), and FN1 (GS2335) were prepared from Qiagen (Hilden, Germany). ATN-161, an integrin α5β1 receptor antagonist (Cat# 6058), was purchased from R&D Systems (Minneapolis, MN, USA). Inhibitors targeting PI3K (S1109), Akt (S1113), NF-κB (S4902), p38 (S1076), and JNK (S1460) were purchased from Selleck Chemicals LLC (Houston, TX, USA). The primary antibodies used in Western blot (WB) analysis included IRAK-M (Cat# 4369), IRAK-1 (Cat# 4504), IRAK-2 (Cat# 4367), IRAK-4 (Cat# 4363), TRAF (Cat# 8028), TAK-1 (Cat# 4505), phospho-p38 (Cat# 4511), phospho-JNK (Cat# 9251), phospho-IκBα (Cat# 2859), phospho-Akt (Cat# 4060), phospho-c-Jun (Cat# 3270), and phospho-NF-κB p65 (Cat# 3033). These antibodies were acquired from Cell Signaling Technology (Danvers, MA, USA). Rabbit anti-vimentin antibody was purchased from Abcam (ERP3776, Cambridge, UK).

4.2 Cell culture

The human immortalized epidermal keratinocyte cell line HaCaT was maintained in Dulbecco's Modified Eagle's Medium (DMEM) supplemented with 10% heat-inactivated fetal bovine serum (FBS), 2 mM L-glutamine, 100 U/ml penicillin, and 100 µg/ml streptomycin. These cells were cultured at 37°C in a humidified incubator with 5% CO_2, and the medium was changed every 3 to 4 days. To investigate the induction of vimentin expression by *S. aureus* in HaCaT cells, live and heat-killed *S. aureus* were treated to HaCaT cells at specified concentrations and durations. Isolation culture was conducted using a transwell chamber (Corning® Transwell® 6-well plates, CLS3428, Sigma-Aldrich).

4.3 Bacteria preparation

Lactiplantibacillus plantarum K8 (KCTC10887BP) was cultured in 1 L of MRS broth (BD Biosciences, USA) at 37°C overnight. The cells were then harvested by centrifugation at 8000× g for 8 min. *L. plantarum* K8 was washed three times with Dulbecco's phosphate-buffered saline (DPBS) and resuspended in DMEM to achieve the desired concentration. *S. aureus* (ATCC 29523), obtained from the American Type Culture Collection, was inoculated in Brain Heart Infusion (BHI) broth (BD Difco, NJ, USA) and incubated at 37°C for 16 to 18 h in a shaking incubator maintained at 220 rpm. After 24 h, the *S. aureus* culture was transferred to fresh BHI medium and cultured until the exponential phase (OD600 = 1.0) was reached. The bacteria were harvested by centrifugation at 4,000 x g for 10 min and washed three times with DPBS. The resulting pellets were resuspended in DMEM to achieve the desired concentration. To prepare heat-killed bacteria, a separate *S. aureus* culture was subjected to the same conditions and then heat-treated at 90°C for 30 min, with vortexing at 5-min intervals during the heat treatment.

Escherichia coli and *Shigella flexneri* were cultured overnight in a shaking incubator at 37°C using Luria Broth (LB) medium. Each bacterium was diluted 1:100 into 100 mL of fresh LB broth and subcultured at 37°C for 6 h. The cultured bacteria were harvested by centrifugation at 4,000 x g for 10 min and washed three times with DPBS. The resulting pellets were resuspended in DMEM to achieve the desired concentration.

4.4 Construction of CRISPR/Cas9-Based knockdown of vimentin

The construction of the GRISPR/Cas9 vector that targeted vimentin was carried out according to the protocol provided by the vector vendor Toolgen (Seoul, Korea). The CRISPR guide RNA (gRNA) for human vimentin (TCC TAC CGC AGG ATG TTC GGC GG) was designed using the gRNA design tool from GenScript (NJ, USA) and subsequently cloned into the pRGEN-Cas9-CMV expression vector (Bioneer, Daejeon, Korea). Synthesized gRNA vectors (1 μg, 2 μg, 3 μg) and Lipofectamine were mixed with Opti-MEM and added to HaCaT cells (1 x 10^5 cells/mL) that had been stabilized through overnight culture. Subsequently, 1 μg of donor DNA was incorporated into the mixture and allowed to react at room temperature for 30 min. The resulting gRNA/DNA mixture was then transfected into HaCaT cells and incubated at 37°C for 42 h. Following this incubation period, *S. aureus* was introduced at a multiplicity of infection (MOI) of 200. The cells were harvested after 6 h and the reduction in vimentin levels was confirmed via Western blot analysis. After lysing the HaCaT cells with a hypertonic buffer, the cells were plated on BHI plates and the *S. aureus* colonies that had entered the cells were counted.

4.5 HaCaT cell infection with *S. aureus*

HaCaT cells were transfected with siRNA, pretreated with inhibitors, or left untreated before being infected with *S. aureus*. For siRNA transfection, HaCaT cells were seeded in 6-well plates (6 x 10^5 cells/well) and transfected with indicated dose of vimentin siRNA using 6 μl of G-fectin (Genolution, Seoul, Korea). The cells were then incubated for 48 h in a humidified incubator at 37°C with a 5% CO_2 atmosphere. For the inhibitor assays, HaCaT cells were pretreated with the indicated doses of inhibitors for 30 min prior to *S. aureus* infection. The indicated dose of *S. aureus* was added to HaCaT cell cultures and incubated at 37°C in a humidified 5% CO_2 incubator for 6 h. After incubation, the cells were washed three times with DPBS and replaced with fresh DMEM medium containing gentamicin (100 μg/mL), followed by an additional incubation for 1 h to eliminate any remaining extracellular *S. aureus*. The cells were then washed three times with DPBS, and 1 mL of hypertonic buffer [20 mM Tris (pH 7.5), 5 mM MgCl2, 5 mM CaCl2, 1 mM DTT, 1 mM EDTA, 0.1% Triton X-100] was added and incubated at 4°C for 5 min to lyse the infected HaCaT cells. Cell lysates were spread on BHI agar plates, incubated at 37°C, and colonies were counted the following day.

4.6 Western blot analysis

HaCaT cells infected with *S. aureus* were lysed with 2X reducing sample buffer and separated by 10% (v/v) denaturing sodium dodecyl sulfate-polyacrylamide gel electrophoresis (SDS-PAGE) for 2 h at 80 V. Following migration, the proteins were transferred onto a polyvinylidene difluoride (PVDF) membrane (GE Healthcare, Chicago, IL, USA) for 1 h at 100V. The membrane was pre-incubated in blocking buffer [5% (w/v) non-fat dried milk in Tris-buffered saline with 0.05% (v/v) Tween-20 (TBS-T)] for 1 h at room temperature (RT). Subsequently, the membranes were incubated overnight at 4 ˚C with first antibodies. After washing the membranes three times with TBS-T (20 mM Tris-HCl, 150 mM NaCl, 0.05% Tween-20), they were incubated with horseradish peroxidase (HRP)-conjugated anti-rabbit IgG (ab205718, Abcam) secondary antibody for 2 h at RT. Following five washes with TBS-T, the protein bands were detected using ECL Select™ Western Blotting Detection Reagent (Cytiva, MA, USA) and exposed on X-ray film. β-actin (sc-47778, Santa Cruz Biotechnology, CA, USA) was used as an internal loading control.

4.7 Immunofluorescence

HaCaT cells (2 x 10^4 cell/well) were seeded in glass-bottom culture dishes (NEST, China) and infected with *S. aureus* (MOI 200) for 6 h. The cells were washed three times with DPBS and treated with gentamicin (50 μg/mL) for 1 h. After treatment, the cells were rinsed three times with PBST and incubated with ice-cold 4% formaldehyde in PBS for 15 min at RT. To visualize the cytosol, the cells were permeabilized with 5% Triton X-100 in PBS for 10 min and then rinsed with PBST for 5 min. Samples were blocked using 1% BSA in PBST for 1 h and then incubated overnight at 4°C with anti-vimentin guinea pig polyclonal antibody (GP53, PROGEN, Heidelberg, Germany) and anti-*Staphylococcus aureus* antibody (ab20920, Abcam). The samples were then reacted with Alexa 488-conjugated anti-guinea pig secondary antibody (ab150185) and Alexa 594-conjugated anti-rabbit secondary antibody (ab150080, Abcam) in the dark for 2 h. A washing step with 0.1% Tween 20 in PBS was performed between each step. To stain the nucleus, the cells were incubated with 0.5 μg/mL DAPI (D9594, Sigma Aldrich) for 1 min. All plates were scanned at 100x magnification using a Leica SP8 CLSM (Leica Biosystems, Vista, CA, USA) at Sungkyunkwan University (Gyeonggi-do, Korea).

4.8 Flow cytometry

S. aureus-infected HaCaT cells were fixed with 4% formaldehyde at RT for 30 min. After cooling for 5 min, cells were centrifuged at 14,000 rpm for 5 min at 4°C. The supernatants were removed, and the cells were washed 3 times with PBS. 500 μl of ice-cold 0.1% Triton X-100 was added to each tube and incubated at RT for 30 min. The cells were then centrifuged at 14,000 rpm for 5 min at 4°C and washed three times. Following this, 500 μl of blocking buffer was added to each tube, briefly vortexed, and incubated on ice for 30 min. The supernatants were removed by centrifugation and aspiration. The cells were treated with vimentin monoclonal antibody (MA5-16409, Invitrogen) and incubated overnight at 4°C. After washing three times with PBS, the cells were treated with goat anti-rabbit IgG H&L (Alexa Fluor 488) (ab150077, Abcam) for 1 h and then washed with PBS. Flow cytometry

analysis was performed at the Gyeonggido Business & Science Accelerator (GBSA, Gyeonggi-do, Korea) using a FACSAria II cell sorter (BD).

4.9 Fluorescence activated cell sorting (FACS) analysis

HaCaT cells were infected with *S. aureus* for the indicated times and subsequently fixed using 4% formaldehyde at 37°C for 20 min. After cooling for 5 min, the cells were incubated with an anti-vimentin antibody (diluted 1:200 in PBS) at RT for 1 h. Following a wash with 0.5 mL of ice-cold PBS, the cells were treated with anti-mouse IgG Alexa Fluor® 568 (diluted 1:1000; Abcam, ab202504) for 30 min. After resuspending the cells in 0.5 mL of PBS, flow cytometry analysis was conducted at the Gyeonggido Business & Science Accelerator (GBSA, Suwon, Korea) using a FACSAria II cell sorter (BD).

4.10 Cell viability assay

HaCaT cells were seeded at 60% confluence in 96-well white/clear plates and cultured overnight. The cells were treated with *S. aureus* prepared at a concentration of 10^8 CFU/mL in DPBS solution and incubated for the indicated times. EZ-Cytox reagent (Daeil Lab Service, Seoul, Korea) was added to each well and incubated for 30 min. Absorbance was measured at a wavelength of 590 nm using an EL800 microplate reader (Biophotometer, Eppendorf, Hamburg, Germany).

4.11 Data analysis

Significant differences in means between the groups were assessed using one-way analysis of variance (ANOVA), followed by Tukey's honestly significant difference (HSD) *post hoc* test, or two-way ANOVA. The data presented represent the mean ± standard deviation (SD) from triplicate experiments. Differences were considered statistically significant when the p-value was less than 0.05.

Data availability statement

The original contributions presented in the study are included in the article/Supplementary Material. Further inquiries can be directed to the corresponding authors.

Ethics statement

Ethical approval was not required for the studies on humans in accordance with the local legislation and institutional requirements because only commercially available established cell lines were used.

Author contributions

KJ: Data curation, Visualization, Writing – original draft, Investigation, Methodology. HK: Data curation, Visualization, Writing – original draft, Conceptualization, Formal analysis, Validation, Writing – review & editing. DC: Investigation, Writing – original draft. SJ: Conceptualization, Formal analysis, Funding acquisition, Project administration, Supervision, Validation, Writing – review & editing. D-KC: Conceptualization, Formal analysis, Project administration, Resources, Supervision, Writing – review & editing.

Funding

The author(s) declare financial support was received for the research, authorship, and/or publication of this article. This research was supported by the National Research Foundation (NRF) funded by the Korean government (MSIT) (No. RS-2024-00398073).

Conflict of interest

Authors HK and D-KC were employed by Skin Biotechnology Center Co. Ltd.

The remaining authors declare that the research was conducted in the absence of any commercial or financial relationships that could be construed as a potential conflict of interest.

Generative AI statement

The author(s) declare that no Generative AI was used in the creation of this manuscript.

Publisher's note

Supplementary material

The Supplementary Material for this article can be found online at: https://www.frontiersin.org/articles/10.3389/fcimb.2025.1543186/full#supplementary-material

References

Al Kindi, A., Alkahtani, A. M., Nalubega, M., El-Chami, C., O'Neill, C., Arkwright, P. D., et al. (2019). *Staphylococcus aureus* internalized by skin keratinocytes evade antibiotic killing. *Front. Microbiol.* 10. doi: 10.3389/fmicb.2019.02242

Alexander, E. H., and Hudson, M. C. (2001). Factors influencing the internalization of *Staphylococcus aureus* and impacts on the course of infections in humans. *Appl. Microbiol. Biotechnol.* 56, 361–366. doi: 10.1007/s002530100703

Babrak, L., Danelishvili, L., Rose, S. J., Kornberg, T., and Bermudez, L. E. (2015). The environment of "Mycobacterium avium subsp. hominissuis" microaggregates induces synthesis of small proteins associated with efficient infection of respiratory epithelial cells. *Infect. Immun.* 83, 625–636. doi: 10.1128/IAI.02699-14

Bur, S., Preissner, K. T., Herrmann, M., and Bischoff, M. (2013). The *Staphylococcus aureus* extracellular adherence protein promotes bacterial internalization by keratinocytes independent of fibronectin-binding proteins. *J. Invest. Dermatol.* 133, 2004–2012. doi: 10.1038/jid.2013.87

Cebrián, G., Condón, S., and Mañas, P. (2017). Physiology of the inactivation of vegetative bacteria by thermal treatments: mode of action, influence of environmental factors and inactivation kinetics. *Foods* 6, 107. doi: 10.3390/foods6120107

Chen, Y., Song, Y., Wang, Z., Lai, Y., Yin, W., Cai, Q., et al. (2024). The chemerin-CMKLR1 axis in keratinocytes impairs innate host defense against cutaneous *Staphylococcus aureus* infection. *Cell Mol. Immunol.* 21, 533–545. doi: 10.1038/s41423-024-01152-y

Chi, F., Jong, T. D., Wang, L., Ouyang, Y., Wu, C., Li, W., et al. (2010). Vimentin-mediated signalling is required for IbeA+ E. coli K1 invasion of human brain microvascular endothelial cells. *Biochem. J.* 427, 79–90. doi: 10.1042/BJ20091097

Clebak, K. T., and Malone, M. A. (2018). Skin infections. *Prim. Care* 45, 433–454. doi: 10.1016/j.pop.2018.05.004

David, M. Z., and Daum, R. S. (2017). Treatment of *staphylococcus aureus* infections. *Curr. Top. Microbiol. Immunol.* 409, 325–383. doi: 10.1007/82_2017_42

Edwards, A. M., Potter, U., Meenan, N. A., Potts, J. R., and Massey, R. C. (2011). *Staphylococcus aureus* keratinocyte invasion is dependent upon multiple high-affinity fibronectin-binding repeats within FnBPA. *PloS One* 6, e18899. doi: 10.1371/journal.pone.0018899

Fournier, B. (2013). The function of TLR2 during staphylococcal diseases. *Front. Cell Infect. Microbiol.* 2. doi: 10.3389/fcimb.2012.00167

Fuyuhiro, Y., Yashiro, M., Noda, S., Kashiwagi, S., Matsuoka, J., Doi, Y., et al. (2010). Clinical significance of vimentin-positive gastric cancer cells. *Anticancer Res.* 30, 5239–5243.

Gehrke, A.-K. E., Giai, C., and Gómez, M. I. (2023). *Staphylococcus aureus* adaptation to the skin in health and persistent/recurrent infections. *Antibiotics (Basel)* 12, 1520. doi: 10.3390/antibiotics12101520

Geoghegan, J. A., Irvine, A. D., and Foster, T. J. (2018). *Staphylococcus aureus* and atopic dermatitis: A complex and evolving relationship. *Trends Microbiol.* 26, 484–497. doi: 10.1016/j.tim.2017.11.008

Gophna, U., Barlev, M., Seijffers, R., Oelschlager, T. A., Hacker, J., and Ron, E. Z. (2001). Curli fibers mediate internalization of *Escherichia coli* by eukaryotic cells. *Infect. Immun.* 69, 2659–2665. doi: 10.1128/IAI.69.4.2659-2665.2001

Gotland, N., Uhre, M. L., Sandholdt, H., Mejer, N., Lundbo, L. F., Petersen, A., et al. (2020). Increased risk of incident primary cancer after *Staphylococcus aureus* bacteremia: A matched cohort study. *Med. (Baltimore)* 99, e19984. doi: 10.1097/MD.0000000000019984

Grunfeld, C., Marshall, M., Shigenaga, J. K., Moser, A. H., Tobias, P., and Feingold, K. R. (1999). Lipoproteins inhibit macrophage activation by lipoteichoic acid. *J. Lipid Res.* 40, 245–252. doi: 10.1016/S0022-2275(20)33363-0

Guignot, J., and Servin, A. L. (2008). Maintenance of the Salmonella-containing vacuole in the juxtanuclear area: A role for intermediate filaments. *Microb. Pathog.* 45, 415–422. doi: 10.1016/j.micpath.2008.09.007

Guo, M., Ehrlicher, A. J., Mahammad, S., Fabich, H., Jensen, M. H., Moore, J. R., et al. (2013). The role of vimentin intermediate filaments in cortical and cytoplasmic mechanics. *Biophys. J.* 105, 1562–1568. doi: 10.1016/j.bpj.2013.08.037

Henderson, P., Wilson, D. C., Satsangi, J., and Stevens, C. (2014). A role for vimentin in Crohn disease. *Autophagy* 8, 1695–1696. doi: 10.4161/auto.21690

Humphreys, D., Hume, P. J., and Koronakis, V. (2009). The Salmonella effector SptP dephosphorylates host AAA+ ATPase VCP to promote development of its intracellular replicative niche. *Cell Host Microbe* 5, 225–233. doi: 10.1016/j.chom.2009.01.010

Icenogle, L. M., Hengel, S. M., Coye, L. H., Streifel, A., Collins, C. M., Goodlett, D. R., et al. (2012). Molecular and biological characterization of Streptococcal SpyA-mediated ADP-ribosylation of intermediate filament protein vimentin. *J. Biol. Chem.* 287, 21481–21491. doi: 10.1074/jbc.M112.370791

Igawa, S., Choi, J. E., Wang, Z., Chang, Y. L., Wu, C. C., Werbel, T., et al. (2019). Human Keratinocytes Use Sphingosine 1-Phosphate and its Receptors to Communicate *Staphylococcus aureus* Invasion and Activate Host Defense. *J. Invest. Dermatol.* 139, 1743–52.e5. doi: 10.1016/j.jid.2019.02.010

Ivaska, J. (2011). Vimentin: Central hub in EMT induction? *Small GTPases* 2, 51–53. doi: 10.4161/sgtp.2.1.15114

Jiang, S., He, J., Zhang, L., Zhao, Q., and Zhao, S. (2023). Bacterial lipoprotein plays an important role in the macrophage autophagy and apoptosis induced by *Salmonella typhimurium* and *Staphylococcus aureus*. *Open Life Sci.* 18, 20220739. doi: 10.1515/biol-2022-073

Josse, J., Laurent, F., and Diot, A. (2017). Staphylococcal adhesion and host cell invasion: fibronectin-binding and other mechanisms. *Front. Microbiol.* 8. doi: 10.3389/fmicb.2017.02433

Kielian, T., Esen, N., and Bearden, E. D. (2005). Toll-like receptor 2 (TLR2) is pivotal for recognition of *S. aureus* peptidoglycan but not intact bacteria by microglia. *Glia* 49, 567–576. doi: 10.1002/glia.20144

Miao, C., Zhao, S., Etienne-Manneville, S., and Jiu, Y. (2023). The diverse actions of cytoskeletal vimentin in bacterial infection and host defense. *J. Cell Sci.* 136, jcs260509. doi: 10.1242/jcs.260509

Mor-Vaknin, N., Punturieri, A., Sitwala, K., and Markovitz, D. M. (2003). Vimentin is secreted by activated macrophages. *Nat. Cell Biol.* 5, 59–63. doi: 10.1038/ncb898

Muller, M., Bhattacharya, S. S., Moore, T., Prescott, Q., Wedig, T., Herrmann, H., et al. (2009). Dominant cataract formation in association with a vimentin assembly disrupting mutation. *Hum. Mol. Genet.* 18, 1052–1057. doi: 10.1093/hmg/ddn440

Murli, S., Watson, R. O., and Gala, J. E. (2001). Role of tyrosine kinases and the tyrosine phosphatase SptP in the interaction of Salmonella with host cells. *Cell Microbiol.* 3, 795–810. doi: 10.1046/j.1462-5822.2001.00158.x

Ngo, Q. V., Faass, L., Sähr, A., Hildebrand, D., Eigenbrod, T., Heeg, K., et al. (2022). Inflammatory Response Against *Staphylococcus aureus* via Intracellular Sensing of Nucleic Acids in Keratinocytes. *Front. Immunol.* 13. doi: 10.3389/fimmu.2024.1330357

Nguyen, M. T., Peisl, L., Barletta, F., Luqman, A., and Götz, F. (2018). Toll-like receptor 2 and lipoprotein-like lipoproteins enhance *staphylococcus aureus* invasion in epithelial cells. *Infect. Immun.* 86, e00343–e00318. doi: 10.1128/IAI.00343-18

Odunitan, T. T., Apanisile, B. T., Akinboade, M. W., Abdulazeez, W. O., Oyaronbi, A. O., Ajayi, T. M., et al. (2024). Microbial mysteries: *Staphylococcus aureus* and the enigma of carcinogenesis. *Microb. Pathog.* 194, 106831. doi: 10.1016/j.micpath.2024.106831

Parsonnet, J. (1995). Bacterial infection as a cause of cancer. *Environ. Health Perspect.* 103 Suppl 8, 263–268. doi: 10.1289/ehp.95103s8263

Paulin, D., Lilienbaum, A., Kardjian, S., Agbulut, O., and Li, Z. (2022). Vimentin: regulation and pathogenesis. *Biochimie* 197, 96–112. doi: 10.1016/j.biochi.2022.02.003

Pereira, M., and Gazzinelli, R. T. (2023). Regulation of innate immune signaling by IRAK proteins. *Front. Immunol.* 14. doi: 10.3389/fimmu.2023.1133354

Ramos, I., Stamatakis, K., Oeste, C. L., and Pérez-Sala, D. (2020). Vimentin as a multifaceted player and potential therapeutic target in viral infections. *Int. J. Mol. Sci.* 21, 4675. doi: 10.3390/ijms21134675

Ridge, K. M., Eriksson, J. E., Pekny, M., and Goldman, R. D. (2022). Roles of vimentin in health and disease. *Genes Dev.* 36, 391–407. doi: 10.1101/gad.349358.122

Satelli, A., and Li, S. (2011). Vimentin in cancer and its potential as a molecular target for cancer therapy. *Cell Mol. Life Sci.* 68, 3033–3046. doi: 10.1007/s00018-011-0735-1

Sayedyahossein, S., Xu, S. X., Rudkouskaya, A., McGavin, M. J., McCormick, J. K., and Dagnino, L. (2015). *Staphylococcus aureus* keratinocyte invasion is mediated by integrin-linked kinase and Rac1. *FASEB J.* 29, 711–723. doi: 10.1096/fj.14-262774

Schroeder, G. N., and Hilbi, H. (2008). Molecular pathogenesis of Shigella spp.: controlling host cell signaling, invasion, and death by type III secretion. *Clin. Microbiol. Rev.* 21, 134–156. doi: 10.1128/CMR.00032-07

Snavely, E. A., Kokes, M., Dunn, J. D., Saka, H. A., Nguyen, B. D., Bastidas, R. J., et al. (2014). Reassessing the role of the secreted protease CPAF in Chlamydia trachomatis infection through genetic approaches. *Pathog. Dis.* 71, 336–351. doi: 10.1111/2049-632X.12179

Soong, G., Chun, J., Parker, D., and Prince, A. (2012). *Staphylococcus aureus* activation of caspase 1/calpain signaling mediates invasion through human keratinocytes. *J. Infect. Dis.* 205, 1571–1579. doi: 10.1093/infdis/jis244

Stenzel, W., Soltek, S., Sanchez-Ruiz, M., Akira, S., Miletic, H., Schlüter, D., et al. (2008). Both TLR2 and TLR4 are required for the effective immune response in *Staphylococcus aureus*-induced experimental murine brain abscess. *Am. J. Pathol.* 172, 132–145. doi: 10.2353/ajpath.2008.070567

Su, L., Pan, P., Yan, P., Long, Y., Zhou, X., Wang, X., et al. (2019). Role of vimentin in modulating immune cell apoptosis and inflammatory responses in sepsis. *Sci. Rep.* 9, 5747. doi: 10.1038/s41598-019-42287-7

Yusuf, K., Sampath, V., and Umar, S. (2023). Bacterial infections and cancer: exploring this association and its implications for cancer patients. *Int. J. Mol. Sci.* 24, 3110. doi: 10.3390/ijms24043110

Zhao, S., Miao, C., Gao, X., Li, Z., Eriksson, J. E., and Jiu, Y. (2024). Vimentin cage - A double-edged sword in host anti-infection defense. *Curr. Opin. Cell Biol.* 86, 102317. doi: 10.1016/j.ceb.2023.102317

Zhu, Q., Wen, W., Wang, W., and Sun, B. (2019). Transcriptional regulation of virulence factors Spa and ClfB by the SpoVG-Rot cascade in *Staphylococcus aureus*. *Int. J. Med. Microbiol.* 309, 39–53. doi: 10.1016/j.ijmm.2018.10.006

Zou, Y., He, L., and Huang, S. H. (2006). Identification of a surface protein on human brain microvascular endothelial cells as vimentin interacting with Escherichia coli invasion protein IbeA. *Biochem. Biophys. Res. Commun.* 351, 625–630. doi: 10.1016/j.bbrc.2006.10.091

frontiers | Frontiers in Cellular and Infection Microbiology

TYPE Original Research
PUBLISHED 09 May 2025
DOI 10.3389/fcimb.2025.1524820

OPEN ACCESS

EDITED BY
Maurizio Sanguinetti,
Catholic University of the Sacred Heart, Italy

REVIEWED BY
Divyashri Baraniya,
Temple University, United States
Anne Lise Lund Håheim,
University of Oslo, Norway

*CORRESPONDENCE
Ryota Yamasaki
r18yamasaki@fa.kyu-dent.ac.jp

RECEIVED 08 November 2024
ACCEPTED 17 April 2025
PUBLISHED 09 May 2025

CITATION
Inui I, Mochizuki S, Hirabayashi-Nishimuta F, Yoshioka Y, Takahashi O, Sasaguri M, Habu M, Ariyoshi W and Yamasaki R (2025) *In vitro* impact of *Streptococcus mitis* on the inhibition of oral cancer cell proliferation via mitotic modulation.
Front. Cell. Infect. Microbiol. 15:1524820.
doi: 10.3389/fcimb.2025.1524820

In vitro impact of *Streptococcus mitis* on the inhibition of oral cancer cell proliferation via mitotic modulation

Inori Inui[1,2], Shinichi Mochizuki[3], Fumika Hirabayashi-Nishimuta[4], Yoshie Yoshioka[1], Osamu Takahashi[2], Masaaki Sasaguri[2], Manabu Habu[2], Wataru Ariyoshi[1] and Ryota Yamasaki[1,5]*

[1]Division of Infections and Molecular Biology, Department of Health Promotion, Kyushu Dental University, Kitakyushu, Fukuoka, Japan, [2]Division of Maxillofacial Surgery, Department of Science of Physical Functions, Kyushu Dental University, Kitakyushu, Fukuoka, Japan, [3]Department of Chemistry and Biochemistry, The University of Kitakyushu, Kitakyushu, Fukuoka, Japan, [4]Division of Oral Medicine, Department of Science of Physical Functions, Kyushu Dental University, Kitakyushu, Fukuoka, Japan, [5]Collaborative Research Centre for Green Materials on Environmental Technology, Kyushu Institute of Technology, Kitakyushu, Fukuoka, Japan

Introduction: Recent studies have elucidated a potential correlation between oral carcinogenesis and the oral microbiome. However, few reports exist on the interaction between *Streptococcus* spp., the most common oral microflora bacterium, and oral cancer. In this study, we aimed to elucidate the effects of *Streptococcus* spp. on oral squamous cell carcinoma (OSCC) cells *in vitro*.

Methods: HSC-3 (tongue carcinoma) and Ca9-22 (gingival carcinoma) cells were used as models of OSCC cells, and their responses were examined after adding major oral *Streptococcus* species—*S. mitis*, *S. sanguinis*, *S. anginosus*, *S. salivarius*, and *S. mutans*—to the culture medium. Cell viability was assessed using the CCK-8 assay. Gene expression changes were analyzed using RNA sequencing and RT-qPCR followed by Gene Ontology analysis. Flow cytometry was used to observe the effects of bacteria on the cell cycle.

Results: Among all examined *Streptococcus* species, *S. mitis* had the strongest inhibitory effect on the growth of OSCC cells. RNA sequencing and RT-qPCR revealed an increase in the number of genes involved in mitotic nuclear division, especially *DUSP1*, in HSC-3 cells treated with *S. mitis.* Flow cytometry showed that *S. mitis* caused a decreased number of HSC-3 cells in the G0/G1 phase and an increased number in the G2/M phase, suggesting cell cycle arrest in the G2/M phase. Various treatments of *S. mitis* were used to examine the effects of intact bacteria and bacterial components on cancer cells, indicating the involvement of structural bacterial proteins.

Conclusions: This study, investigating the association between oral cancer cells and bacteria of the genus *Streptococcus*, revealed that *S. mitis* may play an important role in the inhibition of cancer cells.

10.3389/fcimb.2025.1524820

KEYWORDS

oral microbiota, *Streptococcus* spp., oral cancer, carcinoma, cell cycle, DUSP1, mitotic nuclear division, *Streptococcus mitis*

1 Introduction

Oral cancer encompasses a group of malignant neoplasms localized within the jaw and oral cavity. As the mucosa consists of squamous epithelium covering the entire oral cavity apart from the teeth, 90% of all oral cancer cases are classified as squamous cell carcinoma (Bagan et al., 2010). In 2020, 377,713 cases of oral cancer and 177,757 related deaths were reported worldwide (Sung et al., 2021). According to the Global Cancer Observatory (GCO), the incidence of oral squamous cell carcinoma (OSCC) is projected to rise by approximately 40% by 2040, with increasing mortality rates (Tan et al., 2023). The primary treatment for oral cancer is surgical resection, but tissue loss from surgery can affect the dentition, muscles, and nerves. Since these tissues are involved in important functions, such as chewing, swallowing, and speech, the quality of life after treatment is significantly reduced in cases that require extensive resection (Vermaire et al., 2022).

In addition to smoking, alcohol consumption, and improper oral hygiene, various systemic predisposing factors such as nutritional deficiencies, immunodeficiency, and genetic disorders are intricately involved as major risk factors in the pathogenesis of oral cancer (Chamoli et al., 2021; Tan et al., 2023). The mechanisms of pathogenesis also vary, and unidentified risk factors may exist. Cancer is a multifactorial disease caused by various genetic abnormalities (Hanahan and Weinberg, 2011), and its pathogenesis can involve the induction of an oncogenic inflammatory environment, DNA damage, and the production of molecules involved in tumorigenic signaling by the surrounding bacterial flora (Plottel and Blaser, 2011; Cho and Blaser, 2012). *Helicobacter pylori* has been found to cause gastric cancer (Polk and Peek, 2010); since this discovery, studies have also focused on the involvement of specific microorganisms in cancer development. Examples include typhoid bacteria as a possible risk factor for gallbladder cancer (Espinoza et al., 2016) and human papillomavirus (HPV) being associated with cancers at various sites, including the cervix and mid-pharynx (Egawa, 2023). Furthermore, recent studies have demonstrated that oral microbiota are involved in tumor development and progression (Sun et al., 2020). In addition to the involvement of HPV (Sun et al., 2020) and *Candida albicans* (Wang et al., 2023), the major periodontopathogenic bacteria *Fusobacterium nucleatum* and *Porphyromonas gingivalis* are particularly relevant. These bacteria trigger excessive inflammatory responses, evade the immune system, have anti-apoptotic activity, cause cellular transformation, and promote cancer (Karpiński, 2019; Li et al., 2023).

More than 700 species of bacteria are present in the oral cavity and play an important role in maintaining a healthy oral environment by forming complex commensal flora; however, some bacteria are pathogenic and can cause oral diseases. Among the commensal bacteria inhabiting the oral cavity, *Streptococcus* is the most abundant at the genus level (Costalonga and Herzberg, 2014). Bacteria of the genus *Streptococcus* can exhibit both beneficial effects and pathogenicity in the oral cavity. While *Streptococcus salivarius* and *Streptococcus mitis* inhibit the growth of pathogenic bacteria, *Streptococcus sanguinis* and *S. mitis* are known to cause infective endocarditis (Okahashi et al., 2022; Jenkinson, 2011). *Streptococcus anginosus* is a causative agent of odontogenic infections (Asam and Spellerberg, 2014), whereas *Streptococcus mutans* and *Streptococcus sobrinus* metabolize sugars to produce acid, contributing to dental caries (Jenkinson, 2011). Thus, *Streptococcus* species are closely associated with other microorganisms and various diseases; however, their relationship with oral cancer remains largely unknown. In a previous study, saliva from patients with OSCC lesions contained more *Capnocytophaga gingivalis*, *Prevotella melaninogenica*, and *S. mitis* than saliva from cancer-free individuals, although the reasons for this difference are unclear. As mentioned above, the interaction of *F. nucleatum* and *P. gingivalis* with oral cancer has been demonstrated. However, the influence of *Streptococcus* spp., the most abundant genus in the oral cavity, on OSCC remains unclear, and its exact role in the pathogenesis of cancer remains unknown, although the association of the latter with *S. anginosus* has been pointed out (Sasaki et al., 2005). Reports on other *Streptococcus* species are also limited. Considering that the effects of the main components of oral flora on oral cancer should be taken into account, the present study aimed to elucidate the effects of *Streptococcus* spp. on oral cancer cells *in vitro*.

2 Materials and methods

2.1 Cell and bacterial culture

The OSCC strains HSC-3 (from human tongue carcinoma) and Ca9-22 (from human gingival carcinoma) were obtained from the Japanese Collection of Research Bioresources (JCRB; Osaka, Japan). HSC-3 cells were cultured in Eagle's Minimum Essential Medium (E-MEM; FUJIFILM Wako Pure Chemical Co., Osaka, Japan) supplemented with 10% fetal bovine serum (FBS) and 1% penicillin/streptomycin (SMPC). Ca9-22 cells were cultured in Minimum Essential Medium α (MEMα; FUJIFILM Wako Pure Chemical Co.) with 10% FBS and 1% SMPC. Both strains were incubated at 37°C in a 5% CO_2 environment.

The model bacterial strains used were *S. mitis* ATCC 49456, *S. sanguinis* ATCC 10556, *S. anginosus* ATCC 33379, *S. salivarius* ATCC BAA- 1024, and *S. mutans* UA 159. Brain Heart Infusion

(BHI; BD, Franklin Lakes, NJ) agar medium containing 1% yeast extract (BD) was used for all bacterial cultures, and the bacteria were incubated for 1 to 2 days at 37°C in a 5% CO_2 environment. Single colonies were seeded on BHI liquid medium and incubated for 12 h at 37°C, 5% CO_2. The culture medium (5 mL) was prepared to achieve a turbidity of 0.4 at 600 nm, and all precipitates were resuspended in an equal volume of E-MEM or MEMα with FBS and 1% SMPC after centrifugation at 3500 × *g* for 10 min. The centrifugation and resuspension processes were repeated twice to wash the pellets. After washing, the colony-forming units (CFUs) were counted by plating the culture onto BHI agar.

2.2 Cell viability assay

Cell viability was assessed using a Cell Counting Kit-8 with WST-8 (CCK-8; Dojin Chemical Laboratory, Kumamoto, Japan). Briefly, HSC-3 and Ca9-22 cells were cultured and adhered in 96-well plates at 2000 cells/well for 6 h. Each bacterial solution, resuspended in cell culture medium, was prepared 100–0.1 v/v% by 2-fold serial dilution in a separate 96-well plate. Then 50 µL of each bacterial solution was added to 50 µL of cancer cells (100 µL total). After 48 h of incubation, 10 µL of CCK-8 was added and incubated at 37°C for 2 h. The absorbance of each well at 450 nm was measured using a microplate reader (Multiskan FD, Thermo Fisher Scientific, Waltham, MA). All experiments were conducted with at least three biological replicates.

2.3 Changes in gene expression

Total RNA was extracted from each sample using the Cica Geneus RNA Prep Kit (for tissue) (Kanto Chemical, Tokyo, Japan). After culturing the cells for 48 h in the presence of bacterial solution, RNA was extracted. The quality and quantity (concentration ≥ 40 ng/µL, A260/A230 ≥ 2.0, and A260/A280 = 1.8–2.2) were evaluated using a Nanodrop (Thermo Fisher Scientific). Total RNA was provided to Novogene (China) for RNA sequencing using Nova Seq 6000 (Illumina Inc., San Diego, CA, USA). The raw data in FASTQ format were processed using Novogene's Perl script and cleaned by removing adapter-containing reads, poly-N-containing reads, and low-quality reads. The reference genome index was constructed using Hisat2 v2.0.5, and paired-end clean 1 read were aligned to the reference genome using Hisat2 v2.0.5. Gene expression levels were quantified using featureCounts v1.5.0-p3. Differential expression was analyzed using the DESeq2R package (1.20.0). Genes with adjusted *p*-values of < 0.05 in DESeq2 were considered differentially expressed genes. Gene Ontology (GO) functional analysis was performed using the clusterProfiler R package with gene length bias correction. GO terms with adjusted *p*-values of < 0.05 were considered to have significantly changed functions due to differentially expressed genes. For real-time RT-qPCR, RNA was reverse-transcribed and amplified according to previously described methods (Ariyoshi et al., 2017). RNA expression was analyzed by real-time RT-qPCR using the AriaMx Real-Time PCR system (Agilent Technologies, Santa Clara, CA). The primer sequences used for RT-qPCR are listed in Table 1.

2.4 Flow cytometry analysis of bacterial effects on the cell cycle

After a 6 h pre-culture, 7×10^5 HSC-3 cells were seeded per Petri dish (10 cm in diameter) for 24 h. Then, the *S. mitis* bacterial solution was added, and the cells were fixed in 70% ethanol for 2 h. The fixed cells were treated with PI/RNase solution (IMMUNOSTEP, Salamanca, Spain). The fluorescence intensity of the cells was observed using a flow cytometer (CytoFLEX; Beckman Coulter, Brea, CA).

2.5 Effects of intact bacteria and bacterial components on cancer cells

Live bacteria, secretions of live bacteria, and dead bacteria (sonicated and treated with isopropanol) were used as samples. Culture supernatants were prepared to achieve an optical density of 0.4 at 600 nm of the bacterial culture medium, and the supernatant fluid after centrifugation was extracted by passing it through a 0.2 µm filter. Samples of dead bacteria were obtained by treating live bacteria with 70% isopropanol for 1 h. The bacterial solution was sonicated using an ultrasonic homogenizer (SFX150, Branson Ultrasonics, Brookfield, CT) at 15-second intervals for 5 min, and the solution containing the disrupted bacterial cells was further centrifuged (3500 × *g* for 10 min) to separate the internal components of the bacteria (supernatant) from other bacterial structures (precipitate). The sonicated bacteria were treated with Proteinase K at 65°C for 2 h, then the protease was inactivated at 98°C for 10 min to prepare samples of the bacterial components excluding proteins. Each bacterial solution was added to HSC-3 cells for the cell viability assay. The LIVE/DEAD Viability/Cytotoxicity Kit (Thermo Fisher Scientific) was used to stain live and dead bacteria (sonicated and treated with isopropanol) to observe them under a fluorescence microscope.

2.6 Statistical analysis

All data were expressed as mean ± standard deviation (SD). Student's t-test was used for comparisons between two groups using

TABLE 1 The primer sequences used for RT-qPCR.

Gene name		Primer sequence (5′-3′)
GAPDH	Forward	GAC GGC CGC ATC TTC TTG T
	Reverse	CAC ACC GAC CTT CAC CAT TTT
DUSP1	Forward	CCA TCT GCC TTG CTT ACC TTA T
	Reverse	GCT GAA GTT GGG AGA GAT GAT G

Microsoft Excel. For comparisons between three or more groups, the statistical analysis software EZR was used to perform one-way analysis of variance (ANOVA) with Tukey's *post hoc* test.

3 Results

3.1 *Streptococcus mitis* most effectively inhibits cancer cell growth

To compare the effects of different bacterial species, bacterial solutions of *S. mitis*, *S. mutans*, *S. sanguinis*, *S. anginosus*, and *S. salivarius* were added for 48 h to HSC-3 cells pre-cultured two-dimensionally in 96-well plates. The number of viable cells was evaluated using the CCK-8 assay. The results are shown in Figures 1A–E.

Most bacteria inhibited HSC-3 growth in a dose-dependent manner. *S. mitis* significantly inhibited growth at concentrations above 0.78% (Figure 1A); *S. mutans and S. salivarius* significantly inhibited only at the highest concentration of 50% (Figures 1B, E); *S. sanguinis* significantly inhibited at concentrations of > 25% (Figure 1C); and *S. anginosus* significantly inhibited cell growth at concentrations of > 6.25% (Figure 1D). The concentrations at which cancer cells were inhibited by 80% (IC80) compared to the control group (0%) are shown in Table 2. Among these, *S. mitis* showed the highest inhibition of cancer cell growth. The results of the WST-8 assay when *S. mitis* was added to Ca9-22 cells are shown in Figure 2. Although the sensitivity of Ca9-22 cells was inferior to that of HSC-

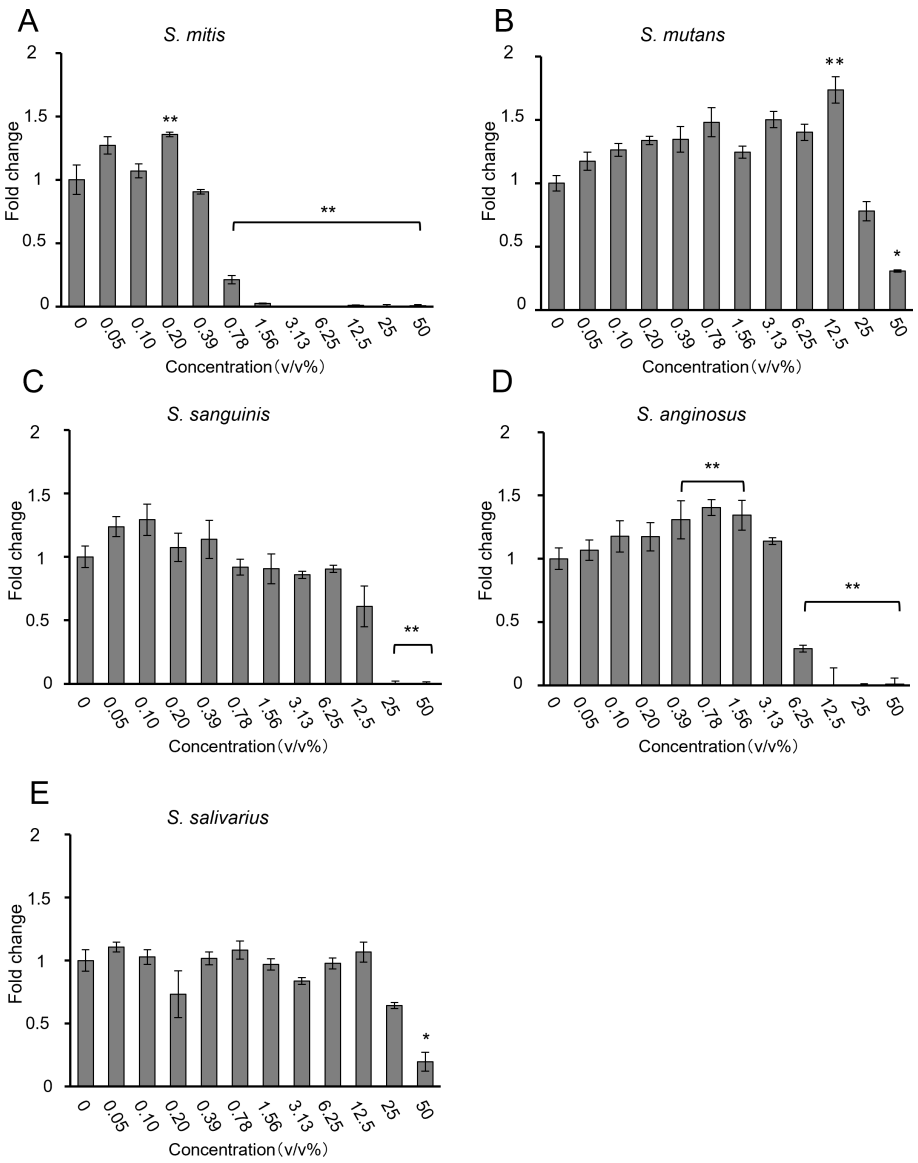

FIGURE 1
Proliferation of HSC-3 cells, as assessed using the CCK-8 assay, when **(A)** *S. mitis*, **(B)** *S. mutans*, **(C)** *S. sanguinis*, **(D)** *S. anginosus*, and **(E)** *S. salivarius* were added (n = 3). The vertical axis represents the bacterial solution concentration (v/v%), and the horizontal axis shows the fold change. *$p < 0.05$, **$p < 0.01$ (Tukey's test after one-way analysis of variance).

10.3389/fcimb.2025.1524820

3 cells, significant inhibition of cell proliferation was observed with bacterial concentrations above 3.13%.

3.2 A group of genes involved in mitosis and nuclear division

S. mitis was added to HSC-3 cells at 1.56%, a concentration that significantly inhibited HSC-3 cell growth (see section 3.1), and RNA was extracted from these cells. The CFU of *S. mitis* at 1.56% was 3.8×10^6 CFU/mL. The multiplicity of infection (MOI) was calculated to be 190. The effects of the bacterial species on gene expression were verified via RNA sequencing. The results of the GO enrichment analysis are shown in Figure 3A where the 30 most important GO terms are displayed. The color represents the level of significance, and the dot size represents the number of genes. The number of genes involved in mitosis and nuclear division was significantly increased in the group incubated with *S. mitis* (Figure 3A). The specific genes included in this gene group are shown in Supplementary Figure 1. DUSP1 expression, which satisfied the conditions $|\log2(\text{Fold Change})| \geq 1$ and adjusted $p \leq 0.05$, was validated by RT-qPCR (Figure 3B).

The results showed a significant increase in *DUSP1* gene expression in the *S. mitis-added* group, which was consistent with the RNA sequencing results. In addition, the directed acyclic graph of biological processes allowed us to visualize the enriched GO terms of differentially expressed genes and their hierarchy (Supplementary Figure 2). The functional range in this figure becomes more specific from top to bottom. Given the presence of cell cycle genes high up in this hierarchy, we next investigated the cell cycle of stimulated cancer cells.

3.3 *S. mitis* treatment decreases the percentage of HSC-3 cells in the G0/G1 phase and increases that in the G2/M phase

In flow cytometry experiments, HSC-3 cells were incubated with a 1.56% dilution of *S. mitis* bacterial suspension (see section 3.2), and changes in the cell cycle were measured. Figure 4A shows a histogram of the flow cytometry results of the cell cycle changes induced by *S. mitis*. The percentage of cells in the G0/G1 phase decreased and that in the G2/M phase increased in the *S. mitis-treated* group (Figure 4B). As the proliferation of cancer cells was inhibited by *S. mitis*, these bacteria may have inhibited the proliferation of HSC-3 cells by arresting them in the G2/M phase.

TABLE 2 IC80 of HSC-3 cells following the addition of *S. mitis*, *S. mutans*, *S. sanguinis*, *S. anginosus*, and *S. salivarius*.

Bacteria	IC80 (v/v%)
S. mitis	0.78
S. mutans	–
S. sanguinis	25
S. anginosus	12.5
S. salivarius	50

3.4 Live and dead *S. mitis*, but not secretions of *S. mitis*, inhibit the growth of cancer cells

To identify the mechanism by which *S. mitis* inhibits the growth of HSC-3 cells, samples with various concentrations of live and dead *S. mitis* were added to HSC-3 cells. The supernatant of centrifuged culture media comprised BHI medium and bacterial secretions. The supernatants containing bacterial secretions at concentrations of 12.5% and 25% showed a significant decrease in growth inhibition compared to supernatants containing only BHI. These results suggest that most of the growth-inhibitory effect of the culture supernatant was due to BHI, whereas bacterial secretions had only a minor contribution (Figure 5A). The WST-8 results (Figure 5B) are similar to those for viable *S. mitis* (section 3.1). Ultrasonically disrupted *S. mitis* samples inhibited cell growth at concentrations of > 0.78%, similar to live *S. mitis* samples (Figure 5C). However, chemical disruption of bacteria by isopropanol treatment did not inhibit HSC-3 growth at any concentration (Figure 5D).

The ultrasonicated material was separated by centrifugation into cell wall components (precipitate) and bacterial contents (supernatant) to examine their separate effects. After sonication and centrifugation, the precipitate inhibited growth at ≥ 0.78%, as did the viable and sonicated samples (Figure 5E). Similarly, the supernatant inhibited cell growth at concentrations of > 12.5%, indicating that supernatants were less effective than the precipitate (Figure 5F). This suggests that the cell wall components of *S. mitis* are important for inhibiting cell growth. Cell wall components include lipid bilayers and membrane proteins. To determine which

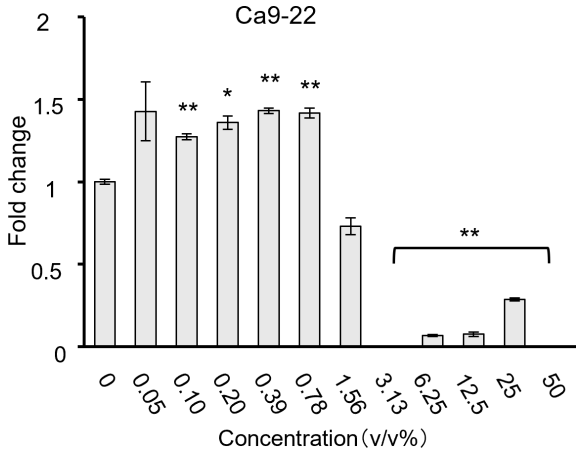

FIGURE 2
Cell proliferation when *S. mitis* bacteria were added to Ca9-22 cells, as assessed using the CCK-8 assay (n = 3). The vertical axis represents the concentration of bacterial solution (v/v%), and the horizontal axis shows the fold change. *$p < 0.05$, **$p < 0.01$ (Tukey's test after one-way analysis of variance).

10.3389/fcimb.2025.1524820

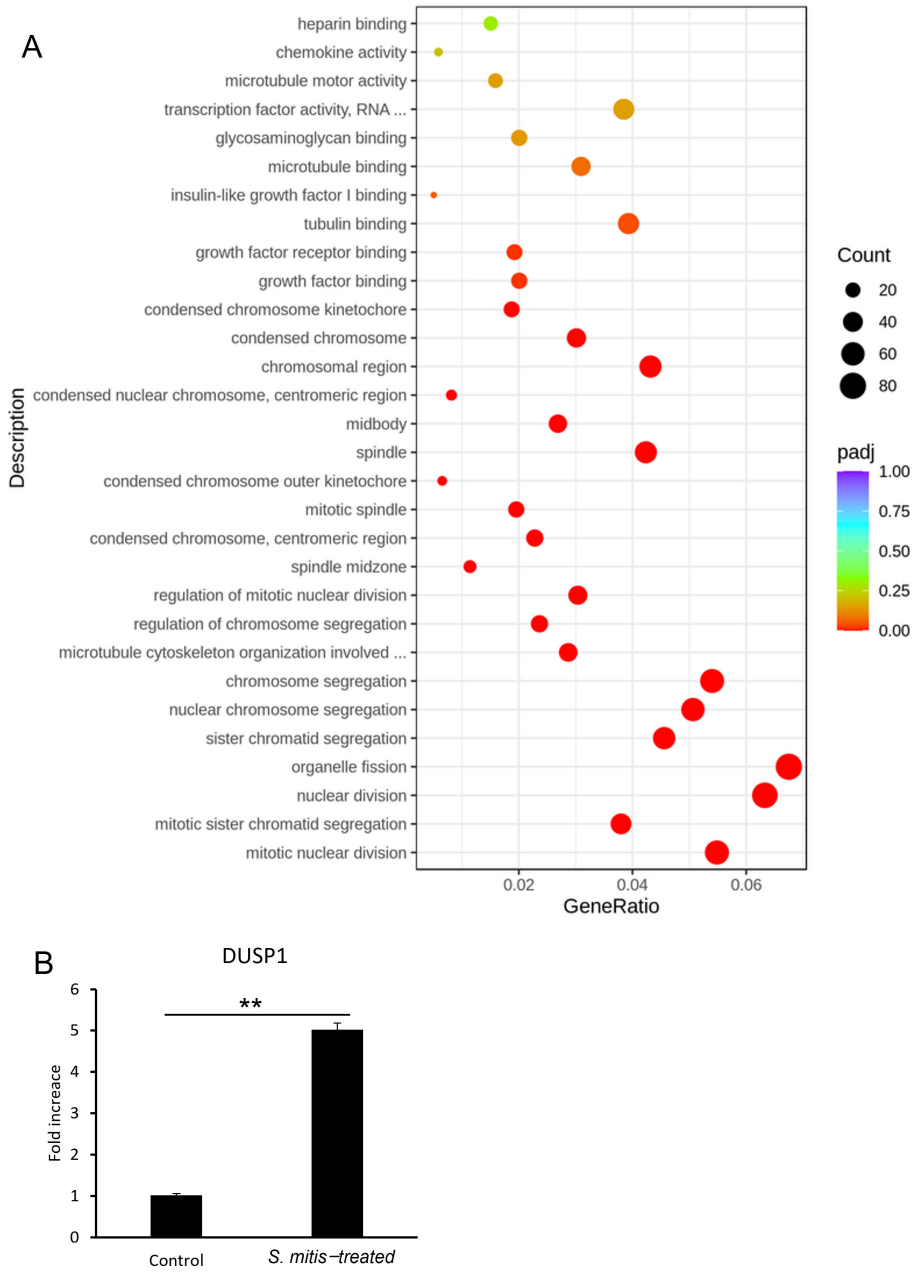

FIGURE 3
(A) Gene expression in HSC-3 cells treated with *S. mitis*. The vertical axis shows the most significant GO term from the bottom up. The horizontal axis shows the ratio of the number of differentially expressed genes linked to the GO term to the total number of differentially expressed genes. The size of the points indicates the number of genes annotated to a specific GO term, and the color indicates the significant level of enrichment. **(B)** *DUSP1* mRNA levels in HSC-3 cells treated with *S. mitis* (n = 3). *$p < 0.05$, **$p < 0.01$ (Student's t-test).

components are particularly important, the proteins were inactivated. Ultrasonically crushed bacteria treated with Proteinase K to degrade proteins achieved cell growth inhibition at concentrations of > 25% (Figure 5G). Protein degradation resulted in a decreased growth inhibition, indicating that protein components of the bacterial cell wall affect the growth inhibition of cancer cells. The viability of bacteria after isopropanol treatment and sonication was confirmed using LIVE/DEAD staining (Supplementary Figure 3). Based on the above results of the WST-8 assay, the IC80 concentrations for cancer cell inhibition compared to control conditions are summarized in Table 3.

4 Discussion

In the present study, we investigated the effects of major strains of the genus *Streptococcus* on oral cancer cells *in vitro*. We found that *S. mitis* inhibited the growth of oral cancer cells *in vitro*.

10.3389/fcimb.2025.1524820

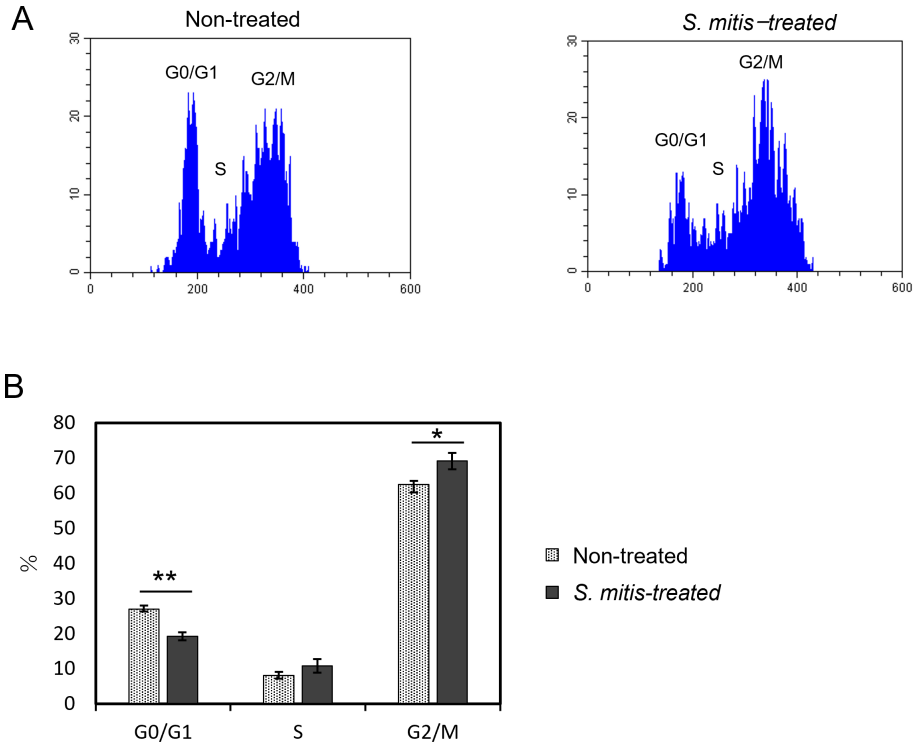

FIGURE 4
Cell cycle changes of HSC-3 cells treated with *S. mitis*. The cells were stained with propidium iodide (PI) and analyzed using a flow cytometer. **(A)** The DNA content and cell count of the cell population are shown. The vertical axis represents the cell count, and the horizontal axis shows the DNA fluorescence intensity. **(B)** Comparison of the percentage of cells in each region analyzed by flow cytometry. *$p < 0.05$, **$p < 0.01$ (Student's t-test).

Furthermore, we observed that *S. mitis* increased the expression of mitosis-related genes in HSC-3 cells and caused cell cycle arrest in the G2/M phase. This activity of *S. mitis* was related to structural bacterial proteins. By matching the absorbance of the culture medium to equalize the number of bacteria, we compared five species, *S. mitis, S. salivarius, S. sanguinis, S. anginosus, and S. mutans*, and found that *S. mitis* had the strongest inhibitory effect on the growth of HSC-3 cells (Figure 1). Previous studies have shown that *S. anginosus* inhibits the proliferation of the OSCC cells SCC15 after 16 h of stimulation (Xu et al., 2021) and *S. mitis* reduces the proliferation of OSCC CAL27 cells to less than 50%; *S. sanguinis* inhibits cell proliferation to the same extent as *S. mitis*; and *S. mutans* does not inhibit cell proliferation within 24–72 h stimulation (Baraniya et al., 2020). These results are consistent with many of our findings; however, the lack of similar effects of *S. mitis and S. sanguinis* treatments may be partly due to differences in susceptibility between the two cell lines used in both studies.

Although *S. mitis* can cause bloodstream infections in immunocompromised patients, it is a relatively harmless oral *Streptococcus* (Mitchell, 2011) and a health-related commensal organism. *S. mitis* is most common in the oral cavity of healthy adults with periodontal pockets less than 4 mm deep, and its percentage decreases in patients with periodontitis and periodontal pockets greater than 4 mm (Costalonga and Herzberg, 2014). In relation to oral cancer, *S. mitis* was significantly more frequently detected in the saliva of patients with OSCC (Mager et al., 2005), while a significant decrease in *S. mitis* abundance has been observed as the cancer progresses (Yang et al., 2018). Predictors of these causes include the species specificity of oral colonization by *Streptococcus* (Mager et al., 2005) and changes in the oral microenvironment of patients with advanced tumors (Yang et al., 2018). Our results suggest that *S. mitis* may play a protective role in patients with oral cancer by increasing the frequency of these bacteria in the oral cavity.

To confirm whether *S. mitis* effectively prevents the proliferation of oral cancer cells, we examined HSC-3 and Ca9-22 cells and found that the growth of both cell lines was suppressed by *S. mitis* (Figure 2). In a previous study, *S. mitis* was co-cultured with the OSCC cell lines CAL27, SCC25, and SCC4, and growth suppression was confirmed in all cases. Therefore, we can assume that *S. mitis* suppresses the growth of various oral cancer cells (Baraniya et al., 2020). In all experiments in this study, antibiotics were added to the culture medium used for cancer cells; therefore, we believe that abnormal bacterial growth did not occur.

A comprehensive survey of gene expression showed that the number of genes involved in mitotic nuclear division was significantly increased in HSC-3 cells treated with *S. mitis* (Figure 3A). In this study, we focused on *DUSP1*, which showed the most significant changes among the specific genes included in the analyzed GO terms. DUSP1 is a dual-specificity phosphatase

10.3389/fcimb.2025.1524820

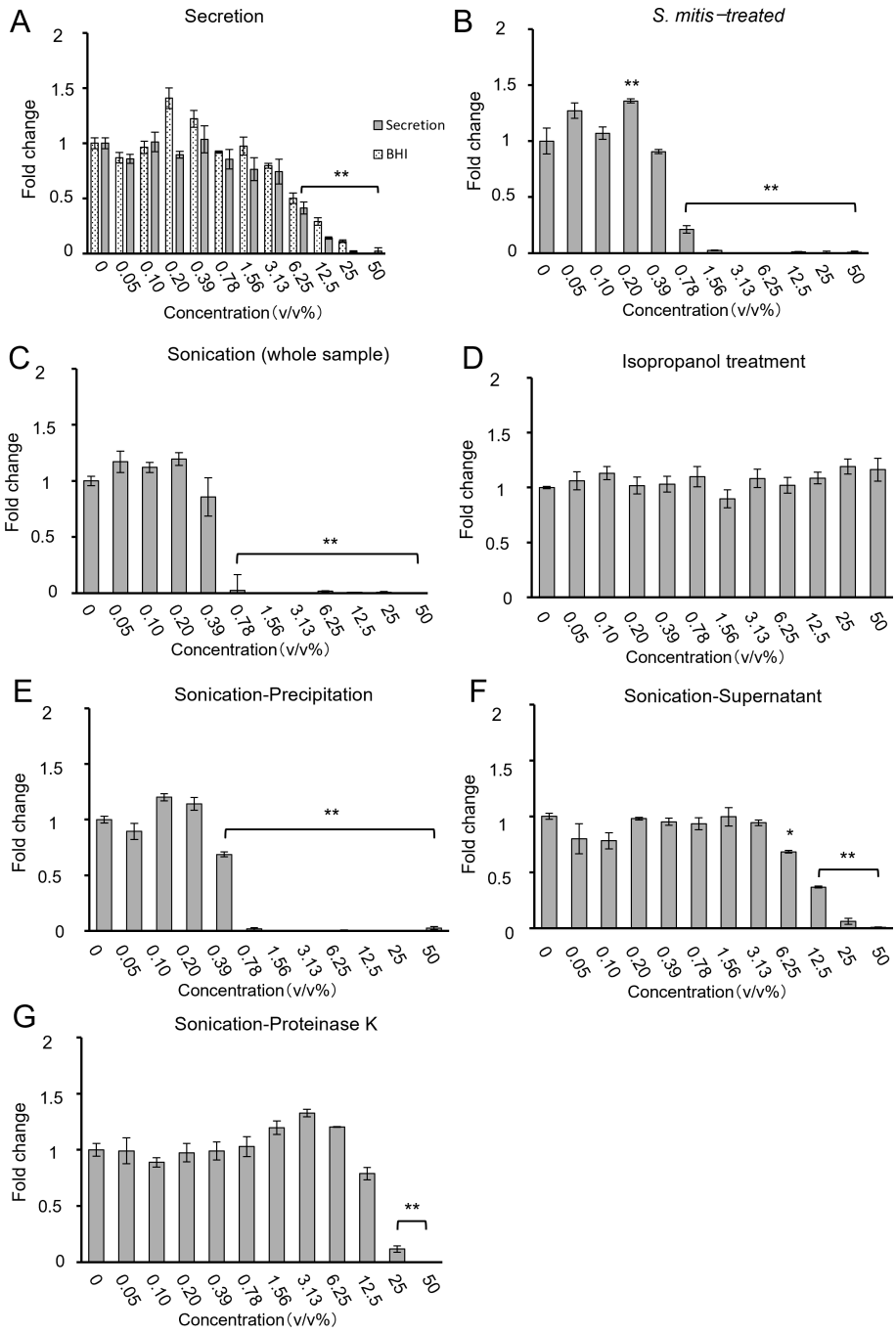

FIGURE 5
Cell proliferation when processed *S. mitis* (**(A)** secretion, **(B)** intact *S. mitis*, **(C)** sonication (whole sample), **(D)** isopropanol, **(E)** sonication-precipitate, **(F)** sonication-supernatant, and **(G)** sonication-Proteinase K) was added to HSC-3. Cell proliferation was evaluated using the CCK-8 assay (n = 3). The vertical axis shows the concentration of the bacterial solution (v/v%), and the horizontal axis represents the fold change. *$p < 0.05$, **$p < 0.01$ (Tukey's test after one-way analysis of variance).

that regulates mitogen-activated protein kinase (MAPK) activity (Lawan et al., 2013). DUSP1 expression is decreased in OSCC (Tomioka et al., 2006), and DUSP1 downregulation promotes the progression of head and neck squamous cell carcinoma (Zhang et al., 2014). In the present study, *DUSP1* expression was increased in HSC-3 cells whose growth was suppressed by *S. mitis* (Figure 3B), suggesting that changes in MAPK signaling by DUSP1 are an important mechanism for growth suppression. According to reports on cell cycle regulation, an increase in DUSP1 expression in gastric cancer leads to a cell cycle arrest in the G1 phase (Li et al., 2003), and it has been reported that DUSP1 expression in cumulus cells is reduced in the G0/G1 phase and increased in the S phase (Fu

TABLE 3 IC80 of HSC-3 cells following the addition of intact *S. mitis* or its components.

Bacterial component	IC80 (v/v%)
Secretion	–
S. mitis	0.78
Isopropanol treatment	–
Sonication (whole sample)	0.78
Sonication-precipitation	0.78
Sonication-supernatant	25
Sonication-Proteinase K	25

et al., 2019). However, specific reports regarding the involvement of DUSP1 in the cell cycle of oral cancer cells have not been published. In the future, the effects of increased DUSP1 expression on the growth of oral cancer cells should be investigated.

According to the results of the cell cycle assay (Figure 4), the number of HSC-3 cells stimulated with *S. mitis* in the G0/G1 phase decreased, whereas the number of cells in the G2/M phase increased; the proportion of cells in the S phase did not change significantly. This suggests that *S. mitis* induces G2/M phase arrest during the cell cycle progression of HSC-3 cells, thereby inhibiting proliferation. To the best of our knowledge, this is the first report on changes in the cell cycle following *S. mitis* infection of oral cancer cells. Previously, it has been reported that CAL27 cells treated with *F. nucleatum* showed increased proliferation and an increased G2/M phase ratio. Furthermore, when the phosphorylation inhibitor genistein was added, neither the proliferation rate nor the proportion of cells in the G2/M phase increased; however, the detailed mechanism of action is unclear (Li et al., 2024). Thus, *S. mitis* may affect each stage of the cell cycle, but further investigations are required.

To elucidate the mechanism of action underlying the effects of *S. mitis* on HSC-3 cells, we investigated the effects of intact bacteria and bacterial components of *S. mitis* on cancer cells. Previous studies have reported that many of the cytotoxic effects of bacteria are caused by H_2O_2 produced by them (Baraniya et al., 2020). Our study findings show that culture supernatants containing bacterial secretions had almost no growth-inhibiting effect (Figure 5A). Using a hydrogen peroxide test paper, we confirmed that the hydrogen peroxide concentration in the bacterial solution after resuspending the pellets and sonication was almost the same as that in E-MEM, the culture medium for cancer cells (Supplementary Figure 4). The growth-inhibiting effect did not differ when alive *S. mitis* was added, after it had been killed by ultrasound treatment, or when the bacterial cytoplasm content was extracted by centrifugation. Proteinase K degradation of proteins (Ebeling et al., 1974) reduced this inhibitory effect of *S. mitis*, albeit not completely. These findings strongly indicate that structural proteins within *S. mitis* contribute significantly to its anti-proliferative effects on cancer cells. Isopropanol (70%) is used as a disinfectant and is effective against Gram-positive bacteria. Protein denaturation is believed to occur in bacteria treated with isopropanol (Rutala and Weber, 2019). The differences in the effects of protein degradation by Proteinase K and that by isopropanol may provide clues for elucidating the structure of specific types of structural proteins involved in the observed inhibitory effects of *S. mitis*.

Oral cleaning is important in the treatment of periodontal diseases (Loesche and Grossman, 2001). Without periodontal disease, the proportion of *S. mitis* is high in the oral cavity (Costalonga and Herzberg, 2014). Therefore, the fact that *S. mitis* suppresses oral cancer may support the importance of oral cleaning in patients with oral cancer. However, the possibility of unknown adverse effects of *S. mitis* on living organisms cannot be completely ruled out since many effects of *S. mitis*' functions remain unknown. Because the inhibitory effect of *S. mitis* does not depend on whether the bacteria are alive or dead, it may be preferable to extract and use only the components that are important for the desired result.

This research has some limitations. First, the effects on non-cancer cells have not been investigated. It is necessary to examine whether *S. mitis* exerts cytotoxicity against non-cancerous cells of oral origin and to investigate the effects of *S. mitis* under conditions more similar to those of living organisms by using murine models of oral cancer. Second, the specific components of the bacteria that inhibit cancer cell growth have not been identified. We have shown in this study that protease treatment of the bacterial components attenuates their inhibitory effect, suggesting that structural proteins of the bacteria are important. Therefore, it would be necessary to further elucidate which proteins are important by recombining the genes involved in the expression of structural proteins of *S. mitis*. Third, the mechanism of action against oral cancer has not yet been fully explained. The investigation of receptors and signals on the cancer cell side and the clarification of inhibitory mechanisms may lead to the discovery of new cancer treatments.

5 Conclusion

This study revealed that *S. mitis*, a *Streptococcus* species that is the most common oral bacterium, suppresses the growth of oral cancer cells. The mechanism by which *S. mitis* suppresses cancer cell growth mainly involves the growth arrest of mitotic oral cancer cells, as revealed by RNA sequencing and flow cytometry. Our findings suggest that structural proteins of *S. mitis* are involved in these effects. This indicates that *S. mitis* may carry out an important role in the prevention and treatment of oral cancer, and we assume that increasing the number of *S. mitis* in the oral cavity may reduce the risk of oral cancer development.

Data availability statement

The sequencing data have been deposited in the DDBJ Sequence Read Archive under the accession number DRR665257-DRR665262.

Ethics statement

Ethical approval was not required for the studies on humans in accordance with the local legislation and institutional requirements because only commercially available established cell lines were used. Ethical approval was not required for the studies on animals in accordance with the local legislation and institutional requirements because only commercially available established cell lines were used.

Author contributions

II: Writing – original draft, Formal Analysis, Investigation, Methodology, Validation. SM: Formal Analysis, Investigation, Methodology, Writing – review & editing. FH: Funding acquisition, Writing – review & editing. YY: Writing – review & editing. OT: Conceptualization, Writing – review & editing. MS: Supervision, Writing – review & editing. MH: Project administration, Writing – review & editing. WA: Conceptualization, Project administration, Supervision, Writing – review & editing. RY: Conceptualization, Data curation, Funding acquisition, Investigation, Methodology, Project administration, Supervision, Validation, Writing – review & editing.

Funding

The author(s) declare that financial support was received for the research and/or publication of this article. This study was funded by JSPS KAKENHI, Grant Numbers 23K17147 and 23K09317 and partially supported by JSPS KAKENHI, Grant Number 24K12888.

Acknowledgments

We would like to thank Editage (www.editage.jp) for English language editing.

Conflict of interest

The authors declare that the research was conducted in the absence of any commercial or financial relationships that could be construed as a potential conflict of interest.

Generative AI statement

The author(s) declare that no Generative AI was used in the creation of this manuscript.

Publisher's note

Supplementary material

The Supplementary Material for this article can be found online at: https://www.frontiersin.org/articles/10.3389/fcimb.2025.1524820/full#supplementary-material

References

Ariyoshi, W., Okinaga, T., Chaweewannakorn, W., Akifusa, S., and Nisihara, T. (2017). Mechanisms involved in enhancement of matrix metalloproteinase-9 expression in macrophages by interleukin-33. *J. Cell. Physiol.* 232, 3481–3495. doi: 10.1002/jcp.25809

Asam, D., and Spellerberg, B. (2014). Molecular pathogenicity of *Streptococcus anginosus*. *Mol. Oral. Microbiol.* 29, 145–155. doi: 10.1111/omi.12056

Bagan, J., Sarrion, G., and Jimenez, Y. (2010). Oral cancer: clinical features. *Oral. Oncol.* 46, 414–417. doi: 10.1016/j.oraloncology.2010.03.009

Baraniya, D., Jain, V., Lucarelli, R., Tam, V., Vanderveer, L., Puri, S., et al. (2020). Screening of health-associated oral bacteria for anticancer properties in *vitro*. *Front. Cell. Infect. Microbiol.* 10. doi: 10.3389/fcimb.2020.575656

Chamoli, A., Gosavi, A. S., Shirwadkar, U. P., Wangdale, K. V., Behera, S. K., Kurrey, N. K., et al. (2021). Overview of oral cavity squamous cell carcinoma: Risk factors, mechanisms, and diagnostics. *Oral. Oncol.* 121, 105451. doi: 10.1016/j.oraloncology.2021.105451

Cho, I., and Blaser, M. J. (2012). The human microbiome: at the interface of health and disease. *Nat. Rev. Genet.* 13, 260–270. doi: 10.1038/nrg3182

Costalonga, M., and Herzberg, M. C. (2014). The oral microbiome and the immunobiology of periodontal disease and caries. *Immunol. Lett.* 162, 22–38. doi: 10.1016/j.imlet.2014.08.017

Ebeling, W., Hennrich, N., Klockow, M., Metz, H., Orth, H. D., and Lang, H. (1974). Proteinase K from *Tritirachium album* limber. *Eur. J. Biochem.* 47, 91–97. doi: 10.1111/j.1432-1033.1974.tb03671.x

Egawa, N. (2023). Papillomaviruses and cancer: commonalities and differences in HPV carcinogenesis at different sites of the body. *Int. J. Clin. Oncol.* 28, 956–964. doi: 10.1007/s10147-023-02340-y

Espinoza, J. A., Bizama, C., García, P., Ferreccio, C., Javle, M., Miquel, J. F., et al. (2016). The inflammatory inception of gallbladder cancer. *Biochim. Biophys. Acta* 1865, 245–254. doi: 10.1016/j.bbcan.2016.03.004

Fu, X. H., Chen, C. Z., Li, S., Han, D. X., Wang, Y. J., Yuan, B., et al. (2019). Dual-specificity phosphatase 1 regulates cell cycle progression and apoptosis in cumulus cells by affecting mitochondrial function, oxidative stress, and autophagy. *Am. J. Physiol. Cell Physiol.* 317, C1183–C1193. doi: 10.1152/ajpcell.00012.2019

Hanahan, D., and Weinberg, R. A. (2011). Hallmarks of cancer: the next generation. *Cell* 144, 646–674. doi: 10.1016/j.cell.2011.02.013

Jenkinson, H. F. (2011). Beyond the oral microbiome. *Environ. Microbiol.* 13, 3077–3087. doi: 10.1111/j.1462-2920.2011.02573.x

Karpiński, T. M. (2019). Role of oral microbiota in cancer development. *Microorganisms* 7, 20. doi: 10.3390/microorganisms7010020

Lawan, A., Shi, H., Gatzke, F., and Bennett, A. M. (2013). Diversity and specificity of the mitogen-activated protein kinase phosphatase-1 functions. *Cell. Mol. Life Sci.* 70, 223–237. doi: 10.1007/s00018-012-1041-2

Li, Z., Liu, Y., Huang, X., Wang, Q., Fu, R., Wen, X., et al. (2024). *F. Nucleatum* enhances oral squamous cell carcinoma proliferation via E-cadherin/β-Catenin pathway. *BMC Oral. Health* 24, 518. doi: 10.1186/s12903-024-04252-3

Li, R., Xiao, L., Gong, T., Liu, J., Li, Y., Zhou, X., et al. (2023). Role of oral microbiome in oral oncogenesis, tumor progression, and metastasis. *Mol. Oral. Microbiol.* 38, 9–22. doi: 10.1111/omi.12403

Li, M., Zhou, J. Y., Ge, Y., Matherly, L. H., and Wu, G. S. (2003). The phosphatase MKP1 is a transcriptional target of p53 involved in cell cycle regulation. *J. Biol. Chem.* 278, 41059–41068. doi: 10.1074/jbc.M307149200

Loesche, W. J., and Grossman, N. S. (2001). Periodontal disease as a specific, albeit chronic, infection: diagnosis and treatment. *Clin. Microbiol. Rev.* 14, 727–752. doi: 10.1128/CMR.14.4.727-752.2001

Mager, D. L., Haffajee, A. D., Devlin, P. M., Norris, C. M., Posner, M. R., and Goodson, J. M. (2005). The salivary microbiota as a diagnostic indicator of oral cancer: a descriptive, non-randomized study of cancer-free and oral squamous cell carcinoma subjects. *J. Transl. Med.* 3, 27. doi: 10.1186/1479-5876-3-27

Mitchell, J. (2011). *Streptococcus mitis*: walking the line between commensalism and pathogenesis. *Mol. Oral. Microbiol.* 26, 89–98. doi: 10.1111/j.2041-1014.2010.00601.x

Okahashi, N., Nakata, M., Kuwata, H., and Kawabata, S. (2022). Oral mitis group streptococci: A silent majority in our oral cavity. *Microbiol. Immunol.* 66, 539–551. doi: 10.1111/1348-0421.13028

Plottel, C. S., and Blaser, M. J. (2011). Microbiome and Malignancy. *Cell Host Microbe* 10, 324–335. doi: 10.1016/j.chom.2011.10.003

Polk, D. B., and Peek, R. M. (2010). *Helicobacter pylori*: gastric cancer and beyond. *Nat. Rev. Cancer* 10, 403–414. doi: 10.1038/nrc2857

Rutala, W. A., and Weber, D. J. (2019). Guideline for disinfection and sterilization in healthcare facilitie. Available online at: https://stacks.cdc.gov/view/cdc/134910 (Accessed October 14, 2024).

Sasaki, M., Yamaura, C., Ohara-Nemoto, Y., Tajika, S., Kodama, Y., Ohya, T., et al. (2005). *Streptococcus anginosus* infection in oral cancer and its infection route. *Oral. Dis.* 11, 151–156. doi: 10.1111/j.1601-0825.2005.01051.x

Sun, J., Tang, Q., Yu, S., Xie, M., Xie, Y., Chen, G., et al. (2020). Role of the oral microbiota in cancer evolution and progression. *Cancer Med.* 9, 6306–6321. doi: 10.1002/cam4.3206

Sung, H., Ferlay, J., Siegel, R. L., Laversanne, M., Soerjomataram, I., Jemal, A., et al. (2021). Global Cancer Statistics 2020: GLOBOCAN estimates of incidence and mortality worldwide for 36 cancers in 185 countries. *CA Cancer J. Clin.* 71, 209–249. doi: 10.3322/caac.21660

Tan, Y., Wang, Z., Xu, M., Li, B., Huang, Z., Qin, S., et al. (2023). Oral squamous cell carcinomas: state of the field and emerging directions. *Int. J. Oral. Sci.* 15, 44. doi: 10.1038/s41368-023-00249-w

Tomioka, H., Morita, K., Hasegawa, S., and Omura, K. (2006). Gene expression analysis by cDNA microarray in oral squamous cell carcinoma. *J. Oral. Pathol. Med.* 35, 206–211. doi: 10.1111/j.1600-0714.2006.00410.x

Vermaire, J. A., Partoredjo, A. S. K., de Groot, R. J., Brand, H. S., and Speksnijder, C. M. (2022). Mastication in health-related quality of life in patients treated for oral cancer: A systematic review. *Eur. J. Cancer Care (Engl.)* 31, e13744. doi: 10.1111/ecc.13744

Wang, X., Wu, S., Wu, W., Zhang, W., Li, L., Liu, Q., et al. (2023). *Candida albicans* promotes oral cancer via IL-17A/IL-17RA-macrophage axis. *mBio* 14, e0044723. doi: 10.1128/mbio.00447-23

Xu, Y., Jia, Y., Chen, L., Gao, J., and Yang, D. (2021). Effect of *Streptococcus anginosus* on biological response of tongue squamous cell carcinoma cells. *BMC Oral. Health* 21, 141. doi: 10.1186/s12903-021-01505-3

Yang, C. Y., Yeh, Y. M., Yu, H. Y., Chin, C. Y., Hsu, C. W., Liu, H., et al. (2018). Oral microbiota community dynamics associated with oral squamous cell carcinoma staging. *Front. Microbiol.* 9. doi: 10.3389/fmicb.2018.00862

Zhang, X., Hyer, J. M., Yu, H., D'Silva, N. J., and Kirkwood, K. L. (2014). DUSP1 phosphatase regulates the proinflammatory milieu in head and neck squamous cell carcinoma. *Cancer Res.* 74, 7191–7197. doi: 10.1158/0008-5472.CAN-14-1379

frontiers | Frontiers in Cellular and Infection Microbiology

TYPE Review
PUBLISHED 14 May 2025
DOI 10.3389/fcimb.2025.1516237

OPEN ACCESS

EDITED BY
Maurizio Sanguinetti,
Catholic University of the Sacred Heart, Italy

REVIEWED BY
Paweł Krzyżek,
Wroclaw Medical University, Poland
Katie A. Lloyd,
University of Chester, Chester,
United Kingdom
Mahmoud Mohammed Bendary,
Port Said University, Egypt

*CORRESPONDENCE
Renitta Jobby
renitta7@gmail.com
Vinothkannan Ravichandran
vrvinothan@gmail.com
Sohinee Sarkar
sohinee.sarkar@mcri.edu.au

RECEIVED 24 October 2024
ACCEPTED 21 April 2025
PUBLISHED 14 May 2025

CITATION
Patil S, Yu S, Jobby R, Ravichandran V and Sarkar S (2025) A critical review on *In Vivo* and *Ex Vivo* models for the investigation of *Helicobacter pylori* infection.
Front. Cell. Infect. Microbiol. 15:1516237.
doi: 10.3389/fcimb.2025.1516237

A critical review on *In Vivo* and *Ex Vivo* models for the investigation of *Helicobacter pylori* infection

Shwetlaxmi Patil[1], Songmin Yu[2,3], Renitta Jobby[1,4]*, Vinothkannan Ravichandran[1,5]* and Sohinee Sarkar[2,3]*

[1]Amity Institute of Biotechnology, Amity University Maharashtra, Mumbai, India, [2]Murdoch Children's Research Institute, Parkville, VIC, Australia, [3]Department of Pediatrics, University of Melbourne, Parkville, VIC, Australia, [4]Amity Centre of Excellence in Astrobiology, Amity University Maharashtra, Mumbai, India, [5]Center for Drug Discovery and Development (CD3), Amity Institute of Biotechnology, Amity University Maharashtra, Mumbai, India

Helicobacter pylori is a stomach-dwelling bacterium with a crude global prevalence of nearly 45% in adults and 35% in children and adolescents. Chronic *H. pylori* infection and the resulting inflammation are major causes of gastritis, peptic ulcer disease and gastric cancer. Since its discovery in 1982, various animal models have been proposed to recreate the specific pathophysiological interactions between *H. pylori* and the human host. These infection models have been instrumental in dissecting the key drivers of *H. pylori* colonization, persistence and mediators of host immune responses. However, a comprehensive understanding of the molecular triggers for malignant transformation of the gastric mucosa is still lacking. Vaccine development in this area has stalled, as promising candidates identified through animal studies have failed in advanced human clinical trials. Currently, *H.* pylori eradication is heavily reliant on different antimicrobial agents. As with other bacterial pathogens, the growing antimicrobial resistance in *H. pylori* remains a major challenge, making eradication therapy increasingly complex and prolonged, over time. Recent drug approvals have mostly been for newer combinations of conventional antibiotics and proton pump inhibitors. Thus, the development of novel treatments and innovative models are crucial for advancing the drug development pipeline. This review encompasses the development and recent advances in animal and non-animal models of *H. pylori* gastric infection and its applications in investigating novel therapeutics and vaccine candidates.

KEYWORDS

***Helicobacter pylori*, animal models, antimicrobial resistance, gastritis, peptic ulcer disease, gastric cancer, gastric organoids**

Introduction

The microaerobic *Helicobacter pylori* is a Gram-negative, spiral rod-shaped bacterium that predominantly colonizes the human gastric mucosal surface and is associated with acute and chronic gastritis, peptic ulcers, and other upper gastrointestinal disorders (Aihara et al., 2014; Chen et al., 2024). Recent estimates of *H. pylori* colonization show a crude global prevalence of nearly 45% in adults and 35% in children and adolescents (Chen et al., 2024). Despite the high prevalence, in 80%-85% of cases, the bacteria's existence is unrelated to any clinically symptomatic disease (Elbehiry et al., 2023). However, individuals with *H. pylori*-associated chronic gastritis have a 1%-3% chance of developing gastric cancer (Uemura et al., 2001) and a 10%–20% chance of developing peptic ulcers (Peek, 2008). The World Health Organization (WHO) has designated *H. pylori* infection as a class I carcinogen due to its ability to cause gastric adenocarcinoma (stomach cancer) and mucosa-associated lymphoid tissue (MALT) lymphoma (Vogiatzi et al., 2007). Presently, gastric cancer ranks as the fifth most common cancer worldwide and the fifth leading cause of cancer-related deaths (Bray et al., 2024).

The prevalence of *H. pylori* varies between and within countries, but it is generally estimated to range from 30% to 50% in developed countries and from 60% to 80% in underdeveloped regions (Chen et al., 2024; Poddar, 2019). These estimates are based on stratified variables like geography, age, socioeconomic status, and ethnicity, which result in significant regional and national variations. In India, the prevalence of *H. pylori* infection has been reported to be relatively high, with studies indicating that up to 80% of children under the age of 10 may be infected (Poddar and Yachha, 2007). The high prevalence of *H. pylori* infection in India can be attributed to factors such as poor sanitation, overcrowding, and lack of access to clean water (Thirumurthi and Graham, 2012). *H. pylori* is typically acquired very early on in childhood via oral-oral, fecal-oral or iatrogenic routes of transmission (Brown, 2000). Having evolved with the human host for thousands of years (Linz et al., 2007), these bacteria demonstrate a remarkable ability to survive in the harsh acidic environment of the stomach, localizing within the gastric mucosal layer during chronic infection (Figure 1) and potentially persisting for the host's lifetime. *H. pylori* have an arsenal of different colonization and virulence factors that facilitate its persistence within the gastric niche. Bacterial factors such as urease production, chemotactic motility, and the capacity to adjust to the changing gastric environment, all contribute to its ability to survive in the stomach for decades (Yamaoka, 2010). However, the more severe disease states are associated with presence of the cytotoxin-associated gene A (*cagA*) and vacuolating cytotoxin A (*vacA*) genes, both which encode for corresponding polymorphic cytotoxins that are injected and secreted by *H. pylori* and contribute significantly to its pathogenesis (Jones et al, 2010). *H. pylori* can further produce diverse classes of lytic enzymes, including lipases, phospholipases, and proteases, which degrade gastric mucus by altering its viscosity and hydrophobicity (Asante et al., 1997; Celli et al., 2009). The compromised mucus barrier allows *H. pylori* to closely associate with the gastric epithelium while making the latter more susceptible to gastric acid. It has recently been proposed that biofilm

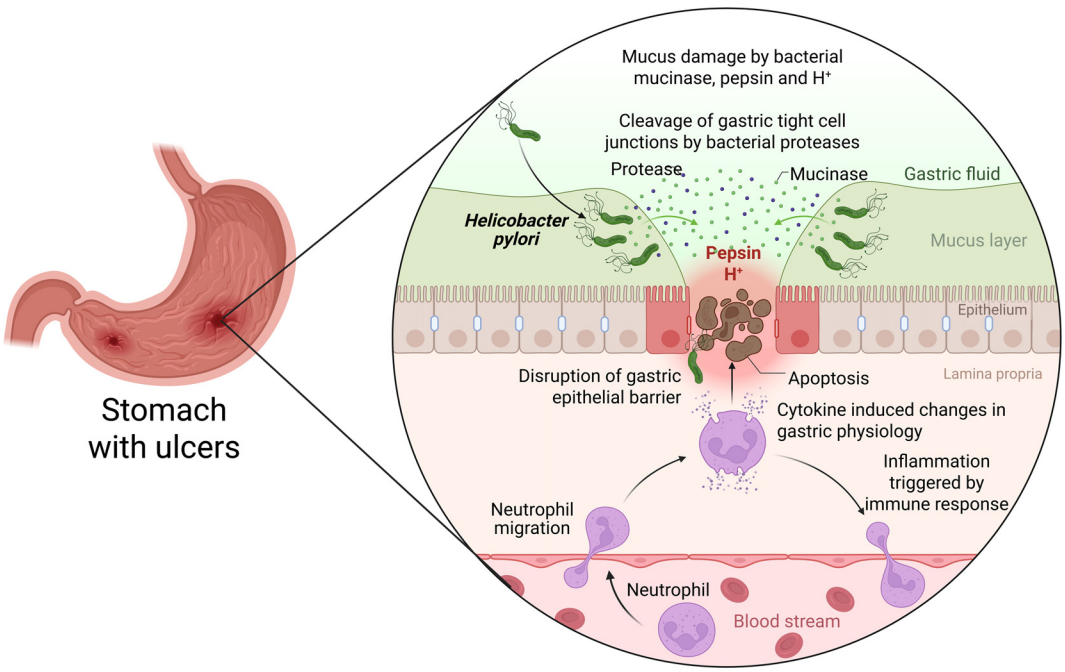

FIGURE 1
Pathogenesis of *H. pylori* infection within the gastric epithelium. Three main stages of *H. pylori* pathogenesis can be studied: i) bacterial attachment to and colonization of the stomach mucosa; ii) the host's immune response and *H. pylori's* immune-evasive mechanisms; and iii) the pathological consequences of chronic infection (Elbehiry et al., 2023) *Created with BioRender*.

development also contributes to chronic colonization (Carron et al., 2006; Cole et al., 2004).

H. pylori and the gastric precancerous cascade

Gastric cancer is the most serious pathological consequence of *H. pylori* infection, although exact steps leading up to it are poorly understood. While gastric cancer can be broadly divided into diffuse and intestinal types, it is the latter that is most commonly associated with *H. pylori* infection (Uemura et al., 2001; Hanada and Graham, 2014). The progression of chronic gastritis towards the development of the gastric ulcers and eventually, gastric cancer, is associated with mucosal pH variations (Brawner et al, 2014) and distinct, sequential changes within the tissue. This precancerous process takes place, presumably over several decades, before any clinical presentation of cancer. First delineated by Pelayo Correa in 1992 (Correa, 1992), specific stages of the precancerous cascade have been refined over the years. The 'Correa Cascade' describes the transition of the gastric mucosa from chronic active gastritis → chronic atrophic gastritis → intestinal metaplasia → dysplasia and ultimately, invasive carcinoma (Correa, 2013). This process is triggered by *H. pylori* infection and sustained by the resultant chronic inflammation. It was initially proposed that eradication of *H. pylori* till the stage of intestinal metaplasia can successfully halt the progression towards gastric cancer. However, more recent evidence suggests that while *H. pylori* eradication is still the most important method for preventing gastric cancer globally, its effect on established gastric intestinal metaplasia is limited (Cheng et al., 2023; Zhu et al., 2024). Thus, early and successful eradication of *H. pylori* is critical for the prevention of gastric cancer.

Current challenges in treatment of *H. pylori*: rise in antimicrobial resistance

The sole and current therapy for *H. pylori* infection in humans is the use of antibiotics (Suzuki et al., 2022). The triple and quadruple therapy regimens are used as the first line of defense against *H. pylori* infection depending on local resistance profiles and treatment guidelines. According to worldwide recommendations, the most commonly used first-line treatment for *H. pylori* infection involves a 'triple therapy' that includes a proton pump inhibitor (PPI) combined with two broad spectrum antibiotics (amoxicillin, clarithromycin, levofloxacin, and metronidazole) for 7 to 14 days (Chey et al., 2024). However, because of the prevalence of antibiotic resistance, the eradication rates of therapy have declined to <80% in many countries (Jiang et al., 2022; Aumpan et al., 2023). The addition of Bismuth to the PPI-antibiotic combination constitutes the 'quadruple therapy' regimen that is being increasingly used as a first line treatment in areas with high resistance (Chey et al., 2024).

Antimicrobial resistance is acknowledged as a significant public health issue with worldwide implications, particularly considering that the rate of advent of multidrug resistant bacteria has vastly outpaced and the slow discovery of novel antibiotics (Ortiz et al., 2019; Aumpan et al., 2023). Antimicrobial resistance may be more prevalent in developing nations than in high-income countries, even though statistics are scarce in low- and middle-income countries (Jaka et al., 2018; Ortiz et al., 2019). Despite concerted stewardship efforts, antimicrobials are increasingly being consumed worldwide, often without appropriate prescription or compliance (Zarauz et al., 2022; Ventola, 2015). Global antimicrobial usage grew by at least 35% in the last ten years, with only a handful of countries responsible for 75% of this growth (Collaborators, 2024). In many nations with significant antimicrobial usage, the high rates of self-medication and the availability of antimicrobials over the counter are of particular concern (Ortiz et al., 2019). In addition to variations in antibiotic resistance rates, there can be differences in the prevalence of the infection within and across different topographical regions within a country (Jiang et al., 2022).

Within the context of *H. pylori* eradication therapy, the results of a recent meta-analysis study released in 2018 show that the rates of primary and secondary resistance to levofloxacin, metronidazole, and clarithromycin have already reached alarming levels (>15%) in nearly all WHO areas (Shah et al, 2021). This has led to the failure rate of triple therapy rising to more than 20% in many regions of the world (Shah et al, 2021). Considering the poor prognosis of gastric cancer and the significant morbidity and costs associated with earlier stages of *H. pylori* pathologies (such as peptic ulcer disease), there is a critical need to create novel therapeutic approaches to combat antimicrobial resistance in *H. pylori*. Even though *H. pylori* has been excluded from the most recent iteration of WHO's priority pathogen list for urgent drug development, the report acknowledges the increasing complexity of treatment and associated adverse effects and failure rates, which necessitates a renewed focus by researchers and drug developers, alike.

Here in this review, we have discussed various animal models, including knock-out and transgenic models, available for the study of various stages of *H. pylori* pathophysiology (Figure 1). We have further emphasized the *ex vivo* models such as gastric and intestinal organoids along with their advantages and limitations that can be a valuable addition to the resources that can be utilized for the development of novel therapeutics and vaccine candidates.

Animal models

While animal models have been instrumental in identifying some of the key features of *H. pylori* pathogenesis that underpins chronic gastritis and the development of ulcers, the exact triggers for gastric carcinogenesis remain under investigation (Ansari and Yamaoka, 2022). The natural history of infection in animals is unknown, and *H. pylori* does not readily infect the gastric mucosa of animals, despite the fact that it is well adapted to colonize the human stomach (Go, 2002). Investigations during early infection in humans are often hindered by the natural pathophysiology of the disease as gastric cancer takes decades to develop due to the complicated interactions between *H. pylori* and the stomach epithelium (Correa and Piazuelo,

2008). The pathogenesis of *H. pylori* infection and the immunological responses brought on by this bacterium have been difficult to ascertain due to the close co-evolution of this pathogen with its human host. However, animal models must be used in order to fully understand the role of host's microenvironment in various *H. pylori*-induced disease states, including gastric cancer. These models have indeed been very helpful in understanding the pathophysiology of *H. pylori* colonization (Peek, 2008) with an emphasis on the comprehension of host immune responses and the natural history of infection (Figure 2). Animals like pigs, rodents, mice, Mongolian gerbils, and guinea pigs have all been mentioned as potential reservoirs for *H. pylori* (Peek, 2008). Thus, appropriate animal models must be used to enable a thorough understanding of the role of the host's microenvironment that sustains and drives *H. pylori*-induced inflammation and gastric cancer. Although these animal models have been beneficial in understanding the host, bacterial, and environmental variables involved in gastritis and gastric carcinogenesis, no single model stands as the definitive standard for mimicking natural human infection (Table 1).

Early animal models

Gnotobiotic piglets were probably the first animals to undergo successful infection with *H. pylori* (Lambert et al., 1987; Krakowka et al., 1987; Eaton et al, 1989). While these animals have been instrumental in studying the role of urease and motility in the mediation of *H. pylori* infection induced pathology, key immune features observed in this model can vary significantly from humans. Despite its early applications, researchers have moved away from using this model, likely due to economic limitations and the need for specialized breeding and experimental facilities.

Beagle dogs, both gnotobiotic pups and conventional animals, have been investigated for experimental *H. pylori* infection. Gnotobiotic pups, infected at 7 days of age, showed successful *H. pylori* colonization for at least a month post-infection, albeit at a lower level compared to humans (Radin et al., 1990). Gastric lesions were observed upon gross examination with microscopic evidence of immune cell infiltration into the gastric lamina propria. Antibodies specific to *H. pylori* were developed in conventional

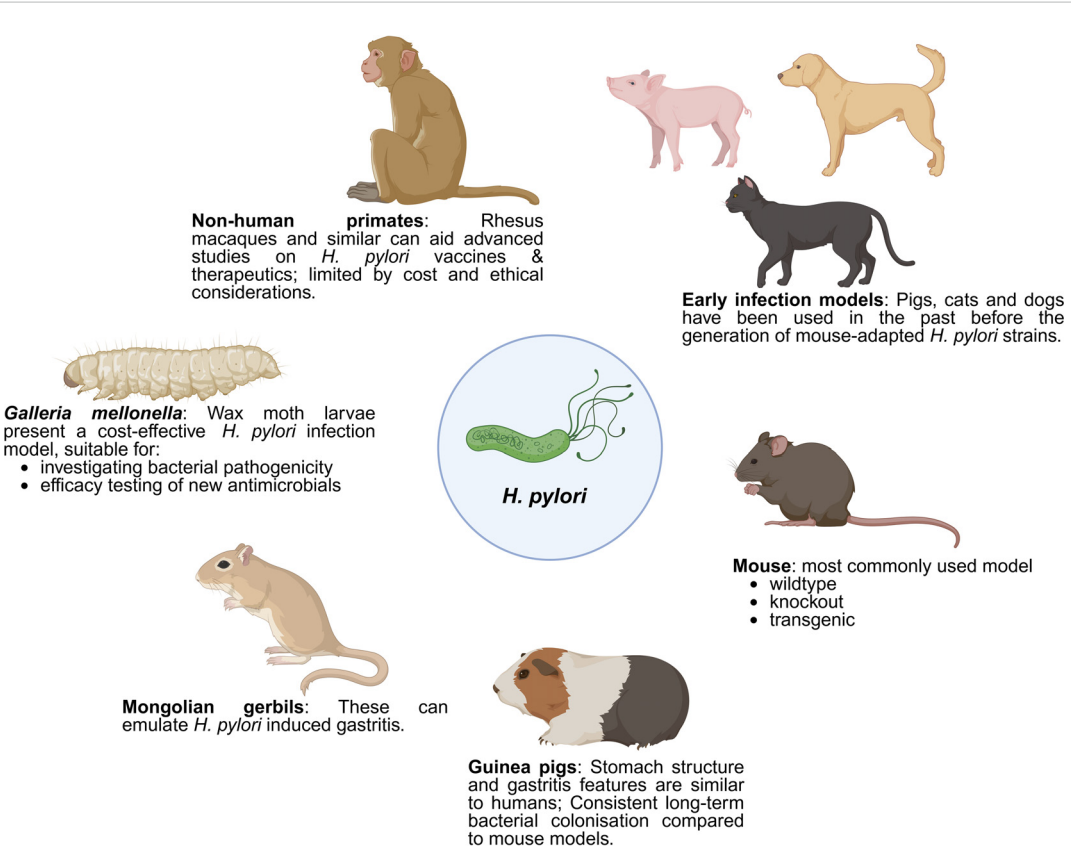

FIGURE 2
Various *in vivo* models for the study of *H. pylori* pathogenesis. This figure illustrates various animal models employed in the study of *H. pylori* infection and its pathogenesis. Early infection models, including pigs, cats, and dogs, were initially used before the development of mouse-adapted *H. pylori* strains. Mice remain the most commonly used model, available in wildtype, knockout, and transgenic varieties. *Mongolian gerbils* are effective in emulating *H. pylori*-induced gastritis, while guinea pigs, with stomach structures and gastritis features similar to humans, allow for consistent, long-term bacterial colonization studies. Non-human primates, such as rhesus macaques, are useful for advanced studies on *H. pylori* vaccines and therapeutics, despite limitations due to cost and ethical considerations. Wax moth larvae (*Galleria mellonella*) present a cost-effective infection model, suitable for investigating bacterial pathogenicity and testing new antimicrobials. Created with BioRender.

TABLE 1 Summary of different *in vivo* models used to study *H. pylori* pathogenesis with its advantages, limitations and applications in research.

Animal Model	Characteristics/Advantages	Research Focus	Limitations	References
Early models (gnotobiotic pigs, dogs and cats)	Used in early *H. pylori* research prior to the establishment of mouse infection models	Instrumental in identifying critical bacterial virulence factors such as urease and motility Early characterization of lymphofollicular gastritis	Significant immune differences from humans; economic and logistical challenges. Lower colonization levels, acute infection symptoms, and not widely adopted.	(Fox et al., 1995; Handt et al., 1995; Radin et al., 1990; Eaton et al., 1989; Krakowka et al., 1987)
Galleria mellonella (wax moth larvae)	Quick determination of *in vivo* toxicity. Cost-effective model for *H. pylori* virulence factors.	Screening clinical *H. pylori* strains. Discriminating between virulent and avirulent strains. Studying pathogenic mechanisms.	Incomplete recapitulation of mammalian infection; supplementary to more physiologically relevant models.	(Giannouli et al., 2014; Krzyżek et al., 2025; Ochoa et al., 2021)
Mouse models	Widely used for modelling different stages of pathogenesis and genetic disorders. Humanized models available for physiological similarity. Vast resource of molecular tools for genetic manipulation and immunological studies.	Testing *H. pylori* mediated gastric pathology Investigation of novel antimicrobials and phytochemicals. Limited insight into severe *H. pylori* illnesses. Investigating immune responses and vaccination strategies.	Milder gastritis and slow disease progression; variability in bacterial virulence; complex pathogenic mechanisms.	(Lee et al., 1997; Dey et al., 2021; Jiang and Yu, 2017; Menheniott et al., 2016; Ohnishi et al., 2008; Sawai et al., 1999; Stair et al., 2023)
Mongolian gerbils	Mirror *H. pylori*-induced human symptoms and diseases. Cost-effective model for studying probiotics.	Validating vaccines and mutation analysis. Studying gastritis, Cag T4SS, and microbiota changes. Testing proton pump inhibitor therapy.	Varied cancer development timelines; lack of molecular resources.	(Guo et al., 2019; Isobe et al., 2012; Jeremy et al., 2006; Kuo et al., 2013; Lin et al., 2020)
Non-human primates	Ideal for physiological studies due to similarities with humans. Chronic gastritis observed in pigtailed macaques and rhesus monkeys.	Testing late-stage vaccine candidates against *H. pylori* prior to human clinical trials Genetic analysis of complex physiological traits.	High cost, time and labor-intensive, ethical concerns, and limited widespread use.	(Semrau et al., 2017; Solnick et al., 2003, Solnick et al, 2006, Solnick et al, 2001)
Guinea pigs	Useful model for studying antral gastritis caused by *H. pylori.* Similar gastric anatomy and physiology to humans.	Modeling *H. pylori*-induced stomach diseases. Studying pathogenesis and host immune response. Examining IL-8 expression and epithelial cell changes.	Limited widespread use despite anatomical and pathophysiological similarities to humans.	(Shomer et al., 1998; Sturegård et al., 1998; Tomaszewska et al., 2024)

beagle dogs that were infected between four and six months of age and observed for up to 24 weeks (Rossi et al., 1999). Animals with an acute infection experienced vomiting and diarrhea. This was followed by polymorphonuclear cell infiltration and subsequent development of gastritis with epithelial changes linked to the development of MALT lymphoma in humans. Even though the pathophysiology of *H. pylori* infection in dogs closely resembles that of humans, this model has not been adopted more widely. Similarly, there are not many reported studies on feline infections. The initial descriptions of feline *H. pylori* infection demonstrated the development of lymphofollicular gastritis (Fox et al., 1995; Handt et al., 1995). According to a vaccination study, cats that received the urease antigen orally were protected against the *H. pylori* challenge (Handt et al., 1995). However, there have not been wider studies with this host species other than reports of isolation and characterization of non-*H. pylori Helicobacter* isolates.

Galleria mellonella larvae

Insects can be employed to quickly determine *in vivo* toxicity and efficacy of novel antimicrobial compounds, which makes it possible to conduct more targeted mammalian testing. *Galleria mellonella* is a wax moth present throughout the world and its larvae have been used as animal model in several research studies for over two decades (Tsai et al, 2016). The larvae of *G. mellonella* are being utilized more frequently as miniature hosts to study the pathogenesis and virulence components of many bacterial and fungal human pathogens from humans despite the fact that they do not recapitulate all elements of mammalian infection. This has the following benefits: i) adaptation to the human physiological temperature (37°C), ii) presence of a well-characterized phagocytic system, and iii) availability of a comprehensive transcriptome and immune gene repertoire. Several pathogens, including

Pseudomonas aeruginosa, Staphylococcus aureus, Acinetobacter baumannii, Klebsiella pneumoniae, and *Campylobacter jejuni*, have been shown to be pathogenic in *G. mellonella* larvae (Tsai et al, 2016). Due to their susceptibility to *H. pylori* infection and relatively lower thresholds of legal or ethical considerations, *G. mellonella* larvae have been proposed as a simple *in vivo* model for the study of *H. pylori* virulence factors and pathogenic pathways (Giannouli et al., 2014). The experimental paradigm that has been developed can be helpful for screening a relatively large number of clinical *H. pylori* strains and for correlating the disease state of patients with the virulence of these strains (Giannouli et al., 2014). Recently this model was utilized to demonstrate biofilm formation by multidrug resistant *H. pylori* strain during its exposure to stress caused by clarithromycin (Krzyżek et al., 2025). The *G. mellonella* larval infection model recapitulates important aspects of *H. pylori* pathophysiology and is cost-effective in comparison to mammalian infection models. While it could be useful for the initial evaluation of the impact of *H. pylori* virulence parameters factors on particular cellular functions, it is unable to completely substitute the well-established and more physiologically relevant *in vivo* models in the analysis of the complex pathogenic mechanisms underlying *H. pylori*-related human disease (Giannouli et al., 2014; Ochoa et al., 2021) and the efficacy of therapeutics (Almeida Furquim de Camargo et al., 2020). In summary, the *G. mellonella* model may lessen reliance on mammalian infection models based on its ability to differentiate between virulent and non-virulent *H. pylori* isolates, determine putative genes associated with virulence through genome-wide association studies and identify novel molecular targets for antimicrobial therapy.

Mouse models

Mice have been a crucial model organism to study different human infectious diseases and genetic disorders. The predominantly used wildtype mouse strains in *H. pylori* infection are C57BL/6 and BALB/c, followed by less commonly used Swiss albino, ICR and Kunming mice (Ansari and Yamaoka, 2022; Wei et al., 2019; Kimura et al., 1998). These models are used to study the effects of *H. pylori* colonization and to test the efficacy of different antimicrobials, phytochemicals, and probiotics. The bacterial strain used to infect these mice presents another important facet to the infection as mice do not get colonized by *H. pylori* as readily as humans (Salama et al, 2013). It is interesting to note that before *H. pylori* infection models were developed, mouse infection models and vaccination trials extensively employed a feline *Helicobacter* isolate named *H. felis*. *H. felis* lacks the *cag* pathogenicity island and produces severe atrophic gastritis in C57BL/6 mice, but only mild disease in BALB/c mice (Zhang and Moss, 2012). In 1997, Lee et al., introduced the first standardized mouse infection model of *H. pylori* with the Sydney strain SS1 derived from an individual with duodenal ulcers (Lee et al., 1997). The original strain was cag^+ vac^+ (PMSS1) but underwent modification during experimental infection to yield the type 4 secretion system (T4SS) deficient SS1 strain widely used in infection studies nowadays. The parental PMSS1 strain is often used to study the effect of a functional cagPAI system (Arnold et al., 2011) although it has been reported that this genetic island is susceptible to genetic rearrangement and disruption leading to variability in bacterial virulence features (Dyer et al., 2018). Overall, *H. pylori* infection in wildtype mice frequently results in milder gastritis or slowly progressive illnesses, and these models offer less insight into the toxicity of clinical *H. pylori* strains. Furthermore, while these wildtype mice infected with *H. pylori* and *H. felis* develop lymphocytic gastritis, they generally do not advance to more severe conditions such as peptic ulcers or stomach cancer (Zhang and Moss, 2012).

To compensate for the deficiencies of the wildtype mouse models, several knockout and transgenic mice have been developed over the years. These have incrementally paved the way for the identification of critical host factors implicated in *H. pylori* pathogenesis and the development of gastric cancer. Some examples are reviewed below.

H. pylori infection-induced gastric inflammation is largely mediated by IFN-gamma and double-knockout mice have been demonstrated to allow longer colonization by strains that are unable to infect wildtype mice (Sawai et al., 1999). Chronic infection is typically associated with significantly lower inflammation in this model which has been used for many vaccine studies. Similar observations have been made in mice deficient in TNF-alpha signaling (Yamamoto et al., 2004).

H. pylori infection has a synergistic effect on the development of gastric cancer in individuals with IL-1β gene polymorphisms with the most severe gastric pathology being observed in patients with both host and bacterial high-risk genotypes (El-Omar et al., 2000). IL-1 receptor knockout mice have lower gastritis scores and associated pathology markers such as nitric oxide production (Huang et al., 2013). Gastrokine-2 is an anti-inflammatory protein produced in the gastric epithelium and its deletion drives premalignant gastric inflammation and tumor progression in mice that is accelerated by *H. pylori* infection (Menheniott et al., 2016). Furthermore, GKN-2 expression is progressively lost during the progression of gastric cancer, and it plays a causal role in its development (Chung Nien Chin et al., 2020). During early *H. pylori* infection, Fas-antigen mediated apoptosis depletes gastric parietal and chief cells which are then replaced by metaplastic glandular lineages resistant to Fas-apoptosis. This has been modelled in Fas antigen–deficient (*lpr*) mice that develop invasive stomach lesions post *H. pylori* infection (Cai et al., 2005).

Transgenic mice are genetically engineered mice that harbor gene insertions from different species. Humanized insulin/Gastrin (INS-GAS) transgenic mice are frequently used to model stomach cancer as they have high circulating levels of pancreatic gastrin (Jiang and Yu, 2017). These mice spontaneously develop atrophic gastritis and intestinal metaplasia which then progress to corpus-centric cancer. PMSS1 infection in IN-GAS mice results in invasive carcinoma whereas SS1 infection causes only dysplasia (Lofgren et al., 2011; Stair et al., 2023), thus demonstrating the importance of bacterial factors in determining disease progression. Transgenic expression of *H. pylori* CagA in mice has been shown to induce gastrointestinal and hematopoietic neoplasms (Ohnishi et al., 2008).

Mongolian Gerbils

Mongolian gerbils are small rodents that show similar symptoms to humans, such as appetite and weight loss, and recount many attributes of *H. pylori*-induced gastric colonization, inflammation, ulcers, and cancers (Noto et al., 2016). After it was discovered that Mongolian gerbils can mirror several characteristics of *H. pylori*-induced human stomach inflammation and cancer, these rodents captured considerable interest and attracted a lot of attention, particularly for vaccine studies (Jeremy et al., 2006; Guo et al., 2019; Lv et al., 2014; Noto et al., 2016; Wu et al., 2008). However, the timeline for cancer development varies greatly between studies and appears to be contingent on the infecting *H. pylori* strain. Gerbil infection by a modified *H. pylori* strain with an inducible T4SS has demonstrated that while an infectious trigger can be instrumental for cancer development, cancer progression does not necessarily depend on the persistent presence of the infectious agent (Lin et al., 2020). Comparative genomic studies in this model have shown that the genomes of three strains recovered from infected gerbil stomachs showed mutations in *babA*, *tlpB*, and *gltS* genes, all of which are linked to host adaptation (Suzuki et al., 2019).

This model has also been used in the study of probiotics in *H. pylori* eradication (Kuo et al., 2013; Zheng et al., 2024). Probiotics have been shown to inhibit *H. pylori* growth, adhesion, and the production of virulence factors *in vitro*. In the gerbil infection model, probiotics have been demonstrated to prevent the colonization of *H. pylori* (Zheng et al., 2024; Kuo et al., 2013; Isobe et al., 2012). This model has also demonstrated that the presence of *H. pylori* and related inflammation can alter microbiome composition in the non-inflamed regions of the gastrointestinal tract (Heimesaat et al., 2014). While the Mongolian gerbil infection model has been instrumental in dissecting the critical determinants mediating host-pathogen interactions during *H. pylori* infection, the lack of molecular resources has stymied its wider application within the research community.

Guinea pigs

The guinea pig stomach structure is akin to that of humans with a dietary requirement for vitamin C like humans and other primates. *H. pylori* infection in this model, first described in the late 1990's, produces an inflammatory response driven by IL-8 secretion by gastric epithelial cells (Sturegård et al., 1998; Kleanthous et al, 1998). Infections with either the rodent adapted SS1 strain or clinical *H. pylori* isolates from gastric biopsies were able to establish lasting colonization and induce seroconversion in infected animals. Chronic infection was associated with the development of antral gastritis and lymphoid follicles like that of *H. pylori*-infected humans. Epithelial cell proliferation as evidenced by the presence of a large population of Ki67-positive gastric cells, is readily observed in this model (Gonciarz et al., 2019). This model has been used in a recent study delineating the role of *H. pylori* in driving metabolic syndrome (Tomaszewska et al., 2024). Despite the similarities with human gastric anatomy and *H. pylori* related pathophysiology, this model has not been widely used.

Non-human primates

Non-human primates, such as macaques, can be a suitable model for *H. pylori* infections due to their physiological and anatomical similarities with humans. Rhesus macaques *(Macaca mulatta)* acquire *H. pylori* in the stomach mucosa and experience chronic gastritis (Solnick et al., 2003, Solnick et al., 2001) and glandular atrophy, the precursor to stomach cancer (Dubois et al., 1999). However, it remains unclear if macaques naturally harbor *H. pylori* and act as a reservoir in wildlife or whether they acquire the bacteria upon contact with humans, after capture (Solnick et al., 2003, Solnick et al., 2006). Non-human primates are mostly used in testing vaccines against *H. pylori* (Lee, 2001). The genetic and physiological parallels between primates and humans make this model appealing and practical for research on *H. pylori*-related gastritis, but the high cost, time and labor requirements along with ethical considerations prevent its widespread use in *Helicobacter* research (Barnhill et al, 2016).

Non-animal (*ex vivo*) models

The preceding sections discuss various *in vivo* infection models that facilitate extended bacterial exposure in the host, proving crucial in identifying key factors driving *H. pylori* pathogenesis. However, these animal models do not precisely mirror the pathophysiological responses observed in humans (Table 1). Additionally, the large numbers of animals required have raised concerns about animal welfare and cost (Burkitt et al., 2017). *In vitro* studies using the widely available gastric cancer cell lines, on the other hand, do not have the complex cellular and architectural details of the intact gastric epithelium (Wagner et al., 1994; Birkness et al., 1996; Saberi et al., 2018). However, they do provide a more controlled environment for studying the intricate details of how hosts and pathogens interact.

Organoids are simplified, tissue-engineered *in vitro* model systems that replicate various features of the complex structures and function found in corresponding biological tissues (Chakrabarti and Zavros, 2020; Hofer and Lutolf, 2021; Idowu et al, 2022). Organoids can be generated from pluripotent or tissue-resident stem cells, whether embryonic or adult, or from differentiated cells isolated from healthy or diseased tissues (Hofer and Lutolf, 2021). More recently, organoids derived from primary cells have gained traction as suitable models for *ex vivo* studies, primarily due to their ability to closely mimic human gastrointestinal physiology. Recent advancements in gastric organoid models to study *H. pylori* infection could reduce an overdependence on 'abnormal' cancer cell lines and enhance the exploration of the initial stages of gastric carcinogenesis (Figure 3), thereby facilitating a deeper understanding of its pathogenesis (Idowu et al, 2022).

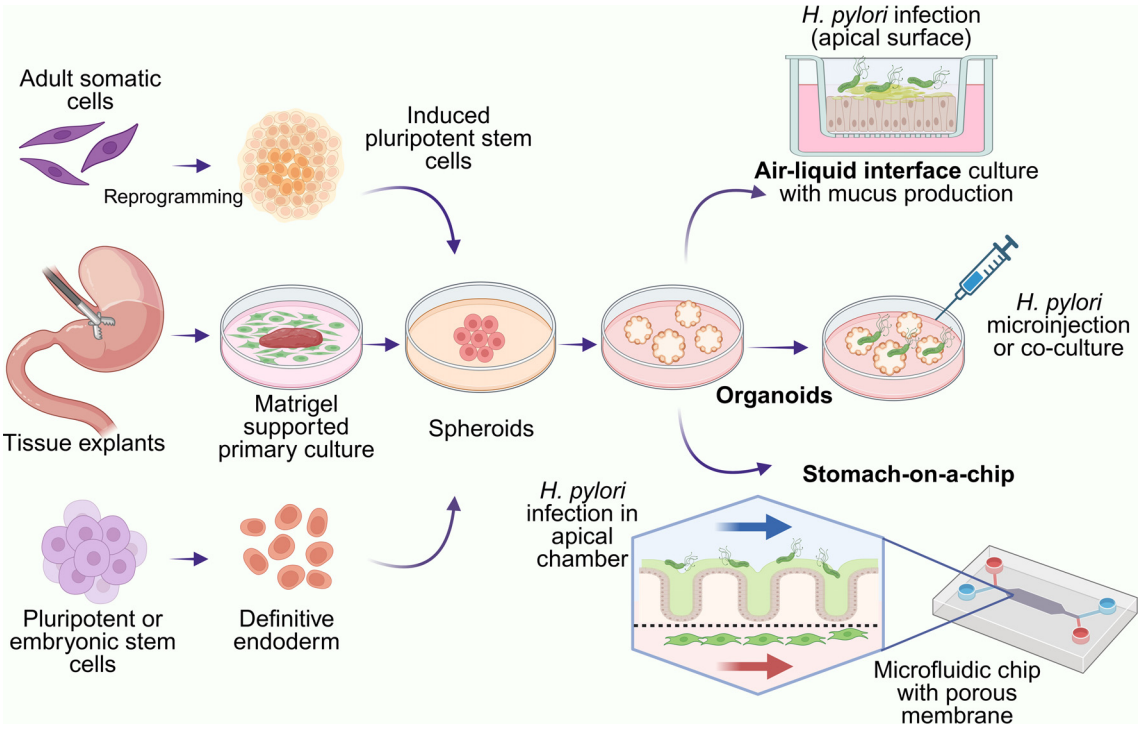

FIGURE 3
Organoid-based models of *H. pylori* infection. Gastric organoids can be derived from mouse or human tissue explants, adult somatic cells or stem cells. Created with BioRender.

Gastric organoids

Induced pluripotent stem cells (iPSC) are derived from adult somatic cells that undergo genetic reprogramming to attain a state akin to embryonic stem cells, achieved through the enforced expression of specific genes and factors crucial for maintaining pluripotency (Ye et al, 2013). Organoid models, a relatively recent advancement in three-dimensional (3D) cell cultivation systems, can be derived from iPSCs by controlled differentiation steps (Pellegrino and Gutierrez, 2021; Seidlitz et al, 2021). Gastric organoids can effectively mimic the cellular diversity and architectural complexity of the stomach, encompassing various epithelial cell types like mucous-secreting cells, chief cells, parietal cells, and enteroendocrine cells (Seidlitz et al, 2021). Given that the stomach serves as the primary site for *H. pylori* colonization and infection in humans, gastric organoids have emerged as invaluable tools for modeling infection and related gastric diseases such as cancer or ulcers (Ku et al., 2022). Compared to immortalized gastric cancer cell lines, organoid cultures offer a closer recapitulation of *in vivo* conditions, particularly in studying interactions between *H. pylori* and the apical-junctional complex (Uotani et al., 2019).

Modeling *H. pylori* infection in gastric organoids

Upon infection, gastric organoids recapitulate key aspects of *H. pylori*-induced diseases, including inflammation, epithelial damage, and dysregulation of tissue homeostasis (Idowu et al, 2022; Jeong et al., 2023; Seidlitz et al, 2021). A study by McCracken et al. demonstrated that microinjection of *H. pylori* into human iPSC-derived gastric organoids led to enhanced epithelial cell proliferation (McCracken et al., 2011). This finding further implied that *H. pylori* infection stimulates the proliferation of gastric epithelial cells, which might contribute to tissue repair mechanisms or pathological changes associated with chronic infection. During infection, CagA was injected into organoid cells via the T4SS and phosphorylated CagA bound to the Src homology 2 (SH2) domain-containing tyrosine phosphatase 2 (SHP-2) (Higashi et al, 2002). Such binding resulted in the activation of the Ras-extracellular signal-regulated kinase (Erk) signaling pathway, promoting cell proliferation, migration and survival. A similar study provided insights into the role of the Cag-SHP-2 interaction in *H. pylori*-induced gastric carcinogenesis using a similar gastric organoid model (Higashi et al, 2002).

Organoids infected with *H. pylori* exhibit alterations in glandular morphology, release of pro-inflammatory cytokines, and activation of signaling pathways associated with host defense and immune responses (Aguilar et al., 2022; Chakrabarti et al., 2021). Gastric organoid models have provided insights into the mechanisms underlying host-pathogen interactions during *H. pylori* infection, including bacterial adhesion, invasion, and modulation of host cell signaling pathways (Chakrabarti et al., 2021; Chakrabarti and Zavros, 2020). Due to the fact that organoids can be infected with *H. pylori* either by direct exposure to the bacterium or by incubation with specific bacterial components, gastric organoids have emerged as valuable tools for studying *H. pylori* infection and its pathogenesis.

Intestinal organoids

Intestinal organoids, also known as enteroids or colonoids, are derived from intestinal stem cells and mimic the cellular composition and architecture of the intestine (Lee et al., 2018; Mahe et al., 2013; Ohki et al., 2020). Although *H. pylori* primarily infects the stomach, studies suggest that it can transiently colonize the duodenum and colon (Fujimori, 2021). A model of mouse intestinal organoids generated from isolated intestinal crypts demonstrated the role of gastric hormones in inflammation and repair thus showing that endocrine cells within these organoids closely resemble those in the gut (Ohki et al., 2020). Given the roles played by gastric hormones in *H. pylori*-associated disease manifestation, intestinal organoids can be infected with *H. pylori* to study its interaction with the intestinal epithelium and investigate potential extra-gastric effects of the infection (Becher et al., 2010; Walduck and Becher, 2012) including alterations in gut microbiota composition and gastrointestinal symptoms such as diarrhea and irritable bowel syndrome (Tan and Goh, 2012; Tohumcu et al., 2024; Cui et al., 2025).

Co-culture of organoid and immune cells

To recapitulate the host immune response to *H. pylori* infection, researchers can co-culture organoids with immune cells such as macrophages, dendritic cells, and T cells. Co-culture systems grow stomach organoids with immune cells from the same host. This helps us learn more about the roles that innate and adaptive immune cells play in *H. pylori* infection (Idowu et al., 2022). Sebrell et al., 2019, investigated the recruitment of dendritic cells during *H. pylori* infection using human gastric organoids co-cultured with monocyte-derived dendritic cells and cataloged the various chemokines that were expressed in response to infection (Sebrell et al., 2019). The effect of *H. pylori* infection on cytokine production by innate immune cells using co-cultured gastric organoids and macrophages from infected mice has been studied as well (Suarez et al., 2019). These studies revealed a remarkable increase in cytokine production in Nod1-deficient cells, particularly when both macrophages and organoids lacked Nod1, suggesting that functional Nod1 suppresses cytokine production (Suarez et al., 2019).

Additionally, changes in mucin and antimicrobial peptide expression resulting from activation of innate and adaptive immunity have been investigated in these models. The bactericidal activity of mucus in a two-dimensional mucosoid culture model was demonstrated where it also acts as a physical barrier against *H. pylori* attachment (Boccellato et al., 2019). A co-culture of mucosoid organoids offers the potential to explore the effects of CD4+ T cell subsets and innate lymphoid cells on epithelial antimicrobial activity and offers opportunities to generate vaccinated organoids to test specific cytokines or hormone's roles in protective responses as well as its associated mechanisms. Research employing co-culture organoids containing immune cells from the same host sheds light on the interaction between *H. pylori* and the host immune system during infection and advances our knowledge of the immunopathogenesis of diseases brought on by *H. pylori*.

Organoid-on-a-chip

Patient and stem cell derived gastrointestinal organoids have become an important tool for the study of *H. pylori* associated pathophysiology. Further advancements in these models have concentrated on integrating microfluidics to regulate the movement of cells, signaling molecules, and physical stimuli through channels and membranes that are bolstered by an extracellular matrix (ECM) constituent (Moses et al., 2021). These additional features introduce a significant layer of complexity, enhancing the resemblance of these models to the native structure and function of the stomach. The stomach-on-a-chip model is based on a sandwich' structure that consists of two microchannels divided by a porous membrane to simulate the mucosal and basal surfaces of the stomach epithelium. Jeong et al., 2023 have described a human stomach micro-physiological system (hsMPS)-on-a-chip with epithelial cells derived from human antral organoids and primary mesenchymal stromal cells extracted from stomach tissue, co-cultivated under controlled flow (Jeong et al., 2023). This model recreated the maturation of gastric epithelial cells, leading to the formation of a mesh-like mucus layer with mucus protective peptides and functional epithelial junctional complexes that exhibited gastroprotective effects against *H. pylori*. Although this model has been proposed as a platform for evaluating the antibacterial drug candidates, the porous membrane used for barrier separation can be prone to non-specific absorption of small molecules which can hinder the study. Another elegant model of the human stomach-on-a-chip demonstrated long-term growth of cannulated gastric organoids with biochemical agents delivered through the lumen using a peristaltic pump (Lee et al., 2018). This system recreated the rhythmic stretch and contraction of the organoid, reminiscent of gastric motility. Overall, with recent advances in stem cell technology and 3D matrices for supporting organotypic cultures, there is significant potential for these *ex vivo* models in identifying and validating novel therapeutic and vaccine targets (Li et al., 2022), while reducing an over-reliance on animal models.

Advantages and limitations

Animal models

The use of animal models has greatly advanced our understanding of the critical determinants of *H. pylori* pathology and factors involved in mediating host response to the infection, particularly the many drivers of the different phases leading to the development of gastric cancer (Ansari and Yamaoka, 2022). These models have also enabled the testing of many antimicrobials and vaccines over the years. Although early research on *H. pylori* infection was conducted mostly on non-rodent models, the isolation and generation of the mouse-adapted *H. pylori* strain has made the mouse model the cornerstone of *H. pylori* infection

studies. However, there are several limitations to using mice as a surrogate for human pathophysiology and anatomy. Mouse metabolic processes are much faster compared to humans, and they can tolerate higher doses of most administered substances due to a quicker rate of kidney filtration and excretion (Sharma and McNeill, 2009). Furthermore, the mouse stomach is quite distinct from the human organ. Mice have a squamous glandular epithelium rather than the oxyntic type found in humans and typically display gastritis features within the stomach corpus as opposed to the antral gastritis observed more typically in humans, following *H. pylori* infection. Stomach cancer is also not easily modeled in this host without interfering with the expression of specific genes. Mongolian gerbils and guinea pigs have been suggested as alternatives, but they have not had the same success as the mouse models, perhaps due to the lack of molecular resources and relevant expertise.

Non-animal models

In recent years, the complexity of non-animal models, particularly 3D organoids, has increased tremendously, putting these at par with traditional animal models. In some instances, human organoids are superlative to animal models with the added benefit of being more efficient and cost-effective. The 3Rs' (replace, reduce and refine) objectives that underpin the ethical frameworks governing animal research in most countries today can be complemented by an increased reliance on non-animal models in the coming years. These models can further encompass *in silico* simulations, which can inform subsequent *in vitro* or animal studies, as well as advanced 2D/3D cell cultures and *ex vivo* tissue explant cultures. This review focuses specifically on the emerging popularity and application of 3D organoid models within the *H. pylori* research community.

Organoids derived from genetically modified stem cells or patient-derived iPSCs allow for the investigation of host genetic factors influencing susceptibility to *H. pylori* infection and disease outcomes. Current iPSC derived gastric organoids closely resemble the cellular composition and architecture of the stomach. Technological advances have made it possible to generate adult stem cell-derived organoids from tissues obtained from a healthy or diseased donor (Pellegrino and Gutierrez, 2021). Donor-matched organoids have diverse applications in the development of precision medicine, particularly for gastric cancer, which continues to have a poor five-year survival rate. Furthermore, gastric organoids can be adapted for high-throughput screening assays to identify novel therapeutics targeting *H. pylori* infection and associated diseases (Du et al., 2020; Lukonin et al, 2021; Li et al., 2022). Organoid-based screening platforms enable the evaluation of drug efficacy, toxicity, and mode of action in a scalable and cost-effective manner. The added dimension of immune cell co-culture allows for the investigation of both innate and adaptive immune responses to *H. pylori* infection, providing a more detailed understanding of host-pathogen interactions. This approach permits the study of immune cell recruitment, activation, and function within the context of the gastric or intestinal epithelium during *H. pylori* infection and provides opportunities to study vaccine-induced immune responses against *H. pylori*.

Obvious limitations of these models are related to the availability and accessibility to the organoid model of interest besides the difficulties pertaining to the optimization of culture conditions and the reproducibility of experimental results (Eicher et al, 2018; Pang et al., 2022). Adult stem cells and iPSCs from genetically and phenotypically well-characterized donor pools may be difficult to source. Culture media for any organoid must be carefully optimized to support the growth and differentiation of stem cells while maintaining the physiological relevance of the model (Sato et al., 2009). Achieving the appropriate balance of growth factors, signaling molecules, and nutrients is crucial for the long-term maintenance of organoid cultures, while also avoiding the common pitfall of batch variation in media components. The composition and stiffness of the extracellular matrix (ECM) used for embedding gastric organoids can influence their growth, differentiation, and functionality. Optimization of ECM components, such as Matrigel® or synthetic hydrogels, is necessary to better mimic the native gastric microenvironment (Pang et al., 2022). Furthermore, most organoids lack vasculature which can lead to necrosis of underlying cells and hypoxia-induced stress responses unrelated to infection pathophysiology.

Summary

Ever since the association between *H. pylori* infection and the development of gastritis, ulcers, and ultimately gastric cancer was first identified, considerable progress has been made in understanding the complex interplay between bacterial, host, and environmental factors that affect the course of disease. Currently, clinical presentations of *H. pylori* related gastritis and ulcers can be effectively managed with triple or quadruple antimicrobial therapy in most cases. However, the rising emergence of antibiotic resistance among *H. pylori* clinical isolates is a grave concern and gastric cancer remains a leading cause of cancer-related deaths. Despite decades of efforts and the continually elevated prevalence of the bacteria in developing parts of the worldwide, there is still no vaccine available against *H. pylori*. The eradication of *H. pylori* remains a key issue because of several factors. The emergence of antibiotic-resistant strains, complex treatment regimens combined with poor compliance, high infection and reinfection rates, and limitations in diagnostic methods all contribute to the difficulty in successfully achieving bacterial eradication. Additionally, host factors such as immune response and genetic predisposition influence the treatment outcomes. Consequently, further research is imperative to develop novel antibiotics, identify biomarkers for early detection and treatment prediction, and explore non-antibiotic therapies.

Animal models play a crucial role in advancing our understanding of *H. pylori* pathogenesis, testing new drugs, and

developing vaccines. They aid in the translation of preclinical research into clinical practice by offering insights into host-pathogen interactions, bacterial virulence, and the safety and effectiveness of possible treatments. This review has summarized advanced models available to researchers for investigating new therapeutics and vaccines against *H. pylori*, addressing a significant unmet need, particularly in regions where *H. pylori* is endemic. Studies in animal models have been instrumental in dissecting the correlates of protection and make the case for targeting *H. pylori* mediated inflammation to prevent or treat the pathological outcomes rather than aiming for complete eradication of the bacteria (Sarkar et al., 2023). Despite the lack of progress on *H. pylori* vaccines due to its complex relationship with the human host, mouse and non-human primate models remain invaluable resources for further studies. On the other hand, the precise environments for studying *H. pylori* infection and pathogenesis afforded by *ex vivo* models support high-throughput screening of therapeutics while reducing the reliance on animal testing and adhering to ethical principles. Due to their advantages over conventional *in vitro* procedures in terms of polarization, longevity, amenability, and accessibility, the use of gastric organoids has increased our understanding of *H. pylori* infection. Consequently, previously unattainable in other models, key features of chemotaxis, the intracellular effects of *H. pylori* virulence factors, interactions with the apical-junctional complex, innate immune activation, and the initiation of inflammation by *H. pylori* have been unraveled using gastric organoids.

Future perspectives

Future research on *H. pylori* infection and its associated diseases should include both animal and non-animal systems, to address current challenges and unserved needs. The development of novel therapeutics is vitally important, particularly in view of the increasing prevalence of antibiotic-resistant *H. pylori* strains. Researchers should focus on identifying new antimicrobial compounds and exploring alternative therapeutic strategies, such as bacteriophage therapy, antimicrobial peptides, and host-targeted approaches. The assimilation of precision medicine, using donor-matched organoids and advanced *ex vivo* models, can facilitate personalized treatment regimens and improve therapeutic outcomes. These models can also aid in high-throughput screening of potential therapeutics, accelerating the discovery and development process. Furthermore, considering the increasing numbers of aging populations around the world, the identification of biomarkers for early detection of gastric cancer and prediction of treatment response will be crucial in reducing the associated mortality. Therefore, continued collaboration between multidisciplinary research teams and the integration of cutting-edge technologies will be essential for overcoming the persistent challenges in *H. pylori* eradication and improving global health outcomes in the coming decades.

Author contributions

SP: Data curation, Writing – original draft, Writing – review & editing. SY: Data curation, Writing – original draft, Writing – review & editing. RJ: Conceptualization, Data curation, Supervision, Writing – review & editing. VR: Conceptualization, Data curation, Supervision, Writing – original draft, Writing – review & editing. SS: Conceptualization, Data curation, Resources, Supervision, Visualization, Writing – review & editing.

Funding

The author(s) declare that financial support was received for the research and/or publication of this article. Contributions by SP, RJ and VR are supported by the Science & Engineering Research Board (SERB), Department of Science and Technology (DST), Government of India, (GOI) New Delhi (SRG/2022/001512).

Acknowledgments

The authors acknowledge the infrastructural support extended by Amity University Maharashtra, Mumbai, Maharashtra, India. SS and SY acknowledge the infrastructure support received from the Murdoch Children's Research Institute and The University of Melbourne.

Conflict of interest

The authors declare the research was conducted in the absence of any commercial or financial relationships that could be construed as a potential conflict of interest.

The author(s) declared that they were an editorial board member of Frontiers, at the time of submission. This had no impact on the peer review process and the final decision.

Generative AI statement

The author(s) declare that no Generative AI was used in the creation of this manuscript.

Publisher's note

References

Aguilar, C., Pauzuolis, M., Pompaiah, M., Vafadarnejad, E., Arampatzi, P., Fischer, M., et al. (2022). Helicobacter pylori shows tropism to gastric differentiated pit cells dependent on urea chemotaxis. *Nat. Commun.* 13, 5878 doi: 10.1038/s41467-022-33165-4

Aihara, E., Closson, C., Matthis, A. L., Schumacher, M. A., Engevik, A. C., Zavros, Y., et al. (2014). Motility and chemotaxis mediate the preferential colonization of gastric injury sites by Helicobacter pylori. *PloS Pathog* 10, e1004275. doi: 10.1371/journal.ppat.1004275

Almeida Furquim de Camargo, B., Soares Silva, D. E., Noronha da Silva, A., Campos, D. L., MaChado Ribeiro, T. R., Mieli, M. J., et al. (2020). New Silver(I) Coordination Compound Loaded into Polymeric Nanoparticles as a Strategy to Improve *In Vitro* Anti-Helicobacter pylori Activity. *Mol. Pharm.* 17, 2287–2298. doi: 10.1021/acs.molpharmaceut.9b01264

Ansari, S., and Yamaoka, Y. (2022). Animal models and helicobacter pylori infection. *J. Clin. Med.* 11. doi: 10.3390/jcm11113141

Arnold, I. C., Lee, J. Y., Amieva, M. R., Roers, A., Flavell, R. A., Sparwasser, T., et al. (2011). Tolerance rather than immunity protects from Helicobacter pylori-induced gastric preneoplasia. *Gastroenterology* 140, 199–209. doi: 10.1053/j.gastro.2010.06.047

Asante, M., Ahmed, H., Patel, P., Davis, T., Finlayson, C., Mendall, M., et al. (1997). Gastric mucosal hydrophobicity in duodenal ulceration: role of Helicobacter pylori infection density and mucus lipids. *Gastroenterology* 113, 449–454. doi: 10.1053/gast.1997.v113.pm9247463

Aumpan, N., Issariyakulkarn, N., Mahachai, V., Graham, D., Yamaoka, Y., and Vilaichone, R. K. (2023). Management of Helicobacter pylori treatment failures: A large population-based study (HP treatment failures trial). *PloS One* 18, e0294403. doi: 10.1371/journal.pone.0294403

Barnhill, A., Joffe, S., and Miller, F. G. (2016). The ethics of infection challenges in primates. *Hastings Cent Rep.* 46, 20–26. doi: 10.1002/hast.2016.46.issue-4

Becher, D., Deutscher, M. E., Simpfendorfer, K. R., Wijburg, O. L., Pederson, J. S., Lew, A. M., et al. (2010). Local recall responses in the stomach involving reduced regulation and expanded help mediate vaccine-induced protection against Helicobacter pylori in mice. *Eur. J. Immunol.* 40, 2778–2790. doi: 10.1002/eji.200940219

Birkness, K. A., Gold, B. D., White, E. H., Bartlett, J. H., and Quinn, F. D. (1996). *In vitro* models to study attachment and invasion of Helicobacter pylori. *Ann. N Y Acad. Sci.* 797, 293–295. doi: 10.1111/j.1749-6632.1996.tb52983.x

Boccellato, F., Woelffling, S., Imai-Matsushima, A., Sanchez, G., Goosmann, C., Schmid, M., et al. (2019). Polarised epithelial monolayers of the gastric mucosa reveal insights into mucosal homeostasis and defence against infection. *Gut* 68, 400–413. doi: 10.1136/gutjnl-2017-314540

Brawner, K. M., Morrow, C. D., and Smith, P. D. (2014). Gastric microbiome and gastric cancer. *Cancer J.* 20, 211–216. doi: 10.1097/PPO.0000000000000043

Bray, F., Laversanne, M., Sung, H., Ferlay, J., Siegel, R. L., Soerjomataram, I., et al. (2024). Global cancer statistics 2022: GLOBOCAN estimates of incidence and mortality worldwide for 36 cancers in 185 countries. *CA Cancer J. Clin.* 74, 229–263. doi: 10.3322/caac.21834

Brown, L. M. (2000). Helicobacter pylori: epidemiology and routes of transmission. *Epidemiol. Rev.* 22, 283–297. doi: 10.1093/oxfordjournals.epirev.a018040

Burkitt, M. D., Duckworth, C. A., Williams, J. M., and Pritchard, D.M. (2017). Helicobacter pylori-induced gastric pathology: insights from *in vivo* and ex vivo models. *Dis. Models Mech.* 10, 89–104. doi: 10.1242/dmm.027649

Cai, X., Stoicov, C., Li, H., Carlson, J., Whary, M., Fox, J. G., et al. (2005). Overcoming Fas-mediated apoptosis accelerates Helicobacter-induced gastric cancer in mice. *Cancer Res.* 65, 10912–10920. doi: 10.1158/0008-5472.CAN-05-1802

Carron, M. A., Tran, V. R., Sugawa, C., and Coticchia, J. M. (2006). Identification of Helicobacter pylori biofilms in human gastric mucosa. *J. Gastrointest Surg.* 10, 712–717. doi: 10.1016/j.gassur.2005.10.019

Celli, J. P., Turner, B. S., Afdhal, N. H., Keates, S., Ghiran, I., Kelly, C. P., et al. (2009). Helicobacter pylori moves through mucus by reducing mucin viscoelasticity. *Proc. Natl. Acad. Sci. U S A* 106, 14321–14326. doi: 10.1073/pnas.0903438106

Chakrabarti, J., Koh, V., So, J. B. Y., Yong, W. P., and Zavros, Y. (2021). A preclinical human-derived autologous gastric cancer Organoid/Immune cell Co-culture model to predict the efficacy of targeted therapies. *JoVE (Journal Visualized Experiments)* 173, e61443. doi: 10.3791/61443

Chakrabarti, J., and Zavros, Y. (2020).Generation and use of gastric organoids for the study of Helicobacter pylori pathogenesis in *Methods in cell biology* (Elsevier). Available online at: https://www.sciencedirect.com/science/article/abs/pii/S0091679X20300753.

Chen, Y. C., Malfertheiner, P., Yu, H. T., Kuo, C. L., Chang, Y. Y., Meng, F. T., et al. (2024). Global prevalence of helicobacter pylori infection and incidence of gastric cancer between 1980 and 2022. *Gastroenterology* 166, 605–619. doi: 10.1053/j.gastro.2023.12.022

Cheng, H. C., Yang, Y. J., Yang, H. B., Tsai, Y. C., Chang, W. L., Wu, C. T., et al. (2023). Evolution of the Correa's cascade steps: A long-term endoscopic surveillance among non-ulcer dyspepsia and gastric ulcer after H. pylori eradication. *J. Formos Med. Assoc* 122, 400–410. doi: 10.1016/j.jfma.2022.11.008

Chey, W. D., Howden, C. W., Moss, S. F., Morgan, D. R., Greer, K. B., Grover, S., et al. (2024). ACG clinical guideline: treatment of helicobacter pylori infection. *Am. J. Gastroenterol.* 119, 1730–1753. doi: 10.14309/ajg.0000000000002968

Chung Nien Chin, S., O'Connor, L., Scurr, M., Busada, J. T., Graham, A. N., Alipour Talesh, G., et al. (2020). Coordinate expression loss of GKN1 and GKN2 in gastric cancer via impairment of a glucocorticoid-responsive enhancer. *Am. J. Physiol. Gastrointest Liver Physiol.* 319, G175–Gg88. doi: 10.1152/ajpgi.00019.2020

Cole, S. P., Harwood, J., Lee, R., She, R., and Guiney, D. G. (2004). Characterization of monospecies biofilm formation by Helicobacter pylori. *J. Bacteriol* 186, 3124–3132. doi: 10.1128/JB.186.10.3124-3132.2004

Collaborators, GBD (2021). Antimicrobial Resistance. 2024. Global burden of bacterial antimicrobial resistance 1990-2021: a systematic analysis with forecasts to 2050. *Lancet* 404, 1199–1226. doi: 10.1016/S0140-6736(24)01867-1

Correa, P. (1992). Human gastric carcinogenesis: a multistep and multifactorial process–First American Cancer Society Award Lecture on Cancer Epidemiology and Prevention. *Cancer Res.* 52, 6735–6740.

Correa, P., and Piazuelo, M. B. (2008). Natural history of Helicobacter pylori infection. *Dig Liver Dis.* 40, 490–496. doi: 10.1016/j.dld.2008.02.035

Correa, P. (2013). Gastric cancer: overview. *Gastroenterol. Clin. North Am.* 42, 211–217.

Cui, S., Liu, X., Han, F., Zhang, L., Bu, J., Wu, S., et al. (2025). Helicobacter pylori CagA+ strains modulate colorectal pathology by regulating intestinal flora. *BMC Gastroenterol.* 25, 54. doi: 10.1186/s12876-025-03631-6

Dey, T. K., Karmakar, B. C., Sarkar, A., Paul, S., and Mukhopadhyay, A. K. (2021). A mouse model of helicobacter pylori infection. . *Methods Mol. Biol.* 2283, 131–151. doi: 10.1007/978-1-0716-1302-3_14

Du, Y., Li, X., Niu, Q., Mo, X., Qui, M., and Ma, T. (2020). Development of a miniaturized 3D organoid culture platform for ultra-high-throughput screening. *J. Mol. Cell Biol.* 12, 630–643. doi: 10.1093/jmcb/mjaa036

Dubois, A., Berg, D. E., Incecik, E. T., Fiala, N., Heman-Ackah, L. M., Del Valle, J., et al. (1999). Host specificity of Helicobacter pylori strains and host responses in experimentally challenged nonhuman primates. *Gastroenterology* 116, 90–96. doi: 10.1016/S0016-5085(99)70232-5

Dyer, V., Brüggemann, H., Sörensen, M., Kühl, A. A., Hoffman, K., Brinkmann, V., et al. (2018). Genomic features of the Helicobacter pylori strain PMSS1 and its virulence attributes as deduced from its *in vivo* colonisation patterns. *Mol. Microbiol* 110, 761–776. doi: 10.1111/mmi.2018.110.issue-5

Eaton, K. A., Morgan, D. R., and Krakowka, S. (1989). Campylobacter pylori virulence factors in gnotobiotic piglets. *Infect. Immun.* 57, 1119–1125. doi: 10.1128/iai.57.4.1119-1125.1989

Eicher, A. K., Berns, H.M., and wells, j. M. (2018). Translating developmental principles to generate human gastricáOrganoids. *Cell. Mol. gastroenterology hepatology* 5, 353–363. doi: 10.1016/j.jcmgh.2017.12.014

Elbehiry, A., Marzouk, E., Aldubaib, M., Abalkhail, A., Anagreyyah, S., Anajirih, N., et al. (2023). Helicobacter pylori infection: current status and future prospects on diagnostic, therapeutic and control challenges. *Antibiotics (Basel)* 12(191). doi: 10.3390/antibiotics12020191

El-Omar, E. M., Carrington, M., Chow, W. H., McColl, K. E., Bream, J. H., Young, H. A., et al. (2000). Interleukin-1 polymorphisms associated with increased risk of gastric cancer. *Nature* 404, 398–402. doi: 10.1038/35006081

Fox, J. G., Batchelder, M., Marini, R., Yan, L., Handt, L., Li, X., et al. (1995). Helicobacter pylori-induced gastritis in the domestic cat. *Infect. Immun.* 63, 2674–2681. doi: 10.1128/iai.63.7.2674-2681.1995

Fujimori, S. (2021). Progress in elucidating the relationship between Helicobacter pylori infection and intestinal diseases. *World J. Gastroenterol.* 27, 8040–8046. doi: 10.3748/wjg.v27.i47.8040

Giannouli, M., Palatucci, A. T., Rubino, V., Ruggiero, G., Romano, M., Triassi, M., et al. (2014). Use of larvae of the wax moth Galleria mellonella as an *in vivo* model to study the virulence of Helicobacter pylori. *BMC Microbiol* 14, 228. doi: 10.1186/s12866-014-0228-0

Go, M. F. (2002). Review article: natural history and epidemiology of Helicobacter pylori infection. *Aliment Pharmacol. Ther.* 16 Suppl 1, 3–15. doi: 10.1046/j.1365-2036.2002.0160s1003.x

Gonciarz, W., Krupa, A., Hinc, K., Obuchowski, M., Moran, A. P., Gajewski, A., et al. (2019). The effect of Helicobacter pylori infection and different H. pylori components on the proliferation and apoptosis of gastric epithelial cells and fibroblasts. *PloS One* 14, e0220636. doi: 10.1371/journal.pone.0220636

Guo, L., Hong, D., Wang, S., Zhang, F., Tang, F., Wu, T., et al. (2019). gTherapeutic protection against H. pylori infection in Mongolian gerbils by oral immunization with a tetravalent epitope-based vaccine with polysaccharide adjuvant. *Front. Immunol.* 10, 1185. doi: 10.3389/fimmu.2019.01185

Hanada, K., and Graham, D. Y. (2014). Helicobacter pylori and the molecular pathogenesis of intestinal-type gastric carcinoma. *Expert Rev. Anticancer Ther.* 14, 947–954. doi: 10.1586/14737140.2014.911092

Handt, L. K., Fox, J. G., Stalis, I. H., Rufo, R., Lee, G., Linn, J., et al. (1995). Characterization of feline Helicobacter pylori strains and associated gastritis in a colony of domestic cats. *J. Clin. Microbiol* 33, 2280–2289. doi: 10.1128/jcm.33.9.2280-2289.1995

Heimesaat, M. M., Fischer, A., Plickert, R., Wiedemann, T., Loddenkemper, C., Göbel, U. B., et al. (2014). Helicobacter pylori induced gastric immunopathology is associated with distinct microbiota changes in the large intestines of long-term infected Mongolian gerbils. *PloS One* 9, e100362. doi: 10.1371/journal.pone.0100362

Higashi, H., Tsutsumi, R., Higashi, S., Sugiyama, T., Takeshi, A., and Masahiro, H. (2002). SHP-2 tyrosine phosphatase as an intracellular target of Helicobacter pylori CagA protein. *Science* 295, 683–686. doi: 10.1126/science.1067147

Hofer, M., and Lutolf, m. P. (2021). Engineering organoids. *Nat. Rev. Materials* 6, 402–420. doi: 10.1038/s41578-021-00279-y

Huang, F. Y., Chan, A. O., Lo, R. C., Rashid, A., Wong, D. K., Cho, C. H., et al. (2013). Characterization of interleukin-1β in Helicobacter pylori-induced gastric inflammation and DNA methylation in interleukin-1 receptor type 1 knockout (IL-1R1(-/-)) mice. *Eur. J. Cancer* 49, 2760–2770. doi: 10.1016/j.ejca.2013.03.031

Idowu, S., Bertrand, P. P., and Walduck, A. K. (2022). Gastric organoids: Advancing the study of H. pylori pathogenesis and inflammation. *Helicobacter* 27, e12891. doi: 10.1111/hel.12891

Isobe, H., Nishiyama, A., Takano, T., Higuchi, W., Nakagawa, S., Taneike, I., et al. (2012). Reduction of overall Helicobacter pylori colonization levels in the stomach of Mongolian gerbil by Lactobacillus johnsonii La1 (LC1) and its *in vitro* activities against H. pylori motility and adherence. *Biosci Biotechnol. Biochem.* 76, 850–852. doi: 10.1271/bbb.110921

Jaka, H., Rhee, J. A., Östlundh, L., Smart, L., Peck, R., Mueller, A., et al. (2018). The magnitude of antibiotic resistance to Helicobacter pylori in Africa and identified mutations which confer resistance to antibiotics: systematic review and meta-analysis. *BMC Infect. Dis.* 18, 193. doi: 10.1186/s12879-018-3099-4

Jeong, H. J., Park, J. H., Kang, J. H., Sabaté Del Río, J., Kong, S. H., and Park, T. E. (2023). Organoid-based human stomach micro-physiological system to recapitulate the dynamic mucosal defense mechanism. *Adv. Sci. (Weinh)* 10, e2300164. doi: 10.1002/advs.202300164

Jeremy, A. H., Du, Y., Dixon, M. F., Robinson, P. A., and Crabtree, J. E. (2006). Protection against Helicobacter pylori infection in the Mongolian gerbil after prophylactic vaccination. *Microbes Infect.* 8, 340–346. doi: 10.1016/j.micinf.2005.06.025

Jiang, F., Guo, C. G., Cheung, K. S., Li, B., Law, S. Y. K., and Leung, W. K. (2022). Age of eradication and failure rates of clarithromycin-containing triple therapy for Helicobacter pylori: A 15-year population-based study. *Helicobacter* 27, e12893. doi: 10.1111/hel.12893

Jiang, Y., and Yu, Y. (2017). Transgenic and gene knockout mice in gastric cancer research. *Oncotarget* 8, 3696–3710. doi: 10.18632/oncotarget.12467

Jones, K. R., Whitmire, J. M., and Merrell, D. S. (2010). A tale of two toxins: helicobacter pylori cagA and vacA modulate host pathways that impact disease. *Front. Microbiol* 1, 115. doi: 10.3389/fmicb.2010.00115

Kimura, N., Ariga, M., Icatlo, F. C. Jr., Kuroki, M., Ohsugi, M., Ikemori, Y., et al. (1998). A euthymic hairless mouse model of Helicobacter pylori colonization and adherence to gastric epithelial cells *in vivo*. *Clin. Diagn. Lab. Immunol.* 5, 578–582. doi: 10.1128/CDLI.5.4.578-582.1998

Kleanthous, H., Lee, C. K., and Monath, T. P. (1998). Vaccine development against infection with Helicobacter pylori. *Br. Med. Bull.* 54, 229–241. doi: 10.1093/oxfordjournals.bmb.a011673

Krakowka, S., Morgan, D. R., Kraft, W. G., and Leunk, R. D. (1987). Establishment of gastric Campylobacter pylori infection in the neonatal gnotobiotic piglet. *Infect. Immun.* 55, 2789–2796. doi: 10.1128/iai.55.11.2789-2796.1987

Krzyżek, P., Dudek, B., Brożyna, M., Krzyżanowska, B., and Junka, A. (2025). Galleria mellonella larvae as a model for Helicobacter pylori biofilm formation under antibiotic stress. *Microb Pathog* 198, 107121. doi: 10.1016/j.micpath.2024.107121

Ku, C.-C., Wuputra, K., Pan, J.-B., Li, C.-P., Liu, C.-J., Liu, Y.-C., et al. (2022). Generation of human stomach cancer iPSC-derived organoids induced by helicobacter pylori infection and their application to gastric cancer research. *Cells* 11, 184. doi: 10.3390/cells11020184

Kuo, C. H., Wang, S. S., Lu, C. Y., Hu, H. M., Kuo, F. C., Weng, B. C., et al. (2013). Long-term use of probiotic-containing yogurts is a safe way to prevent helicobacter pylori: based on a Mongolian gerbil's model. *Biochem. Res. Int.* 2013, 594561. doi: 10.1155/2013/594561

Lambert, J. R., Borromeo, M., Pinkard, K. J., Turner, H., Chapman, C. B., and Smith, M. L. (1987). Colonization of gnotobiotic piglets with Campylobacter Pyloridis–an animal model? *J. Infect. Dis.* 155, 1344. doi: 10.1093/infdis/155.6.1344

Lee, C. K. (2001). Vaccination against Helicobacter pylori in non-human primate models and humans. *Scand. J. Immunol.* 53, 437–442. doi: 10.1046/j.1365-3083.2001.00911.x

Lee, K. K., McCauley, H. A., Broda, T. R., Kofron, M. J., Wells, J. M., and Hong, C. I. (2018). Human stomach-on-a-chip with luminal flow and peristaltic-like motility. *Lab. Chip* 18, 3079–3085. doi: 10.1039/C8LC00910D

Lee, A., O'Rourke, J., De Ungria, M. C., Robertson, B., Daskalopoulos, G., and Dixon, M. F. (1997). A standardized mouse model of Helicobacter pylori infection: introducing the Sydney strain. *Gastroenterology* 112, 1386–1397. doi: 10.1016/S0016-5085(97)70155-0

Li, X., Fu, G., Zhang, L., Guan, R., Tang, P., Zhang, J., et al. (2022). Assay establishment and validation of a high-throughput organoid-based drug screening platform. *Stem Cell Res. Ther.* 13, 219. doi: 10.1186/s13287-022-02902-3

Lin, A. S., McClain, M. S., Beckett, A. C., Caston, R. R., Harvey, M. L., Brea Dixon, A. M., et al. (2020). Temporal control of the helicobacter pylori cag type IV secretion system in a Mongolian gerbil model of gastric carcinogenesis. *mBio* 11, e01296-20. doi: 10.1128/mBio.01296-20

Linz, B., Balloux, F., Moodley, Y., Manica, A., Liu, H., Roumagnac, P., et al. (2007). An African origin for the intimate association between humans and Helicobacter pylori. *Nature* 445, 915–918. doi: 10.1038/nature05562

Lofgren, J. L., Whary, M. T., Ge, Z., Muthupalani, S., Taylor, N. S., Mobley, M., et al. (2011). Lack of commensal flora in Helicobacter pylori-infected INS-GAS mice reduces gastritis and delays intraepithelial neoplasia. *Gastroenterology* 140, 210–220. doi: 10.1053/j.gastro.2010.09.048

Lukonin, I., Zinner, M., and Liberali, P. (2021). Organoids in image-based phenotypic chemical screens. *Exp. Mol. Med.* 53, 1495–1502. doi: 10.1038/s12276-021-00641-8

Lv, X., Yang, J., Song, H., Li, T., Guo, L., Xing, Y., et al. (2014). Therapeutic efficacy of the multi-epitope vaccine CTB-UE against Helicobacter pylori infection in a Mongolian gerbil model and its microRNA-155-associated immuno-protective mechanism. *Vaccine* 32, 5343–5352. doi: 10.1016/j.vaccine.2014.07.041

Mahe, M. M., Aihara, E., Schumacher, M. A., Zavros, Y., Montrose, M. H., Helmrath, M. A., et al. (2013). Establishment of gastrointestinal epithelial organoids. *Curr. Protoc. Mouse Biol.* 3, 217–240. doi: 10.1002/9780470942390.2013.3.issue-4

McCracken, K. W., Howell, J. C., Wells, J. M., and Jason R, S. (2011). Generating human intestinal tissue from pluripotent stem cells *in vitro*. *Nat. Protoc.* 6, 1920–1928. doi: 10.1038/nprot.2011.410

Menheniott, T. R., O'Connor, L., Chionh, Y. T., Däbritz, J., Scurr, M., Rollo, B. N., et al. (2016). Loss of gastrokine-2 drives premalignant gastric inflammation and tumor progression. *J. Clin. Invest.* 126, 1383–1400. doi: 10.1172/JCI82655

Moses, S. R., Adorno, J. J., Palmer, A. F., and Song, J. W. (2021). Vessel-on-a-chip models for studying microvascular physiology, transport, and function *in vitro*. *Am. J. Physiol. Cell Physiol.* 320, C92–c105. doi: 10.1152/ajpcell.00355.2020

Noto, J. M., Romero-Gallo, J., Piazuelo, M. B., and Peek, R. M. (2016). The Mongolian gerbil: A robust model of helicobacter pylori-induced gastric inflammation and cancer. *Methods Mol. Biol.* 1422, 263–280. doi: 10.1007/978-1-4939-3603-8_24

Ochoa, S., Fernández, F., Devotto, L., France Iglesias, A., and Collado, L. (2021). Virulence assessment of enterohepatic Helicobacter species carried by dogs using the wax moth larvae Galleria mellonella as infection model. *Helicobacter* 26, e12808. doi: 10.1111/hel.12808

Ohki, J., Sakashita, A., Aihara, E., Inaba, A., Uchiyama, H., Matsumoto, M., et al. (2020). Comparative analysis of enteroendocrine cells and their hormones between mouse intestinal organoids and native tissues. *Biosci Biotechnol. Biochem.* 84, 936–942. doi: 10.1080/09168451.2020.1713043

Ohnishi, N., Yuasa, H., Tanaka, S., Sawa, H., Miura, M., Matsui, A., et al. (2008). Transgenic expression of Helicobacter pylori CagA induces gastrointestinal and hematopoietic neoplasms in mouse. *Proc. Natl. Acad. Sci. U S A* 105, 1003–1008. doi: 10.1073/pnas.0711183105

Ortiz, V., Estevez-Ordonez, D., Montalvan-Sanchez, E., Urrutia-Argueta, S., Israel, D., Krishna, U. S., et al. (2019). Helicobacter pylori antimicrobial resistance and antibiotic consumption in the low-resource Central America setting. *Helicobacter* 24, e12595. doi: 10.1111/hel.2019.24.issue-4

Pang, M.-J., Burclaff, J. R., Jin, R., Adkins-Threats, M., Osaki, L. H., Han, Y., et al. (2022). Gastric organoids: progress and remaining challenges. *Cell. Mol. gastroenterology hepatology* 13, 19–33. doi: 10.1016/j.jcmgh.2021.09.005

Peek, R. M. (2008). Helicobacter pylori infection and disease: from humans to animal models. *Dis. Model Mech.* 1, 50–55. doi: 10.1242/dmm.000364

Pellegrino, E., and Gutierrez, M. G. (2021). Human stem cell-based models for studying host-pathogen interactions. *Cell. Microbiol.* 23, e13335. doi: 10.1111/cmi.13335

Poddar, U. (2019). Helicobacter pylori: a perspective in low- and middle-income countries. *Paediatr. Int. Child Health* 39, 13–17. doi: 10.1080/20469047.2018.1490100

Poddar, U., and Yachha, S. K. (2007). Helicobacter pylori in children: an Indian perspective. *Indian Pediatr.* 44, 761–770.

Radin, M. J., Eaton, K. A., Krakowka, S., Morgan, D. R., Lee, A., Otto, G., et al. (1990). Helicobacter pylori gastric infection in gnotobiotic beagle dogs. *Infect. Immun.* 58, 2606–2612. doi: 10.1128/iai.58.8.2606-2612.1990

Rossi, G., Rossi, M., Vitali, C. G., Fortuna, D., Burroni, D., Pancotto, L., et al. (1999). A conventional beagle dog model for acute and chronic infection with Helicobacter pylori. *Infect. Immun.* 67, 3112–3120. doi: 10.1128/IAI.67.6.3112-3120.1999

Saberi, S., Pournasr, B., Farzaneh, Z., Esmaeili, M., Hosseini, M. E., Baharvand, H., et al. (2018). A simple and cost-efficient adherent culture platform for human gastric primary cells, as an *in vitro* model for Helicobacter pylori infection. *Helicobacter* 23, e12489. doi: 10.1111/hel.2018.23.issue-4

Salama, N. R., Hartung, M. L., and Müller, A. (2013). Life in the human stomach: persistence strategies of the bacterial pathogen Helicobacter pylori. *Nat. Rev. Microbiol* 11, 385–399. doi: 10.1038/nrmicro3016

Sarkar, S., Talesh, G. A., menheniott, T. R., and sutton, p. (2023). Targeting host sulphonyl urea receptor 2 can reduce severity of helicobacter pylori associated gastritis. *Gastro Hep Adv.* 2, 721–732. doi: 10.1016/j.gastha.2023.03.007

Sato, T., Vries, R. G., Snippert, H. J., Wetering, M. V., Barker, N., Stange, D. E., et al. (2009). Single Lgr5 stem cells build crypt-villus structures *in vitro* without a mesenchymal niche. *Nature* 459, 262–265. doi: 10.1038/nature07935

Sawai, N., Kita, M., Kodama, T., Tanahashi, T., Yamaoka, Y., Tagawa, Y., et al. (1999). Role of gamma interferon in Helicobacter pylori-induced gastric inflammatory responses in a mouse model. *Infect. Immun.* 67, 279–285. doi: 10.1128/IAI.67.1.279-285.1999

Sebrell, T. A., Hashimi, M., Sidar, B., Wilkinson, R. A., Kirpotina, L., Quinn, M. T., et al. (2019). A novel gastric spheroid co-culture model reveals chemokine-dependent recruitment of human dendritic cells to the gastric epithelium. *Cell. Mol. gastroenterology hepatology* 8, 157–71. e3. doi: 10.1016/j.jcmgh.2019.02.010

Seidlitz, T., Koo, B.-K., and Stange, D. E. (2021). Gastric organoids—an *in vitro* model system for the study of gastric development and road to personalized medicine. *Cell Death Differentiation* 28, 68–83. doi: 10.1038/s41418-020-00662-2

Semrau, A., Gerold, S., Frick, J. S., and Iglauer, F. (2017). Non-invasive detection and successful treatment of a Helicobacter pylori infection in a captive rhesus macaque. *Lab. Anim* 51, 208–211. doi: 10.1177/0023677216669179

Shah, S. C., Iyer, P. G., and Moss, S. F. (2021). AGA clinical practice update on the management of refractory helicobacter pylori infection: expert review. *Gastroenterology* 160, 1831–1841. doi: 10.1053/j.gastro.2020.11.059

Sharma, V., and McNeill, J. H. (2009). To scale or not to scale: the principles of dose extrapolation. *Br. J. Pharmacol.* 157, 907–921. doi: 10.1111/j.1476-5381.2009.00267.x

Shomer, N. H., Dangler, C. A., Whary, M. T., and Fox, J. G. (1998). Experimental Helicobacter pylori infection induces antral gastritis and gastric mucosa-associated lymphoid tissue in Guinea pigs. *Infect. Immun.* 66, 2614–2618. doi: 10.1128/IAI.66.6.2614-2618.1998

Solnick, J. V., Chang, K., Canfield, D. R., and Parsonnet, J. (2003). Natural acquisition of Helicobacter pylori infection in newborn rhesus macaques. *J. Clin. Microbiol* 41, 5511–5516. doi: 10.1128/JCM.41.12.5511-5516.2003

Solnick, J. V., Fong, J., Hansen, L. M., Chang, K., Canfield, D. R., and Parsonnet, J. (2006). Acquisition of Helicobacter pylori infection in rhesus macaques is most consistent with oral-oral transmission. *J. Clin. Microbiol* 44, 3799–3803. doi: 10.1128/JCM.01482-06

Solnick, J. V., Hansen, L. M., Canfield, D. R., and Parsonnet, J. (2001). Determination of the infectious dose of Helicobacter pylori during primary and secondary infection in rhesus monkeys (Macaca mulatta). *Infect. Immun.* 69, 6887–6892. doi: 10.1128/IAI.69.11.6887-6892.2001

Stair, M. I., Winn, C. B., Burns, M. A., Holcombe, H., Artim, S. C., Ge, Z., et al. (2023). Effects of chronic Helicobacter pylori strain PMSS1 infection on whole brain and gastric iron homeostasis in male INS-GAS mice. *Microbes Infect.* 25, 105045. doi: 10.1016/j.micinf.2022.105045

Sturegård, E., Sjunnesson, H., Ho, B., Willén, R., Aleljung, P., Ng, H. C., et al. (1998). Severe gastritis in Guinea-pigs infected with Helicobacter pylori. *J. Med. Microbiol* 47, 1123–1129. doi: 10.1099/00222615-47-12-1123

Suarez, G., Romero-Gallo, J., Piazuelo, M. B., Sierra, J. C., Delgado, A. G., Washington, M. K., et al. (2019). Nod1 Imprints Inflammatory and Carcinogenic Responses toward the Gastric Pathogen Helicobacter pylori. *Cancer Res.* 79, 1600–1611. doi: 10.1158/0008-5472.CAN-18-2651

Suzuki, S., Kusano, C., Horii, T., Ichijima, R., and Ikehara, H. (2022). The ideal helicobacter pylori treatment for the present and the future. *Digestion* 103, 62–68. doi: 10.1159/000519413

Suzuki, R., Satou, K., Shiroma, A., Shimoji, M., Teruya, K., Matsumoto, T., et al. (2019). Genome-wide mutation analysis of Helicobacter pylori after inoculation to Mongolian gerbils. *Gut Pathog* 11, 45. doi: 10.1186/s13099-019-0326-5

Tan, H.-J., and Goh, K.-L. (2012). Extragastrointestinal manifestations of Helicobacter pylori infection: facts or myth? A critical review. *J. Digestive Dis.* 13, 342–349. doi: 10.1111/j.1751-2980.2012.00599.x

Thirumurthi, S., and Graham, D. Y. (2012). Helicobacter pylori infection in India from a western perspective. *Indian J. Med. Res.* 136, 549–562.

Tohumcu, E., Kaitsas, F., Bricca, L., Ruggeri, A., Gasbarrini, A. , Cammarota, G., et al. (2024). Helicobacter pylori and the human gastrointestinal microbiota: A multifaceted relationship. . *Antibiotics (Basel)* 13–584. doi: 10.3390/antibiotics13070584

Tomaszewska, A., Gonciarz, W., Rechcinski, T., Chmiela, M., Kurdowska, A. K., and Krupa, A. (2024). Helicobacter pylori components increase the severity of metabolic syndrome and its hepatic manifestations induced by a high fat diet. *Sci. Rep.* 14, 5764. doi: 10.1038/s41598-024-56308-7

Tsai, C. J., Loh, J. M., and Proft, T. (2016). Galleria mellonella infection models for the study of bacterial diseases and for antimicrobial drug testing. *Virulence* 7, 214–229. doi: 10.1080/21505594.2015.1135289

Uemura, N., Okamoto, S., Yamamoto, S., Matsumura, N., Yamaguchi, S., Yamakido, M., et al. (2001). Helicobacter pylori infection and the development of gastric cancer. *N Engl. J. Med.* 345, 784–789. doi: 10.1056/NEJMoa001999

Uotani, T., Murakami, K., Uchida, T., Tanaka, S., Nagashima, H., Zeng, X.-L., et al. (2019). Changes of tight junction and interleukin-8 expression using a human gastroid monolayer model of Helicobacter pylori infection. *Helicobacter* 24, e12583. doi: 10.1111/hel.2019.24.issue-3

Ventola, C. L. (2015). The antibiotic resistance crisis: part 1: causes and threats. *P t* 40, 277–283.

Vogiatzi, P., Cassone, M., Luzzi, I., Lucchetti, C., Otvos, L. Jr., and Giordano, A. (2007). Helicobacter pylori as a class I carcinogen: physiopathology and management strategies. *J. Cell Biochem.* 102, 264–273. doi: 10.1002/jcb.v102:2

Wagner, S., Beil, W., Mai, U. E., Bokemeyer, C., Meyer, H. J., and Manns, M. P. (1994). Interaction between Helicobacter pylori and human gastric epithelial cells in culture: effect of antiulcer drugs. *Pharmacology* 49, 226–237. doi: 10.1159/000139238

Walduck, A. K., and Becher, o. (2012). Leptin, CD4+ Treg and the prospects for vaccination against H. pylori infection. *Front. Immunol.* 3, 29262. doi: 10.3389/fimmu.2012.00316

Wei, X., Feng, X. P., Wang, L. Y., Huang, Y. Q., Liang, L. L., Mo, X. Q., et al. (2019). Improved method for inducing chronic atrophic gastritis in mice. *World J. Gastrointest Oncol.* 11, 1115–1125. doi: 10.4251/wjgo.v11.i12.1115

Wu, C., Shi, Y., Guo, H., Zou, W. Y., Guo, G., Xie, Q. H., et al. (2008). Protection against Helicobacter pylori infection in Mongolian gerbil by intragastric or intramuscular administration of H. pylori multicomponent vaccine. *Helicobacter* 13, 191–199. doi: 10.1111/j.1523-5378.2008.00609.x

Yamamoto, T., Kita, M., Ohno, T., Iwakura, Y., Sekikawa, K., and Imanishi, J. (2004). Role of tumor necrosis factor-alpha and interferon-gamma in Helicobacter pylori infection. *Microbiol Immunol.* 48, 647–654. doi: 10.1111/j.1348-0421.2004.tb03474.x

Yamaoka, Y. (2010). Mechanisms of disease: Helicobacter pylori virulence factors. *Nat. Rev. Gastroenterol. Hepatol* 7, 629–641. doi: 10.1038/nrgastro.2010.154

Ye, L., Swingen, C., and Zhang, J. (2013). Induced pluripotent stem cells and their potential for basic and clinical sciences. *Curr. Cardiol. Rev.* 9, 63–72. doi: 10.2174/157340313805076278

Zarauz, J. M., Zafrilla, P., Ballester, P., and Cerda, B. (2022). Study of the drivers of inappropriate use of antibiotics in community pharmacy: request for antibiotics without a prescription, degree of adherence to treatment and correct recycling of leftover treatment. *Infect. Drug Resist.* 15, 6773–6783. doi: 10.2147/IDR.S375125

Zhang, S., and Moss, S. F. (2012). Rodent models of Helicobacter infection, inflammation, and disease. *Methods Mol. Biol.* 921, 89–98. doi: 10.1007/978-1-62703-005-2_12

Zheng, Y., Zhang, S., Zhang, T., Teng, X., Ling, X., Li, B., et al. (2024). A Bifidobacterium animalis subsp. lactis strain that can suppress Helicobacter pylori: isolation, *in vitro* and *in vivo* validation. *Lett. Appl. Microbiol* 77(1), ovae005. doi: 10.1093/lambio/ovae005

Zhu, H. Y., Wu, J., Zhang, Y. M., Li, F. L., Yang, J., Qin, B., et al. (2024). Characteristics of early gastric tumors with different differentiation and predictors of long-term outcomes after endoscopic submucosal dissection. *World J. Gastroenterol.* 30, 1990–2005. doi: 10.3748/wjg.v30.i14.1990

Frontiers in
Cellular and Infection Microbiology

Investigates how microorganisms interact with their hosts

Explores bacteria, fungi, parasites, viruses, endosymbionts, prions and all microbial pathogens as well as the microbiota and its effect on health and disease in various hosts.

Discover the latest Research Topics

See more →

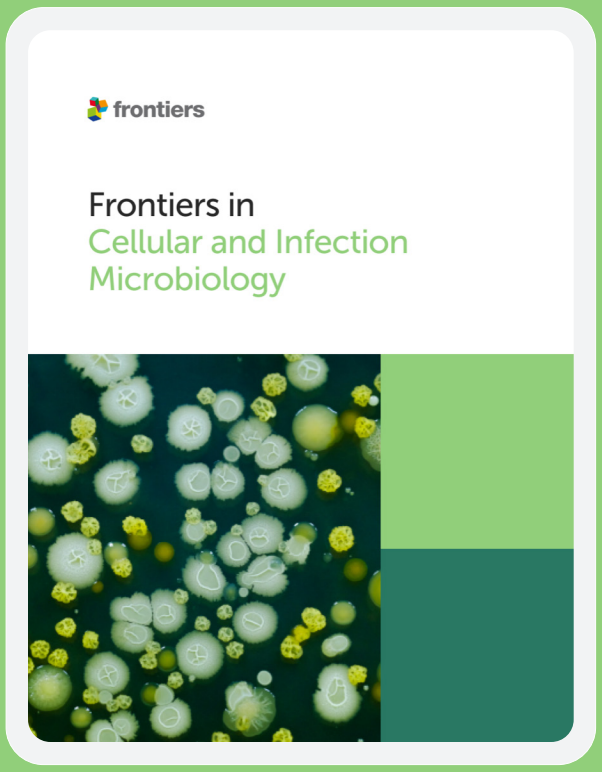

Frontiers

Avenue du Tribunal-Fédéral 34
1005 Lausanne, Switzerland
frontiersin.org

Contact us

+41 (0)21 510 17 00
frontiersin.org/about/contact